

August 2017

Part – I: Development of a Two-step Regiospecific Synthetic Route for Multigram Scale Synthesis of B-carboline Analogs for Studies in Primates as Anti-alcohol Agents, part – II: Design and Synthesis of Novel Antimicrobials for the Treatment of Drug Resistant Bacterial Infections Part – Iii: A Novel Synthetic Method for the Synthesis of the Key Quinine Metabolite (3S)-3-Hydroxyquinine

Veera Venkata Naga Phani Babu Tiruveedhula
University of Wisconsin-Milwaukee

Follow this and additional works at: <https://dc.uwm.edu/etd>

 Part of the [Analytical Chemistry Commons](#), [Biochemistry Commons](#), and the [Organic Chemistry Commons](#)

Recommended Citation

Tiruveedhula, Veera Venkata Naga Phani Babu, "Part – I: Development of a Two-step Regiospecific Synthetic Route for Multigram Scale Synthesis of B-carboline Analogs for Studies in Primates as Anti-alcohol Agents, part – II: Design and Synthesis of Novel Antimicrobials for the Treatment of Drug Resistant Bacterial Infections Part – Iii: A Novel Synthetic Method for the Synthesis of the Key Quinine Metabolite (3S)-3-Hydroxyquinine" (2017). *Theses and Dissertations*. 1710.
<https://dc.uwm.edu/etd/1710>

**PART – I: DEVELOPMENT OF A TWO-STEP REGIOSPECIFIC SYNTHETIC
ROUTE FOR MULTIGRAM-SCALE SYNTHESIS OF β -CARBOLINE ANALOGS
FOR STUDIES IN PRIMATES AS ANTI-ALCOHOL AGENTS**

**PART – II: DESIGN AND SYNTHESIS OF NOVEL ANTIMICROBIALS FOR THE
TREATMENT OF DRUG RESISTANT BACTERIAL INFECTIONS**

**PART – III: A NOVEL SYNTHETIC METHOD FOR THE SYNTHESIS OF THE
KEY QUININE METABOLITE (3S)-3-HYDROXYQUININE**

by

Veera Venkata Naga Phani Babu Tiruveedhula

A Dissertation Submitted in
Partial Fulfillment of the
Requirements for the Degree of

Doctor of Philosophy

in Chemistry

at

The University of Wisconsin-Milwaukee

August 2017

ABSTRACT

PART – I: DEVELOPMENT OF A TWO-STEP REGIOSPECIFIC SYNTHETIC ROUTE FOR MULTIGRAM SCALE SYNTHESIS OF β -CARBOLINE ANALOGS FOR STUDIES IN PRIMATES AS ANTI-ALCOHOL AGENTS
PART – II: DESIGN AND SYNTHESIS OF NOVEL ANTIMICROBIALS FOR THE TREATMENT OF DRUG RESISTANT BACTERIAL INFECTIONS
PART – III: A NOVEL SYNTHETIC METHOD FOR THE SYNTHESIS OF THE KEY QUININE METABOLITE (3S)-3-HYDROXYQUININE

by

Veera Venkata Naga Phani Babu Tiruveedhula

The University of Wisconsin-Milwaukee, 2017
Under the Supervision of Distinguished Professor James M. Cook

PART – I

Development of a Two-Step Regiospecific Synthetic Route for Multigram-Scale Synthesis of β -Carboline Analogs for Studies in Primates as Anti-Alcohol Agents

β -Carboline and their derivatives are important structural motifs in synthetic organic and medicinal chemistry because of their novel biological activity, especially in regard to the reduction of alcohol self-administration [binge drinking (BD)], a major problem increasing day by day in modern society. This anti-alcohol effect is proposed to be due to the activity of ligands at the benzodiazepine site of the GABA_A receptor in the central nervous system acting as antagonists at the $\alpha 1$ subunit. The past evidence by June, Gondre-Lewis, and Weerts et al. of the biological importance of β -carbolines for the treatment of alcohol abuse has prompted the design and synthesis of a new series of analogs to improve the *in vitro* and *in vivo* pharmacological properties. Initial SAR studies on these β -carbolines revealed that β CCt (**3**) and the more water soluble analog, 3-PBC·HCl (**1·HCl**) were lead ligands for they had been shown to reduce alcohol self-administration in alcohol preferring (P) and high alcohol drinking (HAD) rats by June et al. with little or no effect on sucrose self-administration and no anhedonia nor depression. With this important activity, further studies were designed in higher animal models such as non-human primates (Weerts). However, the availability of these ligands for biological studies was the limiting step because of the long synthetic route and overall low yields. Consequently, a novel short two-step palladium catalyzed protocol was developed which consisted of a combined regioselective Buchwald-Hartwig amination and an intramolecular Heck-type cyclization to gain regiospecific access to 3,6-disubstituted β -carbolines. This regiospecific two-step synthetic protocol reduced the number of steps from 6 to 2 and permitted execution in excellent yields on a large scale (50 - 80 grams). To obtain ligands with anti-alcohol effects that were more water soluble than the active anti-alcohol compound β CCt (**3**) by using 3-PBC·HCl (**1·HCl**) as the guide, 3-ISOPBC·HCl

(**2•HCl**) was synthesized which showed more potent activity in the reduction of alcohol self-administration than **1•HCl** in a maternally deprived (MD) rat model for binge drinking. Later pre-clinical studies were conducted in non-human primate models such as baboons which required 80-100 grams of 3-ISOPBC•HCl. This can now be accomplished with ease using the new Pd chemistry. The pronounced activity of **2•HCl** in non-human primates does imply it is a potential ligand to treat human alcoholics without the side effects of diazepam (one of the drugs employed now). These results led to the synthesis of 3-cycloPBC•HCl (**20•HCl**) which was active, to date, in MD rats without effecting the sucrose responding. The 3-cycloPBC•HCl was not cytotoxic at all when compared to β CCt, 3-PBC•HCl, 3-ISOPBC•HCl; the latter 3 ligands of which did exhibit some toxicity but only at very high concentrations. The microsomal stability studies on human and mouse liver microsomes of **20•HCl** revealed it was longer lived *in vitro* than 3-PBC•HCl, and 3-ISOPBC•HCl. Further studies will need to be carried out in primate models to see if **20•HCl** is a potential novel therapeutic agent to combat alcohol drinking and substance use disorders.

PART – II

Design and Synthesis of Novel Antimicrobials for the Treatment of Drug Resistant Bacterial Infections

The alarming increase in bacterial resistance over the last decade along with a dramatic decrease in new treatments for infections has led to problems in the healthcare industry. A world-wide threat with HIV co-infected with multi and extensively drug-resistant strains of tuberculosis (TB) and methicillin-resistant *Staphylococcus aureus* (MRSA) has emerged and is responsible for several million deaths per year. In this regard, herein, novel acrylic acid ethyl ester derivatives were synthesized in simple, efficient routes, and evaluated as potential agents against a panel of gram positive, negative, mycobacterial, and clinically significant resistant strains including *M. tuberculosis* (Mtb) for minimum inhibitory concentrations (MIC). In depth structure activity

relationship (SAR) studies of acrylic acid ethyl ester derivatives revealed that the ethyl esters **59** and **63** were found to be very potent (MIC = 0.72 and 0.69 $\mu\text{g/mL}$) against actively replicating Mtb. Importantly, scaffolds **59** and **63** exhibited six and four fold greater inhibition, respectively, against nonreplicating persistent (dormant) phenotypes under low oxygen conditions than isoniazid; this is essential to decrease the duration of tuberculosis treatment from many months to less time. Further evaluation of these selected analogs **59** and **63** against a panel of single-drug resistant Mtb strains indicated a similar level of activity as against wild type Mtb. This encouraging safety profile is key with a selective index greater than 10. Gratifyingly, the ethyl ester **59** retained excellent inhibition with MIC values of 0.25-4.0 $\mu\text{g/mL}$ against a wide variety of virulent antibiotic-resistant clinical isolates (MRSA, MDR MRSA, VISA MRSA, and VRE). This exciting activity provided a path to determine the molecular target for this novel class of compounds with the copper catalyzed azide-alkyne 1,3-dipolar cycloaddition (CuAAC) Click reaction because of the availability of alkyne functionality in **59**. By treating *Staphylococcus aureus* lysates with Alexa fluor 647 picolyl azide (AF647), one identified *S. aureus* proteins that had been covalently modified by propargyl ligand **59**. SDS-PAGE analysis of the fluorescently labeled proteins showed that only two proteins were labeled. Encouraged by the results, AF647 was replaced with biotin azide to isolate the target proteins using streptavidin beads. Later, the purified protein fractions were subjected to peptide mass fingerprinting for protein identification. Data analysis of these samples using MaxQuant 1.4.1.2 against the Uniport database for *E. coli* and *S. aureus* identified three enzymes as potential targets: enolase (Uniprot ID: P64079), dihydrolipoyllysine-residue acetyltransferase (Uniprot ID: Q8NX76), and glyceraldehyde-3-phosphate dehydrogenase (Uniprot ID: P0A037). These enzymes are well-known to be involved in glycolysis and act as virulence factors responsible for the pathogenicity of *S. aureus*. Thus far, attempts to validate the structure of *S. aureus* enolase by X-ray diffraction analysis have been unsuccessful, since one has

been unable to obtain diffraction-quality crystals of this protein; however, protein docking experiments with *S. aureus* enolase have been successful. Further work on these potent antimicrobial agents would benefit from the knowledge of the binding site as well as interactions between the ligand and the proteins; the mode of inhibition. The identification of the bimolecular interaction between the ligand **59** and target proteins would potentially result in new drugs to treat drug resistant infections from bacteria, including MRSA, MDR VISA, and VRE. The investigation of ADMET medicinal chemistry properties of select agents including **59** and **63** is ongoing in our laboratories.

Part – III

A Novel Synthetic Method for the Synthesis of the Key Quinine Metabolite (3*S*)-3-Hydroxyquinine

The Cinchona alkaloid quinine (**1**) remains unique among the thousands of natural products isolated and characterized to date because it still remains the drug of choice for the treatment of severe and complicated malaria in most parts of the world. Apart from biological activity, Cinchona alkaloids play a vital role in organic chemistry from racemate resolutions to promote enantioselective transformations in both homogeneous and heterogeneous catalysis. The synthesis of the major metabolite of quinine (**1**), 3(*S*)-3-hydroxyquinine (**7**) has been accomplished by a shorter route, devoid of the previously employed toxic reagent (HBr gas) and separated from its epimeric mixture [4(*S*):1(*R*)] at C-3 by conversion into the 9-aceto analogue followed by flash column chromatography. The molecular structure of the major acetate diastereomer **9** was further confirmed by X-ray crystallographic analysis, and this unambiguously confirms the absolute configuration of 3(*S*)-3-hydroxyquinine (**7**). The new synthetic protocol increased the overall yield from 16% to 53% and makes essential metabolite **7** more readily available now for scientists and doctors to study drug-drug interactions when using quinine with another agent to treat, malaria

combined with HIV (ritonavir) or other comorbid situations. For instance, a doctor in Nigeria, using **7** found that in healthy volunteers, to treat patients with HIV and malaria one needed a ratio of ~5:1 ritonavir and quinine, not 1:1, as used previously.

To
my family,
my better half Revathi,
and princess Jesri Tiruveedhula

TABLE OF CONTENTS

List of Figures.....	xix
List of Tables.....	xxiv
List of Schemes.....	xxv
Part - I: Development of a Two-Step Regiospecific Synthetic Route for Multigram-Scale Synthesis of β-Carboline Analogs for Studies in Primates as Anti-Alcohol Agents....	1-116
Chapter 1: Synthesis of Aza and Carbocyclic β -Carbolines for the Treatment of Alcohol Abuse. Regiospecific Solution to the Problem of 3,6-Disubstituted β - and Aza- β -Carboline Specificity	2
1.1. Abstract.....	2
1.2. Introduction.....	2
1.3. Results and Discussion	4
1.4. Conclusion	12
1.5. Experimental.....	13
1.5.1. General conditions.....	13
1.5.2. General procedure for the Buchwald-Hartwig coupling reaction between substituted aniline and substituted pyridines: Representative procedure for the synthesis of <i>N</i> -(2-chlorophenyl)-6-propoxy-pyridin-3-amine (7a)	13
1.5.3. <i>N</i> -(2-Chlorophenyl)-6-isopropoxy-pyridin-3-amine (7b)	14
1.5.4. <i>tert</i> -Butyl 5-[(2-chlorophenyl)amino]picolinate (7c).....	15
1.5.5. <i>N</i> -(3-Chloropyridin-4-yl)-6-propoxy-pyridin-3-amine (7d).....	15
1.5.6. <i>N</i> -(3-Chloropyridin-4-yl)-6-isopropoxy-pyridin-3-amine (7e)	15
1.5.7. General procedure for the intramolecular Heck cyclization: Representative procedure for the synthesis of 3-propoxy-9 <i>H</i> -pyrido[3,4- <i>b</i>]indole (3-PBC, 1) and 2-propoxy-5 <i>H</i> -pyrido[3,2- <i>b</i>]indole (9a)	16
1.5.8. 3-Isopropoxy-9 <i>H</i> -pyrido[3,4- <i>b</i>]indole (3-ISOPBC, 2) and 3-isopropoxy-5 <i>H</i> -pyrido[3,2- <i>b</i>]indole (9b)	17
1.5.9. <i>tert</i> -Butyl 9 <i>H</i> -pyrido[3,4- <i>b</i>]indole-3-carboxylate (β CCt, 3) and <i>tert</i> -butyl 5 <i>H</i> -pyrido[3,2- <i>b</i>]indole-3-carboxylate (9c)	18

1.5.10. 8-Propoxy-5 <i>H</i> -pyrrolo[2,3- <i>c</i> :4,5- <i>c'</i>]dipyridine (6-Aza-3-PBC, 4) and 2-Propoxy-5 <i>H</i> -pyrrolo[3,2- <i>b</i> :4,5- <i>c'</i>]dipyridine (9d).....	19
1.5.11. 8-Isopropoxy-5 <i>H</i> -pyrrolo[2,3- <i>c</i> :4,5- <i>c'</i>]dipyridine (6-Aza-3-ISOPBC, 5) and 2-Isopropoxy-5 <i>H</i> -pyrrolo[3,2- <i>b</i> :4,5- <i>c'</i>]dipyridine (9e)	19
1.5.12. <i>tert</i> -Butyl (2-chlorophenyl)(6-isopropoxy-pyridin-3-yl)carbamate (10).....	20
1.5.13. (9 <i>H</i> -Fluoren-9-yl)methyl (2-chlorophenyl)(6-isopropoxy-pyridin-3-yl)carbamate(11)	21
1.5.14. 4-Chloro-6-isopropoxy- <i>N</i> -phenylpyridin-3-amine (16).....	21
1.5.15. 4-Chloro-6-propoxy- <i>N</i> -phenylpyridin-3-amine (15).....	22
1.5.16. 4-Chloro-6-propoxy- <i>N</i> -(pyridin-4-yl)pyridine-3-amine (17).....	22
1.5.17. 4-Chloro-6-isopropoxy- <i>N</i> -(pyridin-4-yl)pyridine-3-amine (18).....	23
1.5.18. 3-propoxy-9 <i>H</i> -pyrido[3,4- <i>b</i>]indole (3-PBC, 1).....	23
1.5.19. 3-Isopropoxy-9 <i>H</i> -pyrido[3,4- <i>b</i>]indole (3-ISOPBC, 2)	24
1.5.20. 8-Propoxy-5 <i>H</i> -pyrrolo[2,3- <i>c</i> :4,5- <i>c'</i>]dipyridine (6-Aza-3-PBC, 4)	24
1.5.21. 8-Isopropoxy-5 <i>H</i> -pyrrolo[2,3- <i>c</i> :4,5- <i>c'</i>]dipyridine (6-Aza-3-ISOPBC, 5)	24
1.5.22. Large-Scale Synthesis of 3-ISOPBC (2).....	24
1.5.22.1. Step 1: Synthesis of 4-Chloro-6-isopropoxy- <i>N</i> -phenylpyridin-3-amine (16).....	24
1.5.22.2. Step 2: Synthesis of 3-isopropoxy-9 <i>H</i> -pyrido[3,4- <i>b</i>]indole (2).....	25
1.6. References.....	25
Chapter 2: Biological Evaluation of β-Carboline Analogs	29
2.1. Introduction.....	29
2.2. Biological Studies	29
2.2.1. Determination of efficacy studies in HEK 293 cells	30
2.2.2. Efficacy studies in <i>Xenopus laevis</i> frog oocytes and receptor binding.....	36
2.2.3. Effect of 3-isopropoxy- β -carboline hydrochloride (2 ·HCl) on alcohol seeking and self-administration in baboons.....	38
2.3.3.1. Effects of acute administration of 3-ISOPBC·HCl (2 ·HCl)	39
2.3.3.2. Effects of chronic administration of 3-ISOPBC·HCl (2 ·HCl).....	40

2.2.4. Potential role of the $\alpha 1$ Bz/GABA _A subunit-containing receptor in a rhesus monkey model of alcohol drinking and effect of β CCt and 3-PBC·HCl	43
2.2.4.1. Drinking behavior.....	44
2.2.4.2. Effect of $\alpha 1\beta 3\gamma 2$ Bz/GABA(A)ergic preferring compounds on alcohol drinking.....	45
2.2.4.3. Effect of nonselective benzodiazepines ligands on alcohol drinking.....	47
2.2.4.4. Observable behavioral effects with $\alpha 1$ preferring compounds.....	49
2.2.5. The potential effect of 3-PBC·HCl in early life stress induced impulsivity and excessive alcohol drinking in adult MS rats	50
2.2.5.1. Measurement of baseline operant responding	52
2.2.5.2. Antalarmin decreases impulsivity and binge drinking in MS rats	53
2.2.5.3. Increased expression of GABA _A $\alpha 2$ receptors in the CeA and mPFC of naïve MS rats	55
2.2.5.4. 3-PBC·HCl (1·HCl) decreases the impulsivity and binge alcohol drinking in MS rats	56
2.2.6. Effect of PBC isoforms (3-PBC·HCl, 3-ISOPBC·HCl, β CCt, and 3-CycloPBC·HCl) on alcohol drinking in P rats and effect of 3-CycloPBC·HCl and 3-ISOPBC·HCl in maternally deprived (MD) rats	58
2.2.7. The effect of β CCt, 3-PBC·HCl (1·HCl), and 3-ISOPBC·HCl (2·HCl) on the spontaneous locomotor Activity (SLA) and Diazepam Induced Sedation in Mice....	65
2.2.8. Determination of CNS (Central Nervous System) sensorimotor effects using rotarod studies	72
2.2.9. <i>In-vitro</i> metabolic stability studies of β -carboline on human liver microsomes (HLM) and mouse liver microsomes (MLM).....	73
2.2.10. Evaluation of cytotoxicity of β -carboline in HEK 293 and HEPG2 Cells.....	77
2.2.11. Psychoactive drug screening program (PDSP) analysis of 3-ISOPBC·HCl	79
2.3. Conclusion	82
2.4. Experimental Methods	86
2.4.1. Determination of efficacy studies in HEK 293T Cells - general methods for electrophysiological recordings from transiently transfected HEK-293T cells	86
2.4.2. Efficacy studies in <i>Xenopus laevis</i> frog oocytes.....	87
2.4.3. Effect of 3-Isopropoxy- β -carboline hydrochloride (3-ISOPBC) on alcohol seeking and self-administration in baboons	89

2.4.4. Role of $\alpha 1$ GABA _A subunit-containing receptors in a rhesus monkey model of alcohol drinking and effect of β CCt and 3-PBC with Dr. Platt.....	93
2.4.5. Effect of 3-PBC in an early life stress-induced impulsivity model and excessive alcohol drinking in adults MS rats.....	98
2.4.6. Effect of PBC isoforms on alcohol drinking in P rats and effect of 3-CycloPBC and 3-ISOPBC in maternally deprived (MD) rats with Dr. Marjorie Gonde-Lewis.....	104
2.4.7. Effect of β CCt, 3-PBC, and 3-ISOPBC on the spontaneous locomotor activity (SLA) and diazepam induced sedation in mice with Dr. Savic	105
2.4.8. Determination of CNS (Central Nervous System) sensorimotor effects using rotarod studies with Nicholas Zahn.....	107
2.4.9. <i>In-vitro</i> metabolic stability studies in human liver and mouse liver derived microsomes with Revathi Kodali at UWM	107
2.4.10. Evaluation of cytotoxicity of β -carboline in HEK 293 and HEPG2 cells with Dr. Michael Rajesh Stephen at UWM	109
2.4.11. Synthesis of 3-cycloPBC·HCl (20 ·HCl) and WYS8.....	109
2.4.11.1. 3-Cyclopropoxy-9H-pyrido[3,4- <i>b</i>]indol-2-ium chloride (20).....	110
2.5. References.....	111
Part - II: Design and Synthesis of Novel Antimicrobials for the Treatment of Drug Resistant Bacterial Infections	117-276
Chapter 3: Introduction to Antibiotics	118
3.1. Brief History of Antibiotics and Classification	118
3.1.1. Sulfonamides.....	120
3.1.2. β -lactams	120
3.1.2.1. Penicillins	121
3.1.2.2. Cephalosporins	121
3.1.2.3. Carbapenems	122
3.1.3. Aminoglycosides.....	123
3.1.4. Macrolides.....	124
3.1.5. Tetracyclines	124
3.1.6. Rifamycins	125
3.1.7. Quinolones	126

3.1.8. Glycopeptides	128
3.1.9. Polymyxins	129
3.1.10. Oxazolidinones	130
3.1.11. Streptogramins	131
3.1.12. Amphenicols	132
3.1.13. Lipopeptides.....	132
3.2. Tuberculosis.....	136
3.2.1. Pathophysiology.....	137
3.2.2. Clinical manifestations.....	140
3.2.2.1. Latent tuberculosis	140
3.2.2.2. Primary disease (active)	140
3.2.2.3. Primary progressive tuberculosis	141
3.2.2.4. Extrapulmonary tuberculosis.....	141
3.2.3. Treatment for tuberculosis	142
3.2.3.1. First line anti-TB drugs	142
3.2.3.2. Second line anti-TB drugs.....	143
3.2.3.3. Third line anti-TB drugs.....	144
3.2.4 Tuberculosis drugs in the pipeline.....	146
3.3. Methicillin-Resistant <i>Staphylococcus Aureus</i> (MRSA).....	150
3.3.1. Factors causing virulence.....	151
3.3.2. MRSA infections	153
3.3.3. Treatment options for MRSA infections.....	153
3.4. Antibiotic Resistance	155
3.4.1. Origin of resistance in bacteria	155
3.4.2. Different mechanisms of bacterial resistance	158
3.4.2.1. Enzymatic and chemical modification of a drug.....	158
3.4.2.2. Prevention of access to the target by efflux pump mechanisms.....	161

3.4.2.3. Alteration of molecular target by mutation	162
3.4.2.4. Target site protection	163
3.5. References	166
Chapter 4: Design and Synthesis of Novel Antimicrobials with Activity against Gram-positive Bacteria and Mycobacterial species, including <i>M. tuberculosis</i>.....	175
4.1. Abstract	175
4.2. Introduction	175
4.3. Results	177
4.4. Chemistry	183
4.5. Biology	185
4.6. Discussion	186
4.7. Conclusion	188
4.8. Experimental	189
4.8.1. Chemistry	189
4.8.1.1. General method for the synthesis of acids 2 and 3	190
4.8.1.1.1. (Z)-3-(4-(<i>tert</i> -butyl)phenylthio)acrylic acid (2).....	190
4.8.1.1.2. (Z)-3-(Benzo[<i>d</i>]thiazol-2-ylthio)acrylic acid (3)	191
4.8.1.2. (Z)-Cyclopropylmethyl 3-((4-(<i>tert</i> -butyl)phenylthio)acrylate (4)	191
4.8.1.3. General method for the synthesis of amides 5-11	192
4.8.1.3.1. (Z)-3-(Benzo[<i>d</i>]thiazol-2-ylthio)- <i>N,N</i> -diisopropylacrylamide (5).....	192
4.8.1.3.2. (Z)-3-((4-(<i>tert</i> -butyl)phenylthio)- <i>N</i> -phenylacrylamide (6).....	193
4.8.1.3.3. (Z)-3-((4-(<i>tert</i> -butyl)phenylthio)- <i>N</i> -methyl- <i>N</i> -phenylacrylamide (7)	193
4.8.1.3.4. (Z)-3-((4-(<i>tert</i> -butyl)phenylthio)- <i>N</i> -methylacrylamide (8).....	193
4.8.1.3.5. (Z)-3-((4-(<i>tert</i> -butyl)phenylthio)- <i>N,N</i> -dimethylacrylamide (9).....	193
4.8.1.3.6. (Z)-3-((4-(<i>tert</i> -butyl)phenylthio)- <i>N,N</i> -diisopropylacrylamide (10)....	194
4.8.1.3.7. (Z)-3-((4-(<i>tert</i> -butyl)phenylthio)- <i>N</i> -cyclopropylacrylamide (11).....	194
4.8.1.4. General method for the preparation of propargylic alcohols 26 and 27	194
4.8.1.4.1. Ethyl 4-(4-(<i>tert</i> -butyl)phenyl)-4-hydroxybut-2-ynoate (26).....	195

4.8.1.4.2. Ethyl 4-(4-(benzo[<i>b</i>]thiophen-2-yl)-4-hydroxybut-2-ynoate (27)	195
4.8.1.5. The method for the preparation of enones 12 and 13	195
4.8.1.6. (<i>Z</i>)-Ethyl 4-(benzo[<i>b</i>]thiophen-2-yl)-4-oxobut-2-enoate (20).....	196
4.8.1.7. Ethyl 4-(4-(<i>tert</i> -butyl)phenyl)-4-oxobut-2-ynoate (25).....	197
4.8.1.8. Ethyl 4-(4-(<i>tert</i> -butyl)phenyl)-4-oxobutanoate (14)	197
4.8.1.9. Ethyl 4-(4-(<i>tert</i> -butyl)phenyl)butanoate (15)	198
4.8.1.10. (<i>E</i>)-4-(4-(<i>tert</i> -butyl)phenyl)-4-oxobut-2-enoic acid (16)	198
4.8.1.11. (<i>E</i>)-3-methylbut-2-en-1-yl 4-(4-(<i>tert</i> -butyl)phenyl)-4-oxobut-2-enoate (17)	199
4.8.1.12. (<i>E</i>)-Ethyl 4-(4-(<i>tert</i> -butyl)phenyl)but-2-enoate (18)	199
4.8.1.13. Ethyl 2-(4-(<i>tert</i> -butyl)benzoyl)benzoate (19).....	200
4.8.1.14. 3-(4- <i>tert</i> -butyl-phenylsulfanyl)-propionic acid ethyl ester (24).....	201
4.8.1.15. (1 <i>R</i> ,2 <i>R</i>)-ethyl 2-(4-(<i>tert</i> -butyl)benzoyl)cyclopropanecarboxylate (28).....	201
4.8.1.16. (2 <i>R</i> ,3 <i>R</i>)-ethyl 3-(4-(<i>tert</i> -butyl)benzoyl)oxirane-2-carboxylate (29)	202
4.8.2. Microbiology.....	203
4.8.2.1. MIC determinations	203
4.9. References and Notes.....	204
Chapter 5: Extension of SAR and Biological Evaluation of Novel Aroylacrylic Acid Derivatives as Antimicrobial Agents	209
5.1. Background.....	209
5.2. Results and Discussion	209
5.3. Conclusion	222
5.4. Experimental.....	224
5.4.1. General procedure for the Friedel-Crafts acylation between substituted benzenes and maleic anhydride: Synthesis of aroylacrylic acids 16 , 30-34	224
5.4.2. General procedure for esterification of aroylacrylic acid: synthesis of aroylacrylic esters 13 , 42 and 46-54 , representative procedure for the synthesis of ethyl (<i>E</i>)-4-(4- (<i>tert</i> -butyl)phenyl)-4-oxobut-2-enoate (13).....	225
5.4.2.1. Methyl (<i>E</i>)-4-(4-(<i>tert</i> -butyl)phenyl)-4-oxobut-2-enoate (42).....	225

5.4.2.2. Methyl (<i>E</i>)-4-(4-hydroxyphenyl)-4-oxobut-2-enoate (41).....	225
5.4.2.3. (<i>E</i>)-(<i>E</i>)-3,7-Dimethylocta-2,6-dien-1-yl 4-(4-(<i>tert</i> -butyl)phenyl)-4-oxobut-2-enoate (46).....	226
5.4.2.4. (<i>E</i>)-(<i>2E,6E</i>)-3,7,11-Trimethyldodeca-2,6,10-trien-1-yl 4-(4-(<i>tert</i> -butyl)phenyl)-4-oxobut-2-enoate (47).....	226
5.4.2.5. (<i>E</i>)-3-Methylbut-2-en-1-yl 4-(4-chlorophenyl)-4-oxobut-2-enoate (52)	227
5.4.2.6. (<i>E</i>)-3-Methylbut-2-en-1-yl 4-(4-Bromophenyl)-4-oxobut-2-enoate (53) ...	227
5.4.2.7. (<i>E</i>)-3-Methylbut-2-en-1-yl 4-(4-Iodophenyl)-4-oxobut-2-enoate (54)	228
5.4.2.8. (<i>E</i>)-Ethyl 4-(4-methoxyphenyl)-4-oxobut-2-enoate (48)	228
5.4.2.9. (<i>E</i>)-Ethyl 4-(4-chlorophenyl)-4-oxobut-2-enoate (49).....	229
5.4.2.10. (<i>E</i>)-Ethyl 4-(4-bromophenyl)-4-oxobut-2-enoate (50).....	229
5.4.2.11. (<i>E</i>)-Ethyl 4-(4-iodophenyl)-4-oxobut-2-enoate (51)	229
5.4.3. General procedure for the acid catalyzed esterification of aroylacrylic acid; synthesis of aroylacrylic esters 43-45 . Representative procedure for the synthesis of isopropyl (<i>E</i>)-4-(4-(<i>tert</i> -butyl)phenyl)-4-oxobut-2-enoate (43)	230
5.4.3.1. <i>Tert</i> -Butyl (<i>E</i>)-4-(4-(<i>tert</i> -butyl)phenyl)-4-oxobut-2-enoate (44)	230
5.4.3.2. 2,2,2-Trifluoroethyl (<i>E</i>)-4-(4-(<i>tert</i> -butyl)phenyl)-4-oxobut-2-enoate (45) .	231
5.4.4. General procedure for the synthesis of ethyl esters 56 and 57 . Representative procedure for the synthesis of ethyl (<i>E</i>)-4-((4-(<i>tert</i> -butyl)phenyl)amino)-4-oxobut-2-enoate (56)	231
5.4.4.1. 4-(<i>tert</i> -Butyl)phenyl ethyl fumarate (57)	232
5.4.5. Ethyl (<i>E</i>)-4-(4-(<i>tert</i> -butyl)phenyl)-4-hydroxybut-2-enoate (58).....	232
5.4.6. Ethyl (<i>E</i>)-4-oxo-4-(4-(prop-2-yn-1-yloxy)phenyl)but-2-enoate (59)	233
5.4.7. Ethyl (<i>E</i>)-4-oxo-4-(4-(trifluoromethyl)phenyl)but-2-enoate (60).....	234
5.4.8. (<i>E</i>)-10-Hydroxydecyl 4-(4-(<i>tert</i> -butyl)phenyl)-4-oxobut-2-enoate (61)	234
5.4.9. (<i>E</i>)-10-((Diethoxyphosphoryl)oxy)decyl 4-(4-(<i>tert</i> -butyl)phenyl)-4-oxobut-2-enoate (62).....	235
5.4.10. Ethyl (<i>E</i>)-4-(benzo[<i>b</i>]thiophen-2-yl)-4-oxobut-2-enoate (63).....	236

5.4.11. (2 <i>S</i> ,3 <i>R</i>)-Ethyl 4-(benzo[<i>b</i>]thiophen-2-yl)-2,3-dihydroxy-4-oxobutanoate (64)	236
5.4.12. (<i>E</i>)-3-(Benzo[<i>b</i>]thiophen-2-yl)-2-cyanoacrylamide (65).....	237
5.4.13. (<i>E</i>)-1,6-Bis(benzo[<i>b</i>]thiophen-2-yl)hex-3-ene-1,6-dione (66).....	237
5.4.14. Ethyl (<i>E</i>)-3-((4-(<i>tert</i> -butyl)phenyl)sulfinyl)acrylate (68)	238
5.4.15. Ethyl (<i>E</i>)-3-((4-(<i>tert</i> -butyl)phenyl)sulfonyl)acrylate (69)	239
5.4.16. MIC vs. replicating <i>M. tuberculosis</i> H ₃₇ Rv (MABA Assay).....	239
5.4.17. Activity against non-replicating persistent (NRP) <i>M. tuberculosis</i> (LORA Assay)	240
5.4.18. Cytotoxicity.....	241
5.5. References.....	241
Chapter 6: Identification of Molecular Targets for the Antimicrobial Agent 59 (Ethyl (<i>E</i>)-4-oxo-4-(4-(prop-2-yn-1-yloxy)phenyl)but-2-enoate	244
6.1. Introduction.....	244
6.2. Results and Discussion	249
6.3. Role of Targeted Proteins in <i>Staphylococcus</i> Bacteria which were Identified.....	258
6.3.1. Enolase.....	258
6.3.2. Dihydrolipoyllysine Residue Acetyltransferase	264
6.3.3. Glyceraldehyde-3-Phosphate	265
6.4. Methods.....	268
6.4.1. HPLC conditions for the compound, 59 (Ethyl (<i>E</i>)-4-oxo-4-(4-(prop-2-yn-1-yloxy)phenyl)but-2-enoate)	268
6.4.2. Preparation of <i>Staphylococcus aureus</i> cell lysate	268
6.4.3. Labeling of 59 with AF647/biotin azide using the CuAAC reaction in <i>S. aureus</i> lysate	269
6.4.4. Purification after the Click reaction.....	270
6.4.5. Purification of <i>Sa</i> _enolase	270
6.4.6. In-solution trypsin digestion	271
6.4.7. Desalting of tryptic peptides	271
6.4.8 Analysis by LC-MS/MS	272

6.4.9. Enolase crystallization	273
6.5. References	273
Part - III: A Novel Synthetic Method for the Synthesis of the Key Quinine Metabolite (3S)-3-Hydroxyquinine	277-288
Chapter 7: A Novel Synthetic Method for the Synthesis of the Key Quinine Metabolite (3S)-3-Hydroxyquinine	278
7.1. Introduction.....	278
7.2. Results and Discussion	280
7.3. Conclusion	284
7.4. Experimental	285
7.4.1. (R)-((1S,2S,4S)-5-ethylidenequinuclidin-2-yl)(6-methoxyquinolin-4-yl)methanol (2).....	285
7.4.2. (R)-((1S,2S,4S)-5-ethylidenequinuclidin-2-yl)(6-methoxyquinolin-4-yl)methyl acetate (3).....	285
7.4.3. (R)-((1S,2S,4S)-5-hydroxy-5-(1-hydroxyethyl)quinuclidin-2-yl)(6-methoxyquinolin-4-yl)methyl acetate (4).....	286
7.4.4. (R)-(6-Methoxyquinolin-4-yl)((1S,2S,4S)-5-oxoquinuclidin-2-yl)methyl acetate (5).....	286
7.5. References.....	287
APPENDIX A. Identification of <i>Staphylococcus aureus</i> Cellular Pathways Affected by the Stilbenoid Lead Drug SK-03-92 Using a Microarray	289
APPENDIX B. Midazolam Tolerance Data	332
APPENDIX C. Synthesis and Biology Data for β -and Aza- β -Carbolines	334
Curriculum Vitae	495

LIST OF FIGURES

Figure 1-1. Structures of 3-PBC (1), 3-ISOPBC (2), β CCt (3), 6-Aza-3-PBC (4) and 6- Aza-3-ISOPBC (5).....	3
Figure 1-2. ORTEP view of the crystal structure of substituted carbolines 3, 9a, and 9d	5
Figure 2-1. The average enhancement of the current evoked due to GABA alone and GABA with positive allosteric modulators 3-PBC·HCl (1·HCl), 3-ISOPBC·HCl (2·HCl) and 3-cycloPBC·HCl (20·HCl) on α 1-, α 2-, α 3-, α 4-, α 5-, and α 6- subtype GABA _A receptors.....	31
Figure 2-2. The average enhancement of the current evoked by GABA alone and GABA with positive allosteric modulators 3-PBC·HCl (1·HCl), 3-ISOPBC·HCl (2·HCl) and 3-CycloPBC·HCl (20·HCl) on α 1-, α 2-, α 3-, α 4-, α 5-, and α 6- subtype receptors was indicated all in one graph at concentrations of 10 μ M	33
Figure 2-3. Cells were transiently transfected with the α 6 subtype, as indicated, along with β 3 and δ , and voltage clamped at -50 mV	35
Figure 2-4. Augmentation of GABA-induced currents in oocytes expressing GABA _A receptors of specified subunit composition by 3-ISOPBC·HCl and 3-PBC·HCl	36
Figure 2-5. Effects of chronic (5 days) administration of 3-ISOPBC·HCl (2·HCl, 5.0–20.0 mg/kg) on consumption in Component 3 of the chained schedule of reinforcement in the (A) Alcohol Group and (B) Control Group	41
Figure 2-6. Effects of chronic (5 days) administration of 3-ISOPBC·HCl (5.0–20.0 mg/kg) on the pattern of drinking in the first drinking bout in Component 3 of the chained schedule of reinforcement in the (A) Alcohol Group and (B) Control Group	42
Figure 2-7. The effects of varying doses of α 1 GABA _A preferring compounds on intake (top) and latency to first sipper extension (bottom) for alcohol (closed symbols) and sucrose (open symbols).....	46
Figure 2-8. The effects of varying doses of nonselective benzodiazepine receptor ligands on intake (top) and latency to first sipper extension (bottom) for alcohol (closed symbols) and sucrose (open symbols)	48
Figure 2-9. Baseline operant responding for alcohol, blood alcohol concentration and delay discounting (impulsivity) of MS versus CTL rats	53
Figure 2-10. Effects of antalarmin injected into the CeA on delay discounting, operant binge drinking, sucrose drinking	54
Figure 2-11. Effects of antalarmin injected into the mPFC on delay discounting, operant binge drinking and sucrose drinking	54

Figure 2-12. GABA _A α 2 protein concentration in CeA and mPFC of MS versus CTL rats	55
Figure 2-13. Effects of 3-PBC·HCl in the CeA and mPFC on delay discounting, operant binge drinking, and sucrose drinking	57
Figure 2-14. The rat is lever pressing and drinking alcohol/sucrose from the dipper cup which is dispensed near the top of the chamber	59
Figure 2-15. Effect of β CCt, 3-ISOPBC·HCl, 3-PBC·HCl, and 3-cycloPBC·HCl on binge drinking in P rats	60
Figure 2-16. Effect of 3-cycloPBC·HCL on binge drinking in MD rats and effect of 3-ISOPBC·HCl on binge drinking and sucrose drinking in MD rats	62
Figure 2-17. Effect of 3-cycloPBC·HCl on binge drinking in female and male P rats and in female and male P MD rats	64
Figure 2-18. The effects of diazepam (2 mg/kg), β CCt (10 mg/kg), 3-PBC·HCl (10 mg/kg) and 3-ISOPBC·HCl (10 mg/kg) in presented combinations on total distance travelled (left scale, triangles) and total time immobile (right scale, circles) in 0–90 (black symbols) and 0–60 (white symbols) min time periods in mice in SLA	67
Figure 2-19. The effects of diazepam (2 mg/kg) in combination with SOL, 3-PBC·HCl (30 mg/kg) and 3-ISOPBC·HCl (30 mg/kg), respectively, on total distance traveled (a) and total time immobile (b) in 0–90 and 0–60 min time periods in mice in SLA ...	70
Figure 2-20. Effect of compounds on sensorimotor coordination. Swiss Webster mice (Balb/c in case of 3-ISOPBC·HCl) were tested on the rotarod at 15 rpm for 3 min at 10, (5 min for 3-ISOPBC·HCl) 30, and 60 min, respectively following compound exposure	72
Figure 2-21. Oxidative metabolism of the β -carboline alkaloids norharman and harman by human cytochrome P450 enzymes and human liver microsomes.....	76
Figure 2-22. The <i>in-vitro</i> cytotoxicity of β -carboline analogs on HEK 293 and HEPG2 cell lines with LD ₅₀ values which indicates 3-cycloPBC·HCl (20·HCl) is the safest in these assays.....	78
Figure 3-1. Structures of Salvarsan and Neosalvarsan	118
Figure 3-2. Paul Ehrlich (1854-1915) and Sahachiro Hata (1873-1938), Frankfurt 1910.....	119
Figure 3-3. Structures of sulphonamides, and trimethoprim	120
Figure 3-4. β -lactams target interactions and associated cell death.....	120
Figure 3-5. Structures of penicillin antibiotics.....	121
Figure 3-6. Structures of cephalosporin antibiotics and tazobactam	122

Figure 3-7. Structures of carbapenem antibiotics	122
Figure 3-8. Aminoglycosides target 30S ribosome interactions and associated cell death mechanism	123
Figure 3-9. Structures of Aminoglycoside antibiotics	123
Figure 3-10. Structures of macrolide antibiotics.....	124
Figure 3-11. Structures of tetracycline antibiotics	125
Figure 3-12. Structures of rifamycin antibiotics	126
Figure 3-13. Quinolone drug interactions and associated cell death mechanism	127
Figure 3-14. Structures of quinolone antibiotics.....	127
Figure 3-15. Structures of glycopeptide antibiotics	129
Figure 3-16. Structures of polymyxin antibiotics	130
Figure 3-17. Structures of oxazolidinone antibiotics	131
Figure 3-18. Structures of streptogramin antibiotics	132
Figure 3-19. Structure of chloramphenicol	132
Figure 3-20. Structures of lipopeptide antibiotics.....	133
Figure 3-21. An overview of different classes of antibiotics according to their mode of action.....	134
Figure 3-22. An overview of different classes of antibiotics	135
Figure 3-23. Microscopic structure of <i>Mycobacterium tuberculosis</i> cell wall	136
Figure 3-24. Pathophysiology of tuberculosis infection	139
Figure 3-25. First line treatment of TB for Drug Sensitive TB	143
Figure 3-26. Multidrug Resistant Tuberculosis and second line treatments	144
Figure 3-27. Mechanism of action of current tuberculosis drugs	146
Figure 3-28. Discovery of drugs for tuberculosis	147
Figure 3-29. Research and development pipeline for new anti-tuberculosis drugs	147
Figure 3-30. Antitubercular drugs in the pipeline.....	149
Figure 3-31. Microscopic structure of Methicillin resistant <i>Staphylococcus aureus</i> bacteria	150

Figure 3-32. Pathogenic factors of <i>Staphylococcus aureus</i> , with structural and secreted products both play a role as virulence factors.....	152
Figure 3-33. The evolution and genetics of bacterial resistance.....	156
Figure 3-34. Mechanisms of antibiotic resistance strategies in bacteria.....	158
Figure 3-35. Penicillin inactivation by β -lactamase.....	159
Figure 3-36. Enzymatic and chemical modification	160
Figure 3-37. Alteration of molecular target	163
Figure 3-38. Antibiotic targets and mechanisms of resistance	165
Figure 4-1. Lead Compounds.....	177
Figure 4-2. ORTEP view of the crystal structure of acrylic acid 2	178
Figure 5-1. Lead compounds	209
Figure 6-1. Structure of ligands for biocompatible copper-catalyzed azide-alkyne cycloaddition reactions.....	245
Figure 6-2. Coomassie Blue stained SDS-PAGE with pure MRSA lysate, pure lysostaphin, 59 incubated with MRSA lysate and 59 incubated with lysostaphin and fluorescence visualized image of same gel at 635 nm.....	251
Figure 6-3. Coomassie Blue stained SDS-PAGE with pure MRSA lysate, MRSA membrane fraction, MRSA cytoplasmic fraction, 59 incubated with MRSA membrane fraction and 59 incubated with MRSA cytoplasmic fraction and fluorescence visualized image of same gel at 635 nm	251
Figure 6-4. Coomassie blue stained SDS-PAGE gel with pure lysate with CuAAC reaction, protein eluents, and washouts from FPLC.....	252
Figure 6-5. Coomassie Blue stained SDS-PAGE involved in proteolysis.....	254
Figure 6-6. Enolase enzymatic activity with TI-I-100 (59) and DMSO (control).....	254
Figure 6-7. Coomassie Blue stained SDS-PAGE with expressed enolase, enolase incubated with 59 , different concentration of 59 incubated with enolase and fluorescence visualized image of same gel at 635 nm	255
Figure 6- 8A. Representative MS/MS spectrum of Enolase sample (E) with identified peptide. A single letter abbreviation was used to assign the peptide sequence based on fragment ions observed for the peptide. N-terminus b ions and C-terminus y ions are labelled that resulted from peptide bond cleavage.....	256

Figure 6- 8B. Representative MS/MS spectrum of 59 incubated Enolase sample (EL) with identified peptide. A single abbreviation was used to assign the peptide sequence based on fragment ions observed for the peptide segment. N-terminus b ions and C-terminus y ions are labelled that resulted from peptide bond cleavage. *Denotes the 59 adduct on lysine residue of the peptide sequence	256
Figure 6-9A. Molecular docking conformation of 59 in enolase protein	257
Figure 6-9B. The closer view of 59 at binding site residues (lysine) in the enolase protein	258
Figure 6-10. Summary of the glycolytic metabolic pathway and the role of enolase (highlighted) in carbohydrate metabolism	260
Figure 6-11. The ribbon diagram of the overall structure of <i>Sa</i> _enolase, dimeric structure of <i>Sa</i> _enolase, octameric structure, and PEP-bound form of <i>Sa</i> _enolase	261
Figure 6-12. Extracellular matrix (ECM) of host	263
Figure 6-13. Simplified overview of plasminogen system and utilization by bacteria, as well as degradation of ECM components which enables bacterial migration through tissue barriers	263
Figure 6-14. The conversion of pyruvate from glycolysis to acetyl CoA required for the Krebs cycle pathway catalyzed by PDC	264
Figure 6-15. Flow diagram illustrating the overall activity of pyruvate dehydrogenase complex protein with role of dihydrolipoyl transacetylase	265
Figure 6-16. Catalytic conversion using glyceraldehyde-3-phosphate dehydrogenase in the glycolysis	266
Figure 6-17. SaGDAPH overall structure	267

LIST OF TABLES

Table 1-1. Optimization of conditions for regiospecific synthesis of intermediate 16 from 14	9
Table 2-1. The binding affinity of 3-ISOPBC (2·HCl) at $\alpha\beta\gamma 2$ GABA _A receptor subtypes using [3H]-flumazenil displacement studies	37
Table 2-2. Behavioral categories, abbreviations, and definitions	44
Table 2-3. Average baseline intake for each monkey across the duration of the study	45
Table 2-4. The effects of benzodiazepine receptor ligands on alcohol and sucrose drinking parameters.....	47
Table 2-5. Summary of drug effects on selected observable behaviors.....	49
Table 2-6. The significant post hoc comparisons (Student-Newman-Keuls (SNK) test) after the performance of one-way ANOVAs	68
Table 2-7. The results of the two-way ANOVAs. The influence of 3-ISOPBC·HCl and 3-PBC·HCl (10 mg/kg respectively) on the total distance travelled (m) and total time immobile (min) in spontaneous locomotor activity assay was assessed in the 0-90 and 0-60 min time period together with the use of the positive control (β CCt) in a full factorial design	69
Table 2-8. The results of one-way ANOVAs. The influence of 3-ISOPBC·HCl and 3-PBC·HCl (30 mg/kg, respectively) on total distance traveled (m) and total time immobile (min) in SLA was assessed in the 0–90 and 0–60 min period in a partial factorial design..	71
Table 2-9. The <i>in-vitro</i> metabolic stability studies with % remaining at the end of 1 hour.....	74
Table 2-10. Results of Psychoactive Drug Screening Program (PDSP) Analysis of 3-ISOPBC·HCl	80
Table 3-1. Differences in the stages of tuberculosis	141
Table 4-1. Minimum inhibitory concentrations (MIC) of acrylic acid ethyl ester analogs against common bacterial species ($\mu\text{g/mL}$).....	180
Table 4-2. Minimum inhibitory concentrations (MIC) of select compounds against additional <i>mycobacterial</i> species ($\mu\text{g/mL}$)	181
Table 5-1. Minimum inhibitory concentrations (MIC) of compounds 30-31 , 35-54 , 56-66 , and 68-69 against common bacterial species ($\mu\text{g/mL}$)	214
Table 5-2. Minimum inhibitory concentrations (MIC) of compounds 38-39 , 40 , 46-48 , 56-57 , 59 , 63-64 , 68-69 and single drug-resistant strains against <i>Mycobacterium tuberculosis</i> H ₃₇ Rv; Vero cell line cytotoxicity (IC ₅₀ in $\mu\text{g/mL}$), and selective index (SI)	219
Table 5-3. Minimum inhibitory concentrations (MIC) of compounds 38-39 , 41 , 46 , and 59 against clinically significant drug resistant strains ($\mu\text{g/mL}$).....	220

LIST OF SCHEMES

Scheme 1-1. Synthesis of substituted carboline analogs	5
Scheme 1-2. Synthesis of the carbamate protected analogs from intermediate 7b	7
Scheme 1-3. Retrosynthetic analysis of 3,6-disubstituted β -carbolines	8
Scheme 1-4. Regiospecific synthesis of β -carbolines (1-2) and Aza- β -carbolines (4-5)	11
Scheme 1-5. Large-scale regiospecific synthesis of β -carbolines 3-ISOPBC (2)	11
Scheme 2-1. The bioluminescence reaction between the cells and Cell Titer-GLO™	77
Scheme 4-1. Synthesis of <i>cis</i> acrylic acids, amides and esters.....	178
Scheme 4-2. Synthesis of 4-oxo substituted acrylic acid ethyl esters	179
Scheme 4-3. Synthesis of acrylic acid ester derivatives.....	182
Scheme 4-4. Synthesis of acrylic acid ethyl ester derivatives.....	182
Scheme 5-1. Synthesis of aroylacrylic acid derivatives	210
Scheme 5-2. Synthesis of aroylacrylic ethyl ester derivatives	212
Scheme 5-3. Synthesis of aroylacrylic ethyl ester derivatives	213
Scheme 5-4. Synthetic pathway to compounds 64-66 and 68-69	214
Scheme 6-1. Comparison between the thermally-induced and Cu (I) catalyzed Huisgen cycloaddition reaction conditions.....	244
Scheme 6-2. Classification of Click chemistry reactions.....	246
Scheme 6-3. The initial mononuclear mechanism of CuAAC proposed by Sharpless, Fokin, and co-workers.....	247
Scheme 6-4. Up-to-date dinuclear mechanism of CuAAC, X is a bridging ligand	248
Scheme 6-5. CuAAC reaction between 59 and Alexa Fluor 647 picolyl azide in <i>Staphylococcus aureus</i>	250
Scheme 7-1. Synthesis of 3(<i>S</i>)-3-hydroxyquinine (7)	283
Scheme 7-2. Attempts to synthesize 3(<i>S</i>)-3-hydroxyquinine (7) by one step using SeO ₂	283
Scheme 7-3. Proposed mechanism for converting an epimeric mixture at C-3 of 3- hydroxyquinine diastereomers to a single 3(<i>S</i>)-3-hydroxyquinine (7) by a Mislow- Evans rearrangement.....	284

ACKNOWLEDGEMENTS

It is true that to endeavor success in one's life, it is always an incredible journey with the support of amazing people along the way. In this regard, first and foremost, I am ever grateful to my supervisor, Dr. James M. Cook, for providing me the opportunity, strategic guidance and continuous encouragement to complete my doctorate in synthetic organic and medicinal chemistry. It was through his skillful advice, and moral support in both the pleasant and frustrating days that I have grown both today professionally and personally.

My whole hearted thanks go to members of my doctoral committee Dr. Alexander E. Arnold, Dr. Alan W. Schwabacher, Dr. Nicholas Silvaggi, and Dr. Arsenio Pacheco for their insightful suggestions and instructions. Here, I would also like to extend my thanks to Dr. Douglas Stafford for an amazing facility the Milwaukee Institute for Drug Discovery and his efforts to help students gain knowledge in advanced technology.

I also wish to thank Dr. James M. Cook, Dr. Alexander E. Arnold, and Dr. Douglas Stafford for their support for my wife Revathi who worked with them and their continued assistance in her choice of a career in Pharmacy. I thank Professor Arnold for his open door policy and valuable time even after hours with fruitful discussions and recommendations for my research. I also thank Dr. Schwabacher and Dr. Silvaggi for their important instruction, which allowed me to complete my projects with exciting results.

It was my pleasure working with our numerous collaborators that helped me gain knowledge in diversified fields. I especially thank Dr. Sonia L. Bardy (UW-Milwaukee), Dr. Elise M. Weerts (Johns Hopkins University), Dr. Gondre-Lewis Majorie (Howard University), Dr. Miroslav Savic (University of Belgrade), Dr. Margot Ernst (Medical University of Vienna), Dr. Donna M. Platt (Mississippi Medical School), Dr. William Schwann (UW-Lacrosse), Dr. Aaron

Monte (UW-Lacrosse), Dr. Scott G. Franzblau and Ms. Baojie Wan at the University of Illinois-Chicago, and Dr. Shama P. Mirza (UW-Milwaukee). I thank the UWM Research Foundation Senior Licensing Manager, Dr. Jessica Silvaggi, for sharing her knowledge about patents and grant applications.

I would like to express my gratitude to Dr. Sreenivasa Mundla, Managing Director of Sreeni Labs, India, for his advice and assistance to advance my career and the suggestion to pursue a chemistry doctorate in Dr. Cook's research lab. I would also like to thank alumni and current members of Dr. Cook's research group for their helpful discussions (especially Saturday morning group meetings) in a friendly environment which made work both day and night a joy, and a bundle of fond memories to recollect.

I also thank all Professors and staff at the Chemistry and Biochemistry Department at UW-Milwaukee who helped me in many ways to successfully study at UWM. I express deep gratitude to Dr. Frank H Holger for his invaluable help for NMR and Mr. Neal Korfhage for the design and fabrication of very specific glassware. I would like to extend my special thanks to all my friends in Milwaukee and Chicago for being supportive from day one and helped me in my marvelous journey.

I would like to express my love to my own and Revathi's family members for their trust in me and I always felt blessed to have such a wonderful big family. I am ever grateful for all the sacrifices and dedication you made for my happiness and it is in my heart to return a little whenever I can. I extend all my love to my soulmate, Revathi, and especially my little angel Jesri Tiruveedhula, both of which have driven me forward in every respect with their cheerfulness at all times and words cannot express their role in my every achievement. At the outset, I thank the Almighty for his blessings and rendering this an outstanding journey for me.

PREFACE

Chapters 1 and 4 of this dissertation have been adopted from the following articles

- **Tiruvedhula, V. V. N. Phani Babu.**; Methuku, K. R.; Deschamps, J. R.; Cook, J. M. *Org. Biomol. Chem.* **2015**, *13*, 10705-10715.
- **Tiruvedhula, V. V. N. Phani Babu.**; Witzigmann, C. M.; Verma, R.; Kabir, M. S.; Rott, M.; Schwan, W. R.; Medina-Bielski, S.; Lane, M.; Close, W.; Polanowski, R. L.; Sherman, D.; Monte, A.; Deschamps, J. R.; Cook, J. M. *Bioorg. Med. Chem.* **2013**, *21*, 7830-7840.

PART - I

DEVELOPMENT OF A TWO-STEP REGIOSPECIFIC SYNTHETIC ROUTE FOR
MULTIGRAM-SCALE SYNTHESIS OF β -CARBOLINE ANALOGS FOR
STUDIES IN PRIMATES AS ANTI-ALCOHOL AGENTS

CHAPTER 1

SYNTHESIS OF AZA AND CARBOCYCLIC β -CARBOLINES FOR THE TREATMENT OF ALCOHOL ABUSE. REGIOSPECIFIC SOLUTION TO THE PROBLEM OF 3,6-DISUBSTITUTED β - AND AZA- β -CARBOLINE SPECIFICITY

1.1. ABSTRACT

A novel two step protocol was developed to gain regiospecific access to 3-substituted β - and aza- β -carbolines, 3-PBC (**1**), 3-ISOPBC (**2**), β CCt (**3**), 6-Aza-3-PBC (**4**) and 6-Aza-3-ISOPBC (**5**). These β -carbolines (**1-3**) are potential clinical agents to reduce alcohol self-administration, especially 3-ISOPBC·HCl (**2·HCl**) which appears to be a potent anti-alcohol agent active against binge drinking in a rat model of maternally deprived (MD) rats. The method consists of two consecutive palladium-catalyzed reactions: a Buchwald-Hartwig amination followed by an intramolecular Heck-type cyclization in high yield.

1.2. INTRODUCTION

β -Carbolines, aza- β -carbolines and their derivatives are important targets in synthetic chemistry.¹ In addition, they are found in a large number of natural products, many of which demonstrate novel biological activity, especially in regard to the reduction of alcohol self-administration [binge drinking (BD)]. This is proposed to be due to the activity at the benzodiazepine site of the GABA_A receptor.² Surprisingly, BD kills six people a day, most of which are men, and approximately 88,000 people die from alcohol related issues annually making it the third leading preventable cause of death in the United States.³ In 2006, this alcohol misuse cost the US government approximately \$223.5 billion dollars.³ BD (Blood-alcohol level \geq 0.08 g% in a 2 hour period) is one

form of excessive drinking and because of it, alcohol addiction and dependence remain a significant public health concern.⁴ Maternal separation and early life events can cause profound neurochemical and behavioral alterations in childhood that persist into adulthood, enhance the risk to develop alcohol use disorders and excessive drinking.⁵⁻⁷ Consequently, the development of clinically safe and cost effective therapeutic agents to reduce alcohol addiction and dependence remain essential for the future treatment of alcoholism.^{8,9}

One influence on alcohol abuse is known to be mediated by GABA_A receptors, the major inhibitory chloride ion gated channels with γ -aminobutyric acid (GABA) as the endogenous ligand in the central nervous system. It plays a vital role in several neuronal disorders including anxiety, epilepsy, insomnia, depression, bipolar disorder, schizophrenia, as well as mild cognitive impairments and Alzheimer's disease.¹⁰⁻¹⁵ The pentameric structure of the GABA_A receptor is made up of 2 α , 2 β and 1 γ subunits, with a higher distribution of the α 1-subunit in the mesolimbic system of the ventral pallidum (VP) possibly playing an important role in regulating alcohol abuse.¹⁶⁻²⁰ However, the precise neuromechanisms of regulating alcohol-seeking behavior remain unknown. In addition to the ventral pallidum, there is now compelling evidence that the GABA_A receptors within the striatopallidal and extended amygdala system are involved in the 'acute' reinforcing actions of alcohol.²¹⁻²³

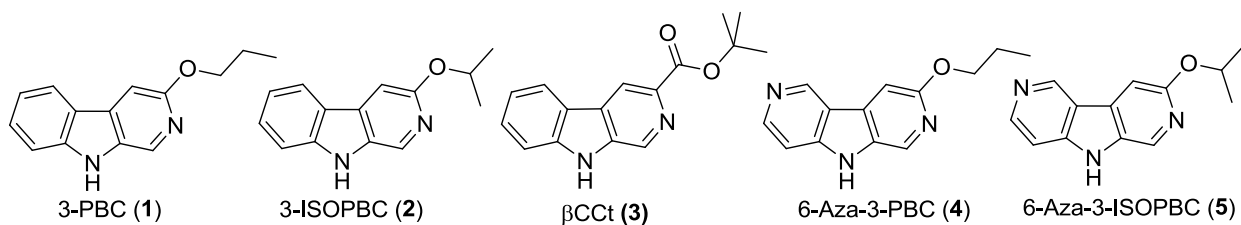


Figure 1-1. Structures of 3-PBC (1), 3-ISOPBC (2), β CCt (3), 6-Aza-3-PBC (4) and 6-Aza-3-ISOPBC (5)

To evaluate the role of the α 1 receptor in regulating alcohol reinforcement, the orally active β -carboline 3-propoxy- β -carboline hydrochloride **1·HCl** (3-PBC·HCl) and β -carboline-3-

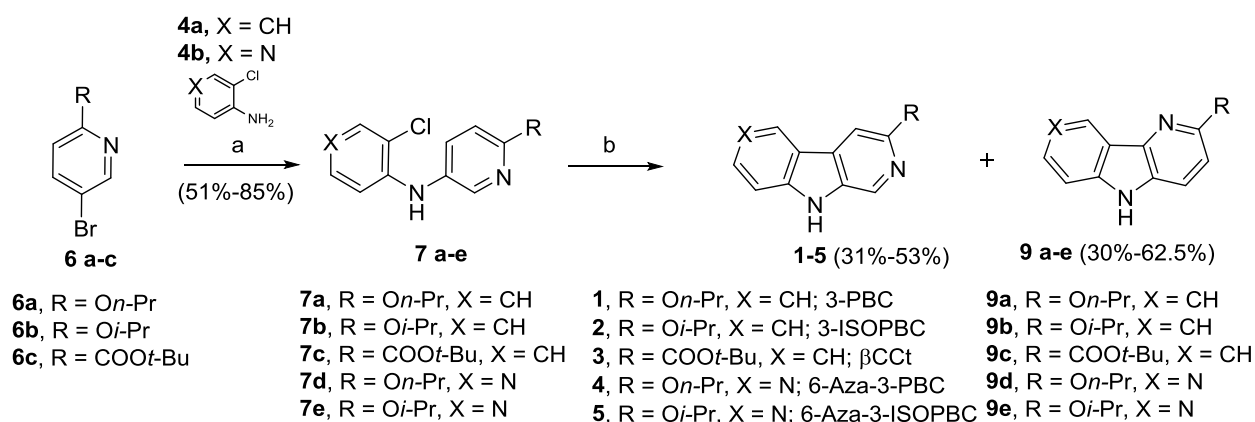
carboxylate-*tert*-butyl ester **3** (β CCt, α 1 antagonist), the mixed benzodiazepine (BDZ) agonist-antagonists with binding selectivity at the α 1 Bz/GABA_A receptor were developed (see Figure 1-1).^{18,24,25} Behavioral studies in several species (e.g., rats, mice, primates) show that these ligands were BDZ antagonists, at the α 1 Bz/GABA_A subtype exhibiting competitive binding-site interactions with BDZ agonists over a broad range of doses.^{18,24,26} In studies which involved the α 1 subtype, they were shown to selectively reduce alcohol-motivated behaviors and more importantly, 3-PBC·HCl significantly reduced alcohol self-administration and reduced craving in baboons.²⁶ β -Carbolines **1·HCl** and **3** displayed mixed weak agonist-antagonist profiles *in vivo* in alcohol preferring (P) and high alcohol drinking (HAD) rats.^{18,26-28} Therefore, in addition to their use to study the molecular basis of alcohol reinforcement, α 1 Bz β -carboline ligands which display mixed pharmacological antagonist-agonist activity in alcohol P and HAD rats may be capable of reducing alcohol intake while eliminating or greatly reducing the anxiety associated with habitual alcohol, abstinence or detoxification.^{18,28-30} Consequently, these types of ligands may be ideal clinical agents for the treatment of alcohol dependent individuals.

1.3. RESULTS AND DISCUSSION

Previously, the β -carbolines **1** and the potent α 1 antagonist **3** have been synthesized from DL-tryptophan. The overall yield of **1** (via 6 steps) as reported previously was 8%, while the combined yield of **3** (5 steps) was 35%. A few key steps occurred in low yields, which was something we sought to improve on³¹⁻³⁴ in a continued effort to find more potent subtype selective ligands for GABA_A receptors. This interest resulted in a short and concise synthesis of **1** and **3**. In 2011, a palladium catalyzed two-step protocol for the synthesis of **1**, and **3**, as well as analogs of **1** was reported.³⁵ In the search for a more potent subtype selective ligand for the GABA_A receptor, with the knowledge that many 3-substituted β -carbolines and more water soluble aza- β -carbolines

might exhibit greater subtype selectivity at $\alpha 1\beta 2/3\gamma 2$ BZR/GABAergic receptors,^{31-33,36-38} the ligands 3-ISOPBC (**2**), 6-Aza-3-PBC (**4**), and 6-Aza-3-ISOPBC (**5**) were designed (see Figure 1-1) and synthesized using a two-step protocol (Scheme 1-1).

Scheme 1-1. Synthesis of Substituted Carboline Analogues



Reagents and conditions: (a) Pd(OAc)₂, X-Phos, Cs₂CO₃, toluene, 100 - 140 °C, 15 - 24 h
 (b) Pd(OAc)₂, (*t*-Bu)₃P·HBF₄, K₂CO₃, DMA, 120 °C, 16 h

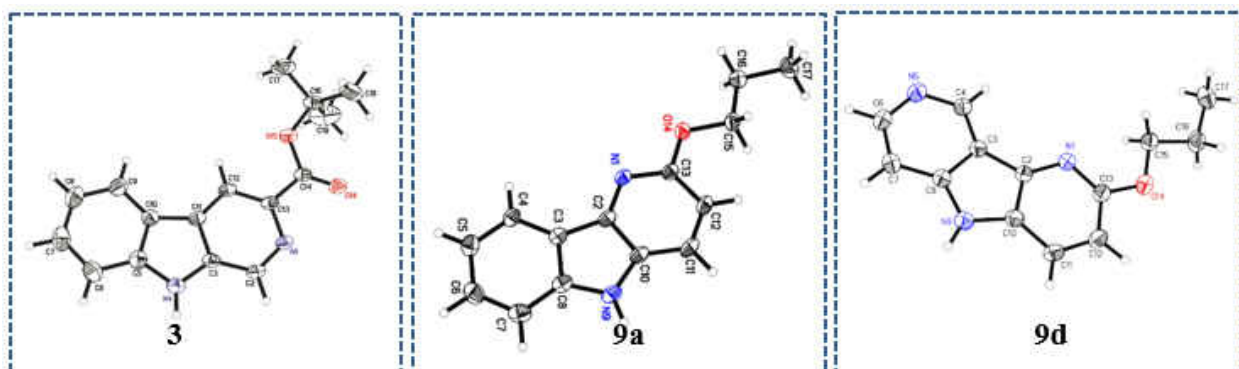


Figure 1-2. ORTEP view of the crystal structure of substituted carbolines **3**, **9a**, and **9d** (Displacement ellipsoids are at the 50% level (β -carboline numbering not followed))

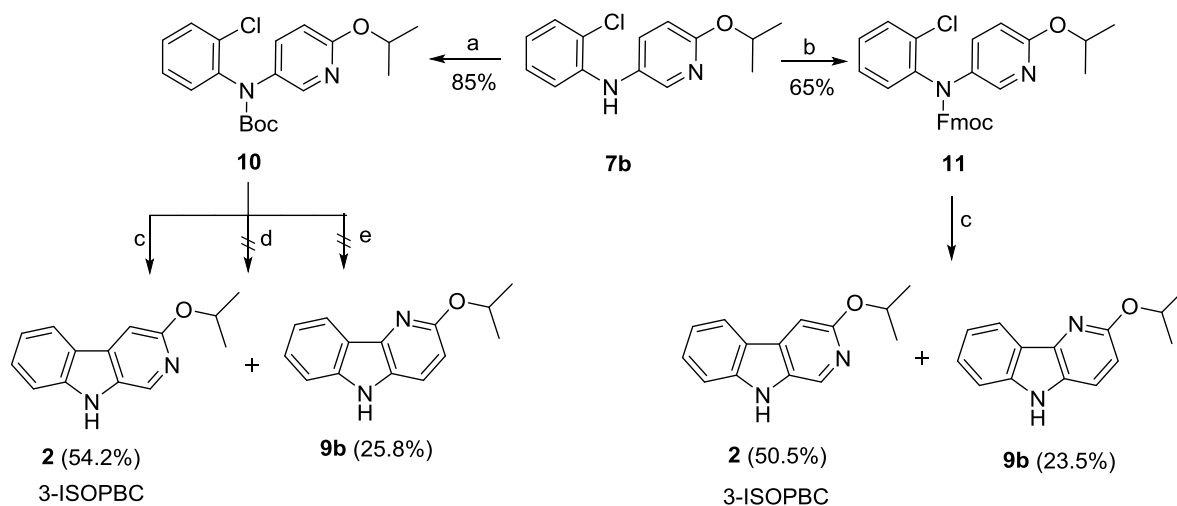
As shown in Scheme 1-1, bromopyridines **6a-c**^{39,40} were reacted with anilines **4a-b** in toluene at 100-140 °C in the presence of 5 mol% Pd(OAc)₂ and 7.5 mol% X-Phos to obtain the corresponding diarylamines **7a-e** in moderate to good yields. Unfortunately, the intramolecular Heck cyclization [Pd(OAc)₂, (*t*-Bu)₃P·HBF₄, K₂CO₃, DMA, 120 °C] of **7a-e** afforded both the β -carbolines **1-5** (individually) and their regioisomeric δ -carbolines **9a-e**, respectively. Carbolines **2**, **3**, **9a**, and **9d** were subjected to X-ray crystallographic analysis (see Figure 1-2, Scheme 1-4, and

the ESI) to confirm the regiochemistry. Although this protocol permitted synthesis of β -carbolines on gram scale for *in vivo* studies, occasionally the first step in the Buchwald-Hartwig coupling failed to give complete conversion into the carboline. This complicated purification for the diarylamine was difficult to purify via column chromatography because the diarylamine and one of the starting anilines had almost identical R_f values. Furthermore, in the case of the water soluble aza- β -carboline the yields (51%) were very poor and importantly, since the second step was not regiospecific, this required careful purification to remove the unwanted δ -carboline present in 30 to 62.5% yield (Scheme 1-1). Interestingly, the *in vivo* results (unpublished) for 3-isopropoxy- β -carboline hydrochloride **2**·HCl (3-ISOPBC·HCl) carried out in maternally deprived rats for binge drinking decreased dramatically this self-administration compared to **1**·HCl without affecting the overall activity of the rats (i.e. no sedation). This important finding led to the interest in a regiospecific synthesis of 3-ISOPBC (**2**) on large scale.

The revised synthetic strategy for the regiospecific synthesis of **2** began with the protection of the intermediate amine **7b** ($N_a - H$) with bulkier groups such as *tert*-butyloxycarbonyl (Boc) **10** or a fluorenylmethylenoxy group (Fmoc) **11**, which might block the formation of the Pd^{II} π -complex that is required to obtain the undesired regioisomeric δ -carboline. The Boc protected amine **10** was easily accessible by treating the amine **7b** with di-*tert*-butyl dicarbonate (Boc)₂O and 4-(dimethylamino)pyridine (DMAP) in good yield (85%). The Fmoc protected amine **11** was synthesized under solvent free conditions by reaction of the amine **7b** and Fmoc-Cl by microwave irradiation at 80 °C in moderate yield (65%, Scheme 1-2).⁴¹ Once protected, diarylamines **10** and **11** were subjected to a palladium catalyzed Heck-type cyclization using similar conditions to those from above. Unfortunately, both reactions afforded the deprotected regioisomers 3-ISOPBC (**2**) and δ -isomer **9b** in approximately the same 2:1 ratio, as compared to cyclization with the previously unprotected diarylamine **7b** (see Scheme 1-1 above). It was felt that deprotection of the

carbamate occurred once the indole ring had formed (Scheme 1-2) which provided the better indole leaving group. To test the thermal stability of the carbamate starting materials, diarylamines **10** and **11** were heated at 120 °C in DMA; they were stable to these conditions. In addition, the cyclization with PdCl₂(PPh₃)₂ as a palladium source was also attempted using standard Heck-type reaction conditions with a milder base (NaOAc), but this failed to give the cyclized product. One also explored the reaction by varying the water content using NaOAc·3H₂O as a base; however, there was no cyclization (Scheme 1-2).

Scheme 1-2. Synthesis of the Carbamate Protected Analogs from Intermediate 7b

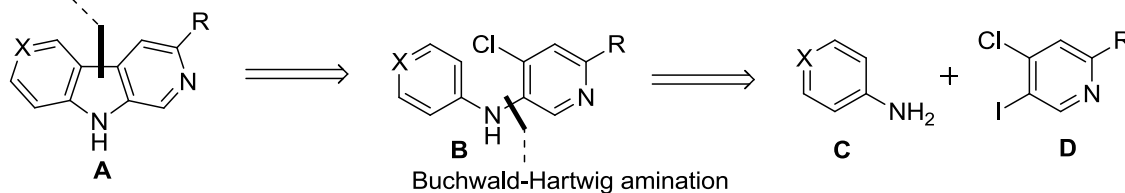


Reagents and conditions: (a) (Boc)₂O, DMAP, THF, rt, 24 h; (b) Fmoc-Cl, 80 °C, Microwave, 1 h; (c) Pd(OAc)₂, (t-Bu)₃P·HBF₄, K₂CO₃, DMA, 120 °C, 16 h; (d) PdCl₂(PPh₃)₂, NaOAc·3H₂O, DMA, 120 °C, 14 h; (e) PdCl₂(PPh₃)₂, NaOAc, DMA, 120 °C, 14 h

The second approach rested on the important switch of the chlorine atom from the benzene ring to the pyridine ring in amine **7b**. Retrosynthetically, it was envisioned that the core structure of 3,6-disubstituted β-carboline **A** could be obtained from diarylamine **B** via an intramolecular Heck cyclization and it was anticipated that diarylamine **B** could arise from a substituted aniline **C** and a substituted pyridine derivative **D** via a Buchwald-Hartwig amination (Scheme 1-3).

Scheme 1-3. Retrosynthetic Analysis of 3,6-Disubstituted- β -carbolines

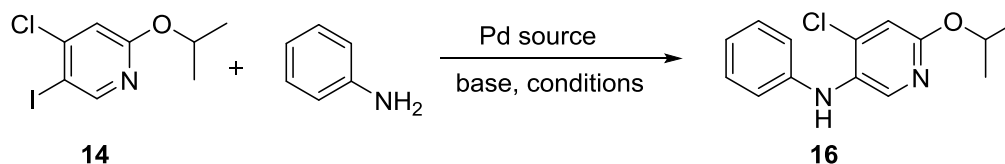
Intramolecular Heck Cyclization



At this point it was decided to explore the regioselective palladium catalyzed Buchwald-Hartwig coupling between aniline and pyridine **14**⁴² for the synthesis of diarylamine **16** (Table 1-1). With the previous history in mind,³⁵ the initial attempt was made with 5 mol% Pd(OAc)₂, 7.5 mol% X-Phos and Cs₂CO₃ (1.5 equiv) in toluene at 110 °C which gave only 18% of the diarylamine **16** with a large excess of unreacted starting material even after heating for 24 hours (Table 1-1, entry 1). However, the catalyst based on the combination of Pd₂(dba)₃, Xantphos and Pd(OAc)₂, Xantphos with Cs₂CO₃ in toluene and dioxane gave the desire product diarylamine **16** in up to 62% yield (Table 1-1, entries 2-3). The ligand Xantphos has been shown to be efficient in cross coupling reactions of C-N bond formation because of a wider bite angle,⁴³ which facilitates the reductive elimination. In addition, the excess base may also play a role in the improvement of the yield.⁴³ In recent years rapid synthesis with microwave technology has attracted a considerable amount of attention for C-N bond formation.⁴⁴⁻⁴⁶ All three previous cyclizations were attempted with microwave irradiation (for 1 hour) in order to decrease the duration of the reaction time, as well as increase the selectivity under similar reaction conditions. However, the results were the same except that in the Xantphos-based ligand systems the cyclizations were completed in 1 hour. During continuation of the study of this selective amination, recent reports from Buchwald and co-workers⁴⁷ demonstrated air- and moisture-stable palladacyclic precatalysts, when employed with aryl iodides and heteroaryliodides were attractive substrates in Pd-catalyzed C-N cross-coupling reactions. This process works by preventing formation of the stable bridging iodide dimers and

also using a solvent system in which iodide salts were insoluble. These complexes easily undergo deprotonation and reductive elimination to generate LPd(0) along with relatively inert indoline (for generation of 1) or carbazole (for generation of 2 and 3). These conditions also permit the successful coupling of aryl iodides with amines at ambient temperature.⁴⁷⁻⁵⁰

Table 1-1. Optimization of Conditions for Regioselective Synthesis of Intermediate 16 from 14^a



entry	Pd source	ligand	base (equiv)	solvent	temp (time)	Yield(%) ^b
1	Pd(OAc) ₂	X-Phos	Cs ₂ CO ₃ (1.5)	toluene	110 °C (24 h)	18 ^c
2	Pd ₂ (dba) ₃	Xantphos	Cs ₂ CO ₃ (2)	dioxane	110 °C (6 h)	51
3	Pd(OAc) ₂	Xantphos	Cs ₂ CO ₃ (4)	toluene	110 °C (6 h)	62
4	BrettPhos Pd G3	BrettPhos	Cs ₂ CO ₃ (1.5)	toluene	110 °C (14 h)	45
5	BrettPhos Pd G3	BrettPhos	Cs ₂ CO ₃ (3)	toluene	110 °C (5 h)	66
6	BrettPhos Pd G3	BrettPhos	NaOt-Bu (1.5)	toluene	110 °C (5 h)	52
7	BrettPhos Pd G3	BrettPhos	Cs ₂ CO ₃ (5)	toluene	110 °C (5 h)	0 ^e
8	Pd ₂ (dba) ₃	Xantphos	Cs ₂ CO ₃ (5)	toluene	110 °C (3 h)	74
9	Pd(OAc) ₂	<i>rac</i> -BINAP	Cs ₂ CO ₃ (5)	toluene	110 °C (5 h)	80
10	Pd(OAc) ₂	<i>rac</i> -BINAP	K ₂ CO ₃ (5)	toluene	110 °C (24 h)	22
11	Pd(OAc)₂	<i>rac</i> -BINAP	Cs₂CO₃ (5)	toluene	110 °C (5 h)	92^d

^a **14** (0.1 mmol), aniline (0.12 mmol), Pd (3 mol%), ligand (3 mol%), base, and solvent (1 mL)

^b Isolated yields

^c Pd (5 mol%), ligand (7.5 mol%)

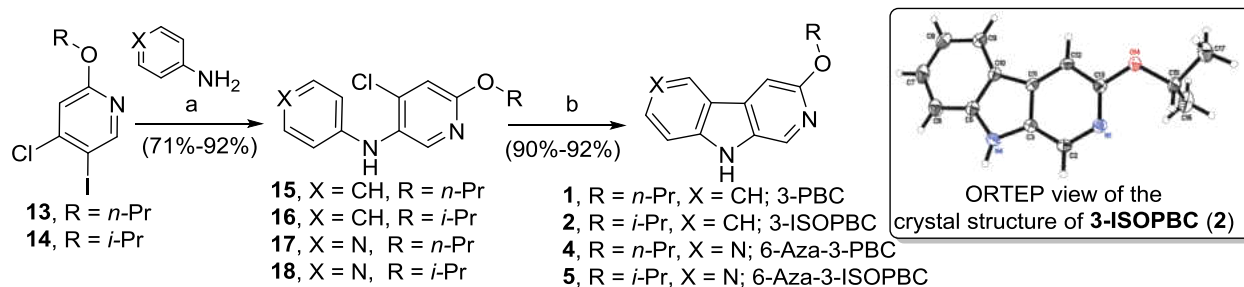
^d aniline (0.1 mmol)

^e 90% of diaminated product [6-isopropoxy-*N*³, *N*⁴-diphenylpyridine-3,4-diamine] was observed

The first attempt in this modification was to use the Buchwald 3rd generation palladacycle precatalyst (BrettPhos Pd G3) with the BrettPhos ligand in the presence of Cs₂CO₃ or NaOt-Bu in toluene at room temperature. This failed to give the desired product and there was no consumption of starting material. Following this attempt, the temperature was raised to reflux, with the addition of 3 equivalents of Cs₂CO₃ and the reaction went to completion within 5 hours. However, it only gave the desired amine **16** in 66% yield (Table 1-1, entry 5). When the same experiment was performed using only 1.5 equiv of Cs₂CO₃ the process took a longer time to go to completion with

an isolated yield of 45% of the desired amine **16**. This was accompanied by the diaminated product [6-isopropoxy-*N*³, *N*⁴-diphenylpyridine-3,4-diamine] in ~18% yield (Table 1-1, entry 4). Unfortunately, when the stronger base NaOt-Bu was employed comparable results to the above reaction (Table 1-1, entry 4) were obtained accompanied by more decomposed material [TLC (silica gel; Table 1-1, entry 6)]. The use of excess base (Cs₂CO₃) gave only the unwanted diaminated product in 90% yield (Table 1-1, entry 7). It was found the Pd(OAc)₂, *rac*-BINAP and K₂CO₃ combination, unfortunately, did not lead to full conversion even after heating for 24 hours (Table 1-1, entry 10). Interestingly, the catalyst system Pd₂(dba)₃ and Xantphos with a large excess of base [Cs₂CO₃ (5 equiv)] gave a 74% yield of **16**, whereas the catalyst system Pd(OAc)₂, *rac*-BINAP under similar reaction conditions yielded 80% (Table 1-1, entry 8 and 9) of the desired amine **16**. Remarkably, these data indicated a large excess of mild base was essential to obtain good yields, as well as selectivity. Furthermore, a rate-limiting interphase deprotonation of the Pd(II)-amine complex intermediate has occurred in the catalytic cycle.⁵¹⁻⁵³ Encouraged by these promising results, efforts turned toward lowering the aniline loading from 1.2 equivalents to 1 equivalent for regioselectivity. In doing so one achieved selective amination of pyridine **14** with aniline. Interestingly, neither a 4- nor 4,5-diaminated pyridine product was obtained. Using this catalyst-base combination in refluxing toluene, the desired cross-coupling proceeded smoothly to provide the desired anilinyridine **16** in excellent yield (92%, Table 1-1, entry 11). Interestingly, the same reaction conditions gave good yields in the case of the more polar starting 4-amino pyridine (Scheme 1-4); however, the temperature was necessarily increased to 140 °C to increase the solubility of the starting material, 4-amino pyridine. In contrast, when a more polar solvent such as DMA was employed, the result was either inferior yields and/or deiodination of pyridine **16**, as mentioned above.

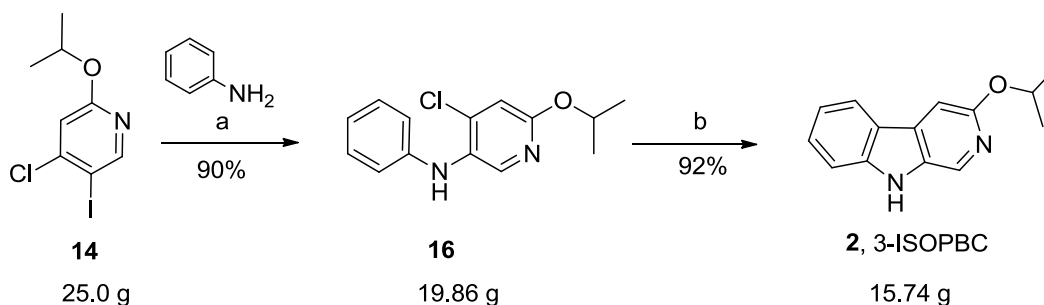
Scheme 1-4. Regiospecific Synthesis of β -Carbolines (1-2) and Aza- β -Carbolines (4-5)



Reagents and conditions: (a) Pd(OAc)₂, *rac*-BINAP, Cs₂CO₃, toluene, 110 - 140 °C, 5 - 6 h
 (b) Pd(OAc)₂, (*t*-Bu)₃P·HBF₄, K₂CO₃, DMA, 120 °C, 16 h

Once the diarylamines **15-18** were in hand in good to excellent yields, the previously applied Heck-type conditions [Pd(OAc)₂, (*t*-Bu)₃P·HBF₄, K₂CO₃, DMA, 120 °C] were employed for cyclization. Gratifyingly, this catalyst system gave excellent yields of 91-92% and 90-92% for β -carbolines **1-2** and aza- β -carbolines **4-5**, respectively (Scheme 1-4). The switch of the position of the chlorine atom from the benzene ring to the pyridine ring worked regiospecifically and completely eliminated the corresponding unwanted δ regioisomer. This completely eliminated the difficult chromatography required to separate β and δ carbolines. The 3-ISOPBC **2** has now been prepared on 15-25 gram scale for studies *in vivo* (Scheme 1-5) and it is very easy to scale up to 50-100 gram level. Finally, the overall yield increased from 43% to 84% compared to the previous syntheses.^{33,35}

Scheme 1-5. Large-Scale Regiospecific Synthesis of β -Carboline 3-ISOPBC (2)



Reagents and conditions: (a) Pd(OAc)₂, *rac*-BINAP, Cs₂CO₃, toluene, 110 °C, 15 h
 (b) Pd(OAc)₂, (*t*-Bu)₃P·HBF₄, K₂CO₃, DMA, 120 °C, 16 h

1.4. CONCLUSION

In conclusion, a novel two-step regiospecific route to the four anti-alcohol agents of biological interest, 3-PBC (**1**), 3-ISOPBC (**2**), 6-Aza-3-PBC (**4**) and 6-Aza-3-ISOPBC (**5**), has been developed. The process provides improved yields when compared to the earlier reported syntheses.^{33,35} This two-step protocol consists of the combination of a regioselective Buchwald-Hartwig amination and an intramolecular Heck-type cyclization. The first step, regioselective arylamination, was achieved by using a Pd-BINAP catalytic system in combination with a large excess of Cs₂CO₃, while the latter intramolecular Heck-type cyclization went smoothly with Pd(OAc)₂ in combination with the air-stable monodentate ligand (*t*-Bu)₃·HBF₄ and K₂CO₃. These conditions permit the presence of base sensitive functional groups in the substrates. Regiospecific synthesis of β- and aza-β-carbolines was achieved by simply changing the chlorine position from the benzene ring to the pyridine derivatives. Importantly, these reactions are capable of scale-up to multigram quantities and were performed on 25 gram scale for *in vivo* biology. We observed similar results except in the case of the Buchwald-Hartwig amination step, where it required an increase of the catalyst loading from 3 to 6 mol% whenever the starting material was not consumed. This new process reported here provides the material necessary to study alcohol self-administration and reduction thereof in MD rats and in primates. This regiospecific two-step synthetic protocol increased the overall yield from 43 % to 84 % in the case of β-carbolines **1-2** and from 16 % to 66 % for Aza-β-carbolines **4-5** respectively, and negated the need for a difficult chromatographic step.

1.5. EXPERIMENTAL

1.5.1. General Considerations

All reactions were carried out in oven-dried, round-bottom flasks or in resealable screw-cap test tubes or heavy-wall pressure vessels under an argon atmosphere. The solvents were anhydrous unless otherwise stated. Stainless steel syringes were used to transfer air-sensitive liquids. Organic solvents were purified when necessary by standard methods or purchased from commercial suppliers. Anhydrous solvents of toluene, dioxane and *N,N*-dimethylacetamide (DMA) were subjected to the freeze-thaw method to render them oxygen free to execute the Buchwald-Hartwig coupling and intramolecular Heck reactions. All chemicals purchased from commercial suppliers were employed as is, unless stated otherwise in regard to purification. Silica gel (230 - 400 mesh) for flash chromatography was utilized to purify the analogues. The ¹H and ¹³C NMR data were obtained on the NMR spectrometer (300 MHz / 500 MHz) instrument with chemical shifts in δ (ppm) reported relative to TMS. The HRMS were obtained on a LCMS-IT-TOF mass spectrometer by Dr. Mark Wang.

1.5.2. General procedure for the Buchwald-Hartwig coupling reaction between substituted anilines and substituted pyridines: Representative procedure for the synthesis of *N*-(2-chlorophenyl)-6-propoxypyridin-3-amine (7a)

A heavy-wall pressure tube was equipped with a magnetic stir bar and fitted with a rubber septum. It was then charged with 5-bromo-2-propoxypyridine **6a** (1.3 g, 6 mmol), Pd(OAc)₂ (67.4 mg, 0.3 mmol), X-Phos (214 mg, 0.45 mmol) and Cs₂CO₃ (2.34 g, 7.2 mmol). The vessel was evacuated and backfilled with argon (this process was repeated a total of 3 times). The 2-chloroaniline **4a** (0.8 g, 6.3 mmol) and freeze-thawed toluene (20 mL) was injected into the tube with a degassed syringe under a positive pressure of argon. The rubber septum was replaced with

a screw-cap by quickly removing the rubber septum under the flow of argon and the sealed tube was introduced into a pre-heated oil bath at 110 °C. The reaction mixture was maintained at this temperature for 15 h. At the end of this time period, the pressure tube was allowed to cool to rt. The reaction mixture was filtered through a short pad of celite, and the pad was washed with ethyl acetate (until no more product could be obtained; \approx 100 mL; TLC, silica gel). The combined organic fractions were washed with water (100 mL), brine (100 mL), dried (Na₂SO₄) and concentrated under reduced pressure. The crude product was purified by flash column chromatography (silica gel, 20:1 hexanes/ethyl acetate) to afford **7a** (0.64 g, 81 %) as a pale yellow oil: ¹H NMR (300 MHz, CDCl₃) δ 8.04 (d, J = 2.6 Hz, 1H), 7.47 (dd, J = 8.8, 2.8 Hz, 1H), 7.33 (dd, J = 7.9, 1.4 Hz, 1H), 7.12 – 7.02 (m, 1H), 6.84 (dd, J = 8.2, 1.3 Hz, 1H), 6.74 (dd, J = 11.5, 5.1 Hz, 2H), 5.88 (br, 1H), 4.24 (t, J = 6.7 Hz, 2H), 1.90 – 1.72 (m, 2H), 1.04 (t, J = 7.4 Hz, 3H); ¹³C NMR (75 MHz, CDCl₃) δ 161.2, 142.1, 141.9, 135.3, 131.0, 129.7, 127.6, 120.1, 119.5, 113.5, 111.4, 67.9, 22.4, 10.6; HRMS (ESI-TOF) (m/z): [M+H]⁺ calcd for C₁₄H₁₆ClN₂O: 263.0951, found: 263.0958.

1.5.3. *N*-(2-Chlorophenyl)-6-isopropoxy pyridin-3-amine (**7b**)

Following the general procedure, 5-bromo-2-isopropoxy pyridine **6b** (0.44 g, 2.0 mmol) with 2-chloroaniline **4a** (0.268 g, 2.1 mmol), Pd(OAc)₂ (22.4 mg, 0.1 mmol), X-Phos (71.4 mg, 0.15 mmol), and Cs₂CO₃ (0.78 g, 2.4 mmol) were heated to 110 °C in toluene. After flash chromatography (silica gel, 20:1 hexane/ethyl acetate), the process afforded **7b** (0.215 g, 82%) as a pale yellow oil: ¹H NMR (300 MHz, CDCl₃) δ 8.06 (d, J = 2.7 Hz, 1H), 7.47 (dd, J = 8.7, 2.8 Hz, 1H), 7.34 (dd, J = 7.9, 1.3 Hz, 1H), 7.13 – 7.04 (m, 1H), 6.87 (dd, J = 8.2, 1.2 Hz, 1H), 6.81 – 6.67 (m, 2H), 5.90 (br, 1H), 5.36 – 5.24 (m, 1H), 1.39 (d, J = 6.2 Hz, 6H); ¹³C NMR (75 MHz, CDCl₃) δ 160.6, 142.3, 142.0, 135.3, 130.7, 129.6, 127.6, 120.1, 119.5, 113.5, 111.9, 68.2, 22.1; HRMS (ESI-TOF) (m/z): [M+H]⁺ calcd for C₁₄H₁₆ClN₂O: 263.0951, found: 263.0935.

1.5.4. *tert*-Butyl 5-[(2-chlorophenyl)amino]picolinate (**7c**)

Following the general procedure, *tert*-butyl 5-bromopicolinate **6c** (5 g, 19.4 mmol) with 2-chloroaniline **4a** (2.6 g, 20.3 mmol), Pd(OAc)₂ (0.22 g, 0.97 mmol), X-Phos (0.69 g, 1.45 mmol), and Cs₂CO₃ (7.59 g, 23.3 mmol) was heated to 110 °C in toluene. After flash chromatography (silica gel, 5:1 hexanes/ethyl acetate), this process afforded **7c** (5.02 g, 85%) as an off-white solid; mp 148-149 °C: ¹H NMR (300 MHz, CDCl₃) δ 8.54 (d, *J* = 2.7 Hz, 1H), 8.00 (d, *J* = 8.6 Hz, 1H), 7.45 (dd, *J* = 8.1, 1.7 Hz, 2H), 7.39 (dd, *J* = 8.1, 1.2 Hz, 1H), 7.27 – 7.20 (m, 1H), 7.02 (td, *J* = 7.9, 1.4 Hz, 1H), 6.45 (br, 1H), 1.65 (s, 9H); ¹³C NMR (75 MHz, CDCl₃) δ 163.8, 141.5, 141.3, 139.3, 137.3, 130.3, 127.7, 125.9, 124.6, 123.7, 122.6, 118.8, 81.9, 28.2; HRMS (ESI-TOF) (*m/z*): [M+Na]⁺ calcd for C₁₆H₁₇ClN₂O₂Na: 327.0876, found: 327.0857.

1.5.5. *N*-(3-Chloropyridin-4-yl)-6-propoxypyridin-3-amine (**7d**)

Following the general procedure for 24 h at 140 °C, 5-bromo-2-propoxypyridine **6a** (13.45 g, 62.50 mmol) was heated with 4-amino-3-chloropyridine **4b** (8.0 g, 62.5 mmol), Pd(OAc)₂ (697 mg, 3.1 mmol), X-Phos (1.46 g, 3.1 mmol) and Cs₂CO₃ (40.6 g, 125 mmol) in refluxing toluene to yield the crude diaza material **7d**. After flash chromatography (silica gel, 1:1 ethyl acetate/hexane), this afforded the pure diaza material **7d** (8.29 g, 51%) as a white solid; mp 71.6 – 72.6 °C: ¹H NMR (300 MHz, CDCl₃): δ 8.35 (s, 1H), 8.10-8.07 (m, 2H), 7.48 (dd, *J* = 6.0, 3.0 Hz, 1H), 6.80 (d, *J* = 6.0 Hz, 1H), 6.60 (d, *J* = 6.0 Hz, 1H), δ 6.45 (br, 1H), 4.25 (t, *J* = 6.9, Hz, 2H), 1.87-1.75 (m, 2H), 1.03 (t, *J* = 7.2, Hz, 3H); ¹³C NMR (75 MHz, CDCl₃): δ 162.3, 148.8, 148.3, 148.2, 144.0, 136.56, 128.2, 117.1, 111.7, 106.9, 68.0, 22.3, 10.5; HRMS (ESI-TOF) (*m/z*): [M+H]⁺ calcd for C₁₃H₁₅ClN₃O 264.0904, found 264.0893.

1.5.6. *N*-(3-Chloropyridin-4-yl)-6-isopropoxypyridin-3-amine (**7e**)

Following the general procedure for 24 h at 140 °C, 5-bromo-2-isopropoxypyridine **6b** (8.09 g, 37.20 mmol) was heated with 4-amino-3-chloropyridine **4b** (4.74 g, 37.20 mmol),

Pd(OAc)₂ (419 mg, 1.87 mmol), X-Phos (608 mg, 1.87 mmol), Cs₂CO₃ (15.25 g, 46.80 mmol) in refluxing toluene to afford a crude solid which was purified by flash chromatography (silica gel, 1:1 ethyl acetate/hexane) to furnish a white solid **7e** (5.20 g, 52.4 %); mp 76 – 78 °C: ¹H NMR (300 MHz, CDCl₃): δ 8.35 (s, 1H), 8.10-8.06 (m, 2H), 7.46 (dd, *J* = 6.0, 3.0 Hz, 1H), 6.74 (d, *J* = 6.0 Hz, 1H), 6.61 (d, *J* = 6.0 Hz, 1H), 6.42 (br s, 1H), 5.35-5.23 (m, 1H), 1.36 (d, *J* = 6.0 Hz, 6H); ¹³C NMR (75 MHz, CDCl₃): δ 161.7, 148.7, 148.3, 144.0, 136.5, 127.9, 117.0, 112.2, 106.9, 68.5, 22.0; HRMS (ESI-TOF) (*m/z*): [M+H]⁺ calcd for C₁₃H₁₅ClN₃O 264.0904, found 264.0909.

1.5.7. General procedure for the intramolecular Heck cyclization: Representative procedure for the synthesis of 3-propoxy-9H-pyrido[3,4-*b*]indole (3-PBC, **1) and 2-propoxy-5H-pyrido[3,2-*b*]indole (**9a**).**

A heavy-wall pressure tube was equipped with a magnetic stir bar and fitted with a rubber septum and loaded with *N*-(2-chlorophenyl)-6-propoxypyridin-3-amine **7a** (526 mg, 2.0 mmol), Pd(OAc)₂ (44.8 mg, 0.2 mmol), (*t*-Bu)₃P·HBF₄ (116 mg, 0.4 mmol) and K₂CO₃ (552 mg, 4.0 mmol). The vessel was evacuated and backfilled with argon (this process was repeated a total of 3 times) and degassed DMA (8 mL) was injected into the tube with a degassed syringe under a positive pressure of argon. The rubber septum was replaced with a screw-cap by quickly removing the rubber septum under the flow of argon and the sealed tube was introduced into a pre-heated oil bath at 120 °C. The reaction mixture was maintained at this temperature for 16 h. At the end of this period, the reaction mixture was allowed to cool to rt. The dark brown mixture which resulted was then passed through a short pad of celite. The celite pad was further washed with ethyl acetate (150 mL) until no more product (TLC; silica gel) was detected in the eluent. The combined filtrate was washed with water (100 mL x 3), brine (100 mL), dried (Na₂SO₄) and concentrated under reduced pressure. The crude product was purified by flash column chromatography (silica gel, 5:1 hexanes/ethyl acetate) to afford 3-PBC (**1**) (235 mg, 52%) as an off white solid. mp 120.5-121.5

°C (lit.³⁵ mp 119.3-120.5 °C) : **1**, ¹H NMR (300 MHz, CDCl₃) δ 8.66 (br, 1H), 8.42 (s, 1H), 8.05 (d, *J* = 7.9 Hz, 1H), 7.50 (t, *J* = 7.6 Hz, 1H), 7.45 – 7.38 (m, 1H), 7.35 (s, 1H), 7.21 (t, *J* = 7.4 Hz, 1H), 4.28 (t, *J* = 6.7 Hz, 2H), 1.94 – 1.78 (m, 2H), 1.06 (t, *J* = 7.4 Hz, 3H); ¹³C NMR (75 MHz, CDCl₃) δ 157.9, 142.4, 133.8, 132.7, 128.9, 128.7, 122.0, 121.4, 119.5, 111.5, 99.1, 68.6, 22.7, 10.6; HRMS (ESI-TOF) (*m/z*): [M+H]⁺ calcd for C₁₄H₁₅N₂O: 227.1184, found: 227.1174. A hydrochloride salt of **1** was prepared by the reported method³¹ to obtain 3-PBC·HCl (**1·HCl**): yellow solid; mp 194.5-195.5 °C (lit³¹ 194.0-195.0 °C). The spectral data for this **1·HCl** were in excellent agreement with the reported values (mp, ¹H NMR).³¹

9a (145 mg, 32%) as a white solid; mp 125-126 °C: ¹H NMR (300 MHz, CDCl₃) δ 8.28 (t, *J* = 8.8 Hz, 1H), 8.20 (br, 1H), 7.60 (d, *J* = 8.7 Hz, 1H), 7.51 – 7.34 (m, 2H), 7.27 (t, *J* = 7.3 Hz, 1H), 6.83 (d, *J* = 8.7 Hz, 1H), 4.46 (t, *J* = 6.7 Hz, 2H), 1.99 – 1.80 (m, 2H), 1.10 (t, *J* = 7.4 Hz, 3H); ¹³C NMR (75 MHz, CDCl₃) δ 159.5, 140.2, 138.2, 128.4, 126.8, 122.3, 121.6, 120.6, 119.7, 111.3, 108.6, 67.9, 22.6, 10.7; HRMS (ESI-TOF) (*m/z*): [M+H]⁺ calcd for C₁₄H₁₅N₂O: 227.1184, found: 227.1180.

1.5.8. 3-Isopropoxy-9H-pyrido[3,4-*b*]indole (3-ISOPBC, **2**) and 3-isopropoxy-5H-pyrido[3,2-*b*]indole (**9b**)

Following the general procedure for the intramolecular Heck cyclization, **7b** (526 mg, 2.0 mmol) was heated with Pd(OAc)₂ (45 mg, 0.2 mmol), (*t*-Bu)₃P·HBF₄ (116 mg, 0.4 mmol) and K₂CO₃ (552 mg, 4.0 mmol) in DMA at 120 °C to afford a mixture of regioisomers **2** and **9b**. After flash chromatography (silica gel, 5:1 hexanes/ethyl acetate), this procedure yielded pure 3-ISOPBC (**2**) and the byproduct **9b**.

2 (239.5 mg, 53%): off-white solid; mp 134-136 °C: ¹H NMR (300 MHz, CDCl₃) δ 8.41 (s, 1H), 8.19 (br, 1H), 8.04 (d, *J* = 7.8 Hz, 1H), 7.50 (t, *J* = 7.6 Hz, 1H), 7.40 (d, *J* = 8.1 Hz, 1H), 7.34 (s, 1H), 7.21 (t, *J* = 7.4 Hz, 1H), 5.35 – 5.23(m, 1H), 1.40 (d, *J* = 6.1 Hz, 6H); ¹³C NMR (75 MHz,

CDCl₃) δ 157.4, 142.1, 133.7, 132.5, 128.9, 128.8, 122.0, 121.6, 119.5, 111.3, 100.5, 68.6, 22.3; HRMS (ESI-TOF) (m/z): [M+H]⁺ calcd for C₁₄H₁₅N₂O: 227.1184, found: 227.1184. A hydrochloride salt of **2** was prepared by the reported method³⁷ to obtain 3-ISOPBC·HCl (**2·HCl**): light greenish yellow solid; mp 169-171 °C (lit.³⁷ 168-172 °C). The data for this compound matched in all respects (¹H NMR, mp) with that reported in the literature.³⁷

9b (163.1 mg, 36%): light brown solid; mp 110.4 - 111.5 °C: ¹H NMR (300 MHz, CDCl₃) δ 8.27 (d, J = 7.8 Hz, 1H), 7.99 (br, 1H), 7.67 (d, J = 8.7 Hz, 1H), 7.49 – 7.45 (m, 2H), 7.30 – 7.25 (m, 1H), 6.79 (d, J = 8.7 Hz, 1H), 5.60 – 5.48 (m, 1H), 1.45 (d, J = 6.1 Hz, 6H); ¹³C NMR (75 MHz, CDCl₃) δ 158.9, 140.1, 138.4, 128.1, 126.7, 122.6, 121.3, 120.5, 119.7, 111.1, 109.4, 67.9, 22.2; HRMS (ESI-TOF) (m/z): [M+H]⁺ calcd for C₁₄H₁₅N₂O: 227.1184, found: 227.1185.

1.5.9. *tert*-Butyl 9*H*-pyrido[3,4-*b*]indole-3-carboxylate (β CCt; **3**) and *tert*-butyl 5*H*-pyrido[3,2-*b*]indole-3-carboxylate (**9c**)

Following the general procedure for the intramolecular Heck cyclization, **7c** (2 g, 16.4 mmol), was heated with Pd(OAc)₂ (147 mg, 0.656 mmol), (*t*-Bu)₃P·HBF₄ (380 mg, 0.4 mmol) and K₂CO₃ (1.8 g, 13.12 mmol) in DMA at 120 °C to afford crude **3** and **9c**. After flash chromatography (silica gel, 1:1 hexanes/ethyl acetate), this afforded pure β CCt (**3**) and **9c**.

3 (885 mg, 50%), white solid; mp 302.5 - 304.5 °C (lit³³ 301-303 °C): ¹H NMR (300 MHz, CDCl₃) δ 10.35 (br, 1H), 9.23 (s, 1H), 8.86 (s, 1H), 8.25 (d, J = 7.9 Hz, 1H), 7.80 (d, J = 8.3 Hz, 1H), 7.66 – 7.61 (m, 1H), 7.38 (t, J = 7.5 Hz, 1H), 1.75 (s, 9H); ¹³C NMR (75 MHz, CD₃COCD₃) δ 164.9, 141.2, 139.2, 137.7, 133.4, 128.6, 128.1, 121.8, 121.5, 120.3, 116.9, 112.2, 80.1, 27.6; HRMS (ESI-TOF) (m/z): [M+H]⁺ calcd for C₁₆H₁₇N₂O₂: 269.1290, found: 269.1286. The spectral data are in excellent agreement with the published values.³³

9c (531 mg, 30%), fluffy white solid; mp 216.0 – 218.2 °C: ¹H NMR (300 MHz, CDCl₃) δ 9.46 (br, 1H), 8.38 (d, J = 7.8 Hz, 1H), 8.18 (d, J = 8.5 Hz, 1H), 7.82 (d, J = 8.5 Hz, 1H), 7.53 – 7.49

(m, 2H), 7.25 – 7.23 (m, 1H), 1.67 (s, 9H); ^{13}C NMR (75 MHz, CDCl_3) δ 164.9, 142.4, 141.4, 141.1, 134.7, 128.6, 122.0, 121.9, 121.0, 120.8, 117.4, 111.5, 81.9, 28.2; HRMS (ESI-TOF) (m/z): $[\text{M}+\text{H}]^+$ calcd for $\text{C}_{16}\text{H}_{17}\text{N}_2\text{O}_2$: 269.1290, found: 269.1289.

1.5.10. 8-Propoxy-5H-pyrrolo[2,3-c:4,5-c']dipyridine (6-Aza-3-PBC, 4) and 2-Propoxy-5H-pyrrolo[3,2-b:4,5-c']dipyridine (9d)

Following the general procedure for the intramolecular Heck cyclization, the diaza compound **7d** (3.0 g, 11.30 mmol) was heated with $\text{Pd}(\text{OAc})_2$ (255.0 mg, 1.13 mmol), (*t*-Bu) $_3\text{P}\cdot\text{HBF}_4$ (657.0 mg, 2.26 mmol) and K_2CO_3 (3.2 g, 22.60 mmol) in DMA at 120 °C to afford crude **4** and **9d**. After flash chromatography (silica gel, 1:24 methanol/dichloromethane) this process afforded the pure regioisomers 6-Aza-3-PBC (**4**) and **9d** as white solids.

4 (820 mg, 31.8%): mp 166-168 °C: ^1H NMR (300 MHz, $(\text{CD}_3)_2\text{SO}$): δ 12.13 (br, 1H), 9.51 (s, 1H), 8.57 (br, 2H), 7.68 (s, 1H), 7.61 (d, $J = 5.7$ Hz, 1H), 4.26 (t, $J = 6.0$ Hz, 2H), 1.83-1.71 (m, 2H), 1.01 (t, $J = 6.0$ Hz, 3H); ^{13}C NMR (75 MHz, $(\text{CD}_3)_2\text{SO}$): δ 158.4, 147.0, 144.5, 143.4, 133.0, 131.5, 130.7, 118.2, 108.1, 100.4, 68.0, 22.5, 10.9; HRMS (ESI-TOF) (m/z): $[\text{M}+\text{H}]^+$ calcd for $\text{C}_{13}\text{H}_{14}\text{N}_3\text{O}$: 228.1137, found: 228.1144.

9d (1.62 g, 62.5%): mp 192-194 °C: ^1H NMR (300 MHz, $(\text{CD}_3)_2\text{SO}$): 11.70 (s, 1H), 9.25 (s, 1H), 8.43 (d, $J = 6.0$ Hz, 1H), 7.94 (d, $J = 9.0$ Hz, 1H), 7.51 (d, $J = 6.0$ Hz, 1H), 6.93 (d, $J = 9.0$ Hz, 1H), 4.36 (t, $J = 6.0$ Hz, 2H), 1.84-1.77 (m, 2H), 1.03 (t, $J = 6.0$ Hz, 3H); ^{13}C NMR (75 MHz, $(\text{CD}_3)_2\text{SO}$): δ 159.7, 145.2, 143.8, 142.8, 136.0, 128.8, 123.5, 118.5, 110.2, 107.6, 67.4, 22.4, 11.0; HRMS (ESI-TOF) (m/z): $[\text{M}+\text{H}]^+$ calcd for $\text{C}_{13}\text{H}_{14}\text{N}_3\text{O}$: 228.1137, found: 228.1140.

1.5.11. 8-Isopropoxy-5H-pyrrolo[2,3-c:4,5-c']dipyridine (6-Aza-3-ISOPBC, 5) and 2-Isopropoxy-5H-pyrrolo[3,2-b:4,5-c']dipyridine (9e)

Following the general procedure for the intramolecular Heck cyclization, pyridine **7e** (3.0 g, 11.30 mmol) was heated with $\text{Pd}(\text{OAc})_2$ (255.0 mg, 1.13 mmol), (*t*-Bu) $_3\text{P}\cdot\text{HBF}_4$ (657.0 mg, 2.26

mmol) and K_2CO_3 (3.2 g, 22.60 mmol) in DMA at 120 °C to afford crude **5** and **9e**. After flash chromatography (silica gel, 1:24 methanol/dichloromethane) this afforded the regioisomeric 6-Aza-3-ISOPBC (**5**) and **9e** as white solids.

5 (800 mg, 31.0%); mp 180.2–183.2 °C: 1H NMR (300 MHz, $(CD_3)_2SO$): δ 11.66 (s, 1H), 9.37 (s, 1H), 8.51 (s, 1H), 8.48 (d, $J = 6.0$ Hz, 1H), 7.56 (s, 1H), 7.46 (d, $J = 6.0$ Hz, 1H), 5.32–5.20 (m, 1H), 1.32 (d, $J = 6.0$ Hz, 6H); ^{13}C NMR (125 MHz, $(CD_3)_2SO$): δ 157.4, 147.3, 146.3, 145.4, 132.7, 131.6, 130.1, 118.2, 107.4, 100.0, 68.0, 22.6; HRMS (ESI-TOF) (m/z): $[M+H]^+$ calcd for $C_{13}H_{14}N_3O$: 228.1137, found: 228.1150.

9e (1.6 g, 62.3%); mp 207.4–208.6 °C: 1H NMR (500 MHz, $(CD_3)_2SO$): δ 11.85 (s, 1H), 9.28 (s, 1H), 8.44 (d, $J = 3.0$ Hz, 1H), 7.94 (d, $J = 6.0$ Hz, 1H), 7.55 (d, $J = 3.0$ Hz, 1H), 6.89 (d, $J = 6.0$ Hz, 1H), 5.49–5.41 (m, 1H), 1.36 (d, $J = 3.0$ Hz, 6H); ^{13}C NMR (125 MHz, $(CD_3)_2SO$): δ 159.2, 144.2, 144.0, 142.1, 136.0, 128.9, 123.7, 111.1, 107.8, 67.8, 22.4; HRMS (ESI-TOF) (m/z): $[M+H]^+$ calcd for $C_{13}H_{14}N_3O$: 228.1137, found: 228.1140.

1.5.12. *tert*-Butyl (2-chlorophenyl)(6-isopropoxy-pyridin-3-yl)carbamate (**10**)

To the amine **7b** (275 mg, 1.05 mmol) in THF (6 mL) was added the di-*tert*-butyl dicarbonate (320 mg, 1.46 mmol) and 4-(dimethylamino)pyridine (DMAP, 51.1 mg, 0.42 mmol) and this mixture was stirred at rt for 24 h. The organic solvent was removed under reduced pressure and the crude product which resulted was purified by flash column chromatography (silica gel, 1:9 ethylacetate/hexane) to give the pure BOC protected amine **10** (323 mg, 85%):

1H NMR (300 MHz, $CDCl_3$) δ 8.03 (d, $J = 2.6$ Hz, 1H), 7.60 (s, 1H), 7.44 (dd, $J = 8.1, 5.9$ Hz, 1H), 7.32 – 7.20 (m, 3H), 6.62 (d, $J = 8.9$ Hz, 1H), 5.30 – 5.16 (m, 1H), 1.43 (s, 9H), 1.31 (d, $J = 6.2$ Hz, 6H); ^{13}C NMR (75 MHz, $CDCl_3$) δ 160.9, 153.3, 143.9, 139.8, 136.7, 133.3, 132.2, 130.4, 130.3, 128.6, 127.7, 111.1, 81.6, 68.2, 28.1; HRMS (ESI-TOF) (m/z): $[M+H]^+$ calcd for $C_{19}H_{24}ClN_2O_3$: 363.1475, found: 363.1469.

1.5.13. (9H-Fluoren-9-yl)methyl (2-chlorophenyl)(6-isopropoxy-pyridin-3-yl)carbamate (**11**)

The microwave tube was loaded with amine **7b** (300 mg, 1.14 mmol) and Fmoc chloride (325 mg, 1.25 mmol). The tube was sealed and placed into a microwave apparatus (with a power of 100 W) at 80 °C for 1 h with stirring. At the end of this period, the reaction was directly purified, without quenching, by flash column chromatography (silica gel, 1:4 ethylacetate/hexane) to give pure Fmoc protected pyridine **11** (360 mg, 65%).

¹H NMR (300 MHz, CDCl₃) δ 8.08 (d, *J* = 2.7 Hz, 1H), 7.70 (d, *J* = 7.6 Hz, 3H), 7.50 (d, *J* = 3.8 Hz, 1H), 7.42 – 7.28 (m, 5H), 7.20 – 7.06 (m, 4H), 6.64 (d, *J* = 8.5 Hz, 1H), 5.33 – 5.15 (m, 1H), 4.49 – 4.41 (m, 2H), 4.16 – 4.09 (m, 1H), 1.34 (d, *J* = 6.1 Hz, 6H); ¹³C NMR (75 MHz, CDCl₃) δ 154.3, 143.6, 141.3, 139.2, 139.1, 131.6, 130.60, 130.5, 129.2, 127.9, 127.7, 126.9, 125.0, 119.9, 111.4, 68.4, 68.2, 46.9, 22.1; HRMS (ESI-TOF) (*m/z*): [M+Na]⁺ calcd for C₂₉H₂₅ClN₂O₃Na: 507.1451, found: 507.1448.

1.5.14. 4-Chloro-6-isopropoxy-*N*-phenylpyridin-3-amine (**16**)

A heavy-wall pressure tube was equipped with a magnetic stir bar and fitted with a rubber septum that had been charged with 4-chloro-5-iodo-2-isopropoxy-pyridine **14** (75 mg, 0.252 mmol), aniline (27.6 μL, 0.256 mmol) and Cs₂CO₃ (410 mg, 1.26 mmol). The vessel was evacuated and backfilled with argon (this process was repeated a total of 3 times) and degassed toluene (1 mL) was injected into the tube with a degassed syringe under a positive pressure of argon. In another round bottom flask fitted with a rubber septum, Pd(OAc)₂ (1.7 mg, 0.0076 mmol) and *rac*-BINAP (4.7 mg, 0.0076 mmol) was charged. This flask was evacuated and backfilled with argon (this process was repeated a total of 3 times) and then degassed toluene (0.5 mL) was added under a positive pressure of argon. This mixture was stirred for 10 min and then the mixture which resulted was added to the above pressure tube. The rubber septum was replaced with a screw-cap by quickly removing the rubber septum under the flow of argon and the sealed tube was introduced

into a pre-heated oil bath at 110 °C. The reaction mixture was maintained at this temperature for 5 h. At the end of this time period the pressure tube was allowed to cool to rt. The reaction mixture was filtered through a short pad of celite, and the pad was washed with ethyl acetate (until no more product could be obtained; \approx 50 mL). The combined organic eluents were washed with water (50 mL), brine (50 mL), dried (Na_2SO_4) and concentrated under reduced pressure. The crude product was purified by flash column chromatography (silica gel, 20:1 hexanes/ethyl acetate) to afford only **16** (61 mg, 92 %) as a pale yellow oil.

^1H NMR (300 MHz, CDCl_3) δ 8.18 (s, 1H), 7.28 (t, $J = 7.9$ Hz, 2H), 6.98 – 6.92 (m, 3H), 6.83 (s, 1H), 5.52 (s, 1H), 5.29 – 5.17 (m, 1H), 1.36 (d, $J = 6.2$ Hz, 6H); ^{13}C NMR (75 MHz, CDCl_3) δ 159.2, 143.5, 139.1, 138.2, 130.4, 129.5, 121.1, 116.8, 111.9, 68.8, 22.1; HRMS (ESI-TOF) (m/z): $[\text{M}+\text{H}]^+$ calcd for $\text{C}_{14}\text{H}_{16}\text{ClN}_2\text{O}$: 263.0951, found: 263.0958.

1.5.15. 4-Chloro-6-propoxy-*N*-phenylpyridin-3-amine (**15**)

Following the above general procedure for 5 h at 110 °C, 4-chloro-5-iodo-2-propoxypyridine **13** (75 mg, 0.252 mmol), aniline (27.6 μL , 0.256 mmol), $\text{Pd}(\text{OAc})_2$ (1.7 mg, 0.0076 mmol), *rac*-BINAP (4.7 mg, 0.0076 mmol) and Cs_2CO_3 (410 mg, 1.26 mmol) were heated in toluene at reflux to afford a crude liquid which was purified by flash chromatography (silica gel, 20:1 hexanes/ethyl acetate) to furnish a pale yellow oil **15** (60.33 mg, 91 %).

^1H NMR (300 MHz, CDCl_3) δ 8.20 (s, 1H), 7.28 (t, $J = 7.9$ Hz, 2H), 6.98 – 6.93 (m, 3H), 6.89 (s, 1H), 5.57 (s, 1H), 4.26 (t, $J = 6.6$ Hz, 2H), 1.89 – 1.77 (m, 2H), 1.06 (t, $J = 7.2$ Hz, 2H); ^{13}C NMR (75 MHz, CDCl_3) δ 159.9, 143.6, 139.3, 138.1, 130.6, 129.5, 121.1, 116.7, 111.4, 68.1, 22.4, 10.5; HRMS (ESI-TOF) (m/z): $[\text{M}+\text{H}]^+$ calcd for $\text{C}_{14}\text{H}_{16}\text{ClN}_2\text{O}$: 263.0951, found: 263.0946.

1.5.16. 4-Chloro-6-propoxy-*N*-(pyridin-4-yl)pyridine-3-amine (**17**)

Following the above general procedure for 6 h at 140 °C, 4-chloro-5-iodo-2-propoxypyridine **13** (214 mg, 0.72 mmol), 4-aminopyridine (68.8 mg, 0.73 mmol), $\text{Pd}(\text{OAc})_2$ (4.8 mg,

0.0216 mmol) and *rac*-BINAP (13.4 mg, 0.0216 mmol) as well as Cs₂CO₃ (1.17 g, 3.6 mmol) were heated in toluene at reflux to afford a crude solid which was purified by flash chromatography (silica gel, ethyl acetate) to furnish a white solid **17** (137 mg, 72 %); mp 119-120 °C, ¹H NMR (300 MHz, CDCl₃): δ 8.28 (d, *J* = 4.8 Hz, 2H), 8.19 (s, 1H), 6.92 (s, 1H), 6.65 (d, *J* = 5.4 Hz, 2H), 6.18 (br, 1H), 4.27 (t, *J* = 6.6 Hz, 2H), 1.88 – 1.76 (m, 2H), 1.04 (t, *J* = 7.5 Hz, 2H); ¹³C NMR (75 MHz, CDCl₃): δ 162.3, 151.7, 150.0, 144.6, 142.0, 126.9, 111.9, 108.9, 68.4, 22.3, 10.5; HRMS (ESI-TOF) (*m/z*): [M+H]⁺ calcd for C₁₃H₁₅ClN₃O 264.0904, found 264.0898.

1.5.17. 4-Chloro-6-isopropoxy-*N*-(pyridin-4-yl)pyridine-3-amine (**18**)

Following the above general procedure for 6 h at 140 °C, 4-chloro-5-iodo-2-isopropoxy-pyridine **13** (214 mg, 0.72 mmol), 4-aminopyridine (68.8 mg, 0.73 mmol), Pd(OAc)₂ (4.8 mg, 0.0216 mmol) and *rac*-BINAP (13.4 mg, 0.0216 mmol) as well as Cs₂CO₃ (1.17 g, 3.6 mmol) were heated in toluene at reflux to afford a crude solid which was purified by flash chromatography (silica gel, ethyl acetate) to furnish a white solid **18** (135 mg, 71 %); ¹H NMR (300 MHz, CDCl₃): δ 8.24 (d, *J* = 4.2 Hz, 2H), 8.18 (s, 1H), 6.87 (s, 1H), 6.74 (d, *J* = 5.7 Hz, 2H), 5.36-5.23 (m, 1H), 1.37 (d, *J* = 6.3 Hz, 6H); ¹³C NMR (75 MHz, CDCl₃): δ 161.9, 152.4, 148.9, 144.8, 142.1, 126.4, 112.4, 108.9, 69.3, 22.0; HRMS (ESI-TOF) (*m/z*): [M+H]⁺ calcd for C₁₃H₁₅ClN₃O 264.0904, found 264.0910.

1.5.18. 3-propoxy-9*H*-pyrido[3,4-*b*]indole (3-PBC, **1**)

Following the general procedure for the Heck cyclization for 16 h at 120 °C, 4-Chloro-6-propoxy-*N*-phenylpyridin-3-amine **15** (526 mg, 2.0 mmol), Pd(OAc)₂ (44.8 mg, 0.2 mmol), (*t*-Bu)₃P·HBF₄ (116 mg, 0.4 mmol) and K₂CO₃ (552 mg, 4.0 mmol) were heated in DMA to give a solid which was purified by a wash column (silica gel, 5:1 hexanes/ethyl acetate) to yield 3-PBC **1** (416.80 mg, 92%).

1.5.19. 3-Isopropoxy-9H-pyrido[3,4-*b*]indole (3-ISOPBC, 2)

Following the general procedure for the Heck cyclization for 16 h at 120 °C, 4-Chloro-6-isopropoxy-N-phenylpyridin-3-amine **16** (526 mg, 2.0 mmol), Pd(OAc)₂ (44.8 mg, 0.2 mmol), (*t*-Bu)₃P·HBF₄ (116 mg, 0.4 mmol) and K₂CO₃ (552 mg, 4.0 mmol) were heated in DMA to give a solid which was purified by a wash column (silica gel, 5:1 hexanes/ethyl acetate) to yield 3-ISOPBC **2** (412.30 mg, 91%).

1.5.20. 8-Propoxy-5H-pyrrolo[2,3-*c*:4,5-*c'*]dipyridine (6-Aza-3-PBC, 4)

Following the general procedure for the Heck cyclization for 16 h at 120 °C, 4-Chloro-6-propoxy-N-(pyridin-4-yl)pyridine-3-amine **17** (125 mg, 0.475 mmol), Pd(OAc)₂ (10.7 mg, 0.047 mmol), (*t*-Bu)₃P·HBF₄ (27.6 mg, 0.095 mmol) and K₂CO₃ (131.3 mg, 0.95 mmol) were heated in DMA to give a solid which was purified by a wash column (silica gel, 1:24 methanol/dichloromethane) to yield 6-Aza-3-PBC **4** (97.15 mg, 90%).

1.5.21. 8-Isopropoxy-5H-pyrrolo[2,3-*c*:4,5-*c'*]dipyridine (6-Aza-3-ISOPBC, 5)

Following the general procedure for the Heck cyclization for 16 h at 120 °C, 4-Chloro-6-isopropoxy-N-(pyridin-4-yl)pyridine-3-amine **18** (125 mg, 0.475 mmol), Pd(OAc)₂ (10.7 mg, 0.047 mmol), (*t*-Bu)₃P·HBF₄ (27.6 mg, 0.095 mmol) and K₂CO₃ (131.3 mg, 0.95 mmol) were heated to give a solid which was purified by a wash column (silica gel, 1:24 methanol/dichloromethane) to yield 6-Aza-3-ISOPBC **5** (99.31 mg, 92%)

1.5.22. Large-Scale Synthesis of 3-ISOPBC (2)

1.5.22.1. Step 1: Synthesis of 4-Chloro-6-isopropoxy-N-phenylpyridin-3-amine (16)

4-Chloro-5-iodo-2-isopropoxy-pyridine **14** (25 g, 84.03 mmol), aniline (7.65 mL, 84.03 mmol), Pd(OAc)₂ (0.57 g, 2.52 mmol) and *rac*-BINAP (1.57 g, 2.52 mmol) as well as Cs₂CO₃ (136.84 g, 420 mmol) were added to a three-neck flask with a reflux condenser. The flask was evacuated and backfilled with argon. Degassed toluene (300 mL) was added via a cannula, and the

flask was introduced into a preheated oil bath at 110 °C. After 15 h at 110 °C the reaction mixture was cooled to rt and filtered through a short pad of celite, and the pad was washed with ethyl acetate. The combined organic eluents were washed with water and brine, dried (Na₂SO₄), and concentrated under reduced pressure. The crude product was purified by flash chromatography (silica gel, 20:1 hexanes/ethyl acetate) to afford only **16** (19.86 g, 90 %) as a pale yellow oil.

1.5.22.2. Step 2: Synthesis of 3-isopropoxy-9H-pyrido[3,4-b]indole (**2**)

A heavy-wall pressure tube was equipped with a magnetic stir bar and fitted with a rubber septum loaded with 4-chloro-6-isopropoxy-*N*-phenylpyridin-3-amine **16** (19.86 g, 75.58 mmol), Pd(OAc)₂ (1.70 g, 7.558 mmol), (*t*-Bu)₃P·HBF₄ (4.39 g, 15.12 mmol) and K₂CO₃ (20.89 g, 151.16 mmol). The vessel was evacuated and backfilled with argon (this process was repeated a total of 3 times) and degassed DMA (200 mL) was added to this vial via a cannula. The rubber septum was replaced with a screw-cap by quickly removing the rubber septum under the flow of argon and the sealed tube was introduced into a pre-heated oil bath at 120 °C. The reaction mixture was maintained at this temperature for 16 h. At the end of this period, the reaction mixture was allowed to cool to rt. The dark brown mixture which resulted was then passed through a short pad of celite. The celite pad was further washed with ethyl acetate until no product (TLC; silica gel) was detected in the eluent. The combined filtrate was washed with water, brine, dried (Na₂SO₄) and concentrated under reduced pressure. The solid product was purified by wash column (silica gel, 5:1 hexanes/ethyl acetate) to afford 3-ISOPBC (**2**) (15.74 g, 92%) as an off white solid.

1.6. REFERENCES

- (1) Cao, R.; Peng, W.; Wang, Z.; Xu, A. *Curr. Med. Chem.* **2007**, *14*, 479.
- (2) Venault, P.; Chapouthier, G. *Sci. World J.* **2007**, *7*, 204.
- (3) Stahre, M.; Roeber, J.; Kanny, D.; Brewer, R. D.; Zhang, X. *Prev. Chronic Dis.* **2014**, *11*, E109.

- (4) Yang, A. R.; Liu, J.; Yi, H. S.; Warnock, K. T.; Wang, M.; June, H. L., Jr.; Puche, A. C.; Elnabawi, A.; Sieghart, W.; Aurelian, L.; June, H. L., Sr. *Front. Neurosci.* **2011**, *5*, 123.
- (5) Moffett, M. C.; Vicentic, A.; Kozel, M.; Plotsky, P.; Francis, D. D.; Kuhar, M. J. *Biochem. Pharmacol.* **2007**, *73*, 321.
- (6) Nylander, I.; Roman, E. *Psychopharmacology (Berl.)* **2013**, *229*, 555.
- (7) Jaworski, J. N.; Francis, D. D.; Brommer, C. L.; Morgan, E. T.; Kuhar, M. J. *Psychopharmacology (Berl.)* **2005**, *181*, 8.
- (8) Johnson, B. A.; Ait-Daoud, N. *Psychopharmacology* **2000**, *149*, 327.
- (9) Kranzler, H. R. *Alcohol Alcohol.* **2000**, *35*, 537.
- (10) Davies, M. J. *Psychiatry Neurosci.* **2003**, *28*, 263.
- (11) Kalsi, G.; Prescott, C. A.; Kendler, K. S.; Riley, B. P. *Trends Genet.* **2009**, *25*, 49.
- (12) Koob, G. F. *Biochem. Pharmacol.* **2004**, *68*, 1515.
- (13) Sieghart, W.; Ernst, M. *Curr.Med.Chem.-Central Nervous Syst. Agents* **2005**, *5*, 217.
- (14) Silveri, M. M.; Sneider, J. T.; Crowley, D. J.; Covell, M. J.; Acharya, D.; Rosso, I. M.; Jensen, J. E. *Biol. Psychiatry* **2013**, *74*, 296.
- (15) Kumar, S.; Porcu, P.; Werner, D. F.; Matthews, D. B.; Diaz-Granados, J. L.; Helfand, R. S.; Morrow, A. L. *Psychopharmacology (Berl.)* **2009**, *205*, 529.
- (16) Churchill, L.; Bourdelais, A.; Austin, M. C.; Lolait, S. J.; Mahan, L. C.; O'Carroll, A. M.; Kalivas, P. W. *Synapse* **1991**, *8*, 75.
- (17) Duncan, G. E.; Breese, G. R.; Criswell, H. E.; McCown, T. J.; Herbert, J. S.; Devaud, L. L.; Morrow, A. L. *Neuroscience* **1995**, *64*, 1113.
- (18) Harvey, S. C.; Foster, K. L.; McKay, P. F.; Carroll, M. R.; Seyoum, R.; Woods, J. E., 2nd; Grey, C.; Jones, C. M.; McCane, S.; Cummings, R.; Mason, D.; Ma, C.; Cook, J. M.; June, H. L. *J. Neurosci.* **2002**, *22*, 3765.
- (19) Wisden, W.; Laurie, D. J.; Monyer, H.; Seeburg, P. H. *J. Neurosci.* **1992**, *12*, 1040.
- (20) Liu, J.; Yang, A. R.; Kelly, T.; Puche, A.; Esoga, C.; June, H. L., Jr.; Elnabawi, A.; Merchenthaler, I.; Sieghart, W.; June, H. L., Sr.; Aurelian, L. *Proc. Natl. Acad. Sci. U. S. A.* **2011**, *108*, 4465.
- (21) Koob, G. F.; Le Moal, M. *Nat. Neurosci.* **2005**, *8*, 1442.
- (22) Koob, G. F.; Roberts, A. J.; Schulteis, G.; Parsons, L. H.; Heyser, C. J.; Hyytia, P.; Merlo-Pich, E.; Weiss, F. *Alcohol. Clin. Exp. Res.* **1998**, *22*, 3.

- (23) McBride, W. J.; Li, T. K. *Crit. Rev. Neurobiol.* **1998**, *12*, 339.
- (24) June, H. L.; Foster, K. L.; McKay, P. F.; Seyoum, R.; Woods, J. E., II; Harvey, S. C.; Eiler, W. J. A., II; Grey, C.; Carroll, M. R.; McCane, S.; Jones, C. M.; Yin, W.; Mason, D.; Cummings, R.; Garcia, M.; Ma, C.; Sarma, P. V. V. S.; Cook, J. M.; Skolnick, P. *Neuropsychopharmacology* **2003**, *28*, 2124.
- (25) Cox, E. D.; Hagen, T. J.; Mckernan, R. M.; Cook, J. M. *Med. Chem. Res.* **1995**, *5*, 710.
- (26) Sawyer, E. K.; Moran, C.; Sirbu, M. H.; Szafir, M.; Van Linn, M.; Namjoshi, O.; Tiruveedhula, V. V. N. P. B.; Cook, J. M.; Platt, D. M. *Alcohol. Clin. Exp. Res.* **2014**, *38*, 1108.
- (27) O'Tousa, D. S.; Warnock, K. T.; Matson, L. M.; Namjoshi, O. A.; Linn, M. V.; Tiruveedhula, V. V.; Halcomb, M. E.; Cook, J.; Grahame, N. J.; June, H. L. *Addict. Biol.* **2015**, *20*, 236.
- (28) Rowlett, J. K.; Spealman, R. D.; Lelas, S.; Cook, J. M.; Yin, W. *Psychopharmacology* **2003**, *165*, 209.
- (29) Kovacevic, J.; Timic, T.; Tiruveedhula, V. V.; Batinic, B.; Namjoshi, O. A.; Milic, M.; Joksimovic, S.; Cook, J. M.; Savic, M. M. *Brain Res. Bull.* **2014**, *104*, 1.
- (30) Divljakovic, J.; Milic, M.; Namjoshi, O. A.; Tiruveedhula, V. V.; Timic, T.; Cook, J. M.; Savic, M. M. *Brain Res. Bull.* **2013**, *91*, 1.
- (31) Allen, M. S.; Hagen, T. J.; Trudell, M. L.; Coddling, P. W.; Skolnick, P.; Cook, J. M. *J. Med. Chem.* **1988**, *31*, 1854.
- (32) Hagen, T. J.; Guzman, F.; Schultz, C.; Cook, J. M.; Skolnick, P.; Shannon, H. E. *Heterocycles* **1986**, *24*, 2845.
- (33) Yin, W.; Majumder, S.; Clayton, T.; Petrou, S.; VanLinn, M. L.; Namjoshi, O. A.; Ma, C.; Cromer, B. A.; Roth, B. L.; Platt, D. M.; Cook, J. M. *Biorg. Med. Chem.* **2010**, *18*, 7548.
- (34) Yin, W.; Sarma, P. V. V. S.; Ma, J.; Han, D.; Chen, J. L.; Cook, J. M. *Tetrahedron Lett.* **2005**, *46*, 6363.
- (35) Namjoshi, O. A.; Gryboski, A.; Fonseca, G. O.; Van Linn, M. L.; Wang, Z.-j.; Deschamps, J. R.; Cook, J. M. *J. Org. Chem.* **2011**, *76*, 4721.
- (36) Allen, M. S.; LaLoggia, A. J.; Dorn, L. J.; Martin, M. J.; Costantino, G.; Hagen, T. J.; Koehler, K. F.; Skolnick, P.; Cook, J. M. *J. Med. Chem.* **1992**, *35*, 4001.
- (37) Allen, M. S.; Tan, Y. C.; Trudell, M. L.; Narayanan, K.; Schindler, L. R.; Martin, M. J.; Schultz, C.; Hagen, T. J.; Koehler, K. F.; Coddling, P. W.; Skolnick, P.; Cook, J. M. *J. Med. Chem.* **1990**, *33*, 2343.

- (38) Cook, J. M.; Van Linn, M. L.; Yin, W.; U.S. Patent No. 8268854, September 18: 2012.
- (39) Bailey, J. M.; Bruton, G.; Huxley, A.; Milner, P. H.; Orlek, B. S.; PCT Int. Patent. 2005014571, February 17: 2005.
- (40) Jansen, J.-R.; Fuesslein, M.; Hallenbach, W.; Ort, O.; Arnold, C.; Franken, E.-M.; Malsam, O.; Reckmann, U.; Sanwald, E.; Goergens, U.; PCT Int. Patent 2009068194, June 4: 2009.
- (41) Godoi, M.; Botteselle, G. V.; Rafique, J.; Rocha, M. S. T.; Pena, J. M.; Braga, A. L. *Asian J. Org. Chem.* **2013**, *2*, 746.
- (42) Heffron, T.; Safina, B.; Staben, S.; Sutherlin, D. P.; Wei, B.; Elliott, R.; Heald, R.; Seward, E. M.; Gancia, E.; Waskowycz, B.; U.S. Patent No. 20120245144, September 27, 2012.
- (43) Birkholz, M.-N.; Freixa, Z.; van Leeuwen, P. W. N. M. *Chem. Soc. Rev.* **2009**, *38*, 1099.
- (44) Loones, K. T. J.; Maes, B. U. W.; Rombouts, G.; Hostyn, S.; Diels, G. *Tetrahedron* **2005**, *61*, 10338.
- (45) Hostyn, S.; Maes, B. U. W.; Van Baelen, G.; Gulevskaya, A.; Meyers, C.; Smits, K. *Tetrahedron* **2006**, *62*, 4676.
- (46) Kappe, C. O. *Angew. Chem. Int. Ed.* **2004**, *43*, 6250.
- (47) Bruno, N. C.; Buchwald, S. L. *Org. Lett.* **2013**, *15*, 2876.
- (48) Fors, B. P.; Davis, N. R.; Buchwald, S. L. *J. Am. Chem. Soc.* **2009**, *131*, 5766.
- (49) Fors, B. P.; Watson, D. A.; Biscoe, M. R.; Buchwald, S. L. *J. Am. Chem. Soc.* **2008**, *130*, 13552.
- (50) Wolfe, J. P.; Buchwald, S. L. *J. Org. Chem.* **1997**, *62*, 6066.
- (51) Maes, B. U. W.; Loones, K. T. J.; Jonckers, T. H. M.; Lemière, G. L. F.; Dommissie, R. A.; Haemers, A. *Synlett* **2002**, *2002*, 1995.
- (52) Meyers, C.; Maes, B. U. W.; Loones, K. T. J.; Bal, G.; Lemière, G. L. F.; Dommissie, R. A. *J. Org. Chem.* **2004**, *69*, 6010.
- (53) Sunesson, Y.; Limé, E.; Nilsson Lill, S. O.; Meadows, R. E.; Norrby, P.-O. *J. Org. Chem.* **2014**, *79*, 11961.

CHAPTER 2

BIOLOGICAL EVALUATION OF ANALOGS OF β -CARBOLINE FOR POTENTIAL TREATMENT OF ALCOHOL ABUSE

2.1. INTRODUCTION

The β -carboline¹ analogs which were synthesized were evaluated to determine the biological activity in regard to the reduction of alcohol self-administration as a preclinical analysis for the treatment of human alcoholics. To determine the importance of the application of these GABA_A (Gamma amino butyric acid) receptor ligands to treat disease states *in-vivo*, *in-vitro* studies were carried out. The efficacy at various GABA_A receptor subtypes was determined using oocytes² and HEK (Human Embryonic Kidney) 293T cells³ for the determination of GABAergic subtype selective efficacy. Many β -carboline are known to possess anti-alcohol properties and reduce alcohol self-administration in rodent models. This data is required to show the ligands are not toxic and paves the way to test these in these higher primate animal models such as baboons and rhesus monkeys.^{1,4-7} In order to determine the metabolic stability of these new ligands and safety they were assayed on human liver and mouse liver microsomes⁸ (Revathi Kodali), sensorimotor coordination on the rotarod,⁹ and righting reflex (Nicholas Zahn) as well as cell viability studies (cytotoxicity) by Dr. Stephen.¹⁰ The importance of the biological effects of these β -carboline and their profound actions in *in-vitro* and *in-vivo* are described below.

2.2. BIOLOGICAL STUDIES

The numbering for the β -carboline analogs are as follows 3-PBC (**1**), 3-ISOPBC (**2**), 3-cycloPBC (**20**), 3-PBC·HCl (**1·HCl**), 3-ISOPBC·HCl (**2·HCl**), and 3-cycloPBC·HCl (**20·HCl**)

and in some case the HCl was omitted for clarity. They were all administered *in-vivo* as HCl salts for they had a much longer shelf life.

2.2.1. Determination of Efficacy Studies in HEK (Human Embryonic Kidney) 293 Cells

Historically the β -carbolines and their analogs are known to be modulators of GABA_A receptor subtypes.¹¹ To determine the subtype specific efficacy of these compounds, electrophysiological recordings were performed on HEK 293T cells by expressing different α subunit subtype GABA_A receptors.¹² This was carried out by Dr. Janet Fischer (Medical College of South Carolina). The **1•HCl**, **2•HCl**, and **20•HCl** compounds were applied to the HEK 293T subtype selective GABA_A receptors at 0.1 μ M, 1 μ M, and 10 μ M concentrations to determine the effect of sensitivity to modulation in HEK 293T cells with co-application of GABA. The concentration of GABA represented an EC < 5 μ M for each isoform¹² and actually was 0.1 μ M (α 6), 0.3 μ M (α 4, α 5), 1 μ M (α 1, α 2) or 3 μ M (α 3).

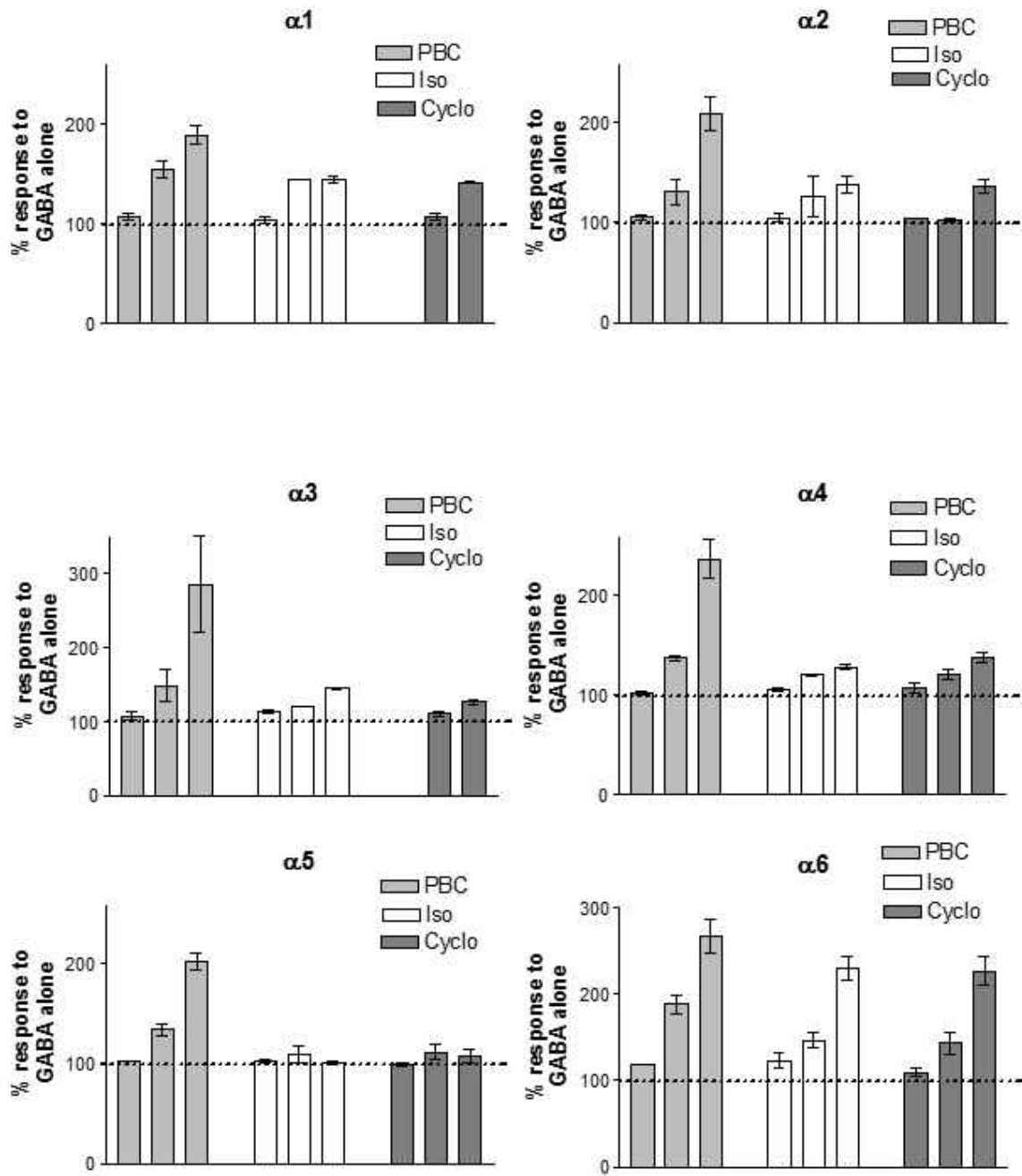


Figure 2-1. The average enhancement of the current evoked due to GABA alone and GABA with positive allosteric modulators 3-PBC·HCl (1·HCl), 3-ISOPBC·HCl (2·HCl) and 3-cycloPBC·HCl (20·HCl) on $\alpha 1$ -, $\alpha 2$ -, $\alpha 3$ -, $\alpha 4$ -, $\alpha 5$ -, and $\alpha 6$ - subtype GABA_A receptors was illustrated. The concentrations tested were 0.1 μ M, 1 μ M, and 10 μ M, respectively, for each compound (except 1 μ M for 3-cycloPBC (20·HCl) for $\alpha 1$ and $\alpha 3$). The peak current amplitude was divided by the response to GABA alone for each cell. The dashed line at 100% indicates the response to GABA alone. Bars represent mean \pm SEM (n = 4–8). EC < 5 μ M of GABA [0.1 μ M ($\alpha 6$), 0.3 μ M ($\alpha 4$, $\alpha 5$), 1 μ M ($\alpha 1$, $\alpha 2$) or 3 μ M ($\alpha 3$)]

The HEK 293T cells were transiently transfected with one of six different α subunit subtypes ($\alpha 1$ to $\alpha 6$) as well as the same β ($\beta 3$) and γ ($\gamma 2L$) subunits. The HEK 293T cells were patch clamped at -50 mV with the application of GABA alone [EC < 5 μ M, 0.1 μ M ($\alpha 6$), 0.3 μ M ($\alpha 4$, $\alpha 5$), 1 μ M ($\alpha 1$, $\alpha 2$) or 3 μ M ($\alpha 3$)] or GABA plus modulator for 5 sec to assess the whole cell recording. The amount of GABA applied to determine sensitivity to modulation was less than the submaximal concentration of 0.1 μ M to $\alpha 6$, 0.3 μ M to $\alpha 4$ and $\alpha 5$, 1 μ M to $\alpha 1$ and $\alpha 2$, and 3 μ M to $\alpha 3$ subtypes. The modulation of the GABA alone on different subtypes was considered as 100 % indicated by the horizontal dashed line in Figure 2-1. The effects of all three modulators on $\alpha 1$ to $\alpha 6$ subtypes at all concentrations tested are represented in Figure 2-1. The **1·HCl** ligand had shown an enhanced positive modulation on all α subtypes compared to GABA alone, and this was observed at higher concentrations of 10 μ M of ligand in relation to 0.1 μ M and 1 μ M. However, even at 1 μ M this is a much higher concentration than a pharmacologically relevant dose (0.10 – 0.25 μ M). For all practical purposes the efficacy of **1·HCl** was zero except at the $\alpha 6$ subtype in this assay. The **1·HCl** had a significant potentiation compared to GABA alone, but it was less than the potentiation at 10 μ M, as expected. The **1·HCl** also exhibited higher similar potentiation with $\alpha 3$ and $\alpha 6$ subtypes at higher concentrations. In contrast, the **2·HCl** and **20·HCl** had significant potentiation at $\alpha 6\beta 3\gamma 2$ subunit, and these compounds have less prominent modulation on $\alpha 1$ to $\alpha 5$ subtypes at all concentrations studied. All three compounds tested have a positive modulatory potentiation on the $\alpha 6$ subtype, which signifies the high efficacy of these compounds selective to GABA_A receptors containing $\alpha 6$ subunits acting as positive allosteric modulators (PAM). However, the efficacy at $\alpha 6$ was not very potent except at 10 μ M which is a much higher concentration than every reached at a pharmacologically relevant dose. The potentiation of the **2·HCl** and **20·HCl** was less pronounced compared to **1·HCl** at concentrations of 1 μ M and 10 μ M. The combined modulatory effects with the whole cell recording currents due to the three

compounds on different subtypes at 10 μM concentration are represented in Figure 2-2. The efficacy pattern for all three ligands was the same except at 10 μM which clearly indicated **1·HCl** was more potent. The major difference was only significant at the highest concentration of ligand. The ligands 3-ISOPBC·HCl, and 3-cycloPBC·HCl are clearly less potent in this assay than 3-PBC·HCl (see below).

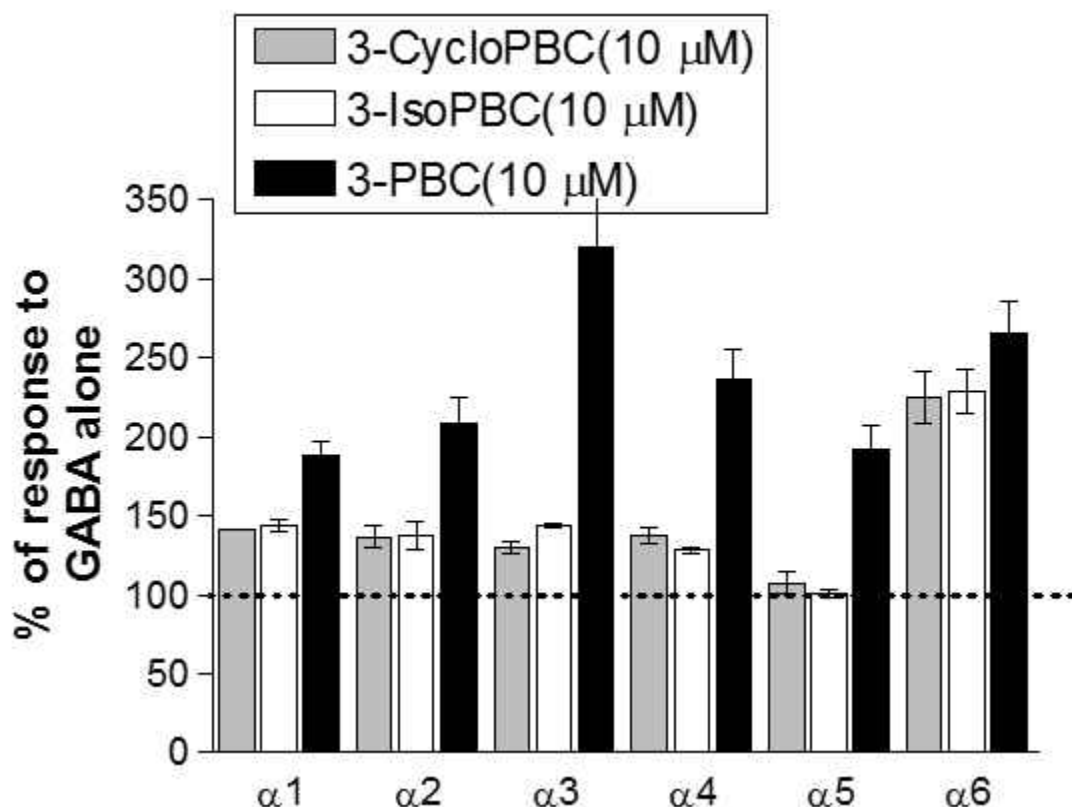


Figure 2-2. The average enhancement of the current evoked by GABA alone and GABA with positive allosteric modulators 3-PBC·HCl (1·HCl), 3-ISOPBC·HCl (2·HCl) and 3-CycloPBC·HCl (20·HCl) on $\alpha 1$ -, $\alpha 2$ -, $\alpha 3$ -, $\alpha 4$ -, $\alpha 5$ -, and $\alpha 6$ - subtype receptors was indicated all in one graph at concentrations of 10 μM . The peak current amplitude was divided by the response to GABA alone for each cell. The dashed line at 100% indicates the response to GABA alone. Bars represent mean \pm SEM (n = 4–8). The 10 μM concentration far exceeds a pharmacologically relevant dose and so does 1 μM . EC < 5 μM of GABA [0.1 μM ($\alpha 6$), 0.3 μM ($\alpha 4$, $\alpha 5$), 1 μM ($\alpha 1$, $\alpha 2$) or 3 μM ($\alpha 3$)]

The GABA_A receptor ligands studied here do not have any significant positive modulation on the $\alpha 1$ through $\alpha 5$ receptor subtypes at pharmacologically relevant concentrations nor do they exert a decrease in sensitivity that would provide negative currents. The null effects of these β -

carbolines at 0.1 μ M indicate that at these particular GABA_A receptor subtypes and concentrations these ligands may act as antagonists. This may be the mechanism of the anti-alcohol effects of these analogs similar to that proposed by June et al. for β CCt and 3-PBC·HCl earlier in rats.^{13,14} The decreased consumption of alcohol in the pre-clinical models are may be due to antagonist activity of these β -carbolines at α 1⁷ and perhaps α 2⁶ GABA_A receptors in the central nervous system. The exact mechanism of action in rats and in non human primates is not fully understood at this time, but it is an important preclinical result. This is because α 1 β 3 γ 2 subtypes are found in the ventral tegmental area (especially α 1 GABA_A receptors).

Because of the slightly more positive modulation and selective efficacy of these β -carbolines at α 6 subtypes in HEK 293T cells, initially the **2·HCl** and **20·HCl** were tested in a different GABA_A receptor isoform (α 6 β 3 δ) which contains the delta (δ) subunit. Delta subunits have been implicated previously in reduction of alcohol self-administration in some rodent models, but these results are not unambiguously established. The whole cell current recordings of HEK 293T cells for **2·HCl** and difference in the potentiation between α 6 β 3 γ 2 and α 6 β 3 δ receptor subtypes for **2·HCl** and **20·HCl**, are shown in Figure 2-3. In addition to the discussion above, these α 6 β 3 δ subtype receptors are insensitive to benzodiazepines (such as diazepam) and different than most conventional modulators that require gamma subunits. The δ subunit GABA_A receptors are highly distributed in the cerebellum which mediates the effects of alcohol on motor coordination function.^{15,16} Moreover α 6 GABA_AR have been implicated in drugs involved in alcohol abuse in some reports, as mentioned.¹⁷

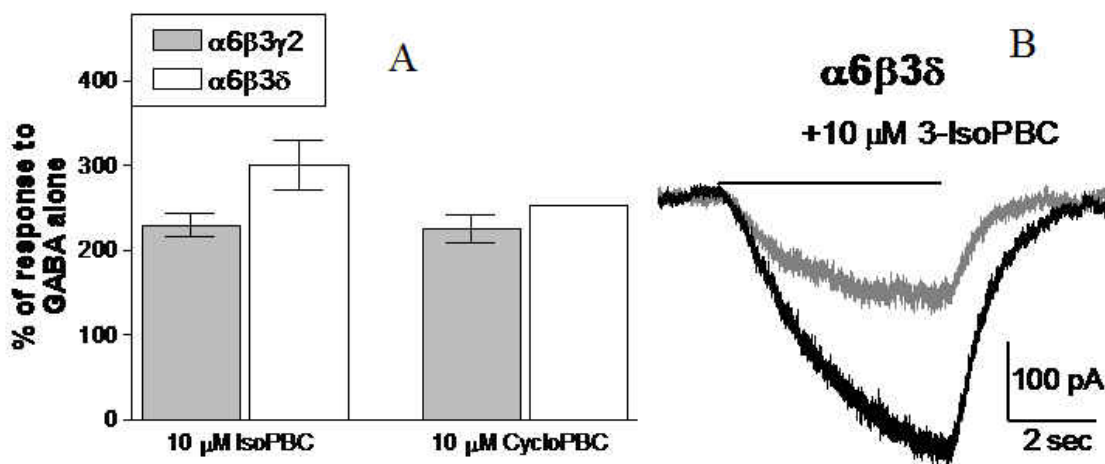


Figure 2-3. Cells were transiently transfected with the $\alpha 6$ subtype, as indicated, along with $\beta 3$ and δ , and voltage clamped at -50 mV. Representative whole-cell currents are shown for 5 sec applications of GABA alone (gray) or GABA + 0.1 μ M modulator (black). EC < 5 μ M of GABA [0.1 μ M ($\alpha 6$), 0.3 μ M ($\alpha 4$, $\alpha 5$), 1 μ M ($\alpha 1$, $\alpha 2$) or 3 μ M ($\alpha 3$)]

The whole cell currents with only GABA applied for 5 seconds are represented by the gray color, and the signal from the potentiated current with both GABA and positive modulator **2·HCl** are represented in black (Figure 2-3B). The application of **2·HCl** and **20·HCl** at 10 μ M had increased the modulatory currents at the $\alpha 6\beta 3\delta$ receptor subtype. However, the sensitivity and response were similar to the other $\alpha 6\beta 3\gamma 2$ GABA_A receptor subtypes at 0.1 μ M which indicated the efficacy towards $\alpha 6\beta 3\delta$ and $\alpha 6\beta 3\gamma 2$ receptor subtypes was about the same (Figure 2-3A). The other β -carboline analogs will be studied further if they exhibit any high potential efficacies towards the δ subtype containing GABA_A receptors for their ability to mediate alcohol self-administration. In addition to potential effects of these compounds mediated by $\alpha 1$ and $\alpha 2$ GABA_A receptors,^{5,6} these PBC isoforms (**1·HCl**, **2·HCl**, β CCt, and **20·HCl**) have shown the same efficacy towards $\alpha 6$ subtype GABA_A receptor but only at extremely high ligand concentrations. Our hypothesis (right or wrong) has been that the β -carbolines act as antagonists at $\alpha 1$ subtypes (50 % of GABA subtypes) similar to the $\alpha 1$ antagonist β CCt and stabilize the antagonist conformation of $\alpha 1$ Bz/GABA receptor thereby interfering slightly with the tonic control of the GABA system. This results in a slight decrease in chloride flux in the ventral tegmental area, which results in a

slight decrease in dopamine levels on exposure to alcohol rather than a big increase in this level. The result is less reason (dopamine) to drink but without the anhedonia and depression sometimes associated from naltrexone and other anti-alcohol agents.

2.2.2. Efficacy Studies in *Xenopus laevis* Frog Oocytes and Receptor Binding

The β -carboline analogs **2·HCl** and **1·HCl** were assayed to determine their efficacy in *Xenopus laevis* oocytes expressing specific GABA_A receptor subunits ($\alpha(1,4,5 \text{ and } 6)\beta 3\gamma 2$) as shown in Figure 2-4.² The efficacy studies included the measurement of chloride currents using a two-electrode voltage patch clamp at GABA 3% effective concentration (EC₃).

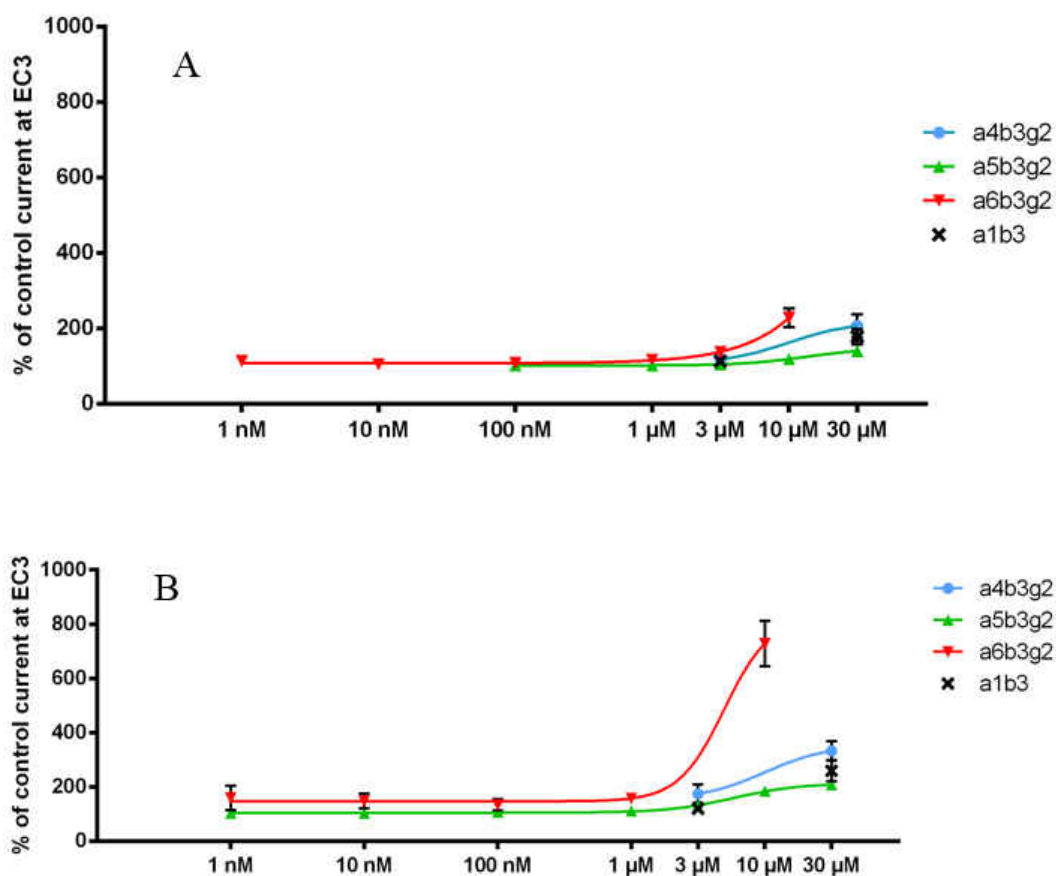


Figure 2-4. A, Augmentation of GABA-induced currents in oocytes expressing GABA_A receptors of specified subunit composition by 3-ISOPBC·HCl (**2·HCl**). B, Augmentation of GABA-induced currents in oocytes expressing GABA_A receptors of specified subunit composition by 3-PBC·HCl (**1·HCl**).

From the electrophysiological experiments conducted with oocytes expressing heterologous GABA_A receptor systems at varying concentration of 1 nM to 30 μM, it was observed that the **1·HCl** and **2·HCl** had shown some functional agonist efficacy at α6 GABA_A receptor subunits. However, the concentrations of the ligands had to be so high (> 3 μM) to see an agonist response, these data really have no pharmacological relevance (100 nM-200 nM; M.Savic, W.Sieghart, private communication). The activity of **2·HCl** at the α6 subunit was in the agonist direction at 10 μM but was much less than the classic 3-PBC·HCl (**1·HCl**) at the same concentration (10 μM) which confirms neither of these are potent agonists at α6β3γ2 subtypes. The importance of the data in this assay demonstrates the two ligands **1·HCl** and **2·HCl** do not exhibit potent agonist potentiation at the α1 subunit in agreement with the previous hypothesis. In earlier studies the anti-alcohol properties of β-carbolines were felt due to the antagonist properties of βCCt and mixed antagonist-agonist properties of **2·HCl**. In agreement with this these two compounds **1·HCl** and **2·HCl** exhibited none of the side effects of diazepam even at concentrations of 30 μM. As indicated in Figure 2-4, there was little or no efficacy of **2·HCl** nor **1·HCl** at α4 or any other subtype studied. In this regard **2·HCl** did resemble known the anti-alcohol agent **1·HCl** at pharmacologically relevant concentrations.

Table 2-1. The binding affinity of 3-ISOPBC (2·HCl) at αxβ3γ2 GABA_A receptor subtypes using [3H]-flumazenil displacement studies.

compound	K _i ± SEM (nM)			
	α1	α2	α3	α5
3-ISOPBC·HCl (2·HCl)	330 ± 160	2300 ± 150	1300 ± 110	10000 ± 1100

The *in-vitro* binding of 3-ISOPBC·HCl (**2·HCl**) was carried out on α(1,2,3 and 5)β3γ2 GABA_A receptor subunits¹⁸ and K_i values were determined, as shown in Table 2-1, by Dr. Petra Scholze. The **2·HCl** analog did bind to the α1 subunits with a moderate K_i value of 330 ± 160 nM which was more potent in relation to the concentration required to displace flumazenil at the other

receptor subunits. This did indicate a moderate binding affinity for **2·HCl** at $\alpha 1\beta 3\gamma 2$ GABA_A receptors as opposed to little or no affinity at the other subtypes. The lead 3-PBC·HCl (**1·HCl**) also bound more potently at $\alpha 1\beta 3\gamma 2$ GABA_A and did reduce alcohol self-administration in primates.^{7,19}

2.2.3. Effect of 3-Isopropoxy- β -carboline Hydrochloride (2·HCl) on Alcohol Seeking and Self-administration in Baboons⁷

Because Dr. Majorie Gondre-Lewis had shown **2·HCl** decreased alcohol self-administration in maternally deprived rats⁶, moreover, there were no overt adverse behavioral effects, this ligand was cleared for study in primates. Because the pharmacological effect of GABA_A receptor ligands depends mainly on the selectivity of compounds to a specific subunit, this controls various behavioral effects to drugs including alcohol.²⁰ The $\alpha 1$ subunit of benzodiazepine GABA_A, which has been shown earlier^{13,21} to be involved in the reinforcing and abuse related effects of alcohol,^{6,11,22} is the most widely expressed subunit in the brain. The mechanism of $\alpha 1$ receptor involvement with alcohol responding was tested in $\alpha 1$ GABA_A knock out mice and indicated a decreased response to alcohol over water. In a self-administration study with these mice, the alcohol intake was reduced but was also associated with the low intake of saccharin and sucrose drinking.^{23,24} The systemic or microinfusions of **1·HCl** (3-propoxy- β -carboline hydrochloride) and β CCt (β -carboline-3-carboxylate-*tert*-butyl ester) into the ventral pallidum region of high alcohol drinking (HAD) rats significantly decreased alcohol intake.^{13,21} In another study with primate models, 3-PBC·HCl (**1·HCl**) was given by chronic administration to baboons and demonstrated multiple effects; 3-PBC·HCl decreased the alcohol self-administration responding, decreased the volume of alcohol consumption, (g/kg alcohol intake), and had positive effects on the control non-alcohol (sucrose) reinforcement.²⁵

Because of the confirmation of the $\alpha 1$ antagonistic activity for **2·HCl** and β CCt in primates,²⁶ and in rhesus macaques,²⁷ these *in-vitro and in-vivo* studies,^{13,14} as well as data described above, prompted the synthesis of the new analog, the 3-isopropoxy- β -carboline Hydrochloride (**2·HCl**).¹ There were several advantages observed with the **2·HCl**; it exhibited seven fold selectivity for $\alpha 1\beta 3\gamma 2$ subtypes compared to $\alpha 2$ and $\alpha 3$ subtypes and thirty fold higher selectivity over the $\alpha 5$ GABA_A subunit. Studies of this **2·HCl** on the rotarod did not show signs of ataxia, sedation, or loss of righting reflex. Moreover, it was hoped that the branched isopropyl group would slow down the metabolism by retarding beta (omega-1) oxidation and increase the duration of action of **2·HCl** in the *in-vivo* conditions. The effect of **2·HCl** in both chronic and acute administration was assayed in baboons to address alcohol seeking behavior and self-administration. When the **2·HCl** was given in both chronic and acute studies intramuscularly to determine alcohol consumption and pattern of drinking, it was given at a dose of 5 -20 mg/kg. The drinking sessions were conducted with a continuous scheduled reinforcement procedure,⁷ and stable drinking was observed during the baseline sessions. This is a typical protocol for drug effect studies on alcohol self-administration in baboons by Dr. Elise Weerts.⁷

2.2.3.1. Effects of Acute Administration of 3-ISOPBC·HCl (2·HCl)

The acute administration of **2·HCl** under a chain schedule of reinforcement did not show any significant variation in the self-administration response and consumption pattern of alcohol (g/kg alcohol consumed; base line (1.1 g/kg), vehicle (1.2 g/kg), 10mg/Kg 3-ISOPBC·HCl (1.1 g/kg), 20 mg/kg 3-ISOPBC·HCl (1.0 g/kg), and 30 mg/kg 3-ISOPBC·HCl (1.0 g/kg) at any dose of drug from 10 mg/kg to 30 mg/kg. However, there were no abnormal behavioral patterns observed at the higher dose of 30 mg/kg which indicated the drug was safe with no side effects of sedation, motor in-coordination, gastrointestinal symptoms, or muscle relaxation at the high dose. The lack of significant effect on acute administration and solubility problems encountered at 30

mg/kg together with the necessity of large amounts of **2·HCl** prompted continued studies with chronic administration.

2.2.3.2 Effects of Chronic Administration of 3-ISOPBC·HCl (2·HCl)

The effect of chronic administration of 3-ISOPBC·HCl (**2·HCl**) for five days on the self-administration response and g/kg alcohol consumption was determined and presented in Figure 2-5. There was a significant **decrease** in the alcohol consumption observed at 10 mg/kg as compared to vehicle (50 % saline, 37.5 % propylene glycol, and 12.5% ethanol). The chronic administration led to a **reduction** in the g/kg of alcohol at 5 mg/kg, 10 mg/kg and 20 mg/kg dose of **2·HCl** relative to control groups. The different doses of **2·HCl** did not decrease the responding for the non-alcohol beverage (orange flavored, sugar free, Tang® powder (Kraft food) dissolved in reverse osmosis purified drinking water) in the control groups.

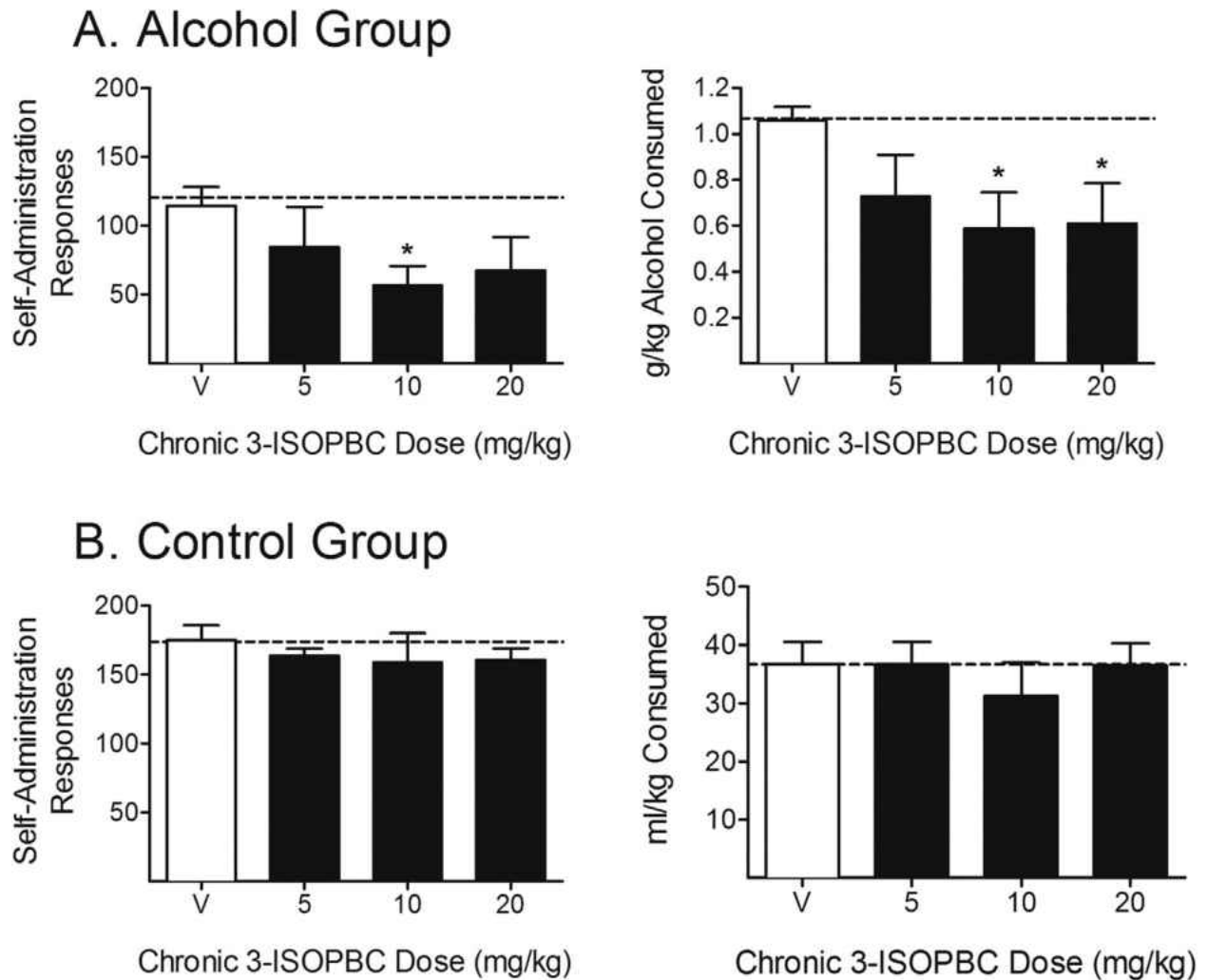
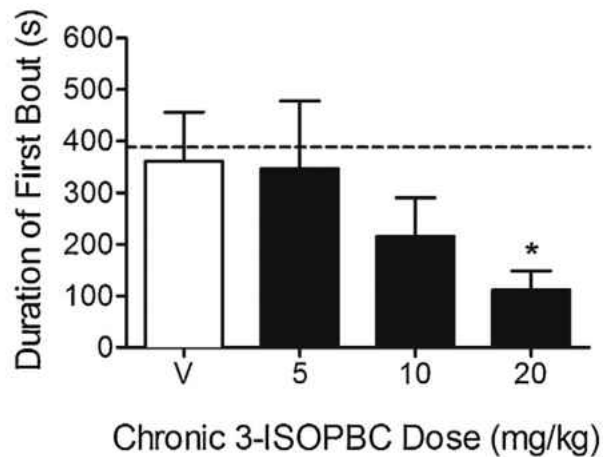
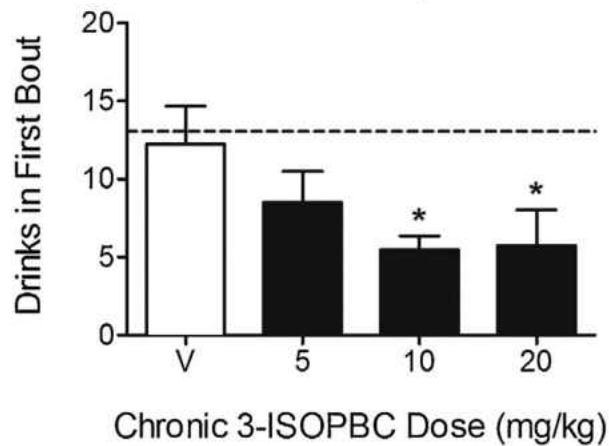


Figure 2-5. Effects of chronic (5 days) administration of 3-ISOPBC·HCl (2·HCl) (5.0–20.0 mg/kg) on consumption in Component 3 of the chained schedule of reinforcement in the (A) Alcohol Group and (B) Control Group. Data shown are the group means (+ SEM) of self-administration responses (left panels), and g/kg alcohol consumed for the alcohol group and ml/kg consumed for the control group (right panel). Baseline responding is indicated by the horizontal, dashed lines. *indicates $p < 0.05$ for pair-wise comparison for each 3-ISOPBC (2·HCl) dose vs. vehicle.

The effect of 2·HCl on the pattern of drinking with the number of drinks in the first bout and duration of the first bout is illustrated in Figure 2-6. In the alcohol group, the 2·HCl at 10 mg/kg and 20 mg/kg decreased the number of drinks in the first bout prominently compared to the 5 mg/kg dose. However, the reduction was seen at all doses. Similarly, there was a reduction in the duration of the first drinking bout and was significant at a dose of 20 mg/kg with chronic administration. In the control group, the 2·HCl did not have any effects on a number of drinks or duration of drinking at any dosage.

A. Alcohol Group



B. Control Group

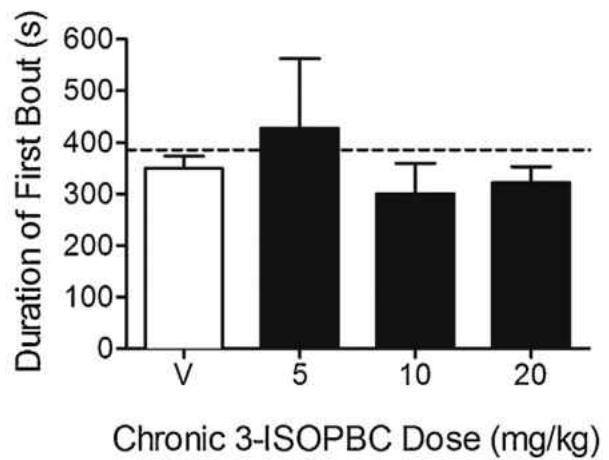
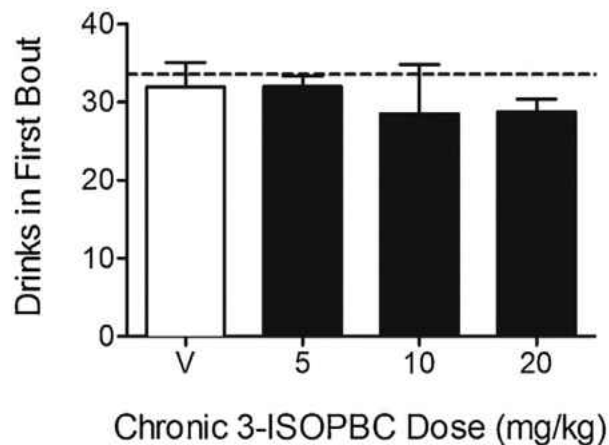


Figure 2-6. Effects of chronic (5 days) administration of 3-ISOPBC·HCl (5.0–20.0 mg/kg) on the pattern of drinking in the first drinking bout in Component 3 of the chained schedule of reinforcement in the (A) Alcohol Group and (B) Control Group. Data shown are the group means (+ SEM) of the number of drinks in the first drinking bout (left panels), and the duration (seconds) of the first drinking bout (right panels). Baseline responding is indicated by the horizontal, dashed lines. *indicates $p < 0.05$ for pair-wise comparison for each 3-ISOPBC·HCl dose vs. vehicle.

The present study focused on the evaluation of the effects **2·HCl** on alcohol seeking behavior in baboons with acute and chronic drug administration in regard to a potential safe treatment for human alcoholics. The **pretreatment** with **2·HCl** did not have any effect on alcohol seeking in the self-administration alcohol groups or self-administration non-alcohol beverage control groups, which was the similar to the case with 3-PBC·HCl (**1·HCl**) under the chain

scheduled reinforcement.²⁵ In contrast, the **2·HCl** given under chronic conditions was highly effective and reduced the alcohol intake in the alcohol group without affecting the consumption of the non-alcohol drinking in the control groups, which demonstrates in these studies in baboons, the effects of **2·HCl** are specific to alcohol drinking. In addition, as discussed elsewhere **2·HCl** had no effects on other receptors in the NIMH-supported 47 panel PDSP screen by Bryan Roth (University of North Carolina; TI-02-IsoPBC·HCl). Moreover, it was more potent than earlier work with 3-PBC·HCl (**2·HCl**) in baboons by Kaminski, Weerts et al.²⁵

2.2.4. Potential Role of the $\alpha 1$ Bz/GABA_A Subunit-Containing Receptor in a Rhesus Monkey Model of Alcohol Drinking and Effect of β CCt and 3-PBC·HCl⁴

Alcohol abuse and dependence are common problems today, and there is a need for proper pharmacotherapy to fight these in the society as described above. There is evidence that GABA_A receptors play a major role in the behavioral effects of alcohol and abuse.^{28,29} Apart from the five different subunit subtypes (see above), $\alpha\beta\gamma 2$ Bz/GABAergic subunits are involved in the behavioral effects due to alcohol abuse and drug dependence.²⁸ In this study, the role of α subunits was evaluated with the $\alpha 1$ preferring ligands and non-selective typical benzodiazepines to determine the effect on alcohol self-administration and behavioral patterns in rhesus monkey models.⁴ The amount of alcohol intake was measured by the blood alcohol levels (BALs), and various behavioral observations with definitions and are summarized in Table 2-2. It must be pointed out at the outset that the work by Weerts et al. was in baboons, while that of Platt et al. was in rhesus monkeys. The strains of animals are different in the two studies, moreover, the paradigms are different.

Table 2-2: Behavioral Categories, Abbreviations, and Definitions^a

Species-typical	
Passive visual (VIS)	Animal is standing or sitting motionless with eyes open
Rest/sleep posture (RSP)	Idiosyncratic posture adopted by monkeys during rest or sleep; eyes closed, easily roused by external stimulation (e.g., tapping on cage)
Locomotion (LOC)	At least 2 directed steps in the horizontal and/or vertical plane
Tactile/oral exploration (TAC)	Any tactile or oral manipulation of the cage or environment
Forage (FOR)	Sweeping and/or picking through wood chip substrate
Self-groom (GRM)	Picking, scraping, spreading, or licking of an animal's own hair
Scratch (SCR)	Vigorous strokes of the hair with the finger or toenails
Vocalization (VOC)	Species-typical sounds emitted by monkey (not differentiated into different types)
Yawn (YWN)	To open mouth wide and expose teeth
Present (PRE)	Posture involving presentation of rump, belly, flank, and/or neck to observer or other monkey
Threat/aggress (THR)	Multifaceted display involving 1 or more of the following: open mouth stare with teeth partially exposed, eyebrows lifted, ears flattened or flapping, rigid body posture, piloerection, attack (e.g., biting, slapping) of inanimate object or other monkey
Fear grimace (FGR)	Grin-like facial expression involving the retraction of the lips exposing clenched teeth; may be accompanied by flattened ears, stiff, huddled body posture, screech/chattering vocalizations
Body spasm (BSP)	An involuntary twitch or shudder of the entire body; also "wet dog" shake
Lip smack (LIP)	Pursing the lips and moving them together to produce a smacking sound; often accompanied by moaning
Cage shake (CSH)	Any vigorous shaking of the cage that may or may not make noise
Stereotypy (STY)	Any repetitive, ritualized pattern of behavior that serves no obvious function
Other (OTH)	Any notable behavior not indicated above (e.g., masturbation, nose rub, lip droop, vomit/retch)
Procedure-related	
Lever press (LVR)	Depression of lever manipulanda on the drinking panel
Drink (DRI)	Mouth contact to fluid delivery sippers
Drug-induced	
Ataxia (ATX)	Any slip, trip, fall, or loss of balance
Procumbent posture (PRO)	Loose-limbed posture (sitting or lying on cage bottom) accompanied by eye closure; not easily aroused by external stimulation (e.g., tapping on cage)

^aAdapted from Ruedi-Bettschen and colleagues,³⁰ Weerts and colleagues,³¹ and Platt and colleagues.^{27,32}

2.2.4.1. Drinking Behavior

The animals were properly trained as previously reported^{27,30-32} and the data was collected over a span of 3-4 years for the baseline drinking conditions of alcohol. The average drinking of alcohol and sucrose by different rhesus monkeys was the same except two individuals and are presented in Table 2-3.^{27,32} Apart from these, there was no significant difference in the volume of alcohol and sucrose consumption by different groups during baseline conditions that were later used to study with different analogs as shown in Table 2-3. The BALs in animals with vehicle administration was above 80 mg/dL, which is the legal driving limit in humans (zolpidem veh: 82.8 ± 9.4 mg/dL; βCCT veh: 93.6 ± 6.1 mg/dL; 3-PBC veh: 99 ± 20.4 mg/dL; triazolam veh: 88.1 ± 13.6 mg/dL; flumazenil 87.6 ± 9.3 mg/ dL; βCCE veh: 97.8 ± 8.3 mg/dL).

Table 2-3. Average Baseline Intake for Each Monkey Across the Duration of the Study.

Monkey	Group	Average intake (ml)	Average intake (g/kg)	p-Value [†]
MM-98	Alcohol	730.1 (24.9)	1.3 (0.05)	0.120
MM-71	Alcohol	629.4 (43.2)	1.2 (0.09)	0.009*
MM-267	Alcohol	902.8 (44.2)	1.5 (0.09)	0.138
MM-247	Alcohol	606.0 (30.1)	1.6 (0.08)	0.059
MM-162	Alcohol	652.6 (20.9)	1.3 (0.04)	0.314
MM-33	Alcohol	821.5 (35.5)	1.5 (0.06)	0.495
MM-488	Sucrose	512.3 (29.8)	N/A	0.559
MM-201	Sucrose	720.4 (46.9)	N/A	0.101
MM-106	Sucrose	1,612 (177.6)	N/A	0.001**
MM-167	Sucrose	684.3 (56.3)	N/A	0.061
MM-354	Sucrose	554.7 (64.9)	N/A	0.393
Alcohol group total		723.74 (48.1)		
Sucrose group total		816.9 (202.7)		0.637

Values are presented as mean (standard error). N/A, not applicable; †p-value reflects results of 1-way ANOVAs for individual animals and results of *t*-test for the group value. *Post hoc tests indicate significant differences between 3-PBC and triazolam baseline intake. **Post hoc tests indicate significant differences in flumazenil versus β CCCT, 3-PBC, and triazolam baseline intakes.

2.2.4.2 Effect of $\alpha 1\beta 3\gamma 2$ Bz/GABA(A)ergic Preferring Compounds on Alcohol Drinking

The amount of alcohol intake was analyzed by employment of three $\alpha 1$ preferring ligands [zolpidem, β CCt, and 3-PBC·HCl (**1·HCl**)]. The treatments were with the $\alpha 1$ preferring agonist zolpidem (0.1 to 10.0 mg/kg), $\alpha 1$ -preferring antagonist β CCCT (0.3 to 3.0 mg/kg) and the antagonist 3-PBC·HCl (**1·HCl**, 0.03 to 10 mg/kg). The three $\alpha 1$ modulators did not cause any significant decrease in alcohol intake or amount of BALs or number of sipper extensions, as illustrated in Figure 2-7 with the top closed symbols.

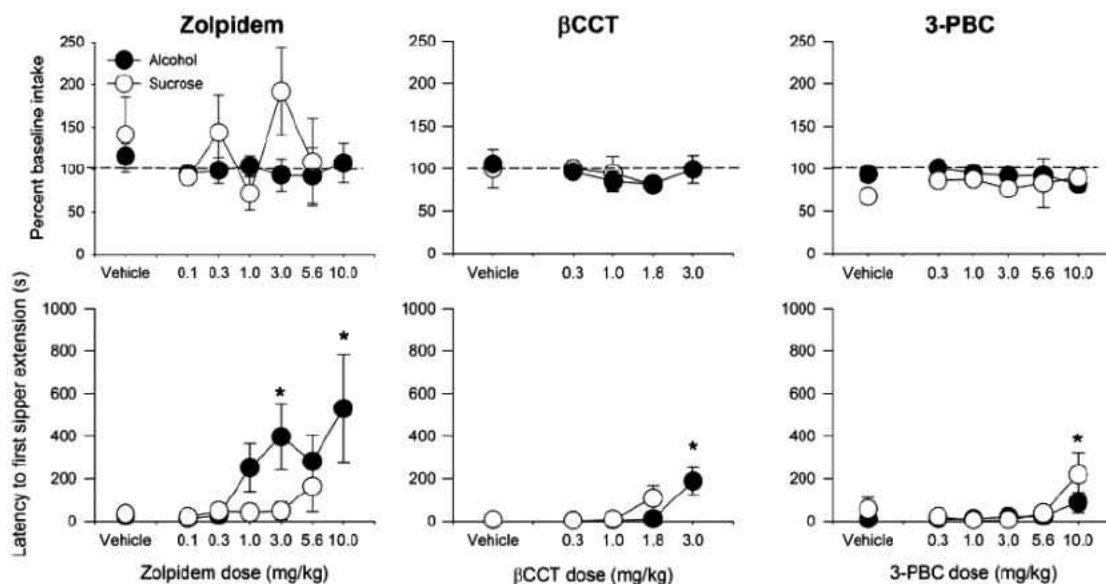


Figure 2-7. The effects of varying doses of $\alpha 1$ GABA_A preferring compounds on intake (top) and latency to first sipper extension (bottom) for alcohol (closed symbols) and sucrose (open symbols). None of the $\alpha 1$ GABA_A preferring compounds significantly affected intake of either alcohol or sucrose. *Indicates $p < 0.05$ compared with respective vehicle baseline.^{27,32}

The increase in latency of first sipper extension was observed with zolpidem in 4/5 monkeys at a dosage of 3 mg/kg and in 3/3 monkeys at 10 mg/kg. The dose of β CCT increased the latency at 3.0 mg/kg in 6/6 monkeys, and **1·HCl** at 10 mg/kg in 6/6 monkeys, as presented in Table 2-4. The compounds did not have any effect on the sucrose drinking (controls) in monkey models, as shown in Figure 2-7 with the open symbols. The lack of $\alpha 1$ antagonistic effects of β CCT and **1·HCl** on the sucrose drinking pattern of monkeys indicate that these compounds are highly selective in increasing the latency specifically for alcohol intake, and the ligands do not have any adverse behavioral effects.

Table 2-4. The Effects of Benzodiazepine Receptor Ligands on Alcohol and Sucrose Drinking Parameters

	α 1-Preferring compounds			Nonselective compounds		
	Zolpidem	3-PBC	β CCT	Triazolam	Flumazenil	β CCE
Alcohol						
Intake	=	=	=	↑(0.003)	=	↓(0.3)
Extensions	=	=	=	=	↑(3.0)	↓(0.18) ^a
Latency	↑(3.0, 10.0)	↑(10.0)	↑(3.0)	↑(0.056)	=	= ^a
Blood alcohol level	=	=	=	↓(0.056)	↓(1.0, 3.0)	= ^a
Sucrose						
Intake	=	=	=	↑(0.1)	=	=
Extensions	=	=	=	=	=	=
Latency	=	=	=	↑(0.56)	=	↑(0.3)

β CCE, β -carboline 3-carboxylate ethyl ester; β CCT, β -carboline-3-carboxylate-*tert*-butyl ester; 3-PBC, 3-propoxy- β -carboline hydrochloride. The direction of significant effects is indicated by ↓ (decrease), and ↑ (increase), or = (no change). Doses at which significant effects occur are indicated in parenthesis and reported in milligram per kilogram. ^aNo blood draws extension or latency recorded for 0.3 mg/kg due to the presence of seizures.

2.2.4.3. Effect of Nonselective Benzodiazepines Ligands on Alcohol Drinking

The rhesus monkeys were also treated with a nonselective typical benzodiazepine to determine that effect on the alcohol and sucrose drinking behavior and are presented in Table 2-4. The nonselective benzodiazepine agonist triazolam given at 0.001 to 10.0 mg/kg, lead to an increase in the alcohol intake (Figure 2-8 top, closed symbols), but increased the latency to first sipper extension (Figure 2-8, bottom) and decreased BAL (Blood Alcohol Level) in the end session of alcohol intake at a higher dose of 0.056 mg/kg. The BAL in the end session with triazolam was 27.3 ± 12.4 mg/dl, whereas in the case of vehicle administration the BAL was 88.1 ± 13.6 mg/dl. The triazolam had an increased effect on sucrose intake and increased latency to the first sipper at higher doses than it produced in the same effect on the alcohol intake, shown in Figure 2-8 top, open symbols. The increased sucrose consumption was observed at 0.1 mg/kg, and increased latency to first sipper extension was noted at 0.56 mg/kg. There was no effect of the nonselective benzodiazepine agonist triazolam on the number of sipper extensions either in the case of alcohol or sucrose.

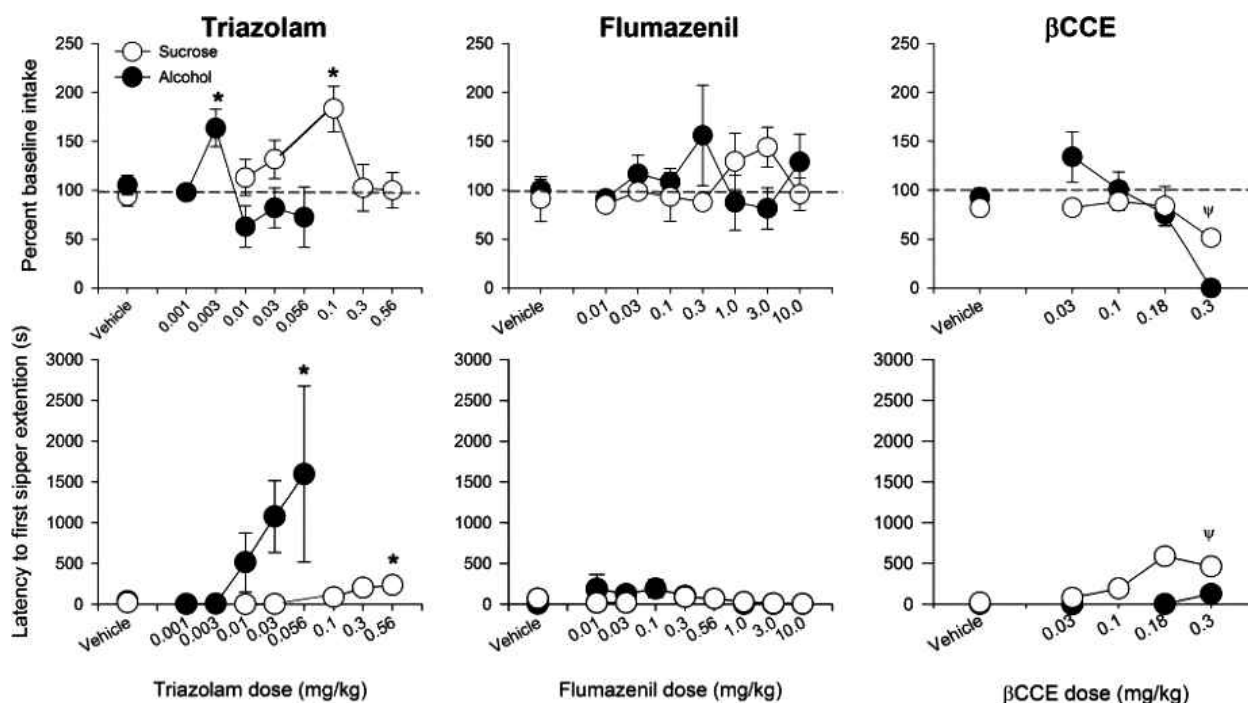


Figure 2-8. The effects of varying doses of nonselective benzodiazepine receptor ligands on intake (top) and latency to first sipper extension (bottom) for alcohol (closed symbols) and sucrose (open symbols). None of the nonselective benzodiazepine compounds significantly affected intake for either alcohol or sucrose. *Indicates $p < 0.05$ compared with respective vehicle baseline. Ψ Indicates data for 0.3 mg/kg, β CCE was not included in statistical analyses due to the presence of seizures in 1 animal at this dose. β CCE, β -carboline 3-carboxylate ethyl ester.

The treatment with nonselective benzodiazepine antagonist flumazenil daily at a dose of 0.1 to 10 mg/kg did not have any profound effect on alcohol intake or the first sipper extension. In addition to the lack of effect, flumazenil further enhanced the number of extensions (Figure 2-8, center) and decreased overall BALs. Flumazenil did not have any effect on the sucrose drinking at any administered dose. The inverse agonist β CCE was given to monkeys at 0.03 to 0.18 mg/kg; it decreased the number of sipper extensions at the highest dose without affecting any other alcohol drinking measurements, as shown in Table 2-4. The other effect observed with the β CCE was increased latency to first sipper extension for sucrose drinking but lacked other drinking effects with sucrose at any dose. There was discontinuation of the study at 0.3 mg/kg (β CCE) for the alcohol group of monkeys due to the appearance of seizures. However, the sucrose group with the same dose administration does not show any seizures in the animals.

2.2.4.4. Observable Behavioral Effects with $\alpha 1$ Preferring Compounds

The effect of $\alpha 1\beta 3\gamma 2$ Bz/GABA(A)ergic ligands on the behavior of rhesus monkeys was observed with the treatment of zolpidem, β CCT, and **1•HCl**. Zolpidem at the dose of 3.0 and 10.0 mg/kg significantly increased the frequency scores for ataxia in the alcohol group of animals. The sucrose group of rhesus monkeys did not show any effect at any dose of zolpidem tested. No, other profound behavior changes were seen in the alcohol group with any dose tested (Table 2-5).

Table 2-5. Summary of Drug Effects on Selected Observable Behaviors

Behavior	Alcohol			Sucrose		
	Zolpidem	3-PBC	β CCT	Zolpidem	3-PBC	β CCT
Ataxia	↑ (3.0, 10.0)	=	=	=	=	=
Tac/oral	=	=	↓	=	=	=
Self-directed	=	↑ (10.0)	↑	=	=	=
Forage	=	↓ (10.0)	=	=	↓	↓ (0.3, 3.0)
Yawn	=	=	=	=	↑ (10.0)	=
Visual explore	=	=	=	=	↑ (5.6, 10.0)	=

β CCT, β -carboline-3-carboxylate-*tert*-butyl ester; 3-PBC, 3-propoxy- β -carboline hydrochloride. The direction of significant effects is indicated by ↓ (decrease), ↑ (increase), or = (no change). Doses at which these effects occur are indicated in parentheses and reported in milligram per kilogram.

β CCt administration significantly decreased the frequency scores for tactile/oral behaviors in alcohol drinking animals. At the dose of 0.3 mg/kg, β CCT decreased frequency for tac/oral behavior in 3/6 monkeys, no monkeys at 1 mg/kg, and 4/6 monkeys at 3.0 mg/kg in the alcohol drinking group. There was an increased score for self-directed behavior such as aggregated self-grooming and scratching at 3.0 mg/kg in alcohol group in comparison to vehicle administration in animals. In the sucrose drinking group, β CCT decreased foraging behavior patterns at 0.3 mg/kg (4/4 monkeys) and 3.0 mg/kg (5/5 monkeys) but did not have any effect on tac/oral or self-directed behavioral observations. The **1•HCl** similar to β CCT increased the self-directed responses at 10.0 mg/kg in the alcohol group compared to vehicle administration. In contrast to β CCt the **1•HCl** decreased the foraging behavior in both alcohol and sucrose groups of rhesus monkeys. The other observation noted with **1•HCl** was increased yawning at 10.0 mg /kg and passive visual behavior

at both 5.6 and 10.0 mg/kg doses only in sucrose group compared to vehicle receiving models but not in alcohol drinking group.

From the findings of this study, it was observed that $\alpha 1$ preferring Bz/GABA_A ligands demonstrated a noticeable effect on increasing the latency to complete the first alcohol drink without affecting the control or sucrose groups. Both β CCT and **1•HCl** demonstrated a profound effect on increasing the time to complete the alcohol drinking. However, these two β -carbolines do not show any effect on the intake number or a number of sipper extensions, or BALs. The response due to β CCT or **1•HCl** administration on the sucrose drinking was nil, which indicated the effects were specific to alcohol use. Interestingly, the behavior of ataxia was not observed with any of the doses that reduced alcohol drinking in the rhesus monkeys. It appears, as expected, the effect of β CCT and **1•HCl** at these doses was as a $\alpha 1$ antagonist. The study of effects of various $\alpha 1$ GABA_A receptor ligands and their effect on the alcohol drinking and behavioral patterns signify the involvement of $\alpha 1\beta 3\gamma 2$ GABAergic receptor subtypes of the GABA receptor system in these studies.

2.2.5. The Potential Effect of 3-PBC•HCl in Early Life Stress Induced Impulsivity and Excessive Alcohol Drinking in Adult MS Rats⁶

The risk of development of drug addiction and dependence in most individuals is related to the experience of stress during their early childhood. The early life stress is often related to the abnormal behavioral mood disorders and increase substance use in adulthood.^{22,33} The stress in infancy leads to neuronal changes in the limbic system and hyperactivity in hypothalamus-pituitary-adrenal (HPA) axis that results in elevated levels of corticosterone, glucocorticoids and their metabolites.³⁴ Even though the defined mechanism is lacking, there is evidence that children under stress are more liable to binge drinking and experience impulsivity especially cognitive impulsivity which is most common with drug addiction.³⁵⁻³⁷ The impulsive nature is associated

with the GABA signaling system in the corticolimbic system and also plays a major role in rodent models exposed to Maternal Separation (MS). The GABA_A α 1 receptors in the amygdala and hippocampus are known to be vital in mediating the binge drinking in MS models. However, there is recent genetic evidence in human linkages that potentially implicates the role of GABA_A α 2 receptors and interference with binge drinking and impulsivity.

MS models exhibit a high expression of corticotropin releasing factor (CRF) in stress loci that lead to neuronal modifications in the prefrontal cortex (PFC), nucleus accumbens, and hippocampus, which are known to constitute the reward and emotional memory circuits.³⁸⁻⁴⁰ The binge drinking and high alcohol consumption are mediated by elevated CRF,^{41,42} with activation of polymorphic CRF1 receptors in the central amygdala.⁴³

The rodent and nonhuman primate models⁴⁴ under MS are known to self-administer more alcohol at the age of adults than controls.^{45,46} In this study the proposed GABA_A α 2 subunit ligand **1·HCl** was used to determine its effects on reducing binge drinking and impulsivity in MS rat models. **It must be pointed out that although Lueddens and Gondre-Lewis term 3-PBC·HCl as α 2 subtype preferring ligand, its activity was not antagonized by flumazenil, consequently, the effect cannot be at the α 2 β 3 γ 2 Bz/GABA site.** According to the National Institutes of Health, binge drinking is defined as an increase in the blood alcohol concentration (BAC) level to ≥ 80 mg% within 2 hours.⁴⁷ Impulsivity is highly linked to numerous neurochemical and anatomical changes in the brain associated with decision making and risky behavior. The tendency to respond prematurely without focusing on the consequences or having no foresight is regarded as impulsivity which is measured by delay discounting (DD) techniques.⁴⁸ The rats separated from their mother every day for 3 hours are used as MS models for early life stress that could result in high alcohol consumption and impulsive behavior. This was developed by Koob et al.,⁴⁷ and employed by many investigators as a model of binge drinking.

2.2.5.1. Measurement of Baseline Operant Responding

The rats were stabilized on an FR8 schedule for 8 days; the responding for alcohol and impulsive behavior was recorded between the control (CTL) and MS rats. The alcohol responses and BAC are presented in Figure 2-9 (A). The MS rats demonstrated a higher level of responding to alcohol compared to controls (CTL). The BAC's are measured in all MS rats for 5 days, in two 45 minute sessions. The level of alcohol in the blood of MS rats was 99.3 ± 3.2 mg%/dL which was 52.9 ± 6.2 mg%/dL in CTL rats (Figure 2-9B). The complex impulsivity behavior was measured using the adjusted amount delay discounting. Impulsive nature is determined based on the reward chosen, the lesser reward chosen faster was denoted as higher impulsivity. From the normal operant conditions, the impulsivity behavior was observed as higher in MS rats in relation to CTL rats, as depicted in Figure 2-9C.

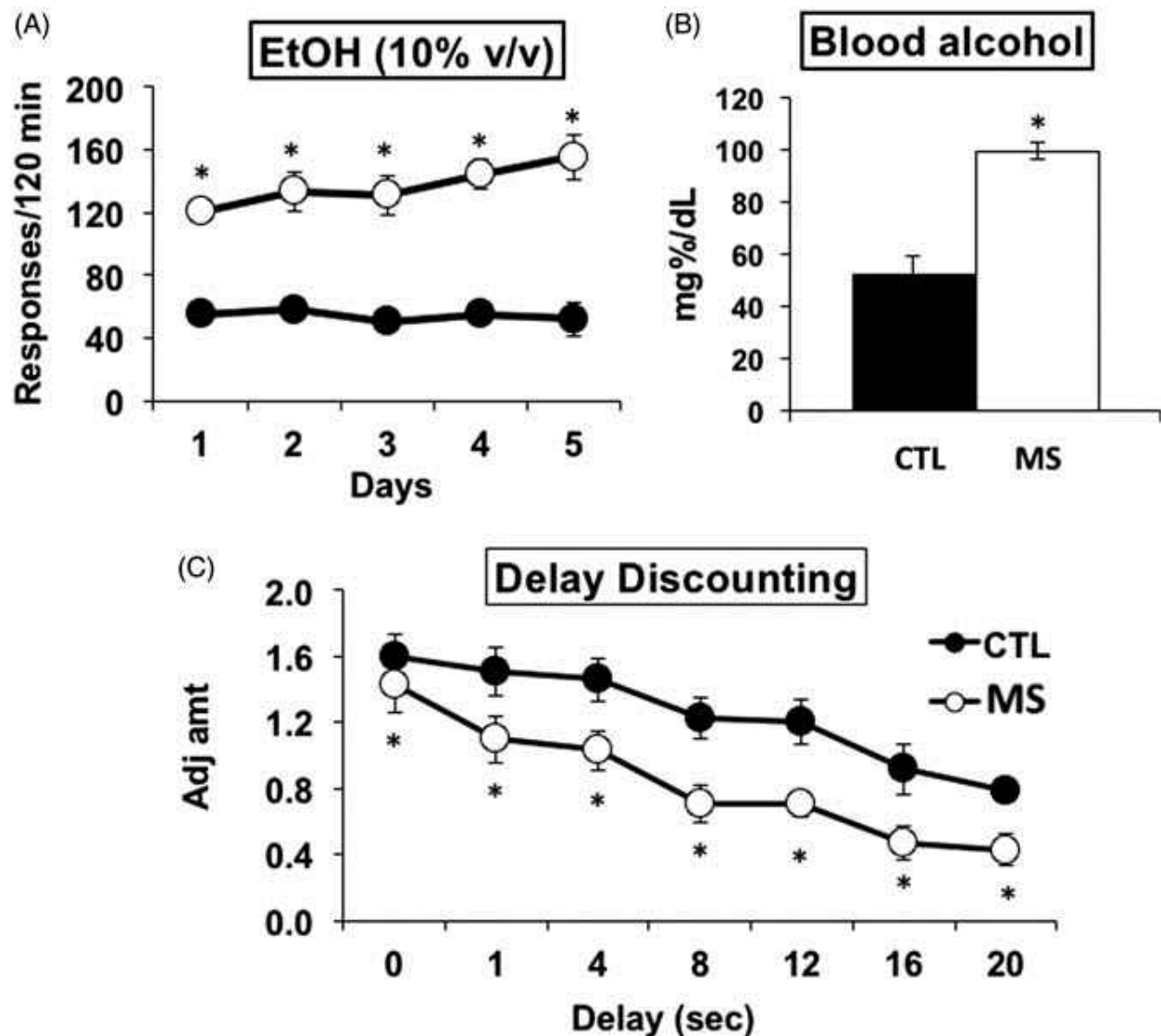


Figure 2-9. Baseline operant responding for alcohol, blood alcohol concentration and delay discounting (impulsivity) of MS versus CTL rats. (A) Responding for alcohol was increased in maternally separated (MS) rats (N=10) compared to control (CTL) rats (N=10). (B) BACs of MS rats (N=4) were elevated above those of CTL rats (N=4) and were > 80 mg%/dL following 2 h of drinking. (C) Adjusted amount was decreased [impulsivity is elevated] in MS rats (N=11) compared to CTL SD rats (N=9). * $p \leq 0.05$ by ANOVA followed by *post-hoc* tests.

2.2.5.2. Antalarmin Decreases Impulsivity and Binge Alcohol Drinking in MS Rats

To determine the role of CRF (corticotropin releasing factor) and elevated levels of CRF in CeA and mPFC of the MS rats, the antalarmin (CRF 1 receptor antagonist)⁶ was directly infused into the CeA and mPFC areas of the brain at 2 μ g and 4 μ g. The two doses of the CRF antagonist were given to alcohol drinking MS and sucrose drinking MS rats to evaluate the effect of

antalarmin in drinking of alcohol and on the non-alcohol beverage. Antalarmin had shown a significant decrease in both the operant responding and impulsivity nature for alcohol when injected into both the CeA and mPFC regions of MS rats without having any effect on sucrose drinking, as represented in Figure 2-10 and 2-11.⁶ The effects of reduction of operant responding and impulsive behavior was confirmed by *post hoc* analysis ($p \leq 0.05$).

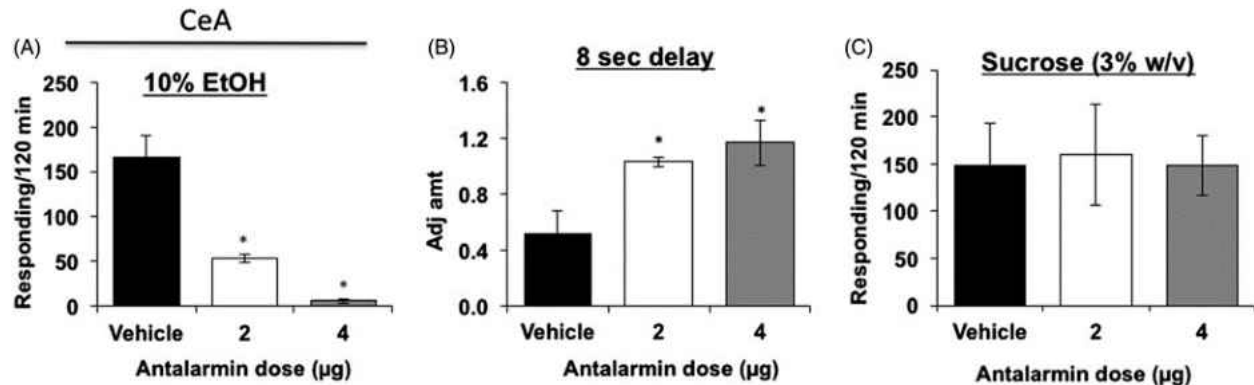


Figure 2-10. Effects of antalarmin injected into the CeA on delay discounting, operant binge drinking, sucrose drinking. (A) Both doses of antalarmin (N=6/dosage group] reduced operant responding for alcohol of MS rats compared to vehicle-treated MS rats (N=6). (B) Both 2 and 4 µg doses of antalarmin (N=6/dosage group] microinjected into the CeA of MS rats elevated adjusted amount (decreased impulsivity) compared to vehicle treatment in MS rats (N=6). (C) Both doses of antalarmin in the CeA (N=5/dosage group) did not alter the responding of MS rats for sucrose as compared to vehicle (N=5). * $p \leq 0.05$ by ANOVA.

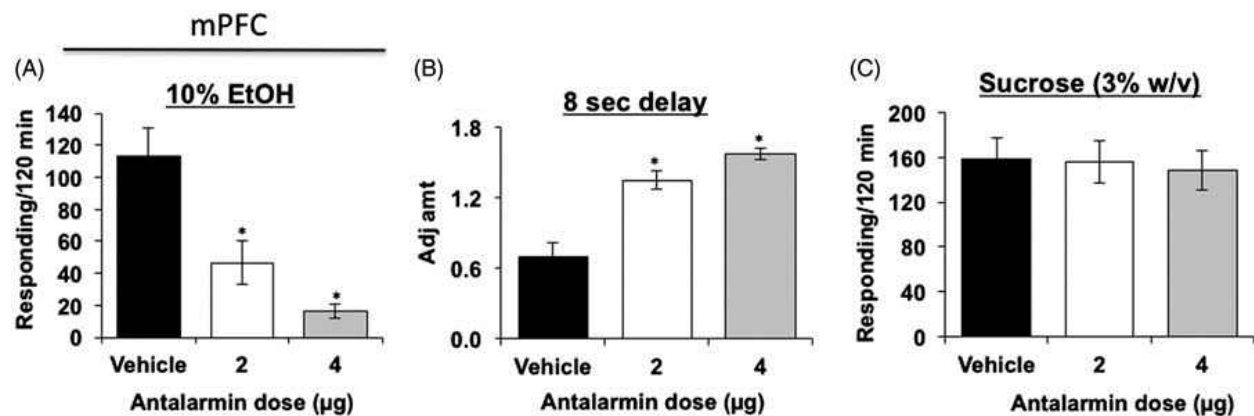


Figure 2-11. Effects of antalarmin injected into the mPFC on delay discounting, operant binge drinking and sucrose drinking. (A) Both 2 and 4 µg doses of antalarmin microinjected into the mPFC decreased impulsivity (elevated adjusted amount) in MS rats (N=6/dosage group) compared to vehicle treatment (N=6). (B) Both doses of antalarmin also reduced responding of MS rats (N=4/dosage group) for alcohol as compared to vehicle (N=4). (C) Both doses of antalarmin in the mPFC (N=5/dosage group) did not alter the responding of MS rats for sucrose compared to vehicle (N=5). * $p \leq 0.05$ by ANOVA.

2.2.5.3. Increased Expression of GABA_A α 2 Receptors in the CeA and mPFC of naïve MS Rats

GABA_A α 2 receptors are known to play an important role in the high alcohol drinking nature of genetically modified alcohol preferring P rats, according to some reports.⁶ Based on the biochemical similarities between the P rats, naïve MS rats, and MS rats the levels of GABA_A α 2 expression were studied in MS rats and the CTL rats. A significantly higher expression of GABA_A α 2 receptors was observed in the MS rats in comparison to CTL rats, as shown in Figure 2-12.

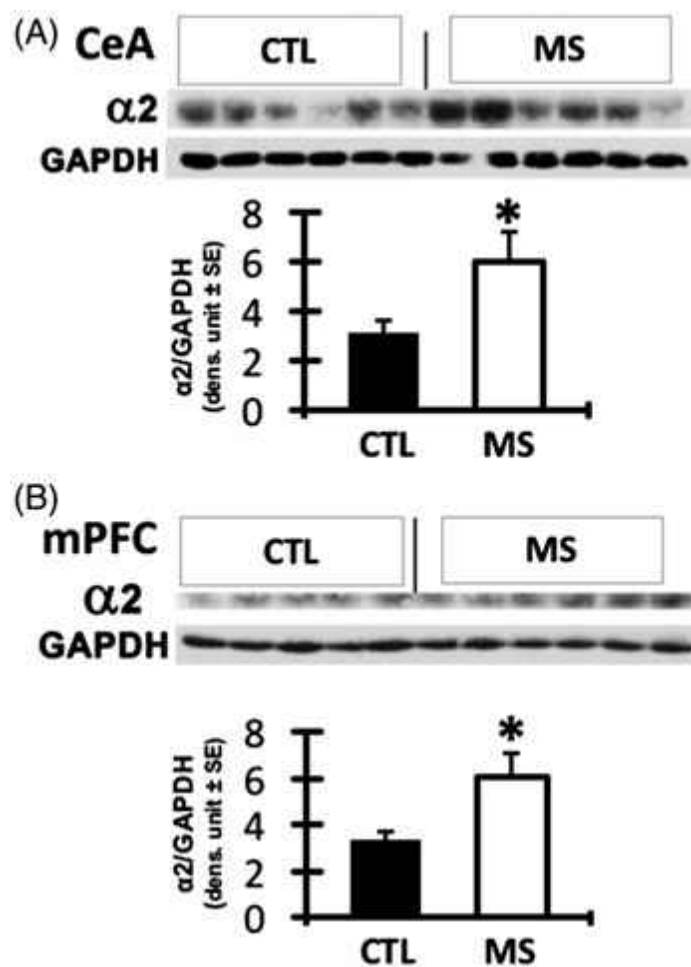


Figure 2-12. GABA_A α 2 protein concentration in CeA and mPFC of MS versus CTL rats. The levels of GABA_A α 2 expression were significantly higher in the CeA (A) and mPFC (B) of MS rats (N=6) compared to CTL rats (N=5 for mPFC, n=6 for CeA). * $p \leq 0.05$ by ANOVA.

2.2.5.4. 3-PBC·HCl (1·HCl) Decreases the Impulsivity and Binge Alcohol Drinking in MS Rats

With the significant involvement and importance of GABA_A α 2 receptors in regulating alcohol drinking, impulsivity, addiction, and stress proposed. The GABA receptor ligand 3-PBC·HCl was tested for its effect on alcohol drinking and impulsivity by microinjecting it directly into the CeA or mPFC of MS rats at 20 μ g and 40 μ g to determine its actions. The **1·HCl** injected into both the CeA and mPFC decreased the alcohol responding and impulsivity as depicted, in Figure 2-13. The 40 μ g of **1·HCl** was known to reverse the alcohol drinking and impulsive nature in rodents and because of this only 40 μ g was tested in mPFC. In both cases, the MS rats did not show any decreased responding to sucrose drinking. The 3-PBC·HCl did not have any aversive effects in the control rats; a necessary control experiment in studies on alcohol addiction to insure the test compound has no aversive or bad side effects that inhibits drinking overall.

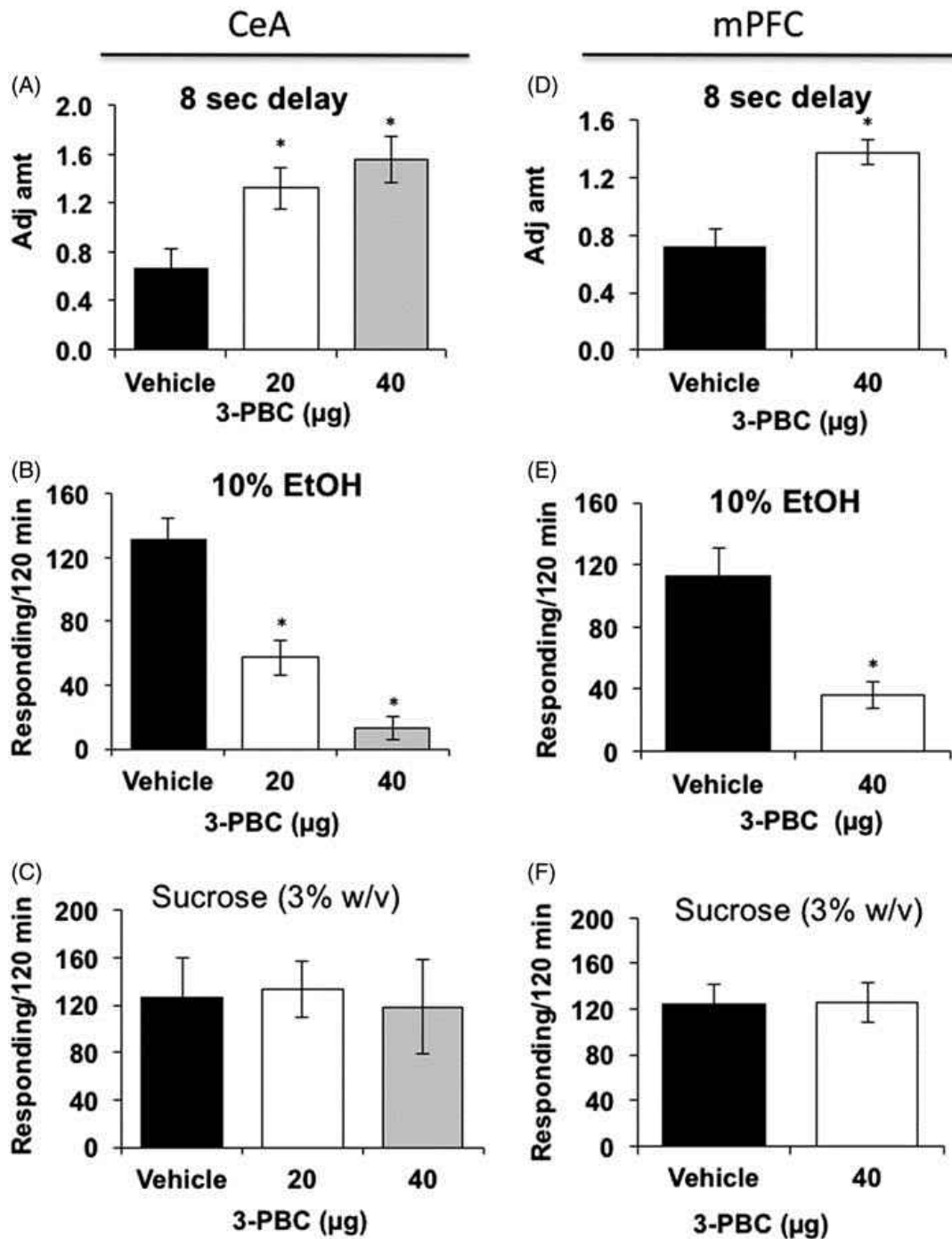


Figure 2-13. Effects of 3-PBC·HCl in the CeA and mPFC on delay discounting, operant binge drinking, and sucrose drinking. (A) Both 20 and 40 µg doses of 3-PBC·HCl micro injected into the CeA, elevated adjusted amounts (decreased impulsivity) in MS rats (N=5/ dosage group) compared to vehicle treatment (N=5). (B) Both doses of 3-PBC·HCl also reduced operant responding of MS rats (N=5/dosage group) for alcohol compared to vehicle (N=5). (C) Neither dose of 3-PBC·HCl in the CeA (N=5/dosage group) altered the responding of MS rats for sucrose compared to vehicle (N=5). (D) The 40 µg dose of 3-PBC·HCl micro injected into the mPFC, elevated adjusted amount (decreased impulsivity) in MS rats (N=4) compared to vehicle treatment (N=4). (E) 40 µg of 3-PBC·HCl also reduced operant responding of MS rats (N=4) for alcohol compared to vehicle (N=4). (F) 3-PBC·HCl in the mPFC (N=5) did not alter the responding of MS rats for sucrose compared to vehicle (N=5). * $p \leq 0.05$ by ANOVA.

The 3-PBC·HCl tested had demonstrated significant effects in reversing the alcohol drinking and impulsivity behavior in these MS rats. The **1·HCl** along with CRF antagonist antalarmin provides a novel way to treat the stress induced alcohol drinking and impulsive life events hopefully in humans.

2.2.6. Effect of PBC Isoforms (3-PBC·HCl, 3-ISOPBC·HCl, β CCt, and 3-cycloPBC·HCl) on Alcohol Drinking in P Rats and Effect of 3-cycloPBC·HCl and 3-ISOPBC·HCl in Maternally Deprived (MD) Rats

The 3-PBC (**1·HCl**) ligand studied in maternally separated (MS) rats had demonstrated effects in decreasing alcohol self-administration and impulsive behavior in these rats.⁶ The studies were further extended to determine the anti-alcohol properties of β -carboline antagonists **1·HCl**, and β CCt, as well as **2·HCl** and **20·HCl** in alcohol preferring P rats. The **2·HCl** and **20·HCl** also were tested in MD rats in addition to P rats and **20·HCl** was tested in male and female rats to determine its effects on different sexes.

The rats were trained under a fixed ratio schedule to lever press to get access to drink ethanol (EtOH) or sucrose (Figure 2-14 A and B). Initially, rats were trained to lever press for the available reinforcer (10% sucrose, W/V) under a fixed ratio (FR1) schedule for 5 to 10 days. The FR1 schedule was subsequently followed by an FR4 schedule for the sucrose drinking. The same fixed ratio was followed for ethanol drinking. Once the rats were stabilized in the operant chamber for ethanol drinking, the rats were allowed to lever press for 10 % EtOH. Rats received the gavage administration of the compound, and after 15 minutes rats were allowed to press the lever for two 30 minute sessions to gain access to alcohol with a 45 minute break. The DIDMSA (drinking-in-the-dark-multiple-scheduled- access) paradigm was followed for all the drinking pattern studies.

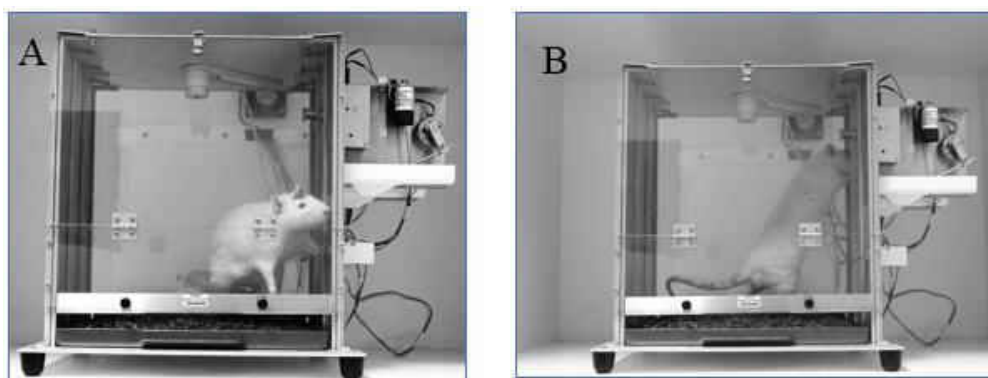


Figure 2-14. A, The rat is lever pressing for ethanol in operant chamber. B, The rat is drinking alcohol/sucrose from the dipper cup which is dispensed near the top of the chamber.

The previous studies done in P rats with these compounds reduced the alcohol drinking at the dose of 40 mg/kg.¹⁴ Now in addition to 40 mg/kg, the compounds were orally given at 5mg/kg, 10 mg/kg, 20 mg/kg, 40 mg/kg and 75 mg/kg to determine the minimum effective dose and most active compound among all PBC isoforms.

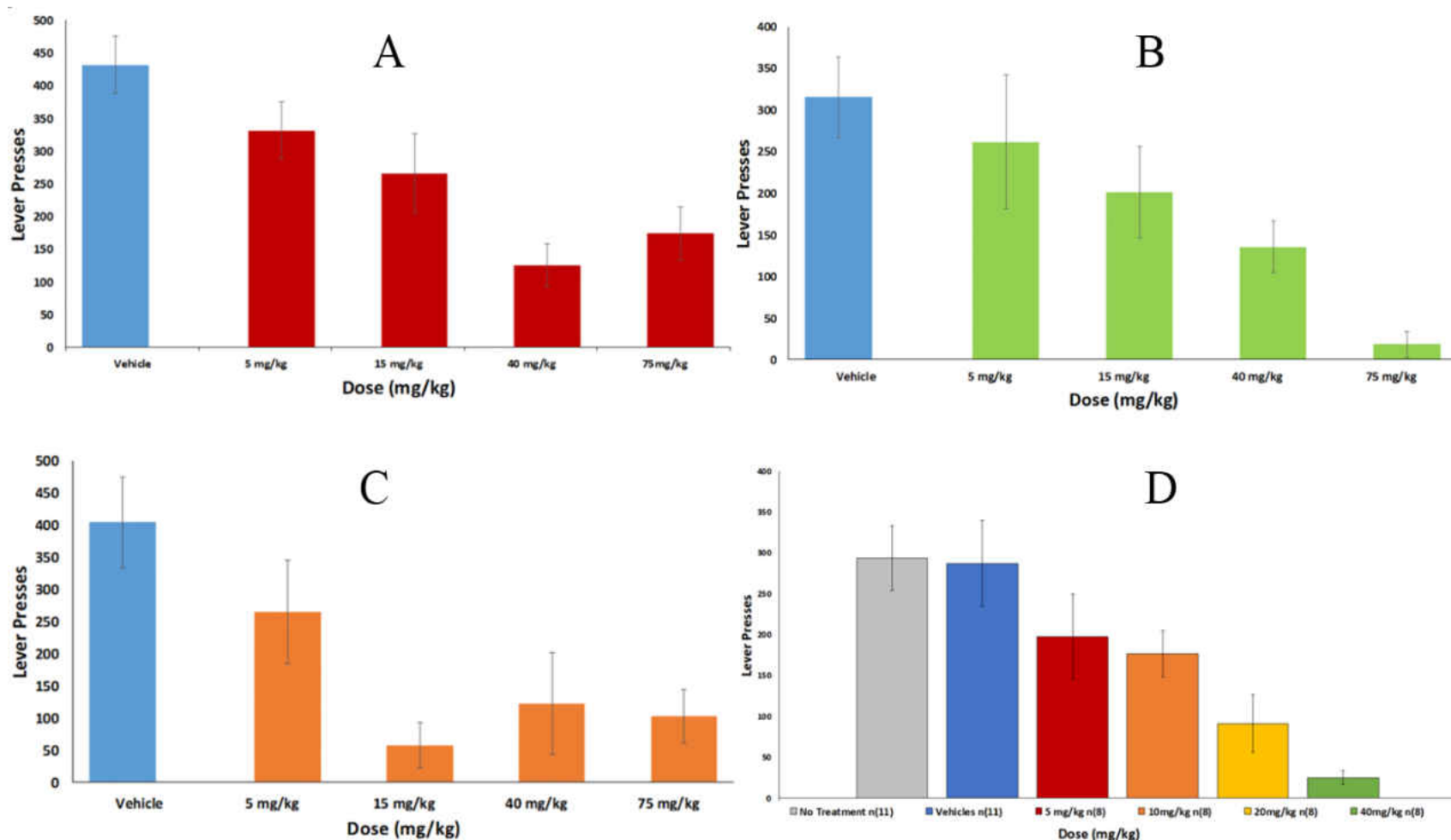


Figure 2-15: A, Effect of β CcT on binge drinking in P rats (N = 6 male rats per group, except for 15 mg/kg where N = 4, N = 8 for vehicle) at 5 mg/kg, 15 mg/kg, 40 mg/kg, and 75 mg/kg. B, Effect of 3-ISOPBC·HCl on binge drinking in P rats (N = 6 male rats per group except for 5 mg/kg where N = 4, N = 8 for vehicle) at 5 mg/kg, 15 mg/kg, 40 mg/kg, and 75 mg/kg. C, Effect of 3-PBC·HCl on binge drinking in P rats (N = 6 male rats per group N = 6 for vehicle) at 5 mg/kg, 15 mg/kg, 40 mg/kg, and 75 mg/kg. D, Effect of 3-cycloPBC·HCl on binge drinking in P rats (N = 8 male rats per group, N = 11 for vehicle) at 5 mg/kg, 15 mg/kg, 20 mg/kg, and 40 mg/kg. N = 11 for no treatment.

All PBC isoforms were given to P rats orally at a dose of 5 mg/kg, 15 mg/kg, 40 mg/kg and 75 mg/kg except **20•HCl** which was tested at a maximum dose of 40 mg/kg. The effect of the compounds on the lever pressings for alcohol for all the compounds administered at different doses are illustrated in Figure 2-15. The α_1 antagonist β CCt reduced the number of lever pressings for alcohol at the initial dose of 5 mg/kg and at 15 mg/kg but had shown a significant reduction at 40 mg/kg. The decrease in lever pressing response at the 75mg/kg dose of β CCt was less but still significant, as shown in Figure 2-15A. The 3-ISOPBC (**2•HCl**) ligand decreased alcohol responding at all dosages, and the response was a sequential decrease from 5 mg/kg to 75 mg/kg (Figure 2-15B). Similar to β CCt and **2•HCl** the number of lever pressings to gain access to alcohol intake was reduced in the case of 3-PBC•HCl (Figure 2-15C). However, the maximum decrease in responding was observed at 15 mg/kg, and there was a slight increase in the lever pressing at 40 mg/kg and 75 mg/kg with **1•HCl**. Again, the reduction in lever pressings was significant. The **20•HCl** was given to rats at the same concentrations as the other three PBC Isoforms except the 75 mg/kg dosage. In the case of 3-cycloPBC (**20•HCl**), the maximum decrease in the alcohol responding was observed at the dose of 40 mg/kg, consequently, a higher dose was not tested (Figure 2-15 D). Although the four different isoforms of PBC demonstrated a prominent reduction in responding for the alcohol intake, the **20•HCl** exhibited a significant decrease at the 40 mg/kg and **1•HCl** at 15 mg/kg, but the increase in the response was observed at higher doses with **1•HCl** but even then it was a significant decrease in lever pressing for alcohol. The **20•HCl** and **2•HCl** were further evaluated for their effectiveness in reducing binge drinking in maternally deprived (MD) rats. For the initial studies **20•HCl** was tested for two 30 minute sessions whereas the **2•HCl** was evaluated for two hours.

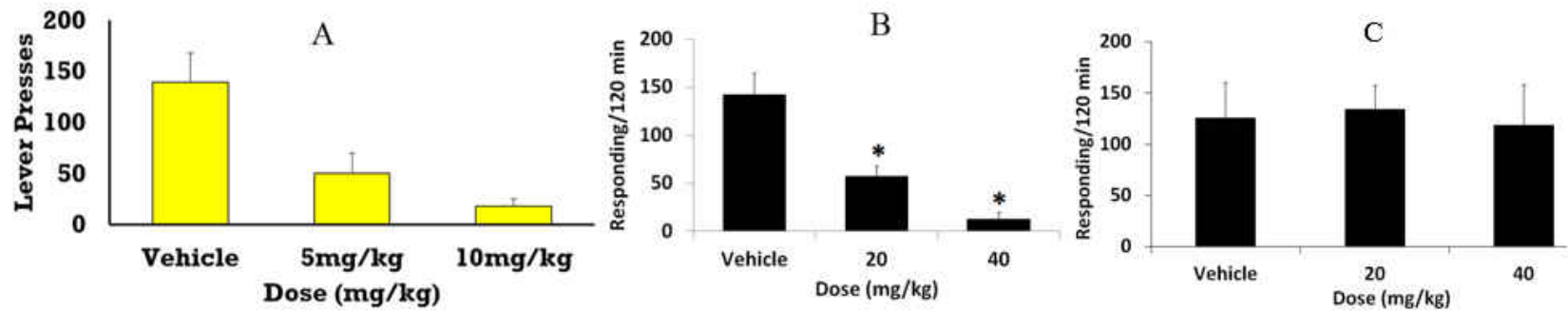


Figure 2-16: A, Effect of 3-cycloPBC·HCL on binge drinking in MD rats (N = 9 male rats per group, N = 8 for vehicle) at 5 mg/kg and 15 mg/kg. B, Effect of 3-ISOPBC·HCl on binge drinking in MD rats (N = 11 male rats per group, N = 11 for vehicle) at 20 mg/kg and 40 mg/kg. C, Effect of 3-ISOPBC·HCl on sucrose drinking in MD rats (N = 11 male rats per group, N = 11 for vehicle) at 20 mg/kg and 40 mg/kg.

The effect of 3-cycloPBC·HCl (**20·HCl**) on the operant responding of lever pressing was shown in Figure 2-16A. There was a significant decrease in the lever press responses for alcohol at 5 mg/kg of **20·HCl**, as compared to vehicle, and it was even less when the 10 mg/kg dose was used (Figure 2-16A). The dose of **20·HCl** that produced a maximum effect in the MD rats was much more potent when compared to the 40 mg/kg dose in P rats. The **2·HCl** given at 20 mg/kg and 40 mg/kg also reduced the alcohol responding compared to vehicle in MD rats (Figure 2-16B) but these doses are higher than the **20·HCl** but still effective. None of the MD rats experienced any decrease in response to sucrose consumption (Figure 2-16C) when given **2·HCl** or **20·HCl**. Gratifyingly, the two ligands **2·HCl** or **20·HCl** had no overt behavioral aversive effects.

Because the **20·HCl** had shown a significant effect in reducing the operant responding for alcohol in both P rats and MD rats, it was tested in both female and male P rats (5 mg/kg, 10 mg/kg, 20 mg/kg, and 40 mg/kg) and MD rats (5 mg/kg and 10 mg/kg), as depicted in Figure 2-17. This was to examine sex differences in the reduction of alcohol self-administration in these rodent models. In male and female P rats the decrease in lever presses was observed at 5 mg/kg as compared to the vehicle treated rats. However, the decrease was more prominent in female P rats at 20 mg/kg and 40 mg/kg. In male P rats the effect was prominent at 40 mg/kg, and the 20 mg/kg drug administration did not cause any decrease in lever pressings in contrast to the 20 mg/kg dose in female P rats (Figure 2-17 A and B).

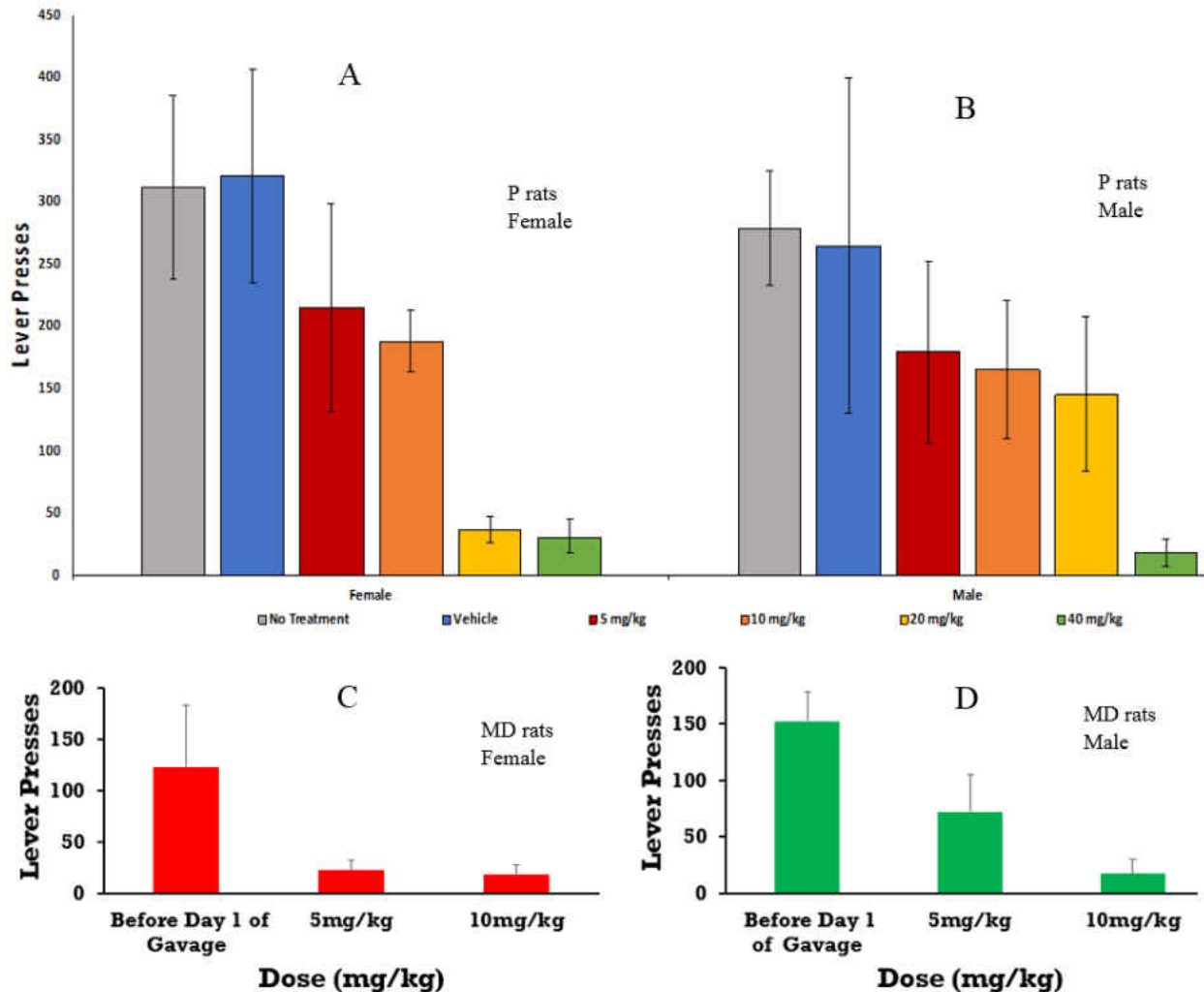


Figure 2-17: A, Effect of 3-cycloPBC·HCl on binge drinking in female P rats (N = 4 female rats per group, N = 5 female for vehicle) at 5 mg/kg, 10 mg/kg, 20 mg/kg and 40 mg/kg. B, Effect of 3-cycloPBC·HCl on binge drinking in male P rats (N = 4 male rats per group, N = 6 male for vehicle) at 5 mg/kg, 10 mg/kg, 20 mg/kg and 40 mg/kg. C, Effect of 3-cycloPBC·HCl on binge drinking in female MD rats (N = 4 female rats per group, N = 4 before day 1 of gavage) at 5 mg/kg and 10 mg/kg. D, Effect of 3-cycloPBC·HCl on binge drinking in male MD rats (N = 5 male rats per group, N = 5 m before day 1 of gavage) at 5 mg/kg and 10 mg/kg.

The **20·HCl** given orally to MD rats at 5 mg/kg and 10 mg/kg in both female and male MD rats had a profound effect on alcohol self-administration at these doses. In female MD rats, the reduction in alcohol responding was observed at both doses and the effect was similar with the 5 mg/kg and 10 mg/kg dose (Figure 2-17C). In male MD rats, the decrease in the responding was observed at the higher dose (10 mg/kg), as compared to administration of the 5 mg/kg of **20·HCl** (Figure 2-17D). Clearly the effect of the **20·HCl** at 5 mg/kg exerted a more potent effect in MD

female rats, as compared to the corresponding male rats. None of the rats showed any decrease in responding to non-alcohol drinks such as sucrose which implies the PBC isoforms are selectively acting against alcohol drinking behaviors with no adverse effects. The **20·HCl** is clearly more potent in female rats against alcohol drinking behaviors than their male counterparts. This is significant in regard to sex difference.

2.2.7. The Effect of β CCt, 3-PBC·HCl (1·HCl), and 3-ISOPBC·HCl (2·HCl) on the Spontaneous Locomotor Activity (SLA) and Diazepam Induced Sedation in Mice

It was demonstrated earlier that alcohol potentiates GABAergic neurotransmission at least in part via action at $\alpha 1$ subunit-containing GABA_A receptors,⁴ and also that an $\alpha 1$ -preferring antagonist such as 3-PBC·HCl (**1·HCl**)¹³ might exhibit a beneficial effect to reduce alcohol drinking.²¹ Recently, an isomer of 3-PBC·HCl and a putative $\alpha 1$ -preferring antagonist 3-ISOPBC·HCl was synthesized and tested.⁷ In the behavioral part of the present study, **2·HCl** and **1·HCl** were tested to answer the question whether both affect spontaneous locomotor activity and the diazepam-induced sedation or antagonize it in mice. It was known the $\alpha 1$ preferring antagonist β CCt (anti-alcohol ligand) was a potent antagonist of the sedative/ataxic effects of diazepam in rhesus monkeys and rodents. Moreover, **1·HCl** has exerted the same effects, albeit weaker. Since the sedative effect of diazepam and other benzodiazepines is mediated mainly by $\alpha 1$ subunit-containing GABA_A receptors, a reversible effect of **2·HCl** or **1·HCl** on diazepam-induced sedation would further support their $\alpha 1$ -preferring antagonistic properties in in-vivo rather than just in-vitro, and encourage their examination in the context of alcohol seeking behavior in other models directed towards human alcoholics.

The study on this subject by Savic et al. in a male C57BL/6 strain of mice included two experiments – the first investigation includes the effects of both **2·HCl** and **1·HCl** at a dose of 10

mg/kg on spontaneous locomotor activity and the diazepam-induced sedation in mice, together with the use of the positive control – a widely studied $\alpha 1$ GABA_A antagonist β CCt designed in Milwaukee. In the second experiment, the same study was carried out, but with the **2·HCl** and **1·HCl** dosed at 30 mg/kg. The results presented here indicated that the application of diazepam at a dose of 2 mg/kg induced a reliable sedation in mice in both experiments. Importantly, the potent $\alpha 1$ preferring antagonist (positive control), β CCt managed to antagonize the sedative effect of diazepam in the first 60 minutes of tracking, while its effect did not reach significance during the complete recording period of 90 min; such subtle differences may be related to the expected shorter elimination half-life of β CCt when compared to diazepam. This drug is known for involvement of active metabolites (nordiazepam) which contributes to the overall behavioral half-life of activity. The 3-ISOPBC·HCl, dosed at both, 10 and 30 mg/kg, had no significant effect on spontaneous locomotor activity on its own but failed to antagonize the sedative effects of diazepam. This finding suggests that **2·HCl** is not an antagonist at $\alpha 1$ -containing GABA_A receptors either from lack of potency or binding affinity but could be at a higher dose. Unexpectedly, the same result was determined for **1·HCl**. This result is in contradiction with others studies which showed 3-PBC·HCl (**1·HCl**) did antagonize some of the properties of diazepam. This result is likely due to animal strain or vehicle differences.

Analysis of the data of this study demonstrated that both **2·HCl** and its more-studied isomer **1·HCl** were devoid of $\alpha 1$ antagonistic properties in the spontaneous locomotor activity assay in these mice in the Dr. Savic laboratory. Since this latter observation with **1·HCl** is in contrast to much literature which indicated **1·HCl** was antagonist at $\alpha 1$ *in-vivo*. These properties may be responsible for the beneficial effects on alcohol drinking behavior. Further work in this area is necessary to unravel these contrasting reports.

In the first SLA experiment (Figure 2-18), analysis by two-way ANOVA revealed a significant effect of factor agonist, except a trend for the parameter total distance traveled when one level of the factor antagonist was 3-PBC·HCl (Table 2-6). When it comes to the factor antagonist, a significant influence was demonstrated for β CCt and the parameter total time immobile at 0–60 min, while for the same parameter at 0–90 min and total distance traveled at 0–60 min a statistical trend was observed. Interaction as a factor was not significant in any case. Post hoc SNK tests revealed significant results after two-way ANOVA and are listed in Table 2-7.

In the second SLA experiment (Figure 2-19), one-way ANOVA demonstrated a highly significant influence of treatment (Table 2-8) by 3-PBC·HCl and 3-ISOPBC·HCl. Significant post hoc SNK comparisons, listed in Table 2-6, revealed that neither 3-PBC·HCl nor 3-ISOPBC·HCl was able to prevent the sedative action of DZP (Diazepam) even when dosed at 30 mg/kg.

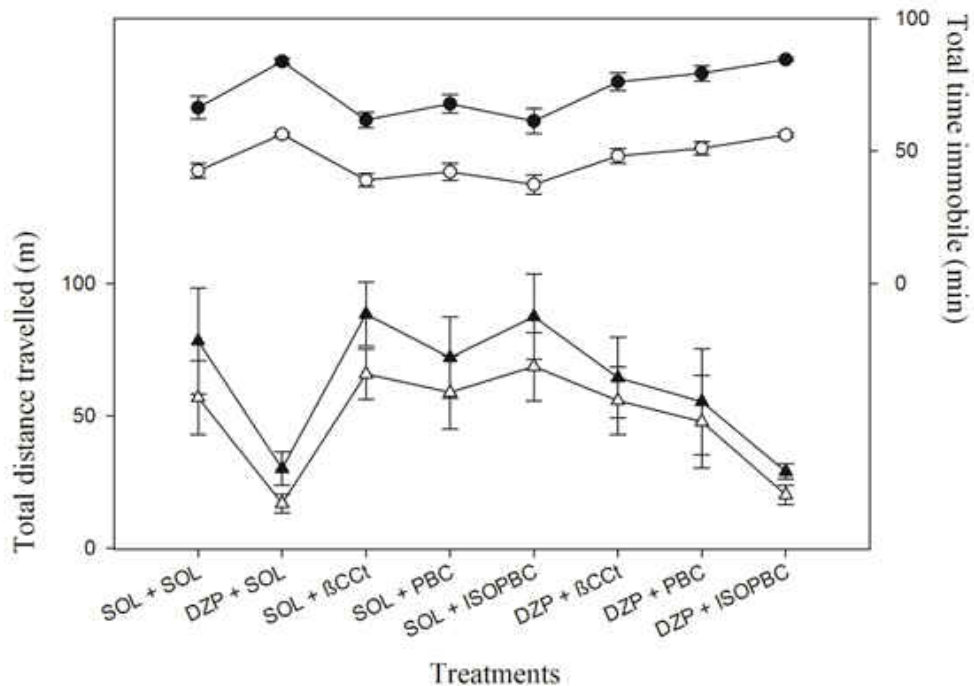


Figure 2-18. The effects of diazepam (2 mg/kg), β CCt (10 mg/kg), 3-PBC·HCl (10 mg/kg) and 3-ISOPBC·HCl (10 mg/kg) in presented combinations on total distance travelled (left scale, triangles) and total time immobile (right scale, circles) in 0–90 (black symbols) and 0–60 (white symbols) min time periods in mice in SLA. All results are presented as means \pm SEM. A number of animals per treatment (for SOL in combination with SOL through DZP in combination with ISOPBC, respectively) was 8, 6, 6, 6, 6, 7, 7 and 6. The significances values are presented in Table 2-7.

Table 2-6. The significant post hoc comparisons (Student-Newman-Keuls (SNK) test) after the performance of one-way ANOVAs. The influence of 3-ISOPBC·HCl and 3-PBC·HCl (30 mg/kg, respectively) on total distance traveled (m) and total time immobile (min) in SLA was assessed in the 0–90 and 0–60 min period in a partial factorial design.

Groups	Behav. param.	Tracking period	Post hoc comparison (SNK test)	Significance
SOL + SOL DZP + SOL DZP + PBC DZP + ISOPBC	Total distance travelled (m)	0–90 min.	SOL + SOL vs. DZP + SOL	p < 0.001
			SOL + SOL vs. DZP + PBC	p = 0.002
			SOL + SOL vs. DZP + ISOPBC	p < 0.001
		0–60 min.	SOL + SOL vs. DZP + SOL	p < 0.001
			SOL + SOL vs. DZP + PBC	p < 0.001
			SOL + SOL vs. DZP + ISOPBC	p < 0.001
	Total time immobile (min.)	0–90 min.	SOL + SOL vs. DZP + SOL	p < 0.001
			SOL + SOL vs. DZP + PBC	p < 0.001
			SOL + SOL vs. DZP + ISOPBC	p < 0.001
		0–60 min.	SOL + SOL vs. DZP + SOL	p < 0.001
			SOL + SOL vs. DZP + PBC	p < 0.001
			SOL + SOL vs. DZP + ISOPBC	p < 0.001

Table 2-7. The results of the two-way ANOVAs. The influence of 3-ISOPBC·HCl and 3-PBC·HCl (10 mg/kg respectively) on the total distance travelled (m) and total time immobile (min) in spontaneous locomotor activity assay was assessed in the 0-90 and 0-60 min time period together with the use of the positive control (βCCt) in a full factorial design (behav. param. –behavioral parameter).

Behav. param.	Tracking period	Factors in the two-way ANOVA	F value and significance for factor Agonist	F value and significance for factor Antagonist	F value and significance for factor Interaction
Total distance traveled (m)	0–90 min	Agonist (SOL and DZP) vs. Antagonist (SOL and βCCt)	F(1,23) = 5.255 p = 0.031	F(1,23) = 2.003 p = 0.170	F(1,23) = 0.584 p = 0.453
		Agonist (SOL and DZP) vs. Antagonist (SOL and PBC)	F(1,23) = 3.361 p = 0.080	F(1,23) = 0.289 p = 0.596	F(1,23) = 0.793 p = 0.382
		Agonist (SOL and DZP) vs. Antagonist (SOL and ISOPBC)	F(1,23) = 12.584 p = 0.002	F(1,23) = 0.073 p = 0.790	F(1,23) = 0.120 p = 0.733
	0–60 min	Agonist (SOL and DZP) vs. Antagonist (SOL and βCCt)	F(1,23) = 4.622 p = 0.042	F(1,23) = 4.199 p = 0.052	F(1,23) = 1.643 p = 0.213
		Agonist (SOL and DZP) vs. Antagonist (SOL and PBC)	F(1,23) = 3.344 p = 0.080	F(1,23) = 1.389 p = 0.251	F(1,23) = 1.071 p = 0.312
		Agonist (SOL and DZP) vs. Antagonist (SOL and ISOPBC)	F(1,23) = 16.539 p < 0.001	F(1,23) = 0.475 p = 0.498	F(1,23) = 0.154 p = 0.699
Total time immobile (min.)	0–90 min	Agonist (SOL and DZP) vs. Antagonist (SOL and βCCt)	F(1,23) = 21.510 p < 0.001	F(1,23) = 3.233 p = 0.085	F(1,23) = 0.215 p = 0.647
		Agonist (SOL and DZP) vs. Antagonist (SOL and PBC)	F(1,23) = 18.410 p < 0.001	F(1,23) = 0.193 p = 0.665	F(1,23) = 0.766 p = 0.391
		Agonist (SOL and DZP) vs. Antagonist (SOL and ISOPBC)	F(1,23) = 33.494 p < 0.001	F(1,23) = 0.366 p = 0.551	F(1,23) = 0.685 p = 0.417
	0–60 min	Agonist (SOL and DZP) vs. Antagonist (SOL and βCCt)	F(1,23) = 21.249 P < 0.001	F(1,23) = 5.618 p = 0.027	F(1,23) = 0.870 p = 0.361
		Agonist (SOL and DZP) vs. Antagonist (SOL and PBC)	F(1,23) = 19.723 P < 0.001	F(1,23) = 1.256 p = 0.274	F(1,23) = 0.911 p = 0.350
		Agonist (SOL and DZP) vs. Antagonist (SOL and ISOPBC)	F(1,23) = 43.926 p < 0.001	F(1,23) = 1.205 p = 0.284	F(1,23) = 1.016 p = 0.324

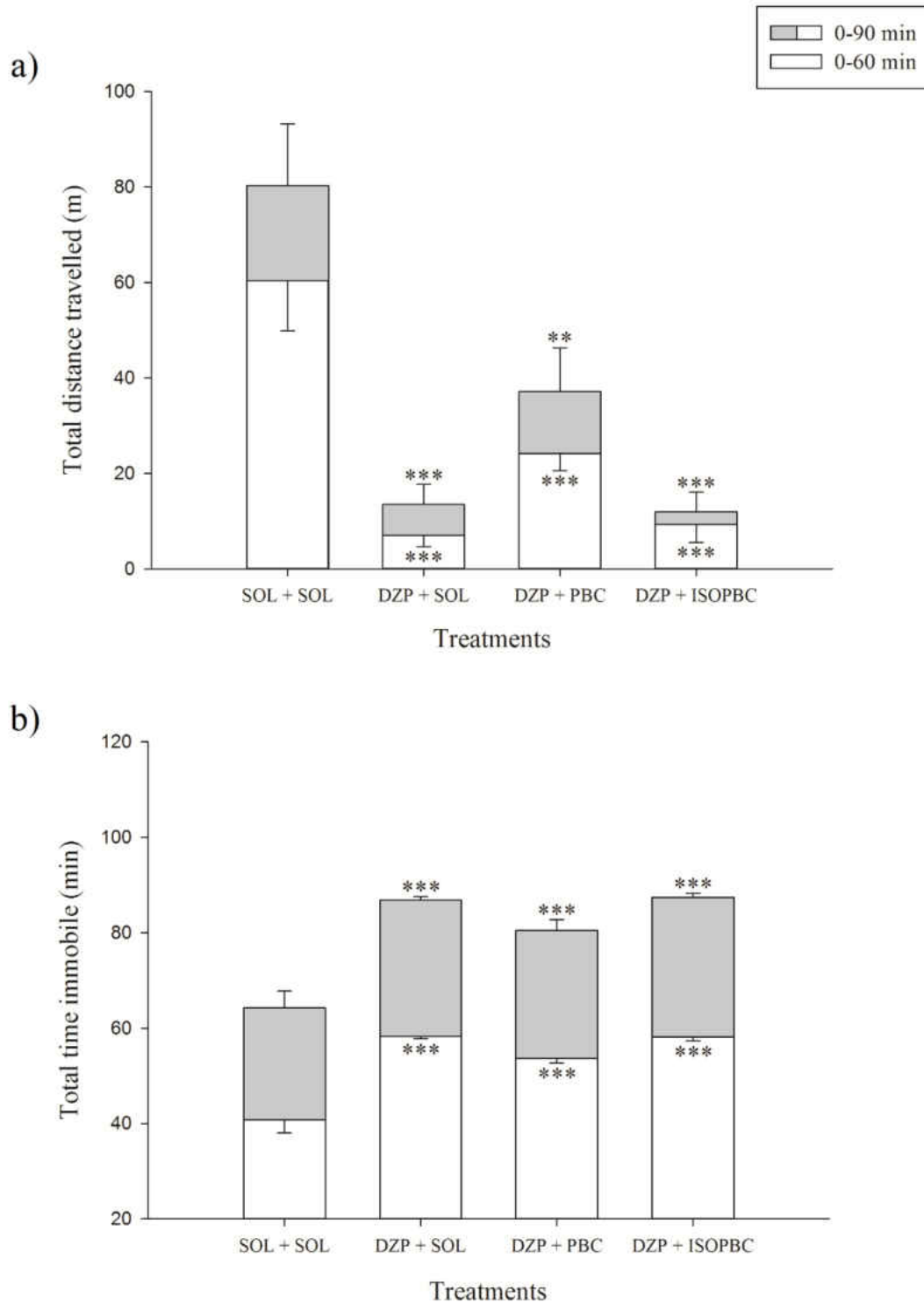


Figure 2-19. The effects of diazepam (2 mg/kg) in combination with SOL, 3-PBC·HCl (30 mg/kg) and 3-ISOPBC·HCl (30 mg/kg), respectively, on total distance travelled (a) and total time immobile (b) in 0–90 and 0–60 min time periods in mice in SLA. All results are presented as means ± SEM.

Table 2-8. The results of one-way ANOVAs. The influence of 3-ISOPBC·HCl and 3-PBC·HCl (30 mg/kg, respectively) on total distance traveled (m) and total time immobile (min) in SLA was assessed in the 0–90 and 0–60 min period in a partial factorial design.

Groups	Behavioral parameter	Tracking period	F value and significance
SOL + SOL DZP + SOL DZP + PBC DZP + ISOPBC	Total distance travelled (m)	0–90 min	F(3,20) = 14.140 p < 0.001
		0–60 min	F(3,20) = 16.854 p < 0.001
	Total time immobile (min.)	0–90 min	F(3,20) = 25.106 p < 0.001
		0–60 min	F(3,20) = 28.091 p < 0.001

2.2.8. Determination of CNS (Central Nervous System) Sensorimotor Effects using Rotarod Studies⁴⁹

Rotarod studies are conducted to examine the possible adverse central nervous system (CNS) sensorimotor effects that include ataxia, sedation, and loss of righting reflex (LORR) due to β -carbolines that behave as Bz/GABA(A)ergic positive allosteric modulators (PAM); as agonists. The compounds were administered to female Swiss Webster mice at 40 mg/kg by oral gavage except for **2-HCl**, which was tested in male Balb/c mice with intraperitoneal (ip) administration. The sensorimotor test was carried out after 10, 30, and 60 minutes (5 min for 3-**2-HCl** instead of 10 min). Diazepam was used as a positive control at 5 mg/kg and vehicle was given to a group of mice to serve as a negative control group. The compounds do not show any adverse effects, as shown in Figure 2-20.

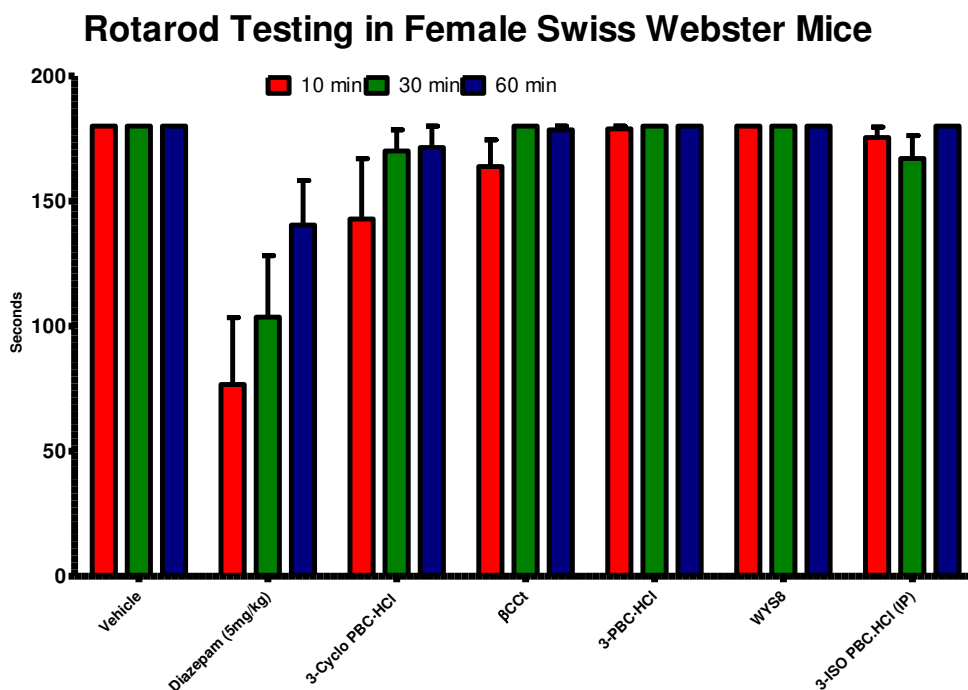


Figure 2-20. Effect of compounds on sensorimotor coordination. Swiss Webster mice (Balb/c in case of 3-ISO PBC-HCl) were tested on the rotarod at 15 rpm for 3 min at 10, (5 min for 3-ISO PBC-HCl) 30, and 60 min, respectively following compound exposure. Mice (N=10) received single oral gavage administration (intraperitoneal for 3-ISO PBC-HCl) of test compound at (40 mg/kg), diazepam (5 mg/kg), or vehicle (50% PBS, 40% propylene glycol, 10% DMSO). The time of fall was recorded if it occurred before 3 min. Data are expressed as mean \pm SEM (N=10).

There was no sedation, ataxia or LORR activity observed with these compounds, except with **2•HCl** which, exhibited only very minor sedation at the 10 minute time point which was also within experimental error. The β CCt, **1•HCl** and WYS8 compounds do not show any significant adverse CNS activity. The **2•HCl** tested ip does not cause any unwanted effects, and there were also no overt CNS effects observed. The rotarod studies clearly indicated that these compounds are safe in rodents even at the concentrations up to 40 mg/kg administration orally. This is necessary to employ these β -carbolines for further studies of alcohol self-administration in nonhuman primates.

2.2.9. *In-vitro* Metabolic Stability Studies of β -carbolines on Human Liver Microsomes (HLM) and Mouse Liver Microsomes (MLM)¹⁰

Drug metabolism is a process of converting hydrophobic xenobiotic agents into more water soluble species by biochemical modification, which facilitates the elimination of drugs from the body primarily by the kidney or bile ducts. Metabolic stability refers to the susceptibility of drugs to biotransformational enzymes such as cytochrome P450, esterases, and hydroxylases which are abundant in the liver.⁵⁰ Microsomes and S9 fractions are subcellular fractions of liver tissue. Microsomes are vesicles derived from the endoplasmic reticulum which contains the CYP 450 enzymes (hydrolases, esterase etc.) responsible for phase I biotransformation reactions.⁵¹ The *in-vitro* metabolic stability assay was carried out in the presence of microsomes derived from human and mouse species.⁵² The stability data was determined at the end of one hour and the half-life values are also presented in Table 2-9.

Table 2-9. The in-vitro metabolic stability studies with % remaining at the end of 1 hour

Compound	Half-life (min) (HLM)	% left after 1 hr. (HLM)^a	Half-life (min) (MLM)^b	% left after 1 hr. (MLM)
3-PBC·HCl	19.95 ± 0.55	13.37 ± 0.17	Compound not detected after 20 minutes	Compound not detected after 20 minutes
3-ISOPBC·HCl	17.41 ± 0.82	11.32 ± 0.31	Compound not detected after 30 minutes	Compound not detected after 30 minutes
3-CycloPBC·HCl	46.6 ± 1.9	40.67 ± 0.23	Compound not detected after 20 minutes	Compound not detected after 20 minutes
βCCt	141.5 ± 8.8	73 ± 0.18	Compound not detected after 20 minutes	Compound not detected after 20 minutes
WYS8	677 ± 148	93.56 ± 0.16	134.2 ± 7.6	75.11 ± 0.18

^aHLM – Human Liver Microsomes, ^bMLM – Mouse Liver Microsomes

On the human liver microsome assay, the stability was in the order of 3-PBC·HCl ~ 3-ISOPBC·HCl < 3-cycloPBC·HCl < βCCt < WYS8. The **1·HCl** and **2·HCl** degraded to less than 20% in an hour, whereas the **20·HCl** contained nearly 50% remaining after one hour which is a significant difference when compared to the active **1·HCl** and **2·HCl**. The longer stability of the 3-cycloPBC·HCl analog (**20·HCl**) was presumably due to the cyclopropyl group, the substitution of which slowed metabolism. The βCCt with the *t*-butyl ester and WYS8 ligands demonstrated better stability and a half-life of more than one hour. The acetylene group present in the WYS8

molecule may have contributed to the higher stability by retarding aromatic hydroxylation in ring A and the branched substituent also had an influence on the increase of the stability of WYS8 and β CCt at C-3. In mouse liver microsomes all of the compounds degraded very rapidly. In less than 20-30 minutes β -carbolines were under the limit of quantification on the analytical mass spectrometer (Shimadzu LCMS -8040). Consequently, the half-life and percent remaining are not calculated for mouse (MLM) assays. It is well known that mouse liver and rat livers are upregulated with detoxification enzymes compared to humans and primates.⁵² **Stability of 1 hour in the rat means approximately four hours in a dog and eight hours in a nonhuman primate.** The metabolic stability samples will be further investigated for metabolic profiling to extend the studies to pre-clinical models such as in baboons, dogs, and rabbits to determine various metabolites formed, their stability and their safety. Reports in the literature which describe the metabolism of the natural β -carboline alkaloids harman and a norharman suggest that these alkaloids are efficiently oxidized to several ring hydroxylated and N-oxidation products.⁵³ The metabolic enzymes CYP 450 1A2, 1A1 catalyzed the formation of 6-hydroxy β -carboline and CYP 450 2D6, 2C19, and 2E1 also contributed to a minor extent (see Figure 2-21 for important details).

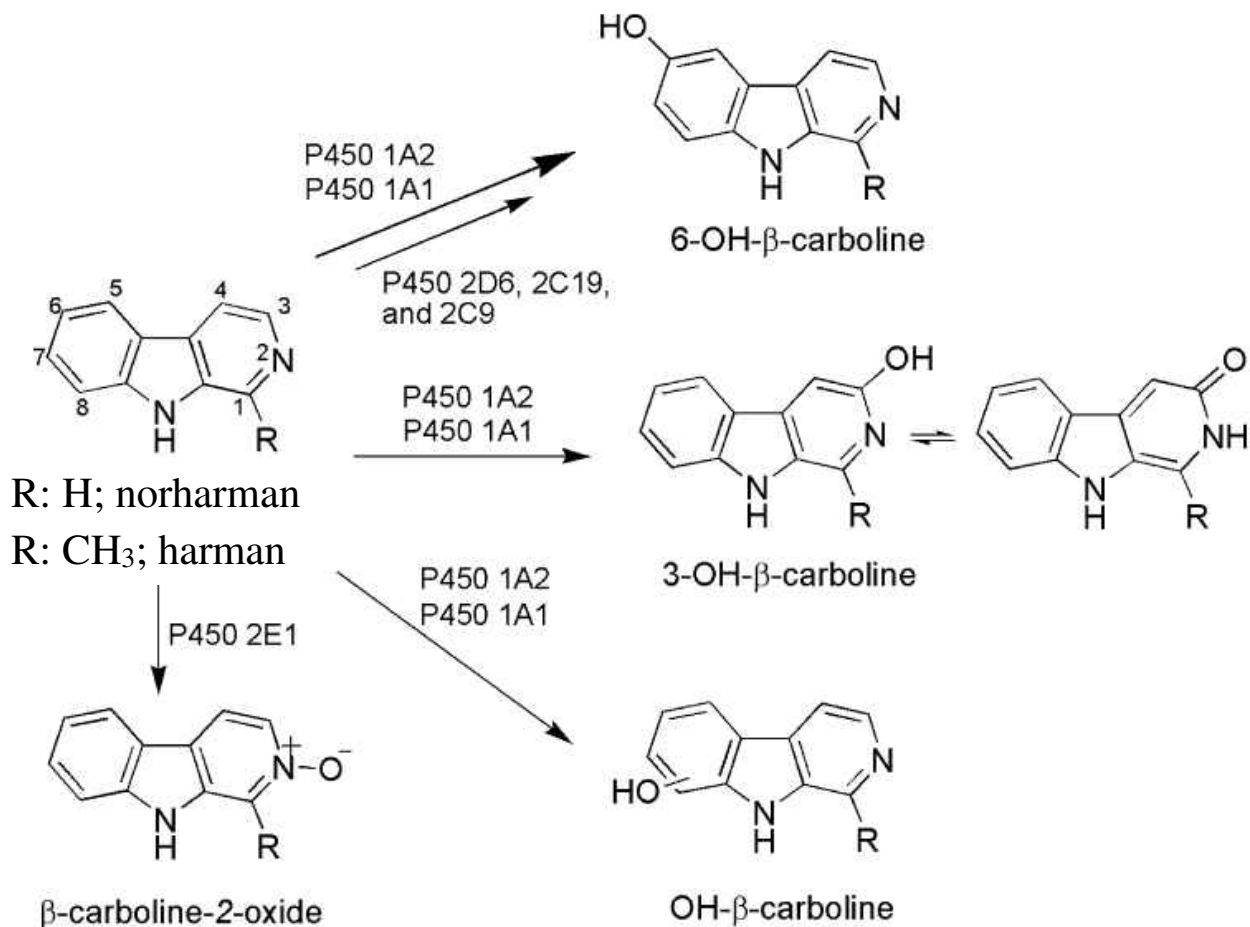


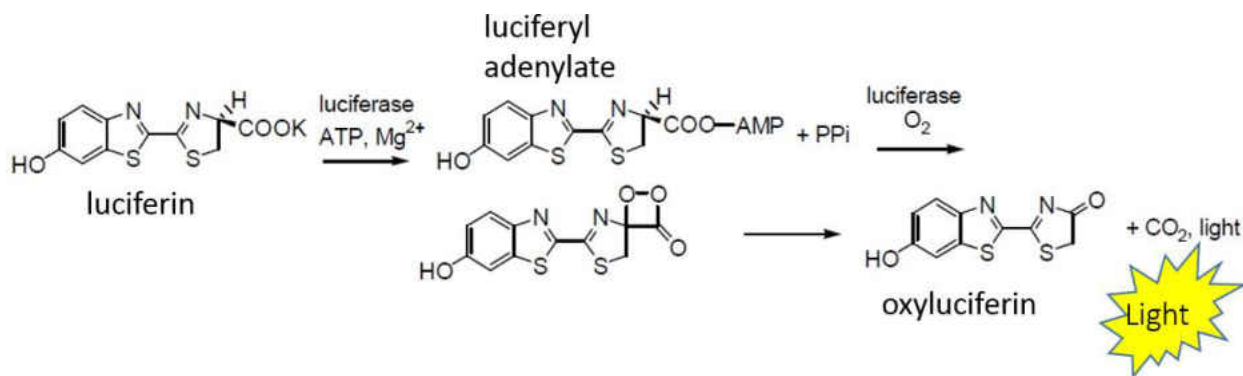
Figure 2-21. Oxidative metabolism of the β -carboline alkaloids norharman and harman by human cytochrome P450 enzymes and human liver microsomes.⁵³

The other metabolite 3-hydroxy β -carboline was formed by enzymes CYP 450 1A1, and 1A2 and the key β -carboline-N (2)-oxide was produced by P450 2E1. Since alkoxy groups in the 3-alkoxy β -carbolines increase the electron density of the β -carboline N-atoms, pathway P450 2E1 to an N-oxide may be involved here. These oxidations are the major route of detoxification for β -carbolines with the involvement of P450 1A1, 1A2, 2D6, 2C19 and 2E1 cytochrome enzymes. The rapid elimination and detoxification reactions of β -carbolines indicate that these act as a good substrates for metabolic enzymes. The mechanism of metabolite formation for β -carbolines compounds is anticipated to be similar to naturally occurring harman and norharman and will be

studied. This is much of the reason one is anxious to see a study in nonhuman primates with 3-cycloPBC·HCl (**20·HCl**).

2.2.10. Evaluation of Cytotoxicity of β -Carbolines in HEK 293 and HEPG2 Cells¹⁰

The PBC isoforms have been characterized for the determination of cytotoxicity in two different cell lines HEK 293 (Human Embryonic Kidney) and HEPG2 (Human Liver Hepatocellular Carcinoma). The cells are incubated with the compounds and the cell viability was measured with the Cell Titer-GLOTM (contains luciferase, Mg, and luciferin) that determines the amount of ATP produced from the living cells. The control reference was the fluorescence of the living cells. The cytotoxicity was the loss of fluorescence because dead cells do not produce ATP. The difference was easy to measure. The reaction that occurs between the Cell Titer-GLOTM assay reagent and ATP from living cells is represented in Scheme 2-1. The LD₅₀ (Lethal Dose) was calculated and compared between the different compounds with the two cell lines and is presented in Figure 2-22.



Scheme 2-1: The bioluminescence reaction between the cells and Cell Titer-GLOTM

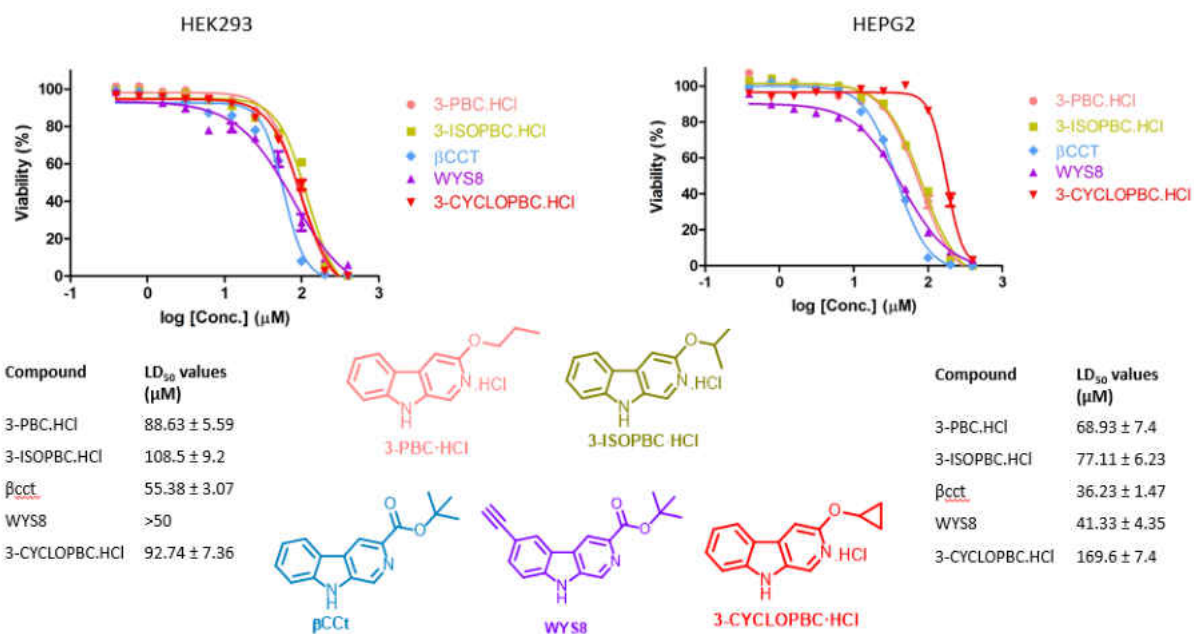


Figure 2-22: The *in-vitro* cytotoxicity of β -carboline analogs on HEK 293 and HEPG2 cell lines with LD₅₀ values which indicates 3-cycloPBC·HCl (20·HCl) is the safest in these assays.

HEK293 cell lines: Analysis of the LD₅₀ values of the above HEK293 viability graphs indicate that the hydrochloride salts of β -carbolines showed almost equal cell viability. The 3-ISOPBC·HCl showed better viability (LD₅₀ = 108.5 ± 9.2 μM) among three hydrochloride compounds except within experimental error, the 3-cycloPBC·HCl ligand was just as safe (93 ± 7 μM). The βCCT and WYS8 were safe and non-toxic up to 50 μM and exhibited toxicity when the concentration was greater than 50 μM. However, an LD₅₀ of 50 micromolar is relatively safe because the concentration in the clinic would not be greater than nanomolar. The other analogs were safe as well.

HEPG2 cell lines: Examination of the LD₅₀ values from the above HEPG2 viability graph indicated that, 3-cycloPBC·HCl was non-toxic (LD₅₀ = 169.6 ± 7.4 μM) compared to all other β -carbolines tested. The 3-PBC·HCl and 3-ISOPBC·HCl demonstrated almost equal viability in HEPG2 cell lines. The βCCT and WYS8 were safe and non-toxic at lower concentration (LD₅₀ =

$36.2 \pm 1.5 \mu\text{M}$ for βCCt ; $\text{LD}_{50} = 41.3 \pm 4.3 \mu\text{M}$ for WYS8) and exhibited toxicity when the concentration increased.

In conclusion, overall 3-cycloPBC·HCl (**20·HCl**) is the safest in these two assays as compared to 3-ISOPBC·HCl, 3-PBC·HCl, βCCt or WYS8 in both cell lines (HEK293 and HEPG2). However, the cytotoxicity at $30 \mu\text{M}$ for βCCt and WYS8 is an order of magnitude, at least, higher than pharmacologically relevant doses of these two agents.

2.2.11. Psychoactive Drug Screening Program (PDSP): Analysis of 3-ISOPBC·HCl

3-ISOPBC·HCl was tested for binding to receptors according to references of the PDSP program^{54,55} at the University of North Carolina-Chapel Hill under the supervision of Dr. Bryan Roth. The results are presented below in the Table 2-10, where data represent mean percentage inhibition (with $n = 4$ determinations) for the ligand tested at the respective receptor subtypes. The data shown in the Table 2-10 are results from primary assays, with the exception of the numbers in parentheses, which are the K_i values in nM as determined from secondary assays. Significant inhibition was considered to be $> 50\%$ in the primary assay. In a primary assay if the binding value was less than 50% this indicated no interaction occurred at 43 of these receptors and a secondary assay was not run (K_i). Where negative inhibition (-) was seen, it represented a stimulation of binding, as in some cases, compounds at high concentrations non-specifically increase binding. The concentration of the compound employed in the primary assays was $10 \mu\text{M}$.

Table 2-10. Results of Psychoactive Drug Screening Program (PDSP) Analysis of 3-ISOPBC·HCl

RECEPTOR ^a	3-ISOPBC (% inhibition)
Adrenergic receptor alpha-1A	2.1
Adrenergic receptor alpha-1B	27
Adrenergic receptor alpha-1D	3.9
Adrenergic receptor alpha-2A	30.4
Adrenergic receptor alpha-2B	-12.8
Adrenergic receptor alpha-2C	13.9
Adrenergic receptor beta-1	10.7
Adrenergic receptor beta-2	3.8
Adrenergic receptor beta-3	-3.9
BZP Rat Brain Site	85.6(251.7) ^b
Dopamine receptor D1	7.2
Dopamine receptor D2	16.4
Dopamine receptor D3	-4
Dopamine receptor D4	0.7
Dopamine receptor D5	-0.9
Dopamine transporter DAT	24.8
Opiate receptor DOR	-4.6
GABA _A receptor	-4.2
Histamine receptor H1	3.7

Histamine receptor H2	34.6
Histamine receptor H3	16
Histamine receptor H4	2.9
Opiate receptor KOR	-2.6
HERG binding	17.6
Opiate receptor MOR	8.7
Muscarinic receptor M1	-5
Muscarinic receptor M2	20.2
Muscarinic receptor M3	-4.4
Muscarinic receptor M4	7.7
Muscarinic receptor M5	23.8
Serotonin receptor 5-HT _{1A}	30.4
Serotonin receptor 5-HT _{1B}	22.4
Serotonin receptor 5-HT _{1D}	1.7
Serotonin receptor 5-HT _{1E}	-9.6
Serotonin receptor 5-HT _{2A}	4.4
Serotonin receptor 5-HT _{2B}	63.9 (1,332.8 nM) ^b
Serotonin receptor 5-HT _{2C}	33.5
Serotonin receptor 5-HT ₃	-4.5
Serotonin receptor 5-HT _{5A}	23.6

Serotonin receptor 5-HT ₆	-3.6
Serotonin receptor 5-HT ₇	-7.2
NET transporter	84.9 (798.7 nM) ^b
SERT transporter	-8.7
Peripheral benzodiazepine receptor	40.2
Sigma-1 receptor	-13.6
Sigma-2 receptor	31

^a Based on the primary (and secondary, if determined) binding assays, 3-ISOPBC·HCl did not significantly bind to the receptors shown here. ^b Secondary binding assay was performed, wherein the number in parentheses is the K_i value in nM.

In the primary receptor binding assay 3-ISOPBC did not bind to 43 receptors as mentioned; demonstrated < 50% binding at 10 μM. Only 3-ISOPBC·HCl demonstrated > 50% binding at 10 μM in the primary receptor binding assays at the serotonin receptor (5-HT_{2B}), BZP rat brain site, and NET transporter, therefore, secondary assay binding data was determined only for these three receptors. The K_i for binding of 3-ISOPBC·HCl at the serotonin receptor (5-HT_{2B}), the BZP rat brain site, and the NET transporter was found to be 1,332.8 nM, 251.7 nM, and 798.7 nM, respectively, which indicated that 3-ISOPBC·HCl does not significantly interact with these receptors.⁵⁶ There is some interaction at the peripheral benzodiazepine receptor site but this is common for most Bz receptor ligands (K_i = 250 μM).

2.3. CONCLUSION

β-carbolines consistently come under scrutiny as important pharmacological targets in natural products and synthetic chemistry.⁵⁷ The β-carboline natural products exhibit a myriad of important biological activity throughout the ages from harman, norharman and others. The β-carbolines here are based on the seminal studies of Braestrap whom incorrectly proposed the

structure of the endogenous ligand for the BzR as a dihydro β -carboline. The structure was incorrect and even the correct structure BCCE was not an endogenous ligand but was an artifact of the isolation process. This error was corrected by Richard Squires. However, Braestrup's discovery was very important for it stimulated interest in β -carbolines as GABA_A receptor ligands with many pharmacological applications. Among the various biological activities, these ligands are known to mediate anti-alcohol effects by acting as antagonists at α subunit subtype GABA_A receptors in the central nervous system as proposed by June et al.¹³ several years ago for β CCt and 3-PBC·HCl.⁵⁸ Ligands such as BCCE and BCCM are important as negative modulators which enhance cognition; however the latter two β -carbolines are convulsant which limits their use.

The past evidence of the biological importance of β CCt and **1·HCl** as potential treatments for alcohol abuse^{4,6,7,14,59} has prompted the design and synthesis of a new series of analogs to reduce the toxicity, extend duration of action and improve the *in-vivo* bioavailability.^{4,5} The efficacy and binding studies carried out on HEK 293T cells and oocytes revealed these molecules act as very weak positive allosteric modulators with efficacy at $\alpha 6\beta 3\delta$ and/or $\alpha 6\beta 3\gamma 2$ GABA_A subunits but only at μ M concentrations. The binding and efficacy studies indicated that **2·HCl** bound tighter to the $\alpha 1$ subunit in contrast to $\alpha 2 - \alpha 6$ subtypes, analogous, to BCCE and **1·HCl** which had antagonistic activity at the $\alpha 1\beta 3\gamma 2$ GABA_A receptor subunits. However, Luddens, Gondre-Lewis reported also an interaction at the $\alpha 2$ subtypes but it was not antagonized by flumazenil, consequently this action at $\alpha 2$ subunits could not be due to the $\alpha 2\beta 3\gamma 2$ studied here. The biological significance of these β -carbolines (**2·HCl**, **20·HCl**) was confirmed by reduction of binge drinking, high alcohol consumption, high alcohol self-administration in alcohol preferring P rats and maternally deprived (MD) rats. Whether this is an $\alpha 1$ or $\alpha 2$ effect or $\alpha 1\alpha 2$ mediated activity has not yet been shown.⁶ The 3-PBC·HCl was known to reduce the impulsive behavior

apart from high alcohol intake¹³ when given to rodent clinical models subjected to stress in early childhood⁶ and was the lead compound for the design and synthesis of **2·HCl** and **20·HCl**.

The role of $\alpha 1$ GABA_A receptors involved in high alcohol consumption and substance use disorders and antagonistic properties of β CCt and 3-PBC·HCl in these disease models were evaluated in baboons by Elise Weerts et al.⁷ Previous studies⁴ in rhesus monkeys with these two ligands demonstrated they were antagonists of the sedation and ataxia exerted by diazepam and alprazolam; hence their designation as $\alpha 1$ antagonists.^{4,13} However, renewed interest in them stems from the use of the related β -carboline (3-ISOPBC·HCl), which was very potent in the reduction of alcohol self-administration and craving in baboons (Weerts et al.)⁷; a very exciting result. Before the study in baboons these β -carboline isomers (**1·HCl**, **2·HCl**, and **20·HCl**) were subjected to studies on the rotarod to determine if there was any adverse CNS sensorimotor effects. These β -carbolines were devoid of sedation, ataxia, and LORR and have safety profiles that extended to high concentrations. Studies of metabolism on HLM and MLM show better stability on human liver microsomes and less stability in mouse liver microsomes. The stability of the 3-cyclopropoxy beta carboline was the best of the alkoxy beta carbolines studied, to date which is a result one was searching for. It was also nontoxic in cytotoxicity assays. Hence further *in-vivo* studies are in order. The stability studies are important to design ligands with enhanced bioavailability and duration of action which enhance pharmacological and pharmacokinetic availability of these as potential drugs. Although the data on the spontaneous locomotor activity and antagonism of diazepam-induced sedation studies *in-vivo* by Dr. Savic in mice using **2·HCl** and **1·HCl** were contradictory to previous findings which involved $\alpha 1$ subtype selective ligands, this difference could be as simple as strain differences between mice and certainly differences in species (mice versus primates) or simply the vehicle employed as well as protocol. The fact remains that 3-PBC·HCl

was efficacious in retarding alcohol self-administration in alcohol P rats, HAD rats, MD rats and baboons. Moreover, 3-ISOPBC·HCl was even more active against alcohol self-administration in these models. Although the science would be clearer if one knew if this anti-alcohol effect (June et. al.,¹³ Gonde-Lewis et. al.,⁶ Weerts et. al.⁷) was mediated by $\alpha 1\beta 3\gamma 2$ subtypes alone, the fact remains BCCt, 3-PBC and 3-ISOPBC·HCl have been shown to reduce alcohol self-administration in many different animal models. These β -carbolines may have clinical potential in human alcoholics because Dr. Harry June showed^{5,13} that some of these beta carbolines reduced alcohol self-administration without the appearance of anhedonia nor depression, which occurs on occasion with naltrexone in some patients.

To get ligands with anti-alcohol effects that were more water soluble than the active anti-alcohol compound β CCt, newer analogs were designed and synthesized. Based on Scott Harvey's work, the 3-PBC·HCl (**1·HCl**) was active in rats, baboons and was more water soluble. However, using this approach 3-ISOPBC·HCl (**2·HCl**) was synthesized and it showed more potency in reduction of alcohol self-administration than 3-PBC·HCl leading on to the synthesis of 3-cycloPBC·HCl which is active to date in MD rats, etc. The 3-cycloPBC·HCl (**20·HCl**) was not cytotoxic at all when compared to β CCt, 3-PBC·HCl, which showed toxicity but only at very higher concentrations. The stability on HLM and MLM revealed **20·HCl** was longer lived than 3-PBC·HCl and 3-ISOPBC·HCl. The 3-cycloPBC·HCl (**20·HCl**) had shown potential activity to reduce the alcohol self-administration in rat models by Gondre-Lewis et al., and studies are being carried out in other higher primate models.

Because of this activity the synthesis and scale up of the new β -carbolines analogs was designed and the number of steps was reduced from 6 to 2 and executed in excellent yields and on large scale (80 g).¹ The biological studies conducted in non-human primate pre-clinical models

such as baboons required 80 -100 grams of ligand which can be done with ease with the new Pd chemistry.¹ The activity in non-human primates does imply potential ligands to treat human alcoholics without diazepam (one of the agents used now) side effects. In summary, the β -carbolines and their analogs have potential to be novel therapeutic agents to combat alcohol drinking and substance use disorders, a major problem increasing day by day in modern society (CNN and FOX NEWS channels!).

2.4. EXPERIMENTAL METHODS

2.4.1. Determination of Efficacy Studies in HEK 293T Cells - General Methods for Electrophysiological Recordings from Transiently Transfected HEK-293T Cells

HEK-293T cells were transiently transfected using calcium phosphate precipitation. Plasmids encoding mammalian GABA_A receptor subunit cDNAs were added to the cells in 1:1:1 ratios (α : β : γ or δ) of 2 μ g each. To allow identification of positively transfected cells, the plasmid encoding the pHook antibody was also included. The selection procedure for pHook expression was performed 18-52 hrs later. The cells were passaged and mixed for 30-60 min with magnetic beads coated with antigen for the pHook antibody (approximately 6×10^5 beads).⁶⁰ The selected cells were plated onto collagen-coated coverslips and used for recordings the next day.

Cells were patch-clamped at -50 mV in the whole-cell recording configuration. The bath solution consisted of (in mM): 142 NaCl, 8.1 KCl, 6 MgCl₂, 1 CaCl₂, and 10 HEPES (4-(2-hydroxyethyl)-1-piperazineethanesulfonic acid) with pH = 7.4 and osmolarity adjusted to 295-305 mOsm. The recording electrodes were filled with a solution of (in mM); 153 KCl, 1 MgCl₂, 5 K-EGTA (ethylene glycol-bis (2-aminoethyl ether N,N,N',N'-tetraacetate), and 10 HEPES with pH = 7.4 and osmolarity adjusted to 295-305 mOsm. GABA was diluted into the bath solution from freshly made or frozen stocks in water. Compounds were dissolved in DMSO and diluted into the

bath solution with the highest DMSO level applied to cells of 0.01%. Patch pipettes were pulled from borosilicate glass (World Precision Instruments, Sarasota, FL) on a two-stage puller (Narishige, Japan) to a resistance of 5-10 M Ω . Solutions containing GABA or GABA plus compounds were applied to cells for 5 sec using a 3-barrelled solution delivery device controlled by a computer-driven stepper motor (SF-77B, Harvard Apparatus, Holliston, MA, open tip exchange time of <50 msec). There was a continuous flow of external solution through the chamber. Currents were recorded with an Axon 200B (Foster City, CA) patch clamp amplifier.

2.4.2. Efficacy Studies in *Xenopus laevis* Frog Oocytes

Two electrode voltage clamp

In-vitro transcription of mRNA was based on the cDNA expression vectors encoding for all indicated GABA_A (rat) receptor subunits.⁶¹ After linearizing the cDNA vectors with appropriate restriction endonucleases, capped transcripts were produced using the mMACHINE[®] T7 transcription kit (Ambion, TX). The capped transcripts were polyadenylated using yeast poly (A) polymerase (USB, OH) and were diluted and stored in diethylpyrocarbonate-treated water at -70°C.

The methods for isolating, culturing, injecting and defolliculating of oocytes were identical with those described by E. Sigel⁶² and were described elsewhere.⁶³ Mature female *Xenopus laevis* (Nasco, WI) were anesthetized in a bath of ice-cold 0.17 % Tricaine (Ethyl-m-aminobenzoate, Sigma, MO) before decapitation and removal of the frog's ovary. Stage 5 to 6 oocytes with the follicle cell layer around them were singled out of the ovary using a platinum wire loop. Oocytes were stored and incubated at 18°C in modified Barths' Medium (88mM NaCl, 10mM HEPES-NaOH (pH 7.4), 2.4 mM NaHCO₃, 1mM KCl, 0.82 mM MgSO₄, 0.41 mM CaCl₂, 0.34 mM Ca(NO₃)₂) that was supplemented with 100 U/ml penicillin and 100 μ g/ml streptomycin. Oocytes

with follicle cell layer still around them were injected with an aqueous solution of mRNA. A total of 2.5ng of mRNA per oocyte was injected. The subunit ratio was 1:1:5 for $\alpha 1\beta 3\gamma 2$ receptors and 1:1 for $\alpha 1\beta 3$ receptors consisting of wild-type or mutated $\alpha 1$ subunit together with wild-type or mutated $\beta 3$ subunit. After injection of mRNA, oocytes were incubated for at least 24 hours for $\alpha 1\beta 3$ receptors and at least 36 hours for $\alpha 1\beta 3\gamma 2$ receptors before the enveloping follicle cell layers were removed. Collagenase-treatment (type IA, Sigma, MO) and mechanically defolliculating of the oocytes was followed, as described previously.⁶³

For electrophysiological recordings, oocytes were placed on a nylon-grid in a bath of Xenopus Ringer solution (XR, containing 90 mM NaCl, 5 mM HEPES-NaOH (pH 7.4), 1 mM $MgCl_2$, 1mM KCl and 1 mM $CaCl_2$). The oocytes were constantly washed by a flow of 6 ml/min XR which could be switched to XR containing GABA and drugs. Drugs were diluted into XR from DMSO-solutions which resulted in a final concentration of 0.1 % DMSO perfusing the oocytes. Drugs were pre-applied for 30 sec before the addition of GABA, which was then co-applied with the drugs until a peak response was observed. Between two applications, oocytes were washed in XR for up to 15 min to ensure full recovery from desensitization. For current measurements, the oocytes were impaled with two microelectrodes (2-3 $M\Omega$) which were filled with 2 M KCl. Maximum currents measured in mRNA injected oocytes were in the microampere range for all subtypes of $GABA_A$ receptors. To test for modulation of GABA induced currents by drugs, a concentration of GABA that was titrated to trigger 3-6% of the respective maximum GABA-elicited current of the individual oocyte (EC_{3-6}), was applied to the cell with various concentrations of drugs, as described previously.⁶¹ Such low GABA concentrations are widely used in the literature. All recordings were performed at rt at a holding potential of -60mV using a Warner OC-725C two-electrode voltage clamp (Warner Instrument, Hamden, CT) or a Dagan CA-1B Oocyte

Clamp or a Dagan TEV-200A two-electrode voltage clamp (Dagan Corporation, Minneapolis, MN). Data were digitized, recorded and measured using a Digidata 1322A data acquisition system (Axon Instruments, Union City, CA). Data were analyzed using GraphPad Prism. Data for dose response curves were fitted (where possible) to the equation $Y = \text{Bottom} + (\text{Top} - \text{Bottom}) / (1 + 10^{(\text{Log}EC_{50} - X) * nH})$, where EC_{50} is the concentration of the compound that increases the amplitude of the GABA-evoked current by 50%, and nH is the Hill coefficient. Data are given as mean \pm S.E. from at least three oocytes and 2 oocyte batches.

2.4.3. Effect of 3-Isopropoxy- β -carboline Hydrochloride (3-ISOPBC) on Alcohol Seeking and Self-Administration in Baboons

Subjects

Eight singly-housed adult male baboons (*Papio anubis*; South-west Foundation for Biomedical Research, San Antonio, TX) weighing on average 28.1 kg (+ 4.2 SD) served as subjects. For the alcohol group (N = 5), the reinforcer delivered was 4% w/v alcohol. For the control group (N = 3), the reinforcer delivered was a preferred non-alcohol beverage (orange-flavored, sugar-free Tang®), diluted to a concentration that functioned as a comparable reinforcer.⁶⁴ All baboons had extensive histories of self-administration of either alcohol or the non-alcoholic beverage under the chained schedule of reinforcement, as reported previously.^{7,19,64,65} Each day the baboons were fed standard primate chow that was adjusted to maintain sufficient caloric intake for normal baboons of their size, age, and activity level (about 50–73 kcals/kg); fresh fruit or vegetables; and a children's chewable multivitamin were also given. Water was available ad libitum except during sessions. The housing room was maintained under a 12-hour light/dark cycle (lights on at 6:00 AM). Facilities were kept in accordance with USDA and AAALAC

standards. The protocol was approved by the JHU Animal Care and Use Committee and followed the Guide for the Care and Use of Laboratory Animals (2011).

Apparatus

Sessions were conducted in modified primate cages as described in detail previously^{19,66} and contained (1) a panel with three colored “cue” lights, (2) an intelligence panel with two vertically operated levers and two different colored “jewel” lights each located above one of the levers, (3) a “drinkometer” connected to a calibrated 1000-ml bottle, and (4) a speaker mounted above the cages for presentation of auditory stimuli (tones). A computer interfaced with Med Associates hardware and software remotely controlled the experimental conditions and data collection.

Chained schedule of reinforcement procedure

Sessions were conducted seven days per week and began at the same time (8:30 AM) each day. The start of a session and the onset of Component 1 was signaled by a 3-s tone. During Component 1, a red cue light was illuminated, and all instrumental responses were recorded but had no programmed consequence. After 20 min, Component 1 ended and Component 2 was initiated. Component 2 was signaled by the illumination of a yellow cue light and consisted of two links. During the first link, the jewel light over the left lever was turned on, and a concurrent fixed interval 10 min, fixed time 20 min (FI 10-min FT 20-min) schedule was in effect. The first link ended either a) with the first response on the left lever after 10 min elapsed or b) automatically after 20 min, whichever occurred first. During the second link, the jewel light over the left lever flashed and a fixed-ratio (FR) 10 schedule was in effect on the left lever. Completion of the FR response requirement ended Component 2; the yellow cue light and the jewel light were turned off, and Component 3 was initiated. If the FR 10 requirement was not completed within 90 min,

the session terminated with-out transitioning to Component 3 (i.e., no access to alcohol or the non-alcoholic beverage for the day). Component 3 was signaled by the illumination of the blue cue light. A blue jewel light over the right lever was also illuminated, and the opportunity to self-administer alcohol or the non-alcoholic beverage (depending on group assignment) was available under an FR 10 schedule on the right lever. Completion of each FR and subsequent contact with the drinkometer spout delivered fluid for the duration of spout contact or for a programmed duration (5 s), whichever came first and is defined as a single drink. Component 3 and the session ended after 120 min.

Drugs

All solutions for oral consumption were mixed using reverse osmosis (RO) purified drinking water. Ethyl alcohol (190 Proof, Pharmco-AAPER, Brookville CT) was diluted with RO water to 4% w/v alcohol. Orange-flavored, sugar-free, Tang® powder (Kraft Foods) was dissolved in RO water as described previously.⁶⁴ The 3-ISOPBC was synthesized in the laboratory of Dr. James Cook (University of Wisconsin-Milwaukee¹). Doses of 3-ISOPBC·HCl **2·HCl** (5.0–30.0 mg/kg) were dissolved in a vehicle of 50% saline, 37.5% propylene glycol, and 12.5% ethanol and administered via the intramuscular route (2–3 ml/injection). Vehicle tests were completed using the same volume and procedures as detailed below.

3-ISOPBC test procedures

The baseline stability criterion was defined as stable self-administration of alcohol or non-alcoholic beverage (i.e., $\pm 20\%$) for three consecutive sessions. To evaluate acute effects of 3-ISOPBC on alcohol-related behaviors and to verify the safety of the dose range, in Experiment 1, doses of 3-ISOPBC (10.0–30.0 mg/kg) or its vehicle were administered acutely in the alcohol group only. The baseline stability criterion was met before each test dose of 3-ISOPBC·HCl. Doses

were tested in mixed order, with active doses tested no more than once per week. In Experiment 2, doses of 3-ISOPBC·HCl (5.0–20.0 mg/kg) or vehicle was administered daily for 5 consecutive days to baboons in both groups. For both experiments, doses of 3-ISOPBC·HCl were administered 30 min before sessions.

Data analysis

The primary variables of interest included measures of seeking (Component 2: FI responses and latency to complete the FI requirement) and measures of consumption (Component 3: FR self-administration responses, drink contacts, and volume consumed). Total g/kg and ml/kg consumed were calculated based on individual body weights, and the total volume of alcohol or non-alcoholic beverage consumed, respectively. The patterning of drinking was analyzed as a function of drinking “bouts” as in our previous study.⁶⁵ A drinking bout was defined as 2 or more drinks with less than 5 min between each drink, beginning with the first drink. For each baboon, the mean of the 3 sessions that preceded each test condition was used as the baseline for comparison with doses of 3-ISOPBC and vehicle. To determine whether there were any differences in baseline responding in the alcohol and control groups, baseline responding in Experiment 2 was compared using independent-sample t-tests (baseline responding of the alcohol group in Experiment 1 is not included because corresponding control group sessions were not conducted). In Experiment 2, data analyzed were the last 3 of the 5 days of 3-ISOPBC or vehicle administration. Data were analyzed using separate statistical analysis of variance (ANOVA) for each group (Alcohol or Control) with 3-ISOPBC dose (BL, 0.0–30.0 mg/kg) as a repeated measure. Bonferroni post-hoc tests were used for pair-wise comparisons of the vehicle with 3-ISOPBC doses.

2.4.4. Role of $\alpha 1$ GABA_A Subunit-Containing Receptors in a Rhesus Monkey Model of Alcohol Drinking and Effect of β CCt and 3-PBC with Dr. Platt

Subjects

Eleven adult male rhesus macaques (*Macaca mulatta*), weighing between 9 and 14 kg, served as subjects. Monkeys were individually housed in a colony room with a 12:12 hour light/dark cycle and were fed monkey chow (Harlan Teklad Monkey Diet; Harlan Teklad, Madison, WI) once daily after the conclusion of the day's experimental session. Diets were supplemented with fresh fruit. Each animal received an additional 2 chow biscuits after the second hour of the 3-hour daily drinking session. Six monkeys participated in the alcohol self-administration studies, and a separate cohort of 5 monkeys participated in the sucrose self-administration studies. All animals had been previously trained to self-administer alcohol or sucrose using an operant panel.^{30,67} The sole exception was 1 sucrose drinker who had prior experience in operant intravenous cocaine self-administration procedures and was naive to the oral self-administration procedures. All procedures were conducted in accordance with the guidelines of the Committee on Animals of the Harvard Medical School and the National Institutes of Health Guide for the Care and Use of Laboratory Animals (Publication No. [NIH] 85-23, revised 1996). Research protocols were approved by the Harvard Medical School Animal Care and Use Committee.

Self-Administration Procedures

Drinking sessions occurred 5 d/wk in the animal's home cage. Each session lasted 3 hours. Access to water (via the standard cage associated sipper) was restricted beginning 1 hour before the start of the day's experimental session and restored 1-hour post session. Animals were trained to drink either alcohol (2%, w/v; n = 6) or sucrose solution (0.3 or 1%, w/v, depending on the

animal; n = 5) using an operant drinking panel mounted on the side of the home cage. The alcohol concentration was chosen because it maintained intake significantly above water levels and is on the ascending limb of the concentration-effect curve³⁰ thus allowing us to detect either increases or decreases in drinking. The sucrose concentrations were chosen because they maintained approximately equal levels of intake to ethanol (EtOH) under baseline conditions. The panel contained 2 retractable sippers (Med Associates, Inc., Georgia, VT) equipped with solenoids to minimize dripping and connected with tygon tubing to stainless steel reservoirs mounted outside of the cage. A response lever (Med Associates) was positioned below each sipper, and a set of colored lights positioned above. Each lever press resulted in an audible click and served as a response. In these experiments, only 1 side of the panel was active. Daily, illumination of white lights signaled the start of the session and alcohol or sucrose availability. Every 10 responses resulted in a switch from the illumination of the white light to illumination of a red light and extension of the drinking spout for 30 seconds. Depression of the spout during extension resulted in a fluid delivery, continuing as long as the sipper was both depressed and extended. Thus, both the actual duration (up to 30 seconds) and volume of intake were controlled by the subject. A brief (1 second) time out followed each spout extension, in which all stimulus lights were dark and responding had no programmed consequences. Responses were recorded and outputs controlled by a software program (MedPC; Med Associates). At the end of each session, reservoirs were drained and the amount of liquid consumed (ml) measured. Experimental compounds were administered as an intramuscular pretreatment 10 minutes before the start of a self-administration session. A range of doses was studied for each compound. Each dose of each compound was studied for a minimum of 5 consecutive sessions and until intake was stable, which was defined as no upward or downward trend in the amount consumed (ml) over 3 consecutive days. Following

evaluation of each dose, monkeys were returned to baseline self-administration conditions (i.e., with no pretreatment injection) until intake stabilized again. Doses were randomized within each treatment condition, and all doses of a particular compound were completed before beginning a new compound.

Observable Behavior

The behavior of each monkey was recorded for 5 minutes each day immediately following the conclusion of the day's self-administration session, using a focal animal approach as described in Platt and colleagues^{32,59} and modified for the rhesus monkey.³⁰ Briefly, a trained observer blind to the drug treatments watched a specific monkey for 5 minutes and recorded each instance that a particular behavior occurred during 15-second intervals.³⁰ Scores for each behavior were calculated as the number of 15-second bins in which the behavior occurred (e.g., a maximum score would be 20). The order in which animals were observed and the observer performing the scoring each day was randomized. Twelve observers participated in the scoring throughout the duration of the study; each observer underwent a minimum of 20 hours of training and met an inter observer reliability criterion of $\geq 90\%$ agreement with all other observers.

Blood Alcohol Levels

Blood alcohol levels (BALs) were determined for monkeys self-administering alcohol once stable self-administration was achieved at each dose of the drug treatments. Monkeys were anesthetized with ketamine (10 mg/kg, intramuscularly) immediately following the day's self-administration and behavioral observation sessions and 3 to 5 ml of blood collected in a sterile 10-ml tube (BD Vacutainer, sodium heparin 158 USP; BD, Franklin Lakes, NJ) from the femoral vein. Samples were then centrifuged at 1,150g for 8 to 12 mins. The plasma was transferred to polypropylene tubes and frozen at -80°C for later analysis. The analysis was conducted using a

rapid high-performance plasma alcohol analysis using alcohol oxidase with an AM1 series analyzer and Analox Kit GMRD-113 (Analox Instruments USA, Lunenburg, MA). This process reliably detects BALs ranging from 0 to 350 mg/dl with an internal standard of 100 mg/dl. BALs were determined in triplicate.

Drugs

Alcohol (95%; Pharmco Products, Brookfield, CT) was diluted to 2% w/v using tap water. Sucrose solutions were also prepared using tap water. The short-acting, nonselective benzodiazepine agonist triazolam^{68,69} and the α 1GABA_A preferring agonist zolpidem were obtained from Sigma/RBI (St. Louis, MO).⁷⁰ The nonselective benzodiazepine antagonist flumazenil,⁷¹ α 1GABA_A preferring antagonist β -carboline-3-carboxylate-*tert*-butyl ester (β CCT),¹⁴ and nonselective benzodiazepine inverse agonist ethyl β -carboline-3-carboxylate⁷² (β CCE) were either purchased from Sigma/RBI or provided by Dr. Jim Cook. The α 1GABA_A preferring antagonist 3- propoxy- β -carboline hydrochloride (3-PBC) was provided by Dr. Cook.¹⁴ All drugs were administered via intramuscular injection. All drugs except 3-PBC and β CCE were dissolved in propylene glycol and then diluted to the desired concentration using a 50% propylene glycol, 50% sterile water solution. 3-PBC required EtOH to be solubilized (final concentration; 10% EtOH, 50% propylene glycol, 40% sterile water), while β CCE was dissolved in a 20% emulphor, 10% EtOH, and 70% water vehicle. The doses for triazolam (0.001 to 1.0 mg/kg), zolpidem (0.1 to 10.0 mg/kg), β CCT (0.3 to 3.0 mg/kg), and 3-PBC (0.03 to 10.0 mg/kg) were chosen based on the previous studies in squirrel monkeys.^{27,73,74} Flumazenil doses (0.01 to 10 mg/kg) were chosen based on the dose range needed to shift the alcohol dose–response function in cynomolgus macaques.⁷⁵ β CCE doses (0.3 to 3.0 mg/ kg) were chosen based on the previous studies,⁷⁶ but tests were halted at the appearance of seizures in 1 animal (see Results). The

appearance of behavioral effects in the observational measures was considered in determining doses for all compounds.

Data Analysis

The alpha level for all statistical analyses was set at 0.05. Daily volumes (ml) served as the measure of intake for individual subjects. Dose was calculated as follows: [volume consumed (ml) alcohol concentration (g/ml)]/weight (kg). Data are expressed as mean intake over 3 sessions. To compare the effects of the test compounds on alcohol and sucrose self-administration, intakes were converted to percent baseline intake. Baseline intake was considered to be the mean amount of alcohol or sucrose consumed across the 3 days immediately prior to beginning pretreatment tests with a given dose of a compound. Separate 1-way repeated-measures analyses of variance (ANOVAs) followed by Bonferroni t-tests compared the effects of the pretreatment drugs to the effect of vehicle on intake and BALs. Given that self-administration sessions lasted 3 hours, one also characterized the pattern of drinking within the session using latency to first sipper extension and a total number of sipper extensions. Latencies and sipper extensions were recorded by the MedPC software system and later extracted manually from each day's data file using cumulative records generated by SoftCR software (MedAssociates). Latencies and extensions are expressed as mean latency or extensions across the treatment and compared using separate 1-way repeated-measures ANOVAs followed by Bonferroni t-tests to evaluate the effects of the pretreatment drugs compared with vehicle. Frequency scores for each observed behavior were averaged separately for the alcohol and sucrose groups and plotted as a function of dose for each of the α 1GABAA-preferring compounds. Normally distributed data (as determined by the Shapiro–Wilk test) were analyzed using a separate 1-way repeated-measures ANOVA (within group factor: dose) for each behavior. Bonferroni-corrected post hoc t-tests were used where appropriate.

2.4.5. Effect of 3-PBC·HCl (1·HCl) in Early Life Stress Induced Impulsivity Model and Excessive Alcohol Drinking in Adults MS Rats

Animals

Pregnant Sprague-Dawley dams were obtained from Harlan Laboratories (Frederick, MD) and offspring used in this study were born on site at the veterinary facility. They were subjected to the MS paradigm as described below and were tested for drinking and impulsivity behaviors as adults. An equivalent number of males and females were used in the binge drinking and impulsivity studies. Subjects were housed in groups of 2–3 per plastic cage until drinking studies began. The vivarium was maintained at an ambient temperature of 21 °C and was on a reverse 12-h light/dark cycle. All rats were provided ad libitum access to food and water. All training and experimental sessions for all subjects took place between 8:30 AM and 5:30 PM. The treatment of all subjects was approved by the IACUC of the Howard University College of Medicine. Moreover, all procedures were conducted in strict adherence with the National Institutes of Health Guide for the Care and Use of Laboratory Animals.

MS regimen

The maternal separation (MS) paradigm was performed as previously published,^{38,40} and was meant to emulate recurrent stressful experiences during the neonatal period. The number of pups in each litter ranged from 10 to 14 pups. To prevent litter effects, pups were sexed, culled to n¼10 with an equal number of males and females, and redistributed to nursing dams at P1. Beginning at P2 until weaning at P21, the separation comprised of removal of pups from their nursing mothers. They were brought to a designated room, separated from the mother, where the temperature was monitored and maintained at 29 °C. Each pup was placed in a cage located on a warmed pad, and visual access to other pups was blocked with cardboard. These conditions were

maintained for 3 h per day from 11:00 AM to 2:00 PM. After the 3 h separation time, they were returned to their home cage and rooms. Non-MS (CTL) pups were not separated from their mothers and were treated according to standard animal facility regulations.

Use of animals

Forty adult rats from 21 litters were used; 12 for western blotting and 28 for the behavioral studies, used over several months. Although these studies were not aimed at examining sex differences, both males and females were always represented. Therefore, this is a mixed-sex study. In any behavioral experiment, to control for litter effects, the maximum number of pups used from a single mother was one male and one female. Therefore, for a n¹/₄10 as an example, the minimum number of dams was 5 for each condition. For the operant binge drinking paradigm, there were n¹/₄10 controls (5F, 5M) and n¹/₄10MS (5M, 5F); 75% of these same animals were reused and added to other animals for the delay discounting experiments; n¹/₄9 controls (5F, 4M) and n¹/₄11 for MS (8F, 3M). For Western blotting analysis, a different cohort of animals was used with the same principle of heterogeneity to reduce litter effects; n¹/₄5–6 controls (2–3F, 3M) and n¹/₄6 for MS (3F and 3M). For drug dosage studies, some animals used were combined with other rats of the same age that had undergone similar sustained operant training to have a sufficient number for surgical implantation of the cannulae and subsequent behavioral testing, n¹/₄5 for CeA drug infusion (3F, 2M) and n¹/₄4 for mPFC studies.

Stereotaxic implantation of cannulae for microinfusions

Adult MS rats were anesthetized via isoflurane/oxygen gas inhalation and placed in a stereotaxic apparatus to allow for bilateral implantation of 22-gauge guide cannulae into the CeA or mPFC. The cannulae were anchored to the skull by four stainless steel screws and dental acrylic. A stylet was inserted into each cannula to maintain its viability and was only removed during

infusion times. The coordinates were based on the rat brain atlas of Paxinos and Watson as follows: CeA: AP, -2.0 mm; ML, \pm 3.6 mm; DV, -8.5mm from bregma; mPFC: AP, +2.7 mm; ML, \pm 1.45 mm; DV, -2.5mm from bregma at a 16° angle to the midline. Each cannula was placed 1.0mm above the intended target. This allowed the injector tip to extend below the cannula tip. The animals were given a 3-day recovery period before re-stabilization on the delay discounting or operant drinking paradigms. After behavioral experiments, cannula placement was confirmed visually by examination of cryostat-generated 300 μ m brain slices post-sacrifice.

Drugs and micro infusion procedure

The 3-propoxy-9H-pyrido [3,4-b]indole hydrochloride, commonly known as 3-propoxy- β -carboline hydrochloride (3-PBC), acting at the GABA_A α 1/ α 2 receptor, was obtained from Dr. James Cook at the University of Wisconsin-Milwaukee.¹ Antalarmin hydrochloride, a CRF antagonist, was obtained from R&D Systems Inc. (Minneapolis, MN). The drugs were mixed into 1mL of sterile PBS with Tween 20 added dropwise until dissolved, and then bilaterally infused into the CeA or mPFC at a rate of 0.1 mL/min for 5 min using a Harvard infusion pump. The overall design of experiments was such that doses of vehicle, 2, and 4 μ g of antalarmin, or 20 or 40 μ g of 3-PBC were injected immediately prior to animals being placed in the operant or delay discounting chambers. Animals rested 1-3 days between doses. The antalarmin infusion studies occurred before the 3-PBC infusion studies and were at least 2 weeks apart for any given animal. Different animals were used for the CeA and mPFC infusions. Antalarmin and 3-PBC were administered to MS rats to test their effects on the heightened operant responding and impulsivity profile of MS, whereas CTL rats do not consume significant levels of alcohol at baseline, nor does their impulsivity profile differ significantly at 8 sec compared to a 0 sec delay.

Delay discounting [impulsivity]

The impulsivity paradigm was executed as described by Oberlin & Grahame.⁷⁷ Impulsivity is operationally defined as choosing a smaller, immediate reward to the exclusion of a larger delayed reward,⁴⁸ and was quantified using the adjusted amount delay discounting (DD) assay.⁷⁸ Operant boxes consisted of a nosepoke light, two levers, a cue light above each lever, a house light, and a 10mL descending sipper tube for saccharin reinforcement [0.03% w/v]. Control of the operant boxes and data collection was with the MedPC IV software (MedAssociates, St. Albans, VT). Before actual testing, rats underwent four stages of behavioral shaping: Stage 1 is run for 1 session, and all center nose pokes are reinforced on a fixed ratio 1 (FR1) schedule with 20 s sipper access, where 1 lever press is required for sipper access. At stage 2, center nose pokes are reinforced on an FR1 schedule with 10 s sipper access, and the animal must complete 20 trials to move on to next stage. Stage 3 also requires 20 trials, but all trials are cued with a center light illuminated for 20 s. There is a 10 s intertrial interval. At stage 4, a nose poke and lever press is required for the 10-second sipper access, and both right and left levers are reinforced equally, 20 trials with a 10 s intertrial interval in 60 min is required.⁷⁷ After shaping, side bias was assessed by averaging the last 3 days' choices on each side. The large reinforcer was then assigned to their non-preferred side, to counter any initial side bias. After shaping had been completed, rats were assessed at 0 s delay. This time point is used as a task to evaluate discrimination of reinforcer (saccharin) magnitude prior to the introduction of any delay to the larger reward. Immediate reward amount started at 1 s of saccharin access, and was adjusted upwards and downwards by 0.1 s based on the rat's choices, i.e. an immediate choice resulted in down-adjustment of the sipper access time by 0.1 s on the next trial, whereas a delayed choice resulted in up-adjustment of the sipper access time by 0.1 s in the next trial. The total adjustments in access were restricted to a minimum

of 0 s and a maximum of 2 s. Average adjusted amounts of the reward over the last 20 trials of the session served as the measure of adjusted amount. All rats received 2- hour water access in their home cages at the end of daily testing.⁷⁷

Phase 1: Following behavioral shaping rats, were tested in the delay discounting paradigm at 0, 1, 4, 8, 12, 16 and 20 s delays. Each delay was tested for two consecutive sessions, and the two-day data for each delay was averaged.

Phase 2: Following completion of Phase 1, rats were randomly separated into treatment groups and bilaterally implanted with cannulae in the mPFC or CeA. After restabilization on the DD paradigm at a delay of 8 s, rats were infused with 3-PBC [20 or 40 µg] or antalarmin [2 or 4 µg] as described above and run in the impulsivity paradigm with an 8 s delay.

Operant drinking apparatus

Animals were tested in 11 standard operant chambers (Coulbourn Instruments, Inc., Lehigh Valley, PA) enclosed in an isolated chamber as previously described.⁷⁹ The operant apparatus contained two levers, two dipper manipulanda, triple cue lights over each lever, and a house light. The dipper cup size which contained the 10% (v/v) alcohol or 3% (w/v) sucrose reinforcers was 0.1 mL. The Coulbourn Graphic State “3” operant software (Coulbourn, Whitehall, PA) was used.

Drinking in the dark multiple scheduled access paradigm

To initiate excessive “binge” alcohol drinking, we employed a modification of the drinking-in-the-dark-multiple-scheduled- access (DIDMSA) protocol.^{79,80} First, the procedure entailed adapting the rats to a reverse 12 h/12 h light/dark cycle which began at 7:00 PM [lights on] and lasted to 7:00 AM [lights off]. Rats were trained to orally self-administer EtOH daily for two 45 min sessions with 30 min rest in between under an FR1 schedule employing the sucrose fading technique.¹³ After a period of stabilization on the FR1 schedule, the response requirement

was then increased to an FR4 schedule, where 4 lever presses were required for access to the reinforcer. For each schedule, responding was considered stable when responses were within $\pm 20\%$ of the average responses for five consecutive days. Stabilization on the FR4 schedule took ~ 8 days. During the stabilization procedures, the animals were never deprived of food or fluid. These procedures are well established in our laboratory.^{38,79} Other cohorts of rats were given a 3% [w/v] concentration of sucrose and trained identically under the FR1, then FR4, schedule. Following stabilization on the FR4 schedule for EtOH/ sucrose, the DIDMSA protocol began using an FR4 schedule where the rats were given access to 10% alcohol, or 3% sucrose on both the left and right levers. To initiate the DIDMSA protocol during the dark phase, rats were given a 45 min operant session. After the session had elapsed, rats were then placed in the home cage with food and water ad libitum for 30 min. Rats were then given a second 45 min operant session and subsequently returned to their home cage. Rats engaged in the alcohol drinking for 21 consecutive days. Using this protocol, the MS rats in the laboratory produced consistent BACs of 99 ± 3 mg%. Sucrose control rats were trained similarly, but lever pressed for a 3% sucrose solution instead of ethanol. The sucrose control rats permitted evaluation of reinforcing specificity following MS and drug treatments. Following 21 days of alcohol or sucrose drinking, rats were surgically implanted with bilateral cannulae into the CeA or mPFC. Rats (N¹/45/6) were then infused with 3-PBC [20 or 40 μ g] or antalarmin [2 or 4 μ g] as described above and were immediately placed in the operant chambers to respond for alcohol or sucrose. A 2-hour session consisted of two 45 min (90 min) access and 30 min of rest.

Blood alcohol concentration measurement

To ensure animals were consuming pharmacologically relevant amounts of EtOH to model human binge drinking (NIH-NIAAA, 2004),^{81,82} ~ 100 μ L of whole blood was collected from the

tail vein of MS and CTL rats (N¹/₄/treatment group) into a heparin-coated tube. After collection, the whole blood was immediately centrifuged for 5 min at 1100 rpm. Plasma samples of 5 mL were analyzed in a GL-5 Analyzer (Analox Instruments, Lunenburg, MA). Microanalysis consisted of measuring the oxygen consumption in the reaction between the sample of alcohol and alcohol oxidase using a Clark-type amperometric oxygen electrode. Alcohol reagent buffer solutions (pH 7.4) and alcohol oxidase enzymes were used in all samples tested. BACs were determined in duplicates after 90 min of drinking.

2.4.6. Effect of PBC Isoforms on Alcohol Drinking in P rats and Effect of 3-CycloPBC and 3-ISOPBC in Maternally Deprived (MD) Rats with Dr. Marjorie Gonde-Lewis

Drug Preparation

Four GABA_A receptor acting isoforms of 3-propoxy- β -carboline hydrochloride (3-PBC), namely β CCt, 3-ISOPBC, and cyclo-PBC, administered as HCl salts at doses of 5, 15, and 40 and 75 mg/kg, were utilized as drug treatments in this study. Each drug was prepared by dissolving the powder in a cocktail of 2% Tween and 99.8% saline solution. A pestle and mortar were commonly used to facilitate the entry of the drug into solution by placing the appropriate amount of Tween and drug in the mortar to create a paste. The volume of saline was added slowly to the mortar to bring it up to the necessary volume. Drugs were administered to each rat via oral gavage. Subsequently, rats were placed into the operant drinking chambers 15 minutes after gavage.

Operant Drinking

The following protocol was approved by the Howard University Animal and Use Committee. The PD72 Sprague-Dawley rats were trained for alcohol drinking using the drinking in the dark multiple schedule access (DIDMSA) paradigm involving multiple scheduled ethanol access sessions during the dark cycle of the rat. To facilitate shaping which induced the propensity

to seek fluid, animals were water-deprived for 23 h/day for the first two to three days of the training period. Rats were removed from their home cages and placed in operant conditioning boxes to begin lever pressing training using a 10% sucrose solution in tap water. Rats were trained for a total of 10-14 days in two 30-min daily sessions with a 45 minute break in between sessions. The drinking sessions are identified by one of two fixed ratio (FR) protocols; namely the FR1 or FR4 schedules which represent one and four lever presses, respectively, for the administration of reinforcer in the operant chamber. The reinforcer is administered in 0.1 mL aliquots. When the animals have been determined to be responding rapidly on the fixed ratio one (FR1) schedule for the 10% sucrose reinforcer solution, the deprivation was discontinued until stabilization was achieved. The response requirement was subsequently increased from FR1 to an FR4 schedule. Once responding stabilized, rats were exposed to 6 successive sessions in which the drinking solution was alternated daily between an EtOH/sucrose cocktail and EtOH (10% v/v) only. After this 6 day alternation procedure, EtOH concentrations in the EtOH/sucrose cocktail solution will be gradually raised from 2% to 5%, 7%, 9% and 10% (v/v) with the concentration of sucrose decreasing from 0.075% to 0.055, 0.025% and 0.0125% (w/v) and eventually eliminated at the 10% EtOH concentration level. All drug studies commenced once lever pressing for 10% EtOH on the FR4 protocol stabilized.

2.4.7. Effect of β CCt, 3-PBC, and 3-ISOPBC on the Spontaneous Locomotor Activity (SLA) and Diazepam Induced Sedation in Mice with Dr. Savic

Materials and methods

To assess the influence of 3-ISOPBC and 3-PBC on basal motor activity and diazepam-induced sedation, spontaneous locomotor activity assay (SLA) was performed in male C57BL/6 mice. The minimal dose of diazepam (DZP) which consistently induces sedation in animals in

given conditions was determined in the pilot dose-response study (data not shown). The SLA study was performed through two independent experiments. Firstly, the influence of 3-ISOPBC, 3-PBC, and β CCt (as the positive control) on basal motor activity and DZP-induced sedation was assessed in a full factorial design. The second experiment used the partial factorial design and the three times higher doses of ISOPBC and 3-PBC combined with DZP.

Spontaneous locomotor activity was assessed in an apparatus consisting of four white and opaque Plexiglas chambers (40×25×35 cm) under dim red light (20 lux). A digital camera mounted on the apparatus recorded animal activity, which was tracked and analyzed using ANY-maze Video Tracking System software (Stoelting Co, Wood Dale, IL, USA). DZP, β CCt, 3-PBC, and 3-ISOPBC were dissolved/suspended with the aid of sonication in the solvent (SOL) containing 85% distilled water, 14% propylene glycol and 1% Tween 80. In the first experiment, eight treatments were applied (n = 6-8 for each): SOL + SOL, DZP + SOL, β CCt + SOL, 3-PBC + SOL, 3-ISOPBC + SOL, β CCt + DZP, 3-PBC + DZP and 3-ISOPBC + DZP, all administered intraperitoneally in two injections one after another at separate sites in a total volume of 20 ml/kg. DZP was applied in a dose of 2 mg/kg, while the administered dose of β CCt, 3-PBC and 3-ISOPBC was 10 mg/kg. The second experiment included four treatments (n = 6 for each): SOL + SOL, DZP + SOL, 3-PBC + DZP and 3-ISOPBC + DZP, with 3-PBC and 3-ISOPBC being dosed at 30 mg/kg. In both experiments, a single mouse was placed in the center of the chamber without the acclimatization period, and its activity was followed for a total of 90 minutes. Chambers were cleaned with 70% ethanol after every trial. The behavioral parameters analyzed were the total distance traveled (m) and total time immobile (min) in two periods of time: 0–90 and 0–60 minutes. Statistical analysis (SigmaPlot 12.0, Systat Software Inc., San Jose, CA, USA) included two-way ANOVA for the first experiment (factors: Agonist (SOL and DZP) and Antagonist (SOL and β CCt

or PBC or ISOPBC), and one-way ANOVA for the second experiment; post hoc Student-Newman-Keuls (SNK) tests were used where applicable.

2.4.8. Determination of CNS (Central Nervous System) Sensorimotor Effects using Rotarod Studies with Nicholas Zahn at UWM

Swiss Webster/Balb/c mice were trained to maintain balance at a constant speed of 15 rpm on the rotarod apparatus (Omnitech Electronics Inc. Nova Scotia, Canada) until mice could perform for 3 min at three consecutive time points. Separate groups of mice received oral gavage administration (Intraperitoneal injections- 3-ISOPBC) of the vehicle (10% DMSO, 40% propylene glycol and 50% PBS) or test compounds. Diazepam was used as a positive control compound (5 mg/kg) in an approximate volume of 100 μ l. Ten minutes (five minutes for 3-ISOPBC·HCL) after each injection, mice were placed on the rotarod for 3 min. The same was repeated for 30 minutes and 60 minutes after administration. A fail was assigned for each mouse that fell from the Rotarod prior to 3 min. Mice were rested two to three days before administration of another dose or a different compound.

2.4.9. *In-vitro* Metabolic Stability Studies in Human Liver and Mouse Liver Derived Microsomes with Revathi Kodali at UWM

Chemicals and Reagents

Test compound (1 mM in DMSO), Verapamil HCl (1 μ M in Acetonitrile), phosphate buffer (0.5 M) pH 7.4, 18 m Ω water, NADPH Regenerating System Solution A (BD Bioscience Cat. No.451220), NADPH Regenerating System Solution B (BD Bioscience Cat. No. 451200), Human pooled liver microsome (BD Gentest, Cat. No. 452156), Mouse liver microsomes (Life Technologies, Cat. No. MSMC-PL).

Microsomal stability assay

Test compounds (10 μM) were incubated with human and mouse liver microsomes at a protein concentration of 0.5 mg/mL in a total volume of 400 μL containing 282 μL of water, 80 μL of phosphate buffer (0.5 M) pH 7.4, 20 μL of NADPH Solution A, 4 μL of NADPH Solution B, 4 μL of test compound (1 mM in DMSO) and 8.8 μL of liver microsomes. After preincubation at 37 $^{\circ}\text{C}$ for 5 minutes, the reaction was initiated by addition of microsomes and vials were stirred using a digital heat-shaking dry bath (Fischer Scientific, Cat. No. S08040). Aliquots of 50 μL were taken at time intervals of 0 (without microsomes), 10, 20, 30, 40, 50 and 60 min. Each aliquot was added to 100 μL of cold acetonitrile solution containing 1 μM of the internal standard verapamil, followed by sonication for 10 seconds and centrifugation at 10,000 rpm for 5 minutes. The 100 μL of the supernatant was transferred into Spin-X HPLC filter tubes and centrifuged at 13,000 rpm for 5 min. The filtrate was diluted and subsequently analyzed by LC-MS/MS (Shimadzu LCMS 8040). The ratio of the peak areas of the internal standard and test compound was calculated for every time point, and the natural log of this ratio was plotted against the time to determine the linear slope (k). The metabolic rate ($k \cdot C_0/C$), half-life ($0.693/k$), and internal clearance ($V \cdot k$) were calculated, where k is the slope, C_0 is the initial concentration of test compound (μM), C is the concentration of microsomes (mg/mL), and V is the volume of incubation (μL)/protein in the incubation (mg). All incubations throughout the study were performed in three experiments carried out in duplicate, and the data was presented as the average value of the standard deviation.

2.4.10. Evaluation of Cytotoxicity of β -Carbolines in HEK 293 and HEPG2 cells (Dr.

Michael Rajesh Stephen at UWM)

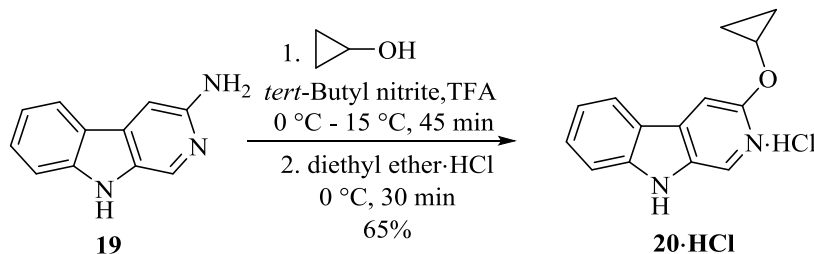
Cytotoxicity Assay Method

Human liver hepatocellular carcinoma (HEPG2) and human embryonic kidney 293T (HEK293T) cell lines were purchased (ATCC) and cultured in 75 cm² flasks (CellStar). Cells were grown in DMEM/High Glucose (Hyclone, #SH3024301) media to which nonessential amino acids (Hyclone, #SH30238.01), 10 mM HEPES (Hyclone, #SH302237.01), 5 x 10⁶ units of penicillin and streptomycin (Hyclone, #SV30010), and 10% of heat inactivated fetal bovine serum (Gibco, #10082147) was added. Cells were harvested using 0.05% Trypsin (Hyclone, #SH3023601), washed with PBS, and dispensed into sterile white, optical bottom 384-well plates (NUNC, #142762). After two hours, small molecule solutions were transferred with a Tecan Freedom EVO liquid handling system equipped with a 100 nL pin tool (V&P Scientific). The controls were 3-dibutylamino-1-(4-hexyl-phenyl)-propan-1-one (25 mM in DMSO, positive control) and DMSO (negative control). The cells were incubated for 48 hours followed by the addition of CellTiter-Glo™, a luminescence-based cell viability assay (Promega, Madison, WI). All luminescence readings were performed on a Tecan Infinite M1000 plate reader. The assay was carried out in quadruplet with three independent runs. The data were normalized to the controls and analyzed by nonlinear regression with GraphPad Prism.

2.4.11. Synthesis of 3-CycloPBC·HCl and WYS8

The amine **19** and WYS8 were synthesized as described previously in the literature.¹⁴

2.4.11.1. 3-Cyclopropoxy-9H-pyrido[3,4-b]indol-2-ium chloride (**20**)



An oven-dried round bottom flask was charged with amine **19** (1 g, 5.5 mmol), cyclopropanol (10 mL), TFA (2.1 mL, 27.72 mmol) added dropwise under a positive pressure of argon and cooled to 0 °C. *Tert*-butyl nitrite (3.3 mL, 27.72 mmol) was added dropwise slowly; the reaction mixture, which resulted, was then stirred for 30 mins at 0 °C, which resulted in a formation of red colored solution. It was then allowed to warm to 15 °C slowly and stirred for 10-15 min, meanwhile the reaction progress was monitored by TLC (silica gel, 50% EtOAc in hexane). After disappearance of starting material, the reaction mixture was diluted with EtOAc and concentrated under vacuum to yield the crude reaction mixture which was quenched with a sat aq NaHCO₃ solution (10 mL), and extracted with ethyl acetate (3 × 20 mL). The combined organic layer was washed with brine (60 mL), dried (Na₂SO₄), and concentrated under vacuum to yield the crude 3-cycloPBC. This material was further purified by flash column chromatography (silica gel, 20-30% EtOAc in hexane) to yield the 3-cycloPBC **20** as a light yellow colored solid (802 mg, 65%).

Caution: To further scale up (> 1.5 g) the reaction may become dangerous and safety precautions must be considered. This material was further converted into the hydrochloride salt, which was prepared by the reported method¹ to furnish a quantitative yield of **20**·HCl (932 mg) as a stable light greenish yellow colored solid; mp: 256-259 °C; ¹H NMR (300 MHz, DMSO-d₆) δ 12.03 (s, 1H), 8.70 (s, 1H), 8.42 (d, *J* = 8.0 Hz, 1H), 8.24 (s, 1H), 7.78 – 7.61 (m, 2H), 7.34-7.29 (m, 1H), 4.41 – 4.30 (m, 1H), 1.03 – 0.91 (m, 2H), 0.92 – 0.82 (m, 2H); ¹³C NMR (75 MHz, DMSO-d₆) δ

154.5, 144.7, 136.3, 132.2, 131.4, 125.3, 123.8, 120.4, 120.2, 112.9, 100.2, 53.2, 6.5; HRMS (ESI-TOF) (m/z): [M+H]⁺ calcd for C₁₄H₁₃N₂O: 225.1023, found: 225.1004 [note: The molecular ion was found devoid of the HCl and this is very common in the mass spectroscopy for salts]

2.5. REFERENCES

- (1) Tiruveedhula, V. V. N. Phani Babu.; Methuku, K. R.; Deschamps, J. R.; Cook, J. M. *Org. Biomol. Chem.* **2015**, *13*, 10705.
- (2) Yocum, G. T.; Gallos, G.; Zhang, Y.; Jahan, R.; Stephen, M. R.; Varagic, Z.; Puthenkalam, R.; Ernst, M.; Cook, J. M.; Emala, C. W. *Am. J. Respir. Cell Mol. Biol.* **2016**, *54*, 546.
- (3) Lewter, L. A.; Fisher, J. L.; Siemian, J. N.; Methuku, K. R.; Poe, M. M.; Cook, J. M.; Li, J. X. *ACS Chem. Neurosci.* **2017**, *8*, 1305.
- (4) Sawyer, E. K.; Moran, C.; Sirbu, M. H.; Szafir, M.; Van Linn, M.; Namjoshi, O.; Phani Babu Tiruveedhula, V. V.; Cook, J. M.; Platt, D. M. *Alcohol. Clin. Exp. Res.* **2014**, *38*, 1108.
- (5) O'Tousa, D. S.; Warnock, K. T.; Matson, L. M.; Namjoshi, O. A.; Linn, M. V.; Tiruveedhula, V. V.; Halcomb, M. E.; Cook, J.; Grahame, N. J.; June, H. L. *Addict. Biol.* **2015**, *20*, 236.
- (6) Gondre-Lewis, M. C.; Warnock, K. T.; Wang, H.; June, H. L., Jr.; Bell, K. A.; Rabe, H.; Tiruveedhula, V. V.; Cook, J.; Luddens, H.; Aurelian, L.; June, H. L., Sr. *Stress* **2016**, *19*, 235.
- (7) Holtyn, A. F.; Tiruveedhula, V. V.; Stephen, M. R.; Cook, J. M.; Weerts, E. M. *Drug Alcohol Depend.* **2017**, *170*, 25.
- (8) Fischer, B. D.; Schlitt, R. J.; Hamade, B. Z.; Rehman, S.; Ernst, M.; Poe, M. M.; Li, G.; Kodali, R.; Arnold, L. A.; Cook, J. M. *Brain Res. Bull.* **2017**, *131*, 62.
- (9) Forkuo, G. S.; Guthrie, M. L.; Yuan, N. Y.; Nieman, A. N.; Kodali, R.; Jahan, R.; Stephen, M. R.; Yocum, G. T.; Treven, M.; Poe, M. M.; Li, G.; Yu, O. B.; Hartzler, B. D.; Zahn, N. M.; Ernst, M.; Emala, C. W.; Stafford, D. C.; Cook, J. M.; Arnold, L. A. *Mol. Pharm.* **2016**, *13*, 2026.
- (10) Jahan, R.; Stephen, M. R.; Forkuo, G. S.; Kodali, R.; Guthrie, M. L.; Nieman, A. N.; Yuan, N. Y.; Zahn, N. M.; Poe, M. M.; Li, G.; Yu, O. B.; Yocum, G. T.; Emala, C. W.; Stafford, D. C.; Cook, J. M.; Arnold, L. A. *Eur. J. Med. Chem.* **2017**, *126*, 550.
- (11) Malatynska, E.; Knapp, R.; Ikeda, M.; Yamamura, H. I. *Brain Res. Bull.* **1989**, *22*, 845.

- (12) Picton, A. J.; Fisher, J. L. *Brain Res.* **2007**, *1165*, 40.
- (13) Harvey, S. C.; Foster, K. L.; McKay, P. F.; Carroll, M. R.; Seyoum, R.; Woods, J. E., 2nd; Grey, C.; Jones, C. M.; McCane, S.; Cummings, R.; Mason, D.; Ma, C.; Cook, J. M.; June, H. L. *J. Neurosci.* **2002**, *22*, 3765.
- (14) Yin, W.; Majumder, S.; Clayton, T.; Petrou, S.; VanLinn, M. L.; Namjoshi, O. A.; Ma, C.; Cromer, B. A.; Roth, B. L.; Platt, D. M.; Cook, J. M. *Bioorg. Med. Chem.* **2010**, *18*, 7548.
- (15) Mody, I.; Glykys, J.; Wei, W. *Alcohol* **2007**, *41*, 145.
- (16) Whissell, P. D.; Lecker, I.; Wang, D. S.; Yu, J.; Orser, B. A. *Neuropharmacology* **2015**, *88*, 24.
- (17) Olsen, R. W. *Proc. Natl. Acad. Sci. U. S. A.* **2011**, *108*, 4699.
- (18) Stamenic, T. T.; Poe, M. M.; Rehman, S.; Santrac, A.; Divovic, B.; Scholze, P.; Ernst, M.; Cook, J. M.; Savic, M. M. *Eur. J. Pharmacol.* **2016**, *791*, 433.
- (19) Kaminski, B. J.; Goodwin, A. K.; Wand, G.; Weerts, E. M. *Alcohol. Clin. Exp. Res.* **2008**, *32*, 1014.
- (20) Olsen, R. W.; Sieghart, W. *Neuropharmacology* **2009**, *56*, 141.
- (21) June, H. L.; Foster, K. L.; McKay, P. F.; Seyoum, R.; Woods, J. E.; Harvey, S. C.; Eiler, W. J.; Grey, C.; Carroll, M. R.; McCane, S.; Jones, C. M.; Yin, W.; Mason, D.; Cummings, R.; Garcia, M.; Ma, C.; Sarma, P. V.; Cook, J. M.; Skolnick, P. *Neuropsychopharmacology* **2003**, *28*, 2124.
- (22) Deminiere, J. M.; Piazza, P. V.; Guegan, G.; Abrous, N.; Maccari, S.; Le Moal, M.; Simon, H. *Brain Res.* **1992**, *586*, 135.
- (23) Blednov, Y. A.; Walker, D.; Alva, H.; Creech, K.; Findlay, G.; Harris, R. A. *J. Pharmacol. Exp. Ther.* **2003**, *305*, 854.
- (24) June, H. L., Sr.; Foster, K. L.; Eiler, W. J., 2nd; Goergen, J.; Cook, J. B.; Johnson, N.; Mensah-Zoe, B.; Simmons, J. O.; June, H. L., Jr.; Yin, W.; Cook, J. M.; Homanics, G. E. *Neuropsychopharmacology* **2007**, *32*, 137.
- (25) Kaminski, B. J.; Van Linn, M. L.; Cook, J. M.; Yin, W.; Weerts, E. M. *Psychopharmacology (Berl.)* **2013**, *227*, 127.
- (26) Licata, S. C.; Platt, D. M.; Cook, J. M.; Van Linn, M. L.; Rowlett, J. K. *Psychopharmacology (Berl.)* **2009**, *203*, 539.
- (27) Platt, D. M.; Rowlett, J. K.; Spealman, R. D.; Cook, J.; Ma, C. *Psychopharmacology (Berl.)* **2002**, *164*, 151.

- (28) Boehm, S. L., 2nd; Ponomarev, I.; Jennings, A. W.; Whiting, P. J.; Rosahl, T. W.; Garrett, E. M.; Blednov, Y. A.; Harris, R. A. *Biochem. Pharmacol.* **2004**, *68*, 1581.
- (29) Kumar, S.; Porcu, P.; Werner, D. F.; Matthews, D. B.; Diaz-Granados, J. L.; Helfand, R. S.; Morrow, A. L. *Psychopharmacology (Berl.)* **2009**, *205*, 529.
- (30) Ruedi-Bettschen, D.; Rowlett, J. K.; Rallapalli, S.; Clayton, T.; Cook, J. M.; Platt, D. M. *Alcohol. Clin. Exp. Res.* **2013**, *37*, 624.
- (31) Weerts, E. M.; Ator, N. A.; Grech, D. M.; Griffiths, R. R. *J. Pharmacol. Exp. Ther.* **1998**, *285*, 41.
- (32) Platt, D. M.; Rowlett, J. K.; Spealman, R. D. *J. Pharmacol. Exp. Ther.* **2000**, *293*, 1017.
- (33) Marinelli, M.; Piazza, P. V. *Eur. J. Neurosci.* **2002**, *16*, 387.
- (34) Koe, A. S.; Salzberg, M. R.; Morris, M. J.; O'Brien, T. J.; Jones, N. C. *Psychoneuroendocrinology* **2014**, *42*, 124.
- (35) Gilpin, N. W.; Karanikas, C. A.; Richardson, H. N. *PLoS One* **2012**, *7*, e31466.
- (36) Vargas, W. M.; Bengston, L.; Gilpin, N. W.; Whitcomb, B. W.; Richardson, H. N. *J. Neurosci.* **2014**, *34*, 14777.
- (37) Robinson, E. S.; Eagle, D. M.; Economidou, D.; Theobald, D. E.; Mar, A. C.; Murphy, E. R.; Robbins, T. W.; Dalley, J. W. *Behav. Brain Res.* **2009**, *196*, 310.
- (38) Gondre-Lewis, M. C.; Darius, P. J.; Wang, H.; Allard, J. S. *J. Chem. Neuroanat.* **2016**, *76*, 122.
- (39) Monroy, E.; Hernandez-Torres, E.; Flores, G. *J. Chem. Neuroanat.* **2010**, *40*, 93.
- (40) Wang, H.; Gondre-Lewis, M. C. *PLoS One* **2013**, *8*, e65517.
- (41) Heilig, M.; Goldman, D.; Berrettini, W.; O'Brien, C. P. *Nat. Rev. Neurosci.* **2011**, *12*, 670.
- (42) Phillips, T. J.; Reed, C.; Pastor, R. *Genes Brain Behav* **2015**, *14*, 98.
- (43) Lowery-Gionta, E. G.; Navarro, M.; Li, C.; Pleil, K. E.; Rinker, J. A.; Cox, B. R.; Sprow, G. M.; Kash, T. L.; Thiele, T. E. *J. Neurosci.* **2012**, *32*, 3405.
- (44) Huggins, K. N.; Mathews, T. A.; Locke, J. L.; Szeliga, K. T.; Friedman, D. P.; Bennett, A. J.; Jones, S. R. *Alcohol* **2012**, *46*, 371.
- (45) Cruz, F. C.; Quadros, I. M.; Planeta Cda, S.; Miczek, K. A. *Psychopharmacology (Berl.)* **2008**, *201*, 459.

- (46) Garcia-Gutierrez, M. S.; Navarrete, F.; Aracil, A.; Bartoll, A.; Martinez-Gras, I.; Lanciego, J. L.; Rubio, G.; Manzanares, J. *Addict. Biol.* **2016**, *21*, 847.
- (47) Crabbe, J. C.; Harris, R. A.; Koob, G. F. *Ann. N. Y. Acad. Sci.* **2011**, *1216*, 24.
- (48) Rachlin, H.; Green, L. *J. Exp. Anal. Behav.* **1972**, *17*, 15.
- (49) Forkuo, G. S.; Nieman, A. N.; Yuan, N. Y.; Kodali, R.; Yu, O. B.; Zahn, N. M.; Jahan, R.; Li, G.; Stephen, M. R.; Guthrie, M. L.; Poe, M. M.; Hartzler, B. D.; Harris, T. W.; Yocum, G. T.; Emala, C. W.; Steeber, D. A.; Stafford, D. C.; Cook, J. M.; Arnold, L. A. *Mol. Pharm.* **2017**, *14*, 2088.
- (50) Zanger, U. M.; Schwab, M. *Pharmacol. Ther.* **2013**, *138*, 103.
- (51) Hill, J. R. *Curr. Protoc. Pharmacol.* **2004**, Chapter 7, Unit 7. 8.
- (52) Perloff, M. D.; von Moltke, L. L.; Court, M. H.; Kotegawa, T.; Shader, R. I.; Greenblatt, D. J. *J. Pharmacol. Exp. Ther.* **2000**, *292*, 618.
- (53) Herraiz, T.; Guillen, H.; Aran, V. J. *Chem. Res. Toxicol.* **2008**, *21*, 2172.
- (54) Besnard, J.; Ruda, G. F.; Setola, V.; Abecassis, K.; Rodriguiz, R. M.; Huang, X. P.; Norval, S.; Sassano, M. F.; Shin, A. I.; Webster, L. A.; Simeons, F. R.; Stojanovski, L.; Prat, A.; Seidah, N. G.; Constam, D. B.; Bickerton, G. R.; Read, K. D.; Wetsel, W. C.; Gilbert, I. H.; Roth, B. L.; Hopkins, A. L. *Nature* **2012**, *492*, 215.
- (55) Huang, X. P.; Mangano, T.; Hufeisen, S.; Setola, V.; Roth, B. L. *Assay Drug Dev Technol* **2010**, *8*, 727.
- (56) Clayton, T.; Poe, M. M.; Rallapalli, S.; Biawat, P.; Savic, M. M.; Rowlett, J. K.; Gallos, G.; Emala, C. W.; Kaczorowski, C. C.; Stafford, D. C.; Arnold, L. A.; Cook, J. M. *Int J Med Chem* **2015**, *2015*, 430248.
- (57) Cao, R.; Peng, W.; Wang, Z.; Xu, A. *Curr. Med. Chem.* **2007**, *14*, 479.
- (58) Venault, P.; Chapouthier, G. *Sci. World J.* **2007**, *7*, 204.
- (59) Platt, D. M.; Duggan, A.; Spealman, R. D.; Cook, J. M.; Li, X.; Yin, W.; Rowlett, J. K. *J. Pharmacol. Exp. Ther.* **2005**, *313*, 658.
- (60) Chesnut, J. D.; Baytan, A. R.; Russell, M.; Chang, M. P.; Bernard, A.; Maxwell, I. H.; Hoeffler, J. P. *J. Immunol. Methods* **1996**, *193*, 17.
- (61) Ramerstorfer, J.; Furtmuller, R.; Vogel, E.; Huck, S.; Sieghart, W. *Eur. J. Pharmacol.* **2010**, *636*, 18.
- (62) Sigel, E.; Baur, R.; Trube, G.; Mohler, H.; Malherbe, P. *Neuron* **1990**, *5*, 703.

- (63) Li, X.; Cao, H.; Zhang, C.; Furtmueller, R.; Fuchs, K.; Huck, S.; Sieghart, W.; Deschamps, J.; Cook, J. M. *J. Med. Chem.* **2003**, *46*, 5567.
- (64) Duke, A. N.; Kaminski, B. J.; Weerts, E. M. *Addict. Biol.* **2014**, *19*, 16.
- (65) Kaminski, B. J.; Weerts, E. M. *Alcohol. Clin. Exp. Res.* **2014**, *38*, 376.
- (66) Weerts, E. M.; Goodwin, A. K.; Kaminski, B. J.; Hienz, R. D. *Alcohol. Clin. Exp. Res.* **2006**, *30*, 2026.
- (67) Vallender, E. J.; Ruedi-Bettschen, D.; Miller, G. M.; Platt, D. M. *Drug Alcohol Depend.* **2010**, *109*, 252.
- (68) Huang, Q.; He, X.; Ma, C.; Liu, R.; Yu, S.; Dayer, C. A.; Wenger, G. R.; McKernan, R.; Cook, J. M. *J. Med. Chem.* **2000**, *43*, 71.
- (69) Ziegler, W. H.; Schalch, E.; Leishman, B.; Eckert, M. *Br. J. Clin. Pharmacol.* **1983**, *16 Suppl 1*, 63S.
- (70) Crestani, F.; Martin, J. R.; Mohler, H.; Rudolph, U. *Br. J. Pharmacol.* **2000**, *131*, 1251.
- (71) Hunkeler, W.; Mohler, H.; Pieri, L.; Polc, P.; Bonetti, E. P.; Cumin, R.; Schaffner, R.; Haefely, W. *Nature* **1981**, *290*, 514.
- (72) Cowen, P. J.; Green, A. R.; Nutt, D. J. *Nature* **1981**, *290*, 54.
- (73) Lelas, S.; Rowlett, J. K.; Spealman, R. D.; Cook, J. M.; Ma, C.; Li, X.; Yin, W. *Psychopharmacology (Berl.)* **2002**, *161*, 180.
- (74) Rowlett, J. K.; Spealman, R. D.; Lelas, S.; Cook, J. M.; Yin, W. *Psychopharmacology (Berl.)* **2003**, *165*, 209.
- (75) Helms, C. M.; Rogers, L. S.; Grant, K. A. *J. Pharmacol. Exp. Ther.* **2009**, *331*, 142.
- (76) McMahon, L. R.; Gerak, L. R.; France, C. P. *J. Pharmacol. Exp. Ther.* **2006**, *318*, 907.
- (77) Oberlin, B. G.; Grahame, N. J. *Alcohol. Clin. Exp. Res.* **2009**, *33*, 1294.
- (78) Wilhelm, C. J.; Mitchell, S. H. *Genes Brain Behav* **2008**, *7*, 705.
- (79) Liu, J.; Yang, A. R.; Kelly, T.; Puche, A.; Esoga, C.; June, H. L., Jr.; Elnabawi, A.; Merchenthaler, I.; Sieghart, W.; June, H. L., Sr.; Aurelian, L. *Proc. Natl. Acad. Sci. U. S. A.* **2011**, *108*, 4465.
- (80) Bell, R. L.; Rodd, Z. A.; Engleman, E. A.; Toalston, J. E.; McBride, W. J. *Alcohol* **2014**, *48*, 225.
- (81) Bell, R. L.; Rodd, Z. A.; Lumeng, L.; Murphy, J. M.; McBride, W. J. *Addict. Biol.* **2006**, *11*, 270.

- (82) Naimi, T. S.; Brewer, R. D.; Mokdad, A.; Denny, C.; Serdula, M. K.; Marks, J. S. *JAMA* **2003**, 289, 70.

PART - II

DESIGN AND SYNTHESIS OF NOVEL ANTIMICROBIALS FOR THE TREATMENT OF DRUG RESISTANT BACTERIAL INFECTIONS

CHAPTER 3

INTRODUCTION TO ANTIBIOTICS

3.1. BRIEF HISTORY OF ANTIBIOTICS AND CLASSIFICATION

“Magic Bullet” as a term was first introduced by Paul Ehrlich¹, the father of chemotherapy, to describe a chemical compound that selectively targets pathogens and toxins in the human body with high affinity at lower concentrations without affecting the host cells.²⁻⁵ Ehrlich was convinced that a chemical compound could be synthesized in the laboratory that targets a parasite living in the other organism without affecting the host cell. This idea paved the way to the design of a drug to treat syphilis caused by *Treponema pallidum*, a terrible disease prominent during the early 1900's.⁶ Ehrlich along with another chemist Alfred Bertheim, and the bacteriologist, Sahachiro Hata discovered the agent during testing of 606 compounds; the drug was the 606th of the series and was employed treat to syphilis (Figure 3-2).⁷ Hoechst marketed this 606th compound under the name Salvarsan, and together with Neosalvarsan, a more soluble and less toxic analog, have remained the most prescribed drugs for syphilis (Figure 3-1).⁸

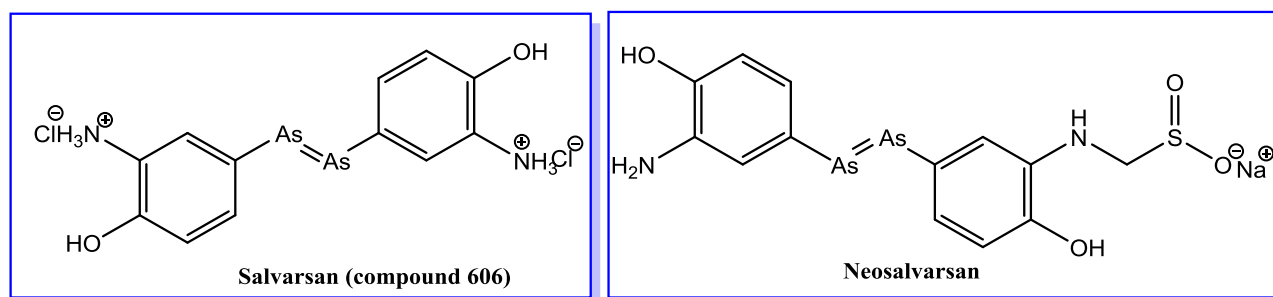


Figure 3-1. Structures of Salvarsan and Neosalvarsan

In the early days of research on antibiotics, two chemists from Bayer, Josef Klarer and Fritz Mietzsch synthesized the sulfa drug, sulfonamidochrysoidine. This medication known as Prontosil was tested for antibacterial activity in many diseases by Domagk.⁹ Despite the development of resistance to sulfa drugs, the derivatives of sulfanilamide remain one of the most successful drugs

even today.¹⁰ In September 1928 another discovery that revolutionized the status of medicine was the discovery of penicillin by Alexander Fleming.¹¹ Penicillin first was isolated from the mold of a *Penicillium* genus and found to be effective against gram-positive bacteria. The development of the purification of penicillin by Howard Florey and Ernest Chain led to mass production of the antibiotic for clinical applications.¹²



Figure 3-2. Paul Ehrlich (1854-1915) and Sahachiro Hata (1873-1938), Frankfurt 1910. Their partnership led to the discovery of a Salvarsan (Credit: Paul-Ehrlich-Institut, Langen, Germany)

Salvarsan, Prontosil, and penicillin stimulated the interest in the discovery of new antibiotics. Many novel drugs have been discovered between 1950 and 1970, which has been called the “golden era” of antibiotics. Later with the emergence of antibiotic resistance, many new antibiotics have been produced by modification of existing drugs to counter emerging drug resistance and reemerging resistance rather than a completely new class of medications.⁶

More than ever today, antibiotics remain essential medicines that effectively fight against life-

threatening illnesses.¹³ There is always a need for new antibiotics to cure infections and save lives. The development of bacterial resistance to previous drugs demands more immediate development of new antibiotics. Several different classes of antibiotics have a unique mode of action and are described below.¹⁴

3.1.1. Sulfonamides

This class of antibiotics contains an aryl sulfonamide moiety as a common structural feature. Prontosil was, as mentioned, the first discovered sulfonamide antibiotic.¹⁵ It acts by inhibiting dihydropteroate synthase, an enzyme involved in folic acid metabolism.¹⁴ In this paradigm DNA replication was repressed due to enzyme inhibition, and the agents which result from this, have shown bacteriostatic activity against gram positive and negative bacteria.¹⁶ Another drug, sulfamethoxazole, in combination with trimethoprim is used to target MRSA (Methicillin resistant *Staphylococcus aureus*) strains (Figure 3-3).¹⁷

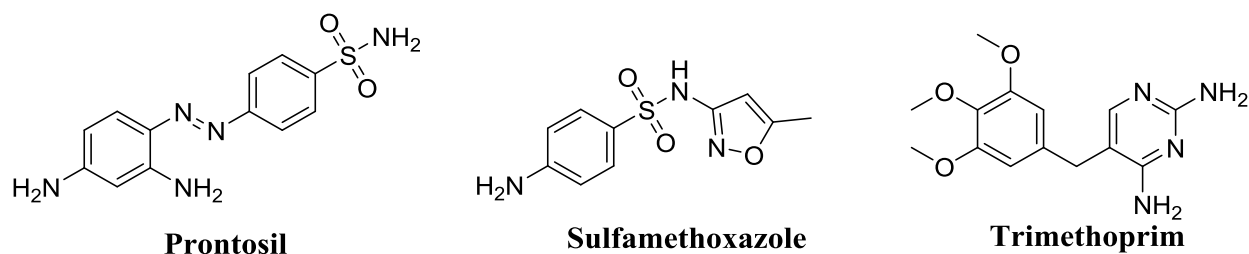


Figure 3-3. Structures of sulphonamides, and trimethoprim

3.1.2. β -lactams

These are very broad spectrum antibiotics active against most aerobic and anaerobic gram-positive and negative bacteria. The four-membered β -lactam ring is the active pharmacophore of these drugs and is critically important in clinical use.¹⁸

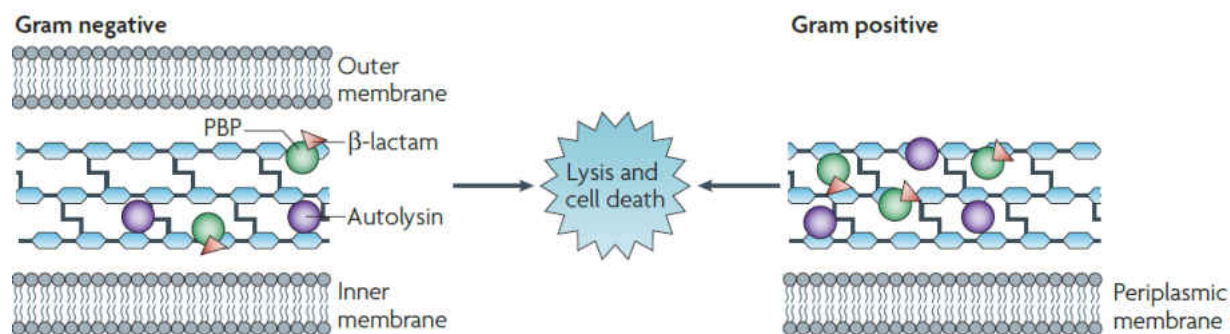


Figure 3-4. β -lactams target interactions and associated cell death¹⁶

3.1.2.1. Penicillins

Benzylpenicillin (penicillin G) was the first β -lactam antibiotic which was discovered; these β -lactam antibiotics are classified as penicillins, cephalosporins, and carbapenems. These antibiotics inhibit cell wall biosynthesis by acting as suicide substrates for penicillin binding proteins (PBP's) specifically affecting the peptidoglycan layer (Figure 3-4).¹⁹

Modifications have been made to penicillin G to increase the stability to penicillinases with bulky side chains in the case of methicillin and oxacillin. The ampicillin and amoxicillin, which are aminopenicillins and ureidopenicillin (such as piperacillin), are modified structures that show an increased spectrum of activity, as compared to penicillin G (Figure 3-5).¹⁴

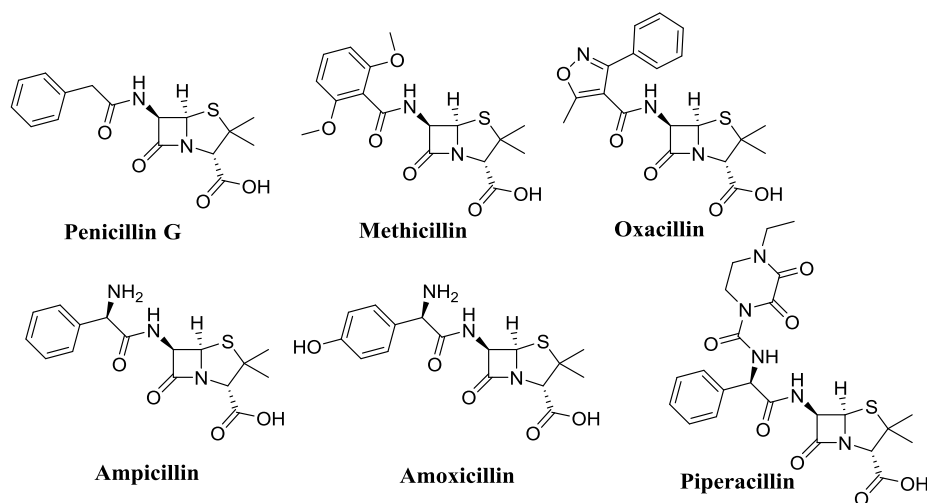


Figure 3-5. Structures of Penicillin antibiotics

3.1.2.2. Cephalosporins

Cephalosporin C was the first cephalosporin that was developed. These agents are thought to have a high pharmacokinetic profile and increased spectrum of activity, particularly against gram-negative bacteria. The FDA has approved the fifth generation cephalosporin, ceftaroline, which is active against MRSA^{20,21} and in combination with tazobactam, it has shown promising activity against resistant strains.²² The ceftolozane, currently in phase III clinical trials, is an

effective antibiotic against multidrug resistance gram-negative bacteria including *E. coli*, *K. pneumoniae*, and with superior activity against *P.aeruginosa* (Figure 3-6).

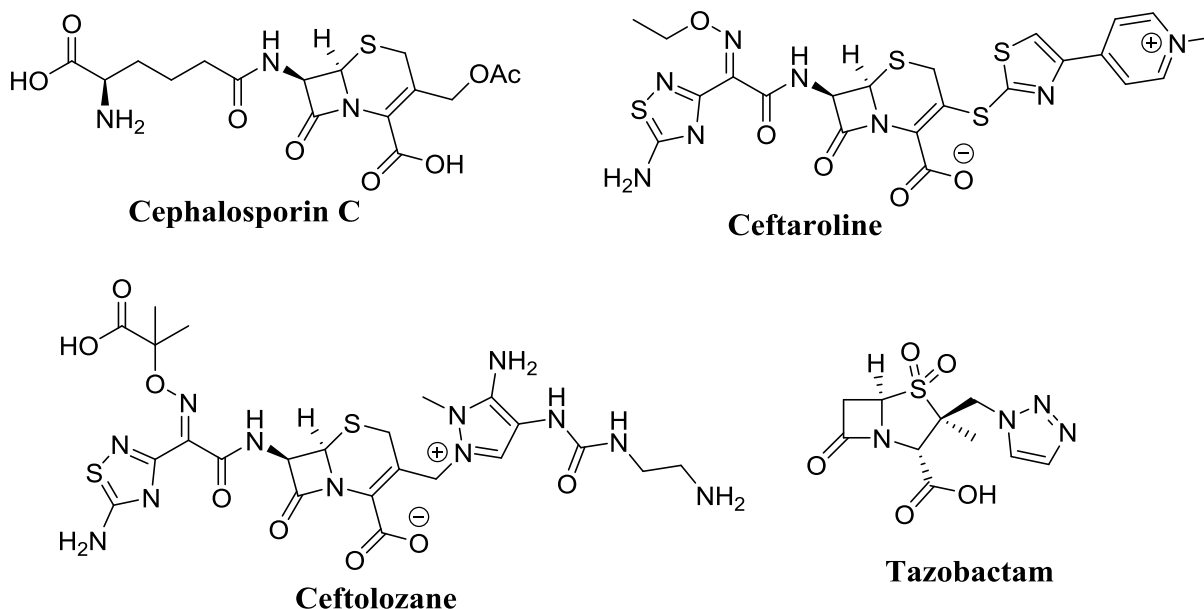


Figure 3-6. Structures of cephalosporin antibiotics and tazobactam

3.1.2.3. Carbapenem

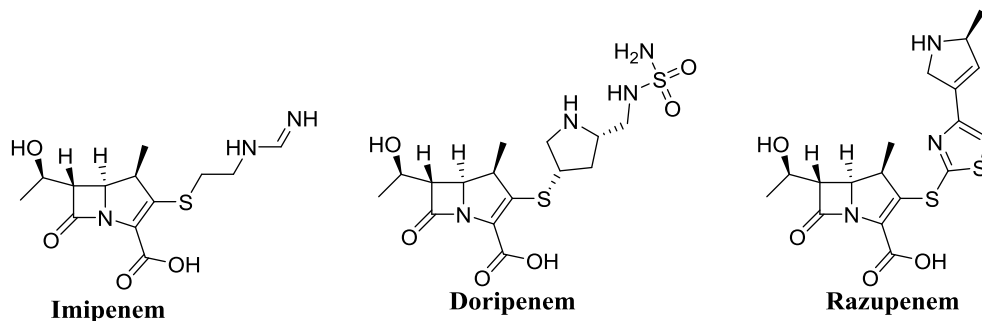


Figure 3-7. Structures of carbapenem antibiotics

Carbapenems are known to exert enhanced activity as drugs because they are resistant to extended broad-spectrum beta-lactamases (ESBLs.). Imipenem was first identified as a carbapenem in 1976.²³ Doripenem was approved in the US (2007) and Japan (2005); it is superior among the carbapenems particularly active against *P.aeruginosa*. However, it lacks activity against MRSA. A phase II carbapenem (razupenem) is known to be very effective against ampicillin resistant *E.faecium* (Figure 3-7).²⁴

3.1.3. Aminoglycosides

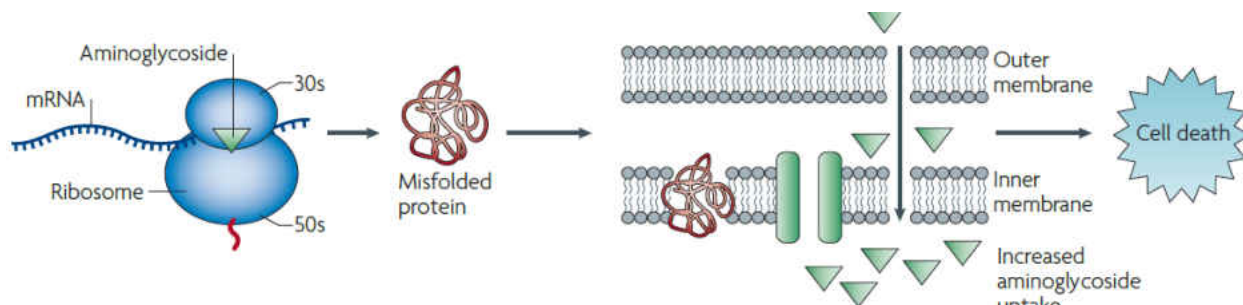


Figure 3-8. Aminoglycosides target 30S ribosome interactions and associated cell death mechanism¹⁶

Aminoglycosides are broad spectrum antibiotics active against most of the gram-negative bacteria including *M. tuberculosis* and some aerobic gram-positive bacteria. These agents consist of amino sugars connected through glycosidic bonds typically to a 2-deoxystreptamine core moiety. Streptomycin was the first important aminoglycoside antibiotic which was developed.¹⁵ The mode of action of these drugs is to target the 30S ribosomal subunit leading to a mistranslation in protein synthesis, which ultimately results in cell death (Figure 3-8).¹⁶

Until the occurrence of the mutation in a 30S ribosomal protein, streptomycin was used as the first-line agent for the treatment of tuberculosis.²⁵ Gentamicin, a natural aminoglycoside obtained from *Micromonospora*, is widely used against infections due to *Enterococci*, *Streptococci*, and *P. aeruginosa*. Tobramycin is unique and demonstrates its effect in cystic fibrosis and resultant *P. aeruginosa* lung infections (Figure 3-9).²⁶

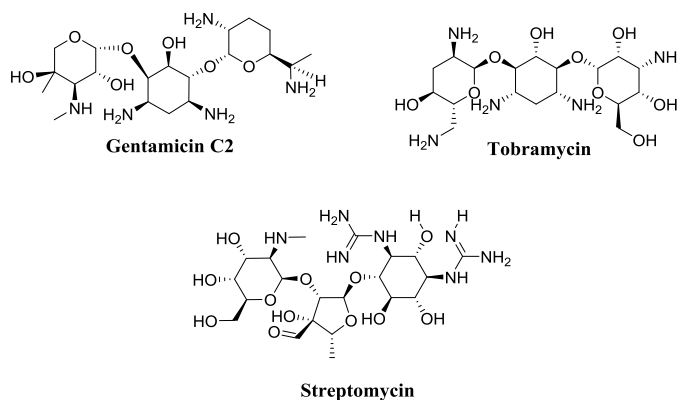


Figure 3-9. Structures of Aminoglycoside antibiotics

3.1.4. Macrolides

Erythromycin was the first macrolide antibiotic and was discovered in 1949. It was introduced into clinical use in 1951. Macrolides contain macrocyclic lactone rings with deoxy sugars, specifically cladinose or dosamine, attached by glycosidic bonds. Similar to aminoglycosides, they also act on ribosomes which interfere with protein synthesis. The binding of macrolides to the 50S subunit of ribosomes blocks the exit channel for peptides which results in the premature dissociation of peptidyl-tRNA from the ribosome and cell death.²⁷

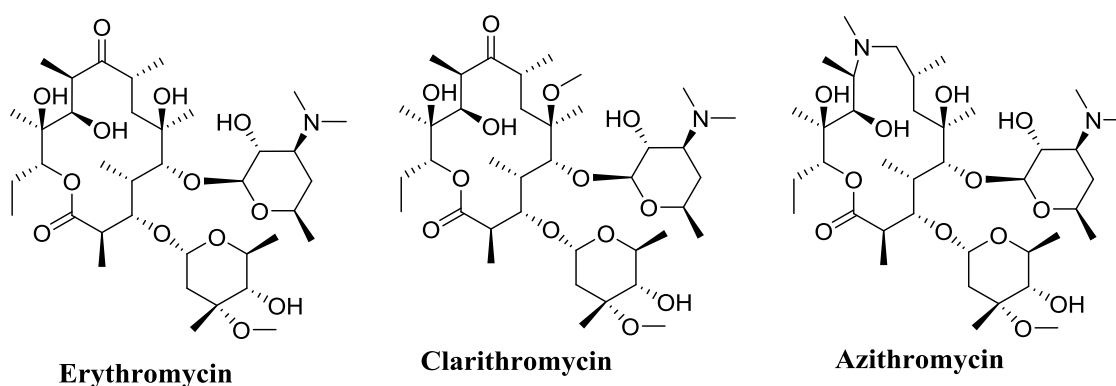


Figure 3-10. Structures of macrolide antibiotics

Macrolides act as bacteriostatic agents with broad spectrum antibacterial activity against aerobic and anaerobic gram-positive and some gram-negative bacteria. Azithromycin at higher concentrations serves as a bactericidal agent against infections caused by *H. influenzae*.²⁸ Improved pharmacokinetics, stability and expanded spectrum of action engender azithromycin and clarithromycin as first line antibiotics (Figure 3-10).²⁹

3.1.5. Tetracyclines

Chlortetracycline was the first tetracycline discovered, and the tetracycline antibiotics contain the octahydro-tetracene skeleton. These bacteriostatic agents attach to the 30S ribosomal subunit blocking aminoacyl-tRNA access to the ribosome during protein synthesis. The low

occurrence of severe side effects make these tetracycline antibiotics the first line therapy to treat many bacterial infections.³⁰

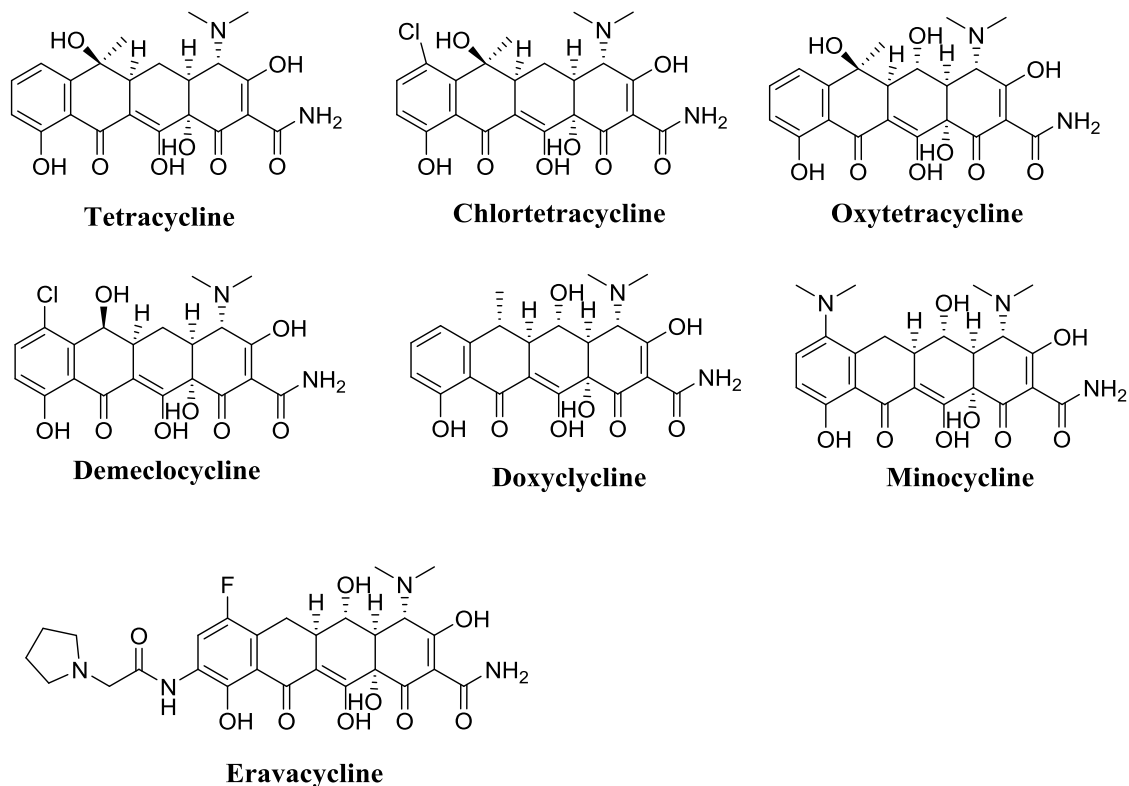


Figure 3-11. Structures of tetracycline antibiotics

Most of the first tetracyclines such as tetracycline, oxytetracycline, and demeclocycline are natural products, but the semisynthetic derivatives such as doxycycline and minocycline have shown good pharmacokinetic profiles.³¹ The fluorocycline, eravacycline in phase III clinical trials, is active against MRSA, vancomycin resistance *Enterococci* (VRE), *C. difficile*, and *Klebsiella pneumoniae* carbapenemase (KPC) producing gram-negative bacteria (Figure 3-11).³²

3.1.6. Rifamycins

Rifampicin is derived semi-synthetically from rifampicin B, a natural product obtained from *Nocardia* in 1957 by Lewis et al. These are ansamycin compounds which contain macrocyclic structures with a bridging aromatic moiety.¹⁵ Rifamycins are active against gram-

positive bacteria and *M. tuberculosis*, and because of low cellular permeability, they act as bacteriostatic agents in gram-negative bacteria.³³

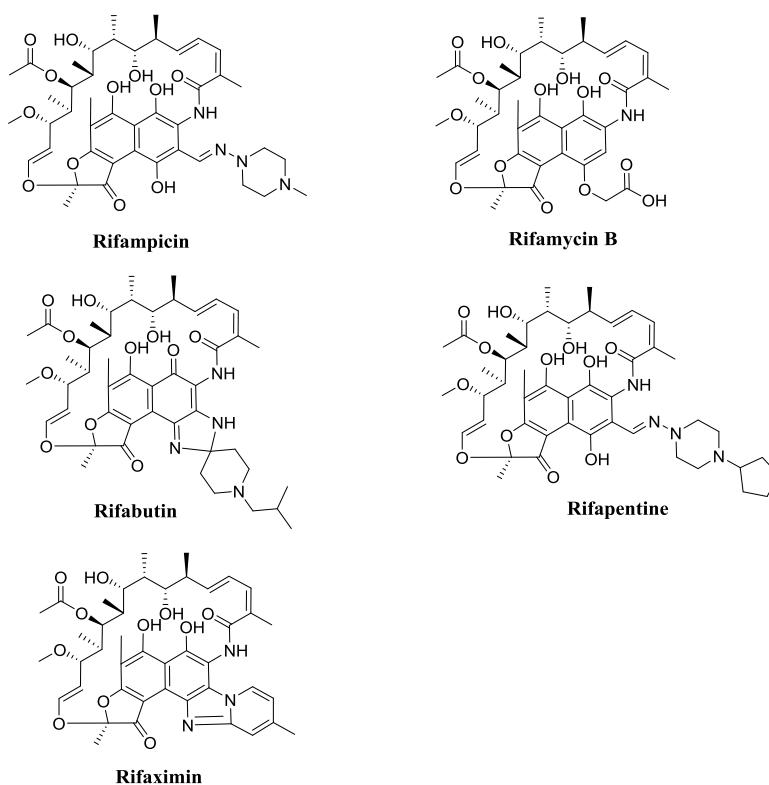


Figure 3-12. Structures of rifamycin antibiotics

Rifamycins interfere with the transcription process by binding with the β - subunit of RNA polymerase preventing the formation of m-RNA required for protein synthesis. Rifampicin is used in combination therapy with isoniazid and pyrazinamide as the first-line therapy in TB (tuberculosis) infections. Because of its high efficacy and common use for TB, rifampicin along with rifabutin and rifapentine are considered by the WHO as essential medications.¹⁸ Rifaximin is the only antibiotic approved by the FDA to treat *E. coli* infections associated with traveler's diarrhea (Figure 3-12).¹⁴

3.1.7. Quinolones

All quinolone antibiotics contain, of course, the basic quinolone core which usually is linked to an N-cyclic heterocycle with different substituents in the aromatic ring – A C (6) and/or

C (7) positions. Even though nalidixic acid (in a technical sense, it is a naphthyridone, not a quinolone) it was the first quinolone one discovered (1968). Ciprofloxacin, the synthetic analog of nalidixic acid, was introduced clinically.¹⁵

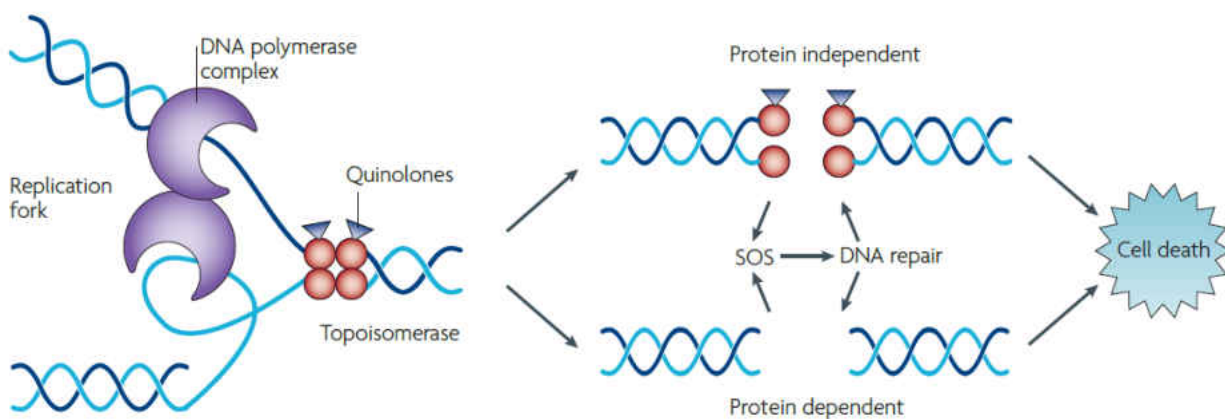


Figure 3-13. Quinolone drug interactions and associated cell death mechanism¹⁶

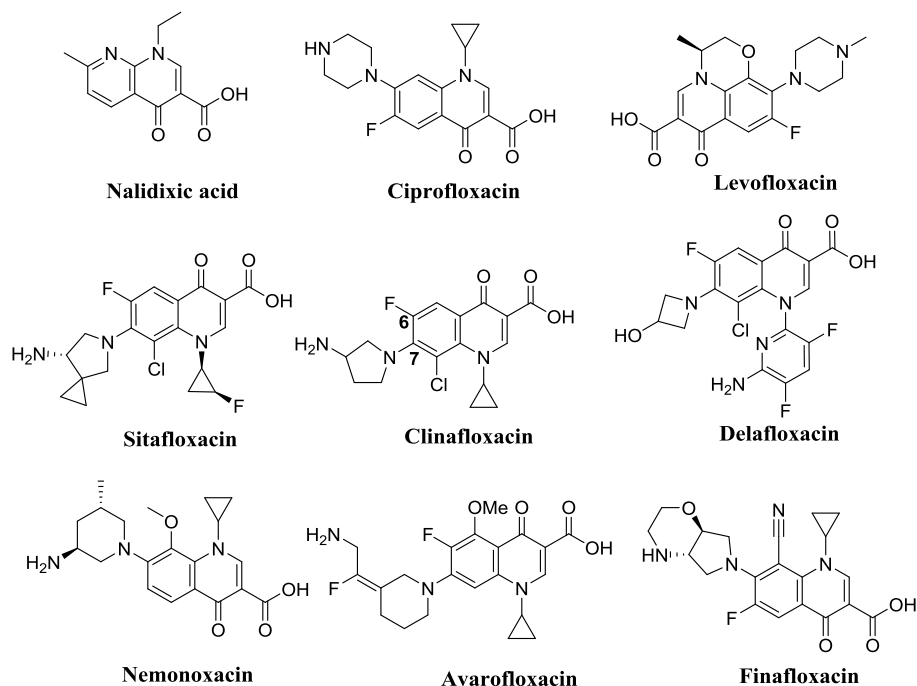


Figure 3-14. Structures of quinolone antibiotics

The unique mode of action of quinolones is to target topoisomerases II (DNA gyrase) and IV. These enzymes are involved in the DNA cleavage stage, consequently inhibiting DNA synthesis (Figure 3-13). The modern quinolones are known for bactericidal activity against most

gram positive and negative organisms. Because of poor biodistribution and a low spectrum of activity, the first-generation quinolones are rarely used today, the second-generation quinolones are characterized with broad spectrum activity in particular to gram-negative organisms. Ciprofloxacin, which belongs to the second generation has gained much attention due to its activity against virulent strains of *Bacillus anthracis* (anthrax) and *Yersinia pestis* (plague). Levofloxacin, the third generation quinolone is active against *Streptococcus* organisms. The fourth generation fluoroquinolones, sitafloxacin and clinafloxacin, target both DNA Gyrase and Topoisomerase IV simultaneously. The fourth generation quinolones exhibit an expanded spectrum of activity against anaerobic bacteria (Figure 3-14).¹⁴

3.1.8. Glycopeptides

The glycopeptides are known to inhibit cell wall biosynthesis, but act differently as compared to β -lactams. These macrocyclic peptides are interspersed with aromatic moieties and saccharide side chains connected through glycosidic bonds. The well-known vancomycin was the first glycopeptide discovered in 1952.¹⁵ Glycopeptides bind sterically to the terminal D-Ala-D-Ala dipeptide unit of peptidoglycan units which render them unsuitable as substrates for PBP's and transglycosylases which interferes with the cell wall synthesis in gram-positive bacteria.³⁴

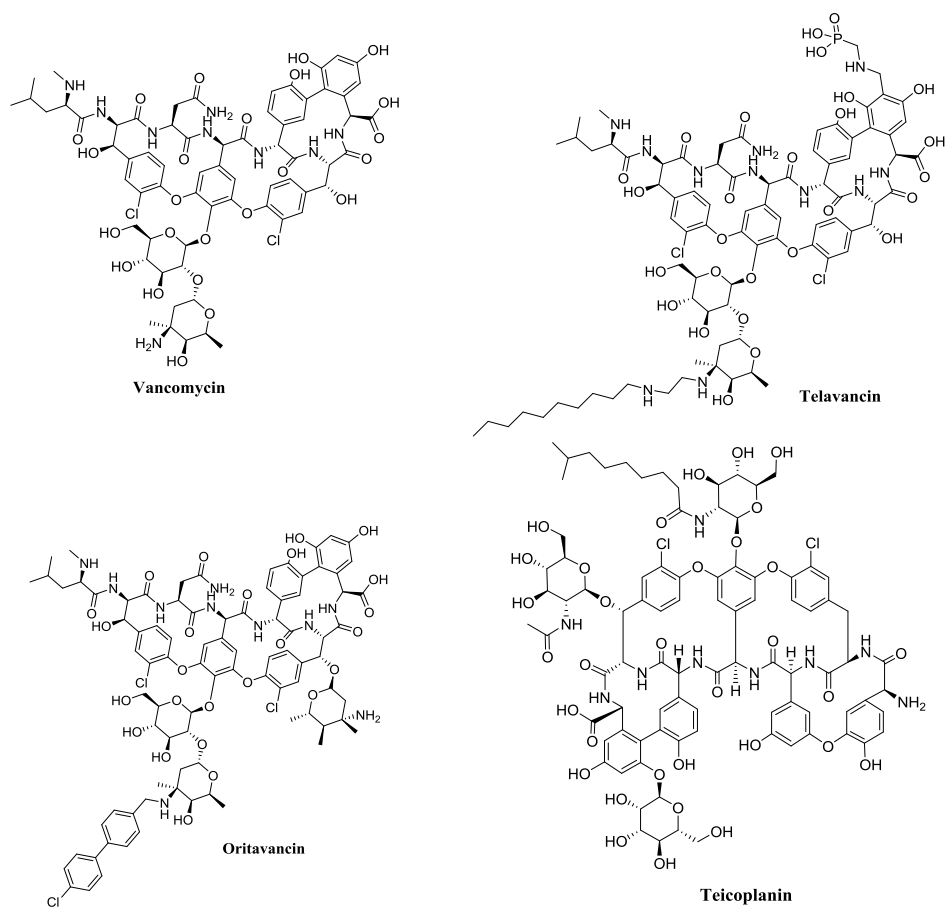


Figure 3-15. Structures of glycopeptide antibiotics

Vancomycin and teicoplanin are two drugs with the same efficacy, but the side chain of teicoplanin helps to overcome the drug resistance due to vancomycin. In 2009, the US FDA approved telavancin for use against MRSA, resistant *Enterococci*.³⁵ Oritavancin, the current drug in Phase III clinical trials is particularly active against Vancomycin Resistant *Staphylococcus aureus*, *S. Pneumoniae*, and Vancomycin-Resistant *Enterococci* (Figure 3-15).³⁶

3.1.9. Polymyxins

Polymyxins A-E are natural products derived from bacillus and were first discovered in 1947.³⁷ These exert broad spectrum activity particularly against gram-negative bacteria, although some strains of *E. coli*, *Klebsiella*, *Enterobacter* and *M. tuberculosis* developed resistance.^{38,39}

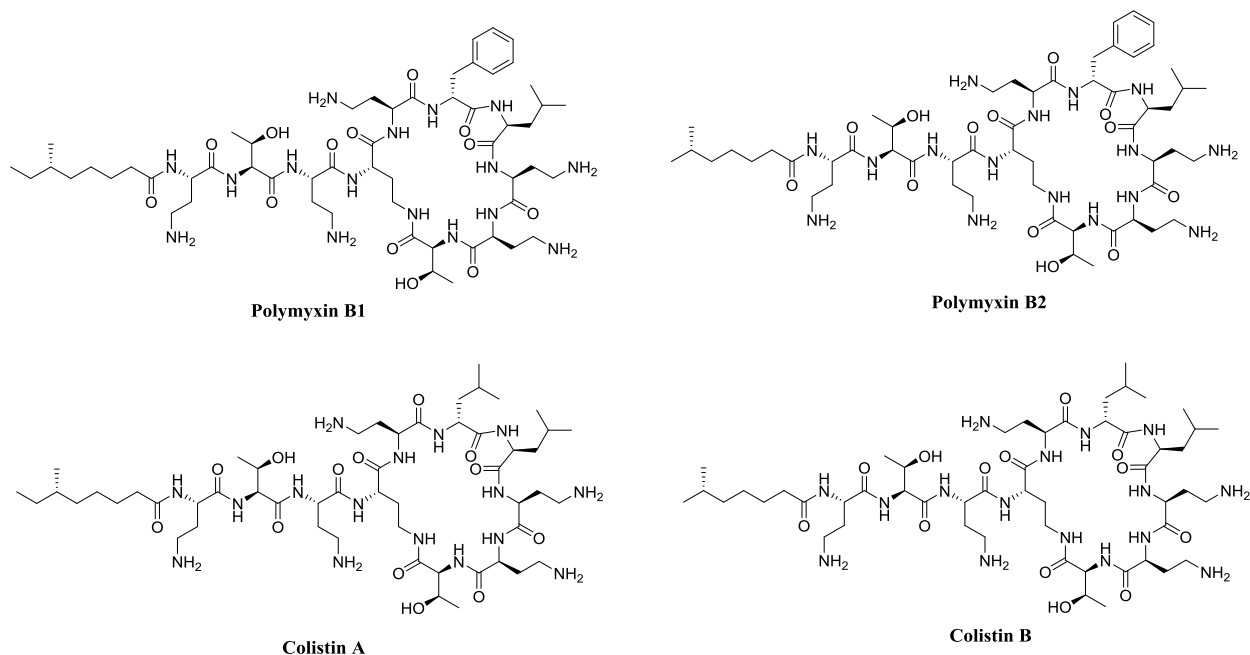


Figure 3-16. Structures of polymyxin antibiotics

Polymyxins are polycationic species that displace the stabilizing magnesium and calcium ions which normally interact, electrostatically, with the anionic lipopolysaccharide (LPS) outer layer in gram-negative membranes. This interaction leads to increased permeability, cell leakage and eventually cell death.⁴⁰ Colistin A and B antibiotics are also known to have potential anti-endotoxin activity⁴¹ as an added benefit to combat infections and are used in the treatment options against MDR *Pseudomonas*, *Klebsiella*, and *Acinetobacter* strains (Figure 3-16).⁴²

3.1.10. Oxazolidinones

The oxazolidinone antibiotics contain a shared oxazolidinone core with N-linked aryl and heterocyclic rings and as well as a short side chain at C-5. The peptidyl transferase center on a 50S ribosomal subunit is a potential target site for these antibiotics, which leads to blockage of peptide bond formation and subsequently interferes with protein translation.⁴³

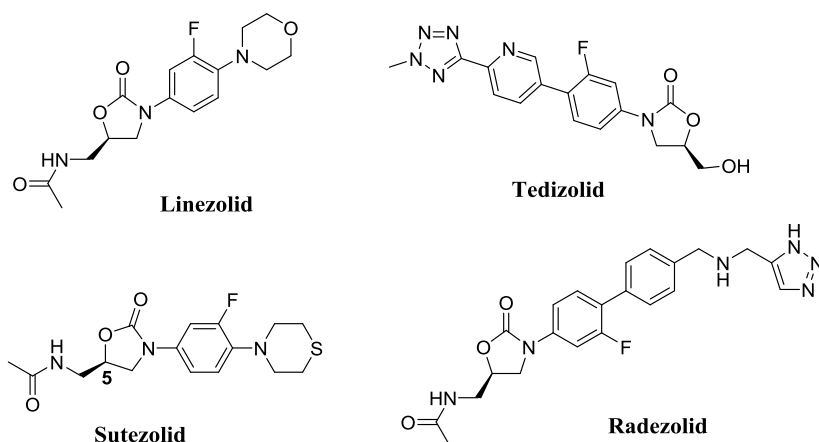


Figure 3-17. Structures of oxazolidinone antibiotics

Linezolid is used to treat infections caused by resistant gram negative bacteria including MRSA and VRE.^{44,45} Many of the oxazolidinones were set back due to poor solubility, pharmacokinetics, and toxicity profiles.⁴⁶ However, tedizolid and radezolid, currently in clinical trials, have shown improved activity even against Linezolid-resistant *Staphylococci* and MRSA strains.⁴⁷ Sutezolid of Pfizer's is in phase II clinical trials and is particularly active against *M. tuberculosis* isolates which are resistant to isoniazid, rifampicin, ethambutol, and streptomycin (Figure 3-17).⁴⁸

3.1.11. Streptogramins

Based on the mechanism of action and structure, the streptogramins are classified into class A, and class B. Class A compounds are 23 membered unsaturated macrocycles which contain peptide and lactone bonds. These Class A antibiotics bind to the PTC (peptidyl transfer center) region of the 50S ribosomal subunit to inhibit initiation and translocation of protein formation. Class B streptogramins are 19 membered depsipeptides which bind at the peptide exit tunnel and further inhibit the elongation stage of translocation during protein synthesis.^{15,16}

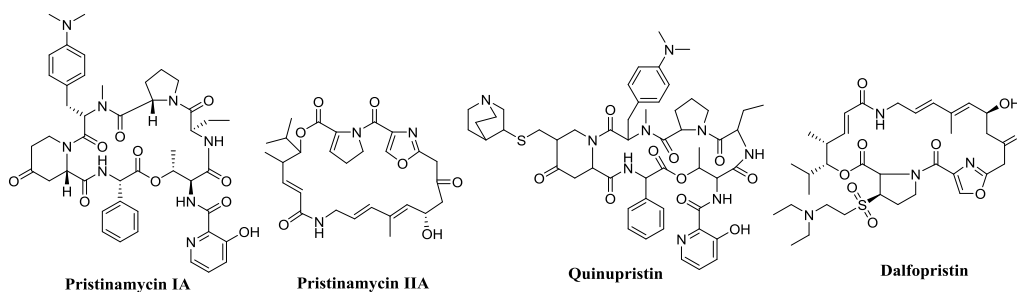
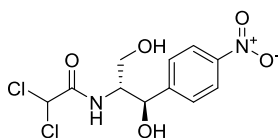


Figure 3-18. Structures of streptogramin antibiotics

These agents are typically used in pairs for clinical applications. Pristinamycin is one among them, and itself is a combination of class A and B molecules. Dalfopristin and pristinamycin exhibit excellent antibacterial properties against MRSA. Quinupristin exerts activity against vancomycin-resistant *E. faecium* and is bacteriostatic in strains which contain erythromycin resistant methylase (*erm*) genes (Figure 3-18).⁴⁹

3.1.12. Amphenicols

Chloramphenicol is the only member of this class to be approved. It is active against gram positive and negative bacteria including anaerobes (Figure 3-19).¹⁶ These phenylpropanoid antibiotics bind to the peptidyl transferase center of the 50S ribosomal subunit to inhibit the elongation step of translation in protein synthesis.⁵⁰ Amphenicols exhibit bactericidal activity against *H. influenzae*, *N. meningitidis*, and *S. pneumoniae*.



Chloramphenicol

Figure 3-19. Structure of chloramphenicol

3.1.13. Lipopeptides

Lipopeptides are complex molecules which contain cyclic depsipeptides with peptidyl side chains capped with a saturated alkyl tail. They disrupt the structural integrity of cell membranes by inserting their lipophilic tails into the cytoplasmic membranes of gram-positive bacteria. This

integration leads to potassium efflux due to depolarization of cell membranes and eventually cell death.¹⁵

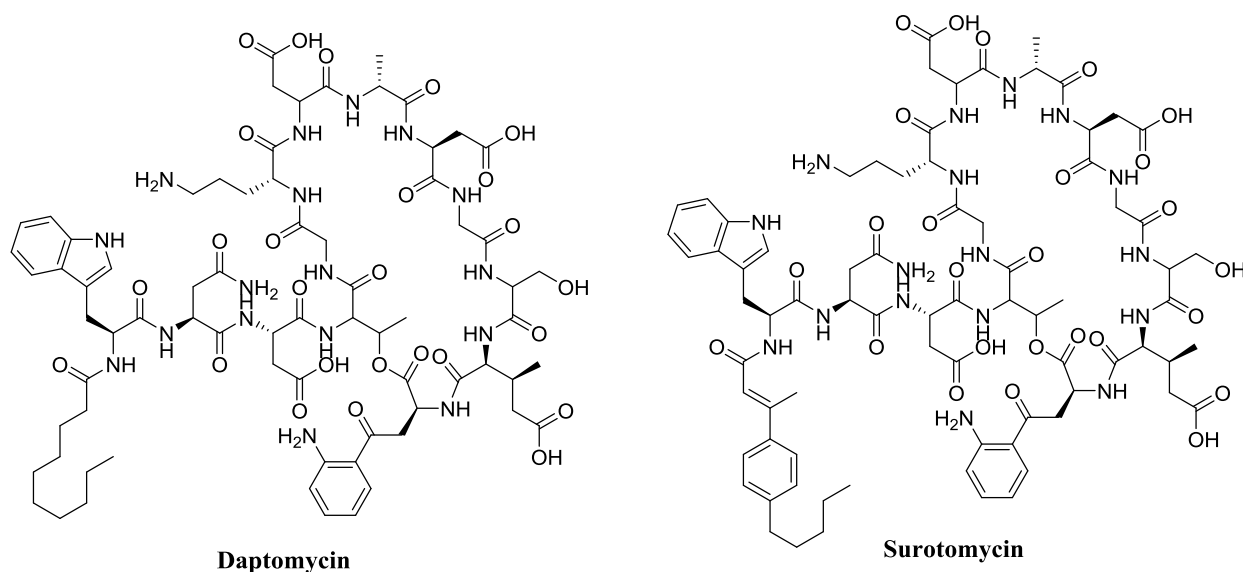


Figure 3-20: Structures of lipopeptide antibiotics

Daptomycin exhibited excellent activity against gram-positive pathogens including MRSA and VRE.⁵¹ Surotomycin is in phase III clinical trials and was found effective against *C. difficile* infections (Figure 3-20).

In addition to the well-known antibiotics described above, there are pleuromutilins,^{52,53} macrolactones,^{15,54} and diarylquinolines^{55,56} which act at the cellular and nuclear level to fight bacterial infections. In recent years due to the widespread emergence of resistance, there has been a shift towards the use of combination drug therapy. Combined therapy has been more effective in the treatment of HIV [Highly Active Anti-Retroviral Therapy (HAART)] and in treatment of *M. tuberculosis* to combat resistance.⁵⁷ An overview of different antibiotic classes and their mode of action is illustrated in Figures 3-21 and 3-22.

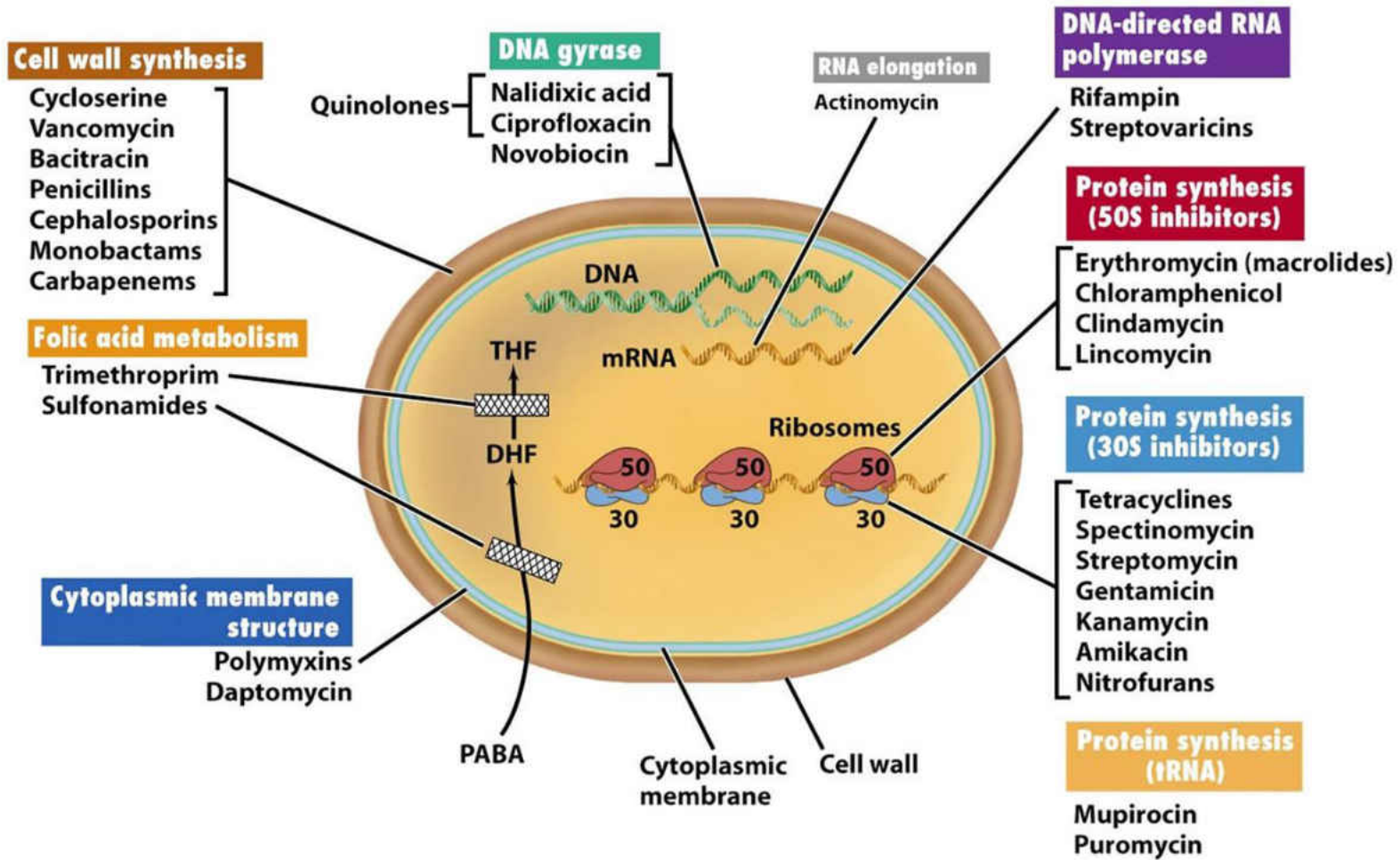


Figure 20-14 Brock Biology of Microorganisms 11/e
 © 2006 Pearson Prentice Hall, Inc.

Figure 3-21. An overview of different classes of antibiotics according to their mode of action

Key: ● COMMONLY ACT AS BACTERIOSTATIC AGENTS, RESTRICTING GROWTH & REPRODUCTION ● COMMONLY ACT AS BACTERICIDAL AGENTS, CAUSING BACTERIAL CELL DEATH

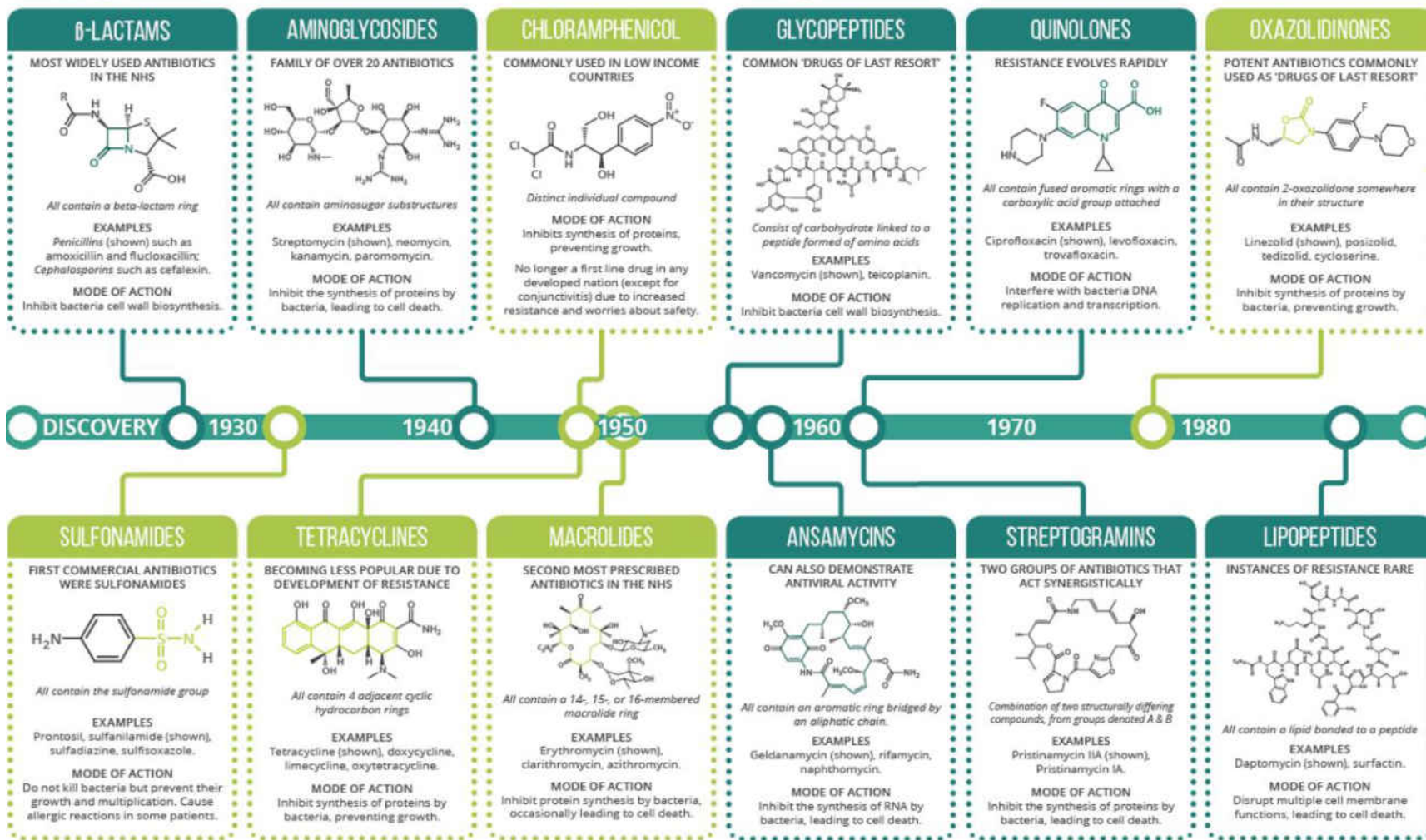


Figure 3-22. An overview of different classes of antibiotics (Credit: www.compoundchem.com)

3.2. TUBERCULOSIS

Tuberculosis is one of the most significant diseases prevailing even today and is fatal to millions of people each year.⁵⁸ In 2015, there were 1.4 million deaths worldwide due to TB, and also the reason for the death of 0.4 million TB infected people living with HIV [World Health Organization (WHO)]. According to the WHO, in 2015 there were 10.4 million new cases of TB worldwide; of these nearly 6 million were men who accounted for 56 %, followed by 3.5million women (34%) and the rest were children. The Sustainable goals (SDGs) and WHO’s End TB strategy now targets the reduction of the global burden of TB infections during the time period 2016-2035. This strategy targets a 35% reduction in deaths from TB and a 20% reduction in the new TB cases by 2020.

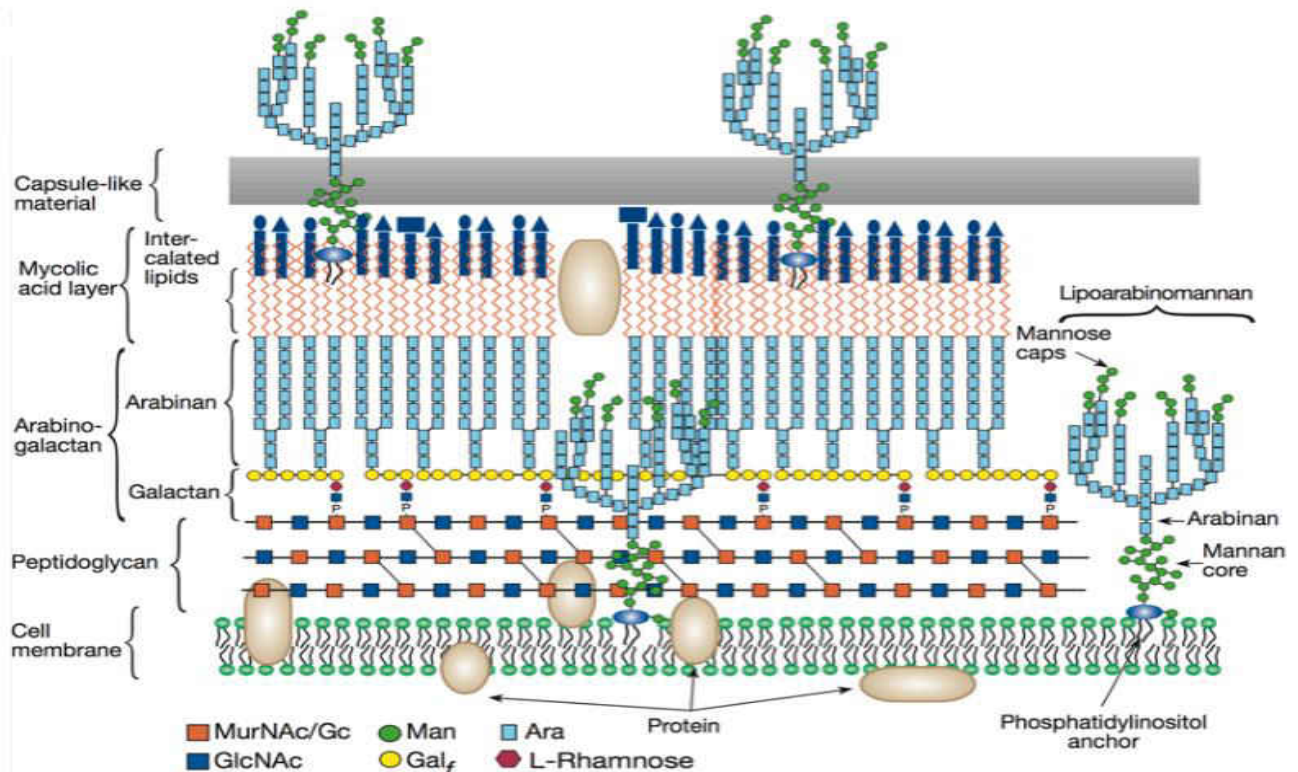


Figure 3-23. Microscopic structure of *Mycobacterium tuberculosis* cell wall

Tuberculosis is caused by *Mycobacterium tuberculosis*, a rod-shaped non-spore-forming bacterium. These are acid-fast bacilli with a distinct cell wall that plays a major role in its survival. The cell wall contains mycolic acid attached to an underlying peptidoglycan layer, bound to a polysaccharide arabinogalactan that provides an extraordinary lipid layer. This unique feature of the cell wall accounts for most of the bacterial virulence, growth, and resistance.⁵⁹ Lipoarabinomannan, the carbohydrate structural antigen is present on the outer side of the bacterial cell wall. This lipoarabinomannan is employed to combat immunogenic effects and promote the survival of the mycobacteria inside the macrophages (Figure 3-23).⁶⁰

Tuberculosis is an airborne infection. *Mycobacterium tuberculosis* is transmitted through the droplet nuclei as a result of coughing, sneezing, talking or singing of a person infected with tuberculosis. The transmission and intensity depend on many factors including the number of bacilli in droplets, virulence of bacilli, bacilli exposure to UV light, and degree of ventilation. Apart from the lungs, the organism can spread to the lymphatic system, pleura, bones, joints, or meninges causing extrapulmonary tuberculosis.⁶⁰

3.2.1. Pathophysiology

Once a healthy person becomes infected with the droplets containing bacilli, the mucus-secreting goblet cells in the upper airway tract trap all the bacteria. Mucus catches the foreign particles, and the cilia on the outer surface of the cells beat vigorously to remove the entrapped particles by expelling upwards.⁶¹ This mucociliary system provides the first line of defense to prevent people from becoming infected with tuberculosis.⁶²

The bacilli which were unaffected by the mucociliary system will find their way to alveoli spaces, which contain alveolar macrophages, the abundant immune cells of the air sacs.⁶³ The bacteria which entered into the air sacs are surrounded and engulfed by macrophages.

Macrophages act as the second line of defense in preventing the invading mycobacteria. The phagocytic macrophages engulf the bacilli and several mechanisms involving the surface receptors act to prevent the infection.⁶⁴ The lipoarabinomannan on the cell surface of bacilli serves as a ligand for the macrophages that help in the recognition of the mycobacteria.⁶⁵ The complement protein C3 enhances recognition of bacilli by the macrophages and helps in opsonization even if it is the first time exposure to the mycobacterium.^{66,67}

The cascade events initiated by macrophages either result in the efficient control of infection or the active disease progresses to tuberculosis. It also depends on the combination of the host defense system and virulence of pathogenic mycobacteria. The preliminary control of TB may also lead to latent tuberculosis, recurring after some time span.

Once ingested by macrophages the mycobacterium continues to multiply every 25 to 32 hours. The macrophages produce numerous amounts of proteolytic enzymes and cytokines to degenerate the bacilli.^{64,65} The release of cytokines acts as a site for the attraction of T-lymphocytes, which are involved in cell-mediated immunity. Once T-lymphocytes reach the infection site, macrophages present the bacterial antigen on their surface to T-Lymphocytes. For about 2 to 12 weeks the primary immune responses take place, and bacteria still continue to divide inside the macrophages. If these reach high numbers, they can be detected by the skin test (Figure 3-24).^{61,64}

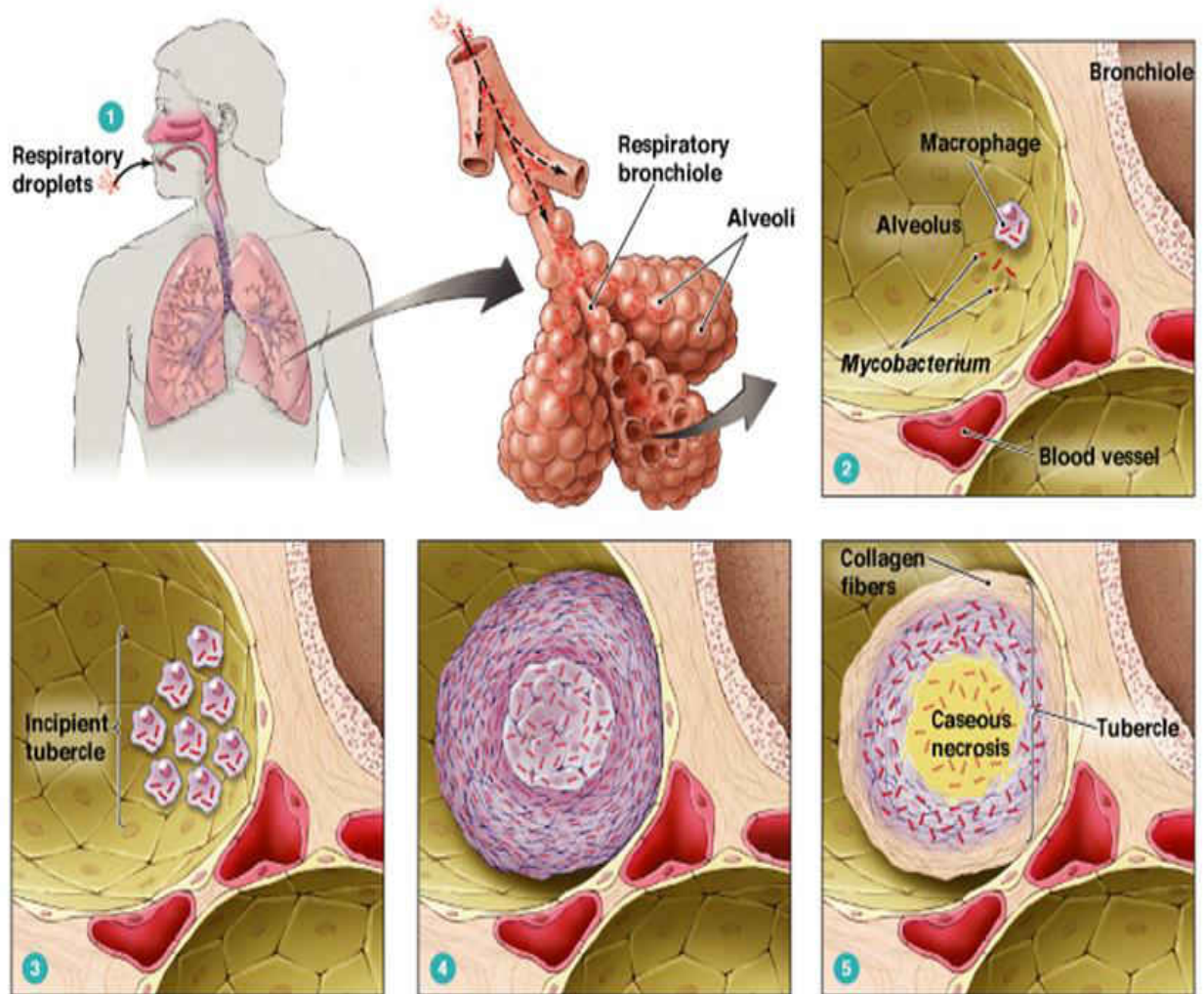


Figure 3-24. Pathophysiology of tuberculosis infection (Credit: <http://novicetoexpert.org/book/tuberculosis>)

Another defensive mechanism in persons with a good immune defense is the formation of granulomas around the mycobacterium. These nodular granulomas contain accumulated T-lymphocytes and macrophages that create a microenvironment to restrict the replication and spread of the bacilli.^{61,65} This microenvironment further kills the macrophages producing the necrotic lesion at the center of the granuloma. With the progression of 2-3 weeks, the necrotic tissue further softens known as caseous necrosis and this constitutes a low pH, low oxygen supply, and decreased nutrients. These conditions lead to the establishment of latency with calcification, and fibrosis containing the bacilli in the dormant lesions. In persons with a weak immune system, the formation

of the granuloma is not complete leaving the disease active. The latent TB infected person, if immunocompromised, the necrotic tissue will become liquefied with the loss of structural integrity in the fibrous lesion wall. This damage allows the bacteria to spread to the bronchi, or to the other parts of the body through blood vessels which causes the extrapulmonary tuberculosis infection (Figure 3-24).⁶⁸

3.2.2. Clinical Manifestations

Tuberculosis grows in different ways in individuals depending on the cellular process progression and immunity system of an infected person. These stages are as follows

3.2.2.1. Latent Tuberculosis

The mycobacterium is enclosed in the fibrous lesion.⁶² There are no signs or symptoms of infection observed. The person does not feel sick and not infectious [Centers for Disease Control and Prevention (CDC)]. Once there is a diminished immune response in these individuals or coinfection with Human Immunodeficiency Virus, the infection is reactivated. There are other conditions such as uncontrolled diabetes mellitus, sepsis, renal failure, malnutrition, smoking, chemotherapy, organ transplantation, and long-term steroid use that can also activate the infection.⁶⁸ According to the CDC, the higher incidence of activation of latent TB usually occurs in people of old age due to the decreased immune system (Table 3-1).

3.2.2.2. Primary Disease (active)

Due to the spread of the mycobacterium through the lymphatic system, the primary disease is characterized by paratracheal lymphadenopathy. The primary disease is associated with pleural effusion inducing fever, chest pains, and dyspnea. This stage is detected by diagnostic tests. The lack of breathing sounds, due to fluid filled pleural spaces are the physical findings at this stage (Table 3-1).

Table 3-1. Differences in the stages of tuberculosis

Early infection	Early primary progressive (active)	Late primary progressive (active)	Latent
Immune system fights infection Infection generally proceeds without signs or symptoms Patients may have fever, paratracheal lymphadenopathy, or dyspnea Infection may be only subclinical and may not advance to active disease	Immune system does not control initial infection Inflammation of tissues ensues Patients often have nonspecific signs or symptoms (eg, fatigue, weight loss, fever) Nonproductive cough develops Diagnosis can be difficult: findings on chest radiographs may be normal and sputum smears may be negative for mycobacteria	Cough becomes productive More signs and symptoms as disease progresses Patients experience progressive weight loss, rales, anemia Findings on chest radiograph are normal Diagnosis is via cultures of sputum	Mycobacteria persist in the body No signs or symptoms occur Patients do not feel sick Patients are susceptible to reactivation of disease Granulomatous lesions calcify and become fibrotic, become apparent on chest radiographs Infection can reappear when immunosuppression occurs

3.2.2.3. Primary Progressive Tuberculosis

Only a few individuals develop active tuberculosis when they are exposed to mycobacterium bacilli. Progressive fatigue, malaise, weight loss and low-grade fever indicates infection. Wasting is the prominent feature that results in the loss of fat and lean muscle.⁵⁸ A cough eventually develops in almost all of the patients. The finger clubbing, which results from poor oxygen supply, is the late indication.⁶⁹ Hemoptysis occurs due to ruptured blood vessels characterized by blood streaks in the sputum. The patients are diagnosed with anemia due to increased leukocytosis as a response to the infection (Table 3-1).

3.2.2.4. Extrapulmonary Tuberculosis

Although the pulmonary system is the primary target for tuberculosis infection, some cases are identified where extrapulmonary organs are infected with bacilli. A few of the fatal conditions are meningitis, the spread of bacilli to the brain and miliary tuberculosis infecting the blood stream involving multiple organ damage. Other affected locations include bone, joints, and pleura, among which lymphatic tuberculosis is the most common.⁵⁸

3.2.3. Treatment for Tuberculosis

Even today the treatment of tuberculosis remains challenging, and there is always a demand for new drugs for effective treatment.⁷⁰ The factors such as early diagnosis and screens for drug resistance help for primitive detection and immediate treatment.⁷¹ The combination of medications based on inhibition of acquired resistance and increased efficiency are considered to treat mycobacterium. The treatment of TB requires particular attention due to the emergence of Multi-Drug Resistance TB (MDR-TB) and Extensively Drug Resistance TB strains (XDR-TB).⁷²

Streptomycin was the first antibiotic, obtained from *Streptomyces griseus*, to be proven effective against *Mycobacterium tuberculosis*.⁷³ During treatment with streptomycin, the improvement in patient health was seen in the initial three months and gradually deteriorated due to the occurrence of streptomycin resistance.⁷⁰ From the 1950's onwards several drugs effective against tuberculosis were discovered initiating treatment for a duration of 18 months or more. This lead (resistance) to the use of combination therapy (Figure 3-27).^{74,75} Based on the potency, drug class, efficiency, application of use, and the TB drugs available, treatments are classified into the following classes:

3.2.3.1. First Line Anti-TB Drugs

These drugs are currently prescribed for the four drug combination regimen to treat drug-susceptible TB. These compounds are taken orally and include isoniazid, which acts by inhibiting mycolic acid synthesis by targeting Enolyl-[acyl-carrier-protein] reductase.⁷⁰ Rifampicin is a transcription inhibitor and acts on the beta subunit of RNA polymerase which prevents formation of m-RNA.⁷⁵ The pyrazinamide discovered in 1954, acts on the 30S ribosomal subunit inhibiting protein formation by interfering with translation.⁷⁴ Ethambutol is one of the agents which acts on

arabinosyl transferases to prevent the biosynthesis of arabinogalactan in the cell walls of mycobacterium (Figure 3-25).

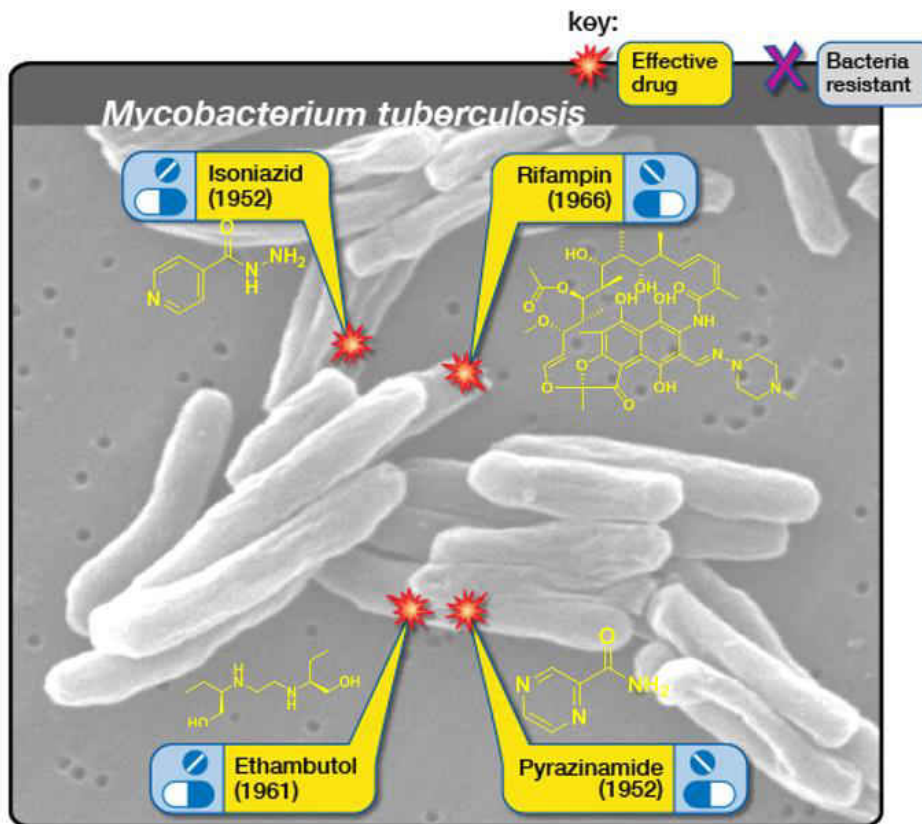


Figure 3-25. First line treatment of TB for Drug Sensitive TB (Credit: NIAID)

3.2.3.2. Second Line Anti-TB Drugs

The second line agents are highly recommended for the treatment of multi-drug resistant mycobacteria. These include injectable aminoglycosides and polypeptides such as streptomycin, kanamycin, amikacin, and capreomycin, or viomycin, respectively.^{76,77} The aminoglycosides are known to inhibit protein synthesis by targeting the 30S ribosomal subunit.⁷⁸ The oral and injectable fluoroquinolones; ciprofloxacin, levofloxacin, moxifloxacin, ofloxacin, and gatifloxacin also fall under this category. The unique mode of action of quinolones is important for inhibiting DNA synthesis by acting on DNA gyrase and topoisomerase IV (QuiM). The other drugs such as para-amino salicylic acid, cycloserine, ethionamide, prothionamide, thioacetazone, and linezolid are

also included in second line agents. Para-aminosalicylic acid works by inhibiting folic acid synthesis by acting on dihydropteroate synthase.⁷⁴ Cycloserine acts on D-alanine racemase and ligase enzymes to prevent the formation of the peptidoglycan layer of the mycobacterial cell wall (Figure 3-26).⁷⁰

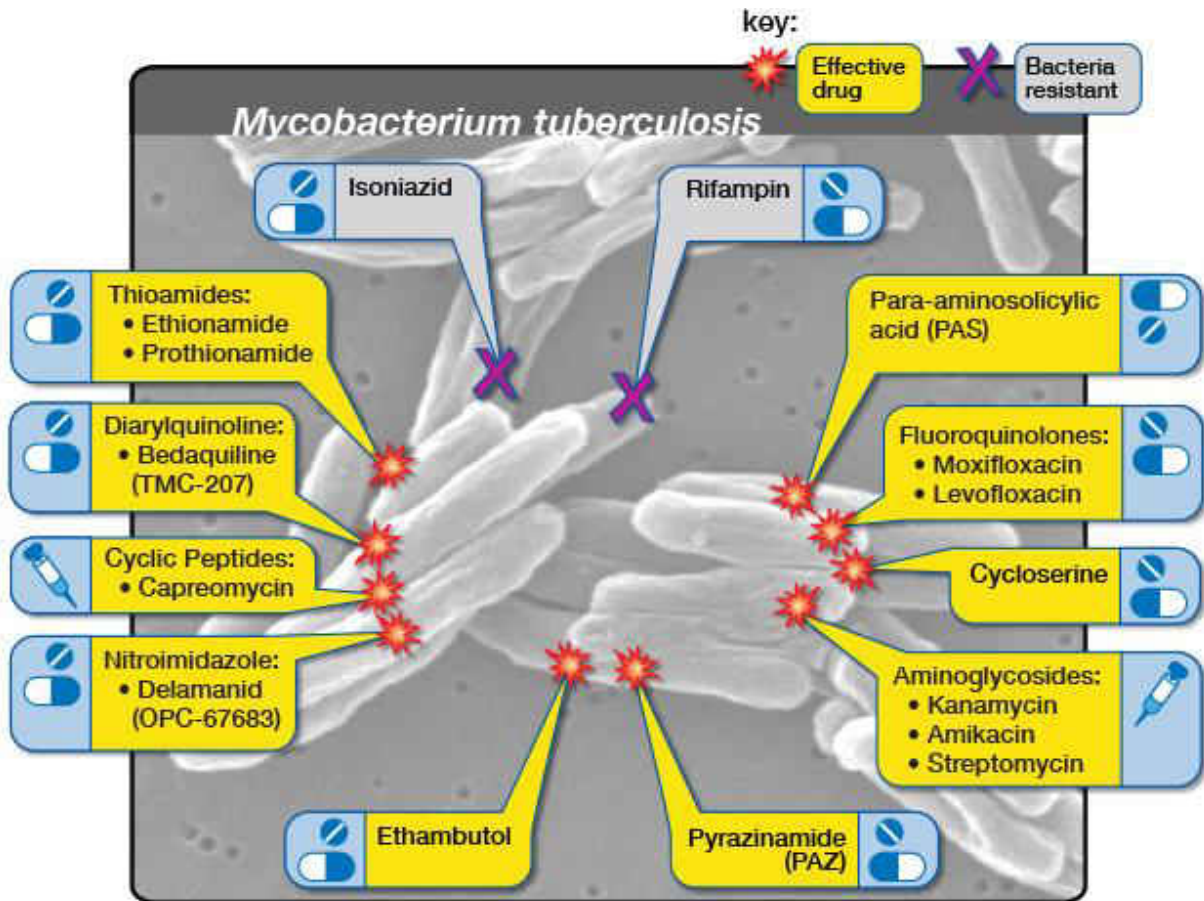


Figure 3-26. Multidrug Resistant Tuberculosis and second line treatments (credit: NIAID)

3.2.3.3. Third Line Anti-TB Drugs

The third line agents are not meant to treat any specific conditions but seem to be effective in some cases with undefined roles. These include clofazimine, linezolid, amoxicillin plus clavulanate, imipenem plus cilastatin, and clarithromycin.

The initial treatment duration time of 18 months or more with the drug cocktail was brought down to 9 months with the clinical introduction of rifampicin and even shortened to 6 months with

the discovery of pyrazinamide.⁷⁹ The current regime enjoys a 95 % success rate with six months duration with Directly Observed Therapy (DOT). It consists of two phases of intensive and then continuous therapy. The initial intensive phase starts with two months of the four drugs: isoniazid, rifampicin, pyrazinamide, and ethambutol. The continuous phase after the initial phase consists of 4 months of isoniazid plus rifampicin. The mycobacterium in infected persons exists in different replication states, metabolically active, relatively rapid replicators, and nearly dormant persisters.⁸⁰ Isoniazid acts particularly on early bacterial activity in the initial five days of therapy, and the active replicators are killed effectively in the first few weeks. To decrease the emergence of resistance and ease of administration the fixed dose combinations of two (isoniazid and rifampicin), three (isoniazid, rifampicin, and pyrazinamide) and four (isoniazid, rifampicin, pyrazinamide and ethambutol) were developed.⁸¹

According to the WHO recommendations, the intensive phase to treat MDR-TB should be at least eight months, with total treatment duration of 20 months. If the same person has prior exposure to multi-drug resistance bacteria, the treatment duration is 28 months.⁸² To treat MDR-TB, the regime should contain at least four-second line agents. In the case of XDR-TB, the treatment is even longer and requires the third line anti-TB agents. Third-line agents are associated with more side effects than others drugs and are also expensive. The XDR-TB is known to be fatal in the case of HIV- people infected with tuberculosis.^{83,84}

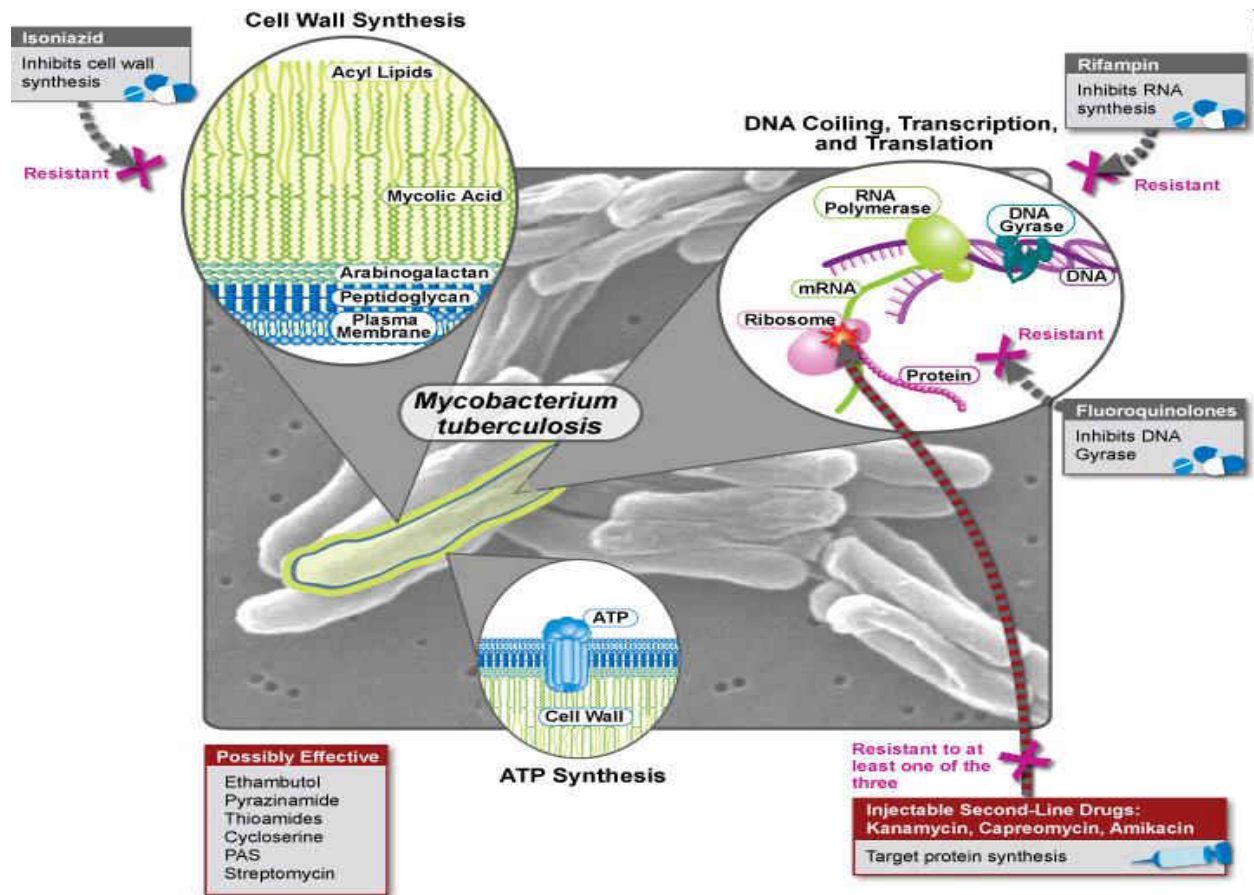


Figure 3-27. Mechanism of action of current tuberculosis drugs (Credit: NIAID)

3.2.4 Tuberculosis Drugs in the Pipeline

There are many challenges to overcome with new drugs to treat TB. Of these, the safety profile, potency against MDR-TB, XDR-TB strains, and reduced duration of treatment are the most important (Figure 3-28).⁸⁵ The need for a new regime always exists since this will result in less tolerance and decreased drug-drug interactions. There are several potential drug candidates currently under investigation in the clinical trial pipeline.⁸⁶

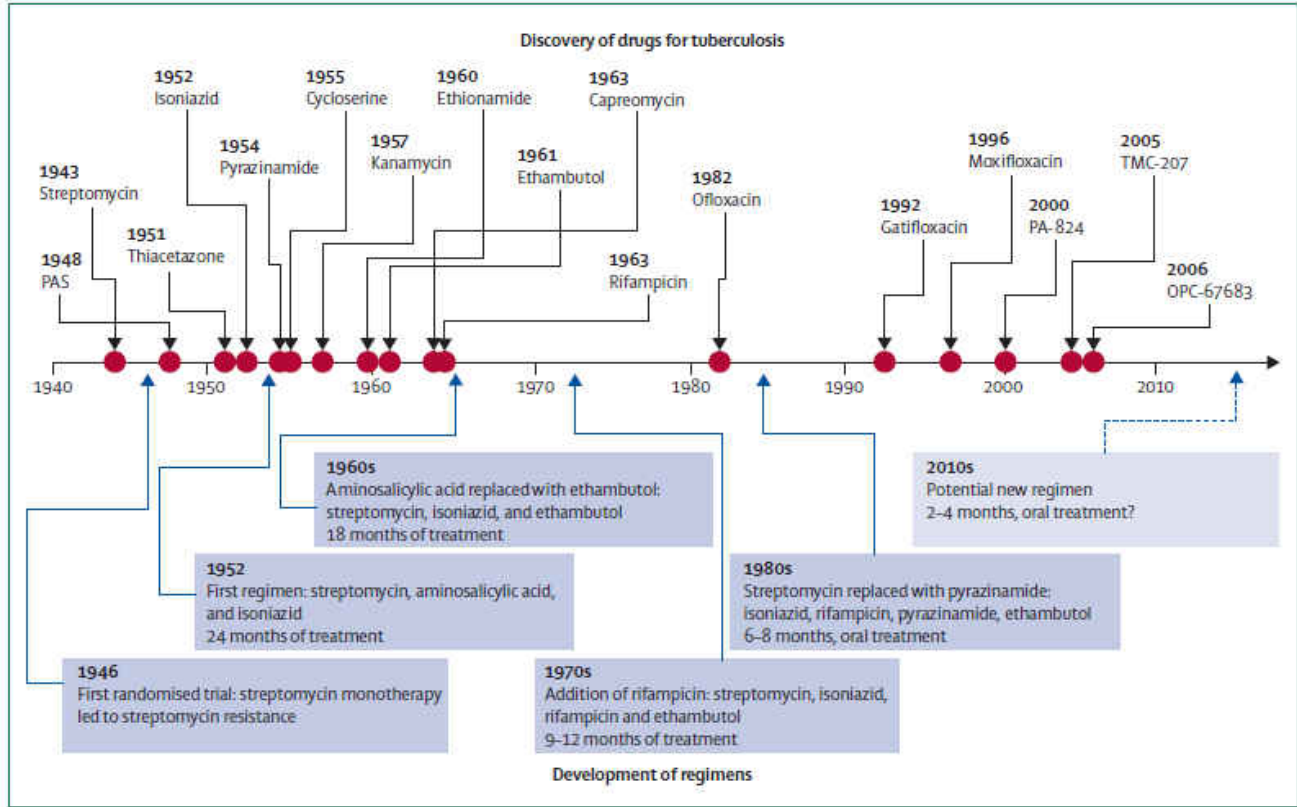


Figure 3-28. Discovery of drugs for tuberculosis

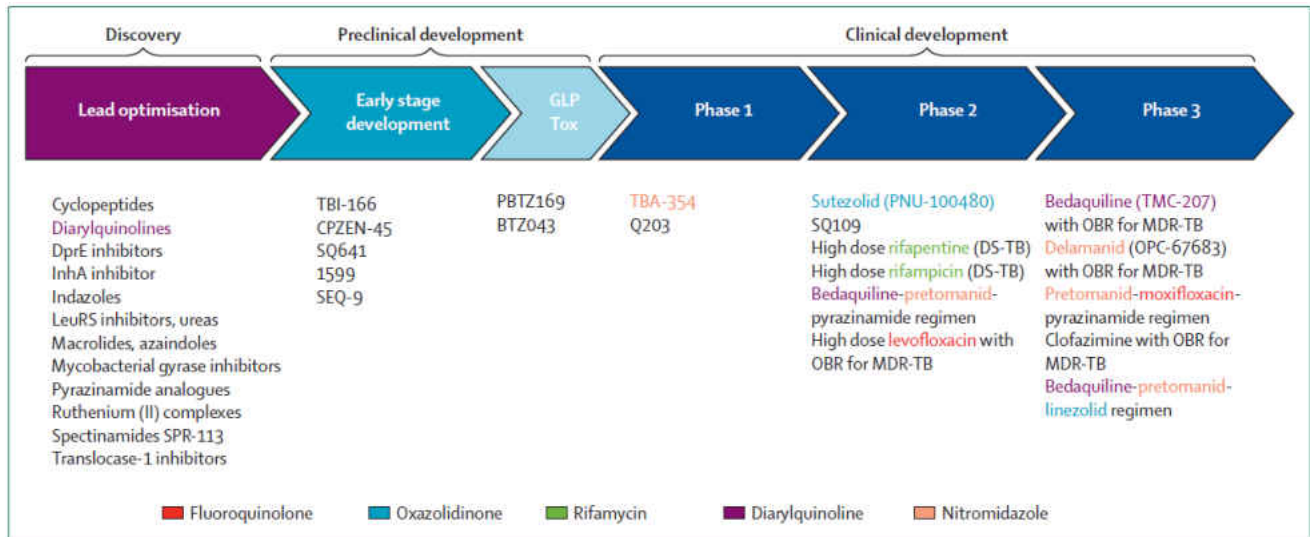


Figure 3-29. Research and development pipeline for new anti-tuberculosis drugs

As seen in Figure 3-29, most of the drugs are in the final stages of Phase 2 and Phase 3 clinical trials. Based on the data from 2012-2014, the two new drugs bedaquiline and delamanid appear to be the best, to date, for MDR-TB, but this must be confirmed. The sutezolid and pretomanid which are in Phase 2 and Phase 3, respectively, are new compounds tested principally for better hepatic safety issues. Most of the first line agents, the long acting rifampicins, and fluoroquinolones are being optimized to further enhance their role in treating drug-susceptible bacilli. The SQ109 agent has not shown any anti-TB activity in sputum either alone or combined with rifampicin within a duration of 14 days. However, the only reason to advance SQ109 testing was to see any pharmacokinetic drug-drug advantage when combined with rifampicin (Figure 3-30).⁸⁷

In Phase 1, TBA-354 is a nitroimidazole and Q203 is a novel ATP synthetase inhibitor. In a study carried out in 39 patients affected by XDR-TB, linezolid has shown efficiency, but high toxicity was reported.⁸⁸ The study is now focused on the toxicity of linezolid without affecting the efficiency. The sutezolid, an analog of linezolid, exerts more potent antibacterial activity both *in-vitro* and *in-vivo* studies against non-replicating mycobacteria.^{48,89} Rifabutin, approved by the FDA, is used to treat *rpoB* mutants of *Mycobacterium avium*; these mutants are susceptible to rifabutin even though resistant to rifampicin.⁹⁰ Rifabutin has many advantages compared to rifampicin due to its decreased ability to induce CYP3A4, making it the best choice to replace rifampicin in combination therapy (Figure 3-30).⁹¹

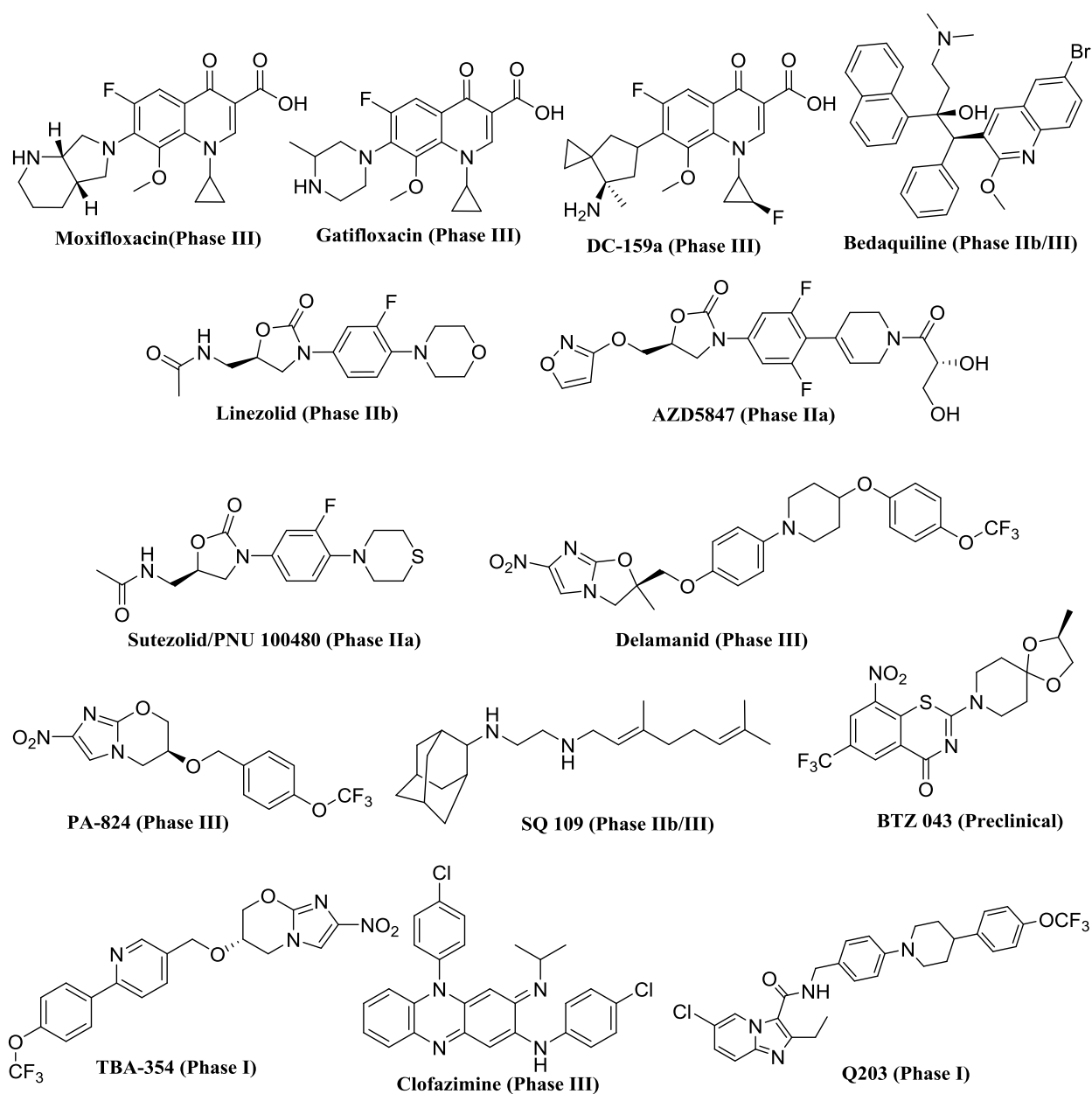


Figure 3-30. Antitubercular drugs in the pipeline⁸⁵

Clofazimine is an antileprotic drug which possesses both anti-bacterial and anti-inflammatory properties. Clofazimine in a study with Balb/c mice⁹² has shown activity against necrotic granulomas.⁹³ Skin discoloration, prolonged QT intervals, pharmacokinetic drug interactions are a few possible concerns studied in the case of clofazimine. Based on the *in-vitro* studies and independent case reports, carbapenems also play a role in treating MDR-TB.⁹⁴

Similarly, many other drugs have been screened for activity against *Mycobacterium tuberculosis* (Figure 3-30).

3.3. Methicillin-Resistant *Staphylococcus Aureus* (MRSA)

MRSA was considered a just born “superbug” in 1961 with the report of the first case in the United Kingdom.⁹⁵ Eventually, MRSA became a significant health concern with a high rate of morbidity and mortality. MRSA infections are not confined to any particular area; it is an alarming worldwide problem.⁹⁶ In the United States, itself, the infection and death rates due to MRSA add up to more than fatalities than caused by AIDS, viral hepatitis and tuberculosis combined.^{97,98} There are two common associated strains of MRSA, the Hospital-acquired MRSA (HA-MRSA)⁹⁹ and Community-acquired MRSA (CA-MRSA).⁹⁷

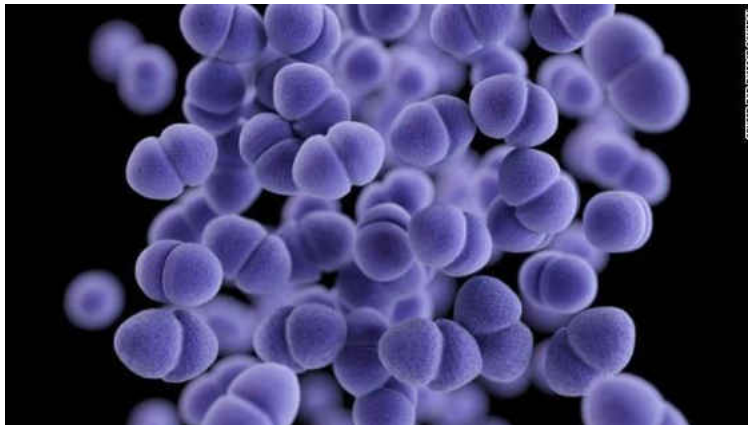


Figure 3-31. Microscopic structure of Methicillin resistant *Staphylococcus aureus* bacteria (credit: CNN)

Staphylococcus aureus is a gram-positive, non-motile, pus forming bacteria, microscopically appearing as grapes when clumped together (Figure 3-31).¹⁰⁰ *S. aureus* is a commensal pathogen; the most common inhabitant of the external nares. Other regions of the body such as axillae, groin and gastrointestinal track are known to contain colonies of *S. aureus*.¹⁰¹

With the discovery of penicillin by Alexander Fleming in 1929, most of the staphylococcus infections were treated using penicillin.¹⁰² *S. aureus* strains developed resistance to penicillin, followed by most of the penicillin derivatives and by 1960's penicillin resistant staphylococcus infections became a pandemic. In 1959, another penicillin derivative methicillin was introduced to treat staphylococcus infections.¹⁰³ However, in 1961 the staphylococcus bacteria were found to evolve resistance to methicillin. The term MRSA is applied to strains of *Staphylococcus aureus* that developed resistance to most common antibiotics; they are also resistant to other named penicillins and cephalosporins.

3.3.1. Factors Causing Virulence

Both the structural components and the secretory substances play a significant role in the pathogenicity of *Staphylococcus aureus* infections. The key surface proteins that are vital for the establishment of infection are microbial surface components which recognize adhesive matrix molecules (MSCRAMMs). Collagen, fibronectin, fibrinogen of the host tissues are the sensitive adhesive surfaces to these proteins. Once attached, these form the source of endovascular infections, as well as bone, and joint infections. The composition of MSCRAMMs differ in various strains which cause a specific type of infection.^{104,105} *S. aureus* has the ability to form a biofilm¹⁰⁶ and small colony variants (SCV)¹⁰⁷ which are mainly responsible for the growth and recurrent infections. The biofilm or slime provide the surface in which these bacteria reside. This is the reason *Staphylococcus aureus* became the main source for the cause of a major problem in infections due to prosthetic devices. The SCV have the ability to hide within host cells which protects them from host immune defense mechanisms and antibiotics. As a result, the hidden bacteria are the reason for persistent *Staphylococcus aureus* infections in cystic fibrosis patients (Figure 3-32).^{107,108}

During the growth cycle of *Staphylococcus aureus*, the MSCRAMMs produced in the logarithmic phase facilitate the early colonization of bacteria in tissues. The secreted proteins during the stationary phase will permit the facile spread of the infection.¹⁰⁹ The degree of staphylococcus virulence is also attributed to accessory gene regulator (*agr*) called the quorum sensing system. The other gene regulators include staphylococcal accessory regulator¹¹⁰, ArIR and ArIS¹¹¹, SaeRS¹¹², Rot¹¹³, and mgr¹¹⁴.

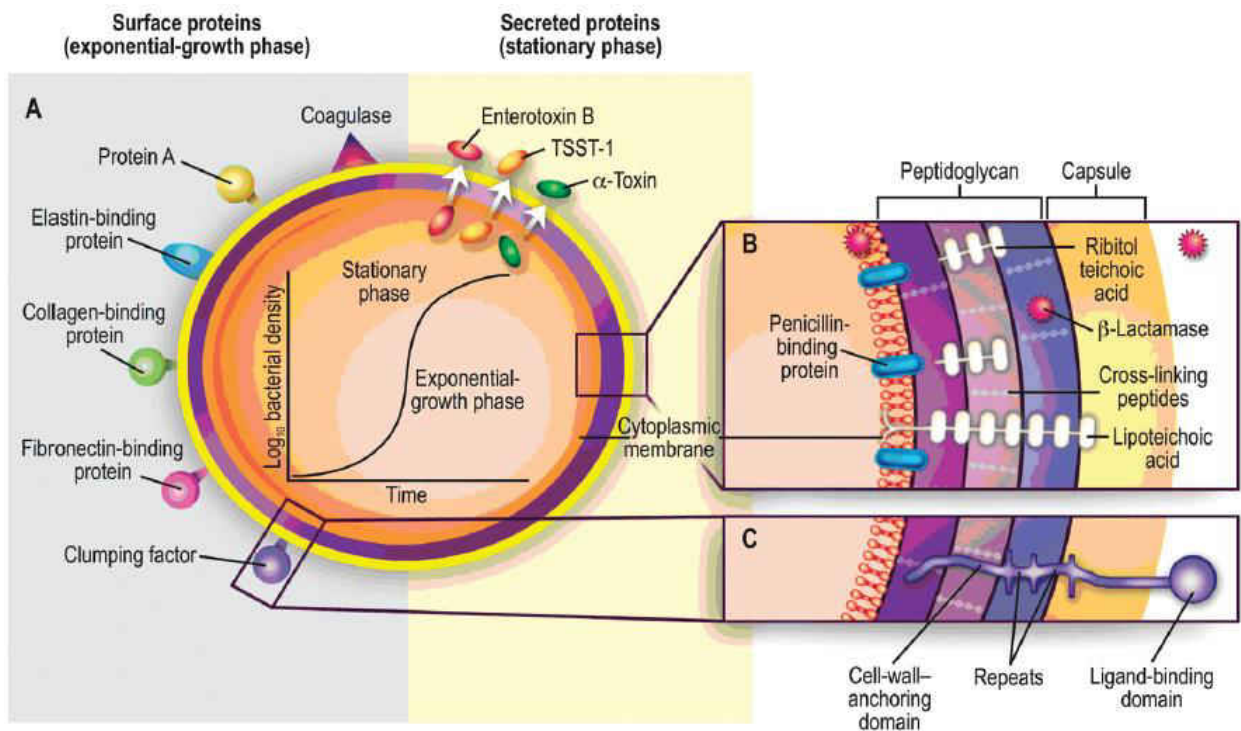


Figure 3-32. Pathogenic factors of *Staphylococcus aureus*, with structural and secreted products both play a role as virulence factors. A, Surface and secreted proteins. B and C, Cross-sections of the cell envelope. TSST-1, toxic shock syndrome toxin 1.¹⁰²

Staphylococcus exhibits various mechanisms to protect itself from the host immune system such as antiphagocytic microcapsule; a zwitterionic capsule that induces the formation of an abscess. To help prevent the opsonization of staphylococcus, the MSCRAMM A protein binds to the Fc portion of an antibody.¹⁰² The secretory enzymes such as proteases, lipases, elastases help bacteria to invade more into the tissues. *Staphylococcus* induces septic shock by interaction with

the host immune system and activation of coagulation pathways. In septic shock, the peptidoglycans, lipoteichoic acid and α -toxins are known to play an important role. Leukocidins are formed to destroy host leukocytes and toxins causing food poisoning and toxic shock syndrome.¹¹⁵

3.3.2. MRSA Infections

Because *Staphylococcus aureus* is a commensal bacterium, this is the reason for many invasive infections. These include severe endocarditis seen in immunocompromised patients and people with increasing resistance due to over use of antibiotics.¹¹² Respiratory infections such as bronchiectasis, cystic fibrosis, and necrotizing pneumonia are increasing these days due to MRSA.¹¹⁶ The skin and soft tissue infections are the first identified infections due to MRSA of which staphylococcal scalded skin syndrome is life threatening. Acute osteomyelitis and septic arthritis are the bone and joint infections which are caused by surgical intervention or by bone replacement procedures. Wounds are the primary targets for MRSA, and rare conditions of urinary tract infections like urethral meatus and pyelonephritis have been reported.^{103,117}

3.3.3. Treatment Options for MRSA Infections

In considering a treatment for MRSA infections, prevention is more important to minimize the spread of the infection. Early screening, identification of carriers, nasal and skin decontamination, staff education, enforcement of hand hygiene, and decontamination of patient wards are factors considered for effective control. MRSA infections are expanding their territory recently including medical devices, faucets, computer keyboards, and stethoscopes. A vaccine being developed for MRSA has proven effective in mice. However, its use in humans will await extensive testing. Even though *Staphylococcus aureus* is an encapsulated bacteria the capsule is not directly involved in virulence *in vivo* like other encapsulated *Staphylococcus pneumoniae*, *H.*

influenzae, and *Neisseria meningitides*. In contrast, *Staphylococcus aureus* do not induce protective humoral immune responses like other encapsulated bacteria. The main immune response to protect from *Staphylococcus aureus* are phagocytes and T-lymphocytes which enhance phagocytic activity, so the antibody antigen mediated neutralization may not be the affective focus for the development of a vaccine against *Staphylococcus aureus*. However, studies to develop a vaccine include selection of multiple antigen targets that induce both cell mediated and humoral immunity to protect against *Staphylococcus aureus*. As a result, antigen antibody interactions may not help to develop effective vaccines and this still requires more research.¹¹⁸

The current antibiotic options for MRSA treatment are limited. Vancomycin has been the drug of last resort for many decades for MRSA infections. Vancomycin is given either continuously or intermittently. However, the intermittent doses appears to be more efficient. Both ways of treatment of MRSA with vancomycin share equally the side effects of nephrotoxicity and mortality. Linezolid, the oxazolidinone antibiotic has proven to be effective and the best alternative to vancomycin in patients with renal problems.¹¹⁹

Daptomycin, derived from *Streptomyces roseosporus* has been given in parental administration for MRSA. The other novel antibiotics such as glycopeptides, (dalbavancin, oritavancin, and telavancin), beta-lactams (ceftobiprole), and are diaminopyrimidines (iclaprim) are in the pipeline and possible future drugs for treatment of MRSA infections.¹²⁰

3.4. ANTIBIOTIC RESISTANCE

Antibiotics are classified as revolutionary discoveries in medicine and have saved millions of lives. At each and every stage there has been the emergence of resistance, followed by its discovery within a few years and this has decreased the effectiveness of antibiotics.¹²¹ Sulfonamide resistance *Streptococcus pyogenes*, penicillin-resistant *Staphylococcus aureus*, and streptomycin-resistant *Mycobacterium tuberculosis* are a few of the initially identified resistance strains reported in hospitals.¹²² The occurrence of resistance is more common in ESKAPE pathogens (*Enterococcus faecium*, *Staphylococcus aureus*, *Klebsiella pneumoniae*, *Acinetobacter baumannii*, *Pseudomonas aeruginosa*, and *Enterobacter* spp.) which cause most lung and urinary tract infections.¹²³

The evolution of resistance is due to many biochemical and genetic factors. The resistance mechanism is generally attributed to changes in cell structure and function. The bacterial resistance may be intrinsic or acquired due to new encoded genes and vectors of transmission.¹²⁴ Resistance mechanisms to antibiotics include the structural modification of targets, enzymatic inactivation of antibiotics, or protection from antibiotics. Mutations in chromosomes allow the bacteria to emerge readily as highly resistant organisms (Figure 3-34).

3.4.1. Origin of Resistance in Bacteria

There are a wide variety of mechanisms by which bacteria develop resistance. It can be intrinsic or acquired resistance. The inherent resistance is a natural mechanism of bacteria that produces genes to evolve resistant strains. This type of protection is seen in bacterial isolates of resistance phenotypes to sulfonamides and trimethoprim.¹²⁵

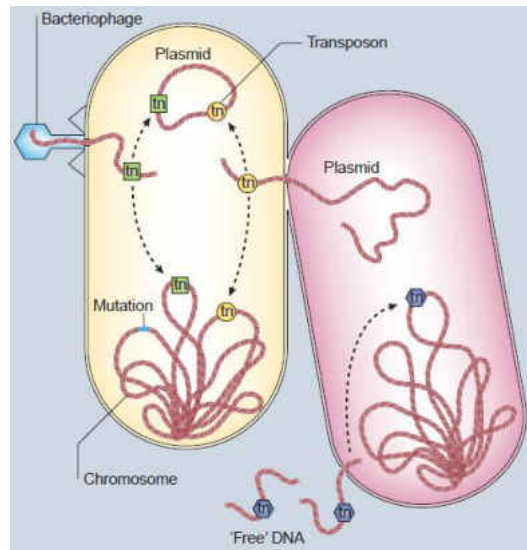


Figure 3-33. The evolution and genetics of bacterial resistance

In general there are two different origins of resistance in bacteria, i.e., vertical transfer and horizontal transfer. Horizontal transfer is further divided into conjugation, transformation, and transduction. Mutations generally occur in vertical transfer during replication of bacteria that are transferred to progeny. If this mutation induces a favorable change, the bacteria retain these mutant alleles that help in their survival (natural selection). These mutations are spontaneous and occur rarely.

In horizontal transfer the genetic material is transferred between two different bacteria. The uptake of naked DNA from the environment/dead bacterial cell and incorporation into its own chromosomal DNA by another bacteria is called transformation. In conjugation, two bacteria become adjacent to each other and transfer plasmids (known to contain resistant genes) with the help of pili present on outer surface of bacteria. In transduction, the bacteriophage (virus that infects bacteria) transfers the genetic material required for resistance from one bacterium to another. The transfer of genetic elements such as plasmids, naked DNA, transposons, and bacteriophages are responsible for the acquisition of resistance between bacteria of different taxonomical classes. Apart from these, during the course of an infection there are a large number

of diverse populations of pathogens. If a single mutation encoding bacterial resistance to antibiotics occurs, these mutants proliferate inside the host leaving the bacteria resistant to antibiotics (Figure 3-33).¹²²

The tet (M) tetracycline resistant gene is an example of a resistance gene spread through transposons¹²⁶ found in gram positive, gram negative, aerobic, and anaerobic bacteria.¹²⁷ The DNA transformation process created the resistant strains of *S. pneumoniae* acquired from penicillin-resistant *S. viridans*.¹²⁸ Even the spread of bacteria from person to person is also responsible for emergence of resistant strains exemplified by the appearance of progeny strains of resistant pneumococci from Spain in Iceland and the United States.¹²⁹

In the absence of genetic transfer of antibiotic resistance, the chromosomal mutation is a principal source of developing high-level resistance. These include mutations in the target enzymes, DNA gyrase and topoisomerase IV, which rendered fluoroquinolones inactive in strains of *E. coli* and *Enterobacteriaceae* with the expression of additional efflux pumps to pump antibiotics to the outside of the bacteria.^{122,130} There are many ecological, anthropogenic, and unknown biological factors which play a crucial role in the development of resistance.

3.4.2. Different Mechanisms of Bacterial Resistance

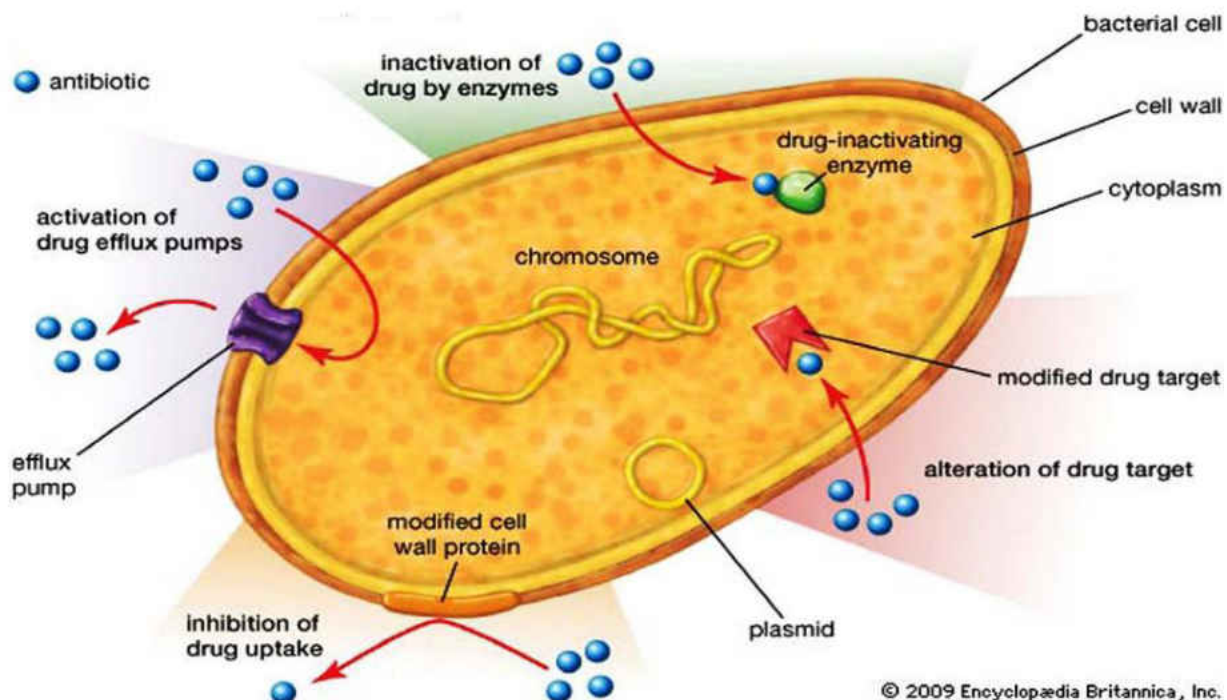


Figure 3-34. Mechanisms of antibiotic resistance strategies in bacteria

3.4.2.1. Enzymatic and Chemical Modification of a Drug

These mechanisms of resistance are generally observed in drugs of natural origin. β -lactam antibiotics and aminoglycosides are more susceptible to bacterial enzymes and key chemical changes that render the drug inactive.¹³¹

3.4.2.1.a. Inactivation by Hydrolysis

The most fundamental mechanism of resistance in β -lactam susceptible organisms is the production of the enzyme β -lactamase that inactivates penicillin (Figure 3-35). These β -lactamases contain serine residues at the active site and some require metal ion cofactors for activation. These are characterized into four classes, Class A, B, C, and D. Class A, C and D are proteins that contain serine residues, and Class B proteins are zinc-dependent metalloenzymes.¹³² These subclasses of

enzymes target different β -lactam antibiotics such as penicillins, cephalosporins, clavams, carbapenems, and monobactams. These resistant β -lactamses are found in various species of *Enterobacteriaceae*, *Pseudomonas*, *Acetivobacter*, and *Aeromonas* genus (Figure 3-36).^{124,133}

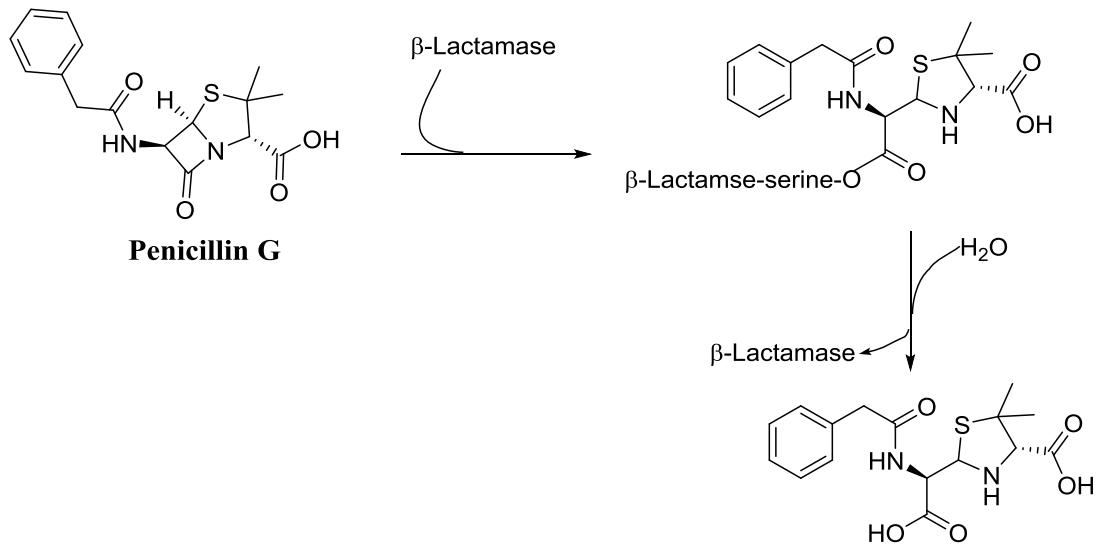


Figure 3-35. Penicillin inactivation by β -lactamase

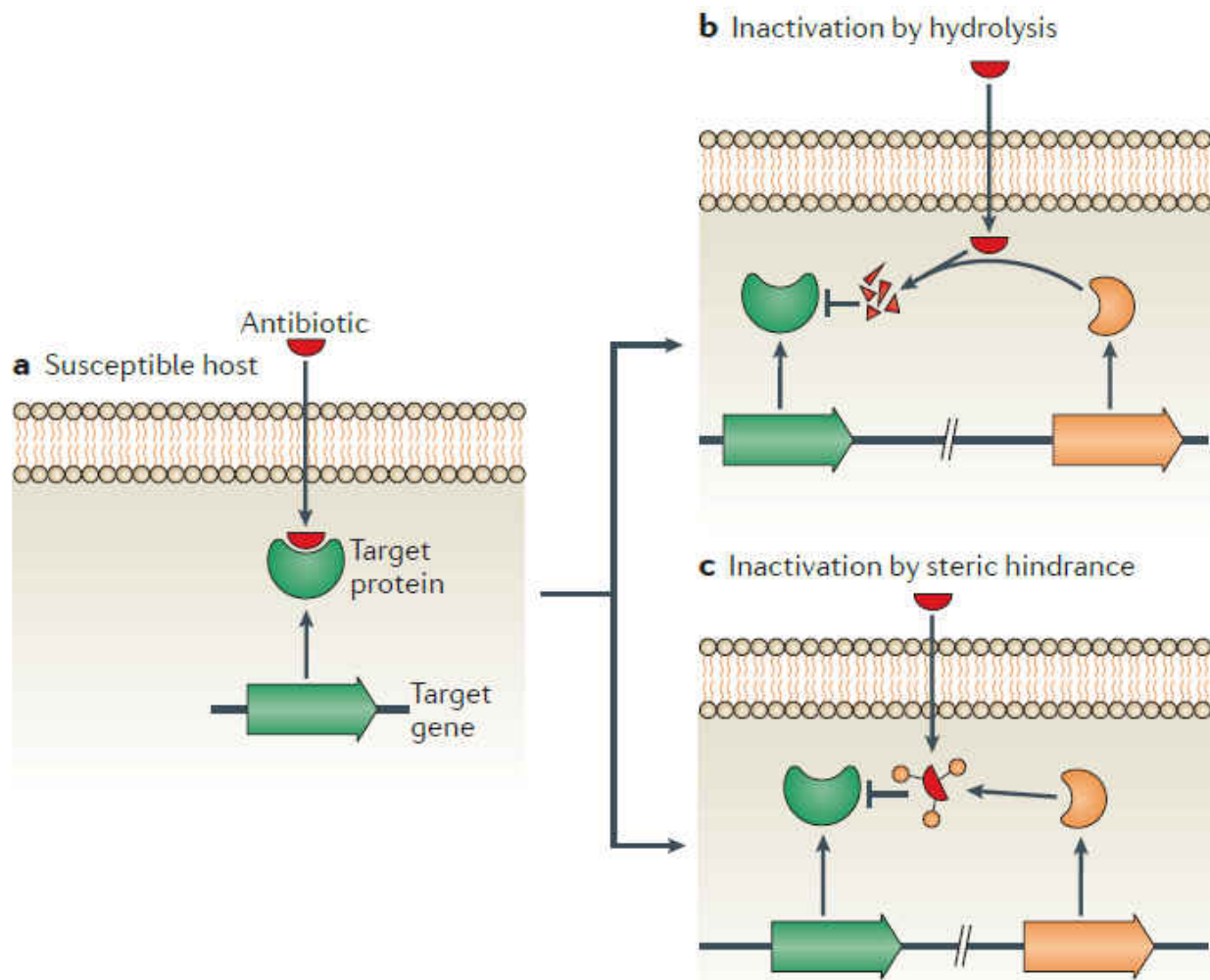


Figure 3-36. Enzymatic and chemical modification. a. A susceptible host with a target that is efficiently inhibited by an antibiotic. b. Acquisition and production of enzymes that destroy the antibiotic preventing binding to the target. c. Acquisition and production of enzymes that modify the structure of the antibiotic can also prevent binding to the target.

3.4.2.1.b. Chemical Modification of the Antibiotic

Aminoglycoside antibiotics are large chemical compounds which render them more susceptible to chemical modifications. There can be a transfer of acetyl, phosphate, nucleotidyl, and ribityl groups onto the aminoglycoside antibiotics making them sterically hindered at the target site.¹³⁴ There are three classes of modifying enzymes, acetyltransferases, phosphotransferases, and nucleotidyl transferases that alter the structure of the specific type and particular location on aminoglycosidic antibiotics. A recent phenomenon observed with the campylobacter infections was the encoding of six modifying enzymes that made it resistant even

to gentamicin.¹²⁴ The resistance in *Actinomycetes* species associated with RAE (rif-associated-element) is due to phosphotransferases (Figure 3-36).¹³⁵

3.4.2.2. Prevention of Access to the Target by Efflux Pump Mechanisms

The drug access to a target can be reduced by decreased permeability or the increased number of efflux pumps. The bacterial cell wall in gram-negative bacteria acts as a real barrier for the incoming antibiotics, as compared to that of wall in gram-positive bacteria. In *Enterobacteriaceae*, the outer membrane proteins, called porins OmpF and OmpC are known to be involved in the transport of drug. In these bacteria the resistance that evolved was due to greater expression of selective channels rather than porins to reduce cell permeability of the outer membrane and limit the antibiotic entry into the cell.^{136,137} The carbapenems in *Pseudomonas* species and *Acetivobacter* species are inactivated due to reduction in porin expression, which usually helps in transport of the drug into the cell irrespective of the carbapenemase production mechanism (Figure 3-34).¹³⁸

The efflux mechanism is the removal of the antibiotic from the cell with the help of efflux pumps (proteins) on the surface.¹³⁹ Gram-negative bacteria show overexpressed efflux proteins that alter the substrate specificity. These provide resistance to many drugs known as Multidrug resistance (MDR) efflux pumps in *Streptococcus mutans*, *Stenotropomonas maltophilia*, and *K. Pneumoniae*. There are five families of efflux proteins of which, the RND (resistance nodulation cell division) are more prevalent in gram-negative bacteria. The RND systems consist of a cell membrane-spanning pump, outer membrane pore and connecting periplasmic adapter protein distributed in *Escherichia coli* and *Pseudomonas aeruginosa*.¹⁴⁰ In MDR-TB, the TetR family transcriptional repressor Rv1219c gene induce the increased expression of the ABC family of transporters Rv1217c- Rv1218c responsible for the outflow of isoniazid and rifampicin.

3.4.2.3. Alteration of Molecular Target by Mutation

The modification of the target by a mutation is the more prominent and efficient method of resistance.¹³⁹ Variations in the target structure prevent the attachment of antibiotics, thus enabling the proper processing of pathogens. Mutation of the gene that codes the antibiotic target is the principal reason for resistance. In the case of linezolid, the antibiotic target 23SrRNA is coded by multiple copies of a gene. The clinical applications of linezolid have shown resistance in *S. pneumoniae* and *S. aureus* because of mutation in one of these gene copies that favored recombination at higher frequencies between homologous alleles, which produced populations carrying mutant alleles resistant to antibiotics (Figure 3-37).¹²⁴

The uptake of naked DNA through transformation and recombination between bacteria of closely related species form the mosaic genes. The transformation of mosaic penicillin binding protein genes from *Streptococcus mitis* to *Streptococcus pneumoniae* encode penicillin insensitive enzymes that cause resistance to penicillin antibiotics in *Streptococcus pneumoniae*.¹⁴¹ Another mechanism is the acquisition of homologous genes from another bacteria that encode the antibiotic target. This mechanism is seen in MRSA, where MRSA acquires staphylococcal cassette chromosome mec (SCCmec) gene. This gene encodes for β -lactam insensitive proteins that allow the cell wall bio-synthesis in MRSA, even though native penicillin binding proteins are inhibited by antibiotics.¹⁴²

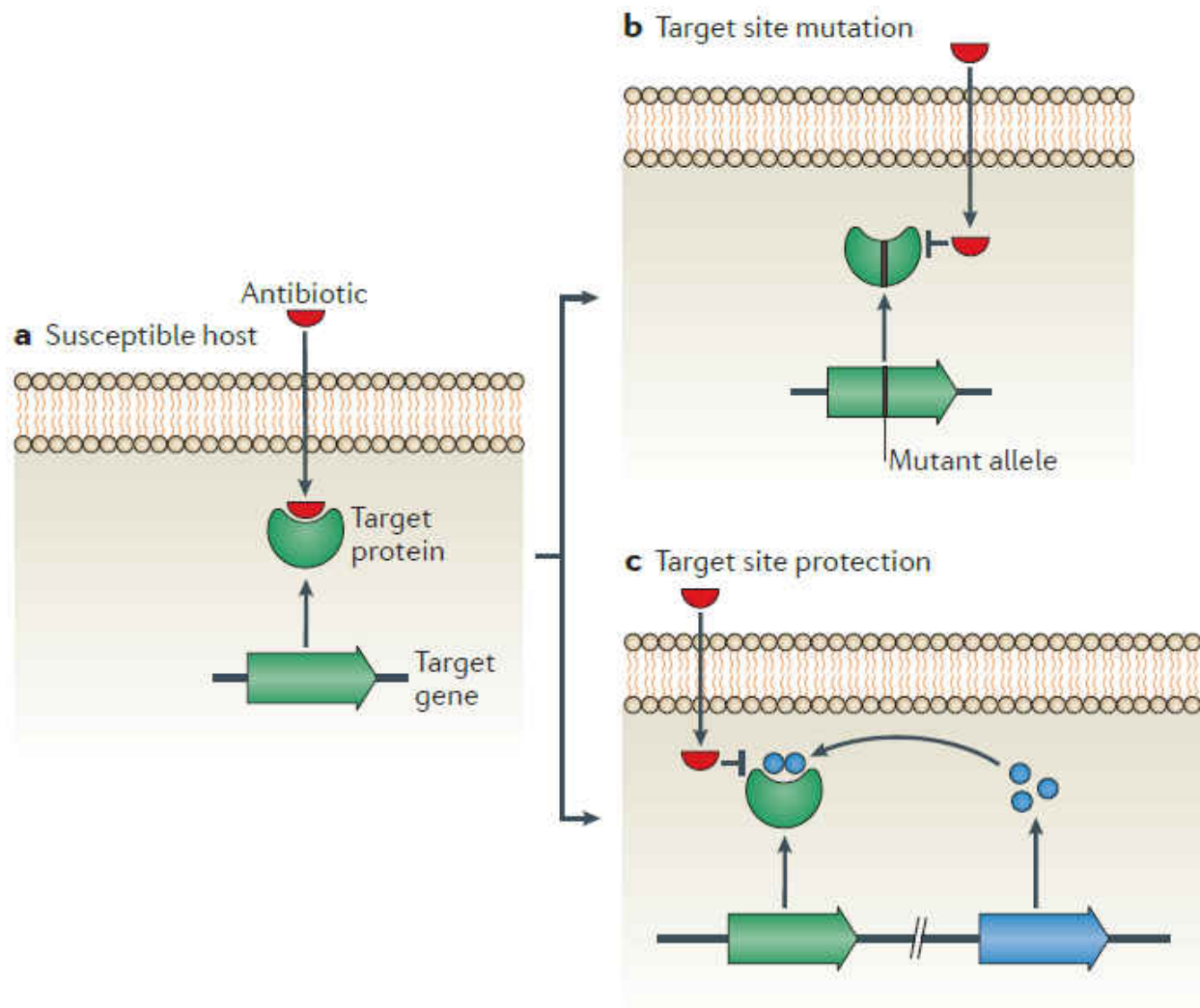


Figure 3-37. Alteration of molecular target. a. A susceptible host in which an antibiotic is able to bind tightly to its specific target and exert an inhibitory effect. b. Mutation of the target site or recombination of mosaic allele results in a functional target with reduced affinity for the antibiotics. c. Modification of target by addition of a chemical group can also prevent the antibiotic binding without altering the primary protein sequence of the target.

3.4.2.4. Target Site Protection

The modification of a target site provides resistance without the involvement of a mutation. This mechanism is observed in many antibiotics such as macrolides, lincosamides, and streptogramins due to methylation of the 16S rRNA by an erythromycin ribosome methylase (*erm*).¹⁴³ The methylation of the A2503 site in the 23S rRNA by chloramphenicol florfenicol resistance methyltransferase (*cfr*) renders pleuromutilins, streptogramins, phenicols, and oxazolidinones inactive.¹⁴⁴ The plasmids carrying *erm* and *cfr* genes act as vectors for the transfer

of resistance between many organisms by conjugation.¹⁴⁵ The methylation of the ribosome by methyltransferase encoded by the *armA* gene is one of the reasons for development of resistance to aminoglycoside antibiotics by *Enterobacteriaceae* (Figure 3-37).¹⁴⁶

A unique mechanism of resistance to quinolone antibiotics was observed with *qnr* genes encoding for pentapeptide repeat proteins that safeguard topoisomerase IV and DNA gyrase.¹⁴⁷ The polymyxins are the lipopolysaccharide (LPS) binding antibiotics which disrupt the cell wall biosynthesis in gram-negative bacteria. The specific binding to LPS is based on high affinity of the hydrophobic tails of polymixin antibiotics. The resistance to these antibiotics is developed by expression of regulators which affect the LPS production that results in alteration of target and reduced binding making an unsuitable binding target.¹⁴⁸ Daptomycin targets anionic phospholipids in the cytoplasmic membrane of gram-positive bacteria and in the presence of calcium ions it causes depolarization and loss of intracellular contents. In *S. aureus*, a point mutation in the *mprF* (multiple peptide resistance factor) gene, encodes, a protein that decorates anionic phospholipid phosphatidylglycerol with L-Lys, which results in a change in phospholipid contents. This in turn changes the membrane polarity and phospholipid composition that reduces the binding of daptomycin.¹⁴⁹ Furthermore, in the case of sulfonamide-resistance, the bacteria do not require para-aminobenzoic acid (PABA), an important precursor for the synthesis of folic acid and nucleic acids in bacteria inhibited by sulfonamides. Instead, like mammalian cells, they turn to use preformed folic acid (alteration of metabolic pathway/by pass). An overview of different antibiotic targets and resistant mechanisms can be seen in Figure 3-38.¹⁵⁰

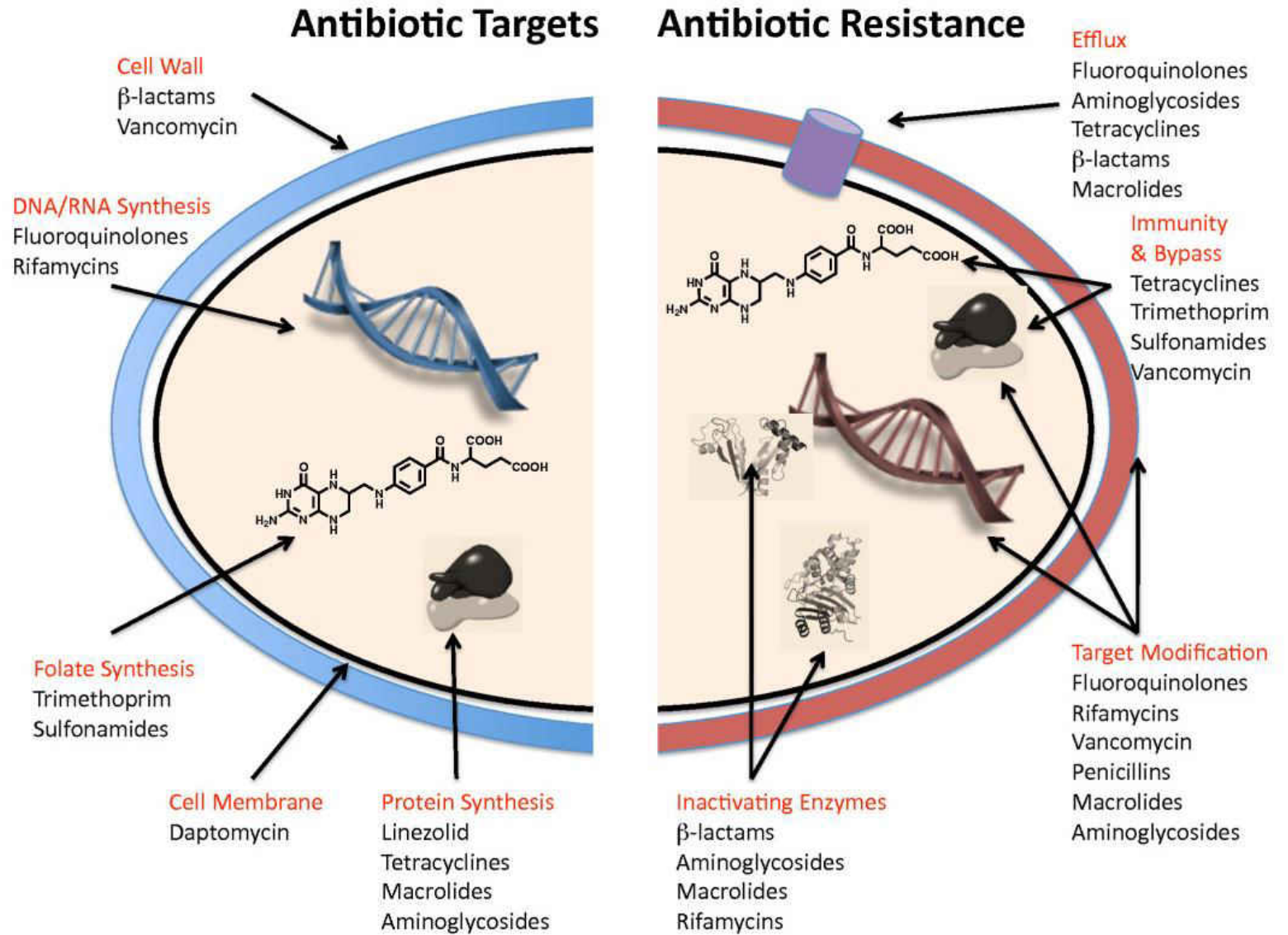


Figure 3-38. Antibiotic targets and mechanisms of resistance

3.5. REFERENCES

- (1) Ellis, H. *Br. J. Hosp. Med. (Lond.)* **2015**, 76, 483.
- (2) Heynick, F. *Br. J. Psychiatry.* **2009**, 195, 456.
- (3) Gelpi, A.; Gilbertson, A.; Tucker, J. D. *Sex. Transm. Infect.* **2015**, 91, 68.
- (4) Strebhardt, K.; Ullrich, A. *Nat. Rev. Cancer* **2008**, 8, 473.
- (5) Winau, F.; Westphal, O.; Winau, R. *Microbes Infect* **2004**, 6, 786.
- (6) Aminov, R. I. *Front. Microbiol.* **2010**, 1, 134.
- (7) Elsner, H. L. *J. Am. Med. Assoc.* **1910**, 55, 2052.
- (8) Mahoney, J. F.; Arnold, R. C.; Harris, A. *Am. J. Public Health Nations Health* **1943**, 33, 1387.
- (9) Domagk, G. *Dtsch. Med. Wochenschr.* **1935**, 61, 250.
- (10) Enne, V. I.; Bennett, P. M.; Livermore, D. M.; Hall, L. M. *J. Antimicrob. Chemother.* **2004**, 53, 958.
- (11) Tan, S. Y.; Tatsumura, Y. *Singapore Med. J.* **2015**, 56, 366.
- (12) Chain, E.; Florey, H. W.; Gardner, A. D.; Heatley, N. G.; Jennings, M. A.; Orr-Ewing, J.; Sanders, A. G. *Clin. Orthop. Relat. Res.* **2005**, 439, 23.
- (13) Butler, M. S.; Blaskovich, M. A.; Cooper, M. A. *J. Antibiot. (Tokyo)* **2017**, 70, 3.
- (14) Fair, R. J.; Tor, Y. *Perspect. Medicin. Chem.* **2014**, 6, 25.
- (15) Lewis, K. *Nat Rev Drug Discov* **2013**, 12, 371.
- (16) Kohanski, M. A.; Dwyer, D. J.; Collins, J. J. *Nat. Rev. Microbiol.* **2010**, 8, 423.
- (17) Jemni, L.; Hmouda, H.; Letaief, A. *Clin. Infect. Dis.* **1994**, 19, 202.
- (18) Collignon, P.; Powers, J. H.; Chiller, T. M.; Aidara-Kane, A.; Aarestrup, F. M. *Clin. Infect. Dis.* **2009**, 49, 132.
- (19) Tomasz, A. *Annu. Rev. Microbiol.* **1979**, 33, 113.
- (20) El Solh, A. *Expert Opin. Pharmacother.* **2009**, 10, 1675.
- (21) Noel, G. J.; Bush, K.; Bagchi, P.; Ianus, J.; Strauss, R. S. *Clin. Infect. Dis.* **2008**, 46, 647.

- (22) Bassetti, M.; Ginocchio, F.; Mikulska, M.; Taramasso, L.; Giacobbe, D. R. *Expert Rev. Anti Infect. Ther.* **2011**, *9*, 909.
- (23) Torres, J. A.; Villegas, M. V.; Quinn, J. P. *Expert Rev. Anti Infect. Ther.* **2007**, *5*, 833.
- (24) Livermore, D. M.; Mushtaq, S.; Warner, M. J. *Antimicrob. Chemother.* **2009**, *64*, 330.
- (25) Gillespie, S. H. *Antimicrob. Agents Chemother.* **2002**, *46*, 267.
- (26) Avent, M. L.; Rogers, B. A.; Cheng, A. C.; Paterson, D. L. *Intern. Med. J.* **2011**, *41*, 441.
- (27) Tenson, T.; Lovmar, M.; Ehrenberg, M. *J. Mol. Biol.* **2003**, *330*, 1005.
- (28) Goldstein, F. W.; Emirian, M. F.; Coutrot, A.; Acar, J. F. *J. Antimicrob. Chemother.* **1990**, *25 Suppl A*, 25.
- (29) Hicks, L. A.; Taylor, T. H., Jr.; Hunkler, R. J. *N. Engl. J. Med.* **2013**, *368*, 1461.
- (30) Roberts, M. C. *FEMS Microbiol. Lett.* **2005**, *245*, 195.
- (31) Agwuh, K. N.; MacGowan, A. J. *Antimicrob. Chemother.* **2006**, *58*, 256.
- (32) Boucher, H. W.; Talbot, G. H.; Benjamin, D. K., Jr.; Bradley, J.; Guidos, R. J.; Jones, R. N.; Murray, B. E.; Bonomo, R. A.; Gilbert, D.; Infectious Diseases Society of, A. *Clin. Infect. Dis.* **2013**, *56*, 1685.
- (33) Sensi, P. *Rev. Infect. Dis.* **1983**, *5 Suppl 3*, S402.
- (34) Cetinkaya, Y.; Falk, P.; Mayhall, C. G. *Clin. Microbiol. Rev.* **2000**, *13*, 686.
- (35) Shaw, J. P.; Seroogy, J.; Kaniga, K.; Higgins, D. L.; Kitt, M.; Barriere, S. *Antimicrob. Agents Chemother.* **2005**, *49*, 195.
- (36) Mercier, R. C.; Hrebickova, L. *Expert Rev. Anti Infect. Ther.* **2005**, *3*, 325.
- (37) Koch-Weser, J.; Sidel, V. W.; Federman, E. B.; Kanarek, P.; Finer, D. C.; Eaton, A. E. *Ann. Intern. Med.* **1970**, *72*, 857.
- (38) Rastogi, N.; Potar, M. C.; David, H. L. *Ann. Inst. Pasteur Microbiol.* **1986**, *137A*, 45.
- (39) Li, J.; Nation, R. L.; Milne, R. W.; Turnidge, J. D.; Coulthard, K. *Int. J. Antimicrob. Agents* **2005**, *25*, 11.
- (40) Schindler, M.; Osborn, M. J. *Biochemistry* **1979**, *18*, 4425.
- (41) Senturk, S. *J. Vet. Pharmacol. Ther.* **2005**, *28*, 57.
- (42) Gootz, T. D.; Marra, A. *Expert Rev. Anti Infect. Ther.* **2008**, *6*, 309.

- (43) Tsiodras, S.; Gold, H. S.; Sakoulas, G.; Eliopoulos, G. M.; Wennersten, C.; Venkataraman, L.; Moellering, R. C.; Ferraro, M. J. *Lancet* **2001**, 358, 207.
- (44) Diekema, D. J.; Jones, R. N. *Lancet* **2001**, 358, 1975.
- (45) Birmingham, M. C.; Rayner, C. R.; Meagher, A. K.; Flavin, S. M.; Batts, D. H.; Schentag, J. J. *Clin. Infect. Dis.* **2003**, 36, 159.
- (46) Bush, K. *Curr. Opin. Pharmacol.* **2012**, 12, 527.
- (47) Rodriguez-Avial, I.; Culebras, E.; Betriu, C.; Morales, G.; Pena, I.; Picazo, J. J. *J. Antimicrob. Chemother.* **2012**, 67, 167.
- (48) Alffenaar, J. W.; van der Laan, T.; Simons, S.; van der Werf, T. S.; van de Kastele, P. J.; de Neeling, H.; van Soolingen, D. *Antimicrob. Agents Chemother.* **2011**, 55, 1287.
- (49) Giamarellou, H. *Expert Rev. Anti Infect. Ther.* **2006**, 4, 601.
- (50) Lewis, K.; Ausubel, F. M. *Nat. Biotechnol.* **2006**, 24, 1504.
- (51) Lawrence, L.; Danese, P.; DeVito, J.; Franceschi, F.; Sutcliffe, J. *Antimicrob. Agents Chemother.* **2008**, 52, 1653.
- (52) Schwendener, S.; Perreten, V. *Antimicrob. Agents Chemother.* **2011**, 55, 4900.
- (53) Kadlec, K.; Pomba, C. F.; Couto, N.; Schwarz, S. *J. Antimicrob. Chemother.* **2010**, 65, 2692.
- (54) Srivastava, A.; Talaue, M.; Liu, S.; Degen, D.; Ebright, R. Y.; Sineva, E.; Chakraborty, A.; Druzhinin, S. Y.; Chatterjee, S.; Mukhopadhyay, J.; Ebright, Y. W.; Zozula, A.; Shen, J.; Sengupta, S.; Niedfeldt, R. R.; Xin, C.; Kaneko, T.; Irschik, H.; Jansen, R.; Donadio, S.; Connell, N.; Ebright, R. H. *Curr. Opin. Microbiol.* **2011**, 14, 532.
- (55) Andries, K.; Verhasselt, P.; Guillemont, J.; Gohlmann, H. W.; Neefs, J. M.; Winkler, H.; Van Gestel, J.; Timmerman, P.; Zhu, M.; Lee, E.; Williams, P.; de Chaffoy, D.; Huitric, E.; Hoffner, S.; Cambau, E.; Truffot-Pernot, C.; Lounis, N.; Jarlier, V. *Science* **2005**, 307, 223.
- (56) Avorn, J. *JAMA* **2013**, 309, 1349.
- (57) Ejim, L.; Farha, M. A.; Falconer, S. B.; Wildenhain, J.; Coombes, B. K.; Tyers, M.; Brown, E. D.; Wright, G. D. *Nat. Chem. Biol.* **2011**, 7, 348.
- (58) Knechel, N. A. *Crit. Care Nurse* **2009**, 29, 34.
- (59) Lee, R. E.; Li, W.; Chatterjee, D.; Lee, R. E. *Glycobiology* **2005**, 15, 139.
- (60) Joe, M.; Bai, Y.; Nacario, R. C.; Lowary, T. L. *J. Am. Chem. Soc.* **2007**, 129, 9885.

- (61) Frieden, T. R.; Sterling, T. R.; Munsiff, S. S.; Watt, C. J.; Dye, C. *Lancet* **2003**, *362*, 887.
- (62) Jensen, P. A.; Lambert, L. A.; Iademarco, M. F.; Ridzon, R.; Cdc *MMWR Recomm. Rep.* **2005**, *54*, 1.
- (63) Korf, J. E.; Pynaert, G.; Tournoy, K.; Boonefaes, T.; Van Oosterhout, A.; Ginneberge, D.; Haegeman, A.; Verschoor, J. A.; De Baetselier, P.; Grooten, J. *Am. J. Respir. Crit. Care Med.* **2006**, *174*, 152.
- (64) van Crevel, R.; Ottenhoff, T. H.; van der Meer, J. W. *Clin. Microbiol. Rev.* **2002**, *15*, 294.
- (65) Nicod, L. P. *Swiss Med. Wkly.* **2007**, *137*, 357.
- (66) Ferguson, J. S.; Weis, J. J.; Martin, J. L.; Schlesinger, L. S. *Infect. Immun.* **2004**, *72*, 2564.
- (67) Li, Y. J.; Petrofsky, M.; Bermudez, L. E. *Infect. Immun.* **2002**, *70*, 6223.
- (68) Dheda, K.; Booth, H.; Huggett, J. F.; Johnson, M. A.; Zumla, A.; Rook, G. A. *J. Infect. Dis.* **2005**, *192*, 1201.
- (69) Ddungu, H.; Johnson, J. L.; Smieja, M.; Mayanja-Kizza, H. *BMC Infect. Dis.* **2006**, *6*, 45.
- (70) Zumla, A.; Nahid, P.; Cole, S. T. *Nat. Rev. Drug Discov.* **2013**, *12*, 388.
- (71) Cohen, J. *Science* **2013**, *339*, 130.
- (72) Hill, A. N.; Becerra, J.; Castro, K. G. *Epidemiol. Infect.* **2012**, *140*, 1862.
- (73) Abubakar, I.; Zignol, M.; Falzon, D.; Raviglione, M.; Ditiu, L.; Masham, S.; Adetifa, I.; Ford, N.; Cox, H.; Lawn, S. D.; Marais, B. J.; McHugh, T. D.; Mwaba, P.; Bates, M.; Lipman, M.; Zijenah, L.; Logan, S.; McNERney, R.; Zumla, A.; Sarda, K.; Nahid, P.; Hoelscher, M.; Pletschette, M.; Memish, Z. A.; Kim, P.; Hafner, R.; Cole, S.; Migliori, G. B.; Maeurer, M.; Schito, M.; Zumla, A. *Lancet Infect. Dis.* **2013**, *13*, 529.
- (74) Chakraborty, S.; Gruber, T.; Barry, C. E., 3rd; Boshoff, H. I.; Rhee, K. Y. *Science* **2013**, *339*, 88.
- (75) Shi, W.; Zhang, X.; Jiang, X.; Yuan, H.; Lee, J. S.; Barry, C. E., 3rd; Wang, H.; Zhang, W.; Zhang, Y. *Science* **2011**, *333*, 1630.
- (76) Sirgel, F. A.; Tait, M.; Warren, R. M.; Streicher, E. M.; Bottger, E. C.; van Helden, P. D.; Gey van Pittius, N. C.; Coetzee, G.; Hoosain, E. Y.; Chabula-Nxiweni, M.; Hayes, C.; Victor, T. C.; Trollip, A. *Microb. Drug Resist.* **2012**, *18*, 193.
- (77) Salian, S.; Matt, T.; Akbergenov, R.; Harish, S.; Meyer, M.; Duscha, S.; Shcherbakov, D.; Bernet, B. B.; Vasella, A.; Westhof, E.; Bottger, E. C. *Antimicrob. Agents Chemother.* **2012**, *56*, 6104.

- (78) Laurenzi, M.; Ginsberg, A.; Spigelman, M. *Infect Disord. Drug Targets* **2007**, *7*, 105.
- (79) Blumberg, H. M.; Burman, W. J.; Chaisson, R. E.; Daley, C. L.; Etkind, S. C.; Friedman, L. N.; Fujiwara, P.; Grzemska, M.; Hopewell, P. C.; Iseman, M. D.; Jasmer, R. M.; Koppaka, V.; Menzies, R. I.; O'Brien, R. J.; Reves, R. R.; Reichman, L. B.; Simone, P. M.; Starke, J. R.; Vernon, A. A.; American Thoracic Society, C. f. D. C.; Prevention; the Infectious Diseases, S. *Am. J. Respir. Crit. Care Med.* **2003**, *167*, 603.
- (80) Johnson, J. L.; Hadad, D. J.; Dietze, R.; Maciel, E. L.; Sewali, B.; Gitta, P.; Okwera, A.; Mugerwa, R. D.; Alcaneses, M. R.; Quelapio, M. I.; Tupasi, T. E.; Horter, L.; Debanne, S. M.; Eisenach, K. D.; Boom, W. H. *Am. J. Respir. Crit. Care Med.* **2009**, *180*, 558.
- (81) Lienhardt, C.; Cook, S. V.; Burgos, M.; Yorke-Edwards, V.; Rigouts, L.; Anyo, G.; Kim, S. J.; Jindani, A.; Enarson, D. A.; Nunn, A. J.; Study, C. T. G. *JAMA* **2011**, *305*, 1415.
- (82) Falzon, D.; Jaramillo, E.; Schunemann, H. J.; Arentz, M.; Bauer, M.; Bayona, J.; Blanc, L.; Caminero, J. A.; Daley, C. L.; Duncombe, C.; Fitzpatrick, C.; Gebhard, A.; Getahun, H.; Henkens, M.; Holtz, T. H.; Keravec, J.; Keshavjee, S.; Khan, A. J.; Kulier, R.; Leimane, V.; Lienhardt, C.; Lu, C.; Mariandyshev, A.; Migliori, G. B.; Mirzayev, F.; Mitnick, C. D.; Nunn, P.; Nwagboniwe, G.; Oxlade, O.; Palmero, D.; Pavlinac, P.; Quelapio, M. I.; Raviglione, M. C.; Rich, M. L.; Royce, S.; Rusch-Gerdes, S.; Salakaia, A.; Sarin, R.; Sculier, D.; Varaine, F.; Vitoria, M.; Walson, J. L.; Wares, F.; Weyer, K.; White, R. A.; Zignol, M. *Eur. Respir. J.* **2011**, *38*, 516.
- (83) Gandhi, N. R.; Moll, A.; Sturm, A. W.; Pawinski, R.; Govender, T.; Lalloo, U.; Zeller, K.; Andrews, J.; Friedland, G. *Lancet* **2006**, *368*, 1575.
- (84) Dheda, K.; Shean, K.; Zumla, A.; Badri, M.; Streicher, E. M.; Page-Shipp, L.; Willcox, P.; John, M. A.; Reubenson, G.; Govindasamy, D.; Wong, M.; Padanilam, X.; Dziwiecki, A.; van Helden, P. D.; Siwendu, S.; Jarand, J.; Menezes, C. N.; Burns, A.; Victor, T.; Warren, R.; Grobusch, M. P.; van der Walt, M.; Kvasnovsky, C. *Lancet* **2010**, *375*, 1798.
- (85) Koul, A.; Arnoult, E.; Lounis, N.; Guillemont, J.; Andries, K. *Nature* **2011**, *469*, 483.
- (86) Donald, P. R.; Diacon, A. H. *Tuberculosis (Edinb)* **2008**, *88 Suppl 1*, S75.
- (87) Wallis, R. S.; Maeurer, M.; Mwaba, P.; Chakaya, J.; Rustomjee, R.; Migliori, G. B.; Marais, B.; Schito, M.; Churchyard, G.; Swaminathan, S.; Hoelscher, M.; Zumla, A. *Lancet Infect. Dis.* **2016**, *16*, e34.
- (88) Lee, M.; Lee, J.; Carroll, M. W.; Choi, H.; Min, S.; Song, T.; Via, L. E.; Goldfeder, L. C.; Kang, E.; Jin, B.; Park, H.; Kwak, H.; Kim, H.; Jeon, H. S.; Jeong, I.; Joh, J. S.; Chen, R. Y.; Olivier, K. N.; Shaw, P. A.; Follmann, D.; Song, S. D.; Lee, J. K.; Lee, D.; Kim, C. T.; Dartois, V.; Park, S. K.; Cho, S. N.; Barry, C. E., 3rd *N. Engl. J. Med.* **2012**, *367*, 1508.
- (89) Williams, K. N.; Stover, C. K.; Zhu, T.; Tasneen, R.; Tyagi, S.; Grosset, J. H.; Nuermberger, E. *Antimicrob. Agents Chemother.* **2009**, *53*, 1314.

- (90) ElMaraachli, W.; Slater, M.; Berrada, Z. L.; Lin, S. Y.; Catanzaro, A.; Desmond, E.; Rodrigues, C.; Victor, T. C.; Crudu, V.; Gler, M. T.; Rodwell, T. C. *Int. J. Tuberc. Lung Dis.* **2015**, *19*, 1222.
- (91) Davies, G.; Cerri, S.; Richeldi, L. *Cochrane Database Syst Rev* **2007**, CD005159.
- (92) Tyagi, S.; Ammerman, N. C.; Li, S. Y.; Adamson, J.; Converse, P. J.; Swanson, R. V.; Almeida, D. V.; Grosset, J. H. *Proc. Natl. Acad. Sci. U. S. A.* **2015**, *112*, 869.
- (93) Irwin, S. M.; Gruppo, V.; Brooks, E.; Gilliland, J.; Scherman, M.; Reichlen, M. J.; Leistikow, R.; Kramnik, I.; Nuermberger, E. L.; Voskuil, M. I.; Lenaerts, A. J. *Antimicrob. Agents Chemother.* **2014**, *58*, 4026.
- (94) De Lorenzo, S.; Alffenaar, J. W.; Sotgiu, G.; Centis, R.; D'Ambrosio, L.; Tiberi, S.; Bolhuis, M. S.; van Altena, R.; Viggiani, P.; Piana, A.; Spanevello, A.; Migliori, G. B. *Eur. Respir. J.* **2013**, *41*, 1386.
- (95) Karchmer, A. W.; Bayer, A. S. *Clin. Infect. Dis.* **2008**, *46 Suppl 5*, S342.
- (96) Carroll, K. C. *Mol. Diagn. Ther.* **2008**, *12*, 15.
- (97) Klevens, R. M.; Morrison, M. A.; Nadle, J.; Petit, S.; Gershman, K.; Ray, S.; Harrison, L. H.; Lynfield, R.; Dumyati, G.; Townes, J. M.; Craig, A. S.; Zell, E. R.; Fosheim, G. E.; McDougal, L. K.; Carey, R. B.; Fridkin, S. K.; Active Bacterial Core surveillance, M. I. *JAMA* **2007**, *298*, 1763.
- (98) Centers for Disease, C.; Prevention *MMWR Morb. Mortal. Wkly. Rep.* **2011**, *58*, 1.
- (99) Deresinski, S. *Clin. Infect. Dis.* **2005**, *40*, 562.
- (100) Deurenberg, R. H.; Stobberingh, E. E. *Infect. Genet. Evol.* **2008**, *8*, 747.
- (101) Kluytmans, J.; van Belkum, A.; Verbrugh, H. *Clin. Microbiol. Rev.* **1997**, *10*, 505.
- (102) Gordon, R. J.; Lowy, F. D. *Clin. Infect. Dis.* **2008**, *46 Suppl 5*, S350.
- (103) Enright, M. C.; Robinson, D. A.; Randle, G.; Feil, E. J.; Grundmann, H.; Spratt, B. G. *Proc. Natl. Acad. Sci. U. S. A.* **2002**, *99*, 7687.
- (104) Menzies, B. E. *Curr. Opin. Infect. Dis.* **2003**, *16*, 225.
- (105) Patti, J. M.; Allen, B. L.; McGavin, M. J.; Hook, M. *Annu. Rev. Microbiol.* **1994**, *48*, 585.
- (106) Ogawa, S. K.; Yurberg, E. R.; Hatcher, V. B.; Levitt, M. A.; Lowy, F. D. *Infect. Immun.* **1985**, *50*, 218.
- (107) Proctor, R. A.; Peters, G. *Clin. Infect. Dis.* **1998**, *27*, 419.

- (108) Kahl, B.; Herrmann, M.; Everding, A. S.; Koch, H. G.; Becker, K.; Harms, E.; Proctor, R. A.; Peters, G. *J. Infect. Dis.* **1998**, *177*, 1023.
- (109) Yarwood, J. M.; Schlievert, P. M. *J. Clin. Invest.* **2003**, *112*, 1620.
- (110) Cheung, A. L.; Koomey, J. M.; Butler, C. A.; Projan, S. J.; Fischetti, V. A. *Proc. Natl. Acad. Sci. U. S. A.* **1992**, *89*, 6462.
- (111) Fournier, B.; Hooper, D. C. *J. Bacteriol.* **2000**, *182*, 3955.
- (112) Liang, X.; Yu, C.; Sun, J.; Liu, H.; Landwehr, C.; Holmes, D.; Ji, Y. *Infect. Immun.* **2006**, *74*, 4655.
- (113) Said-Salim, B.; Dunman, P. M.; McAleese, F. M.; Macapagal, D.; Murphy, E.; McNamara, P. J.; Arvidson, S.; Foster, T. J.; Projan, S. J.; Kreiswirth, B. N. *J. Bacteriol.* **2003**, *185*, 610.
- (114) Luong, T. T.; Newell, S. W.; Lee, C. Y. *J. Bacteriol.* **2003**, *185*, 3703.
- (115) McCormick, J. K.; Yarwood, J. M.; Schlievert, P. M. *Annu. Rev. Microbiol.* **2001**, *55*, 77.
- (116) Wertheim, H. F.; Vos, M. C.; Ott, A.; van Belkum, A.; Voss, A.; Kluytmans, J. A.; van Keulen, P. H.; Vandenbroucke-Grauls, C. M.; Meester, M. H.; Verbrugh, H. A. *Lancet* **2004**, *364*, 703.
- (117) Melles, D. C.; Gorkink, R. F.; Boelens, H. A.; Snijders, S. V.; Peeters, J. K.; Moorhouse, M. J.; van der Spek, P. J.; van Leeuwen, W. B.; Simons, G.; Verbrugh, H. A.; van Belkum, A. *J. Clin. Invest.* **2004**, *114*, 1732.
- (118) Spellberg, B.; Daum, R. *Semin. Immunopathol.* **2012**, *34*, 335.
- (119) Waness, A. *J. Glob. Infect. Dis.* **2010**, *2*, 49.
- (120) Cornaglia, G.; Rossolini, G. M. *Clin. Microbiol. Infect.* **2009**, *15*, 218.
- (121) Davies, J.; Davies, D. *Microbiol. Mol. Biol. Rev.* **2010**, *74*, 417.
- (122) Levy, S. B.; Marshall, B. *Nat. Med.* **2004**, *10*, S122.
- (123) Brown, D. *Nat Rev Drug Discov* **2015**, *14*, 821.
- (124) Blair, J. M. A.; Webber, M. A.; Baylay, A. J.; Ogbolu, D. O.; Piddock, L. J. V. *Nat Rev Micro* **2015**, *13*, 42.
- (125) Kashmiri, S. V.; Hotchkiss, R. D. *Genetics* **1975**, *81*, 21.
- (126) Clewell, D. B.; Gawron-Burke, C. *Annu. Rev. Microbiol.* **1986**, *40*, 635.
- (127) Roberts, M. C. *FEMS Microbiol. Rev.* **1996**, *19*, 1.

- (128) Spratt, B. G. *Science* **1994**, 264, 388.
- (129) Soares, S.; Kristinsson, K. G.; Musser, J. M.; Tomasz, A. *J. Infect. Dis.* **1993**, 168, 158.
- (130) Wang, H.; Dzink-Fox, J. L.; Chen, M.; Levy, S. B. *Antimicrob. Agents Chemother.* **2001**, 45, 1515.
- (131) Nikaido, H. *Annu. Rev. Biochem.* **2009**, 78, 119.
- (132) Alekshun, M. N.; Levy, S. B. *Cell* **2007**, 128, 1037.
- (133) Voulgari, E.; Poulou, A.; Koumaki, V.; Tsakris, A. *Future Microbiol.* **2013**, 8, 27.
- (134) Wright, G. D. *Adv Drug Deliv Rev* **2005**, 57, 1451.
- (135) Spanogiannopoulos, P.; Waglechner, N.; Koteva, K.; Wright, G. D. *Proc. Natl. Acad. Sci. U. S. A.* **2014**, 111, 7102.
- (136) Kojima, S.; Nikaido, H. *Proc. Natl. Acad. Sci. U. S. A.* **2013**, 110, E2629.
- (137) Vargiu, A. V.; Nikaido, H. *Proc. Natl. Acad. Sci. U. S. A.* **2012**, 109, 20637.
- (138) Wozniak, A.; Villagra, N. A.; Undabarrena, A.; Gallardo, N.; Keller, N.; Moraga, M.; Roman, J. C.; Mora, G. C.; Garcia, P. *J. Med. Microbiol.* **2012**, 61, 1270.
- (139) Wright, G. D. *Chemical Communications* **2011**, 47, 4055.
- (140) Blair, J. M.; Piddock, L. J. *Curr. Opin. Microbiol.* **2009**, 12, 512.
- (141) Unemo, M.; Golparian, D.; Nicholas, R.; Ohnishi, M.; Gallay, A.; Sednaoui, P. *Antimicrob. Agents Chemother.* **2012**, 56, 1273.
- (142) Shore, A. C.; Deasy, E. C.; Slickers, P.; Brennan, G.; O'Connell, B.; Monecke, S.; Ehricht, R.; Coleman, D. C. *Antimicrob. Agents Chemother.* **2011**, 55, 3765.
- (143) Kumar, N.; Radhakrishnan, A.; Wright, C. C.; Chou, T. H.; Lei, H. T.; Bolla, J. R.; Tringides, M. L.; Rajashankar, K. R.; Su, C. C.; Purdy, G. E.; Yu, E. W. *Protein Sci.* **2014**, 23, 423.
- (144) Long, K. S.; Poehlsgaard, J.; Kehrenberg, C.; Schwarz, S.; Vester, B. *Antimicrob. Agents Chemother.* **2006**, 50, 2500.
- (145) Zhang, W. J.; Xu, X. R.; Schwarz, S.; Wang, X. M.; Dai, L.; Zheng, H. J.; Liu, S. J. *Antimicrob. Chemother.* **2014**, 69, 385.
- (146) Fritsche, T. R.; Castanheira, M.; Miller, G. H.; Jones, R. N.; Armstrong, E. S. *Antimicrob. Agents Chemother.* **2008**, 52, 1843.

- (147) Vetting, M. W.; Hegde, S. S.; Wang, M.; Jacoby, G. A.; Hooper, D. C.; Blanchard, J. S. *J. Biol. Chem.* **2011**, *286*, 25265.
- (148) Lim, L. M.; Ly, N.; Anderson, D.; Yang, J. C.; Macander, L.; Jarkowski, A., 3rd; Forrest, A.; Bulitta, J. B.; Tsuji, B. T. *Pharmacotherapy* **2010**, *30*, 1279.
- (149) Mishra, N. N.; Yang, S. J.; Chen, L.; Muller, C.; Saleh-Mghir, A.; Kuhn, S.; Peschel, A.; Yeaman, M. R.; Nast, C. C.; Kreiswirth, B. N.; Cremieux, A. C.; Bayer, A. S. *PLoS One* **2013**, *8*, e71151.
- (150) Wright, G. D. *BMC Biol.* **2010**, *8*, 123.

CHAPTER 4

DESIGN AND SYNTHESIS OF NOVEL ANTIMICROBIALS WITH ACTIVITY AGAINST GRAM-POSITIVE BACTERIA AND MYCOBACTERIAL SPECIES, INCLUDING *M. TUBERCULOSIS*

4.1. ABSTRACT

The alarming increase in bacterial resistance over the last decade along with a dramatic decrease in new treatments for infections has led to problems in the healthcare industry. Tuberculosis (TB) is caused mainly by *Mycobacterium tuberculosis* which is responsible for 1.4 million deaths per year. A world-wide threat with HIV co-infected with multi and extensively drug-resistant strains of TB has emerged. In this regard, herein, novel acrylic acid ethyl ester derivatives were synthesized in simple, efficient routes and evaluated as potential agents against several *Mycobacterium* species. These were synthesized via a stereospecific process for structure activity relationship (SAR) studies. Minimum inhibitory concentration (MIC) assays indicated that esters **12**, **13**, and **20** exhibited greater *in vitro* activity against *Mycobacterium smegmatis* than rifampin, one of the current, first-line anti-mycobacterial chemotherapeutic agents. Based on these studies the acrylic ester **20** has been developed as a potential lead compound which was found to have an MIC value of 0.4 µg/mL against *Mycobacterium tuberculosis*. The SAR and biological activity of this series is presented; a Michael – acceptor mechanism appears to be important for potent activity of this series of analogs.

4.2. INTRODUCTION

Surprisingly, tuberculosis (TB) is the second leading lethal infectious disease in the world, following human immunodeficiency virus (HIV). According to a recent global tuberculosis report

by the World Health Organization (WHO), TB caused 1.4 million deaths in 2011 and 9 million newly infected cases are reported each year.¹ TB is a bacterial infection caused by the acid-fast bacillus *M. tuberculosis*. TB mainly infects the lungs (pulmonary TB), although it can affect most organs in the body (extra pulmonary TB) including the liver, brain and kidney.² The traditional current first-line treatment of drug-sensitive TB infections consists of a four-drug regimen that includes rifampin, isoniazid, pyrazinamide, and ethambutol.³⁻⁴ This treatment requires a minimum of six months to be effective.⁵ Due to the extended time course of treatment many patients stop taking the medication as soon as their symptoms decrease long before the infection has been eradicated, allowing the bacteria to develop drug resistance. This potentially leads to multidrug-resistant (MDR) and extensively drug-resistant (XDR) forms of TB. Treatment of these infections may extend to 18-20 months.² The ability to treat TB is further confounded by co-infection with HIV leading to treatment failures as well as a rise in transmission rates and mortality due to TB. Without improvements one billion people will be newly infected, there will be around 125 million people get sick, and 14 million will die in the next ten years.⁶⁻¹¹ Consequently, the development of new chemotherapeutic combinations for TB that eradicate the disease quicker as well as are less complex, cheaper and have fewer side effects are essential for the future.

In our continued efforts to develop new anti-mycobacterial agents, a novel class of acrylic esters was synthesized.¹²⁻¹⁴ In early efforts to increase the molecular diversity in this series of antimicrobial agents, certain acrylic acid ethyl esters such as **1** were synthesized.^{15a} This initial lead compound exhibited a promising MIC of 16 $\mu\text{g/mL}$ against *M. smegmatis*, a safer surrogate of the clinically significant TB causing mycobacteria. Consequently, **1** was assayed against the more virulent strain, *M. tuberculosis*, resulting in an MIC value of 25 $\mu\text{g/mL}$.¹²

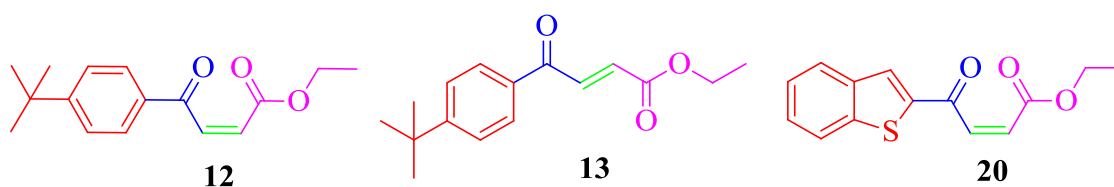
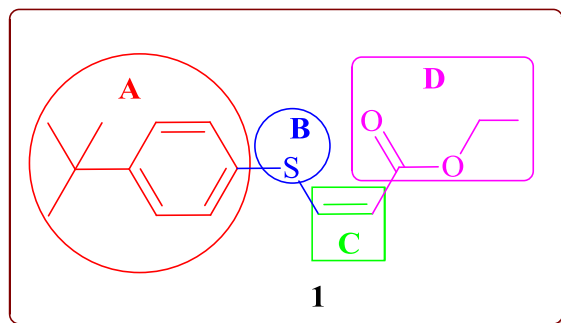
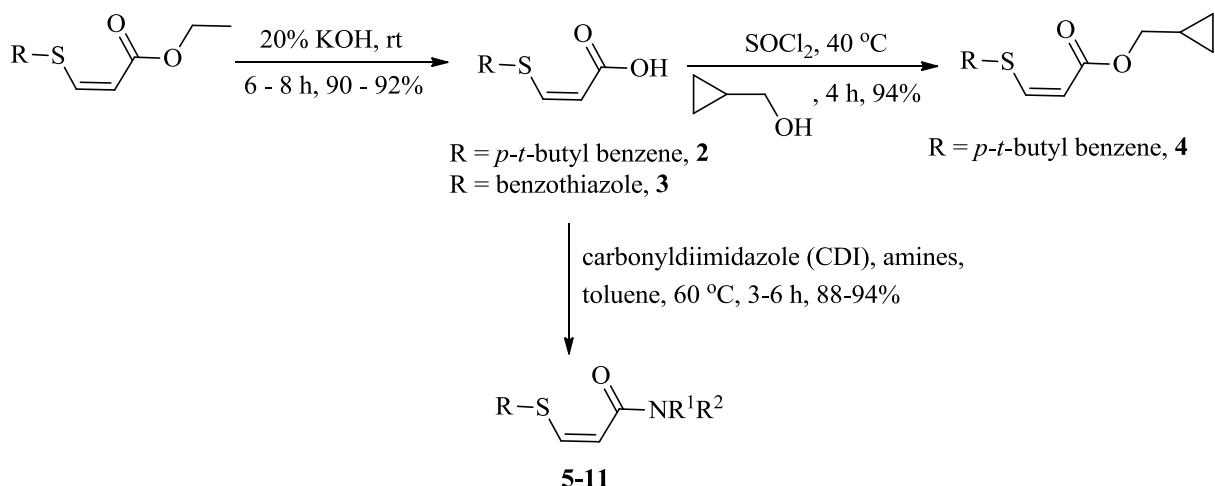


Figure 4-1. Lead Compounds

4.3. RESULTS

The structure-activity relationship (SAR) study of lead compound **1** provided valuable information regarding the basic structural requirements for anti-mycobacterial activity. In addition, manipulations of the basic unit led to increased potency and stability.^{15b} In order to evaluate the effect of structural changes on anti-mycobacterial activity, the esters of **1** at positions **A**, **B**, **C**, and **D** were altered. First, in order to increase the hydrophobic interactions of ester **1** with bacteria the ethyl ester was replaced with a methyl cyclopropyl ester to give **4** (Scheme 4-1) at position **D** in **1**. To increase the stability as well as the water solubility of the ester **1**, the acids **2** and **3** (Scheme 4-1) were prepared. This increased the hydrophilic character of the molecule and the CLoP value went from 5.7 to 4.7 in agreement with Lipinski's rules and the classic QSAR studies of Hansch.¹⁶ Various amides (**5-11**) were synthesized to increase stability and to evaluate steric and electronic effects on the bioavailability and potency (Scheme 4-1) of **1**.



- R = benzothiazole; R¹ = R² = isopropyl: **5**
R = *p-t*-butyl benzene; R¹ = H; R² = phenyl: **6**
R = *p-t*-butyl benzene; R¹ = methyl; R² = phenyl: **7**
R = *p-t*-butyl benzene; R¹ = H; R² = methyl: **8**
R = *p-t*-butyl benzene; R¹ = R² = methyl: **9**
R = *p-t*-butyl benzene; R¹ = R² = isopropyl: **10**
R = *p-t*-butyl benzene; R¹ = H; R² = cyclopropyl: **11**

Scheme 4-1. Synthesis of *cis* acrylic acids, amides and esters

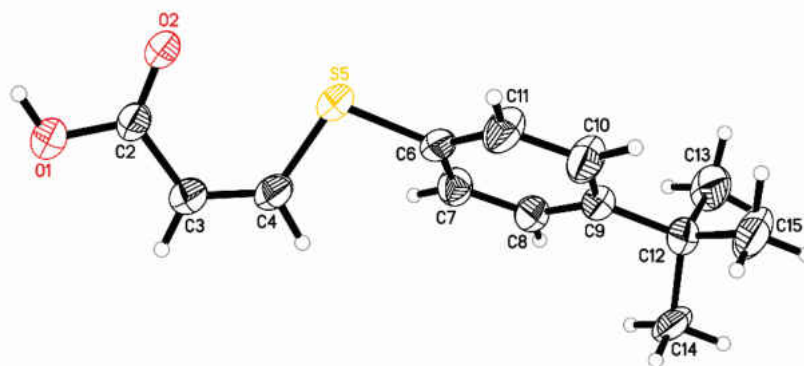
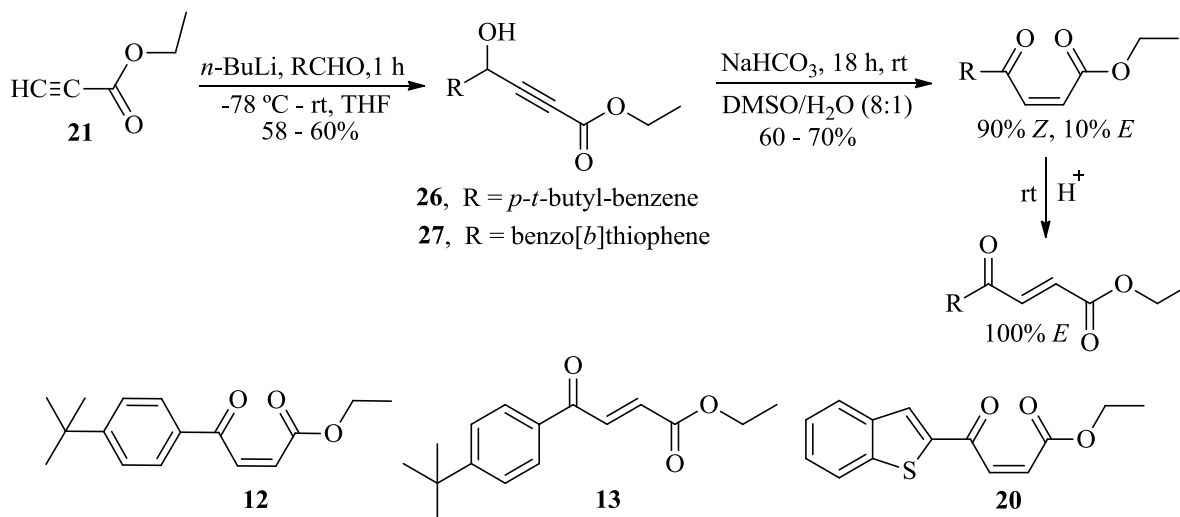


Figure 4-2. ORTEP view of the crystal structure of acrylic acid 2

Further SAR studies on these compounds were carried out with ligands which contained similar functionality. Hence, the sulfur atom in **1** was replaced with the keto group at position **B** to furnish ketones **12** and **13** (Scheme 4-2).¹⁷ This altered the electronic character of the double

bond of analog **1**. These 4-oxo substituted acrylic esters exhibited increased activity against *M. smegmatis* and *M. tuberculosis* (see Tables 4-1 and 4-2).



Scheme 4-2. Synthesis of 4-oxo substituted acrylic acid ethyl esters^a

^a *Z* and *E* isomers were separated by flash chromatography on silica gel.

Table 4-1. Minimum inhibitory concentrations (MIC) of acrylic acid ethyl ester analogs against common bacterial species (µg/mL)

Compound	<i>M. smegmatis</i>	<i>S. aureus</i> ATCC 29213	<i>B.cereus</i>	<i>E. coli</i> ATCC 29522
1	16	>128	>128	>128
2	>128	>128	128	>128
3	>128	>128	>128	>128
4	16	>128	128	>128
5	>128	>128	>128	>128
6	>128	>128	>128	>128
7	32	>128	>128	>128
8	>128	>128	128	>128
9	64	>128	16	>128
10	64	>128	>128	>128
11	>128	>128	>128	>128
12	8	4	8	>128
13	8	2	4	>128
14	>128	>128	ND ^b	>128
15	64	>128	ND ^b	>128
16	>128	32	ND ^b	>128
17	>128	0.5	ND ^b	>128
18	>128	16	ND ^b	>128
19	>128	>128	ND ^b	>128
20	4	1	ND ^b	128
24	>128	>128	>128	>128
25	>128	>128	>128	>128
28	16	64	ND ^b	>128
29	128	32	ND ^b	>128
tetracycline ^a	ND ^b	0.25	ND ^b	1
rifampin ^a	64	ND ^b	ND ^b	ND ^b

^a Positive control

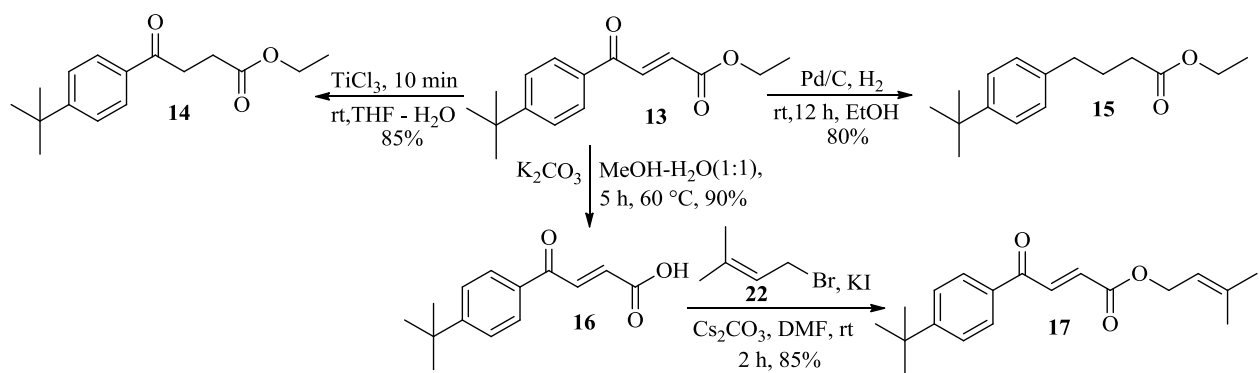
^b ND = Not determined

Table 4-2. Minimum inhibitory concentrations (MIC) of select compounds against additional *mycobacterial* species ($\mu\text{g/mL}$)

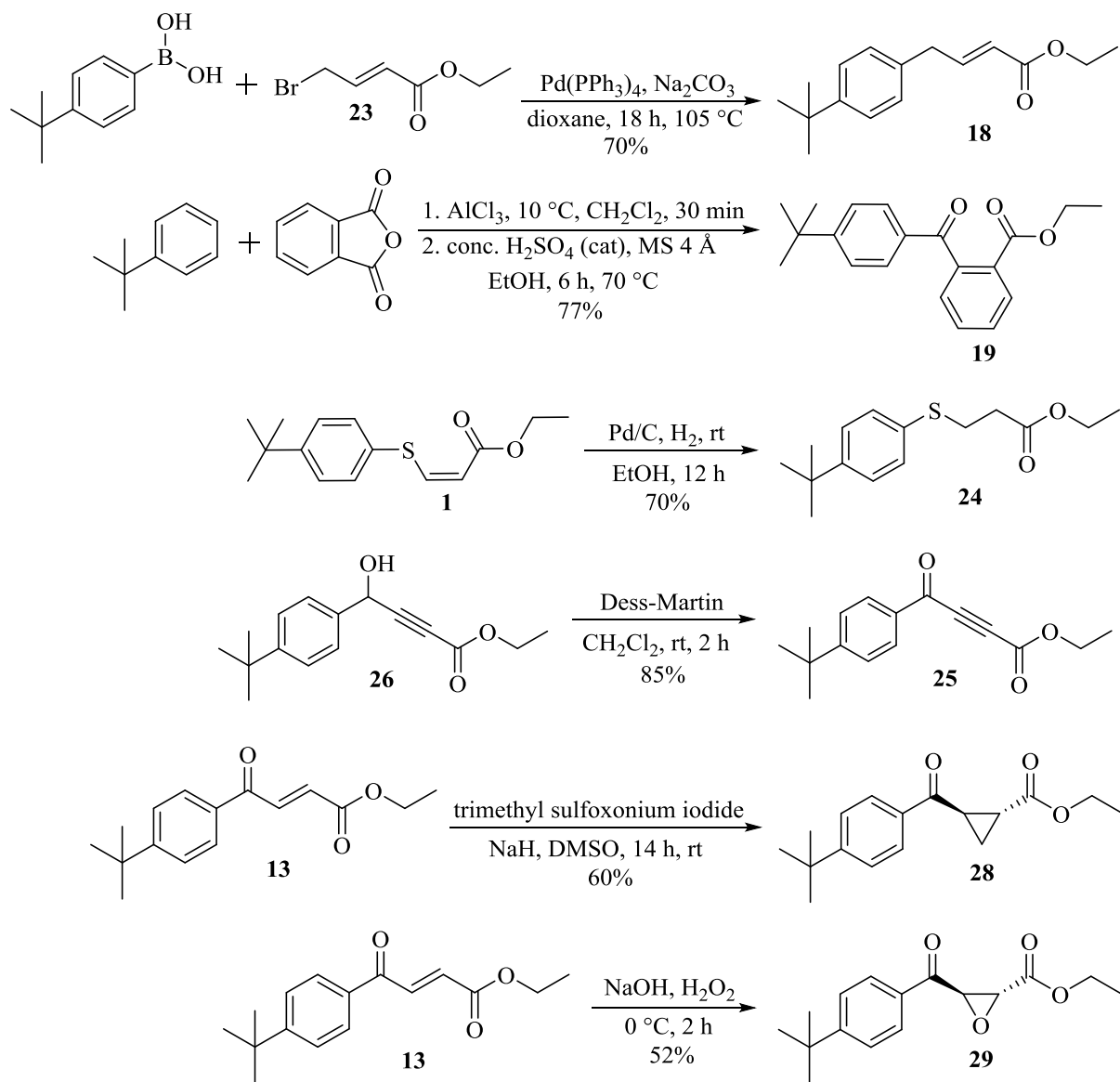
Compound	<i>M. tuberculosis</i>	<i>M. fortuitum</i>	<i>M. kansasii</i>	<i>M. chelonae</i>	<i>M. avium</i>	<i>M. intracellulare</i>
12	0.8	8	64	16	32	8
13	0.8	4	32	8	16	4
14	ND ^b	>128	>128	>128	>128	>128
15	ND ^b	32	128	32	>128	>128
16	ND ^b	>125	ND ^b	ND ^b	ND ^b	ND ^b
17	ND ^b	64	>128	32	>128	>128
18	ND ^b	>128	>128	>128	>128	>128
19	ND ^b	>128	>128	>128	>128	>128
20	0.4	16	8	8	16	4
24	ND ^b	>128	>128	>128	>128	>128
25	ND ^b	>128	>128	>128	>128	>128
28	ND ^b	64	ND ^b	ND ^b	ND ^b	ND ^b
29	ND ^b	>128	ND ^b	ND ^b	ND ^b	ND ^b
ethambutol ^a	1.2	ND ^b	ND ^b	ND ^b	ND ^b	ND ^b
isoniazid ^a	0.25	ND ^b	ND ^b	ND ^b	ND ^b	ND ^b
rifampin ^a	<0.03	32	0.5	32	2	1

^a Positive controls^b ND = Not determined

Presumably, the *trans* ester **13** is more stable *in vivo* than the *cis* ester **12**. Accordingly, a series of analogs were prepared to study the importance of the double bond in regard to the increased potency of **13**. To evaluate the importance of the electronic character of the double bond in keto ester **13**, the saturated compounds **14** and **15** (Scheme 4-3) were synthesized as well as **19**, **28**, and **29**, with a benzene, cyclopropyl and epoxide ring in place of the double bond, as illustrated in Scheme 4-4. To increase the hydrophobic character of the molecule **13**, a prenyl group was substituted for the ethyl function (see reference 31 for a precedent) to provide alkyl ester **17** (Scheme 4-3). The hydrogen bond acceptor properties of the olefin in **13** were decreased via synthesis of an α,β -unsaturated ester **18** (Scheme 4-4). To alter both the geometry of the molecule and the Michael acceptor properties, the alkyne **25** was synthesized (Scheme 4-4). It is well-known that acetylenic ketones do not undergo Michael additions, as rapidly as olefinic ketones or esters.¹⁸⁻



Scheme 4-3. Synthesis of acrylic acid ester derivatives



Scheme 4-4. Synthesis of acrylic acid ethyl ester derivatives

4.4. CHEMISTRY

To study the SAR and establish the pharmacophoric unit of **1**, as mentioned earlier, the molecule was divided into four areas **A**, **B**, **C**, and **D** (Figure 4-1). To alter area **D**, the two esters represented by structure **1** were saponified to provide the corresponding carboxylic acids **2** and **3** in excellent yields (91 and 92%), respectively, using an aqueous solution of 20% KOH (Scheme 4-1). The stereochemistry of acid **2** was assigned by ¹H NMR. The characteristic olefinic hydrogens appeared with a value of the coupling constant of 10.1 Hz and were readily correlated with the *cis* isomer with the help of the available literature on acrylic esters and also confirmed by X-ray crystallographic analysis (Figure 4-2).^{15a, 22-23} In the case of acid **3**, the starting moiety in area **A** had been altered from *t*-butyl benzene to benzothiazole. Due to the presence of the keto group adjacent to the double bond in keto ester **13**, a similar hydrolysis reaction was attempted with 20% KOH but resulted in the disappearance of the alkene protons. The hydrolysis conditions were modified and **16** was prepared from keto ester **13** in 90% yield using K₂CO₃ in refluxing aqueous methanol, as illustrated in Scheme 4-3. The cyclopropyl methyl ester **4** was prepared from the acid using thionyl chloride and then addition of cyclopropylmethyl alcohol in excellent yield 93% (Scheme 4-1).

Additional alteration of the ester moiety in **1** (area **D**) was accomplished using carbonyldiimidazole (CDI) and the corresponding amines in toluene at 60 °C giving amides **5-11** (Scheme 4-1) in good to excellent yields 88-93%. The SAR of area **B** of **1** was explored by introduction of the keto group in place of the sulphur atom in **1** to furnish ketones **12** and **13** (individually). In order to do this the 4-hydroxy-2-alkynoates **26** and **27** were prepared first by the addition of *n*-butyllithium to propynoic acid ethyl ester at low temperature -78 °C and the alkynic anion, which resulted, rapidly added to the corresponding aldehydes (Scheme 4-2) in 58-60%

yield.²⁴ Treatment with sodium bicarbonate as a catalyst for the required isomerization gave a mixture of *cis* and *trans* isomers **12** and **13** (9:1) which were readily separated by flash column chromatography (overall yield 70%). Treatment of the mixture of **12** and **13** with anhydrous HCl(g) in ether gave complete conversion of *cis* **12** into *trans* **13** in excellent yield. In the presence of the benzothiophene heterocyclic ring in **20**, the yield decreased to 60% (Scheme 4-2).²⁵

Alteration of area **C** of **13** from alkene to alkane was slightly more challenging. The classic route using Pd/C in EtOH with hydrogen gas (pressure at 20 psi) furnished saturated analog **15** instead of the desired ketone **14** because the ketone was both benzylic and allylic. However, the reduction procedure of *trans* ester **13** with TiCl₃²⁶ gave ketone **14** in good yield 85% (Scheme 4-3). In the case of thioalkyl **24**, the standard Pd/C (H₂) reduction was readily executed (Scheme 4-4). Prenyl ester **17** was prepared by alkylation of acid **16** with prenyl bromide **22** with cesium carbonate as the base in DMF in 85% yield (Scheme 4-3). The synthesis of **25** was accomplished using the Dess-Martin reagent on propargylic alcohol **26** in good yield (85%, Scheme 4-4). The α,β -unsaturated analog **18** was synthesized by a Suzuki palladium catalyzed cross coupling reaction (Scheme 4-4) with the allylic bromide **23** and the appropriate phenyl boronic acid.²⁷ The benzene substituted compound **19** was synthesized using a Friedel-Crafts acylation reaction between phthalic anhydride and *p-t*-butyl benzene in the presence of a Lewis acid (AlCl₃).²⁸ The subsequent acid was converted into the ethyl ester with EtOH in the presence of a catalytic amount of H₂SO₄ at 70 °C; activated molecular sieves (MS 4 Å) were used for removal of water. Cyclopropanation of **13** to **28** was achieved by the use of dimethylsulfoxonium methylide and *trans* epoxide **29** was prepared by the epoxidation of the *trans* olefin **13** with alkaline hydrogen peroxide.²⁹⁻³⁰

4.5. BIOLOGY

Structure-activity relationship (SAR) studies based on antimicrobial activity in a standard minimum inhibitory concentration (MIC) assay, indicated 42% (10 of 24) of analogs tested showed equal (3 of 24) or greater (7 of 24) potency than the positive control rifampin against *M. smegmatis* (MIC \leq 64 $\mu\text{g/mL}$, Table 4-1). Anti-mycobacterial activity of **1** was abolished by alteration of position **D** to a carboxylic acid (see MIC values for **2** and **3**). Anti-mycobacterial activity of **1** was retained when position **D** was altered to a cyclopropane (**4**), however, anti-mycobacterial activity was abolished by the larger prenyl group (**17**). However, **17** showed potent anti-staphylococcal activity (MIC = 0.5 $\mu\text{g/mL}$) which is exciting via another study. An amide in position **D** either abolished (**5**, **6**, **8**, and **11**) or decreased (**7**, **9**, and **10**) anti-mycobacterial activity.

At position **B**, replacement of the sulfur atom with a keto group (**12** and **13**) doubled the potency of **1** and extended the activity to include the Gram-positive species tested. However, replacement of the ethyl ester (**13**) with a carboxylic acid (**16**) in position **D** again destroyed anti-mycobacterial activity although some anti-staphylococcal activity was retained. In the *cis* keto compound **12**, replacement of the *p-t*-butyl phenyl group (**12**) with a benzo[*b*]thiophene moiety (**20**) in position **A** increased antibacterial potency for all bacteria tested except *M. fortuitum* (Table 4-2). Saturation of the alkene bond in position **C** of the keto esters (**12** and **13**) abolished all antibacterial activity (see **14** and **24**). Reduction of the **C**₁ keto function (**15**) partially restored anti-mycobacterial activity. However, anti-mycobacterial activity was again abolished in the unsaturated alkene with the **C**₁ keto group fully reduced (**18**). When the alkene was replaced by either benzene (**19**) or an alkyne (**25**) activity was abolished. Whereas, the cyclopropyl analog **28** showed decreased potency (MIC = 16 $\mu\text{g/mL}$, Table 4-1) on *M. smegmatis* and epoxide ester **29** showed moderate anti-staphylococcal activity but no activity against mycobacterial species.

Of the compounds active against *M. smegmatis*, the three most potent (**12**, **13**, and **20**) were also active against both the Gram-positive bacteria tested (Table 4-1) as well as the other mycobacterial species that were tested (Table 4-2), including *M. tuberculosis*. In fact, the *in vitro* sub- $\mu\text{g/mL}$ anti-mycobacterial activity of **12**, **13**, and **20** against *M. tuberculosis* indicated an increase in potency over the lead compound **1** of 32- and 64-fold, respectively. Furthermore, both **12** and **13** were 1.5-fold more active than ethambutol against *M. tuberculosis*, whereas **20** was 3-fold more potent than this current first line anti-tuberculosis drug.

4.6. DISCUSSION

The SAR studies clearly show that the structure of the most potent compounds, **12**, **13**, and **20** contain an aromatic ring in area **A** with a Michael acceptor scaffold in areas **B**, **C**, and **D**. In order to study this effect, the saturated analogs (**14**, **15**, **18**), prenyl ester **17**, benzene compound **19**, keto analog **20**, alkyne **25**, cyclopropyl ester **28** and epoxide ester **29** were prepared. Alkyne **25** failed to behave as a Michael acceptor because of the *sp* character in area **C** as compared to the *sp*² character in olefin **13**. It is also possible that the geometry of the molecule plays some role in activity from *sp*² hybridization to *sp* hybridization. To mimic the double bond nature of the active compound **13**, but limit the Michael acceptor properties, the olefin in **13** was replaced by the benzene ring in analog **19**, cyclopropyl ring in analog **28** and epoxide ring in analog **29**. The benzene analog **19** was inactive, presumably because the Michael acceptor properties were decreased because of resonance stabilization. However, the cyclopropyl ethyl ester **28** demonstrated weak activity similar to the thio ester **1** on *M. smegmatis*, whereas epoxide ester **29** showed moderate activity on *S. aureus* ATCC29213 (MIC = 32 $\mu\text{g/mL}$, Table 4-1) but no activity against mycobacterial species. Saturated analogs **14**, **15**, and **18**, devoid of a keto function, were also prepared to examine the importance of the Michael acceptor scaffold (area **B-C**) for activity.

The saturated analogs **14** and **15** were not active and loss of the ketone in olefin **18** completely eliminated activity. When the ethyl ester was transformed into the prenyl ester to give the lipophilic **17**, activity against *M. smegmatis* was completely eliminated, although **17** was nearly as potent (MIC = 0.5 µg/mL, Table 4-1) against *S. aureus* ATCC29213 as compared to the standard tetracycline (MIC = 0.25 µg/mL, Table 4-1) which is of interest in other studies.¹² It is not clear why the prenyl ester is not active since it has been previously demonstrated that hydrophobicity was important for very potent activity.³¹ Since mycolic acid surrounds the mycobacterial cell, it is possible that the prenyl group of olefin **17** adheres to the mycolic acid bilayer and does not penetrate the cell. Further work to explore this result is required. The methyl cyclopropyl ester **4** was still active against *M. smegmatis* (MIC = 16 µg/mL, Table 4-1), but not active on other strains.

It is clear the Michael acceptor property of the active keto targets **12**, **13**, and **20** is very important. In support of this, the acrylic ester amides **5-11** were not active, presumably, because the Michael acceptor properties of the olefin (area **B**) were decreased. In modern medicine, many Michael acceptors are employed in the clinic including several corticosteroids, antibiotics, antiviral and anticancer drugs.³²⁻³⁹ Some Michael acceptor scaffolds have been developed by accident to impart structural rigidity, *e.g.* corticosteroids, while others require Michael acceptors due to the desired mechanism of action for some chronic diseases, such as those used in antiviral and anticancer therapies. In drug discovery, Michael acceptors are used to trap an active intermediate in the biological cycle. One important component of such an intermediate can be a free thiol. An example of this can be found in cysteine protease inhibitors, which can be employed to help treat and prevent many diseases including emphysema, stroke, viral infections, cancer, Alzheimer's disease, inflammation and arthritis.⁴⁰⁻⁴² Acifran,⁴³ affinin,⁴⁴ amcinonide,⁴⁵ betamethasone,⁴⁶ dexamethasone,⁴⁷ are a few examples of Michael acceptor drugs used clinically. Rifampin is also

a Michael acceptor and, as mentioned, is one of the current first line drugs in the tuberculosis treatment regimen. These results suggest that Michael acceptor acrylates **12**, **13**, and **20** could potentially be developed into viable anti-mycobacterial agents providing alternatives to current front line therapies used in the treatment of TB, MRSA, and other less common infections caused by other *Mycobacterium* species. In unpublished work, Schwan *et al.* have given mice a 300 mg/kg dose of **20** and saw no overt toxic effects, showing that such compounds may not be overtly cytotoxic *in vivo*. Much work must be done to follow up these results and gain a clear understanding of the mechanism of action for these extremely active compounds. It is important to note that **12**, **13**, and **20** were not active toward *E. coli* indicating their mode of action is not an indiscriminate interaction with bacteria.

4.7. CONCLUSION

A new series of acrylic acids, including various amides, prenyl and ethyl esters were synthesized by simple, cheap and efficient synthetic routes as compared to those agents employed in first-line therapies for TB, including rifampin.⁴⁸⁻⁵⁰ Due to their simple, unique, and novel scaffold, these analogs have been evaluated and demonstrated antimicrobial activity against a range of Gram-positive bacteria including *M. smegmatis* and the pathogenic *M. tuberculosis*. Keto analogs **12**, **13**, and **20** exhibited the most potent antimicrobial activity; keto olefins **12** and **13** demonstrated an 8-fold greater activity against *M. smegmatis* than rifampin, one of the primary anti-mycobacterial agents currently used to treat TB (Table 4-1). Accordingly, **12** and **13** were assayed against other, more virulent mycobacteria species, including *M. tuberculosis*. Both analogs exhibited an MIC value of 0.8 µg/mL against *M. tuberculosis* (Table 4-2), indicating less potency than isoniazid (MIC = 0.25 µg/mL, Table 4-2) or rifampin (MIC = <0.03 µg/mL, Table 4-2) but greater potency than ethambutol (MIC = 1.2 µg/mL, Table 4-2), all three of which are part of the

current first-line drug regimen for TB. Agents which exhibit MIC values of less than 10 $\mu\text{g/mL}$ are generally considered clinically significant for further study.⁵¹ This activity may signify a new mechanism of action for these readily available small molecules. Analog **20** is unique in that it exhibits an MIC value of 4 $\mu\text{g/mL}$ against *M. smegmatis* with 16 fold greater potency than rifampin against this strain and at the same time is very potent (1 $\mu\text{g/mL}$) against *S. aureus* ATCC2913. The benzothiophene analog **20** exhibited excellent activity against *M. tuberculosis* with an MIC value of 0.4 $\mu\text{g/mL}$, a 64-fold increase in activity over lead compound **1** and 3-fold increase in potency over ethambutol. Although the mechanism of action of the acrylic ethyl esters **12**, **13**, and **20** is not known at this time, experiments are underway to see which biochemical pathway (if any) in the biogenesis of TB was disrupted. These simple scaffolds warrant further study to treat drug resistant antimicrobial strains including those related to *M. tuberculosis*.⁵²

These small molecules are easily and inexpensively synthesized, even in multi-gram quantities, in comparison to other front-line treatments. Further SAR studies to obtain greater potency, in addition to elucidation of the mode of action of the active compounds are ongoing in our laboratories.

4.8. EXPERIMENTAL

4.8.1. Chemistry

All reactions were performed in oven-dried round-bottom flasks under an argon atmosphere unless the reaction conditions were supposed to contain water. Stainless steel syringes were used to transfer air-sensitive liquids. Organic solvents were purified when necessary by standard methods⁵³ or purchased from Sigma-Aldrich.TM All chemicals purchased from Sigma-AldrichTM were employed as is, unless stated otherwise in regard to purification. Silica gel (Dynamic Adsorbents, 230-400 mesh) for flash chromatography was utilized to purify the analogues. The

^1H and ^{13}C NMR data were obtained on Bruker Spectrospin 300 MHz and GE 500 MHz instruments with chemical shifts in δ (ppm) reported relative to TMS. The HRMS and GC/MS spectral data were determined by the laboratory for mass spectrometry, University of Kansas, Lawrence, KS 66045-7582, USA. Melting points were taken on a Stuart melting point apparatus SMP3 manufactured by Barloworld Scientific US Ltd. X-ray crystallographic studies were performed at the Naval Research Laboratory, Code 6930, Washington, D. C. 20375, USA.

4.8.1.1. General method for the synthesis of acids 2 and 3

To the ester **1** (0.1 mmol) was added 20% aq KOH (20 mL) and the mixture was stirred at rt. The reaction progress was monitored by TLC on a silica gel plate (10% EtOAc in hexane). After 6-8 h the starting ester had disappeared on TLC and the mixture was cooled to 0 °C. The acid was precipitated from the solution by addition of cold aq 5% hydrochloric acid until the pH of the solution reached 1.5-2. The slurry which resulted was allowed to stir for 30 min and the acid was filtered off under vacuum. The acid was dissolved in a saturated aq solution of Na_2CO_3 (10 mL) and the aq layer was extracted twice with DCM (15 mL) to remove impurities. The aq layer was cooled to 0 °C while adjusting the pH to 1.5-2. The pure acid precipitated and was filtered and dried in the air with yields ranging from 90-92%.

4.8.1.1.1. (Z)-3-(4-(*tert*-Butyl)phenyl)thio)acrylic acid (2)

The general method above was followed using ester **1** (215 mg, 0.1 mmol) which yielded 171 mg (92%) of acid **2** as a white powder. ^1H NMR (300 MHz, CDCl_3): δ 7.47-7.40 (m, 5H), 5.96-5.93 (d, $J = 10.1$ Hz, 1H), 1.33 (s, 9H); ^{13}C NMR (75 MHz, CDCl_3): δ 170.5, 149.1, 146.4, 132.1, 129.7, 125.4, 112.3, 40.7, 31.1. HRMS (ESI) (M+H) $^+$ calcd. For $\text{C}_{13}\text{H}_{17}\text{O}_2\text{S}$: 237.0949; Found: 237.0942.

4.8.1.1.2. (Z)-3-(Benzo[d]thiazol-2-ylthio)acrylic acid (3)

The general method above was followed using benzothiazole acrylic acid ethyl ester (266 mg, 0.1 mmol) which yielded 215 mg (91%) of acid 3 as an off white powder. ¹H NMR (300 MHz, CDCl₃): δ 8.27-8.23 (d, *J* = 9.75 Hz, 1H), 8.12-8.09 (d, *J* = 7.5 Hz, 1H), 7.99-7.96 (d, *J* = 7.95 Hz, 1H), 7.56 (t, *J* = 6.12 Hz, 1H), 7.47 (t, *J* = 7.5 Hz, 1H), 6.30-6.27 (d, *J* = 9.75 Hz, 1H); ¹³C NMR (75 MHz, CDCl₃): δ 167.8, 167.6, 152.4, 140.3, 135.4, 127.3, 125.8, 122.7, 121.1, 117.6. HRMS (ESI) (M+H)⁺ calcd. For C₁₀H₈NO₂S₂: 237.9996; Found: 237.9989.

4.8.1.2. (Z)-Cyclopropylmethyl 3-((4-(*tert*-butyl)phenyl)thio)acrylate (4)

To a stirred suspension of the acid **1** (236 mg, 0.1 mmol) in DCM (10 mL) was added thionyl chloride (0.1 mL, 0.15 mmol). The reaction mixture was allowed to heat to reflux for 2 h. The reaction mixture was cooled to rt and the appropriate alcohol (0.2 mmol) was added with stirring. The reaction was again heated at reflux for 2 h. The reaction progress was monitored by TLC (silica gel). After complete conversion of the starting acid into the ester, the reaction solution was cooled to 0 °C and water (5 mL) was added slowly. The reaction mixture was stirred further for 15 min and the layers separated. The aq layer was extracted again with DCM (3 x 10 mL). The combined organic extracts were washed with brine (2 x 15 mL) and this was followed by cold water (10 mL). The organic layer was dried (Na₂SO₄) and concentrated under vacuum to yield the crude ester **4**. This material was further purified by flash column chromatography (silica gel). The pure ester **4** (270 mg) was obtained in 93% yield as an oil. ¹H NMR (300 MHz, CDCl₃): δ 7.64-7.61 (m, 4H), 7.58 (d, *J* = 10.38 Hz, 1H), 6.11 (d, *J* = 10.38 Hz, 1H), 4.12 (d, 2H), 1.37 (s, 9H), 0.91-0.89 (m, 1H), 0.38-0.34 (m, 2H), 0.12-0.07 (m, 2H); ¹³C NMR (75 MHz, CDCl₃): δ 168.1, 157.7, 141.4, 132.2, 126.4, 117.9, 114.9, 54.2, 34.2, 28.3, 11.3, 2.7. HRMS (ESI) (M+H)⁺ calcd. For C₁₇H₂₃O₂S: 291.1419; Found: 291.1428.

4.8.1.3. General method for the synthesis of amides 5-11

Acid (**2** or **3**, 0.1 mmol) and toluene (10 mL) were suspended in a clean dry flask. The suspension was allowed to stir and warmed to 60 °C under an inert atmosphere. The CDI (0.178 g, 0.11 mmol) was then added and the mixture allowed to stir for 15 min which yielded a clear solution. The heating was discontinued and the reaction solution was allowed to cool to rt under an inert atmosphere. The appropriate amine (0.11 mmol) was dissolved in dry toluene (5 mL) and transferred to the reaction flask. After completion of the addition, the reaction mixture was stirred for 15 min at rt. The reaction mixture was then heated to 45-60 °C and this temperature was maintained for 3-6 h. The progress of the reaction was followed using TLC (silica gel). On completion by analysis of the mixture by TLC, the reaction mixture was cooled to rt and water (5 mL) was added slowly. The reaction solution was allowed to stir for 10 min and then diluted with EtOAc (10 mL). The layers were separated and the aq layer was extracted with EtOAc (2 x 5 mL). The combined organic layers were washed with brine (2 x 15 mL). The organic layer was dried (Na₂SO₄) and concentrated under reduced pressure. Further purification was carried out by flash column chromatography (silica gel) to yield a pure amide. The yield was typically 88-94% depending on the amine.

4.8.1.3.1. (Z)-3-(Benzo[d]thiazol-2-ylthio)-N,N-diisopropylacrylamide (**5**)

The general method above was followed using acid **3** (237 mg, 0.1 mmol) and diisopropylamine (111 mg, 0.11 mmol) yielding 285 mg (89%) of amide **5**. ¹H NMR (300 MHz, CDCl₃): δ 8.51 (d, *J* = 9.82 Hz, 1H), 8.12 (d, *J* = 8.2 Hz, 2H), 7.38 (d, *J* = 7.8 Hz, 2H), 6.37 (d, *J* = 9.82 Hz, 1H), 3.93 (m, 2H), 1.27 (s, 12H); ¹³C NMR (75 MHz, CDCl₃): δ 161.7, 156.8, 153.0, 145.3, 136.2, 125.3, 124.9, 121.6, 121.3, 116.8, 47.1, 22.3. HRMS (ESI) (M+H)⁺ calcd. For C₁₆H₂₁N₂OS₂: 321.1095; Found: 321.1088.

4.8.1.3.2. (Z)-3-((4-(*tert*-butyl)phenyl)thio)-*N*-phenylacrylamide (6)

The general method above was followed using acid **2** (236 mg, 0.1 mmol) and aniline (102 mg, 0.11 mmol) yielding 289.5 mg (93%) of amide **6**. ¹H NMR (300 MHz, CDCl₃): δ 7.69-7.03 (m, 9H), 7.26 (d, *J* = 10.17 Hz, 1H), 5.88 (d, *J* = 10.17 Hz, 1H), 1.29 (s, 9H); ¹³C NMR (75 MHz, CDCl₃): δ 169.7, 146.8, 145.1, 134.4, 132.0, 129.6, 129.3, 129.1, 125.6, 125.2, 121.7, 121.1, 112.5, 39.9, 31.4. HRMS (ESI) (M+H)⁺ calcd. For C₁₉H₂₂NOS: 312.1422; Found: 312.1411.

4.8.1.3.3. (Z)-3-((4-(*tert*-butyl)phenyl)thio)-*N*-methyl-*N*-phenylacrylamide (7)

The general method above was followed using acid **2** (236 mg, 0.1 mmol) and *N*-methylaniline (118 mg, 0.11 mmol) yielding 296 mg (91%) of amide **7**. ¹H NMR (300 MHz, CDCl₃): δ 7.61-7.00 (m, 9H), 7.28 (d, *J* = 10.05 Hz, 1H), 5.90 (d, *J* = 10.05 Hz, 1H), 2.77 (s, 3H), 1.29 (s, 9H); ¹³C NMR (75 MHz, CDCl₃): δ 161.7, 148.1, 145.7, 134.2, 132.3, 129.9, 129.4, 129.1, 125.4, 125.1, 121.7, 121.3, 112.6, 39.2, 31.7, 30.2. HRMS (ESI) (M+H)⁺ calcd. For C₂₀H₂₄NOS: 326.1579; Found: 326.1586.

4.8.1.3.4. (Z)-3-((4-(*tert*-butyl)phenyl)thio)-*N*-methylacrylamide (8)

The general method above was followed using acid **2** (236 mg, 0.1 mmol) and *N*-methylamine (34 mg, 0.11 mmol) yielding 220 mg (88%) of amide **8**. ¹H NMR (300 MHz, CDCl₃): δ 7.51-7.35 (m, 4H), 7.28 (d, *J* = 10 Hz, 1H), 5.90 (d, *J* = 10 Hz, 1H), 2.84 (s, 3H), 1.29 (s, 9H); ¹³C NMR (75 MHz, CDCl₃): δ 163.9, 151.5, 150.4, 133.7, 131.2, 125.1, 114.5, 60.2, 34.5, 27.0. HRMS (ESI) (M+H)⁺ calcd. For C₁₄H₂₀NOS: 250.1266; Found: 250.1259.

4.8.1.3.5. (Z)-3-((4-(*tert*-butyl)phenyl)thio)-*N,N*-dimethylacrylamide (9)

The general method above was followed using acid **2** (236 mg, 0.1 mmol) and dimethylamine (50 mg, 0.11 mmol) which yielded 243.5 mg (92.5%) of amide **9**. ¹H NMR (300 MHz, CDCl₃): δ 7.67-7.28 (m, 4H), 7.28 (d, *J* = 10.1 Hz, 1H), 5.90 (d, *J* = 10.1 Hz, 1H), 2.77 (s,

6H), 1.32 (s, 9H); ^{13}C NMR (75 MHz, CDCl_3): δ 162.6, 151.2, 150.9, 133.3, 131.7, 125.0, 114.6, 60.7, 34.1, 27.6. HRMS (ESI) (M+H) $^+$ calcd. For $\text{C}_{15}\text{H}_{22}\text{NOS}$: 264.1422; Found: 264.1429.

4.8.1.3.6. (Z)-3-((4-(*tert*-butyl)phenyl)thio)-*N,N*-diisopropylacrylamide (10)

The general method above was followed using acid **2** (236 mg, 0.1 mmol) and diisopropylamine (111 mg, 0.11 mmol) which yielded 300 mg (94%) of amide **10**. ^1H NMR (300 MHz, CDCl_3): δ 7.46-7.39 (m, 4H), δ 7.28 (d, $J = 10.1$ Hz, 1H), 5.90 (d, $J = 10.1$ Hz, 1H), 3.93 (m, 2H), 1.36 (s, 9H), 1.12 (s, 12H); ^{13}C NMR (75 MHz, CDCl_3): δ 161.2, 151.4, 150.9, 132.1, 131.8, 125.3, 114.4, 45.6, 40.7, 34.5, 31.1, 21.4. HRMS (ESI) (M+H) $^+$ calcd. For $\text{C}_{19}\text{H}_{30}\text{NOS}$: 320.2048; Found: 320.2040.

4.8.1.3.7. (Z)-3-((4-(*tert*-butyl)phenyl)thio)-*N*-cyclopropylacrylamide (11)

The general method above was followed using acid **2** (236 mg, 0.1 mmol) and cyclopropylamine (63 mg, 0.11 mmol) which yielded 248 mg (90%) of amide **11**. ^1H NMR (300 MHz, CDCl_3): δ 8.07 (s, 1H), 7.46-7.39 (m, 4H), 7.28 (d, $J = 10$ Hz, 1H), 5.90 (d, $J = 10$ Hz, 1H), 2.32 (m, 1H), 1.56 (s, 9H), 0.38-0.34 (m, 2H), 0.12-0.07 (m, 2H); ^{13}C NMR (75 MHz, CDCl_3): δ 165.4, 146.8, 145.1, 132.0, 129.5, 129.1, 116.7, 40.6, 31.4, 24.2, 7.4. HRMS (ESI) (M+H) $^+$ calcd. For $\text{C}_{16}\text{H}_{22}\text{NOS}$: 276.1422; Found: 276.1424.

4.8.1.4. General method for the preparation of propargylic alcohols **26** and **27**

A round bottom flask was charged with anhydrous THF (5 mL) and propynoic acid ethyl ester **21** (100 mg, 1.02 mmol) after which it was cooled to -78 $^\circ\text{C}$. Then *n*-BuLi (1.6 M of 0.8 mL, 1.22 mmol) was added dropwise. After the addition the mixture which resulted was stirred for 5 min and the appropriate aldehyde (1.02 mmol) was added slowly. The solution which resulted was stirred for 1 h at -78 $^\circ\text{C}$ and then allowed to warm to rt. The reaction mixture was then quenched with a saturated aq solution of NH_4Cl , extracted with EtOAc (2 x 10 mL) and then washed with

brine. The combined organic extracts were dried (Na_2SO_4) and concentrated under reduced pressure. The crude oil was purified by silica gel flash column chromatography (10 - 20% EtOAc in hexanes) to yield pure alcohols.

4.8.1.4.1. Ethyl 4-(4-(*tert*-butyl)phenyl)-4-hydroxybut-2-ynoate (**26**)

The general method above was followed using *t*-butyl benzaldehyde (0.17 mL, 1.02 mmol) which yielded 169 mg (60%) of alcohol **26**. ^1H NMR (300 MHz, CDCl_3): δ 7.44 (m, 4H), 5.57 (s, 1H), 4.24 (q, $J = 6.9$ Hz, 2H), 1.33 (m, 12H); ^{13}C NMR (75 MHz, CDCl_3): δ 153.3, 152.2, 135.6, 126.5, 125.9, 86.04, 77.2, 64.2, 62.3, 34.7, 31.3, 14.0. HRMS (ESI) ($\text{M} + \text{Na}$) $^+$, Calcd. for $\text{C}_{16}\text{H}_{20}\text{O}_3\text{Na}$: 283.1310; Found: 283.1309.

4.8.1.4.2. Ethyl 4-(4-(benzo[*b*]thiophen-2-yl)-4-hydroxybut-2-ynoate (**27**)

The general method above was followed using benzothiophene-2-carboxaldehyde (165 mg, 1.02 mmol) which yielded 154 mg (58%) of alcohol **27**. ^1H NMR (300 MHz, CDCl_3): δ 7.77 (m, 2H), 7.40 (s, 1H), 7.36 (m, 2H), 5.85 (d, $J = 5.7$ Hz, 1H), 4.28 (q, $J = 7.2$ Hz, 2H), 1.33 (t, $J = 7.2$ Hz, 3H); ^{13}C NMR (75 MHz, CDCl_3): δ 155.8, 142.4, 140.1, 139.0, 125.1, 124.7, 124.4, 124.1, 122.8, 84.2, 77.9, 62.5, 60.9, 14.0. HRMS (ESI) ($\text{M} + \text{H}$) $^+$, Calcd. for $\text{C}_{14}\text{H}_{13}\text{O}_3\text{S}$: 283.0585; Found: 283.0572.

4.8.1.5. The method for the preparation of enones **12** and **13**

A round bottom flask was charged with propargylic alcohol **26** (100 mg, 0.3618 mmol), DMSO: H_2O (8:1; 1.25 mL) and then a solution of 0.01 M of hydroquinone in DMSO (0.36 mL, 0.0036 mmol) was added at 23 °C. Subsequently, solid NaHCO_3 (6 mg, 0.0723 mmol) was added in one portion. After the addition the solution which resulted was stirred for 18 h at 23 °C. The reaction mixture was then diluted with H_2O and brought to pH = 3 [to obtain pH = 3 the phosphate buffer which was employed was pH = 7.2 phosphate buffer and an aq solution of HCl (the solution

of 1 N HCl was used to reduce the pH = 7.2 to pH = 3)]. The solution which resulted was extracted with diethyl ether (2 x 10 mL) and the ether layer washed with brine. The combined organic extracts were dried (Na₂SO₄) and concentrated under reduced pressure. The crude oil was purified by silica gel flash column chromatography (5% EtOAc in hexanes) to afford pure cis ester **12** (59 mg, 63%) and trans ester **13** (6.5 mg, 7%). Cis ester **12** ¹H NMR (300 MHz, CDCl₃): δ 7.89 (d, *J* = 8.4 Hz, 2H), 7.50 (d, *J* = 8.4 Hz, 2H), 6.89 (d, *J* = 12.3 Hz, 1H), 6.27 (d, *J* = 12 Hz, 1H), 4.06 (q, *J* = 7.2 Hz, 2H), 1.35 (s, 9H), 1.08 (t, *J* = 6.9 Hz, 3H); ¹³C NMR (75 MHz, CDCl₃): δ 189.1, 165.7, 157.8, 136.6, 134.1, 132.2, 128.9, 125.9, 61.3, 35.3, 31.3, 14.2. HRMS (ESI) (M + Na)⁺, Calcd. for C₁₆H₂₀O₃Na 283.1310; Found 283.1334. Trans ester **13** ¹H NMR (300 MHz, CDCl₃): δ 7.96 (d, *J* = 8.4 Hz, 2H), 7.93 (d, *J* = 15.6 Hz, 1H), 7.55 (d, *J* = 8.4 Hz, 2H), 6.90 (d, *J* = 15.6 Hz, 1H), 4.32 (q, *J* = 7.2 Hz, 2H), 1.38 (m, 12H); ¹³C NMR (75 MHz, CDCl₃): δ 189.0, 165.6, 157.8, 136.6, 134.1, 132.2, 128.9, 125.8, 61.3, 35.2, 31.0, 14.2. HRMS (ESI) (M + Na)⁺, Calcd. for C₁₆H₂₀O₃Na 283.1310; Found 283.1348. When the mixture of **12** and **13** was stirred with anhydrous HCl(g) in ether it was completely converted into trans **13** with no formation of the corresponding acid **16**.

4.8.1.6. (Z)-Ethyl 4-(benzo[*b*]thiophen-2-yl)-4-oxobut-2-enoate (**20**)

The procedure (**5.6.**) was followed. The mixture of 4-benzo[*b*]thiophen-2-yl-4-hydroxybut-2-ynoic acid ethyl ester **27** (157 mg, 0.6031 mmol), a 0.01 M solution of hydroquinone in DMSO (0.6 mL, 0.0060 mmol) and NaHCO₃ (10 mg, 0.1206 mmol) in DMSO: H₂O (8:1; 2 mL) was allowed to stir. Flash column chromatography on silica gel (2% EtOAc in hexane) provided enoate **20** (94 mg, 60% yield). ¹H NMR (300 MHz, CDCl₃): δ 7.89 (m, 3H), 7.47 (m, 2H), 6.95 (d, *J* = 12.3 Hz, 1H), 6.36 (d, *J* = 12 Hz, 1H), 4.12 (q, *J* = 6.9 Hz, 2H), 1.14 (t, *J* = 7.2 Hz, 3H); ¹³C NMR (75 MHz, CDCl₃): δ 187.2, 164.8, 143.0, 142.8, 138.9, 138.3, 131.0, 127.8, 127.6,

126.2, 125.3, 123.1, 61.3, 13.8. HRMS (ESI) (M + Na)⁺, Calcd. for C₁₄H₁₂O₃SNa: 283.0405; Found: 283.0432.

4.8.1.7. Ethyl 4-(4-(*tert*-butyl)phenyl)-4-oxobut-2-ynoate (**25**)

To alcohol **26** (0.5 g, 1.8 mmol) in dry CH₂Cl₂ (10 mL) was added the Dess-Martin periodinane reagent (0.77 g, 1.8 mmol) at rt and the reaction mixture was allowed to stir for 2 h. The volume of the reaction mixture was increased by the addition of CH₂Cl₂ (10 mL). An aq solution (20 mL) containing sodium thiosulfate (100 g/L) and sodium bicarbonate (100 g/L) was added and the mixture which resulted was allowed to stir for 10 min. The organic phase was separated and washed with H₂O (30 mL) and dried (Na₂SO₄). The solvent was removed in vacuo. The residue was purified by flash column chromatography on silica gel (10% ethyl acetate in hexane) to afford ketone **25** (0.39 g, 85%). ¹H NMR (300 MHz, CDCl₃): δ 8.07 (d, *J* = 8.7 Hz, 2H), 7.55 (d, *J* = 8.4 Hz, 2H), 4.37 (q, *J* = 7.2 Hz, 2H), 1.39 (m, 12H); ¹³C NMR (75 MHz, CDCl₃): δ 175.8, 159.4, 152.4, 133.2, 129.8, 125.9, 80.1, 80.0, 62.9, 35.4, 31.0, 13.9. HRMS (EI) (M)⁺, Calcd. for C₁₆H₁₈O₃: 258.1256; Found: 258.1243.

4.8.1.8. Ethyl 4-(4-(*tert*-butyl)phenyl)-4-oxobutanoate (**14**)

The *trans* ester **13** (40 mg, 0.153 mmol) was dissolved in acetone (5 mL) and cold 20% TiCl₃ solution (0.15 mL, 0.306 mmol) was added dropwise with a syringe and the mixture was allowed to stir for 10 min at rt. The solution was then poured into brine (20 mL) and extracted with diethyl ether (2 x 10 mL). The combined extracts were dried (Na₂SO₄) and the solvent removed under reduced pressure. The crude oil was purified by silica gel flash column chromatography (10% EtOAc in hexanes) to afford saturated analog **14** (34 mg, 85%). ¹H NMR (300 MHz, CDCl₃): δ 7.95 (d, *J* = 8.4 Hz, 2H), 7.50 (d, *J* = 8.4 Hz, 2H), 4.18 (q, *J* = 7.2 Hz, 2H), 3.31 (t, *J* = 6.9 Hz, 2H), 2.77 (t, *J* = 6.6 Hz, 2H), 1.36 (s, 9H), 1.28 (t, *J* = 6.9 Hz, 3H); ¹³C NMR (75 MHz, CDCl₃):

δ 197.8, 173.0, 156.9, 134.0, 128.0, 125.5, 60.6, 35.1, 33.2, 31.1, 28.3, 14.2. HRMS (ESI) ($M + H$)⁺, Calcd. for C₁₆H₂₃O₃: 263.1647; Found: 263.1631.

4.8.1.9. Ethyl 4-(4-(*tert*-butyl)phenyl)butanoate (**15**)

A Parr hydrogenation bottle (50 mL) was charged with dry Pd/C (10% by wt, 400 mg, 0.38 mmol) and the *trans* ester **13** (100 mg, 0.38 mmol) in ethanol (3 mL) was added. The mixture was degassed under reduced pressure at rt and back filled with H₂ (3 times) and then flushed with H₂ and pressurized to the desired pressure (20 psi) and stirred with H₂ overnight at rt. The catalyst was removed by filtration (celite) and the solid which remained was washed with ethanol (3 x 10 mL). The combined organic layers were concentrated under reduced pressure to give an oil. This oil was purified by silica gel flash column chromatography (2% EtOAc in hexanes) to afford ester **15** (76 mg, 80%). ¹H NMR (300 MHz, CDCl₃): δ 7.33 (d, $J = 8.1$ Hz, 2H), 7.13 (d, $J = 8.1$ Hz, 2H), 4.14 (q, $J = 7.2$ Hz, 2H), 2.64 (t, $J = 7.5$ Hz, 2H), 2.35 (t, $J = 7.5$ Hz, 2H), 1.97 (m, 2H), 1.33 (s, 9H), 1.27 (t, $J = 7.2$ Hz, 3H); ¹³C NMR (75 MHz, CDCl₃): δ 173.6, 148.7, 138.3, 128.1, 125.3, 60.2, 34.6, 34.4, 33.8, 31.4, 26.5, 14.2. HRMS (ESI) ($M + Na$)⁺, Calcd. for C₁₆H₂₄O₂Na: 271.1674; Found: 271.1657.

4.8.1.10. (*E*)-4-(4-(*tert*-butyl)phenyl)-4-oxobut-2-enoic acid (**16**)

To the *trans* ester **13** (105 mg, 0.4 mmol) in CH₃OH (5 mL) was added K₂CO₃ (0.279 mg, 2 mmol) in H₂O (5 mL). The reaction mixture was allowed to reflux for 5 h and then the CH₃OH was removed under reduced pressure. The residue was then cooled to 0 °C and brought to pH 2 with a solution of cold aq HCl (1M). The mixture, which resulted, was extracted with diethyl ether (2 x 15 mL). The combined extracts were washed with brine (20 mL), dried (Na₂SO₄) and concentrated under reduced pressure to furnish a pale green solid acid **16** (84.3 mg, 90%). mp 118 – 121 °C. ¹H NMR (300 MHz, CDCl₃): δ 8.03 (d, $J = 15.6$ Hz, 1H), 7.98 (d, $J = 7.97$ Hz, 2H),

7.56 (d, $J = 7.97$ Hz, 2H), 6.91 (d, $J = 15.3$ Hz, 2H), 1.38 (s, 9H); ^{13}C NMR (75 MHz, CDCl_3): δ 188.8, 170.5, 158.2, 138.6, 133.8, 131.1, 128.9, 125.9, 35.3, 31.0. HRMS (ESI) ($\text{M} + \text{H}$) $^+$, Calcd. for $\text{C}_{14}\text{H}_{17}\text{O}_3$: 233.1178; Found: 233.1155. This material was employed directly in the next experiment.

4.8.1.11. (*E*)-3-methylbut-2-en-1-yl 4-(4-(*tert*-butyl)phenyl)-4-oxobut-2-enoate (**17**)

The acid **16** (70 mg, 0.3 mmol) was dissolved in anhydrous DMF (1 mL) and cesium carbonate (200 mg, 0.6 mmol) and KI (50 mg, 0.3 mmol) were added. The mixture which resulted was stirred for 5 to 10 min at rt and then a solution of 1-bromo-3-methyl-but-2-ene (**22**) in DMF (0.5 mL) was added with a syringe under a positive pressure of argon. After the addition the mixture, which resulted, was stirred for 2 h at rt. The reaction mixture was then quenched with H_2O and extracted with diethyl ether (2 x 10 mL) as well as washed with brine (2 x 30 mL). The combined organic extracts were dried (Na_2SO_4) and concentrated under reduced pressure. The crude oil was purified by flash column chromatography (5% EtOAc in hexanes) on silica gel to afford prenyl ester **17** (76.5 mg, 85%). ^1H NMR (300 MHz, CDCl_3): δ 7.96 (d, $J = 7.5$ Hz, 2H), 7.93 (d, $J = 15.3$ Hz, 1H), 7.54 (d, $J = 8.7$ Hz, 2H), 6.90 (d, $J = 15.6$ Hz, 1H), 5.43 (t, $J = 7.5$ Hz, 1H), 4.76 (d, $J = 7.5$ Hz, 2H), 1.79 (d, $J = 9.9$ Hz, 6H), 1.37 (s, 9H); ^{13}C NMR (75 MHz, CDCl_3): δ 189.1, 165.7, 157.8, 139.9, 136.6, 134.1, 132.2, 128.9, 125.9, 118.1, 62.2, 35.3, 31.0, 25.8, 18.1. HRMS (ESI) ($\text{M} + \text{Na}$) $^+$, Calcd. for $\text{C}_{19}\text{H}_{24}\text{O}_3\text{Na}$: 323.1623; Found: 323.1627.

4.8.1.12. (*E*)-Ethyl 4-(4-(*tert*-butyl)phenyl)but-2-enoate (**18**)

To a solution of ethyl 4-bromocrotonate **23** (0.9 mL, 5.18 mmol) in anhydrous dioxane (10 mL), palladium triphenyl phosphine tetrakis (300 mg, 0.26 mmol) was added to the round bottom flask. The flask was then evacuated three times at rt and backfilled with argon. The reaction mixture was allowed to stir for 15 min at rt then phenyl boronic acid (1.84 g, 10.36 mmol) and

Na₂CO₃ (2.75 g, 25.9 mmol) were added under a positive pressure of argon. The reaction mixture which resulted was heated at reflux for 18 h and then cooled to rt. It was then passed through a short bed of celite. The celite bed was washed with EtOAc (50 mL) and the combined organic layers were washed with water (50 mL) and brine (30 mL). The organic layer was dried (Na₂SO₄) and concentrated under reduced pressure. The crude oil was purified by flash column chromatography (5% EtOAc in hexanes) on silica gel to afford ester **18** (893 mg, 70%). ¹H NMR (300 MHz, CDCl₃): δ 7.37 (d, *J* = 8.1 Hz, 2H), 7.14 (d, *J* = 7.8 Hz, 2H), 7.12 (d, *J* = 15.6 Hz, 1H), 5.85 (d, *J* = 15.3 Hz, 1H), 4.21 (q, *J* = 7.2 Hz, 2H), 3.52 (d, *J* = 6.9 Hz, 2H), 1.35 (s, 9H), 1.31 (t, *J* = 6.9 Hz, 3H); ¹³C NMR (75 MHz, CDCl₃): δ 166.5, 149.6, 147.5, 134.7, 128.5, 125.6, 122.2, 60.2, 38.0, 34.4, 31.4, 14.3. HRMS (ESI) (M + Na)⁺, Calcd. for C₁₆H₂₂O₂Na: 269.1518; Found: 269.1512.

4.8.1.13. Ethyl 2-(4-(*tert*-butyl)benzoyl)benzoate (**19**)

A round bottom flask was charged with *tert*-butyl-benzene (1.04 mL, 6.7 mmol), phthalic anhydride (1 g, 6.7 mmol), anhydrous CH₂Cl₂ (10 mL) and cooled to 10 °C. Then AlCl₃ (1.8 g, 13.4 mmol) was added portionwise under a positive pressure of argon. The reaction mixture which resulted was then stirred for 15 min at 10 °C. The mixture was poured into an excess of ice-water (100 mL) and the aq phase was extracted with CH₂Cl₂ (2 x 30 mL). It was then washed with brine (50 mL). The organic layer was dried (Na₂SO₄) and concentrated under reduced pressure to furnish an acid (1.62 g, 85%) intermediate. The acid was then dissolved in EtOH (10 mL) and a catalytic amount of H₂SO₄ as well as activated MS (4 Å) were added. The mixture was allowed to stir for 6 h. The EtOH was removed under reduced pressure and the residue dissolved in EtOAc (30 mL). This organic solution was washed with H₂O (50 mL), brine (50 mL), dried (Na₂SO₄) and concentrated under reduced pressure. The crude oil was purified by silica gel flash column

chromatography (10% EtOAc in hexanes) to afford the benzoate **19** (1.9 g, 90%). ¹H NMR (300 MHz, CDCl₃): δ 8.06 (m, 1H), 7.71 (d, *J* = 8.4 Hz, 2H), 7.58 (m, 2H), 7.45 (d, *J* = 8.4 Hz, 2H), 7.38 (m, 1H), 4.10 (q, *J* = 6.9 Hz, 2H), 1.33 (s, 9H), 1.06 (t, *J* = 7.2 Hz, 3H); ¹³C NMR (75 MHz, CDCl₃): δ 196.7, 166.0, 156.9, 142.0, 134.6, 132.2, 130.1, 129.4, 127.7, 125.4, 61.4, 35.1, 31.1, 13.6. HRMS (ESI) (M + H)⁺, Calcd. for C₂₀H₂₃O₃: 311.1647; Found: 311.1649.

4.8.1.14. 3-(4-*tert*-butyl-phenylsulfanyl)-propionic acid ethyl ester (**24**)

The Parr hydrogenation bottle (500 mL) was charged with dry Pd/C (10% by wt, 400 mg, 0.38 mmol), and thio ester **1** (100 mg, 0.38 mmol) in ethanol (3 mL). The mixture, which resulted, was degassed under reduced pressure at rt and back filled with H₂ (3 times) and then flushed with H₂. It was pressurized to the desired pressure (20 psi) with H₂ and stirred overnight at rt. The catalyst was removed by filtration (celite) and washed with ethanol (3 x 10 mL). The solvent was removed under reduced pressure. The crude compound was purified by flash column chromatography (2% EtOAc in hexanes) on silica gel to afford ester **24** (70 mg, 70%). ¹H NMR (300 MHz, CDCl₃): δ 7.34 (s, 4H), 4.15 (q, *J* = 7.2 Hz, 2H), 3.15 (t, *J* = 7.5 Hz, 2H), 2.63 (t, *J* = 7.5 Hz, 2H), 1.33 (s, 9H), 1.27 (t, *J* = 6.9 Hz, 3H); ¹³C NMR (75 MHz, CDCl₃): δ 171.9, 150.0, 131.5, 130.5, 126.1, 60.7, 34.6, 34.5, 31.3, 29.5, 14.2. HRMS (ESI) (M + Na)⁺, Calcd. for C₁₅H₂₂O₂SNa: 289.1238; Found: 289.1227.

4.8.1.15. (1*R*,2*R*)-ethyl 2-(4-(*tert*-butyl)benzoyl)cyclopropanecarboxylate (**28**)

Trimethylsulfoxonium iodide (40 mg, 0.18 mmol) was added portionwise to a slurry of sodium hydride (5 mg, 0.2 mmol) in DMSO (1 mL). The mixture was stirred at rt until a completely clear solution was obtained. The ester **13** was added dropwise and the reaction mixture was then stirred for 14 h at rt. After completion, the reaction mixture was poured on crushed ice (50 g) and the oily product extracted with diethyl ether (2 x 10 mL). The combined organic extracts were

washed with brine (2 x 15 mL). The organic layer was dried over MgSO₄ and concentrated under vacuum to yield the crude cyclopropyl ester. The crude compound was purified by flash column chromatography (5% EtOAc in hexanes) on silica gel to afford *trans* cyclopropyl ester **28** (25.2 mg, 60%). ¹H NMR (300 MHz, CDCl₃): δ 7.99 (d, *J* = 8.4 Hz, 2H), 7.53 (d, *J* = 8.4 Hz, 2H), 4.20 (q, *J* = 7.2 Hz, 2H), 3.20 (ddd, *J* = 5.7, 5.7, 9.3 Hz, 1H), 2.37 (ddd, *J* = 5.7, 5.7, 9.6 Hz, 1H), 1.57 (m, 2H), 1.37 (s, 9H), 1.31 (t, *J* = 7.5 Hz, 3H); ¹³C NMR (75 MHz, CDCl₃): δ 196.6, 172.5, 157.2, 134.5, 128.3, 125.6, 61.1, 35.2, 31.1, 25.9, 24.5, 17.7, 14.2. HRMS (ESI) (M + H)⁺, Calcd. for C₁₇H₂₃O₃: 275.1647; Found: 275.1639.

4.8.1.16. (2*R*,3*R*)-ethyl 3-(4-(*tert*-butyl)benzoyl)oxirane-2-carboxylate (**29**)

A 6 N NaOH (0.1 mL) solution was added dropwise into a solution of **13** (100 mg, 0.38 mmol) and 30% H₂O₂ (0.05 mL) in EtOH (5 mL) at 0 °C. The reaction mixture which resulted, was stirred for 2 h at the same temperature after which water was added to the reaction mixture and it was extracted with CH₂Cl₂ (2 x 10 mL). The combined organic extracts were washed with brine (2 x 15 mL). The organic layer was dried (MgSO₄) and concentrated under vacuum to yield the crude epoxide ethyl ester. The crude compound was purified by flash column chromatography (10% EtOAc in hexanes) on silica gel to afford epoxide ethyl ester **29** (55 mg, 52%). ¹H NMR (300 MHz, CDCl₃): δ 7.99 (d, *J* = 8.4 Hz, 2H), 7.55 (d, *J* = 8.4 Hz, 2H), 4.46 (d, *J* = 1.8 Hz, 1H), 4.32 (m, 2H), 3.70 (d, *J* = 1.8 Hz, 1H), 1.38 (m, 12H); ¹³C NMR (75 MHz, CDCl₃): δ 191.3, 167.31, 158.5, 132.5, 128.6, 126.0, 62.3, 55.2, 53.0, 35.3, 31.0, 14.1. HRMS (ESI) (M + Na)⁺, Calcd. for C₁₆H₂₀O₄Na: 299.1259; Found: 299.1248.

4.8.2. Microbiology

4.8.2.1. MIC determinations

In vitro minimum inhibitory concentration (MIC) determinations were performed according to the Clinical and Laboratory Standards Institute (CLSI) guidelines for *Staphylococcus aureus* ATCC 29213, *Bacillus cereus* (University of Wisconsin-La Crosse culture collection), and *Escherichia coli* ATCC 29522.⁵⁴ Tetracycline was used as a control antibiotic and correlated with established MIC values.

All anti-mycobacterial activity evaluations (except for the *M. tuberculosis* assays) were performed using MIC assays in Middlebrook 7H9 broth with 10% oleic acid albumin dextrose complex (OADC) as previously described.¹² The following mycobacterial species were tested: *M. avium*, *M. chelonae*, *M. fortuitum*, *M. intracellulare* and *M. kansasii*. All of the mycobacterial species that were used were from the University of Wisconsin-La Crosse culture collection. Rifampin was used as the positive control for the mycobacterial MICs. All MIC values reported were a compilation of the geometric means from three separate runs.

For *M. tuberculosis* MIC determinations, *M. tuberculosis* strain H37Rv was used. Briefly, black, clear-bottom, 384-well microtiter plates and Middlebrook 7H12 (7H9 broth supplemented with 0.1% casitone, 5.6 µg/mL palmitate, 0.5% bovine serum albumin and 4 µg/mL catalase) broth were used. The compounds were diluted in assay media to 2x the final test concentration and 25 µL of these diluted compounds were transferred to 384-well plates. Amikacin was included in the positive control wells in every assay plate. Plates containing test compounds and positive control compounds were transferred into the BSL3 facility for bacteria addition and incubation. The bacterial stock was diluted to 1-2 x10⁵ CFU/mL in the assay medium, Middlebrook 7H12 broth and 25 µL was plated over the compounds using a Thermo Scientific Matrix WellMate, inside a

Class 2A Biological Safety Cabinet. Positive and negative control wells were included in each plate. Plates were placed in stacks of two and incubated for 7 days at 37 °C with approximately 95% humidity. After 7 days of incubation, autofluorescence of any test compounds was determined by pre-reading the high dose plate by a bottom read for fluorescence using a Perkin Elmer Envision plate reader at 535 nm excitation and 590 nm emission. The assay plates were removed from the incubator and allowed to equilibrate to room temperature. Twenty-five microliters of Promega BacTiter-Glo™ Microbial Cell Viability (BTG) reagent, one third of the final volume of the well, was added using a WellMate. The plates were incubated for 20 minutes at room temperature, sealed with a Perkin Elmer clear TopSeal A and read from the top using luminescence on a Perkin Elmer Envision. Rifampin, ethambutol, amikacin, isoniazid, and pyrimethamine were used as positive controls.

4.9. REFERENCES AND NOTES

1. Global Tuberculosis Report 2012, http://www.who.int/tb/publications/global_report/en/
2. TB Alliance, <http://www.tballiance.org/>
3. Dover, L. G.; Coxon, G. D. *J. Med. Chem.* **2011**, *54*, 6157.
4. Janin, Y.L. *Bioorg. Med. Chem.* **2007**, *15*, 2479.
5. Harper, C. *Nat. Med.* **2007**, *13*, 309.
6. Maurice, J. *Lancet* **2011**, *378*, 1209.
7. Patpi, S. R.; Pulipati, L.; Yogeewari, P.; Sriram, D.; Jain, N.; Sridhar, B.; Murthy, R.; T, A. D.; Kalivendi, S. V.; Kantevari, S. *J. Med. Chem.* **2012**, *55*, 3911.
8. Loewenberg, S. *Lancet* **2012**, *379*, 205.
9. Boccia, D.; Evans, C.A. *Lancet* **2011**, *378*, 1293.
10. Sacchetti, J. C.; Rubin, E. J.; Freundlich, J. S. *Nat. Rev. Microbiol.* **2008**, *6*, 41.

11. Showalter, H. D. H.; Denny, W. A. *Tuberculosis* **2008**, 88, S3.
12. Kabir, M. S.; Namjoshi, O. A.; Verma, R.; Polanowski, R.; Krueger, S. M.; Sherman, D.; Rott, M. A.; Schwan, W. R.; Monte, A.; Cook, J. M. *Bioorg. Med. Chem.* **2010**, 18, 4178.
13. Kabir, M. S.; Engelbrecht, K.; Polanowski, R.; Krueger, S. M.; Ignasiak R.; Rott, M. A.; Schwan, W. R.; Stemper, M. E.; Reed, K. D.; Sherman, D.; Cook, J. M.; Monte, A. *Bioorg. Med. Chem. Lett.* **2008**, 18, 5745.
14. Kabir, M.; Cook, J. M.; Monte, A.; Rott, M.; Schwan, W.; Witzigmann, C.; Namjoshi, O.; Tiruveedhula, V. V. N. Phani Babu.; Verma, R. Provisional patent filed 14th March (2012), Serial # 61/610, 574.
15. a. Kabir, M.S.; Namjoshi, O. A.; Verma, R.; Lorenz, M.; Tiruveedhula, V.V.N. Phani Babu.; Monte, A.; Bertz, S. H.; Schwabacher, A. W.; Cook, J. M. *J. Org. Chem.* **2012**, 77, 300.
- b. All the compounds are stable at room temperature. Please see the Supporting Information for acid/base stability studies on compounds 12 and 13.
16. a. CLogP values were calculated from ChemDraw Ultra, version 12.0.2, software by Cambridge Soft.
- b. Lipinski, C. A.; Lombardo, F.; Dominy, B. W.; Feeney, P. J. *Adv. Drug Deliv. Rev.* **2001**, 46, 3.
17. a. Meanwell, N. A. *J. Med. Chem.* **2011**, 54, 2529.
- b. Patani, G. A.; Lavoie, E. J. *Chem. Rev.* **1996**, 96, 3147.
18. Lipshutz, B. H.; Sengupta, S. *Org. React.* **1992**, 41, 135.
19. Ihara, M.; Fukumoto, K. *Angew. Chem. Int. Ed. Engl.* **1993**, 32, 1010.
20. Hoz, S. *Acc. Chem. Res.* **1993**, 26, 69.

21. Michael, A. *J. Prakt. Chem.* **1887**, 35, 349.
22. CCDC 949911 [2] contains the supplementary crystallographic data for this paper. These data can be obtained free of charge from The Cambridge Crystallographic Data Centre via www.ccdc.cam.ac.uk/data_request/cif.
23. H. Gunther. *NMR Spectroscopy*, 2nd ed., Wiley, New York, 2001.
24. Midland, M. M.; Tramontano, A.; Cable J. R. *J. Org. Chem.* **1980**, 45, 28.
25. Sonye, J. P.; Koide, K. *J. Org. Chem.* **2007**, 72, 1846.
26. Blaszczyk, L. C.; McMurry J. E. *J. Org. Chem.* **1974**, 39, 258.
27. Bonini, C.; Chiummiento, L.; Bonis, M. D.; Funicello, M.; Lupattelli, P.; Pandolfo, R. *Tetrahedron: Asymmetry*. **2006**, 17, 2919.
28. Tsuge, A.; Hashimoto, I.; Matsuda, T.; Nagano, Y.; Tashiro M. *Eng. Sci. Rep. Kyushu Univ.* **1992**, 13, 361.
29. Hamdouchi, C.; Topolski, M.; Goedken V.; Walborsky H. M. *J. Org. Chem.* **1993**, 58, 3148.
30. Chien, C-S.; Kawasaki, T.; Sakamoto, M.; Tamura, Y.; Kita, Y. *Chem. Pharm. Bull.* **1985**, 33, 2743.
31. De, P.; Yoya G. K.; Constant, P.; Bedos-Belval, F.; Duran, H.; Saffon, N.; Daffe, M.; Baltas, M. *J. Med. Chem.* **2011**, 54, 1449.
32. Avonto, C.; Tagliatalata-Scafati, O.; Pollastro, F.; Minassi, A.; Marzo, V. D.; Petrocellis, L. D.; Appendino, G. *Angew. Chem. Int. Ed.* **2011**, 50, 467.
33. Ahn, B.; Sok, D. *Curr. Pharm. Des.* **1996**, 2, 247.
34. Johansson, M. H. *Mini. Rev. Med. Chemistry.* **2012**, 12, 1330.
35. McGovern, S.L.; Caselli, E.; Grigorieff, N.; Shoichet, B.K. *J. Med. Chem.* **2002**, 45, 1712.

36. Amslinger, S. *ChemMedChem*. **2010**, *5*, 351.
37. Aptula, A.O.; Roberts, D.W. *Chem. Res. Toxicol.* **2006**, *19*, 1097.
38. Petronelli, A.; Pannitteri, G.; Testa, U. *Anti-cancer Drugs*. **2009**, *20*, 880.
39. Nanavati, S.M.; Silverman, R. B. *J. Am. Chem. Soc.* **1991**, *113*, 9341.
40. Powers, J. C.; Asgian, J. L.; Ekici, O. D.; James, K. E. *Chem. Rev.* **2002**, *102*, 4639.
41. Couch, R. D.; Browning, R. G.; Honda, T.; Gribble, G. W.; Wright, D.L.; Sporn, M. B.; Anderson A. C. *Bioorg. Med. Chem. Lett.* **2005**, *15*, 2215.
42. Fukuda, K.; Akao, S.; Ohno, Y.; Yamashita, K.; Fujiwara, H. *Cancer Lett.* **2001**, *164*, 7.
43. Jirkovsky, I.; Cayen, M. N. *J. Med. Chem.* **1982**, *25*, 1154.
44. Boonen, J.; Baert, B.; Roche, N.; Burvenich, C.; Spiegeleer, B. D. *J. Ethnopharmacol.* **2010**, *127*, 77.
45. Overington, J. P.; Al-Lazikani, B.; Hopkins, A. L. *Nat. Rev. Drug Discov.* **2006**, *5*, 993.
46. Tanigawa, K.; Nagase, H.; Ohmori, K.; Tanaka, K.; Miyake, H.; Kiniwa, M.; Ikizawa, K.; *Int. Immunopharmacol.* **2002**, *2*, 941.
47. Funato, H.; Kobayashi, A.; Watanabe, Y. *Brain Res.* **2006**, *1117*, 125.
48. Nagaoka, H.; Rutsch, W.; Schmid, G.; Iio, H.; Johnson, M.R.; Kishi Y. *J. Am. Chem. Soc.* **1980**, *102*, 7962.
49. Nagaoka, H.; Kishi, Y. *Tetrahedron.* **1981**, *37*, 3873.
50. Iio, H.; Nagaoka, H.; Kishi, Y. *J. Am. Chem. Soc.* **1980**, *102*, 7965.
51. Saleem, M.; Nazir, M.; Ali, M. S.; Hussain, H.; Lee, Y. S.; Riaz N.; Jabbar A. *Nat. Prod. Rep.* **2010**, *27*, 238.
52. Center for Disease Control, <http://www.cdc.gov/mrsa/>

53. Armarengo, W. L. F.; Chai, C. L. L. *Purification of Laboratory Chemicals*, 7th ed., Butterworth-Heinemann, New York, 2012.
54. Wayne, P. A. *Methods for dilution antimicrobial susceptibility tests for bacteria that grow aerobically*, 6th ed.; Clinical and Laboratory Standards Institute, 2005. Approved standard M7–A6.

CHAPTER 5

EXTENSION OF THE SAR AND BIOLOGICAL EVALUATION OF NOVEL AROYLACRYLIC ACID DERIVATES AS ANTIMICROBIAL AGENTS

5.1. BACKGROUND

In continued efforts to develop new antimicrobial agents a novel class of aroylacrylic acids and corresponding derivatives were synthesized.¹ As discussed previously in Chapter 4, the initial structure-activity relationship (SAR) studies of the ester **1** resulted in ligand **13** as one of the lead compounds, which exhibited a promising minimum inhibitory concentration (MIC) of 8 $\mu\text{g/mL}$ and 2 $\mu\text{g/mL}$ against *Mycobacterium smegmatis* (*M. smegmatis*), a safer surrogate of the clinically significant mycobacteria that causes tuberculosis and gram positive bacteria *Staphylococcus aureus* (*S. aureus*), respectively, in a testing panel of gram positive, negative, and mycobacterial strains. In addition, the ester **13** was screened for the more virulent strain, *M. tuberculosis*, which resulted in a MIC value of 0.8 $\mu\text{g/mL}$.¹ The exciting activity of these compounds has encouraged the synthesis of several structurally related derivatives, to study the mode of action and improve the antimicrobial activity.

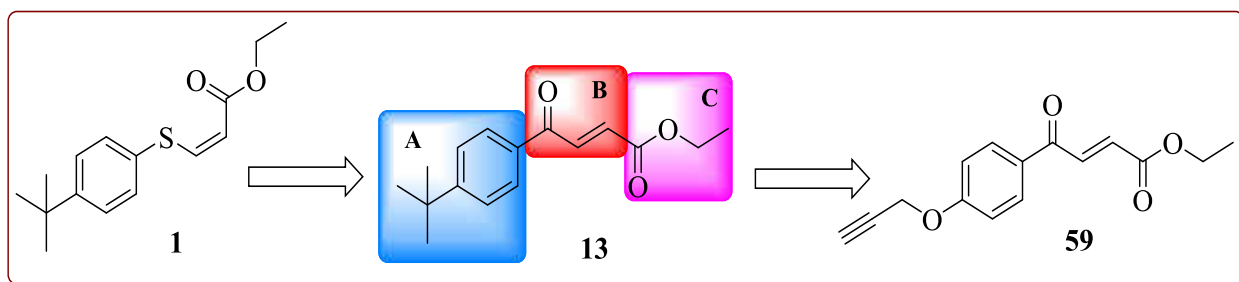
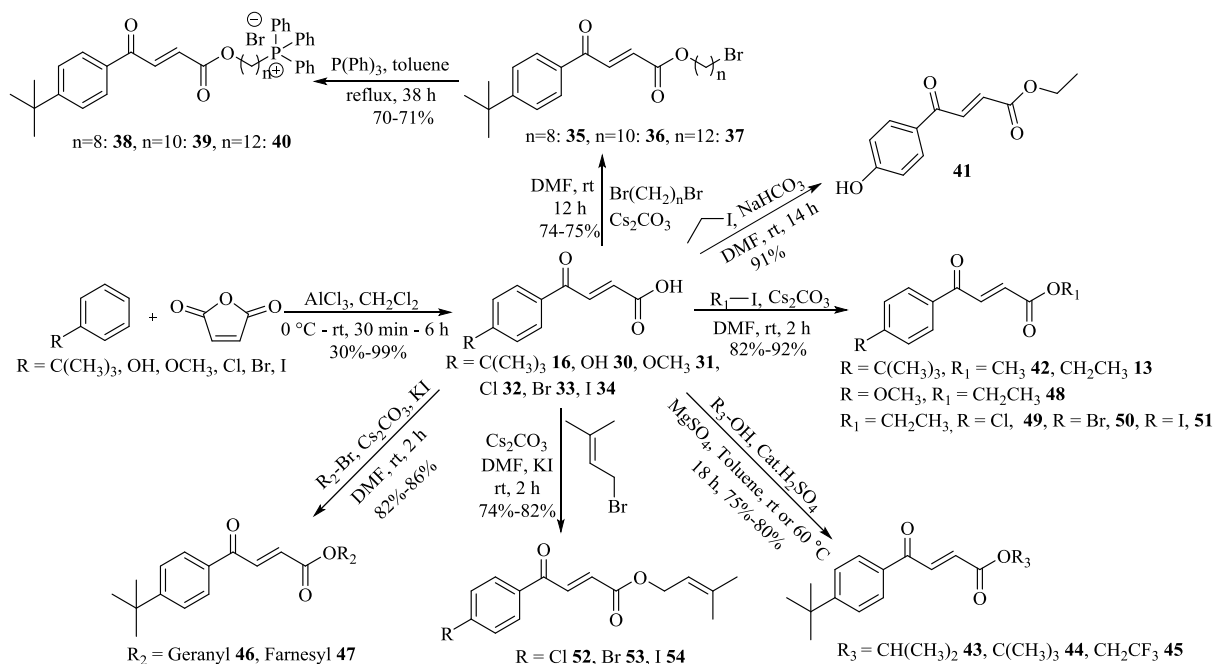


Figure 5-1. Lead compounds

5.2. RESULTS AND DISCUSSION

Based on the past SAR, the ethyl ester **13** was altered at positions A, B, and C, in order to evaluate the structural changes on antimicrobial activity and further develop the SAR to identify

the most potent compounds, as shown in Figure 5-1. To assess the size of the lipophilic pocket of the bacteria at position C, the ethyl ester function in **13** was replaced with methyl **42**, isopropyl **43**, and *t*-butyl esters **44**, respectively. These various esters were synthesized cheaply because the first step was a Friedel-Crafts acylation of *t*-butyl benzene with maleic anhydride using the Lewis acid AlCl₃ in dry CH₂Cl₂ to produce acid **16**^{2,3} in nearly quantitative yield. The acid **16** was then converted into the corresponding esters by Fischer esterification with the exception of the methyl ester **42**. The methyl ester **42** was produced from the acid under basic conditions using methyl iodide as the alkyl halide, as shown in Scheme 5-1. To further increase the lipophilicity and because of the importance of geranyl and farnesyl groups in drug discovery of antibiotics^{4,5} because of the lipid membranes which comprise the cell walls, the geranyl and farnesyl esters **46** and **47** were prepared using Cs₂CO₃ as a base in good yield.

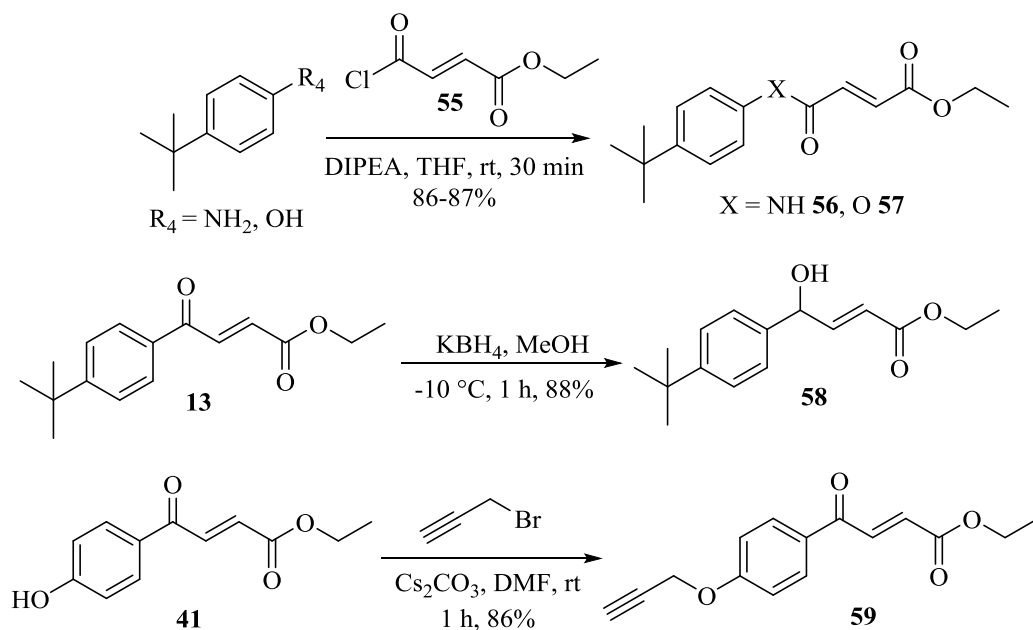


Scheme 5-1. Synthesis of aroylacrylic acid derivatives

It is well-known that triphenyl phosphonium cationic (TPPC) agents target mitochondria to induce anti-proliferative and cytotoxic effects in tumor cells without affecting healthy cells.^{6,7} In addition, TPPC also plays a vital role in cell wall permeability and accumulation within the cells

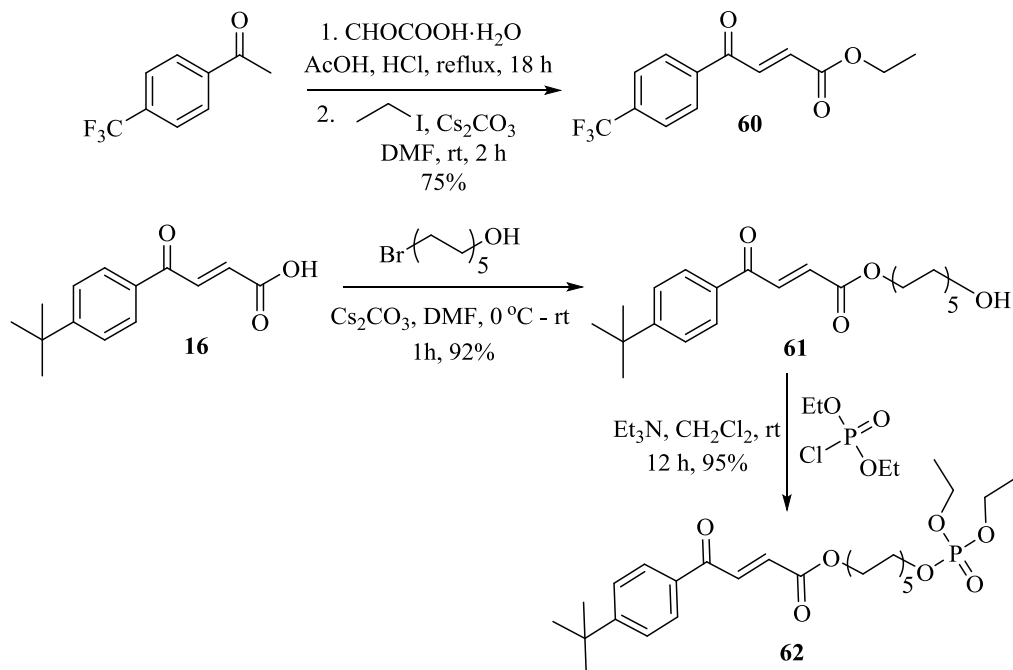
when attached to small molecules.^{8,9} As shown in Scheme 5-1, a number of esters were synthesized which contained terminal TPPC groups with n=8 (**38**), n=10 (**39**), and n=12 (**40**). The first step in the route involved the synthesis of the various bromides **35-37** and they were obtained in good yields by treatment of the acid **16** with the corresponding dibromo alkanes in DMF. With the desired bromides **35-37** (n = 8, 10, 12) in hand, they were subsequently converted into phosphonium salts **38-40** by stirring with triphenyl phosphine in refluxing toluene (70-71% yields). Replacement of the *t*-butyl group in the starting material with a methoxy group at position A in **13**, followed by the analogous Friedel-Crafts acylation with maleic anhydride gave the ether, acid **31** (see Scheme 5-1). This acid was converted into ethyl ester **48** by treatment with ethyl iodide under basic conditions.

To evaluate the steric, electronic, and lipophilic effects on the potency of these compounds, various halogen (Cl, Br, and I) containing analogs **49-51** and **52-54** were prepared by incorporation of these halogens at position A. This was accomplished by judicious choice of starting materials (Cl, Br, I). These acids were transformed into the ethyl and prenyl esters via the route described below employing an established methyl ester **42** protocol. Friedel-Crafts acylation of the commercially available halogenated benzenes with maleic anhydride yielded aroylacrylic acids **32-34**, although prolonged reaction times were needed with these halides, as expected. Subsequently, the acids were converted into esters **49-51** and **52-54** in dry DMF on treatment with ethyl iodide and prenyl bromide, respectively, using Cs₂CO₃ as the base in good yield.



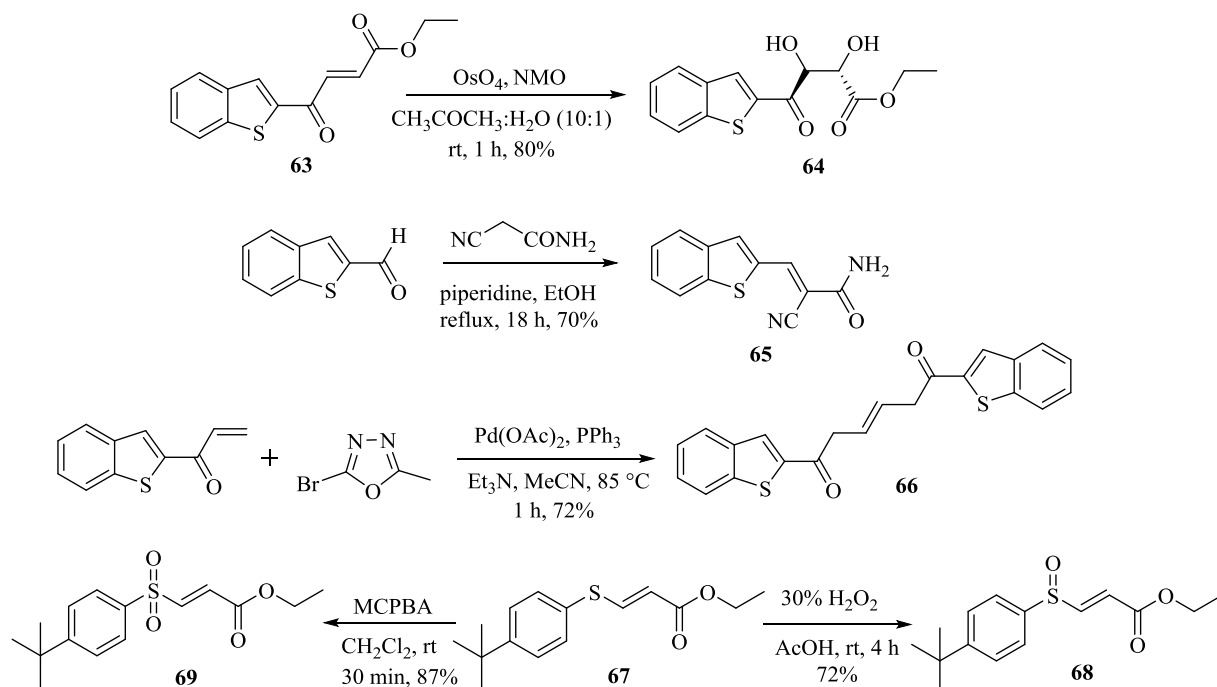
Scheme 5-2. Synthesis of aroylacrylic ethyl ester derivatives

In order to increase the hydrogen bond donor number in these agents in agreement with Lipinski's rule of five¹⁰, the analogs **41**, **58**, **61**, and **64** were synthesized; these altered the positions of **13** at A, B, and C. The analog **41** was readily prepared from the acid **30** by selective esterification of the acid with ethyl iodide employing NaHCO_3 as a base in DMF at ambient temperature with continuous stirring for 14 hours. As shown in Scheme 5-2, the hydroxy derivative **58** was prepared by selective reduction of the ketone function in **13** with KBH_4 in MeOH ¹¹, this altered the electronic character of the double bond. In the case of alcohol **61**, the methyl ester **42** (RX, base) protocol was followed for one hour, and it should be noted that a longer reaction time was found to be detrimental to the reaction yield. The latter trans diol **64** was furnished smoothly from trans olefin **63** by stereoselective dihydroxylation using osmium tetroxide (OsO_4), and *N*-methylmorpholine-*N*-oxide (NMO) as an oxidant (Dr. Stuart Schreiber) with cis addition to the double bond (Scheme 5-4).¹²



Scheme 5-3. Synthesis of aroylacrylic ethyl ester derivatives

To further expand the SAR studies on these compounds, the keto function in ester **13** at position B was replaced with an amide **56** and an ester **57** (Scheme 5-2) to alter the Michael acceptor ability of **13** and to evaluate the effect as well on stability, bioavailability, and potency. As illustrated in Scheme 5-2, these derivatives were conveniently obtained by treatment of aniline and phenol starting materials with acid chloride **55** under basic conditions. This process was carried out in THF at ambient temperature with stirring for 30 minutes in 86-87% yields. To determine if the size of (see A) of the lipophilic pocket in the bacteria would accommodate a longer alkyl group, the propargyl ether **59**, was prepared. In addition, the propargyl group in the **59** if active, would provide the necessary handle for Click chemistry analysis of the proteins involved in the MOA (see Chapter 6 for details). The required **59** was obtained by smooth O-alkylation of phenol **41** with propargyl bromide in DMF with Cs_2CO_3 as the base in good yield.



Scheme 5-4. Synthetic pathway to compounds 64-66 and 68-69

It is well known that CF₃ groups play a major role in medicinal chemistry and drug discovery.¹³ The presence of the CF₃ group retards metabolism and also alters the electronic character of the aromatic ring in region A. To investigate the influence of the CF₃ group on antibacterial activity in the scaffold **13** at positions C and A, the analogs **45** (trifluoro ethyl ester) and **60** (4-CF₃) were designed and synthesized. The -CH₂CF₃ ester analog **45** was obtained by Fischer esterification of the acid **16** with trifluoroethanol; it is worthy of note that the (RX plus base) which gave methyl ester **42** failed when trifluoro ethyl iodide was employed.

Table 5-1. Minimum inhibitory concentrations (MIC) of compounds 30-31, 35-54, 56-66, and 68-69 against common bacterial species (µg/mL)

Compound	<i>M. smegmatis</i>	<i>S. aureus</i> ^a	<i>E. faecium</i> ^a	<i>E. coli</i> ^a	<i>P. aeruginosa</i> ^a
13	8	2	8	>128	>128
30	>128	>128	>128	>128	>128
31	>128	64	>128	>128	>128
35	>128	8	64	>128	>128
36	>128	>128	>128	>128	>128
37	>128	>128	>128	>128	>128
38	64	0.5	1	32	128
39	0.25	0.5	4	64	128
40	16	4	4	>128	>128

41	8	1	8	32	>128
42	ND ^b	2	16	>128	>128
43	ND ^b	4	8	>128	>128
44	ND ^b	2	16	>128	>128
45	4	8	32	>128	>128
46	>128	0.5	128	>128	>128
47	>128	128	128	>128	>128
48	8	2	4	32	>128
49	16	1	8	32	128
50	16	0.5	16	32	128
51	16	1	8	32	128
52	16	2	8	>128	>128
53	16	2	8	>128	>128
54	64	4	8	>128	>128
56	128	64	128	>128	>128
57	>128	128	>128	>128	>128
58	64	8	32	>128	>128
59	8	0.5	4	32	>128
60	16	2	8	32	>128
61	32	1	8	>128	>128
62	32	2	8	>128	>128
63	8	0.25	2	16	128
64	128	32	>128	>128	>128
65	64	>128	>128	>128	>128
66	ND ^b	>128	>128	>128	>128
68	4	4	8	>128	>128
69	4	16	8	>128	>128
Rifampin ^c	16	0.5	ND ^b	ND ^b	ND ^b
Tetracycline ^c	ND ^b	0.25	16	1	16

^a ATCC strains used for *S. aureus*, *E. faecium*, *E. coli*, *P. aeruginosa*;

^b ND = not determined, ^c Positive control

Unfortunately, the Friedel-Crafts acylation reaction between trifluorotoluene and maleic anhydride failed to give the corresponding acrylic acid; presumably, the electron withdrawing nature of the CF₃ substituent remarkably reduced the reactivity of the substrate. The p-trifluorotoluene acrylic acid was synthesized based on the procedure reported by Xu et al. (Scheme 5-3).¹⁴ The process began by coupling (trifluoromethyl)acetophenone with glyoxylic acid monohydrate under acidic conditions to yield the corresponding acrylic acid via the aldol condensation, followed by loss of water. This acid was converted into ethyl ester **60** by using ethyl

iodide as an alkyl halide under basic conditions to furnish the desired analog **60** in 75% yield, as shown in Scheme 5-3. To further mimic the cell wall structure of bacteria, the scaffold **62** was designed and synthesized. The diethylphosphate analog **62** was smoothly obtained by treatment of alcohol **61** with diethyl chloro phosphate in dichloromethane under basic conditions. This gave **62** in nearly quantitative yield, however, several attempts at hydrolysis of this ethyl ester **62** failed to give the desired alkyl substituted phosphoric acid.

As previously reported,¹ the activity of these compounds was due to the Michael acceptor nature and to design a reversible Michael acceptor the amido nitrile **65** was synthesized.^{15,16} As shown in Scheme 5-4, treatment of benzothiophene carboxaldehyde with cyanoacetamide under basic conditions gave the amide **65** in good yield. Replacement of the ethyl ester in **63** with bioisosteres¹⁷ in a PdCl₂/PPh₃ mediated process gave the undesired dimer **66**; it was a palladium-catalyzed reaction between 1-(benzo[*b*]thiophen-2-yl)pro-2-en-1-one and 2-bromo-5-methyl-1,3,4-oxadiazole in acetonitrile with triphenyl phosphine as the ligand, as depicted in Scheme 5-4. Dimer **66** may be product of a radical mediated coupling reaction. Finally, the sulfoxide **68** and sulfone **69** were obtained from sulfur analog **67** when the sulfide was reacted with hydrogen peroxide and 3-chloroperbenzoic acid (MCPBA) in 72% and 87% yields, respectively.¹⁸ The sulfoxide **68** is a bioisoster of ester **13** while sulfone **69** is a doubly activated Michael replacement for the carbonyl. **Caution must be exercised in handling the vinyl sulfones for they are very reactive alkylating agents which may blister the skin or damage the lungs.** With the desired thirty-five new scaffolds in hand, they were tested on a panel of clinically relevant normal and resistant bacterial strains to evaluate their antimicrobial activity (MIC). Initially, the acids **30** and **31** (Scheme 5-1) were tested against common gram positive, gram negative, and *Mycobacterium* strains as shown in Table 5-1. These results were consistent with our previous results¹ which

indicated that altering the ester functionality to an acid at position C in **13** abolished the activity. The ester function clearly lies in a lipophilic pocket. Consequently a series of esters were evaluated with different alkyl chains wherein the aromatic ring (see A) was substituted with electron donating groups such as *t*-butyl, hydroxy, methoxy (**35-37**, **41-48**, **61**) and electron withdrawing groups such as halogens, and a CF₃ group (**49-54**, **60**) at position A. As shown in Table 5-1, increasing the length of the alkyl chain from methyl to *t*-butyl (**13**, **42-48**) at position C was tolerated with moderate MIC values; however, antimicrobial activity was abolished on substitution by the larger geranyl **46**, farnesyl **47**, and alkyl bromo analogs **35-37**. Interestingly, examination of the data on the geranyl ester **46** indicated potent anti-staphylococcal activity with a MIC of 0.5 µg/mL. The 4-phenolic ester **41** (region A) increased the potency twofold over lead ester **13** and the potency was further extended to the gram-negative bacteria *E.coli*. In the case of analogs substituted with electron withdrawing groups (region A) **49-54** and **60** showed similar or potent activity and also exhibited greater than four fold activity against *E.coli*, whereas the iodo prenyl ester **54** exhibited less activity than the lead compound **13**. This may be the result of the increased size of the alkyl iodide which, presumably, prevented it from establishing a potent interaction with the bacteria binding site. Remarkably, the related bromo substituted ester **50** exhibited very potent activity against *S. aureus* with a MIC of 0.5 µg/mL as indicated in Table 5-1. This also suggested alkyl iodides are too large for the binding site of *S. aureus*. The TPPC analogs **38-40** exhibited moderate to excellent activity on an array of bacterial strains, especially the alkyl TPPC analog **39** which showed very potent activity against *M. smegmatis* (MIC = 0.25 µg/mL) and *S. aureus* (MIC = 0.5 µg/mL). This observation stimulated the synthesis of the same length of alkyl chain for phosphate ester **62**, unfortunately the potency was not retained so the observed differences in biological activity must track to other molecular properties. The key here is that alkyl TPPC analog

39 was charged; however, alkyl phosphate **62** was not. This is a big difference. Recall the hydrolysis of **62** failed.

The other region of the molecule examined was at position B in lead compound **13**; the keto group in ester **13** was replaced with an amide **56**, ester **57**, and hydroxy **58** functionality and tested for antibacterial activity. Since these changes altered the electronic character of the Michael acceptor chromophore they decreased activity. This indicated the attack of the bacteria was on the enone system at the position beta to the carbonyl not beta to the ester carbonyl. On the other hand, the alkyne derivate **59** at C-4 (para, Scheme 5-2) of phenolic ester **41** exhibited four fold more potent activity on *S. aureus* (MIC = 0.5 µg/mL) and *E.coli* (MIC = 32 µg/mL) when compared to lead compound **13** (Table 5-1). This significant result provided a path to study the mechanism of action of these novel aroylacrylic ester derivates using Click chemistry (for complete details see Chapter 6). The trans ester **63** (Scheme 5-4) was screened for antimicrobial activity, and as expected, it was very potent against the *S. aureus* strain with an MIC value of 0.25 µg/mL. As previously described the Michael acceptor property was the key feature for the activity of these novel acrylic esters¹ and it was again demonstrated with the analogs **64** and **66**. Interestingly, the structurally unrelated reversible Michael acceptor **65** was not active at all. It simply did not fit the receptor pharmacophore (Table 5-1). Furthermore, the Michael acceptor keto replacements (sulfoxide **68** and sulfone **69**) increased the potency compared to previous lead compound **1**¹, however, these ligands exhibited comparable activity with lead compound **13** except they showed a two fold increase in potency against *M. smegmatis* activity compared to ketone ester **13**.

Table 5-2. Minimum inhibitory concentrations (MIC) of compounds 38-39, 40, 46-48, 56-57, 59, 63-64, 68-69 and single drug-resistant strains against *Mycobacterium tuberculosis* H₃₇Rv; Vero cell line cytotoxicity (IC₅₀ in µg/mL), and selective index (SI)

compound	MIC (µg/mL)		MIC of single drug-resistant strains (µg/mL)					Cytotoxicity (IC ₅₀)	SI (IC ₅₀ /MIC)	
	MABA ^a	LORA ^a	rCS ^a	rINH ^a	rKM ^a	rRMP ^a	rSM ^a	Vero cell	MABA ^a	LORA ^a
13	1.20	4.84	1.17	0.73	0.73	1.35	1.39	17.22	14.35	3.6
38	24.3	>50	ND ^b	ND ^b	ND ^b	ND ^b	ND ^b	ND ^b	NA ^c	NA ^c
39	6.2	>50	ND ^b	ND ^b	ND ^b	ND ^b	ND ^b	ND ^b	NA ^c	NA ^c
40	20.7	>50	ND ^b	ND ^b	ND ^b	ND ^b	ND ^b	ND ^b	NA ^c	NA ^c
46	1.4	40.0	ND ^b	ND ^b	ND ^b	ND ^b	ND ^b	ND ^b	NA ^c	NA ^c
48	1.28	5.32	1.49	1.37	1.43	1.50	2.61	18.63	15.0	3.5
56	>50	>50	ND ^b	ND ^b	ND ^b	ND ^b	ND ^b	>50	NA ^c	NA ^c
57	>50	>50	ND ^b	ND ^b	ND ^b	ND ^b	ND ^b	>50	NA ^c	NA ^c
59	0.72	6.20	1.48	1.36	1.43	1.59	2.70	19.60	27.2	3.1
63	0.69	10.35	1.51	1.32	0.74	4.98	1.44	32.58	47.2	3.1
64	>50	>50	ND ^b	ND ^b	ND ^b	ND ^b	ND ^b	>50	NA ^c	NA ^c
68	2.96	2.88	6.06	5.21	5.85	5.60	5.46	17.01	5.7	5.9
69	5.67	6.00	8.04	3.11	5.78	5.43	5.24	19.87	3.5	3.3
RMP ^d	0.03	0.30	< 0.02	< 0.02	< 0.02	> 6.6	0.04	>150	NA ^c	NA ^c
INH ^d	0.03	> 35.1	0.04	> 1.1	0.07	0.10	> 1.1	ND ^b	NA ^c	NA ^c

^a MABA: microplate alamar blue assay; LORA: low oxygen recovery assay; rCS: resistant to cyclosporine; rINH: resistant to isoniazid; rKM: resistant to kanamycin; rRMP: resistant to rifampicin; rSM: resistant to streptomycin; ^b ND = not determined; ^c NA = Not applicable; ^d Positive control.

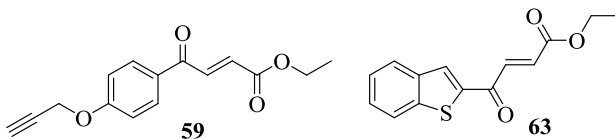


Table 5-3. Minimum inhibitory concentrations (MIC) of compounds 38-39, 41, 46, and 59 against clinically significant drug resistant strains ($\mu\text{g/mL}$)

Resistant strain ^a	38	39	41	46	59	Ox ^b	Van ^b	Gen ^b	Am ^b	Ery ^b	Cip ^b	Tet ^b
MC7827 MDR MRSA	1	0.5	2	>128	1	4	1	8	32	>128	>128	32
MC7769 Rif ^R MRSA	2	0.5	1	>128	0.5	4	1	32	>128	>128	>128	0.5
MC7606 MDR MRSA	1	0.25	2	>128	1	4	1	16	>128	128	32	64
MC7846 VISA MRSA	2	0.5	1	>128	0.5	4	4	32	8	>128	128	0.25
MC7583 MDR MRSA	1	0.25	0.5	>128	0.5	8	1	ND ^c	ND ^c	ND ^c	ND ^c	ND ^c
MW2 MRSA	1	0.25	0.25	>128	0.25	8	1	ND ^c	ND ^c	ND ^c	ND ^c	ND ^c
VRE 1	ND ^c	ND^c	2	>128	2	128	32	128	128	>128	8	4
VRE 14	ND ^c	ND^c	4	>128	4	128	128	128	128	128	64	64

^aMRSA = methicillin-resistant *S. aureus*, MDR = multi-drug resistant, VISA = vancomycin intermediate-resistant *S. aureus*; VRE = vancomycin resistant enterococci; ^b positive controls: Ox = oxacillin, Van = vancomycin, Gen = gentamicin, Am = ampicillin; Ery = erythromycin, Cip = ciprofloxacin, Tet = tetracycline; ^c ND = not determined

To further evaluate the biological profile of the most potent agents, they were tested for MIC values against the more virulent, actively replicating *M. tuberculosis* H₃₇Rv (Mtb) strain. This was carried out by Franzblau et al. at the Institute for Tuberculosis Research, University of Illinois at Chicago using the microplate alamar blue assay (MABA)¹⁹ and for non-replicating (dormant) cultures of Mtb via the low oxygen recovery assay (LORA).²⁰ The *in-vitro* cytotoxicity of these compounds were assessed using the Vero cells (monkey kidney cells), as described previously.²¹ As shown in Table 5-2, TPPC compounds **38-40** did not inhibit the growth of Mtb when compared to lead compound **13** and completely abolished the bactericidal activity against nonreplicating Mtb and unfortunately, the analog **39** did not retain its previous antimycobacterial (MIC = 0.25 $\mu\text{g/mL}$ against *M. smegmatis*) activity. The activity of inhibition of analogs **56-57** and **64** was consistent with the above MIC values (Table 5-1). Compared to the sulfone **69**, the sulfoxide **68** exhibited two fold more potent antibacterial activity against both replicating and dormant Mtb. The sulfoxide is a closer bioisostere to the keto group in **13**. The geranyl **46** and ethyl ester **48** exhibited similar activity against replicating bacilli in the MABA assay. However

the analog **46** was not capable of killing non-replicating Mtb in the LORA assay. Gratifyingly, the key ethyl esters **59** and **63** exhibited excellent antitubercular activity on actively replicating bacteria with a MIC value of 0.72 $\mu\text{g/mL}$, and 0.69 $\mu\text{g/mL}$ respectively, whereas these were not able to kill effectively, as compared to lead compound **13**, in the case of the dormant culture of Mtb. But the ethyl esters **59** and **63** exhibited roughly five and three fold greater potency than isoniazid against dormant Mtb, which is one of the current first-line drug regimens in the four drug cocktail for tuberculosis, as shown in Table 5-2. **This result suggested both compounds have the potential to decrease the time of six month drug regimen employed in patients today and inhibit or retard the bacilli from developing resistance.**

The most representative compounds were also tested against single drug resistance tuberculosis strains (SDRTB) to rule out the possibility of cross-resistance with the commonly used chemotherapeutics such as cyclosporine, isoniazid, kanamycin, rifampicin, and streptomycin. The lead compounds **59** and **63** exhibited a MIC range of 0.74 $\mu\text{g/mL}$ - 4.98 $\mu\text{g/mL}$ against the above SDRTB which implies selective antitubercular activity towards resistant strains. The ethyl ester **48** showed activity similar to lead molecule **13** in each of the single drug resistant strains of Mtb. In the case of sulfoxide **68** and sulfone **69**, the same trend was observed against these clinically significant drug resistant strains of virulent Mtb, as shown in Table 5-2. The prominent analogs described in Table 5-2 were also evaluated in the safety profile towards Vero cell lines.²¹ As shown for lead compounds **59** and **63**, the IC_{50} values are 19.60 $\mu\text{g/mL}$ and 32.58 $\mu\text{g/mL}$ respectively. In general, a selective index ($\text{IC}_{50}/\text{MIC}$) greater than 10 denotes the measure of a valuable lead molecule that can be further optimized to a druggable candidate²², which was true in the case of **59** and **63** in MABA. Also, the same pattern was continued for compound **48**, however,

for the compounds **68** and **69**, the SI values fall below ten, as shown in Table 5-2. Unfortunately, most of the compounds did not show any significant SI values in the LORA assay.

While the initial activity of clinically employed drugs against *S. aureus* was promising, because of emergence of resistant strains, agents which have potential activity against various clinically relevant resistant strains is necessary for any new line of antibiotics. The strains tested with these analogs include methicillin-resistant *S. aureus* (MRSA), multi-drug resistant (MDR) MRSA, vancomycin intermediate-resistant *S. aureus* (VISA), and vancomycin resistant enterococci (VRE) with present antibiotics available on the market as positive controls and the results are listed in Table 5-3. The geranyl ester **46** was detrimental in its activity against these resistant strains, whereas the TPPC analogs **38-39** and the phenolic ester **41** nearly retain their level of activity and especially TPPC analog **39**, which exhibited greater potency against the above tested resistant strains than control antibiotics, as shown in Table 5-3. This is exciting via another study. Remarkably, the propargyl ether **59** retained excellent potent antibacterial activity observed in the MIC range of 0.25 µg/mL to 4 µg/mL against various resistant strains. This propargyl ether **59** was several fold more potent than some present day clinical drug candidates on the market with the capability of development into a novel antibiotic.

5.3. CONCLUSION

A novel new series of aroylacrylic acid derivatives were designed which contained various functionalities and were prepared by simple, economical, and straight forward synthetic routes as compared to some of those first and second line antibiotics in the clinic. This simple chemistry permitted a systematic study of the SAR and evaluation against a panel of gram positive, gram negative and mycobacteria including Mtb and the corresponding clinically important resistant strains. Most notable compounds **59** and **63** exhibited two fold more potent activity against *M.*

smegmatis than rifampin, one of the first line antibiotics for tuberculosis. In addition, both ethyl esters **59** and **63** were found to be very potent (MIC = 0.72 and 0.69 $\mu\text{g/mL}$) against actively replicating Mtb and more importantly, scaffolds **59** and **63** exhibited six and four fold greater inhibition, respectively, toward nonreplicating persistent (dormant) phenotypes in low oxygen conditions than isoniazid; this is essential to decrease duration of tuberculosis treatment from many months to less. Further evaluation of these selected analogs **59** and **63** against a panel of single – drug resistant Mtb strains maintained similar activity as against the wild type with an encouraging safety profile with an SI value greater than 10. This suggests these scaffolds act through a different mechanism from those of the currently used clinical candidates (see next Chapter for complete details) and might not develop resistance. Clinicians all over the world are searching for these types of antimicrobials to treat deadly resistant infections. Gratifyingly, the propargyl ether **59** retained excellent inhibition against a wide variety of virulent antibiotic-resistant clinical isolates (MRSA, MDR MRSA, VISA MRSA, and VRE). According to the SAR, it is clear these lead candidates act through a Michael acceptor mechanism of action. In modern medicine, Michael acceptors are employed to treat chronic illness due to their desired mode of action.²³⁻³⁰ Although there is inherent fear in employing Michael acceptors, several classes of drugs include corticosteroids, antibiotics, antiviral, and anticancer agents used clinically today (see the Merck index for details).³¹ The structural rigidity and planarity of the Michael acceptor scaffold allows them to trap an active intermediate in a biological cycle especially one which contains free thiols.³² The direct covalent modification of protein thiols by Michael acceptor agents is seen in cysteine protease inhibitors used to treat emphysema, stroke, viral infections, cancer, Alzheimer's disease, inflammation, and arthritis.³³⁻³⁵ Rifampin, the first line anti-tubercular drug which has saved millions of lives also contains a Michael acceptor unit, however, this is not actively involved in

the rifampin mode of action. Taken together, these potential applications and importance of Michael acceptor moieties in therapeutic agents suggest these novel acrylic acid ethyl esters **59** and **63** may be preferred options to present clinical antibiotics because of the efficient synthetic routes and ease of scale-up of synthesis. The investigation of ADMET (Absorption, Distribution, Metabolism, Excretion, and Toxicity) medicinal chemistry properties of select agents including **41**, **59**, and **63** are ongoing in our laboratories. It is felt a promising preclinical candidate related to **59** and **63** could evolve into a novel drug molecule in the near future to treat susceptible and resistant strains of bacterial infections.

5.4. EXPERIMENTAL

Agents **16**, **30-40** were synthesized as described previously in the literature.^{1,3,6,9}

5.4.1. General procedure for the Friedel-Crafts acylation between substituted benzenes and maleic anhydride: Synthesis of aroylacrylic acids 16, 30-34.

An oven-dried round bottom flask was charged with maleic anhydride (0.73 g, 7.45 mmol), the aromatic substrates (7.45 mmol), anhydrous CH₂Cl₂, and cooled to 0 °C. Then AlCl₃ (14.90 mmol) was added portionwise under a positive pressure of argon. The reaction mixture which resulted was stirred for 15 min at 0 °C and then allowed to warm to rt and stirred for 30 min – 6 h. The reaction progress was monitored by TLC (silica gel, 30% EtOAc in hexane). After the disappearance of starting materials, the reaction mixture was poured into an excess of ice water and the aq phase was extracted with CH₂Cl₂. The combined organic extracts were washed with brine, dried (Na₂SO₄), and concentrated under vacuum to yield the crude acid **16**, **30-34** (30% - 99%) as a solid which was used for the next reaction without further purification.

5.4.2. General procedure for esterification of aroylacrylic acid: synthesis of aroylacrylic esters **13**, **42** and **46-54**. Representative procedure for the synthesis of ethyl (*E*)-4-(4-(*tert*-butyl)phenyl)-4-oxobut-2-enoate (**13**)

The acid **16**³ (200 mg, 0.86 mmol) was dissolved in anhydrous DMF (2 mL) and Cs₂CO₃ (560 mg, 1.72 mmol) was added at rt under a positive pressure of argon. The reaction mixture which resulted was then stirred for 10-15 min after which ethyl iodide (83 μ L, 1.03 mmol) was added dropwise with a syringe and the mixture stirred for 2 h. The reaction mixture was quenched with water (5 mL) and extracted with ethyl acetate (3 \times 20 mL). The combined organic layer was washed with brine (3 \times 50 mL), dried (Na₂SO₄), and concentrated under vacuum to yield the crude ethyl ester **13**. This material was further purified by flash column chromatography (silica gel, 10% EtOAc in hexane) to yield the ethyl ester **13** as a light yellow colored oil (205 mg, 92%). The spectral data for this material were identical to the published values.¹

5.4.2.1. Methyl (*E*)-4-(4-(*tert*-butyl)phenyl)-4-oxobut-2-enoate (**42**)

The general method above was followed using the acid **16** (200 mg, 0.86 mmol) with methyl iodide (64.2 μ L, 0.87 mmol), Cs₂CO₃ (560 mg, 1.72 mmol) and the mixture stirred for 2 h at rt. After flash column chromatography (silica gel, 10% EtOAc in hexane) this yielded the methyl ester **42** as a light yellow colored oil (193 mg, 91%). ¹H NMR (300 MHz, CDCl₃) δ 8.05 – 7.88 (m, 3H), 7.54 (d, *J* = 8.4 Hz, 2H), 6.90 (d, *J* = 15.6 Hz, 1H), 3.86 (s, 3H), 1.37 (s, 9H); ¹³C NMR (75 MHz, CDCl₃) δ 188.9, 166.1, 157.9, 136.8, 134.0, 131.7, 128.9, 125.9, 52.3, 35.3, 31.0; HRMS (ESI-TOF) (*m/z*): [M+Na]⁺ calcd for C₁₅H₁₈O₃Na: 269.1154, found: 269.1182.

5.4.2.2. Methyl (*E*)-4-(4-hydroxyphenyl)-4-oxobut-2-enoate (**41**)

The general method above was followed using the acid **30** (140 mg, 0.73 mmol) with ethyl iodide (58.5 μ L, 0.73 mmol), NaHCO₃ (67.3 mg, 0.80 mmol) and the mixture stirred for 14 h at

rt. After flash column chromatography (silica gel, 30% EtOAc in hexane) this yielded the ester **41** as an off-white solid (146 mg, 91%); mp: 124-127 °C; ¹H NMR (300 MHz, CDCl₃) δ 8.00 (d, *J* = 8.7 Hz, 2H), 7.93 (d, *J* = 15.5 Hz, 1H), 6.96 (d, *J* = 8.8 Hz, 2H), 6.90 (d, *J* = 15.5 Hz, 1H), 5.57 (s, 1H), 4.33 (q, *J* = 7.1 Hz, 2H), 1.37 (t, *J* = 7.1 Hz, 3H); ¹³C NMR (75 MHz, CDCl₃) δ 188.2, 166.2, 162.1, 136.8, 131.9, 131.8, 129.1, 115.9, 61.7, 14.1; HRMS (ESI-TOF) (*m/z*): [M-H]⁻ calcd for C₁₂H₁₁O₄: 219.0657, found: 219.0632.

5.4.2.3. (*E*)-(*E*)-3,7-Dimethylocta-2,6-dien-1-yl-4-(4-(*tert*-butyl)phenyl)-4-oxobut-2-enoate (46**)**

The general method above was followed using the acid **16** (200 mg, 0.86 mmol) with Cs₂CO₃ (561 mg, 1.72 mmol), KI (142 mg, 0.86 mmol), and geranyl bromide (171 μL, 0.86 mmol) and the mixture was stirred for 2 h at rt. After flash column chromatography (silica gel, 10% EtOAc in hexane) this yielded the geranyl ester as a light yellow colored oil **46** (265 mg, 82%). ¹H NMR (300 MHz, CDCl₃): δ 7.96 (d, *J* = 7.8 Hz, 2H), 7.93 (d, *J* = 15.6 Hz, 1H), 7.54 (d, *J* = 8.1 Hz, 2H), 6.90 (d, *J* = 15.6 Hz, 1H), 5.44 (t, *J* = 7.2 Hz, 1H), 5.10 (m, 1H), 4.78 (d, *J* = 7.2 Hz, 2H), 2.12 (m, 4H), 1.77 (s, 3H), 1.70 (s, 3H), 1.69 (s, 3H), 1.37 (s, 9H); ¹³C NMR (75 MHz, CDCl₃): δ 188.9, 165.7, 157.7, 143.0, 136.6, 134.1, 132.2, 131.8, 128.9, 125.8, 123.7, 117.8, 62.2, 39.5, 35.2, 31.0, 26.3, 25.7, 17.7, 16.5; HRMS (EI) (*m/z*): (M⁺) calcd for C₂₄H₃₂O₃: 368.2351, found: 368.2344.

5.4.2.4. (*E*)-(2*E*,6*E*)-3,7,11-Trimethyldodeca-2,6,10-trien-1-yl 4-(4-(*tert*-butyl)phenyl)-4-oxobut-2-enoate (47**)**

The general method above was followed using the acid **16** (100 mg, 0.43 mmol) with Cs₂CO₃ (281 mg, 0.86 mmol), KI (71 mg, 0.43 mmol), and *trans,trans*-farnesyl bromide (116 μL, 0.43 mmol) and the mixture was stirred for 2 h at rt. After flash column chromatography (silica gel, 10% EtOAc in hexane) this yielded the farnesyl ester as a light yellow colored oil **47** (154 mg,

86%). ¹H NMR (300 MHz, CDCl₃): δ 7.95 (d, *J* = 7.8 Hz, 2H), 7.91 (d, *J* = 15.3 Hz, 1H), 7.52 (d, *J* = 6.0 Hz, 2H), 6.87 (d, *J* = 15.6 Hz, 1H), 5.42 (t, *J* = 7.2 Hz, 1H), 5.09 (m, 2H), 4.76 (d, *J* = 7.2 Hz, 2H), 2.15-1.97 (m, 8H), 1.75 (s, 3H), 1.67 (s, 3H), 1.60 (s, 3H), 1.59 (s, 3H), 1.35 (s, 9H); ¹³C NMR (75 MHz, CDCl₃): δ 189.0, 165.7, 157.8, 143.0, 136.6, 135.5, 134.1, 132.2, 131.3, 128.9, 125.8, 124.3, 123.5, 117.8, 62.2, 39.7, 39.5, 35.2, 31.0, 26.7, 26.2, 25.7, 17.7, 16.6, 16.0; HRMS (ESI-TOF) (M+H)⁺ calcd for C₂₉H₄₁O₃: 437.3056, found: 437.3038.

5.4.2.5. (*E*)-3-Methylbut-2-en-1-yl 4-(4-chlorophenyl)-4-oxobut-2-enoate (**52**)

The general method above was followed using the acid **32** (500 mg, 2.37 mmol) with Cs₂CO₃ (1.54 g, 4.743 mmol), KI (393 mg, 2.37 mmol), and prenyl bromide (274 μL, 0.43 mmol) and the mixture was stirred for 2 h at rt. After flash column chromatography (silica gel, 10% EtOAc in hexane) this yielded the prenyl ester as a greenish yellow colored solid **53** (489 mg, 74%); mp: 55-56 °C; ¹H NMR (300 MHz, CDCl₃): δ 7.96 (d, *J* = 9.0 Hz, 2H), 7.87 (d, *J* = 15.0 Hz, 1H), 7.50 (d, *J* = 9.0 Hz, 2H), 6.91 (d, *J* = 15.0 Hz, 1H), 5.43 (t, *J* = 9.0 Hz, 1H), 4.76 (d, *J* = 6.0 Hz, 2H), 1.81 (s, 3H), 1.78 (s, 3H); ¹³C NMR (75 MHz, CDCl₃): δ 188.3, 165.4, 140.4, 140.1, 135.8, 134.9, 133.1, 130.2, 129.2, 117.9, 62.3, 25.8, 18.1; HRMS (APCI-TOF) (m/z): (M+H)⁺ calcd for C₁₅H₁₆O₃Cl: 279.0782, found: 279.0782.

5.4.2.6. (*E*)-3-Methylbut-2-en-1-yl 4-(4-Bromophenyl)-4-oxobut-2-enoate (**53**)

The general method above was followed using the acid **33** (500 mg, 1.96 mmol) with Cs₂CO₃ (1.28 g, 3.92 mmol), KI (325 mg, 1.96 mmol), prenyl bromide (226 μL, 1.96 mmol) and, the mixture was stirred for 2 h at rt. After flash column chromatography (silica gel, 10% EtOAc in hexane) this yielded the prenyl ester as a shiny white solid **54** (519 mg, 82%); mp: 60-61 °C; ¹H NMR (300 MHz, CDCl₃): δ 7.87 (d, *J* = 9.0 Hz, 2H), 7.83 (d, *J* = 15.0 Hz, 1H), 7.66 (d, *J* = 9.0 Hz, 2H), 6.90 (d, *J* = 15.0 Hz, 2H), 5.41 (t, *J* = 9.0 Hz, 1H), 4.74 (d, *J* = 6.0 Hz, 2H), 1.79 (s, 3H),

1.76 (s, 3H); ^{13}C NMR (75 MHz, CDCl_3): δ 188.5, 165.4, 140.0, 135.7, 135.3, 133.1, 132.2, 130.3, 129.2, 118.0, 62.3, 25.8, 18.1; HRMS (APCI-TOF) (m/z): (M+H) $^+$ calcd for $\text{C}_{15}\text{H}_{16}\text{O}_3\text{Br}$: 323.0277, found: 323.0280.

5.4.2.7. (*E*)-3-Methylbut-2-en-1-yl 4-(4-Iodophenyl)-4-oxobut-2-enoate (**54**)

The general method above was followed using the acid **34** (500 mg, 1.61 mmol) with Cs_2CO_3 (1.05 g, 3.22 mmol), KI (274 mg, 1.96 mmol), and prenyl bromide (191 μL , 1.61 mmol) and the mixture was stirred for 2 h at rt. After flash column chromatography (silica gel, 10% EtOAc in hexane) this yielded the ester as a light yellowish colored solid **55** (471 mg, 79%); mp: 61-63 $^\circ\text{C}$; ^1H NMR (300 MHz, CDCl_3): δ 7.89 (d, $J = 9.0$ Hz, 2H), 7.84 (d, $J = 15.0$ Hz, 1H), 7.70 (d, $J = 9.0$ Hz, 2H), 6.90 (d, $J = 18.0$ Hz, 1H), 5.42 (t, $J = 6.0$ Hz, 1H), 4.75 (d, $J = 6.0$ Hz, 2H), 1.80 (s, 3H), 1.76 (s, 3H); ^{13}C NMR (75 MHz, CDCl_3): δ 188.8, 165.4, 140.0, 138.2, 135.9, 135.7, 133.1, 130.2, 130.1, 118.0, 102.1, 62.3, 25.8, 18.1; HRMS (APCI-TOF) (m/z): (M+H) $^+$ calcd for $\text{C}_{15}\text{H}_{16}\text{O}_3\text{I}$: 371.0139, found: 371.0141.

5.4.2.8. (*E*)-Ethyl 4-(4-methoxyphenyl)-4-oxobut-2-enoate (**48**)

The general method above was followed using the acid **31** (400 mg, 1.941 mmol) with ethyl iodide (200 μL , 2.33 mmol), Cs_2CO_3 (1.26 g, 3.88 mmol) and this was stirred for 2 h at rt. After flash column chromatography (silica gel, 10% EtOAc in hexane) this yielded the ethyl ester **48** as a greenish yellow colored solid (409 mg, 90%). mp: 41-44 $^\circ\text{C}$; ^1H NMR (300 MHz, CDCl_3) δ 8.72 (d, $J = 8.9$ Hz, 2H), 8.63 (d, $J = 15.5$ Hz, 1H), 7.69 (d, $J = 8.9$ Hz, 2H), 7.58 (d, $J = 15.5$ Hz, 1H), 5.01 (q, $J = 7.1$ Hz, 2H), 4.61 (s, 3H), 2.06 (t, $J = 7.1$ Hz, 3H); ^{13}C NMR (75 MHz, CDCl_3) δ 188.4, 166.4, 164.9, 137.2, 132.5, 132.0, 130.4, 114.8, 61.9, 56.3, 14.9; HRMS (ESI-TOF) (m/z): [M+Na] $^+$ calcd for $\text{C}_{13}\text{H}_{14}\text{O}_4\text{Na}$: 257.0790, found: 257.0794.

5.4.2.9. (*E*)-Ethyl 4-(4-chlorophenyl)-4-oxobut-2-enoate (**49**)

The general method above was followed using the acid **32** (500 mg, 3.37 mmol) with Cs₂CO₃ (1.54 g, 6.74 mmol), iodoethane (210, 3.71 mmol) in DMF (3 mL) and the mixture was stirred for 2h at rt. After flash column chromatography (silica gel, 10% EtOAc in hexane) this yielded the ethyl ester **49** as a greenish yellow colored oil (660 mg, 82%). ¹H NMR (500 MHz, CDCl₃) 1.38 (t, *J* = 7.5 Hz, 3H), 4.34 (q, *J* = 7.5 Hz, 2H), 6.92 (d, *J* = 15.5 Hz, 1H), 7.52 (d, *J* = 8.4 Hz, 2H), 7.89 (d, *J* = 15.4 Hz, 1H), 7.98 (d, *J* = 8.4 Hz, 2H); ¹³C NMR (125 MHz, CDCl₃) δ 188.3, 165.4, 140.5, 135.8, 135.0, 133.1, 130.3, 129.3, 129.3, 61.5, 14.2; HRMS (ESI-TOF) (M+H)⁺ calcd for C₁₂H₁₂O₃Cl: 239.0470, found: 239.0445.

5.4.2.10. (*E*)-Ethyl 4-(4-bromophenyl)-4-oxobut-2-enoate (**50**)

The general method above was followed using the acid **33** (500 mg, 1.96 mmol) with Cs₂CO₃ (1.28 g, 3.92 mmol), iodoethane (173.2 μL, 2.16 mmol) in DMF (3 mL) and this was stirred for 2h at rt. After flash column chromatography (silica gel, 10% EtOAc in hexane) this yielded the ethyl ester **50** as a light yellowish colored solid (472 mg, 85%). mp 64-65 °C; ¹H NMR (500 MHz, CDCl₃) δ 1.38 (t, *J* = 7.2 Hz, 3H), 4.38 (q, *J* = 7.1 Hz, 2H), 6.92 (d, *J* = 15.5 Hz, 1H), 7.69 (d, *J* = 8.5 Hz, 2H), 7.88 (d, *J* = 15.5 Hz, 1H), 7.90 (d, *J* = 8.5 Hz, 2H); ¹³C NMR (125 MHz, CDCl₃) δ 188.5, 165.4, 135.8, 135.4, 133.1, 132.3, 130.3, 129.3, 61.5, 14.2; HRMS (ESI-TOF) (m/z): (M+H)⁺ calcd for C₁₂H₁₂O₃Br: 282.9964, found: 283.0001.

5.4.2.11. (*E*)-Ethyl 4-(4-iodophenyl)-4-oxobut-2-enoate (**51**)

The general method above was followed using the acid **34** (500 mg, 1.65 mmol) with Cs₂CO₃ (1.07 g, 3.3 mmol), iodoethane (146 μL, 1.81 mmol) in DMF (3 mL) and this mixture was stirred for 2h at rt. After flash column chromatography (silica gel, 10% EtOAc in hexane) this yielded the ethyl ester **51** as a light yellowish colored solid (463 mg, 85%). m.p. 52-54 °C; ¹H

NMR (300 MHz, CDCl₃) δ 1.37 (t, J = 7.12 Hz, 3H), 4.32 (q, J = 7.10 Hz, 2H), 6.91 (d, J = 15.52 Hz, 1H), 7.72 (d, J = 8.25 Hz, 2H), 7.93-7.82 (m, 3H); ¹³C NMR (75 MHz, CDCl₃) δ 188.8, 165.4, 138.2, 135.9, 135.7, 133.1, 130.1, 102.1, 61.5, 14.2. HRMS (ESI-TOF) (m/z): (M+H)⁺ calcd for C₁₂H₁₂O₃I: 330.9826, found: 330.9809.

5.4.3. General procedure for the acid catalyzed esterification of aroylacrylic acid; synthesis of aroylacrylic esters 43-45. Representative procedure for the synthesis of isopropyl (*E*)-4-(4-(*tert*-butyl)phenyl)-4-oxobut-2-enoate (43)

To a stirred solution of the acid **16** (500 mg, 2.152 mmol) in anhydrous toluene (5 mL) was added isopropyl alcohol (823.4 μ L, 10.76 mmol), conc. H₂SO₄ (65 μ L, 30 μ L/mmol), MgSO₄ (647 mg, 5.38 mmol) at rt under a positive pressure of argon. The reaction mixture, which resulted, was then stirred for 18 h at rt. The reaction mixture was filtered and the residue was washed with toluene (until no more product could be obtained; ~ 5 mL; TLC, silica gel). The combined toluene layer was brought to neutral pH [pH paper] with aq sat NaHCO₃ solution. The solution was subsequently washed with water (30 mL), brine (30 mL), dried (Na₂SO₄), and concentrated under vacuum to yield the crude ester **43**. This material was further purified by flash column chromatography (silica gel, 10% EtOAc in hexane) to yield the ester **43** as a light yellow colored oil (472 mg, 80%). ¹H NMR (300 MHz, CDCl₃) δ 7.94 (d, J = 8.5 Hz, 2H), 7.88 (d, J = 15.6 Hz, 1H), 7.52 (d, J = 8.5 Hz, 2H), 6.85 (d, J = 15.6 Hz, 1H), 5.28 – 4.93 (m, 1H), 1.35 (s, 9H), 1.32 (d, J = 6.3 Hz, 6H); ¹³C NMR (75 MHz, CDCl₃) δ 189.2, 165.2, 157.8, 136.4, 134.1, 132.8, 128.9, 125.9, 68.9, 35.3, 31.1, 21.8; HRMS (ESI-TOF) (m/z): [M+Na]⁺ calcd for C₁₇H₂₂O₃Na: 297.1467, found: 297.1461.

5.4.3.1. *Tert*-Butyl (*E*)-4-(4-(*tert*-butyl)phenyl)-4-oxobut-2-enoate (44)

The general method above was followed using the acid **16** (100 mg, 0.430 mmol) with *tert*-butanol (200 μ L, 2.15 mmol), conc. H₂SO₄ (13 μ L), MgSO₄ (130 mg, 1.1 mmol) and the mixture

was stirred for 18 h at rt. After flash column chromatography (silica gel, 10% EtOAc in hexane) this yielded the *t*-butyl ester **44** as a greenish yellow colored solid (93 mg, 75%). mp: 59-62 °C; ¹H NMR (300 MHz, CDCl₃) δ 7.94 (d, *J* = 8.3 Hz, 2H), 7.82 (d, *J* = 15.6 Hz, 1H), 7.52 (d, *J* = 8.3 Hz, 2H), 6.80 (d, *J* = 15.6 Hz, 1H), 1.54 (s, 9H), 1.35 (s, 9H); ¹³C NMR (75 MHz, CDCl₃) δ 189.4, 164.9, 157.7, 135.8, 134.2, 128.9, 125.8, 81.8, 35.2, 31.1, 28.0; HRMS (ESI-TOF) (*m/z*): [M+Na]⁺ calcd for C₁₈H₂₄O₃Na: 311.1623, found: 311.1617.

5.4.3.2. 2,2,2-Trifluoroethyl (*E*)-4-(4-(*tert*-butyl)phenyl)-4-oxobut-2-enoate (**45**)

The general method above was followed in the absence of the solvent toluene using the acid **16** (100 mg, 0.430 mmol) with 2,2,2-trifluoroethanol (excess), conc. H₂SO₄ (13 μL), MgSO₄ (130 mg, 1.1 mmol) and the mixture was stirred for 18 h at 60 °C. After flash column chromatography (silica gel, 10% EtOAc in hexane) this yielded the ester **45** as an off-white solid (105 mg, 78%). mp: 52-56 °C; ¹H NMR (300 MHz, CDCl₃) δ 8.03 (d, *J* = 15.6 Hz, 1H), 7.97 (d, *J* = 8.4 Hz, 2H), 7.56 (d, *J* = 8.4 Hz, 2H), 6.95 (d, *J* = 15.6 Hz, 1H), 4.65 (q, *J* = 8.3 Hz, 2H), 1.38 (s, 9H); ¹³C NMR (75 MHz, CDCl₃) δ 188.4, 164.0, 158.2, 138.7, 133.8, 129.7, 128.9, 125.9, 122.7 (q, ¹*J*_{C-F} = 277.5 Hz), 60.9 (q, ²*J*_{C-F} = 37.5 Hz), 35.3, 31.0; HRMS (ESI-TOF) (*m/z*): [M+H]⁺ calcd for C₁₆H₁₈F₃O₃: 315.1208, found: 315.1202.

5.4.4. General procedure for the synthesis of ethyl esters **56** and **57**. Representative procedure for the synthesis of ethyl (*E*)-4-((4-(*tert*-butyl)phenyl)amino)-4-oxobut-2-enoate (**56**)

To a stirred solution of ethyl (*E*)-4-chloro-4-oxobut-2-enoate **55** (2.18 g, 13.4 mmol) in anhydrous THF (20 mL) was added 4-(*tert*-butyl)aniline (2 g, 13.4 mmol) slowly dropwise at rt. The formation of a solid was observed and then DIPEA (2.1 g, 16.08 mmol) was added slowly dropwise at rt which gave a clear solution. The reaction mixture, which resulted, was then stirred for 30 min at rt. The reaction progress was monitored by TLC (silica gel, 25% EtOAc in hexane).

After the disappearance of starting materials, the reaction mixture was quenched with water (10 mL) and extracted with ethyl acetate (3 × 50 mL). The combined organic layer was washed with brine (50 mL), dried (Na₂SO₄), and concentrated under vacuum to yield the crude ester **56**. This material was further purified by flash column chromatography (silica gel, 10% EtOAc in hexane) and this yielded the ester **56** as a white solid (3.17 g, 86%). mp: 97-100 °C; ¹H NMR (500 MHz, CDCl₃) δ 8.39 (s, 1H), 7.57 (d, *J* = 8.4 Hz, 1H), 7.37 (d, *J* = 8.4 Hz, 1H), 7.23 (d, *J* = 15.3 Hz, 1H), 6.99 (d, *J* = 15.3 Hz, 1H), 4.30 (q, *J* = 7.1 Hz, 2H), 1.40 – 1.29 (m, 12H); ¹³C NMR (125 MHz, CDCl₃) δ 166.0, 161.7, 148.1, 137.3, 134.9, 130.9, 125.9, 120.0, 61.5, 34.5, 31.3, 14.2; HRMS (ESI-TOF) (m/z): [M-H]⁻ calcd for C₁₆H₂₀NO₃: 274.1448, found: 274.1440.

5.4.4.1. 4-(*tert*-Butyl)phenyl ethyl fumarate (**57**)

The general method above was followed using ethyl (*E*)-4-chloro-4-oxobut-2-enoate **55** (0.4 g, 2.66 mmol) with 4-(*tert*-butyl)phenol (0.38 g, 2.66 mmol), DIPEA (0.41 g, 3.2 mmol) and the mixture was stirred for 30 min at rt. After flash column chromatography (silica gel, 10% EtOAc in hexane) this process yielded the ester **57** as a white solid (639 mg, 87%). mp: 41-44 °C; ¹H NMR (300 MHz, DMSO-*d*₆) δ 7.46 (d, *J* = 8.7 Hz, 2H), 7.14 (d, *J* = 8.7 Hz, 2H), 6.96 (s, 2H), 4.25 (q, *J* = 7.1 Hz, 2H), 1.37 – 1.22 (m, 12H); ¹³C NMR (75 MHz, CDCl₃) δ 164.8, 163.6, 149.1, 147.9, 135.2, 132.9, 126.4, 120.6, 61.5, 34.5, 31.4, 14.1; HRMS (ESI-TOF) (m/z): [M+H]⁺ calcd for C₁₆H₂₁O₄: 277.1440, found: 277.1449.

5.4.5. Ethyl (*E*)-4-(4-(*tert*-butyl)phenyl)-4-hydroxybut-2-enoate (**58**)

To a stirred solution containing ethyl (*E*)-4-(4-(*tert*-butyl)phenyl)-4-oxobut-2-enoate **13** (100 mg, 0.384 mmol) in anhydrous methanol (3 mL) at -10 °C, KBH₄ (20.7 mg, 0.384 mmol) was added and the mixture was stirred for 1 h. The reaction progress was monitored by TLC (silica gel, 25% EtOAc in hexane). After the disappearance of starting material, the reaction mixture was

quenched with a sat aq NH₄Cl solution (5 mL) and extracted with ethyl acetate (3 × 10 mL). The combined organic layer was washed with brine (50 mL), dried (Na₂SO₄), and concentrated under vacuum to yield the crude ester **58**. This material was further purified by flash column chromatography (silica gel, 20% EtOAc in hexane) to yield the ester **58** as a light yellow colored oil (89 mg, 88%). ¹H NMR (300 MHz, CDCl₃) δ 7.42 (d, *J* = 8.2 Hz, 2H), 7.31 (d, *J* = 8.2 Hz, 2H), 7.08 (dd, *J* = 15.6, 4.8 Hz, 1H), 6.18 (d, *J* = 15.6 Hz, 1H), 5.36 (s, 1H), 4.21 (q, *J* = 7.1 Hz, 2H), 2.21 (s, 1H), 1.37–1.22 (m, 12H); ¹³C NMR (75 MHz, CDCl₃) δ 166.5, 151.5, 148.6, 137.9, 126.4, 125.8, 120.1, 73.4, 60.5, 34.5, 31.3, 14.2; HRMS (EI) (*m/z*): [*M*]⁺ calcd for C₁₆H₂₂O₃: 262.1569, found: 262.1543.

5.4.6. Ethyl (*E*)-4-oxo-4-(4-(prop-2-yn-1-yloxy)phenyl)but-2-enoate (**59**)

The phenol **41** (1 g, 4.541 mmol) was dissolved in anhydrous DMF (7 mL) and Cs₂CO₃ (2.22 g, 6.811 mmol) was added at rt under a positive pressure of argon. The reaction mixture which resulted turned to a orange red color and was then stirred for 30 min after which the propargyl bromide (410.2 μL, 5.45 mmol) was added dropwise with a syringe and the mixture then stirred for 1 h. The reaction mixture was quenched with water (10 mL) and extracted with ethyl acetate (3 × 40 mL). The combined organic layer was washed with brine (3 × 100 mL), dried (Na₂SO₄), and concentrated under vacuum to yield the crude ethyl ester **59**. This material was further purified by flash column chromatography (silica gel, 20% EtOAc in hexane) to furnish the ester **59** as an off-white solid (1 g, 86%). mp: 73-76 °C; ¹H NMR (300 MHz, CDCl₃) δ 8.03 (d, *J* = 8.8 Hz, 2H), 7.92 (d, *J* = 15.5 Hz, 1H), 7.08 (d, *J* = 8.8 Hz, 2H), 6.88 (d, *J* = 15.5 Hz, 1H), 4.79 (d, *J* = 2.3 Hz, 2H), 4.31 (q, *J* = 7.1 Hz, 2H), 2.59 (t, *J* = 2.3 Hz, 1H), 1.36 (t, *J* = 7.1 Hz, 3H); ¹³C NMR (75 MHz, CDCl₃) δ 187.7, 165.7, 161.9, 136.4, 132.0, 131.2, 130.4, 114.9, 77.5, 76.4, 61.3, 55.9, 14.2; HRMS (ESI-TOF) (*m/z*): [*M*+Na]⁺ calcd for C₁₅H₁₄O₄Na: 281.0790, found: 281.0788.

5.4.7. Ethyl (*E*)-4-oxo-4-(4-(trifluoromethyl)phenyl)but-2-enoate (**60**)

To a solution of 1-(4-(trifluoromethyl)phenyl)ethenone (2 g, 10.62 mmol) in a mixture of AcOH (10 mL) and HCl (2 mL) was added glyoxylic acid monohydrate (978 mg, 10.62 mmol). The reaction mixture, which resulted, was heated to reflux for 18 h. The reaction progress was monitored by TLC (silica gel, 5% MeOH in CH₂Cl₂). After disappearance of the starting material, the solvents were removed *in vacuo* and the acid was dried (benzene employed as the azeotropic distillation solvent). The crude acid (2.1 g, 81%) was used directly in the next step. The general method for synthesis of ethyl ester **13** was followed using the above acid (620 mg, 2.5 mmol) with ethyl iodide (240 μ L, 3 mmol), Cs₂CO₃ (1.63 g, 5 mmol) and this mixture was stirred for 2 h at rt. After flash column chromatography (silica gel, 10% EtOAc in hexane) this yielded the ester **60** as a light yellow solid (626 mg, 92%). mp: 67-70 °C; ¹H NMR (300 MHz, CDCl₃) δ 8.10 (d, *J* = 6.0 Hz, 2H), 7.88 (d, *J* = 15.0 Hz, 1H), 7.78 (d, *J* = 6.0 Hz, 2H), 6.92 (d, *J* = 15.0 Hz, 1H), 4.32 (q, *J* = 9.0 Hz, 2H), 1.36 (t, *J* = 6.0 Hz, 3H); ¹³C NMR (75 MHz, CDCl₃) δ 188.7, 165.2, 139.3, 135.5, 134.9 (q, ²*J*_{C-F} = 33 Hz), 133.7, 129.1, 125.9 (q, ³*J*_{C-F} = 3.7 Hz), 123.4 (q, ¹*J*_{C-F} = 271.5 Hz), 61.6, 14.1; HRMS (ESI-TOF) (*m/z*): [M-H]⁻ calcd for C₁₃H₁₀F₃O₃: 271.0587, found: 271.0601.

5.4.8. (*E*)-10-Hydroxydecyl 4-(4-(*tert*-butyl)phenyl)-4-oxobut-2-enoate (**61**)

The Cs₂CO₃ (1.75 g, 5.38 mmol) was added to a stirred solution of the acid **16** (500 mg, 2.15 mmol) in anhydrous DMF (8 mL) after which 10-bromo-1-decanol (766 mg, 3.23 mmol) was added slowly with a syringe under a positive pressure of argon. The reaction mixture, which resulted, was then stirred for 1 h (a longer reaction time was found to be detrimental to the yield). After completion of the reaction, as indicated by TLC (silica gel, 30% EtOAc in hexane), the reaction mixture was diluted with EtOAc (60 mL) and poured into water. The organic layer was separated and washed with water (50 mL), brine (3 x 50 mL), and dried (Na₂SO₄). The solvent

was removed under reduced pressure to give a light yellow colored oil. Flash column chromatography with 30% EtOAc in hexane on silica gel furnished the alcohol **61** as a light yellow colored oil (770 mg, 92%). ¹H NMR (500 MHz, CDCl₃) δ 7.97 (d, *J* = 8.37 Hz, 2H), 7.94 (d, *J* = 15.6 Hz, 1H), 7.55 (d, *J* = 8.3 Hz, 2H), 6.91 (d, *J* = 15.5 Hz, 1H), 4.28-4.24 (m, 2H), 3.68-3.64 (m, 2H), 1.76-1.69 (m, 2H), 1.62-1.55 (m, 2H), 1.44-1.31 (m, 21H); ¹³C NMR (125 MHz, CDCl₃): 189.1, 165.8, 157.9, 136.6, 134.1, 132.3, 128.9, 125.9, 65.5, 63.1, 35.3, 32.8, 31.1, 29.5, 29.4, 29.4, 29.2, 28.5, 25.9, 25.7; HRMS (ESI-TOF) (*m/z*): [M+H]⁺ calcd for C₂₄H₃₇O₄: 389.2686, found: 389.2696.

5.4.9. (E)-10-((Diethoxyphosphoryl)oxy)decyl 4-(4-(*tert*-butyl)phenyl)-4-oxobut-2-enoate (62)

To a stirred solution of the alcohol **61** (50 mg, 0.13 mmol) and Et₃N (89.7 μL, 0.64 mmol) in dry CH₂Cl₂ (3 mL), diethyl chlorophosphate (37.1 μL, 0.26 mmol) was added at rt. The reaction mixture, which resulted, was then stirred overnight. After completion of the reaction, as indicated by TLC (silica gel, 50% EtOAc in hexane) and LR-MS, the reaction mixture was diluted with CH₂Cl₂ and water. The organic layer was separated and the aq layer was extracted with CH₂Cl₂ (2 x 10 mL). The combined organic layer was washed with brine (3 x 20 mL) and dried (Na₂SO₄) to provide a light brown oil which upon purification on silica gel (flash chromatography) with 50% EtOAc in hexane provided the pure alkyl diethyl phosphate ester **62** as a colorless oil (64 mg, 95%). ¹H NMR (500 MHz, CDCl₃) δ 7.97 (d, *J* = 8.5 Hz, 2H), 7.93 (d, *J* = 15.6 Hz, 1H), 7.54 (d, *J* = 8.4 Hz, 2H), 6.90 (d, *J* = 15.7 Hz, 1H), 4.25 (t, *J* = 6.7 Hz, 2H), 4.16-4.09 (m, 4H), 4.05 (q, *J* = 6.8 Hz, 2H), 1.75-1.66 (m, 4H), 1.42-1.30 (m, 27H); ¹³C NMR (125 MHz, CDCl₃): 189.1, 165.8, 157.8, 136.6, 134.1, 132.2, 128.9, 125.9, 67.7, 67.6, 65.5, 63.6, 63.6, 35.3, 31.0, 30.3, 30.3, 29.4,

29.2, 29.1, 28.5, 25.9, 25.4, 16.2, 16.1; HRMS (ESI-TOF) (m/z): [M+H]⁺ calcd for C₂₈H₄₆O₇P: 525.2976, found: 525.2985.

5.4.10. Ethyl (*E*)-4-(benzo[*b*]thiophen-2-yl)-4-oxobut-2-enoate (**63**)

The general method for compound **20** was followed using with 4-benzo[*b*]thiophen-2-yl-4-hydroxy-but-2-ynoic acid ethyl ester **27** (157 mg, 0.6031 mmol), a 0.01 M solution of hydroquinone in DMSO (0.6 mL, 0.0060 mmol) and NaHCO₃ (10 mg, 0.1206 mmol) in DMSO:H₂O (8:1, 2 mL) and this mixture was allowed to stir for 18 h. After flash column chromatography on silica gel (2% EtOAc in hexane) this provided enoate **63** as a light pale yellowish colored solid (64 mg, 68%). mp: 71–75 °C; ¹H NMR (300 MHz, CDCl₃) δ 8.11 (s, 1H), 7.95-7.87 (m, 3H), 7.53 – 7.41 (m, 2H), 6.98 (d, *J* = 15.4 Hz, 1H), 4.33 (q, *J* = 7.1 Hz, 2H), 1.38 (t, *J* = 7.1 Hz, 3H); ¹³C NMR (125 MHz, CDCl₃) δ 182.7, 165.5, 143.9, 143.2, 139.1, 135.3, 132.3, 130.9, 128.2, 126.4, 125.3, 123.1, 61.5, 14.2; HRMS (ESI-TOF) (m/z): [M+Na]⁺ calcd for C₁₄H₁₂O₃SNa: 283.0405, found: 283.0413.

5.4.11. (*2S,3R*)-Ethyl 4-(benzo[*b*]thiophen-2-yl)-2,3-dihydroxy-4-oxobutanoate (**64**)

To a solution of ester **63** (37 mg, 0.142 mmol) in acetone (4.5 mL) and H₂O (0.5 mL) at rt, was added NMO (25 mg, 0.213 mmol), and OsO₄ (0.72 mg, 0.0028 mmol). The reaction mixture, which resulted, was stirred for 1 h. The reaction mixture was then quenched with a sat aq solution of Na₂S₂O₄ (5 mL), and stirred for 30 min. The aq layer was extracted with EtOAc (2 x 10 mL) and the combined organic layer was washed with brine (20 mL), dried (Na₂SO₄), and concentrated under vacuum to yield the crude ester **64**. This material was further purified by flash column chromatography (silica gel, 30% EtOAc in hexane) to yield the ester **64** as an off-white solid (33.4 mg, 80%). mp: 108-112 °C; ¹H NMR (300 MHz, CDCl₃) δ 8.14 (s, 1H), 7.95 (dd, *J* = 12.9, 8.0 Hz, 2H), 7.51 (dt, *J* = 14.8, 7.1 Hz, 2H), 5.38 (d, *J* = 1.4 Hz, 1H), 4.76 (d, *J* = 1.4 Hz, 1H), 4.42

(q, $J = 7.1$ Hz, 2H), 1.43 (t, $J = 7.1$ Hz, 3H); ^{13}C NMR (75 MHz, CDCl_3) δ 191.3, 171.4, 142.7, 138.8, 138.6, 130.5, 128.2, 126.3, 125.4, 123.0, 75.4, 73.1, 62.8, 14.3. HRMS (ESI-TOF) (m/z): $[\text{M}+\text{H}]^+$ calcd for $\text{C}_{14}\text{H}_{15}\text{O}_5\text{S}$: 295.0635, found: 295.0662.

5.4.12. (*E*)-3-(Benzo[*b*]thiophen-2-yl)-2-cyanoacrylamide (65)

To a stirred solution of benzo[*b*]thiophene-2-carboxaldehyde (500 mg, 3.08 mmol) in EtOH (12 mL) was added 2-cyanoacetamide (259.1 mg, 3.08 mmol), and piperidine (304.2 μL , 3.08 mmol). The reaction mixture which resulted was then stirred for 18 h and then the EtOH was removed *in vacuo*. The crude residue was subjected to flash column chromatography on silica gel (40% EtOAc in hexane) to yield the amide **65** as a yellow colored solid (492 mg, 70%): mp: 181-184 °C; ^1H NMR (300 MHz, $\text{DMSO}-d_6$) δ 8.51 (s, 1H), 8.19 (s, 1H), 8.13 (d, $J = 7.9$ Hz, 1H), 8.03 (d, $J = 7.7$ Hz, 1H), 7.87 (d, $J = 34.7$ Hz, 2H), 7.52 (dt, $J = 14.4, 6.9$ Hz, 2H); ^{13}C NMR (75 MHz, DMSO) δ 162.8, 144.6, 141.9, 138.3, 136.1, 136.0, 128.3, 126.0, 123.5, 116.8, 105.2; HRMS (ESI-TOF) (m/z): $[\text{M}+\text{H}+\text{CH}_3\text{CN}]^+$ calcd for $\text{C}_{14}\text{H}_{12}\text{N}_3\text{OS}$: 270.0696, found: 270.0678.

5.4.13. (*E*)-1,6-Bis(benzo[*b*]thiophen-2-yl)hex-3-ene-1,6-dione (66)

A heavy-wall pressure tube was equipped with a magnetic stir bar and fitted with a rubber septum. It was then charged with 1-(benzo[*b*]thiophen-2-yl)prop-2-en-1-one (115.4 mg, 0.61 mmol), 2-bromo-5-methyl-1,3,4-oxadiazole (100 mg, 0.61 mmol), $\text{Pd}(\text{OAc})_2$ (2.7 mg, 0.012 mmol), PPh_3 (8 mg, 0.0305 mmol), triethyl amine (40 μL , 0.305 mmol), and freeze-thawed anhydrous MeCN (5 mL) was injected into the tube with a degassed syringe under a positive pressure of argon. The vessel was evacuated and backfilled with argon (this process was repeated a total of three times). The rubber septum was replaced with a screw cap by quickly removing the rubber septum under a flow of argon and the sealed tube was introduced into a pre-heated oil bath at 85 °C. The reaction mixture was maintained at this temperature for 3-4 h. At the end of this time

period, the pressure tube was allowed to cool to rt. The reaction mixture was filtered through a short pad of celite, and the pad was washed with ethyl acetate (until no more product could be obtained; 30 mL; TLC, silica gel). The combined organic fractions were washed with water (50 mL), brine (50 mL), dried (Na₂SO₄), and concentrated under reduced pressure. The crude product was purified by flash column chromatography (silica gel, 25% EtOAc in hexane) to afford **66** as an off-white solid (165 mg, 72%). mp: 126-130 °C; ¹H NMR (300 MHz, CDCl₃) δ 7.98 (s, 1H), 7.92 – 7.79 (m, 5H), 7.53 – 7.31 (m, 4H), 5.98 (s, 2H), 3.31 (t, *J* = 7.3 Hz, 2H), 3.01 (t, *J* = 7.2 Hz, 2H). ¹³C NMR (75 MHz, CDCl₃) δ 193.7, 190.8, 146.3, 143.4, 142.8, 142.7, 142.5, 139.1, 138.9, 131.5, 129.5, 127.5, 127.4, 126.1, 125.9, 125.5, 124.9, 124.9, 122.9, 122.8, 37.6, 28.3. HRMS (ESI-TOF) (*m/z*): [M+Na]⁺ calcd for C₂₂H₁₆O₂S₂Na: 399.0484, found: 399.0469.

5.4.14. Ethyl (*E*)-3-((4-*tert*-butyl)phenyl)sulfinyl)acrylate (**68**)

To a stirred solution of sulfide **67** (100 mg, 0.38 mmol) in glacial acetic acid (1 mL) was added 30% H₂O₂ (173 μL, 1.52 mmol) at rt and the reaction mixture which resulted was stirred for 4 h at the same temperature. The reaction progress was monitored by TLC (silica gel, 10% EtOAc in hexane). After the disappearance of the starting material, the solution which resulted was neutralized with aq NaOH (4 M) and the sulfoxide, which formed, was extracted with CH₂Cl₂ (2 x 10 mL). The combined organic layer was washed with water (30 mL), brine (30 mL), dried (Na₂SO₄) and concentrated under reduced pressure. The crude product was purified by flash column chromatography (silica gel, 10% EtOAc in hexane) to yield sulfoxide **68** as an off-white solid (77 mg, 72%). mp: 60-64 °C; ¹H NMR (500 MHz, CDCl₃) δ 7.62 – 7.55 (m, 4H), 7.51 (d, *J* = 14.9 Hz, 1H), 6.76 (d, *J* = 14.9 Hz, 1H), 4.26 (q, *J* = 6.7 Hz, 2H), 1.36 (s, 9H), 1.33 (t, *J* = 7.1 Hz, 3H); ¹³C NMR (125 MHz, CDCl₃) δ 164.1, 155.7, 151.2, 138.2, 126.9, 124.9, 124.1, 61.4, 35.1, 31.2, 14.2; HRMS (ESI-TOF) (*m/z*): [M+H]⁺ calcd for C₁₅H₂₁O₃S: 281.1206, found: 281.1235.

5.4.15. Ethyl (*E*)-3-((4-(*tert*-butyl)phenyl)sulfonyl)acrylate (**69**)

To a stirred solution of sulfide **67** (100 mg, 0.38 mmol) in CH₂Cl₂ (3 mL), MCPBA (213 mg, 0.95 mmol) was added at rt. The reaction mixture which resulted was stirred for 30 min at the same temperature, and the formation of a white slurry was observed. The reaction progress was monitored by TLC (silica gel, 5% EtOAc in hexane). After the disappearance of the starting material, the reaction mixture was diluted with CH₂Cl₂ (15 mL) and then a sat aq solution of NaHCO₃ (10 mL) was added dropwise. The reaction mixture which resulted was stirred for 10 min and then the organic layer was separated and washed with water (30 mL), brine (30 mL), dried (Na₂SO₄) and concentrated under reduced pressure. The crude product was purified by flash column chromatography (silica gel, 5% EtOAc in hexane) to yield sulfone **69** as an off-white solid (98 mg, 87%). mp: 90-92 °C; ¹H NMR (500 MHz, CDCl₃) δ 7.86 (d, *J* = 8.5 Hz, 2H), 7.62 (d, *J* = 8.4 Hz, 2H), 7.35 (d, *J* = 15.2 Hz, 1H), 6.84 (d, *J* = 15.2 Hz, 1H), 4.27 (q, *J* = 7.1 Hz, 2H), 1.38 (s, 9H), 1.33 (t, *J* = 7.1 Hz, 3H); ¹³C NMR (125 MHz, CDCl₃) δ 163.6, 158.6, 143.5, 135.4, 130.6, 128.3, 126.7, 62.0, 35.4, 31.1, 14.1; HRMS (ESI-TOF) (*m/z*): [M+H+CH₃CN]⁺ calcd for C₁₇H₂₄NO₄S: 338.1420, found: 338.1428.

5.4.16. MIC vs. replicating *M. tuberculosis* H₃₇Rv (MABA Assay)

All compounds were evaluated for MIC vs. *M. tuberculosis* H₃₇Rv (ATCC 27294) using the microplate Alamar Blue assay (MABA) as previously described¹⁹ except that one now uses 7H12 media²¹ (instead of 7H9 + glycerol + casitone + OADC). In the case of compounds which exhibit significant background fluorescence, one also utilizes luciferase reporter strains of *M. tuberculosis* H₃₇Rv, as well as measurement of intracellular adenosine triphosphate. The cultures were incubated in 200 μL medium in 96-well plates for 7 days at 37 °C. Alamar Blue and Tween 80 were added and the incubation continued for 24 hours at 37 °C. Fluorescence was determined

at excitation/emission wavelengths of 530/590 nm, respectively. The MIC was defined as the lowest concentration effecting a reduction in fluorescence (or luminescence) of 90% relative to controls. Six control compounds were run in each experiment including isoniazid, rifampin, moxifloxacin, streptomycin, PA-824 and metronidazole.

5.4.17. Activity against non-replicating persistent (NRP) *M. tuberculosis* (LORA Assay)

This Low Oxygen Recovery Assay (LORA) ²⁰ was designed to detect compounds which may have the potential for shortening the duration of therapy through (more) efficient killing of the non-replicating persister (NRP) populations. The assay involves 1) adaptation of *M. tuberculosis* to low oxygen through gradual, monitored, self-depletion of oxygen during culture in a sealed flask with slow stirring, 2) exposure for 10 days of the low-oxygen adapted culture to test compounds in microplates that are maintained under an anaerobic environment using an Anoxomat system, thus precluding growth and 3) subsequent evaluation of *M. tuberculosis* viability as determined by the ability to recover. Recovery/viability is determined by the extent to which a luciferase-expressing strain can recover the ability to produce luminescence. This assay is HTS-compatible. Compounds such as isoniazid and ethambutol which are considered to be devoid of “sterilizing activity”, are inactive in this assay. Confirmation of new classes with activity is made by immediate subculture (without recovery phase) onto solid, drug-free media and determination of colony forming units. The rifamycins and the more potent fluoroquinolones, which do appear to eliminate some proportion of the persister population and thus can affect treatment duration, are active, albeit at concentrations higher than the MICs for replicating cultures. The correlation between the cfu and luminescence readout has been good with the exception of the fluoroquinolone class for which luminescence underestimated absolute activity but not relative activity.

5.4.18. Cytotoxicity

Compounds were routinely tested for cytotoxicity using VERO cells.²¹ After 72 hours exposure, viability was assessed on the basis of cellular conversion of MTS into a soluble formazan product using the Promega CellTiter 96 Aqueous Non-Radioactive Cell Proliferation Assay. Rifampin is included as a control. For compounds with IC₅₀:MIC >10, cytotoxicity will be repeated, this time using the J774.1 macrophage cell line since these are used in the macrophage assay and are usually somewhat more sensitive than VERO cells. This is important for interpreting data from the macrophage assay. Since much more comparative data is available for VERO cells, we still prefer to use these for primary cytotoxicity testing. Additional cell lines include HepG2 and the new metabolically active HepaRG which can be employed as well in the future.

5.5. REFERENCES

- (1) Tiruveedhula, V. V.; Witzigmann, C. M.; Verma, R.; Kabir, M. S.; Rott, M.; Schwan, W. R.; Medina-Bielski, S.; Lane, M.; Close, W.; Polanowski, R. L.; Sherman, D.; Monte, A.; Deschamps, J. R.; Cook, J. M. *Bioorg. Med. Chem.* **2013**, *21*, 7830.
- (2) Papa, D.; Schwenk, E.; Villani, F.; Klingsberg, E. *J. Am. Chem. Soc.* **1948**, *70*, 3356.
- (3) Vitorovic-Todorovic, M. D.; Eric-Nikolic, A.; Kolundzija, B.; Hamel, E.; Ristic, S.; Juranic, I. O.; Drakulic, B. J. *Eur. J. Med. Chem.* **2013**, *62*, 40.
- (4) Nicolaou, K. C.; Chen, J. S.; Edmonds, D. J.; Estrada, A. A. *Angew. Chem. Int. Ed. Engl.* **2009**, *48*, 660.
- (5) Feng, L.; Maddox, M. M.; Alam, M. Z.; Tsutsumi, L. S.; Narula, G.; Bruhn, D. F.; Wu, X.; Sandhaus, S.; Lee, R. B.; Simmons, C. J.; Tse-Dinh, Y. C.; Hurdle, J. G.; Lee, R. E.; Sun, D. *J. Med. Chem.* **2014**, *57*, 8398.
- (6) Cheng, G.; Zielonka, J.; Ouari, O.; Lopez, M.; McAllister, D.; Boyle, K.; Barrios, C. S.; Weber, J. J.; Johnson, B. D.; Hardy, M.; Dwinell, M. B.; Kalyanaraman, B. *Cancer Res.* **2016**, *76*, 3904.
- (7) Weinberg, F.; Hamanaka, R.; Wheaton, W. W.; Weinberg, S.; Joseph, J.; Lopez, M.; Kalyanaraman, B.; Mutlu, G. M.; Budinger, G. R.; Chandel, N. S. *Proc. Natl. Acad. Sci. U. S. A.* **2010**, *107*, 8788.

- (8) Abu-Gosh, S. E.; Kolvazon, N.; Tirosh, B.; Ringel, I.; Yavin, E. *Mol. Pharm.* **2009**, *6*, 1138.
- (9) Hu, Z.; Sim, Y.; Kon, O. L.; Ng, W. H.; Ribeiro, A. J.; Ramos, M. J.; Fernandes, P. A.; Ganguly, R.; Xing, B.; Garcia, F.; Yeow, E. K. *Bioconjug. Chem.* **2017**, *28*, 590.
- (10) Lipinski, C. A.; Lombardo, F.; Dominy, B. W.; Feeney, P. J. *Adv. Drug Deliv. Rev.* **2001**, *46*, 3.
- (11) Ciclosi, M.; Fava, C.; Galeazzi, R.; Orena, M.; Sepulveda-Arques, J.; Gonzalez-Rosende, M. E. *Heterocycles* **2003**, *60*, 1173.
- (12) Nicolaou, K. C.; Li, H.; Nold, A. L.; Pappo, D.; Lenzen, A. *J. Am. Chem. Soc.* **2007**, *129*, 10356.
- (13) Zhou, Y.; Wang, J.; Gu, Z.; Wang, S.; Zhu, W.; Acena, J. L.; Soloshonok, V. A.; Izawa, K.; Liu, H. *Chem. Rev.* **2016**, *116*, 422.
- (14) Zhao, S.; Lin, J. B.; Zhao, Y. Y.; Liang, Y. M.; Xu, P. F. *Org. Lett.* **2014**, *16*, 1802.
- (15) Krishnan, S.; Miller, R. M.; Tian, B.; Mullins, R. D.; Jacobson, M. P.; Taunton, J. *J. Am. Chem. Soc.* **2014**, *136*, 12624.
- (16) Krenske, E. H.; Petter, R. C.; Houk, K. N. *J. Org. Chem.* **2016**, *81*, 11726.
- (17) Meanwell, N. A. *J. Med. Chem.* **2011**, *54*, 2529.
- (18) Golchoubian, H.; Hosseinpoor, F. *Molecules* **2007**, *12*, 304.
- (19) Collins, L.; Franzblau, S. G. *Antimicrob. Agents Chemother.* **1997**, *41*, 1004.
- (20) Cho, S. H.; Warit, S.; Wan, B.; Hwang, C. H.; Pauli, G. F.; Franzblau, S. G. *Antimicrob. Agents Chemother.* **2007**, *51*, 1380.
- (21) Falzari, K.; Zhu, Z.; Pan, D.; Liu, H.; Hongmanee, P.; Franzblau, S. G. *Antimicrob. Agents Chemother.* **2005**, *49*, 1447.
- (22) Pieroni, M.; Wan, B.; Cho, S.; Franzblau, S. G.; Costantino, G. *Eur. J. Med. Chem.* **2014**, *72*, 26.
- (23) Avonto, C.; Tagliatela-Scafati, O.; Pollastro, F.; Minassi, A.; Di Marzo, V.; De Petrocellis, L.; Appendino, G. *Angew. Chem. Int. Ed. Engl.* **2011**, *50*, 467.
- (24) Ahn, B. Z.; Sok, D. E. *Curr. Pharm. Des.* **1996**, *2*, 247.
- (25) Johansson, M. H. *Mini-Rev Med Chem* **2012**, *12*, 1330.
- (26) McGovern, S. L.; Caselli, E.; Grigorieff, N.; Shoichet, B. K. *J. Med. Chem.* **2002**, *45*, 1712.

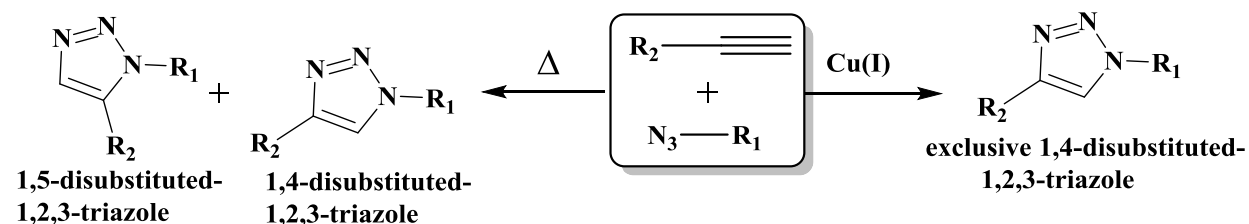
- (27) Amslinger, S. *ChemMedChem* **2010**, *5*, 351.
- (28) Aptula, A. O.; Roberts, D. W. *Chem. Res. Toxicol.* **2006**, *19*, 1097.
- (29) Petronelli, A.; Pannitteri, G.; Testa, U. *Anticancer Drugs* **2009**, *20*, 880.
- (30) Nanavati, S. M.; Silverman, R. B. *J. Am. Chem. Soc.* **1991**, *113*, 9341.
- (31) O'Neil, M. J.; Royal Society of Chemistry (Great Britain) *The Merck index : an encyclopedia of chemicals, drugs, and biologicals*; 15th ed.; Royal Society of Chemistry: Cambridge, UK, 2013.
- (32) Maucher, I. V.; Ruhl, M.; Kretschmer, S. B.; Hofmann, B.; Kuhn, B.; Fettel, J.; Vogel, A.; Flugel, K. T.; Manolikakes, G.; Hellmuth, N.; Hafner, A. K.; Golghalyani, V.; Ball, A. K.; Piesche, M.; Matrone, C.; Geisslinger, G.; Parnham, M. J.; Karas, M.; Steinhilber, D.; Roos, J.; Maier, T. J. *Biochem. Pharmacol.* **2017**, *125*, 55.
- (33) Fukuda, K.; Akao, S.; Ohno, Y.; Yamashita, K.; Fujiwara, H. *Cancer Lett.* **2001**, *164*, 7.
- (34) Couch, R. D.; Browning, R. G.; Honda, T.; Gribble, G. W.; Wright, D. L.; Sporn, M. B.; Anderson, A. C. *Bioorg. Med. Chem. Lett.* **2005**, *15*, 2215.
- (35) Powers, J. C.; Asgian, J. L.; Ekici, Ö. D.; James, K. E. *Chem. Rev.* **2002**, *102*, 4639.

CHAPTER 6

IDENTIFICATION OF MOLECULAR TARGETS FOR THE ANTIMICROBIAL AGENT **59** (ETHYL (*E*)-4-OXO-4-(4-(PROP-2-YN-1-YLOXY)PHENYL)BUT-2-ENOATE)

6.1. INTRODUCTION

In 1963 Rolf Huisgen introduced the concept of 1,3-dipolar cycloadditions of organic azides and alkynes. However, the reaction required long reaction times, high temperatures and/or pressures and resulted in the formation of two products, 1,4- and 1,5-regioisomers.¹ The high potential of this transformation, especially in the case of azides and alkynes to form aromatic triazole cycloaddition products ($\Delta G^\circ \approx -61 \text{ Kcal mol}^{-1}$), was too important to be ignored.² Although many research groups employed this process, it was not before 2001 that the Meldal and Sharpless laboratories independently discovered a Cu (I)-catalyzed variation of the 1,3-dipolar cycloaddition of azides with terminal alkynes. This permitted a very fast, efficient and selective formation of 1,4-disubstituted 1,2,3-triazole regioisomers under milder reaction conditions (Scheme 6-1).^{3,4} The reaction, termed as the copper catalyzed azide-alkyne 1,3-dipolar cycloaddition (CuAAC), proceeded approximately seven times faster than the uncatalyzed reaction. In addition, improved kinetics were achieved with the use of specific ligands for copper (I), as shown in Figure 6-1.^{5,6}



Scheme 6-1. Comparison between the thermally-induced and Cu (I) catalyzed Huisgen cycloaddition reaction conditions

The catchy phrase “Click Chemistry (CC)” proposed by Dr. Barry Sharpless at the 217th American Chemical Society Annual Meeting and his landmark review in 2001 referred to a concept

of the reaction that mimics nature.³ The process, as stated by Sharpless, is Mother Nature's strategy for accomplishing incredible biological diversity from a very limited number of monomers (i.e. the formation of proteins from amino acids, DNA/RNA from nucleotides, polysaccharides from monosaccharides and so on). According to Sharpless, CC refers to a group of reactions that: "must be modular, energetically favored, wide in scope, high yielding, and irreversible. The reaction should be stereospecific but not necessarily enantioselective and generate by-products that can be removed without chromatography. The required process characteristics should include simple reaction conditions (ideally, the process should be insensitive to oxygen and water), readily available starting materials and reagents, application of water as solvent and simple product isolation. Ideally, products are purified by non-chromatographic methods such as crystallization or distillation and products must be stable under physiological conditions".³ The process of CC plays a pivotal role in the quest for function and can be stated in one sentence: "all searches must be restricted to molecules that are easy to make".³

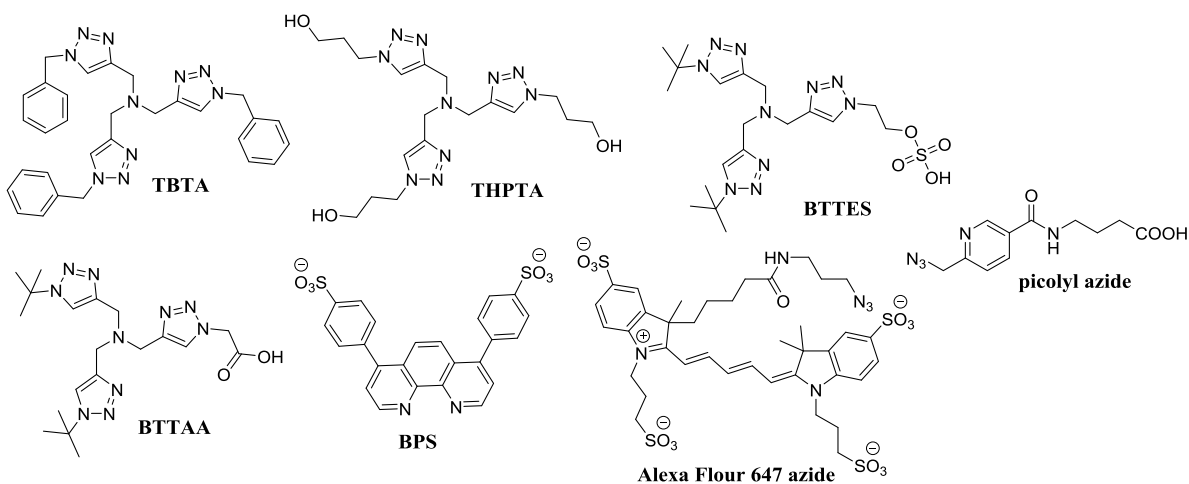
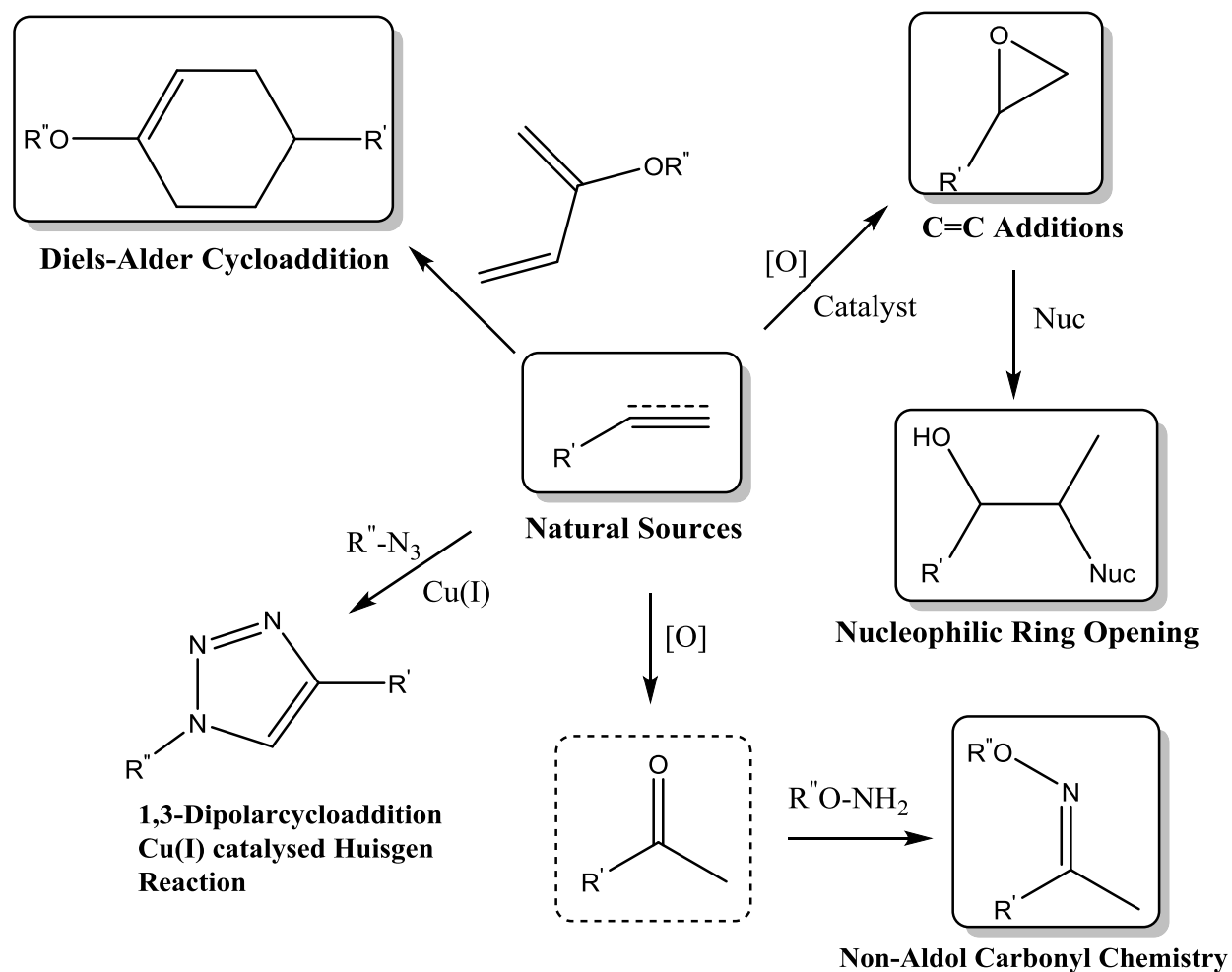


Figure 6-1. Structure of ligands for biocompatible copper-catalyzed azide-alkyne cycloaddition reactions

The concept of CC did not take long before it was applied to many different areas of science such as molecular and chemical biology, materials science, macromolecular chemistry, bioconjugation to drug design and discovery.^{5,7-12} The mild reaction conditions are attractive to

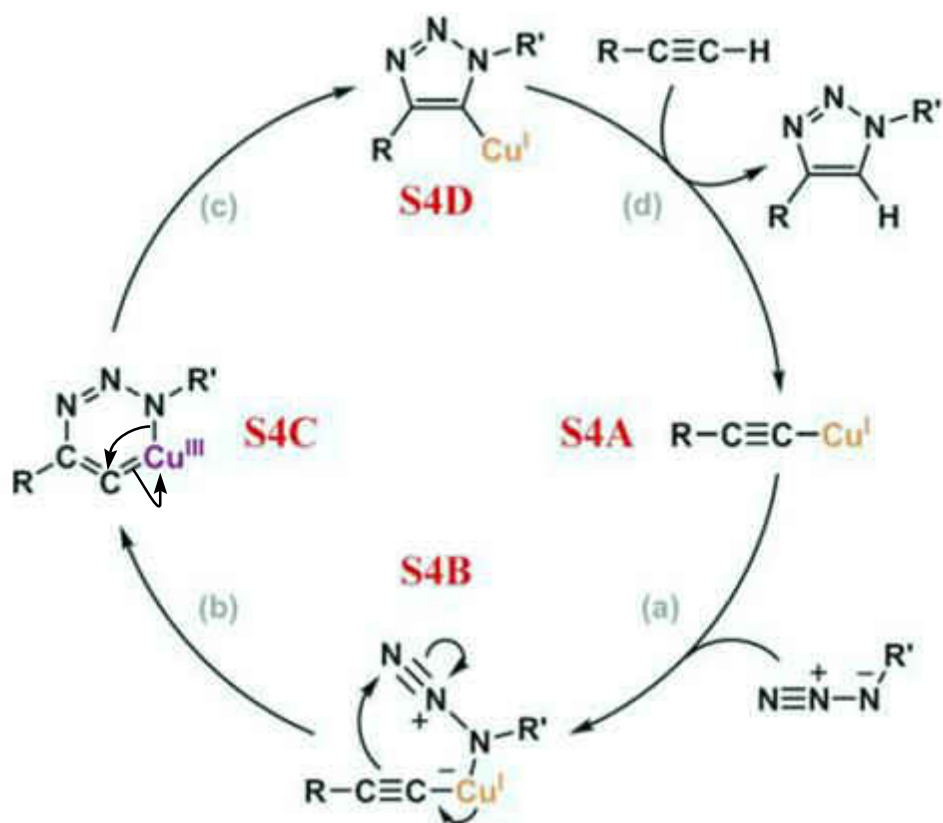
most modern scientists especially in the field of pharmaceutical sciences for drug discovery processes because of the complexity involved in the earlier traditional strategies that were used to label biomolecules.⁸



Scheme 6-2. Classification of Click chemistry reactions

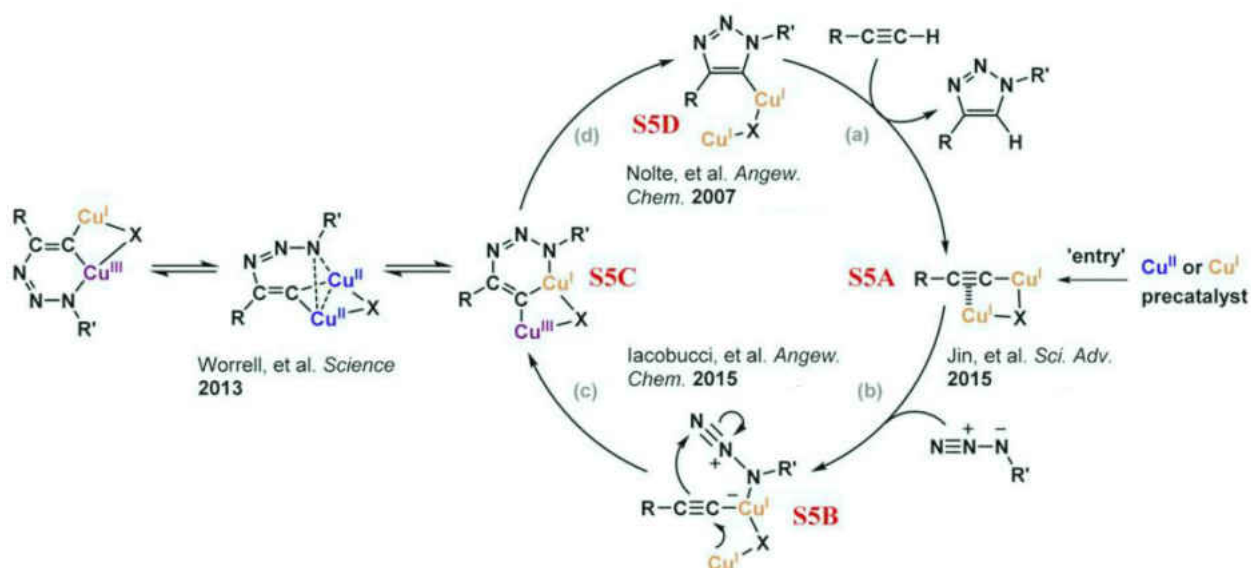
As stated earlier, even though meeting the benchmark of a Click reaction is not easy, a couple of reactions were recognized (Scheme 6-2). To the best of our knowledge Click reactions have been classified into four types: 1) nucleophilic ring opening reactions of aziridines, aziridinium ions and epoxides; 2) the formation of hydrazones, oximes, and urea, etc. for non-aldol carbonyl chemistry; 3) the addition reactions to carbon-carbon multiple bonds for Michael

processes and oxidative additions of nucleophiles. Finally, 4) cycloaddition reactions especially 1,3-dipolar cycloaddition reactions and Diels-Alder reactions.¹⁰



Scheme 6-3. The initial mononuclear mechanism of CuAAC proposed by Sharpless, Fokin, and co-workers

To date, the CuAAC reaction is the most applied reaction among the above processes, probably due to the production of stable products, the wide scope of substrates, compatibility with water, and minimal or no purification.³ In 2002, Sharpless, Fokin, and co-workers¹³ proposed the initial mechanism of CuAAC (Scheme 6-3). It starts with formation of copper(I) acetylide (S4A) followed by coordination with the azide, which results in complex (S4B). Metallacycle (S4C) is generated by the formation of a C-N bond (step b) and oxidation of copper from (I) to (III) in this step. Cuprous triazolide (S4D) is produced by ring contraction reducing copper (III) to copper (I), as shown in Scheme 6-3 (step c). The catalytic cycle completes with the formation of a triazole by protonation (S4D, step d).



Scheme 6-4. Up-to-date dinuclear mechanism of CuAAC, X is a bridging ligand

Subsequent studies on reaction kinetics suggested the presence of two copper ions that interact with one or two alkynes and one azide. Questions were raised about the exact mechanism in which this dinuclear system was involved. Initially, mechanistic studies of CuAAC focused on how to understand the rapid formation of the metallacycle, which resulted in the formation of the first C-N bond (Scheme 6-3, step b). Usually, the formation of a six-membered ring from an sp-hybridized carbon atom requires a very high activation energy.^{6,14} Subsequent kinetic and computational modeling experiments suggested the involvement of an additional copper ion for the metallacycle structure, which could relieve ring strain of S4C; thus lowering the activation barrier of the formation of the metallacycle. The extra copper ion could be introduced during the copper (I) acetylide step based on earlier observations of copper(I) involved in both σ and π bonding with $C\equiv C$ bonds in structures of polymers and clusters.^{15,16}

The most recent understanding of the dinuclear mechanism of CuAAC reactions, initiated by the formation of σ , π -di(copper) acetylide (S5A), is illustrated in Scheme 6-4. Herein the acetylide participates in both σ and π bonding with copper(I) which itself coordinates with the azide (step b) to form an azide/alkyne/copper(I) ternary complex (S5B). This leads to the fast

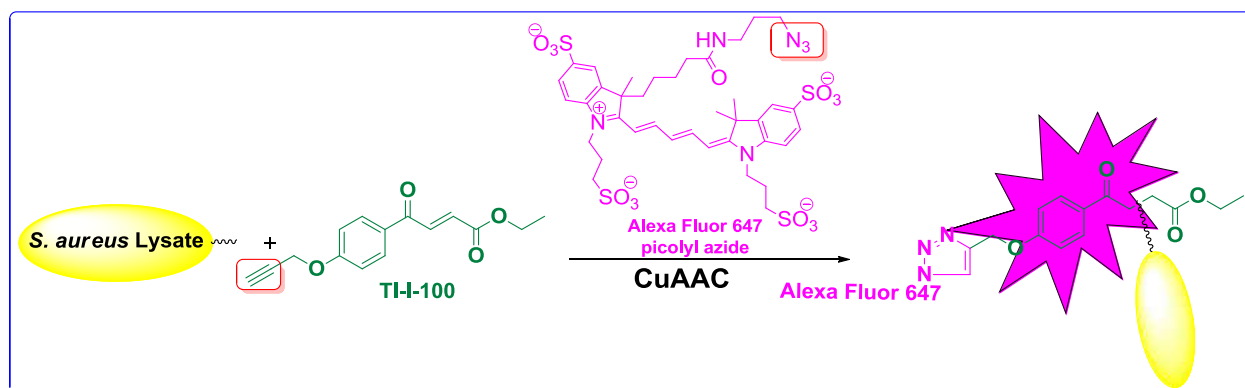
formation of metallacycle (S5C). Triazolide (S5D) is formed by the reductive ring contraction and deprotonation of the alkyne to complete the cycle (step a). The σ , π -di(copper) acetylide (S5A) and the copper(I) triazolide (S5D) structures were fully characterized by X-ray crystallography and verified as feasible intermediates for this reaction.¹⁷⁻²⁰ The (S5B) intermediate was identified by ion-tagged electron spray ionization mass spectrometry.¹⁹ The dinuclear intermediate (S5C) exhibits less ring strain when compared to (S4C) in Scheme 6-3. In 2013, Fokin and colleagues clearly showed that the dicopper metallacycle (S5C) was involved in a rapid internal rearrangement, which scrambled the two copper centers by using a copper isotopic labeling experiment. To avoid ambiguity, the authors did a control experiment to eliminate the probability of copper scrambling at the dinuclear copper(I) acetylide step for their elaborately constructed catalytic cycle.¹⁸

In cells, enzymes employ transition metals to catalyze reactions. The well-known non-natural metal-catalyzed reaction that took center stage in bioorthogonal chemistry in this decade is CuAAC because of its performance under physiological conditions. It employs low reactant concentrations to reduce toxicity, low background labeling at practical time scales while still preserving biological functions. Currently, strain-promoted azide-alkyne Click chemistry reactions and tetrazine-alkene ligations play an important role for copper free *in vivo* labeling.⁵

6.2. RESULTS AND DISCUSSION

Our efforts to develop new antimicrobial agents is based on a novel class of acrylic esters (see the previous section for details).²¹ To determine molecular targets of these acrylic esters, a novel alkyne (**59**) was developed bearing an alkyne as a substrate for the CuAAC reaction (Scheme 6-5). Ligand **59** exhibited a promising MIC of 0.5 $\mu\text{g/mL}$ against *Staphylococcus aureus* and a MIC of 0.25 to 0.5 $\mu\text{g/mL}$ against vancomycin, methicillin, and rifampicin resistant *Staphyloco-*

ccus aureus strains. This finding stimulated the search for molecular targets employing the CuAAC reaction using the Click-iT Plus Alexa Fluor Picolyl Azide Toolkit with fluorescently tagged Alexa Fluor 647 picolyl azide (AF647) in whole cell *Staphylococcus aureus* lysate (Scheme 6-5).



Scheme 6-5. CuAAC reaction between **59** and Alexa Fluor 647 picolyl azide in *Staphylococcus aureus*

Due to the electrophilic nature of **59**, we expected covalent interactions with bacterial proteins that in turn can be detected by fluorescence after Click chemistry and separation by SDS-PAGE (Sodium Dodecyl Sulfate-Polyacrylamide Gel Electrophoresis). For this process, crude cell lysate was prepared from *Staphylococcus aureus* purchased from ATCC (American Type Culture Collection). The digestion of peptide cross-linking, found in gram-positive bacterial peptidoglycan cell walls, was achieved with lysostaphin. The lysate was incubated with **59** for 14 hours and subjected to the CuAAC reaction with fluorescent AF647 followed by separation by SDS-PAGE (Figure 6-2). Fluorescent labeling of proteins was only observed for **59** incubated lysate (lane 4). Control experiments lacking **59** or cell lysate exhibited no fluorescent bands (lane 1 or lane 2 respectively). Direct incubation of lysostaphin and **59** produced fluorescently labeled lysostaphin (lane 3).

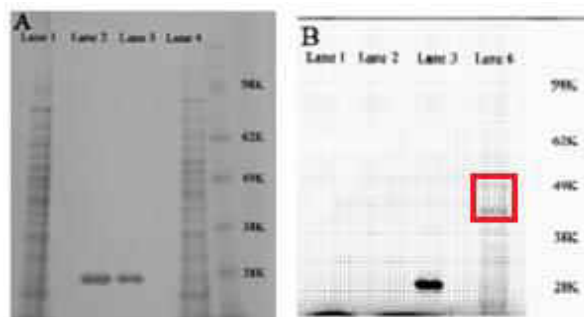


Figure 6-2. A) Coomassie Blue stained SDS-PAGE; Lane 1: MRSA lysate; Lane 2: lysostaphin for lysis; Lane 3: lysostaphin incubated with 59 (14h) used for CuAAC reaction in the presence of AF647; Lane 4: MRSA lysate incubated with 59 (14h) used for CuAAC reaction in the presence of AF647; B) same SDS-PAGE gel visualized by fluorescence imaging at 635 nm.

Further studies included the comparison of whole cell lysate, cytoplasmic, and membrane fractions separated from the *S. aureus* cells (Figure 6-3). Therefore, the incubation time was reduced to 4 hours. The prepared lysate, cytoplasmic, and membrane protein portions were subjected to the CuAAC reaction using AF647 followed by SDS-PAGE separation. A strong fluorescent band was observed for Michael acceptor 59 incubated membrane protein fractions (lane 5-7) that was also seen for the whole cell lysate (lane 4). Two lower molecular weight weak fluorescent bands were observed for the cytoplasmic fraction, which again were seen for the whole cell lysate (lane 8 and 9).

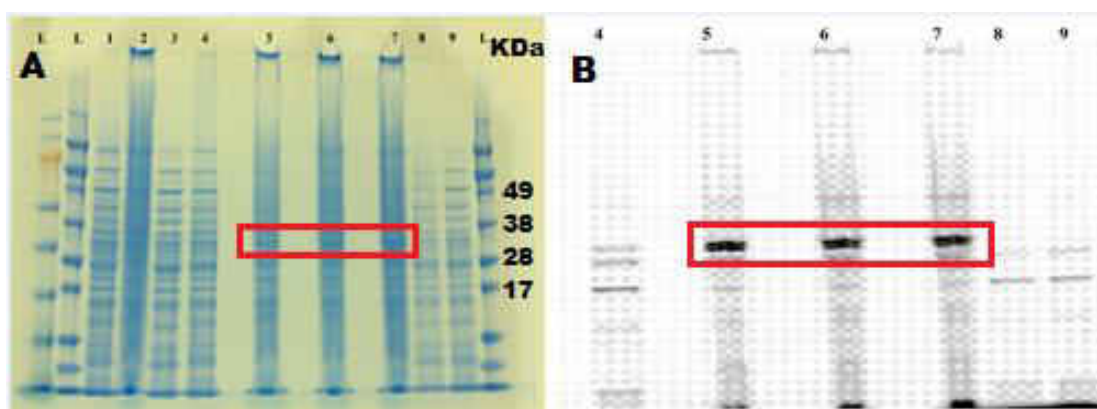


Figure 6-3. A) Coomassie Blue stained SDS-PAGE; L: Ladder; Lane 1: MRSA lysate; Lane 2: MRSA membrane fraction; Lane 3: Cytoplasmic fraction; Lane 4: MRSA lysate incubated with 59 (14h); Lane 5-7; Different concentration of membrane fractions incubated with 59 used for CuAAC reaction in the presence of AF647; Lane 8-9; Different concentrations of cytoplasmic fractions incubated with 59 used for CuAAC in the presence of AF647. B) Same SDS-PAGE gel visualized by fluorescence imaging at 635 nm.

At this point, one focused attention on the isolation of membrane proteins that interact with **59**. Therefore, a CuAAC reaction with a biotin azide was carried out instead of AF647 to enable the isolation with streptavidin conjugated beads. The target protein was separated by affinity chromatography using a streptavidin conjugated column followed by LC-MS/MS mediated identification. Different fractions were collected from FPLC (fast protein liquid chromatography), and the purity fractions were visualized by SDS-PAGE (Figure 6-4). A pronounced band was observed for fraction 3-6 with a molecular weight of around 29 kDa. Gratifyingly, the labelled band had the same molecular weight as the one detected using a fluorescent azide (Figure 6-3).

Some modifications was made to this protocol to overcome some shortcomings. Labelled membrane fractions readily undergo proteolysis during the lysate preparation. This was later resolved by adding a protease inhibitor. As seen in Figure 6-5A (lane 7-8), no protein bands were observed due to proteolysis. Furthermore, we observed that the syringe filter used for FPLC injections can adsorb protein. In Figure 6-5B (lane 2 and 6), the labelled protein bands were absent do to this unwanted interaction. Consequently, high-speed centrifugation, rather than filtration, was employed to prepare the samples for FPLC.



Figure 6-4. Coomassie blue stained SDS-PAGE gel; Lane 1 and 15: Ladder; Lane 2: Pure Lysate after CuAAC reaction without purification; Lane 3-6, 14: Protein eluents from FPLC; Lane 7-10, 12: Washouts from FPLC

The labelled protein bands from the SDS-PAGE (Figure 6-4) and the purified protein fraction collected from affinity FPLC were subjected to in-gel²² and in-solution trypsin digestion, followed by desalting and LC-MS/MS analysis for protein identification. Data analysis of these two samples using MaxQuant 1.4.1.2 and the Uniport database for *E. Coli* and *S. aureus* identified three enzymes as the targets of **59**: enolase (protein ID: P64079), dihydrolipoyllysine-residue acetyltransferase (protein ID: Q8NX76), and glyceraldehyde-3-phosphate dehydrogenase (protein ID: POA037). **These enzymes are known to be involved in glycolysis and act as virulence factors responsible for the pathogenicity of *S. aureus*.**

The enolase protein was observed as one of the top hits from the mass spectral analysis of both in-gel and in-solution trypsin digests. Consequently, enolase from *S. aureus* was constructed in pET 15b vector and expressed in *E. coli* for validation. The His-tagged enolase was purified by FPLC using a nickel column. It is known that enolase catalyzes 2-phosphoglycerate (2-PG) to phosphoenolpyruvate (PEP). To investigate whether ligand **59** affected this activity, the PEP formation rate mediated by enolase after incubation with **59** was determined (Figure 6-6).²³

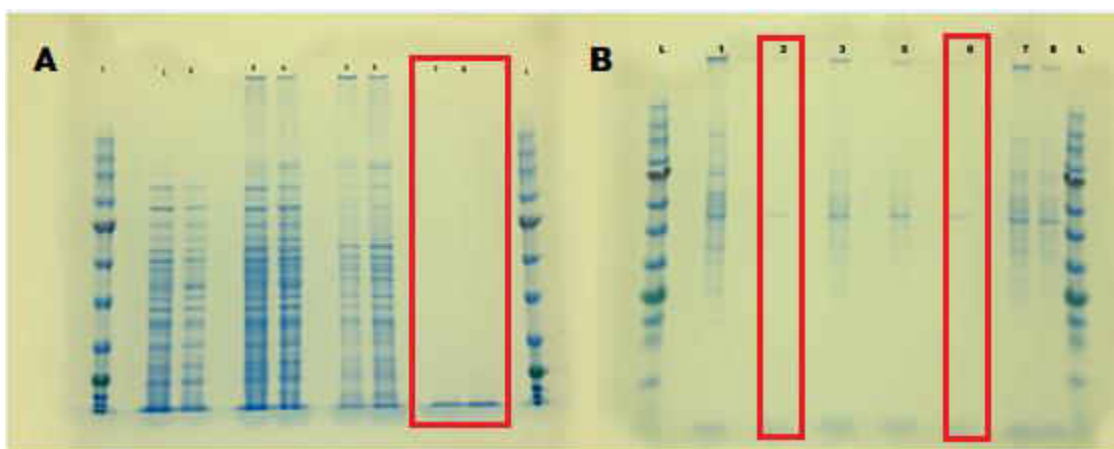


Figure 6-5. Coomassie Blue stained SDS-PAGE; A) L: ladder; Lane 1: unlabelled cytoplasm; Lane 2: labelled cytoplasm; Lane 3: unlabelled lysate; Lane 4: labelled lysate; Lane 5-6: unlabelled membrane; Lane 7-8: labelled membrane; B) L: ladder; Lane 1: pure membrane fraction; Lane 2, 6: Filtered membrane fraction after CuAAC reaction; Lane 3, 7: unfiltered membrane fraction after CuAAC reaction; Lane 5,8: centrifuged membrane fraction after CuAAC reaction.

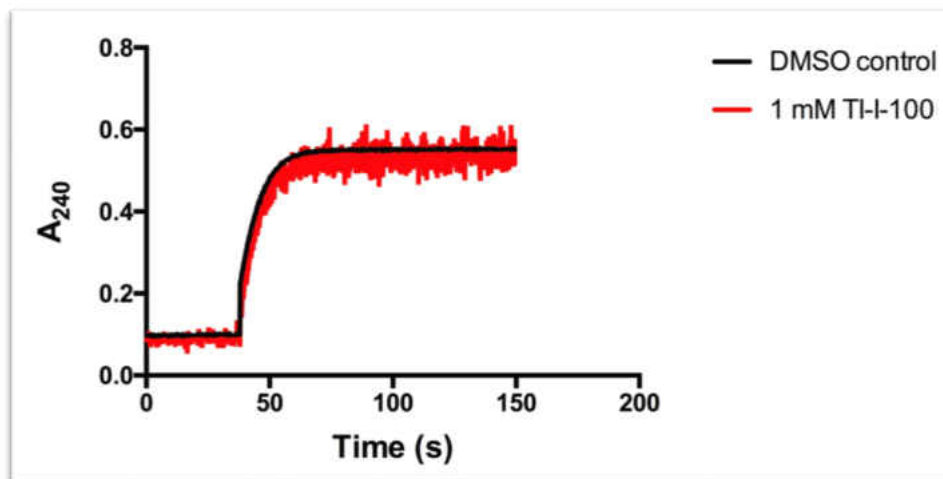


Figure 6-6. Enolase enzymatic activity with TI-I-100 (**59**) and DMSO (control)

Surprisingly, no change in the enolase enzyme kinetics was observed. In addition, different crystallization methods were tried for enolase with compound **59** resulting in the formation of crystals after two weeks. However, these crystals did not diffract well. Currently other crystallization conditions are being tested. There is the possibility that **59** binds at outside the active site, likely on the surface of the protein and consequently inhibits the virulence of *S. aureus* by affecting the binding of the host plasminogen.²⁴ This hypothesis was tested by incubating **59** with recombinantly expressed enolase for 14 hours, and this was followed by the addition of fluorescent tag AF647 performing the standard CuAAC reaction. The analysis of the reaction was carried out by SDS-PAGE gel chromatography, as shown in Figure 6-7. The Coomassie Blue stain gel showed a predominant band at around 50 kDa for enolase that when labeled with **59** followed by CuAAC with AF647 resulted in the fluorescent band with the same molecular weight.

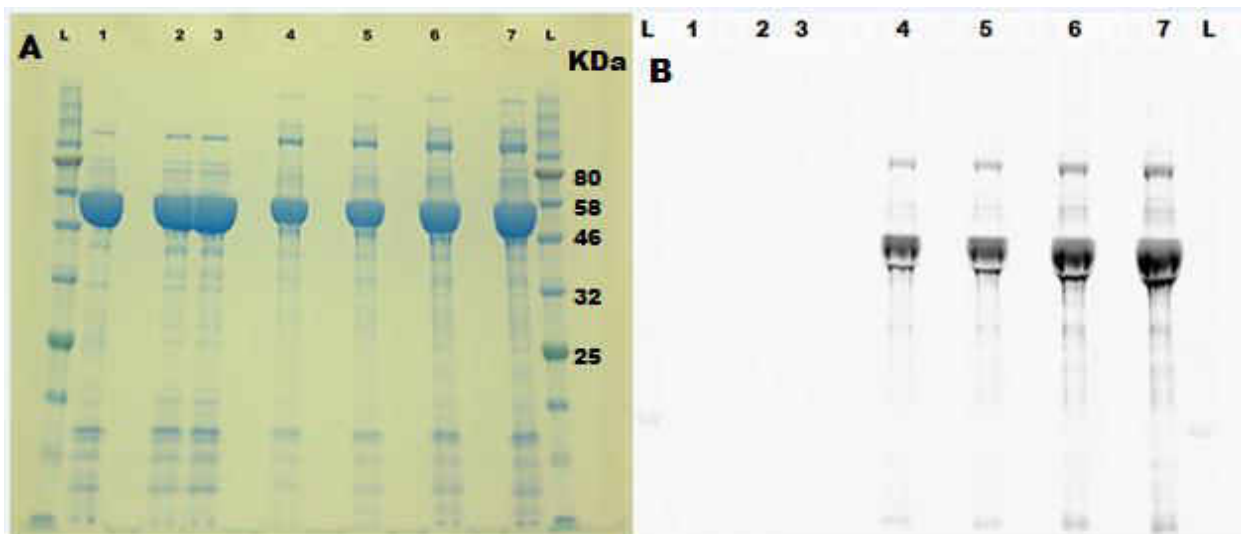


Figure 6-7. Coomassie Blue stained SDS-PAGE; A) L: Ladder; Lane 1: expressed enolase; Lane 2-3: enolase incubated with **59** (14h); Lane 4-7: Different concentration of enolase incubated with **59** used for CuAAC reaction in the presence of AF647; B) Same SDS gel visualized by fluorescence imaging at 635 nm.

To determine the enolase binding site for **59**, pure enolase (E) expressed from *E. coli* and enolase incubated with a ligand **59** (EL) were subjected to in-solution trypsin digestion followed by LC-MS/MS analysis. The search parameters used for protein identification include trypsin cleavage (at lysine and arginine), fixed modifications of cysteine alkylation, differential modification of methionine oxidation and the **59** (addition of 258 Da) molecule adduct on cysteine or lysine. Data analysis was performed with MaxQuant 1.4.1.2 with the Uniprot database for *E. coli* and *S. aureus*. MS/MS spectra of the enolase peptide A[117-128]K without and with the binding of **59** are shown in Figures 6-8A and 6-8B. The peptide without a binding site had a mass of 1258.69 Da. In contrast, the peptide with the binding of **59** was observed at 1516.78 Da (addition of 258 to 1258). The sequence of the peptide was assigned with single letter abbreviations for amino acids with N-terminal b ions and C-terminal y ions resulting from the amide bond cleavage. Specifically, in Figure 6-7B, the MS/MS analysis of the EL sample showed the **59** modified lysine residue at K128 confirmed by the identification of 258 Da adduct on y1 ion (147; lysine) to give a m/z of 405. Inherently, no cysteine modification of **59** was detected.

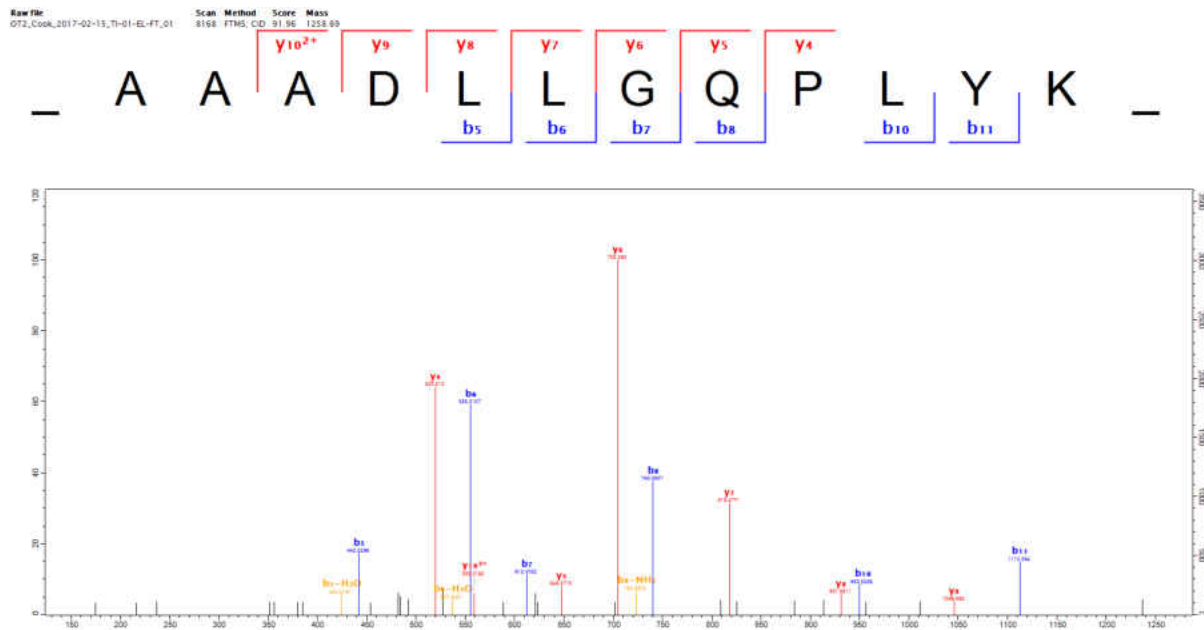


Figure 6-8A. Representative MS/MS spectrum of Enolase sample (E) with identified peptide. A single letter abbreviation was used to assign the peptide sequence based on fragment ions observed for the peptide. N-terminus b ions and C-terminus y ions are labelled that resulted from peptide bond cleavage.

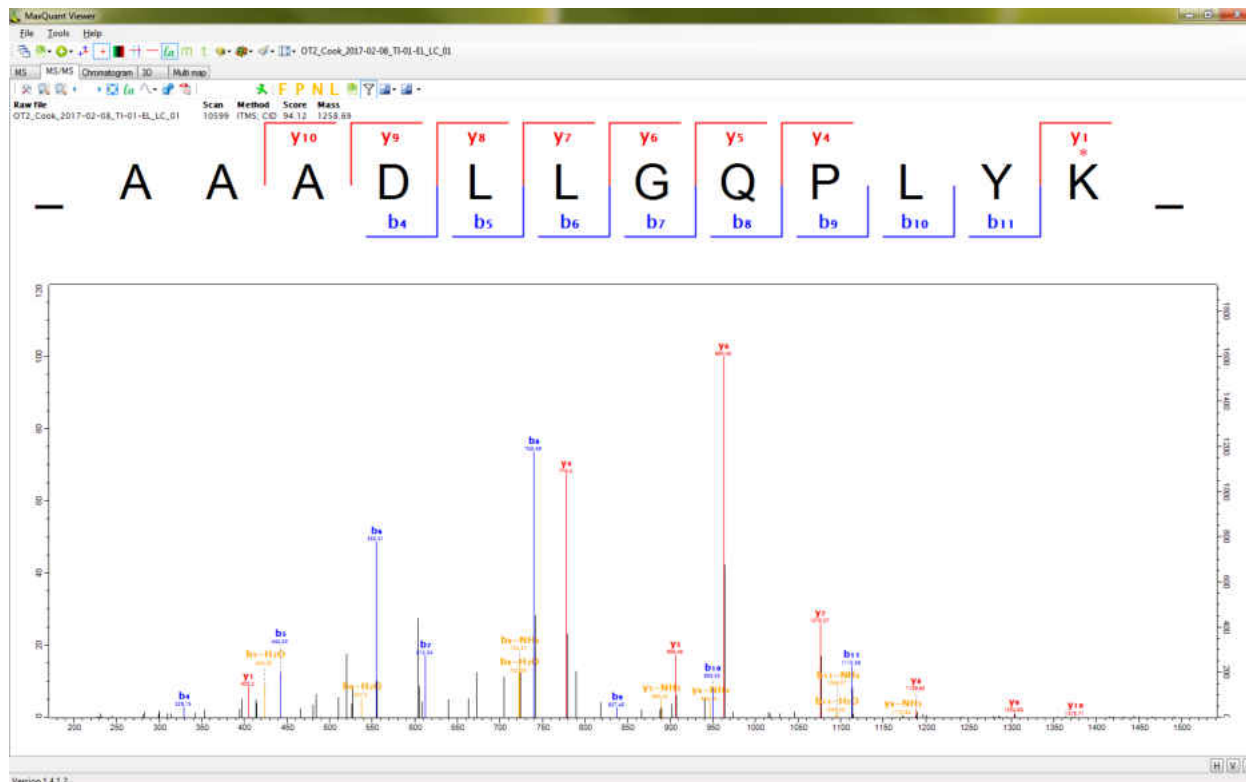


Figure 6-8B. Representative MS/MS spectrum of 59 incubated Enolase sample (EL) with identified peptide. A single abbreviation was used to assign the peptide sequence based on fragment ions observed for the peptide segment. N-terminus b ions and C-terminus y ions are labelled that resulted from peptide bond cleavage. *Denotes the 59 adduct on lysine residue of the peptide sequence

To further validate binding studies from the mass spectrometry, molecular modeling was done enabling **59** to be docked within the known enolase protein using MOE (Molecular Operating Environment) software (Figure 6-9A and 6-9B). The molecular docking structure reveals that **59** binds covalently at the lysine residue in the enolase protein which is similar to binding amino residue data from mass spectrometry.

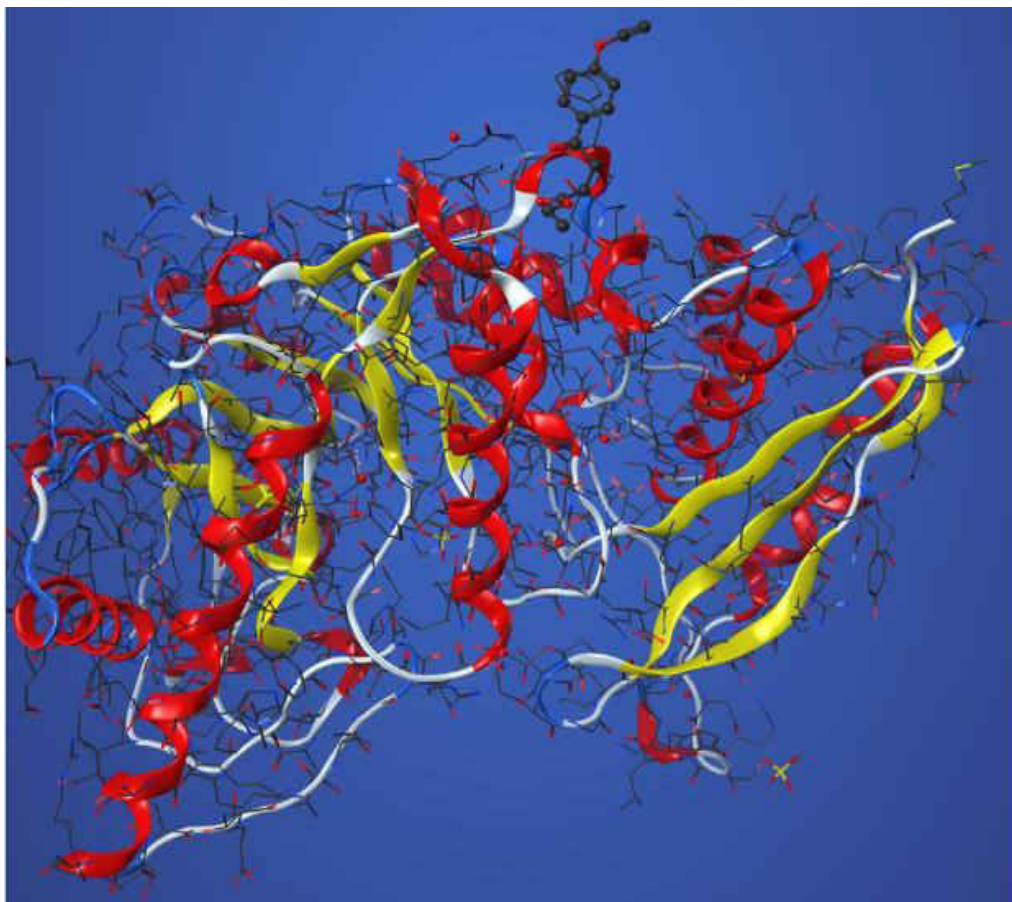


Figure 6-9A. Molecular docking conformation of 59 in enolase protein

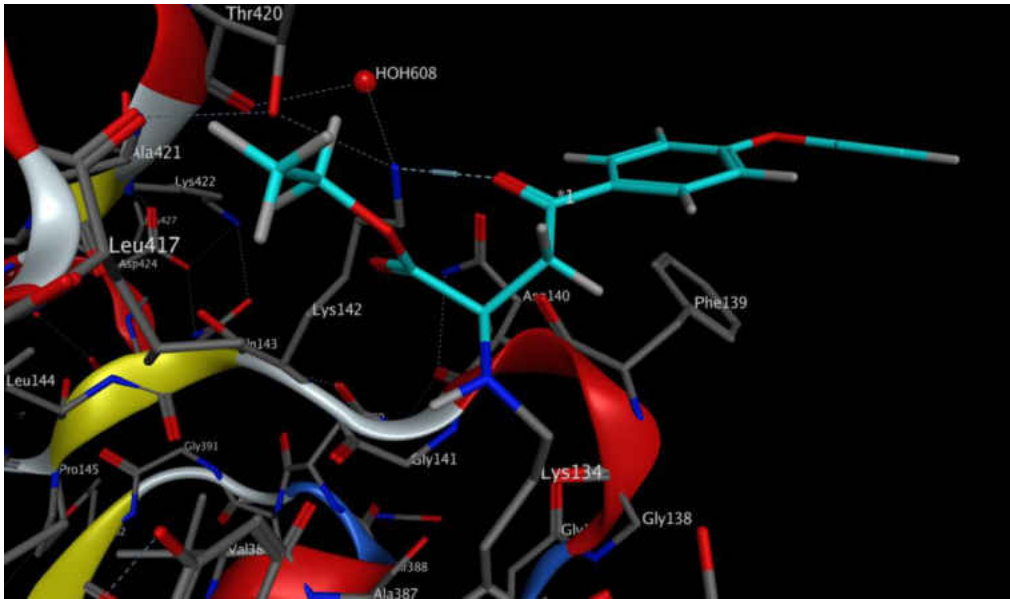


Figure 6-9B. The closer view of 59 at binding site residues (lysine) in the enolase protein

6.3. ROLE OF TARGETED PROTEINS IN *STAPHYLOCOCCUS* BACTERIA WHICH WERE IDENTIFIED

6.3.1. Enolase

Enolase is a universal enzyme found in both prokaryotic and eukaryotic organisms belonging to the enolase superfamily.²⁵ The enolase protein is one of the “moonlighting proteins” because of its multifunctional activity.²⁶ In bacteria such as *Staphylococcus aureus*, *Streptococcus pyogenes*, and *Streptococcus pneumoniae* the enolase protein is well distributed, and is responsible for its survival, as well as virulence.²⁷ The enolase protein is expressed both as a cytoplasmic and a cell surface protein in primitive and higher organisms.²⁸ The cytoplasmic enolase enzyme catalyzes the conversion of 2-phospho-D-glycerate to phosphoenolpyruvate (PEP) in the glycolysis cycle and the conversion of phosphoenolpyruvate to 2-phosph-D-glycerate in the gluconeogenesis cycle, as shown in Figure 6-10. The enolase enzyme is a metalloenzyme that requires the presence of Mg^{2+} divalent cations for this catalytic conversion.²⁹ The enzymatically

active enolase protein occurs as a dimer in eukaryotic organisms and in an octameric form in prokaryotic organisms.^{30,31}

Zhang and Zang's group extensively studied the phosphoenolpyruvate bound and unbound enolase protein crystals from *Staphylococcus aureus*.²³ The dimeric form of the enolase protein is commonly found in many organisms. However, the octamer structure is also present in some bacterial pathogens. The unbound *Staphylococcus aureus* enolase (*Sa_enolase*) belongs to the space group $P4_21_2$, which contains two monomers that form a homodimer in the asymmetric unit. The *Sa_enolase* monomer contains a small N-terminal domain and a large C-terminal barrel domain. The C-terminal domains contain the active site which binds to magnesium and sulfate ions. The larger C-terminal domain has eight β -strands ($\beta 4$ - $\beta 11$) and eight α -helices ($\alpha 5$ - $\alpha 12$). These eight α/β strands are arranged as an inner barrel-like structure with $\beta 4$ - $\beta 11$ surrounded by outer barrels which contains $\alpha 5$ - $\alpha 12$ helices. Besides these α/β barrels, three short helices $3_{10}1$, $3_{10}2$ and $\eta 1$ are located in the C-terminal domain. The interaction between $\beta 1$ - $\beta 3$ and $\alpha 5$ and $\alpha 12$ forms a butterfly-like structure with two monomers. The four dimers of enolase are connected and form a ring-shaped octameric structure in unbound *Sa_enolase* (Figures 6-11A and 11B).²³

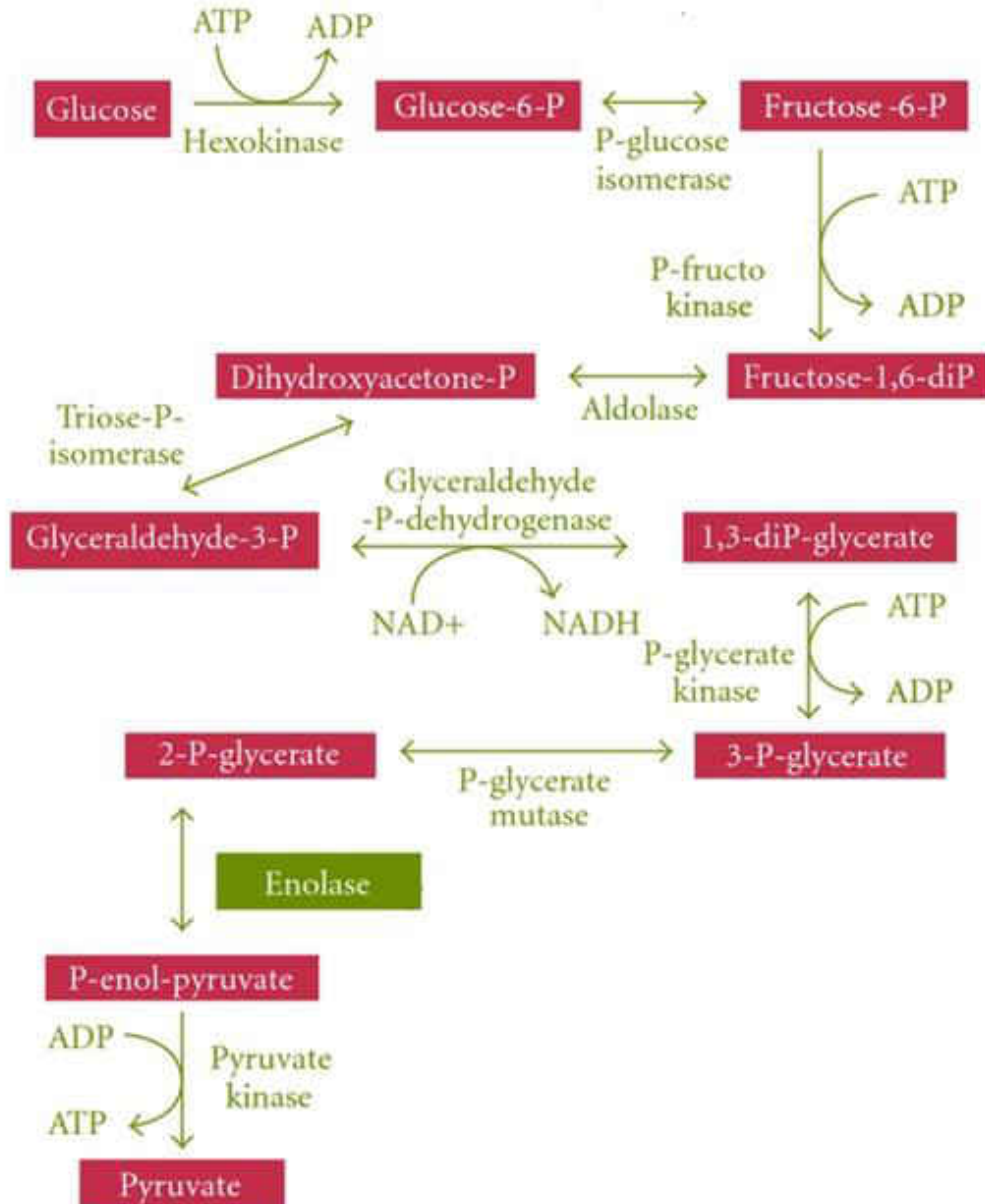


Figure 6-10. Summary of the glycolytic metabolic pathway and the role of enolase (highlighted) in carbohydrate metabolism

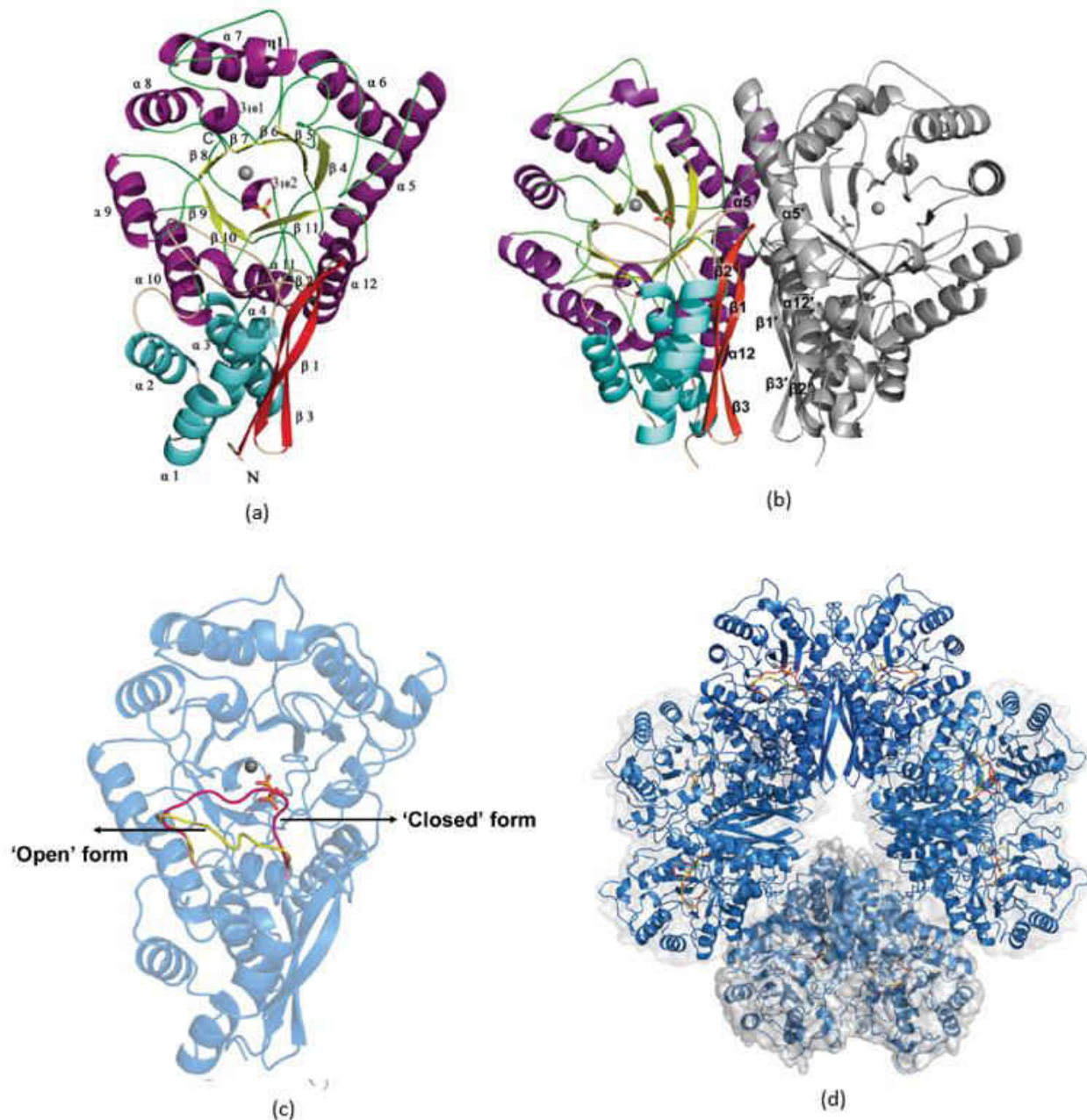


Figure 6-11. (A). The ribbon diagram of the overall structure of *Sa_enolase*. The secondary-structural elements are colored cyan/red for the N-terminal domain and purple/yellow for the C-terminal barrel domain. The α -helices and β -strands are labelled in black. (B). The dimeric structure of *Sa_enolase*. The secondary-structural elements (β 1– β 3, α 5, and α 12) involved in dimerization are labelled in black. PEP-binding site of *Sa_enolase*. Ribbon diagrams of the dimeric structure (C) and the octameric structure (D) of the PEP-bound form of *Sa_enolase*. The two alternative conformations of the catalytic loop 1 are highlighted in red for the closed form and yellow for the open form. PEP is shown as sticks.

The *Sa_enolase* crystals with bound PEP were formed by co-crystallization with 2-PG (phosphoglycerate) as the substrate. The obtained structure of PEP-bound *Sa_enolase* appears

similar to the unbound form except for a conformational change in the loop 1 (L1; residues 38-64) involved in the catalytic loop. The other two loops, loop 2 (L2; residues 154-163) and loop 3 (L3; residues 249-269) do not show any conformational modification.³² The modified conformations of the L1 loop are in the closed and open arrangements. The PEP-binding site located at the center of the C-terminal barrel domain is formed by the interaction of Lys343, Lys394, Asp318, Arg372, and Ser373 together with Ser42 and form loop L1 in the open conformation, whereas in the closed confirmation the interaction with Ser42 of loop L1 is not present (Figures 6-11C and 6-11D).²³

The surface associated enolase protein plays a major role in bacterium-host interactions especially in the commensal pathogens such as *Staphylococcus aureus*, *Lactobacillus crispatus*, and *Lactobacillus johnsonii*.³³ The cell invasiveness of these bacteria require the degradation of the extracellular matrix (ECM) and basement membranes (BMs) to migrate into circulation or adjacent tissues. The extracellular matrix of host cells contains different components such as collagens, proteoglycans, elastin, and glycoproteins (laminin, fibronectin, and enactin; Figure 6-12).³⁴

Enolase plays a major role in the plasminogen-mediated disruption of the ECM and basement membranes. The circulating plasminogen (plg) is bound to the plasminogen receptor on the enolase protein rendering it immobilized. The immobilized plg further enhances the action of bacterial staphylokinase (SK) and host tissue plasminogen activator (uPA/tPA) to convert plasminogen into active plasmin. The formed plasmin degrades laminin, fibronectin, proteoglycans, and gelatin by a cascade of proteolytic reactions, as shown in Figure 6-13. Plasmin also indirectly activates pro-collagenases, latent elastase, and pro-stromelysins to degrade collagen, elastin and other ECM and BMs, proteins, respectively.^{24,35-37} The host controls the degradation by secreting the tissue plasminogen activation inhibitors (PAI) and α 2-plasmin/ α 2

macroglobulin to monitor the activity of plasmin. The complete destruction of ECM and BMs proteins clear the way for bacteria for migration and invasion into the tissues. Also, the enolase on the surface of bacteria is known to bind to laminin, an important constituent of the extracellular matrix. The binding of enolase to laminin helps to destroy the host ECM that helps bacteria to enter into cells.³⁸

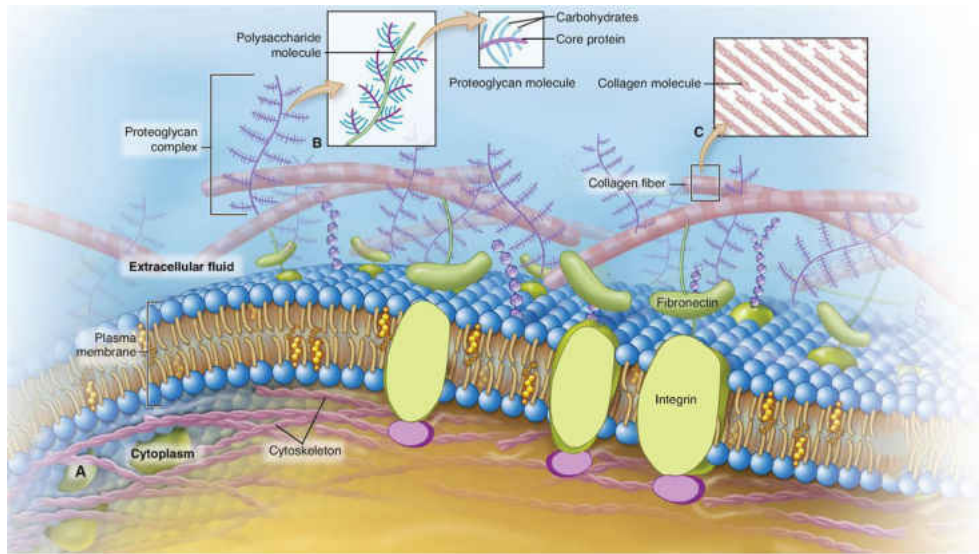


Figure 6-12. Extracellular matrix (ECM) of host. (A). The extracellular matrix is made up of water, proteins/glycoproteins, and proteoglycans that often form large bundles or complexes that bind together and to the cells of the tissue. Although the makeup of ECM varies from tissue to tissue, it usually includes some connections to integrins in the plasma membranes, thereby allowing for structural integrity, as well as communication and coordination within the tissue. **(B).** A detailed view of a proteoglycan complex shows many proteoglycans, each with a protein backbone and attached carbohydrate subunits—all held together by a polysaccharide chain. **(C).** Detailed view of a collagen bundle showing the individual collagen fibers within it. (Credit: basicmedicalkey.com)

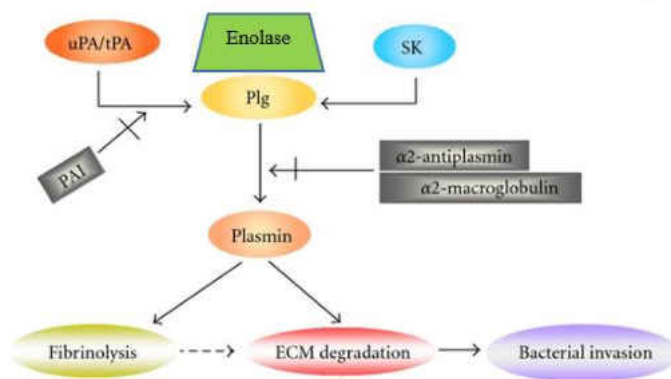


Figure 6-13. Simplified overview of plasminogen system and utilization by bacteria as well as degradation of ECM components which enables bacterial migration through tissue barriers

6.3.2. Dihydrolipoyllysine Residue Acetyltransferase

The pyruvate formed at the end of the glycolysis cycle is further oxidized to acetyl-CoA and CO_2 in aerobic organisms. The formed acetyl-CoA participates in the citric acid cycle which releases stored energy and generates various biological precursors. The conversion of glycolytic pyruvate to acetyl-CoA is catalyzed by a multi-enzyme complex called pyruvate dehydrogenase (PD; Figure 6-14). Pyruvate dehydrogenase is part of a multi-enzyme complex (PDC) that contains three enzymes, pyruvate dehydrogenase (PDH), dihydrolipoyl transacetylase (DLAT), and dihydrolipoyl dehydrogenase (DLD).

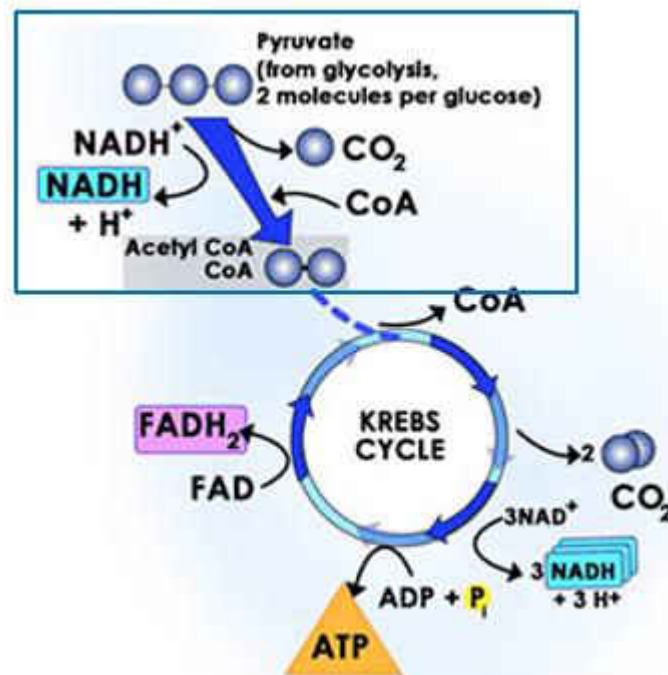


Figure 6-14. The conversion of pyruvate from glycolysis to acetyl CoA required for the Krebs cycle pathway catalyzed by PDC (highlighted in box, credit: sparknotes.com)

The conversion of pyruvate to acetyl-CoA involves five catalytic reactions mediated by DLAT. The acetyltransferase enzyme acts as an acceptor for the hydroxyethyl group from pyruvate dehydrogenase and converts lipoamide (prosthetic group) to acetyl-dihydrolipoamide (step 2 in Figure 6-15). In the next step, DLAT transfers the acetyl group to CoA leading to the formation of acetyl-CoA and dihydrolipoamide (step 3 in Figure 6-15). The enzyme domains for the attachment

of the lipoyl group are known to contain lysine (Lys) residues at the catalytic center (Donald Voet/ Judith G. Voet, Textbook of Biochemistry, 4th Edition, Wiley publisher, 2011).

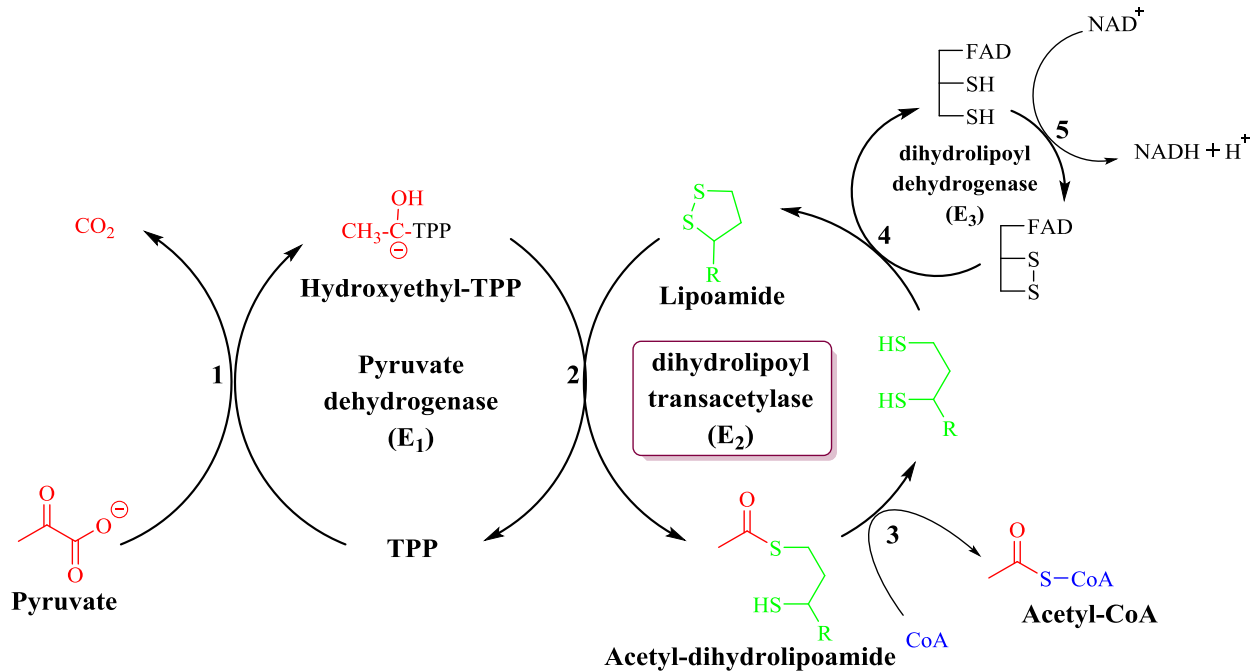


Figure 6-15. Flow diagram illustrating the overall activity of Pyruvate dehydrogenase complex protein with role of dihydrolipoyl transacetylase (highlighted, credit: biochempages.com)

6.3.3. Glyceraldehyde-3-Phosphate

Glyceraldehyde-3-phosphate dehydrogenase is also involved in the production of ATP during glycolysis. It is the sixth enzyme in the glycolysis cycle, which converts glyceraldehyde-3-phosphate (G3P) into 1, 3-bisphosphoglycerate (1, 3-BPG; Figure 6-16).

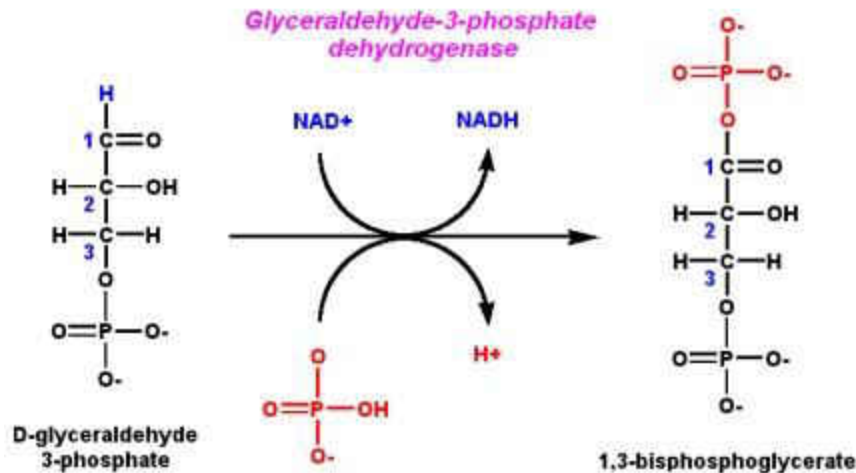


Figure 6-16. Catalytic conversion using Glyceraldehyde-3-phosphate dehydrogenase in the glycolysis

The group of Das et al.³⁹ studied GADPH from MRSA252 (Methicillin Resistant *Staphylococcus aureus*) strains using x-ray protein crystallography. Glyceraldehyde-3-phosphate dehydrogenase (*Sa*GADPH) was crystallized in the p2 space group which contained four molecules in the asymmetric unit⁴⁰ (Figure 6-17A). Each subunit contained a NAD⁺ (Nicotinamide adenine dinucleotide) binding domain and a catalytic domain. The NAD⁺ contains a Rossmann fold which contains a classic α/β dinucleotide binding fold. This NAD⁺ folds into nine β sheets which have β_{A-I} residues interconnected by helices or short loops. The β_D and β_H run antiparallel to other strands. There are four helices, α_B and α_E interspersed in between β_A and β_B and β_F and β_G sheets respectively. The other two helices, α_C connects β_B and β_C , and α_E connects β_E and β_F , as shown in Figure 6-17B.

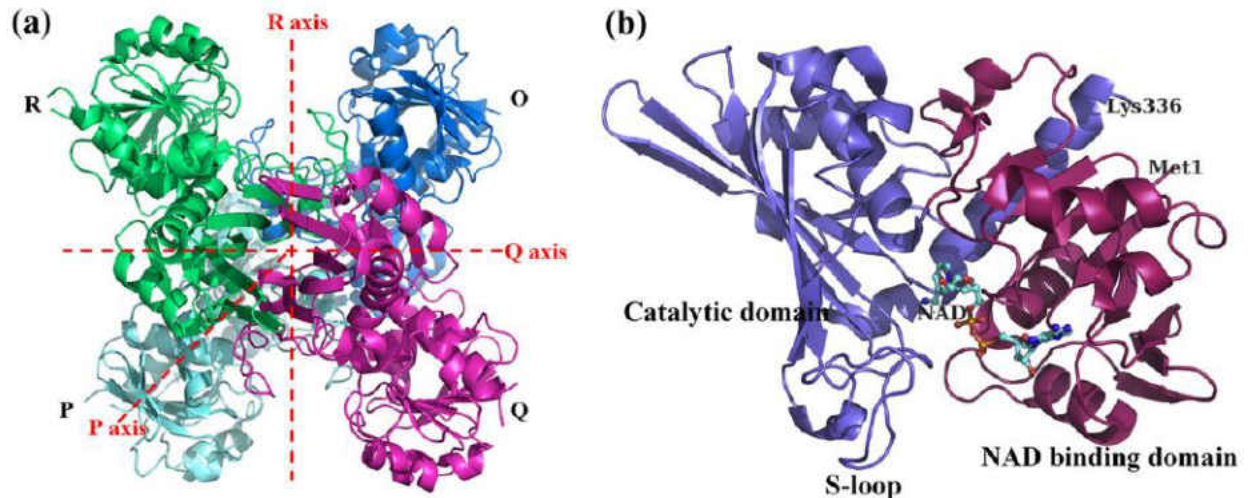


Figure 6-17. SaGDAPH overall structure. (A). Spatial organization of the four subunits in the asymmetric unit: The subunits P (cyan), O (blue), Q (magenta), and R (green) are related by a noncrystallographic 222 plane of symmetry on three mutually perpendicular axes designated as P, Q, and R. The P-axis is orthogonal to the plane of the paper. (B). A cartoon representation of monomeric SaGAPDH1: The N-terminal domain (colored pink) binds NAD⁺ (shown in sticks) while the C-terminal catalytic domain (colored blue) contains the flexible long S loop

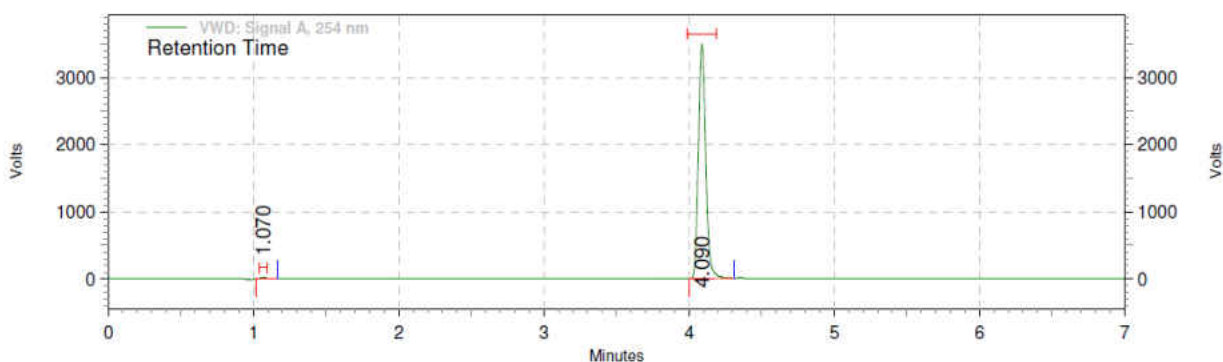
The catalytic domain is comprised of eight mixed β strands ($\beta 1$ to $\beta 8$) and three long α helices ($\alpha 1$ to $\alpha 3$). The $\alpha 1$ links the NAD⁺ domain and catalytic domain. The active Cys151 (Cysteine 151) and His178 (Histidine 178) constitutes the catalytic site. The C-terminal $\alpha 3$ helix fits into the groove of the N-terminal domain associated with various interactions with the coenzyme. The S loop in the catalytic domain is necessary for intersubunit interactions.³⁹

In addition to its application as housekeeping protein for PCR and Western Blots, GADPH plays a role as a surface binding protein.³⁹ This cell surface associated with GADPH is capable of binding to human transferrin to obtain access to iron required for its survival.⁴¹ There is evidence that cell wall activated GADPH immobilizes laminin and fibronectin, making the degradation of ECM and BMs easier to invade the host tissues.⁴²

6.4. METHODS

6.4.1. HPLC conditions for the compound, **59** (Ethyl (*E*)-4-oxo-4-(4-(prop-2-yn-1-yloxy)phenyl)but-2-enoate)

The purity of propargyl ether (C-4, para) **59** was estimated to be 99.52 % using the Agilent Technologies 1220 Infinity LC HPLC system. The chromatographic separations were carried out on a Restek pinnacle II C18 column (100 mm × 4.6 mm, id 5 μm). The mobile phase consisted of water (A) and ACN (B). The gradient elution program was as follow: 0–2 min 20 % B; 2–5 min, 99 % B; 5–7 min, 20 % B. The flow rate of the mobile phase was 0.6 mL/min. The effluents were monitored at 254 nm by a photodiode array detector. A typical injection volume was 5 μL.



VWD: Signal A,
254 nm Results

Retention Time	Area	Area %	Height	Height %
1.070	1086145	0.52	282988	0.48
4.090	206672637	99.48	58578486	99.52
Totals	207758782	100.00	58861474	100.00

6.4.2. Preparation of *Staphylococcus aureus* cell lysate

The *Staphylococcus aureus* ATCC 1683 was grown at 37 °C with aeration for 2.5 h. The grown cells were labelled for 4 h with **59** (8 μg/mL) at rt with shaking, followed by centrifugation at 14,000xg for 10 min. After freezing the cells overnight, they were resuspended in PBS

(phosphate buffered saline) with protease inhibitor (complete, EDTA-free protease inhibitor cocktail, Sigma-Aldrich) to lyse the cells. Lysostaphin to a final concentration of 0.05 mg/mL and DNase was added followed by incubation at 37 °C for 2 hrs. Non-lysed cells were removed by centrifugation (10 min at 14,000xg), and the supernatant was collected which contained cell membranes and cytoplasm. The cell membranes were separated from the cytoplasm by ultracentrifugation (30 min at 90,000 rpm) followed by resuspension in PBS.

6.4.3. Labeling of **59 with AF647/biotin azide using the CuAAC reaction in *S. aureus* lysate**

The single reaction mixture of 100 μ L volume was prepared by adding lysate (78.3 μ L) with 8.7 μ L of 10 X Click-iT reaction buffer (buffer B), 1 μ L of 500 μ M Alexa Fluor PCA solution, 2 μ L CuSO₄-copper protectant pre-mix which included 1.2 μ L of CuSO₄ (Component C) and 0.9 μ L of copper protectant (Component D), and 10 μ L of 1 X Click-iT buffer additive (Click-iT Alexa Fluor647 picoyl azide tool kit, Thermo Fisher Scientific). The reaction mixture was incubated for 30 - 45 mins at rt protected from light. The loading buffer was added to the lysate and denatured by heating at 85°C for 10 min followed by slow-cooling to rt. The denatured protein was then subjected to SDS-PAGE gel (Invitrogen, NuPAGE™ 4-12 % Bis-Tris Protein Gels), followed by fluorescence detection at 635/665 nm and then visualized by Coomassie blue (SimpleBlue Safe stain, Invitrogen) stain. In the case of unlabelled lysate with **59**, the lysate was incubated with 1mM (DMSO) **59** and left on a shaker for 12-14 h and then subjected to the CuAAC reaction. The same lysate procedure was followed for membrane and the cytoplasmic fractions of *Staphylococcus aureus*. In the case of a biotinylation, the biotin azide (500 μ M in DMSO) was used instead of AF647.

6.4.4. Purification after the Click reaction

After the Click reaction, the biotinylated target protein was purified by streptavidin affinity chromatography. The sample was centrifuged at 3000 xg for 10 min and desalted into 100 mM phosphate buffer, pH 7.2 (binding buffer), and 150 mM NaCl buffer. After equilibration with 15 CV with the binding buffer, the sample was loaded onto a 5 mL Pierce Streptavidin Chromatography Cartridge (product No. 87740). The biotinylated proteins were eluted with 8 M guanidine·HCl at pH 1.5. The proteins were concentrated using 3 kDa molecular weight cutoff filters (Millipore) for SDS-PAGE and later trypsin digestion.

6.4.5. Purification of *Sa_enolase*

The coding sequences of *Sa_enolase* (GenBank accession code CEH25490.1) was optimized for expression in *E. coli* and synthesized by GenScript Inc (Piscataway, NJ). The synthetic gene was sub-cloned into the pET15b expression vector (LifeSensors Inc, Malvern, PA) using BamH I and Xho I restriction sites. The His₆-tagged *Sa_enolase* fusion protein was expressed from *E. coli* BL21 Star (DE3) cells (Invitrogen Inc, Carlsbad, CA) carrying the pET15b-*Sa_enolase* plasmid. Cultures were grown in Luria-Bertani medium with 100 µg/mL ampicillin at 37 °C. When the cultures reached an OD₆₀₀ between 0.6-0.8, protein expression was induced with 0.4 mM IPTG. The temperature was reduced to 16 °C and the cultures were grown overnight with shaking at 250 rpm. The cells were harvested by centrifugation, resuspended in 5 mL/g of buffer A (25 mM TRIS pH 8.0, 300 mM NaCl, 10 mM imidazole) supplemented with 0.1 mg/mL DNase I (Worthington Biochemical Corp., Lakewood, NJ). The cells were lysed using a Branson Sonifier S-450 cell disruptor (Branson Ultrasonics Corp., Danbury, CT) for a total of 10 min of sonication at 60 % amplitude with 30 s pulses separated by 50 s rest periods. The temperature was maintained at or below 4 °C by suspending the steel beaker in an ice bath directly over a spinning stir bar. The

lysate was clarified by centrifugation at 39,000 x g for 45 mins and then applied to a 5 mL HisTrap column (GE Lifesciences, Piscataway, NJ) at a flow rate of 5 mL/min to isolate the His₆-Sa_enolase fusion protein. The protein was eluted by a 4-step gradient of buffer B (25 mM TRIS pH 8.0, 300 mM NaCl, and 250 mM imidazole; 5, 15, 50, and 100%). The His₆-Sa_enolase fusion protein eluted in the third and fourth steps and was ~90 % pure, as judged on Coomassie-stained SDS-PAGE gels. The peak fractions were concentrated by using 10 kDa molecular weight cutoff filters. The concentrated enolase protein were loaded on the Hi-Pre Sephacryl 26/60 S-100 HR column to separate the dimer and octamer. The resulting octamer enolase protein was confirmed by SEC 300 (BIO-RAD) and was > 95% pure. The protein was desalted using a HiTrap Desalting column (GE Lifesciences) into 20.0 mM HEPES pH 7.5, 150 mM NaCl and stored at -80 °C.

6.4.6. In-solution trypsin digestion

To the protein sample of 100 µL, an equal volume of 250 mM NH₄HCO₃ (Sigma-Aldrich) was added and vortexed to mix thoroughly. The sample was reduced with the addition of 1 µL of 10 mM dithiothreitol (Sigma-Aldrich) and incubated at 37 °C for 45 mins. After reduction, the sample was alkylated with 5 µL of 55 mM iodoacetamide (Sigma-Aldrich) followed by incubation in the dark for one hour at rt. The digestion was performed with trypsin (Trypsin Gold, Promega) in the ratio of trypsin to sample protein of 1:20 at pH 8 overnight. The next day, the pH of the sample was adjusted to just less than 7.0 with 10% formic acid (Fisher Scientific) and evaporated using speedvac. The sample was stored at -20 °C until followed by ziptip cleanup and analysis by mass spectrometry.

6.4.7. Desalting of tryptic peptides

The trypsin digested samples were dissolved in 25 µL of 0.1% TFA and centrifuged for 5 min at 5000 rpm. The 20 µL of supernatant was taken for desalting with C18 resin-packed ZipTip

pipette tips (EMD Millipore), according to the manufacturer's instructions. The peptides were then dried in a speedvac concentrator almost to complete dryness. The dried peptide samples were dissolved in 30 μ L of 5% acetonitrile/0.1% formic acid solution for analysis by mass spectrometry.

6.4.8. Analysis by LC-MS/MS

The desalted tryptic peptides were separated by a C18 capillary column (10 cm x 75 μ m packed with 3 μ m Michrom Magic C18 AQ) on an AB Sciex Eksigent Nano-2D pump equipped with the 920AS autosampler. The peptides were eluted over a 120 min gradient from buffer A (H₂O, 0.1% formic acid) to buffer B (acetonitrile, 0.1% formic acid) at 300 nl/min. The gradient started with 2 min at 2% B, followed by a 75 min ramp to 30% B, a 10 min ramp to 95% B, 3 min at 95% B, 10 min ramp to 2% B, then a 20 min equilibration in 2% B. The eluted peptides underwent electrospray ionization followed by data acquisition in a Thermo Scientific LTQ-Orbitrap Velos mass spectrometer. MS1 scans were detected in the FTMS section of the Orbitrap Velos in profile mode at a resolution of 60,000 (full width of the peak at half-maximum at 400 m/z). The 10 most abundant parent ions from each MS1 scan were selected for fragmentation via collision-induced dissociation with a normalized collision energy of 35% for MS2 scans in the LTQ section of the instrument. Dynamic exclusion settings omitted any mass observed more than once in a 30 s interval from selection for fragmentation. The data analysis was performed with MaxQuant 1.4.1.2 against the Uniprot database for *Escherichia coli* and *Staphylococcus aureus* (release date June 22, 2016). Search parameters included trypsin cleavage (K, R), and the fixed modification of cysteine alkylation, differential modification of methionine oxidation, and **59** molecule adduct on cysteine and lysine residues.

6.4.9. Enolase Crystallization

Initial crystallization conditions were identified by screening 11.5 mg/mL enolase with 10 fold of **59** against the Index HT screen (Hampton Research) and PEG/Ion screen (Hampton Research). The drops contained 1 μ L of protein solution at 11.5 mg/mL and 1 μ L of crystallization solution. There are 12 conditions showed below: 1, 1.0 M Ammonium sulfate, 0.1 M Bis-Tris pH 5.5, 1% w/v Polyethylene glycol 3350; 2, 0.2 M Ammonium sulfate, 0.1 M BisTris pH 6.5, 25% w/v Polyethylene glycol 3350; 3, 0.2 M Lithium sulfate monohydrate, 0.1 M BisTris pH 6.5, 25% w/v Polyethylene glycol 3350; 4, 0.2 M Lithium sulfate monohydrate, 0.1 M HEPES pH 7.5, 25% w/v Polyethylene glycol 3350; 5, 0.2 M Ammonium sulfate, 0.1 M HEPES pH 7.5, 25% w/v Polyethylene glycol 3350; 6, 0.2 M Potassium chloride, 0.05 M HEPES pH 7.5, 35% v/v Pentaerythritol propoxylate (5/4 PO/OH); 7, 0.2 M Potassium sodium tartrate tetrahydrate, 20% w/v Polyethylene glycol 3350; 8, 0.2 M Lithium citrate tribasic tetrahydrate, 20% w/v Polyethylene glycol 3350; 9, 8% v/v TacsimateTM pH 7.0, 20% w/v Polyethylene glycol 3350; 10, 0.2 M Succinic acid pH 7.0, 20% w/v Polyethylene glycol 3350; 11, 0.2 M Ammonium citrate tribasic pH 7.0, 20% w/v Polyethylene glycol 3350; 12, 0.04 M Citric acid, 0.06 M BIS-TRIS propane (final pH 6.4 after mixing), 20% w/v Polyethylene glycol 3350. Different shapes of crystals were formed in ~2 weeks. These crystals were looped and soaked in the well solution with 20% v/v glycerol. However, these crystals did not diffract well; this may be due to the cryoprotectant or the crystals need more optimization.

6.5. REFERENCES

- (1) Huisgen, R. *Angew. Chem., Int. Ed.* **1963**, 2, 565.
- (2) Meldal, M.; Tornøe, C. W. *Chem. Rev.* **2008**, 108, 2952.
- (3) Kolb, H. C.; Finn, M. G.; Sharpless, K. B. *Angew. Chem., Int. Ed.* **2001**, 40, 2004.

- (4) Tornøe, C. W.; Christensen, C.; Meldal, M. *J. Org. Chem.* **2002**, *67*, 3057.
- (5) Ramil, C. P.; Lin, Q. *Chem. Commun.*, **2013**, *49*, 11007.
- (6) Rodionov, V. O.; Presolski, S. I.; Diaz, D. D.; Fokin, V. V.; Finn, M. G. *J. Am. Chem. Soc.* **2007**, *129*, 12705.
- (7) Gao, P.; Sun, L.; Zhou, J.; Li, X.; Zhan, P.; Liu, X. *Expert Opin. Drug Discov.* **2016**, *11*, 857.
- (8) Hein, C. D.; Liu, X. M.; Wang, D. *Pharm. Res.* **2008**, *25*, 2216.
- (9) Kolb, H. C.; Sharpless, K. B. *Drug Discov. Today* **2003**, *8*, 1128.
- (10) Moses, J. E.; Moorhouse, A. D. *Chem. Soc. Rev.* **2007**, *36*, 1249.
- (11) Thirumurugan, P.; Matusiuk, D.; Jozwiak, K. *Chem. Rev.* **2013**, *113*, 4905.
- (12) Wang, J.; Wong, Y. K.; Zhang, J.; Lee, Y. M.; Hua, Z. C.; Shen, H. M.; Lin, Q. *Methods Enzymol.* **2017**, *586*, 291.
- (13) Rostovtsev, V. V.; Green, L. G.; Fokin, V. V.; Sharpless, K. B. *Angew. Chem. Int. Ed. Engl.* **2002**, *41*, 2596.
- (14) Rodionov, V. O.; Fokin, V. V.; Finn, M. G. *Angew. Chem. Int. Ed. Engl.* **2005**, *44*, 2210.
- (15) Lang, H.; Jakob, A.; Milde, B. *Organometallics* **2012**, *31*, 7661.
- (16) Zhu, L.; Brassard, C. J.; Zhang, X.; Guha, P. M.; Clark, R. J. *Chem. Rec.* **2016**, *16*, 1501.
- (17) Nolte, C.; Mayer, P.; Straub, B. F. *Angew. Chem. Int. Ed. Engl.* **2007**, *46*, 2101.
- (18) Worrell, B. T.; Malik, J. A.; Fokin, V. V. *Science* **2013**, *340*, 457.
- (19) Iacobucci, C.; Reale, S.; Gal, J. F.; De Angelis, F. *Angew. Chem. Int. Ed. Engl.* **2015**, *54*, 3065.
- (20) Jin, L.; Tolentino, D. R.; Melaimi, M.; Bertrand, G. *Sci. Adv.* **2015**, *1*, e1500304.

- (21) Tiruveedhula, V. V.; Witzigmann, C. M.; Verma, R.; Kabir, M. S.; Rott, M.; Schwan, W. R.; Medina-Bielski, S.; Lane, M.; Close, W.; Polanowski, R. L.; Sherman, D.; Monte, A.; Deschamps, J. R.; Cook, J. M. *Bioorg. Med. Chem.* **2013**, *21*, 7830.
- (22) Shevchenko, A.; Tomas, H.; Havlis, J.; Olsen, J. V.; Mann, M. *Nat. Protoc.* **2006**, *1*, 2856.
- (23) Wu, Y.; Wang, C.; Lin, S.; Wu, M.; Han, L.; Tian, C.; Zhang, X.; Zang, J. *Acta Crystallogr. D Biol. Crystallogr.* **2015**, *71*, 2457.
- (24) Molkanen, T.; Tyynela, J.; Helin, J.; Kalkkinen, N.; Kuusela, P. *FEBS Lett.* **2002**, *517*, 72.
- (25) Gerlt, J. A.; Babbitt, P. C.; Rayment, I. *Arch. Biochem. Biophys.* **2005**, *433*, 59.
- (26) Huberts, D. H.; van der Klei, I. J. *Biochim. Biophys. Acta* **2010**, *1803*, 520.
- (27) Antikainen, J.; Kuparinen, V.; Lahteenmaki, K.; Korhonen, T. K. *FEMS Immunol. Med. Microbiol.* **2007**, *51*, 526.
- (28) Miles, L. A.; Dahlberg, C. M.; Plescia, J.; Felez, J.; Kato, K.; Plow, E. F. *Biochemistry* **1991**, *30*, 1682.
- (29) Pancholi, V. *Cell. Mol. Life Sci.* **2001**, *58*, 902.
- (30) Schurig, H.; Rutkat, K.; Rachel, R.; Jaenicke, R. *Protein Sci.* **1995**, *4*, 228.
- (31) Pawluk, A.; Scopes, R. K.; Griffiths-Smith, K. *Biochem. J.* **1986**, *238*, 275.
- (32) Wedekind, J. E.; Reed, G. H.; Rayment, I. *Biochemistry* **1995**, *34*, 4325.
- (33) Lahteenmaki, K.; Kuusela, P.; Korhonen, T. K. *FEMS Microbiol. Rev.* **2001**, *25*, 531.
- (34) Lahteenmaki, K.; Kuusela, P.; Korhonen, T. K. *Methods* **2000**, *21*, 125.
- (35) Korhonen, T. K.; Virkola, R.; Lahteenmaki, K.; Bjorkman, Y.; Kukkonen, M.; Raunio, T.; Tarkkanen, A. M.; Westerlund, B. *FEMS Microbiol. Lett.* **1992**, *100*, 307.

- (36) Boyle, M. D.; Lottenberg, R. *Thromb. Haemost.* **1997**, *77*, 1.
- (37) Sodeinde, O. A.; Subrahmanyam, Y. V.; Stark, K.; Quan, T.; Bao, Y.; Goguen, J. D. *Science* **1992**, *258*, 1004.
- (38) Carneiro, C. R.; Postol, E.; Nomizo, R.; Reis, L. F.; Brentani, R. R. *Microbes Infect* **2004**, *6*, 604.
- (39) Mukherjee, S.; Dutta, D.; Saha, B.; Das, A. K. *J. Mol. Biol.* **2010**, *401*, 949.
- (40) Menichetti, F. *Clin. Microbiol. Infect.* **2005**, *11 Suppl 3*, 22.
- (41) Taylor, J. M.; Heinrichs, D. E. *Mol. Microbiol.* **2002**, *43*, 1603.
- (42) Gozalbo, D.; Gil-Navarro, I.; Azorin, I.; Renau-Piqueras, J.; Martinez, J. P.; Gil, M. L. *Infect. Immun.* **1998**, *66*, 2052.

PART - III

A NOVEL SYNTHETIC METHOD FOR THE SYNTHESIS OF
THE KEY QUININE METABOLITE (3*S*)-3-HYDROXYQUININE

CHAPTER 7

A NOVEL SYNTHETIC METHOD FOR THE SYNTHESIS OF THE KEY QUININE METABOLITE (3S)-3-HYDROXYQUININE

7.1. INTRODUCTION

Cinchona alkaloids remain unique among the thousands of natural products isolated and characterized to date, which comprise quinine, quinidine, cinchonine, and cinchonidine as primary members. Discovery of the antimalarial properties of Cinchona alkaloids resulted early on in the exploration and successful applications of these alkaloids in studies on stereochemistry, asymmetric synthesis, and medicinal chemistry.¹ The role of Cinchona alkaloids in organic chemistry, as discovered by Pateur in 1853, was their ability to resolve racemic mixtures by the crystallization of diastereomeric salts. Apart from racemate resolutions, the Cinchona alkaloids promote enantioselective transformations in both homogeneous and heterogeneous catalysis, as shown by Sharpless and others.²

Malaria is a protozoan disease which infects humans and is caused by five different species of the genus *Plasmodium* (*P. falciparum*, *P. vivax*, *P. ovale*, *P. malariae*, and *P. knowlesi*) and is transmitted by *Anopheles* mosquitos.³ Despite the availability of many effective antimalarial drugs, the prevalence of malaria remains as one of the most common reasons for millions of deaths worldwide.⁴ Among the Cinchona alkaloids quinine was the first, pure and active chemotherapeutic agent which had a high impact on human civilization that saved many lives. Even today with resistance increasing to drugs to treat malaria, quinine can compete with the new novel classes of antiplasmodial agents and still stands out as an important antimalarial drug.¹

The pharmacological response of any drug molecule depends on the properties of the drug and the biotransformation products, of which metabolism plays a significant role. The elimination of quinine from humans is primarily by hepatic metabolism although nearly 20% of the drug is excreted in unchanged form through the urine.^{5,6} Although several metabolites have been isolated and characterized from quinine, the exact contribution of different isoforms of CYP 450 involved in the biotransformation pathway is still not clear. The analysis of quinine metabolites from human urine by Liddle et al. identified 6'-hydroxycinchonidine (O-desmethylquinine), 6'-hydroxydihydrocinchonidine, 3-hydroxydihydroquinine, quinine-10,11-epoxide and quinine-10,11-dihydrodiol as metabolites accompanied by the major metabolite 3-hydroxyquinine.⁷ Studies of *in vitro* human liver microsomal incubation of quinine revealed that (3*S*)-3-hydroxyquinine and the *N*-oxide products are the major metabolites. They are catalyzed by cytochrome P450 3A4 enzymes and CYP2C19 to a minor extent.⁸⁻¹⁰ Quinine and its diastereomer quinidine are known to be metabolized similarly which resulted in the formation of 3(*S*)-3-hydroxyquinidine as the major metabolite of quinidine, as well as the minor metabolites quinidine-*N*-oxide and 2'-quinidinone. Again these transformation were effected by cytochrome P450 enzymes.¹¹ Several studies have been performed to determine the CYP 450 isoforms responsible for the metabolism of quinine and the formation of 3-hydroxyquinine. Both quinine and 3-hydroxyquinine are known to interfere with other drugs when used in combination for they participate in drug-drug interactions with other classes of drugs. The work by Wanwimolruk et al.^{11,12} showed that clearance of quinine by metabolism was increased 77 % by smoking and 69 % by use in combination with rifampicin. The later drug is a CYP 3A4 inducer,¹³ pretreatment of which indicated quinine metabolism was mediated by CYP 450 3A. However, there was also strong evidence that cigarette smoking induces CYP1A^{14,15} rather than CYP3A enzymes. The

potent CYP 450 3A4 enzyme inhibitor ketoconazole¹⁶ reduced the oral clearance of quinine and formation of 3-hydroxy quinine which again demonstrated involvement of cytochrome P450 3A4 isoform, this time in healthy volunteers.¹⁷

In another study by Soyinka et al.,¹⁸ the co-administration of anti-retroviral drug ritonavir (CYP3A4 inhibitor) with quinine in healthy volunteers decreased the metabolism of quinine 4.5 fold rather than subjects receiving quinine alone. The quinine also had increased the clearance of ritonavir four fold, and this was due to the displacement of ritonavir at the inhibition site of CYP 3A4 by quinine. The amount and clearance of quinine in the plasma were quantified using its metabolite 3-hydroxy quinine.¹⁸ Based on this interaction a clear conclusion could be drawn that the doses of quinine should be decreased in the treatment of HIV patients infected with malaria to avoid any toxic side effects. In another study by Igbino et al. explained the influence of honey on the metabolism of the quinine.¹⁹ This indicated that honey in Nigeria altered the drug metabolizing enzymes because of the presence of quercetin, kaempferol, and luteolin. However, the interference of honey on the metabolism of quinine was not prominent even at high and low doses of honey with very little or no effect on the formation of 3-hydroxy quinine.²⁰

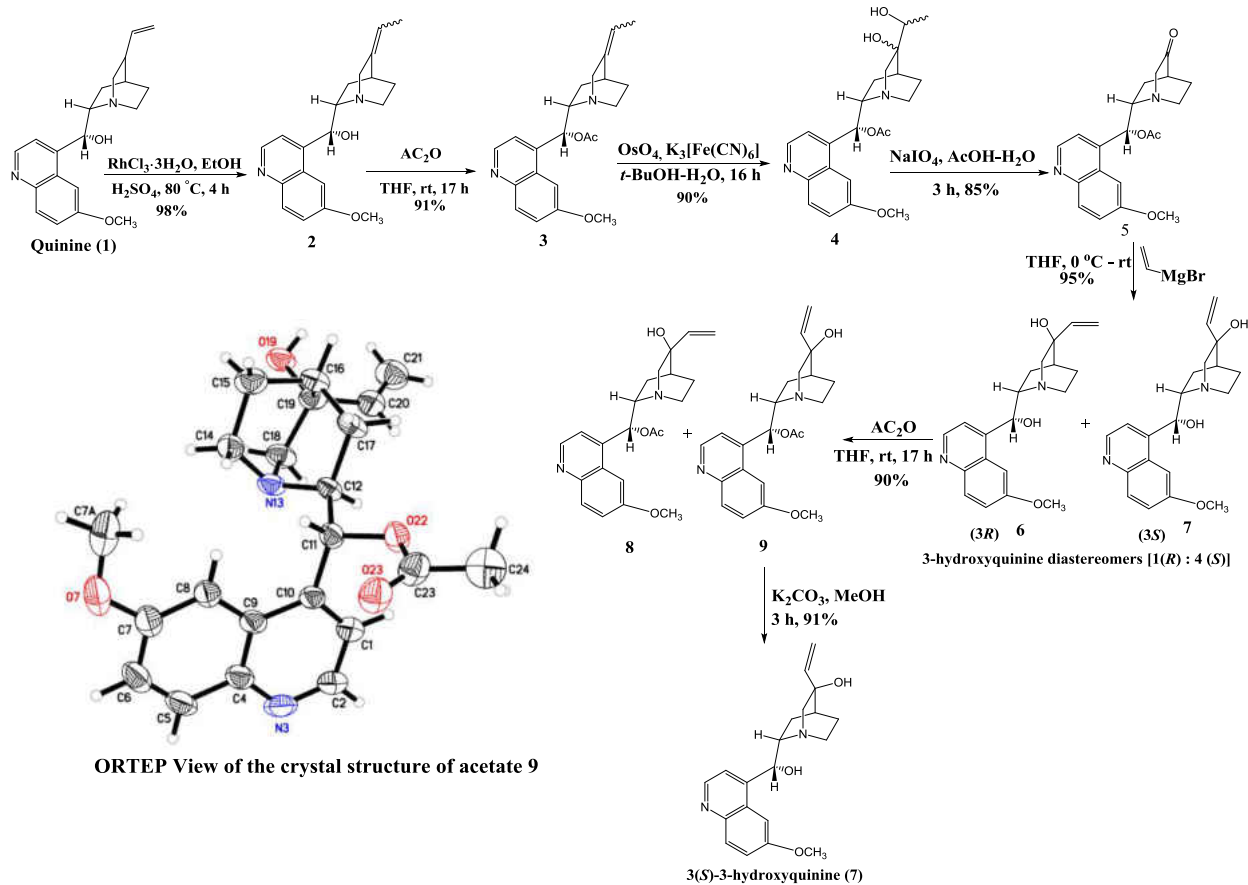
7.2. RESULTS AND DISCUSSION

The metabolic biotransformation of quinine and its interaction with the other drugs primarily effects the *in vivo* biosynthesis of the major metabolite 3-hydroxyquinine. All previous studies reported it as 3(*S*)-3-hydroxyquinine based on very old data and not unambiguous results. Previously, the 3-hydroxyquinine was synthesized from quinine by Diaz-Arauzo et al.²¹ and Sarma et al.²² Interestingly, Sarma, Zeng et al.²² synthesized the major metabolite of quinine, 3(*S*)-3-hydroxyquinine (**7**), and separated it from its epimeric mixture at C-3 by converting it into the corresponding acetate esters (**8** and **9**) and this was followed by column chromatography. The

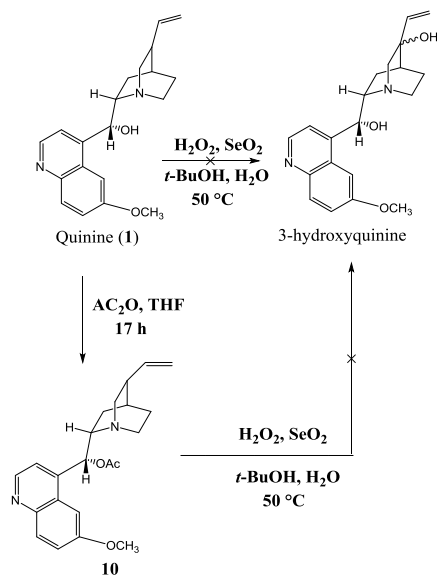
overall yield of **7**, as reported,²² previously was 16% and a few key steps occurred in low yields which one sought to improve on in a continued effort. The approach to **7** was to shorten the number of steps, as well as eliminate the harsh conditions and reagents which had been employed such as aqueous HBr, HBr gas, and pyridine. At first, the search to bypass the use of HBr gas was because of inavailability and numerous Government regulations. After a comprehensive literature survey, RhCl₃·3H₂O catalyzed alkene isomerization was found.²³ As shown in Scheme 7-1, gratifyingly RhCl₃·3H₂O catalyzed isomerization of quinine (**1**) to the C(10)–C(11) olefin and this was followed by protection of the C-9 hydroxy group as its acetate. This gave olefin **3** in excellent yield using only Ac₂O in the absence of base (pyridine). It is likely the quinine N atoms react with Ac₂O to form the corresponding acyl ammonium species, which in turn reacts with the neighboring hydroxy group intramolecularly to give the corresponding acetate **3**. Without further purification, the osmium tetroxide catalyzed dihydroxylation was performed on acetate **3** using K₃[Fe(CN)₆] as an oxidant to give diol **4**. This diol was subsequently converted into the key intermediate carbonyl compound **5** on treatment with NaIO₄ as an oxidative reagent under acidic conditions. This gave the ketone **5** in good yield. As shown in Scheme 7-1, the Grignard reaction with vinyl magnesium bromide on ketone **5** gave an epimeric mixture of hydroxy quinines **6** and **7**, obtained in a 1:4 ratio, with an almost identical R_f value. The two alcohols were inseparable by flash column chromatography on either silica gel or alumina. In order to separate the epimeric mixture **6** and **7**, these alcohols were converted into the acetate analogs **8** and **9** by treatment with Ac₂O in THF at room temperature. As shown in Scheme 7-1, the major acetate diastereomer **9** was crystallized from a two solvent system which contained CH₂Cl₂-hexane. The crystals were subjected to X-ray crystallographic analysis via Cu source at low temperature to confirm the absolute configuration. Subsequent hydrolysis of **9** under basic conditions with K₂CO₃ in methanol furnished pure 3(*S*)-

3-hydroxyquinine (**7**) and the spectrum was identical to that from the previous multistep route.²² Furthermore, the pure two isomers *S* and *R* of 3-hydroxyquinine and corresponding 9-aceto analogues are now available for biological studies of the major and trace metabolites of quinine.

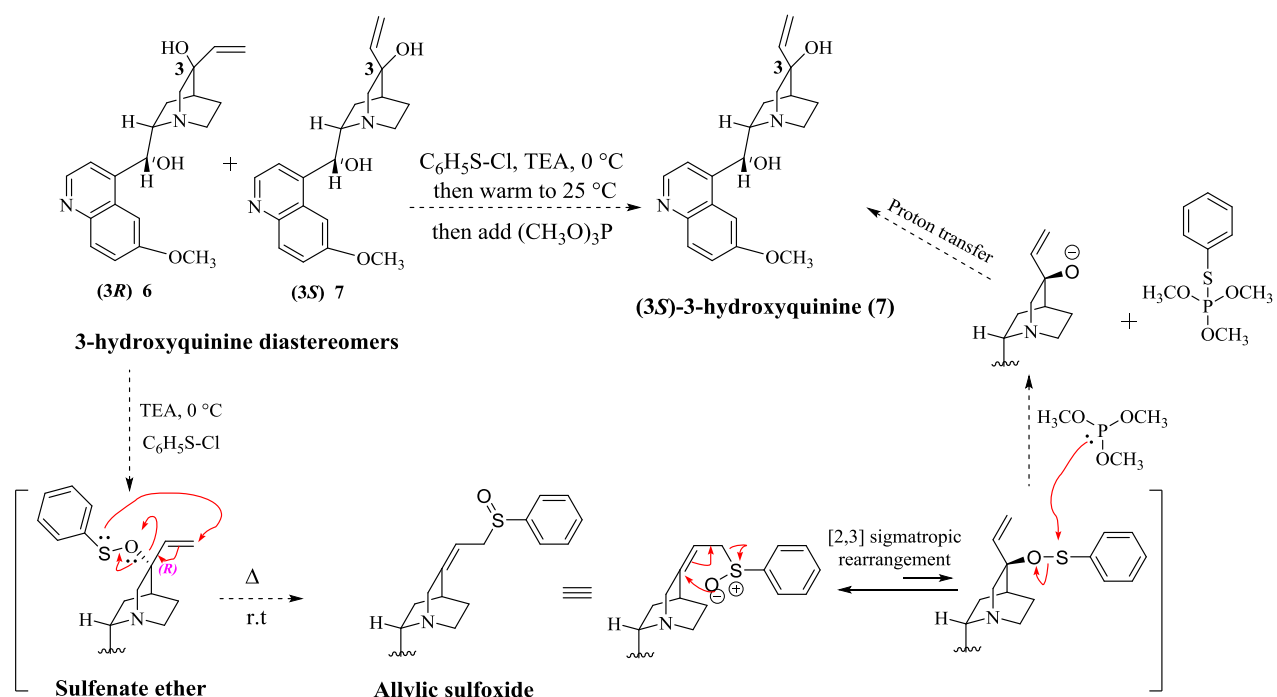
With authentic samples of the hydroxy isomers **6** and **7** (desired) in hand, this stimulated the development of a the short and concise diastereoselective synthetic route which would be a step protocol for allylic hydroxylation on quinine (**1**) by SeO₂, as shown in Scheme 7-2. However, this failed to give the desired hydroxy isomer **7** with quinine (**1**), and acetyl protected quinine (**10**). Extensive review of the literature revealed that an epimeric mixture at C-3 of substituted 3-hydroxyquinine could be converted into single 3(*S*)-3-hydroxyquinine by a Mislow-Evans rearrangement²⁴ using benzenesulfonyl chloride under basic conditions, as shown in Scheme 7-3. This is a possible pathway one can explore but it also fraught with difficulties particularly because of the presence of the 9-hydroxy group. Attention must be paid to the C-9 dehydration reaction and is ongoing in our laboratories.



Scheme 7-1. Synthesis of 3(S)-3-hydroxyquinine (7)



Scheme 7-2. Attempts to synthesize 3(S)-3-hydroxyquinine (7) by one step using SeO_2



Scheme 7-3. Proposed mechanism for converting an epimeric mixture at C-3 of 3-hydroxyquinine diastereomers to a single 3(*S*)-3-hydroxyquinine (**7**) by a Mislow-Evans rearrangement²⁴

7.3. CONCLUSION

The major metabolite of the antimalarial Cinchona alkaloid quinine (**1**) 3(*S*)-3-hydroxyquinine (**7**), has been synthesized by a shorter route and separated from its epimeric mixture (4(*S*): 1(*R*)) at C-3 by conversion into the 9-aceto analogue. This was followed by flash column chromatography and hydrolysis to provide gram quantities of **7**. The synthesis was accomplished devoid of previously employed toxic reagents hydrogen bromide gas and the hard to remove base pyridine. This synthetic protocol increased the overall yield from 16% to 53%. This makes very important metabolite **7** more readily available now for scientists to study drug-drug interactions when using quinine with another agent to treat malaria combined with HIV or other diseases. The development of a diastereoselective synthesis is ongoing for an even shorter synthetic route to 3(*S*)-3-hydroxyquinine (**7**). For instance, a doctor in Nigeria, using **7** found that

in healthy volunteers, to treat patients with HIV and malaria one needed a ratio of ~5:1 ritonavir and quinine, not 1:1, as used previously.

7.4. EXPERIMENTAL

The compounds **6-10** were synthesized as described previously in the literature.²¹⁻²³

7.4.1. (*R*)-((1*S*,2*S*,4*S*)-5-ethylidenequinuclidin-2-yl)(6-methoxyquinolin-4-yl)methanol (**2**)

An oven-dried round bottom flask was charged with quinine **1** (6 g, 18.49 mmol), EtOH (110 mL), conc H₂SO₄ (2 mL) under a positive pressure of argon and the reaction mixture, which resulted, was stirred for 10-15 mins at rt. The formation of a white slurry was observed. The RhCl₃·3H₂O (150 mg, 0.55 mmol) was then added and the mixture was heated at reflux for 4 h under argon. After the evaporation of the EtOH, the mixture was diluted with CHCl₃ (150 mL), brought to the alkaline pH (pH paper) with 10% aq K₂CO₃ solutions. The organic layer was washed with brine, dried (K₂CO₃), and concentrated under vacuum to yield a brown colored amorphous solid **2** (5.9 g, 98%, 5% MeOH in CHCl₃) which was used directly in the next reaction without further purification.

7.4.2. (*R*)-((1*S*,2*S*,4*S*)-5-ethylidenequinuclidin-2-yl)(6-methoxyquinolin-4-yl)methyl acetate (**3**)

The solution of the crude **2** (4.8 g, 15 mmol) in anhydrous THF (50 mL) was cooled to 0 °C and then Ac₂O (1.7 ml, 18.15 mmol) was added under a positive pressure of argon. The reaction mixture, which resulted, was stirred for 10-15 min at 0 °C and then allowed to warm to rt and stirred for 17 h. The reaction progress was monitored by TLC (silica gel, 5% MeOH in CHCl₃). After the disappearance of starting materials, the reaction mixture was diluted with CHCl₃, washed with a sat aq NaHCO₃ solution, brine, dried (K₂CO₃), and concentrated under vacuum to furnish acetate **3** as a yellow colored amorphous solid (5 g, 91%), which was used for the next reaction without further purification.

7.4.3. (*R*)-((1*S*,2*S*,4*S*)-5-hydroxy-5-(1-hydroxyethyl)quinuclidin-2-yl)(6-methoxyquinolin-4-yl)methyl acetate (**4**)

The crude acetate **3** (5.1 g, 14 mmol) was dissolved in *t*-BuOH-H₂O (5:1, 102 mL). To this reaction mixture at rt were added in this order of K₂CO₃ (4.62 g, 33.6 mmol), K₃[Fe(CN)₆] (11 g, 33.6 mmol), and OsO₄ (127.1 mg, 7 mmol). The reaction mixture, which resulted, was stirred for 16 h at rt and the progress was monitored by TLC (silica gel, 10% MeOH in CHCl₃). After the disappearance of starting material, the reaction mixture was quenched by the addition of a sat solution of aq NaHSO₃ and washed with brine. The mixture was diluted with CHCl₃ and filtered through celite which was washed with CHCl₃. The CHCl₃ filtrate and washings were combined, washed with brine, dried (K₂CO₃), and concentrated under vacuum to give diol **4** as a yellow colored amorphous solid (5 g, 90%) which was used for the next reaction without further purification.

7.4.4. (*R*)-(6-Methoxyquinolin-4-yl)((1*S*,2*S*,4*S*)-5-oxoquinuclidin-2-yl)methyl acetate (**5**)

To a solution of crude diol **4** (5.35 g, 13.35 mmol) in AcOH-H₂O (4:1, 100 mL) was added NaIO₄ (3.04 g, 14.22 mmol) at rt under a positive pressure of argon. The reaction mixture which resulted, was then stirred for 3 h at rt. After the disappearance of starting material as indicated by TLC (silica gel, 10% MeOH in CHCl₃), the reaction mixture was subjected to evaporation, then brought to alkaline pH (pH paper) with 10% aq K₂CO₃ solution, and extracted with CHCl₃ (2 × 100 mL). The combined organic extracts were washed with brine, dried (K₂CO₃), and concentrated under vacuum to yield the crude ketone **5**. This material was further purified by flash column chromatography (silica gel, 5% MeOH in CHCl₃) to furnish the ketone **5** as a pale yellow colored solid (4 g, 85%); mp: 149-150 °C (lit²¹ 150 °C); ¹H NMR (500 MHz, CDCl₃) δ 8.77 (d, *J* = 4.5 Hz, 1H), 8.10 (d, *J* = 9.2 Hz, 1H), 7.49 – 7.40 (m, 2H), 7.38 (d, *J* = 4.5 Hz, 1H), 6.66 (d, *J* = 6.6 Hz,

1H), 4.00 (s, 3H), 3.50 (q, $J = 8.3$ Hz, 1H), 3.41-3.35 (m, 1H), 3.32-3.17 (m, 2H), 2.92 – 2.80 (m, 1H), 2.58 (s, 1H), 2.24 – 2.09 (m, 7H); HRMS (ESI-TOF) (M+H)⁺ calcd for C₂₀H₂₃N₂O₄: 355.1652, found: 355.1653. The spectral data of **5** are in excellent agreement with the published values.^{21,22}

7.5. REFERENCES

- (1) Kacprzak, K. M. In *Natural Products: Phytochemistry, Botany and Metabolism of Alkaloids, Phenolics and Terpenes*; Ramawat, K. G., Mérillon, J.-M., Eds.; Springer Berlin Heidelberg: Berlin, Heidelberg, 2013, p 605.
- (2) Song, C. E. In *Cinchona Alkaloids in Synthesis and Catalysis*; Wiley-VCH Verlag GmbH & Co. KGaA: 2009.
- (3) Kantele, A.; Jokiranta, T. S. *Clin. Infect. Dis.* **2011**, *52*, 1356.
- (4) Alonso, P. L.; Brown, G.; Arevalo-Herrera, M.; Binka, F.; Chitnis, C.; Collins, F.; Doumbo, O. K.; Greenwood, B.; Hall, B. F.; Levine, M. M.; Mendis, K.; Newman, R. D.; Plowe, C. V.; Rodriguez, M. H.; Sinden, R.; Slutsker, L.; Tanner, M. *PLoS Med.* **2011**, *8*, e1000406.
- (5) White, N. J. *Br. J. Clin. Pharmacol.* **1992**, *34*, 1.
- (6) Krishna, S.; White, N. J. *Clin. Pharmacokinet.* **1996**, *30*, 263.
- (7) Liddle, C.; Graham, G. G.; Christopher, R. K.; Bhuwathanapun, S.; Duffield, A. M. *Xenobiotica* **1981**, *11*, 81.
- (8) Zhao, X. J.; Yokoyama, H.; Chiba, K.; Wanwimolruk, S.; Ishizaki, T. *J. Pharmacol. Exp. Ther.* **1996**, *279*, 1327.
- (9) Zhang, H.; Coville, P. F.; Walker, R. J.; Miners, J. O.; Birkett, D. J.; Wanwimolruk, S. *Br. J. Clin. Pharmacol.* **1997**, *43*, 245.
- (10) Kolars, J. C.; Schmiedlin-Ren, P.; Schuetz, J. D.; Fang, C.; Watkins, P. B. *J. Clin. Invest.* **1992**, *90*, 1871.
- (11) Wanwimolruk, S.; Wong, S. M.; Zhang, H.; Coville, P. F. *Journal of Liquid Chromatography & Related Technologies* **1996**, *19*, 293.
- (12) Wanwimolruk, S.; Wong, S. M.; Zhang, H.; Coville, P. F.; Walker, R. J. *J. Pharm. Pharmacol.* **1995**, *47*, 957.
- (13) Oesch, F.; Arand, M.; Benedetti, M. S.; Castelli, M. G.; Dostert, P. *J. Antimicrob. Chemother.* **1996**, *37*, 1111.

- (14) Combalbert, J.; Fabre, I.; Fabre, G.; Dalet, I.; Derancourt, J.; Cano, J. P.; Maurel, P. *Drug Metab. Dispos.* **1989**, *17*, 197.
- (15) Ged, C.; Rouillon, J. M.; Pichard, L.; Combalbert, J.; Bressot, N.; Bories, P.; Michel, H.; Beaune, P.; Maurel, P. *Br. J. Clin. Pharmacol.* **1989**, *28*, 373.
- (16) Sai, Y.; Dai, R.; Yang, T. J.; Krausz, K. W.; Gonzalez, F. J.; Gelboin, H. V.; Shou, M. *Xenobiotica* **2000**, *30*, 327.
- (17) Seif El-Din, S. H.; Abdel-Aal Sabra, A. N.; Hammam, O. A.; El-Lakkany, N. M. *Korean J. Parasitol.* **2013**, *51*, 165.
- (18) Soyinka, J. O.; Onyeji, C. O.; Omoruyi, S. I.; Owolabi, A. R.; Sarma, P. V.; Cook, J. M. *Br. J. Clin. Pharmacol.* **2010**, *69*, 262.
- (19) Chen, L.; Mehta, A.; Berenbaum, M.; Zangerl, A. R.; Engeseth, N. J. *J. Agric. Food Chem.* **2000**, *48*, 4997.
- (20) Igbino, S. I.; Akanmu, M. A.; Onyeji, C. O.; Soyinka, J. O.; Owolabi, A. R.; Nathaniel, T. I.; Pullela, S. V.; Cook, J. M. *J. Clin. Pharm. Ther.* **2015**.
- (21) Diaz-Arauzo, H.; Cook, J. M.; Christie, D. J. *J. Nat. Prod.* **1990**, *53*, 112.
- (22) Srirama Sarma, P. V.; Han, D.; Deschamps, J. R.; Cook, J. M. *J. Nat. Prod.* **2005**, *68*, 942.
- (23) Nakano, A.; Ushiyama, M.; Iwabuchi, Y.; Hatakeyama, S. *Adv. Synth. Catal.* **2005**, *347*, 1790.
- (24) Majetich, G.; Song, J. S.; Ringold, C.; Nemeth, G. A.; Newton, M. G. *J. Org. Chem.* **1991**, *56*, 3973.

APPENDIX A
IDENTIFICATION OF *STAPHYLOCOCCUS AUREUS* CELLULAR PATHWAYS
AFFECTED BY THE STILBENOID LEAD DRUG SK-03-92 USING A
MICROARRAY

1 Identification of *Staphylococcus aureus* cellular pathways affected by the stilbenoid lead drug
2 SK-03-92 using a microarray

3
4 William R. Schwan^{1,2*}, Rebecca Polanowski^{1,2}, Paul M. Dunman³, Sara Medina-Bielski^{1,2},
5 Michelle Lane^{1,2}, Marc Rott^{1,2}, Lauren Lipker^{1,2}, Aaron Monte^{2,4}, V. V. N. Phani Babu
6 Tiruveedhula,⁵ Christopher M. Witzigmann⁵, James M. Cook⁵,
7 Greg A. Somerville⁶, Cassandra Mikel^{1,2},

8
9 ¹University of Wisconsin-La Crosse, Department of Microbiology, La Crosse, WI;

10 ²University of Wisconsin-La Crosse Emerging Technology Center

11 for Pharmaceutical Development;

12 ³University of Rochester School of Medicine and Dentistry, Rochester, NY;

13 ⁴University of Wisconsin-La Crosse, Department of Chemistry and Biochemistry,

14 La Crosse, WI;

15 ⁵University of Wisconsin-Milwaukee, Milwaukee, WI;

16 ⁶University of Nebraska, Lincoln, NE

17 ⁷Current affiliation: FDA; U.S. Food and Drug Administration

18
19 Corresponding Author:

20
21 William R. Schwan
22 Department of Microbiology
23 University of Wisconsin-La Crosse
24 1725 State St.
25 La Crosse, WI 54601 U.S.A.
26 (608)-785-6980
27 wschwan@uwlax.edu
28

- 29 Key Words:
30 Stilbene, microarray, *Staphylococcus aureus*, gene regulation, drug mechanism of action, sortase

31 **ABSTRACT**

32 Since the mechanism of action for a new lead stilbene compound coded SK-03-92 with
33 bactericidal activity against methicillin-resistant *S. aureus* (MRSA) is unknown, an mRNA
34 microarray was performed on SK-03-92 treated versus untreated *S. aureus* to examine
35 transcriptional changes occurring after drug treatment. A total of 14 genes were up-regulated
36 and 38 genes down-regulated by SK-03-92 drug treatment. Genes involved in sortase A
37 production, protein metabolism, and transcriptional regulation were up-regulated, whereas genes
38 encoding various transporters, purine synthesis proteins, and a putative two-component system
39 [TCS; *SACOL2360* (*MW2284*) and *SACOL2361* (*MW2285*)] were down-regulated by SK-03-92
40 treatment. Quantitative real-time polymerase chain reaction analyses (qRT-PCR) validated up-
41 regulation of *srtA* and *tdk* as well as down-regulation of the *MW2284/MW2285* and purine
42 biosynthesis genes in the drug treated population. A qRT-PCR analysis of *MW2284* and
43 *MW2285* mutants compared to wild-type cells demonstrated that the *srtA* gene was up-regulated
44 by both putative two-component regulatory gene mutants compared to the wild-type strain.
45 Using a transcription profiling technique, we have identified several cellular pathways regulated
46 by SK-03-92 drug treatment, including a putative TCS that may regulate *srtA* and other genes
47 that could be tied to the SK-03-92 mechanism of action and drug persisters.

48

49 1. INTRODUCTION

50 *Staphylococcus aureus* is a common inhabitant of the human body, but it causes
51 numerous infections that include skin and soft tissue infections as well as more serious
52 infections, such as pneumonia and bacteremia [1]. Presently, around 60% of *S. aureus* clinical
53 isolates are methicillin-resistant *S. aureus* (MRSA)[2], and the species is a leading cause of
54 nosocomial infections in the United States [3]. Many healthcare facilities in the United States
55 have endemic problems with MRSA [3, 4]. In 1997, community-associated methicillin-resistant
56 *S. aureus* (CA-MRSA) strains emerged in the United States, causing infections in younger
57 people, including necrotizing pneumonia [5-7]. Although skins infection caused by CA-MRSA
58 are still very prevalent, invasive MRSA infections have decreased [3, 8]. Besides methicillin
59 resistance, CA-MRSA strains are becoming multidrug resistant at an alarming rate [9-11].
60 Vancomycin-heteroresistant and vancomycin-resistant strains of *S. aureus* have led to
61 vancomycin no longer being effective against all strains of *S. aureus* [12-15]. Tolerance to
62 vancomycin now has been reported to be as low as 3% and as high as 47% [16, 17]. New drugs
63 are needed to treat MRSA infections; however, most of the drugs currently being developed are
64 derivatives of current drugs already being marketed [18, 19]. *S. aureus* is one of the ESKAPE
65 pathogens (*Enterococcus faecium*, *Staphylococcus aureus*, *Klebsiella pneumoniae*, *Acinetobacter*
66 *baumannii*, *Pseudomonas aeruginosa*, and *Enterobacter* species) targeted by the 10 X '20
67 initiative to develop 10 new, safe and effective antibiotics approved by 2020 [20].

68 As part of an endeavor to discover a new antibiotic to treat drug resistant strains of *S.*
69 *aureus*, we identified (*E*)-3-hydroxy-5-methoxystilbene from *Comptonia peregrina* (L.) Coulter
70 (“sweet fern”) [21] with promising activity against *S. aureus*. A structure activity relationship
71 analysis identified our lead compound, (*E*)-3-(2-(benzo[b]thiophen-2-yl)vinyl)-5-

72 methoxyphenol, “SK-03-92”. SK-03-92 was rapidly bactericidal against every Gram-positive
73 species that was tested, including MRSA strains [22]. A combined safety and pharmacokinetic
74 study demonstrated that the SK-03-92 lead drug was safe in mice [23]. Although SK-03-92
75 drug killed 90% of the population in a matter of minutes, a high number of SK-03-92 drug
76 persister cells remained.

77 Drug persisters are phenotypically different than the parent strain, but are not true drug
78 resistant variants because the MICs of the drug persisters are the same as their parent strains [24,
79 25]. Persisters are thought to be a major component of bacterial biofilms, allowing significant
80 drug tolerance [26, 27]. Many drugs used to treat *S. aureus* infections have drug persister
81 population emerge that are recalcitrant to treatment [28-30].

82 In this study, the effect of SK-03-92 on *S. aureus* cells was tested using an RNA
83 microarray that compared SK-03-92 treated versus untreated *S. aureus* MW2 cells. More than
84 twice as many genes were transcriptionally down-regulated as compared to up-regulated,
85 including two genes that may be part of a novel two-component system (TCS) in *S. aureus* that
86 could be tied to the mechanism of action or drug persisters.

87

88 2. RESULTS AND DISCUSSION

89 General transcriptome response of SK-03-92 treatment

90 New drugs to treat *S. aureus* infections are still needed, and a new lead compound,
91 SK-03-92, could be a possibility. SK-03-92 has a stilbenoid backbone [22] and is bactericidal
92 within 20 min. The SK-03-92 lead compound showed promising *in vitro* activity against all
93 strains of *S. aureus* that were tested [22], but the mechanism of action remained elusive. In an
94 attempt to ascertain the effects of SK-03-92 treatment on the transcriptome of *S. aureus* and
95 possibly elucidate the mechanism of action for the drug, total RNA was isolated from *S. aureus*
96 MW2 cells (Table 1) treated for 30 with SK-03-92 drug or untreated cells. A total of 52 genes
97 were dysregulated by the SK-03-92 drug treatment (Table 3), representing a mere 2% of the total
98 *S. aureus* transcriptome. Microarrays done with other bactericidal compounds have shown a
99 much broader effect on the *S. aureus* transcriptome, including ortho-phenylphenol (24%)[31],
100 amicoumacin A (20%)[32], and daptomycin (5 to 32%)[33, 34].

101 Another observation from this analysis was the number of down-regulated genes (38,
102 73%) greatly surpassed the number of up-regulated genes (14, 27%). An examination of genes
103 affected by pterostilbene, another stilbenoid drug, in *Saccharomyces cerevisiae* showed 1189
104 genes that were dysregulated: 1007 up-regulated (85%) and 182 down-regulated (15%) [35].
105 Microarray analysis with resveratrol treated *Schizosaccharomyces pombe* showed 480 genes
106 dysregulated, 377 genes that were up-regulated and 103 that were down-regulated [36]. RNA
107 sequence analysis of resveratrol treated *S. aureus* cells demonstrated 444 dysregulated genes,
108 201 up-regulated and 243 down-regulated [37]. The majority of the genes in our study had a
109 two- to four-fold difference in transcription when comparing SK-03-92 drug treated versus
110 untreated *S. aureus* cells. Only three genes had a 10-fold or higher change in transcription,

111 which included two genes annotated to be part of a putative TCS [*SACOL2360* (annotated as
112 *MW2284* in MW2 strain) = 14.1-fold lower and *SACOL2361* (annotated as *MW2285* in MW2
113 strain) = 26.9-fold lower] as well as the *glpD* gene encoding glycerol-3-phosphate
114 dehydrogenase (10-fold higher).

115 GlpD funnels electrons into the respiratory chain via quinone reduction coupled to the
116 oxidation of glycerol-3-phosphate to glycerone phosphate (dihydroxyacetone phosphate) [38],
117 which can be enzymatically or non-enzymatically transformed into methylglyoxal (MG) [39].
118 Higher concentrations of methylglyoxal are thought to halt bacterial growth by damaging
119 proteins and other cell components by acting as protein glycation agent that affects mainly
120 arginine residues [40, 41] as well as being associated with drug persistence in *Escherichia coli*
121 [42] and *S. aureus* [34]. Overexpression of GlpD increased the number of persisters present in
122 stationary phase in an *E. coli* expression library, whereas deletion of *glpD* decreased persister
123 production in late exponential and stationary phase cells [42]. Endogenous addition of MG
124 increased the number of persisters in a dose-dependent manner in wild-type *E. coli* [43].

125 Dysregulation of transport genes by SK-03-92 drug

126 By inspecting the genes that were differentially expressed, 12 potentially involved in
127 transport were all down-regulated: *SACOL0086*, *SACOL0155*, *SACOL0178* (*scrB*), *SACOL0400*
128 (*ulaA*), *SACOL0454*, *SACOL1018*, *SACOL1872* (*epiE*), *SACOL2146* (*mtlA*), *SACOL2333*,
129 *SACOL2573* (*copZ*), *SACOL2664* (*manA*), and *SACOL2718*. These genes encoded proteins
130 involved in anion transport, a cation efflux family protein, two phosphotransferase system (PTS)
131 transporters, a sodium:alanine symporter, sodium:dicarboxylase symporter family protein, and a
132 copper ion binding protein. Lower expression of these transport proteins may contribute to death
133 of the *S. aureus* cells because toxic intermediates may not be transported out of the bacterial cell

134 (e.g., copper transport)[44] or important biomolecules needed by the bacterial cell are not
135 transported inside.

136 Transcriptional dysregulation of programmed cell death genes by SK-03-92

137 An interesting observation was dysregulation of genes tied to programmed cell death
138 (PCD). Both the *lrgA* and *cidB* genes had decreased transcription, forming a holin/antiholin
139 system mediating autolysis, a form of prokaryotic PCD that is analogous to bcl-2 pro-apoptotic
140 effector and anti-apoptotic family members [45, 46]. The Cid/Lrg (holin/antiholin) system
141 controls autolysis and affects the distribution of extracellular DNA in *S. aureus* during biofilm
142 development [47-49].

143 SK-03-92 drug disrupts metabolic genes

144 A total of 24 genes involved in metabolism were dysregulated by SK-03-92 treatment.
145 Ten of the genes were up-regulated and 14 genes were down-regulated. Three of the genes were
146 tied to lipid metabolism. The *glpD* gene described above was up-regulated, but the other two
147 genes affected (*fabZ* and *pnbA*) were down-regulated by the drug treatment. Following
148 treatment of *S. aureus* with betulinaldehyde (a pentacyclic triterpenoid), *fabZ* transcription was
149 also shown to be down-regulated [50]. The β -hydroxyacyl-dehydratase FabZ is required for lipid
150 synthesis, catalyzing the third step in elongation of the fatty acid chain. FabZ is also involved in
151 beta oxidation of fatty acids. A decrease in FabZ activity would not only decrease fatty acid
152 biosynthesis, disrupting membrane production and repair, but also eliminate fatty acids as a
153 potential source of acetyl Co-A and reducing power [51]. PnbA is a para-nitrobenzyl esterase
154 that causes de-esterification of cephalosporin drugs in *Bacillus* sp. and *S. aureus* [52].

155 Other genes were tied to DNA metabolism as well as purine and pyrimidine synthesis.
156 One DNA metabolism gene, *SACOL2329* (*rpiA*), that was down-regulated encodes for 3.5

157 ribose-5-phosphate isomerase A, the first step in the pentose phosphate pathway that provides
158 precursors for the synthesis of amino acids, vitamins, nucleotides, and cell wall components [53].

159 Three genes associated with purine synthesis were down-regulated: *purD*, *purH*, and
160 *purL*, encoding phosphoribosylformylglycinamide synthase II (step four in *de novo* purine
161 synthesis), phosphoribosylamine-glycine ligase (step two in *de novo* purine biosynthesis), and
162 phosphoribosylaminoimidazolecarboxamide formyltransferase/IMP cyclohydrolase,
163 respectively. Purine metabolism is a necessary part of DNA synthesis and energy production in
164 *S. aureus* [54]. Other studies have demonstrated that genes involved in purine metabolism are
165 down-regulated after treatment with a drug or plant extract [55-57]. Moreover, less purine
166 metabolism is often tied to drug persister populations [58-59]. Disruption of nucleotide
167 metabolism in a library of *S. aureus* transposon insertion mutants caused a decrease in persister
168 formation frequency when treated with rifampicin [60].

169 In addition, one gene associated with pyrimidine synthesis, *tdk*, was up-regulated.
170 Thymidine kinase has roles in nucleotide transport and metabolism by transferring the terminal
171 phosphate from ATP to thymidine or deoxyuridine [61]. A decrease in the synthesis of purines
172 coupled with an increase in phosphorylation of pyrimidines could result in a dramatic
173 reorganization of the intracellular nucleotide pool.

174 Specific protein metabolism genes regulated by SK-03-92 treatment included
175 *SACOL0590 (rplL7)*, *SACOL0877 (gcvH)*, *SACOL1907 (rluD)*, and *SACOL2596* encoding a
176 hypothetical protein with homology to YME1 metallo-dependent amidohydrolase mitochondrial
177 inner membrane protein turnover [62]. GcvH shuttles the methylamine group of glycine from
178 the P-protein to the T protein via a lipoyl group [63]. Daptomycin treatment of *S. aureus* cells

179 leads to dysregulation of the *gcvT* gene, the other half of the glycine cleavage enzyme system
180 (34). Both RplL7 and RluD are tied to translation (64).

181 Genes associated with protein degradation and repair had altered transcript abundance in
182 SK-03-92-treated *S. aureus*. Transcripts encoding a putative repair system for deglycation of
183 Amadori protein adducts derived from ribose-5-P [65] showed altered abundance in SK-03-92-
184 treated *S. aureus*, as did the transcript encoding the enzyme that produces ribose-5-P. In *S.*
185 *aureus*, this repair system is comprised of a low molecular weight phosphatase (PtpA) together
186 with a fructosamine 3-kinase homolog, ribulosamine-3-kinase (SACOL2605). The formation of
187 Amadori protein adducts occurs spontaneously via a dehydrogenation mechanism when ribose-5-
188 P interacts with an amine, such as the lysine residues of proteins. Amadori glycated proteins
189 undergo further spontaneous reactions to become advanced glycation end products (AGEs).
190 AGEs promote protein aggregation [65, 66].

191 PtpA is an exported *S. aureus* signaling molecule controlled by tyrosine phosphorylation
192 which may interfere with host cell signaling by removing the 5' terminal phosphate from these
193 potentially damaging adducts, thereby producing a substrate for the kinase to attach a phosphate
194 to the 3' carbon of the sugar [67]. Phosphorylation of the 3' carbon of the sugar destabilizes the
195 ribulosamine adduct and spontaneous hydrolysis frees the original amine, restoring the original
196 functional protein. Since, the LMW-PTP transcript *ptpA* was increased 2.3-fold and the kinase
197 transcript *SACOL2605* was decreased 9.6-fold, ribulosamine substrates produced were likely not
198 being deglycated, and protein repair was not occurring. Phase-dark and phase-bright inclusions
199 were observed microscopically in SK-03-92-treated *B. subtilis*, consistent with perturbation of
200 proteostasis resulting in visible accumulation of protein aggregates (R. Polanowski and M. Rott,
201 unpublished results). Uncontrolled protein aggregation is toxic to cells [66].

202 Transcript levels for genes involved in energy production were also affected in
203 SK-03-92-treated *S. aureus* (Table 2), one of which has been directly linked to persistence in *E.*
204 *coli*. Besides the *glpD* gene, the *adhE* (*SACOL0135*), *adhP* (*SACOL0660*), and *sdhC*
205 (*SACOL1158*) genes were also dysregulated by SK-03-92 treatment. In *Candida albicans*,
206 ADH1 catalyzes the NAD⁺ linked oxidation of MG to pyruvate and disruption of the *adh1* gene
207 in *C. albicans* caused accumulation of MG followed by inhibition of growth [68]. The
208 dysregulation of *glpD* and *adh* genes suggests that MG was accumulating and glycation was
209 occurring in SK-03-92-treated *S. aureus*. MG glycation of proteins, lipids, and DNA generate
210 AGEs [69].

211 Several genes with unknown function dysregulated by SK-03-92

212 The genes identified above have annotation suggesting a known function for the gene
213 product. However, five genes identified by the microarray are annotated as hypothetical proteins
214 with no known function. These included three genes that were down-regulated (*SACOL2315*,
215 *SACOL2338*, and *SACOL2491*) and two genes that were up-regulated (*SACOL0742* and
216 *SACOL1789*). One other down-regulated gene, *SACOL0089* has annotation as a myosin-reactive
217 antigen, but the function in *S. aureus* is unknown.

218 Few virulence factor genes dysregulated by SK-03-92

219 The only true virulence factor genes affected by SK-03-92 treatment were the
220 *SACOL0151 cap5P* gene that is involved in capsule biosynthesis [70], the *SACOL1872 epiE*
221 gene encoding a gallidermin-class lantibiotic [71], the *SACOL2333* gene encoding a YnfA
222 family protein putative transport small multidrug resistance family -3 protein [72], and the *srtA*
223 gene encoding sortase A that will be described in more detail below [73].

224

225 Few regulatory genes dysregulated by SK-03-92 treatment

226 A surprising microarray result was no known *S. aureus* global regulatory genes were
227 shown to be affected by the drug treatment. Microarray analysis of daptomycin treated *S. aureus*
228 demonstrated that the the *icaR* gene was dysregulated compared to untreated cells [34]. Our
229 microarray showed that a *tetR*-family transcriptional regulator, SACOL2340, and two genes
230 comprising a putative TCS (*SACOL2360* and *SACOL2361*) were dysregulated.

231 Genes of a putative TCS are significantly down-regulated by SK-03-92 treatment

232 The most striking results from the SK-03-92 microarray were the down-regulation of the
233 two genes that comprise a putative TCS in *S. aureus* annotated as *SACOL2360* (*MW2284*, 14.1-
234 fold down-regulated) and *SACOL2361* (*MW2285*, 26.3-fold down-regulated). A bioinformatic
235 analysis of *MW2284* and *MW2285* suggest that they comprise a putative two-component
236 regulatory system where *MW2284* (LytTR superfamily regulator protein) is the response
237 regulator protein and *MW2285* (membrane protein) is the sensor kinase protein. *MW2284* was
238 identified as a 440-bp ORF encoding a putative 14.7-kDa transcriptional regulator protein and
239 *MW2285* was identified as a 455-bp ORF encoding a putative 15.1-kDa histidine kinase sensor
240 protein. The *MW2285* ORF has a 3-bp overlap with the *MW2284* ORF. BLASTP, PSI-BLAST,
241 and BLASTN bioinformatics analyses [74] showed that *MW2284* aligned with other two-
242 component regulatory system regulator proteins and *MW2285* aligned with other two-component
243 regulatory system sensor proteins. Both proteins have homology with LytTR superfamily
244 proteins involved in the regulation of bacterial genes [75]. These LytTR proteins regulate
245 virulence gene expression in a variety of bacterial species including *S. aureus*. The AgrA
246 transcriptional regulator is one of these LytTR-type proteins [76]. Moreover, the *MW2284* and
247 *MW2285* ORFs appeared to be conserved across a wide number of Gram-positive species,

248 including all *Staphylococcus* and *Streptococcus* species, as well as *Bacillus*, *Clostridium*,
249 *Lactobacillus*, and *Leuconostoc*.

250 The same LytTR TCS dysregulated in SK-03-92-treated *S. aureus* was up-regulated in
251 purine synthesis deficient mutants in *S. aureus* [77]. The putative sensor kinase (MW2285) was
252 up-regulated in *purH* mutants and the response regulator (MW2284) was up-regulated in *purA*
253 mutants (adenylosuccinate synthetase involved in purine biosynthesis). The response regulator
254 component transcript was also up-regulated during anaerobic growth in another study [78]. A
255 transposon mutant of the sensor kinase component has been previously shown to be viable,
256 capable of producing a better biofilm, and had a lower LD₅₀ than the parent strain [79, 80]. The
257 mechanistic link between defects in purine synthesis, persister formation, and the LytTR
258 regulatory system remains unclear. Furthermore, RNAseq analysis of resveratrol treated *S.*
259 *aureus* cells showed an almost 8-fold down-regulation of the *MW2284* gene, but no effect on the
260 *MW2285* gene [37].

261 Validation of microarray data by qRT-PCR

262 The microarray results were confirmed using qRT-PCR analyses on RNAs from 8X the
263 MIC SK-03-92 treated MW2 cells versus untreated MW2 cells. Transcription of the *srtA* gene
264 was significantly up-regulated almost 6-fold ($P < 0.006$, Table 4) and the *tdk* gene was also up-
265 regulated 2.1-fold ($P < 0.03$) in SK-03-92 treated cells versus untreated cells. On the other
266 hand, several genes involved in purine biosynthesis (*purD*, *purH*, and *purL*) were shown to be
267 significantly down-regulated 2.2- to 2.4-fold ($P < 0.01$ to 0.04), whereas the *MW2284* and
268 *MW2285* genes were down-regulated 4- ($P < 0.01$) and 3-fold ($P < 0.003$), respectively in the
269 SK-03-92 treated samples. These results confirmed that treatment with the SK-03-92 lead

270 compound caused dysregulation of the *srtA*, *tdk*, *purD*, *purH*, *purL*, *MW2284*, and *MW2285*
271 genes.

272 A sortase A mutant has a lower MIC against SK-03-92 than wild-type

273 Since the putative *MW2284*/*MW2285* TCS appears to repress transcription of the *srtA*
274 gene, this regulatory effect could be tied to the mechanism of action of the SK-03-92 drug.
275 Sortase A was first described in *S. aureus* in 1999 [73]. The protein covalently anchors surface
276 proteins (e.g., fibronectin-binding protein, fibrinogen-binding protein, protein A, clumping
277 factors, collagen adhesion protein) to the cell wall of *S. aureus* and other Gram-positive bacteria
278 [81]. An LPXTG motif [82-84] is common among these anchored proteins and many are
279 important for biofilm formation [85]. A mutation of the *srtA* gene caused less expression of
280 several cell wall anchored surface proteins [86, 87]. Moreover, *srtA* mutants are attenuated
281 compared to the wild-type strain in a variety of murine models of infection [86, 88, 89].

282 Because *srtA* and *MW2284*/*MW2285* transcription were affected by SK-03-92 treatment,
283 MICs were performed using the SK-03-92 lead compound on an *srtA* mutant (NE1787), *srtB*
284 mutant (control, NE1363), *MW2284* mutant (NE671), and *MW2285* mutant (NE272) compared
285 to the wild-type strain JE2 [90]. The *srtB*, *MW2284*, and *MW2285* mutants had MICs that were
286 equal to the wild-type strain (Table 5). However, the *srtA* mutant had an MIC that was 2-fold
287 lower than the wild-type strain. When a *Listeria monocytogenes srtA* mutant was tested [91], the
288 MIC for the *srtA* strain was 8-fold lower than the wild-type strain. A *L. monocytogenes srtB*
289 mutant had the same MIC as the wild-type bacteria.

290 Presumably, SK-03-93 treatment causes down-regulation of the *MW2285* gene with an
291 effect that would be similar to a mutation in the *MW2285* gene. The regulatory effect could be
292 derepression of *srtA* transcription. Either event would create more SrtA protein that in turn

293 would allow greater extracellular presentation of proteins on the surface of *S. aureus* cells. This
294 result may suggest that something tethered to the cell walls by sortase A that is conserved in both
295 species may be tied to the mechanism of action of the SK-03-92 drug, and we are exploring this
296 possibility.

297 Mutations in the *MW2284/MW2285* two-component regulatory genes cause an up-regulation of
298 the *srtA* gene

299 Since the microarray results showed up-regulation of the *srtA* gene and down-regulation
300 of the *MW2284* and *MW2285* genes, we hypothesized that the *MW2284* gene product, a putative
301 transcriptional regulator protein, may be repressing the *srtA* gene. To confirm that the putative
302 two-component regulatory system (*MW2284/MW2285*) may be involved in repressing the *srtA*
303 gene, we obtained transposon mutant strains from the Nebraska Transposon Mutant Library [89]
304 with insertion mutations in the *MW2284* and *MW2285* genes. A qRT-PCR analysis was then
305 undertaken on RNA isolated from the NE272 (*MW2285* mutation) and NE671 (*MW2284*
306 mutation) compared to the wild-type strain JE2, targeting the *srtA* gene. The results showed that
307 mutations in both the *MW2284* and *MW2285* genes led to a 9.2-fold ($P < 0.005$) and 8.1-fold (P
308 < 0.0008) up-regulation of *srtA* transcription, respectively, suggesting that this putative two-
309 component regulatory system may be repressing transcription of the *srtA* gene (Figure 2).

310

311

312 3. EXPERIMENTAL SECTION

313 3.1. SK-03-92 Synthesis

314 SK-03-92 was synthesized as described previously [22].

315 3.2. Bacterial strains and growth conditions

316 The *S. aureus* MW2 strain [7] used for the initial microarray and confirmatory qRT-PCRs
317 (Table 1) was obtained from Jean Lee (Brigham and Young Hospital, Boston, MA). *S. aureus*
318 strains JE2 (wild-type), NE671 (MW2284), and NE272 (MW2285) were obtained from the
319 Network on Antimicrobial Resistance in *Staphylococcus aureus* (NARSA) strain repository
320 (Table 1), representing part of the Nebraska Transposon Mutant Library [90]. Strain JE2 is a
321 plasmid-cured derivative of a USA300 CA-MRSA [92]. Phillip Klebba (Kansas State University,
322 Manhattan, KS)[91] provided the *Listeria montocytogenes* wild-type strain EGD as well as the
323 isogenic *srtA* and *srtB* mutant strains. All strains were grown in brain heart infusion broth
324 (Becton Dickinson, Franklin Lakes, NJ, USA) or trypticase soy broth (Becton Dickinson) shaken
325 250 rpm at 37°C. The transposon mutant strains had 5 µg/mL of erythromycin (Sigma-Aldrich,
326 St. Louis, MO, USA) added to the media.

327 3.3. RNA Extractions

328 Total RNA was isolated from *S. aureus* MW2 cells grown to mid-logarithmic phase
329 either treated with 8X the MIC of SK-03-92 or from dimethyl sulfoxide (DMSO) alone treated
330 cells using TRizol extraction (Life Technologies, Carlsbad, CA, USA) according to
331 manufacturer's instructions with an additional lysostaphin treatment step to lyse the *S. aureus*
332 cell walls. The RNA samples were digested with DNase I (New England Biolabs, Ipswich, MA,
333 USA) followed by phenol and chloroform extractions to remove the protein. RNAs were run on
334 0.8% agarose gels to confirm concentration and integrities of the RNAs. To assess DNA

335 contamination of the samples, PCRs were performed on the RNA samples using SaFtsZ1 and
336 SaFtsZ2 primers (see Table 2). The PCR conditions for amplification with the SaFtsZ1/SaFtsZ2
337 primers was as follows: 94⁰ C, 1 min; 55⁰ C, 1 min; and 72⁰ C, 1 min for 35 cycles.

338 3.4. *Microarray*

339 Total RNAs from cells treated with DMSO or 8X the MIC of SK-03-92 were converted
340 to cDNAs, biotinylated, and hybridized to *S. aureus* GeneChips following the manufacturer's
341 recommendations (Affymetrix, Santa Clara, CA, USA). Agilent GeneSpring GX 7.3 software
342 was used to gauge transcript differences and a two-fold or higher difference in the transcript
343 level for one population over the other was considered significant. Nucleic acid sequences with
344 a ≥ 2 -fold change in transcriptional abundance were mapped to the *Staphylococcus aureus* COL
345 genome (taxid:93062) via BLASTN, BLASTX, or PSI-BLAST analysis [74] through the
346 National Center for Biotechnology Information (NCBI) website, and their products and functions
347 investigated.

348 3.5. *cDNA Synthesis*

349 The cDNAs were synthesized from 5 μ g of total RNA from SK-03-92 treated or
350 untreated *S. aureus* MW2 using a First-Strand Synthesis kit (Life Technologies) according to
351 manufacturer's instructions.

352 3.6. *Real time-quantitative polymerase chain reaction (qRT-PCR)*

353 All of the qRT-PCRs were performed using the LightCycler FastStart DNA Master^{PLUS}
354 SYBR Green kit according to manufacturer's instructions (Roche, Indianapolis, IN, USA).
355 Primers used in this study were based off of the MW2 sequenced genome [93] and synthesized
356 by Integrated DNA Technologies (Coralville, IA, USA) that are shown in Table 2. A
357 LightCycler 1.5 machine (Roche) and a CFX96 machine (BioRad, Hercules, CA, USA) were

358 used throughout the study. The *guaB* and *ftsZ* housekeeping genes were used as standardization
359 controls. Each RT-qPCR run followed the minimum information for publication of quantitative
360 real-time PCR experiments guidelines [94]. The qRT-PCRs were done at least three times under
361 the following conditions: 94⁰ C, 20 sec; 55⁰ C, 30 sec; and 72⁰ C, 1 min for 35 cycles. The level
362 of target gene transcripts in MW2 cells was compared to the *guaB* and *ftsZ* genes. Crossover
363 points for all genes were standardized to the crossover points for *ftsZ* and *guaB* in each sample
364 using the $2^{-\Delta\Delta C_T}$ formula [95].

365 3.7. MICs

366 *In vitro* minimum inhibitory concentration (MIC) determinations were performed on the
367 *S aureus* strains using SK-03-92 according to the Clinical and Laboratory Standards Institute
368 guidelines [96]. All MICs were done a minimum of three times.

369 3.8. Statistical analysis

370 A Student's t-test was used to assess probabilities. P-values < 0.05 were considered
371 significant.

372

373 **4. CONCLUSIONS**

374
375 Drug treatment with the stilbenoid compound SK-03-92 caused more genes to be
376 transcriptionally down-regulated than up-regulated compared to other bactericidal and stilbenoid
377 compounds (e.g., pterostilbene and resveratrol). The methoxy substitution on the main benzene
378 ring at position 5 is likely to be responsible for this effect. A putative TCS, MW2284/MW2285,
379 is clearly affected by SK-03-92 treatment. Is the TCS the prime target of the SK-03-92 lead
380 compound and could targeting this TCS be the mechanism of action for SK-03-92 in Gram-
381 positive bacteria? It is certainly possible that one of the SK-03-92 targets is this putative TCS.
382 Knockouts of both *MW2284* and *MW2285* showed substantial up-regulation of the *srtA* gene that
383 encodes sortase A. Sortase A may present something on the exterior of the *S. aureus* cell that
384 causes rapid cell lysis. Furthermore, the *MW2284* and *MW2285* ORFs lie just upstream of the
385 *MW2286* ORF, which is thought to encode a quinolone biosynthetic gene important for the
386 electron transport chain. If the MW2284/MW2285 TCS positively regulates this gene, then a
387 mutation in either gene or treatment of *S. aureus* with SK-03-92 drug would in turn cause down-
388 regulation of this gene and a disruption of the electron transport chain in *S. aureus*. Evidence
389 presented in this study also suggests the existence of a conserved bacterial pathway, involving
390 PCD and persister formation, which is triggered by protein glycation and aggregation that may
391 be responsible for the killing mechanism of SK-03-92. Could this putative TCS be tied to these
392 phenomenon? Further study may help us determine if the SK-03-92-induced *S. aureus* cell lysis
393 is caused by a disruption of the electron transport chain, an induction of proteostasis, regulation
394 of a conserved prokaryotic PCD pathway, or a combination of two or more of these events.

395 ACKNOWLEDGEMENTS

396 We thank Phillip Klebba, Jean Lee, and the NARSA for several *S. aureus* strains used in
397 this study. This work was funded by an ARG-WiTAG grant to W.R.S., a WiSys grant to W.R.S.
398 and A.M., a National Institute of Neurological Disorders and Stroke grant NS076517 to J.M.C., a
399 UWL Undergraduate Research Grant to M.L., a UWL CSAH supply grant to L.L., WisCAMP
400 scholarships to M.L. and S.M.B., and a McNair Scholarship to M.L.

401

402 AUTHOR CONTRIBUTIONS

403 W.R.S. conceived the experiments, wrote the paper, designed some of the primers, and ran data
404 analysis; P.M.D. ran the microarray analysis and initial microarray annotation; A.M., J.M.C., and
405 M.S.K. synthesized the SK-03-92 lead compound used in the study; S.M.B., M.L., L.L., and
406 A.B. isolated the RNA samples, designed primers, and ran qRT-PCR; G.A.S. analyzed the
407 connections between the annotation and bacterial pathways; and R.P. and M.R. ran bioinformatic
408 analysis of the microarray results.

409 CONFLICT OF INTEREST

410 W.R.S., M.R., M.S.K., A.M., and J.M.C. hold a composition of matter and use patent covering
411 the SK-03-92 lead compound.

412 REFERENCES

- 413 1. Suaya, J. A.; Mera, R. M.; Cassidy, A.; O'Hara, P.; Amrine-Madsen, H.; Burstin, S.; Miller, L.
414 G. Incidence and cost of hospitalizations associated with *Staphylococcus aureus* skin and soft
415 tissue infections in the United States from 2001 to 2009. *BMC Infect. Dis.* **2014**, *14*, 296.
- 416 2. Klein, E.Y.; Sun, L.; Smith, D.L.; Laxminarayan, R. The changing epidemiology of
417 methicillin-resistant *Staphylococcus aureus* in the United States: a national observational study.
418 *Am. J. Epidemiol.* **2013**, *177*, 666-674.
- 419 3. Hidron, A. I.; Edwards, J. R.; Patel, J.; Horan, T. C.; Sievert, D. M.; Pollock, D. A.; Fridkin,
420 S. K.; National Healthcare Safety Network Team, Participating National Healthcare Safety
421 Network Facilities. NHSN annual update: antimicrobial-resistant pathogens associated with
422 healthcare-associated infections: annual summary of data reported to the National Healthcare
423 Safety Network at the Centers for Disease Control and Prevention, 2006–2007. *Infect. Control*
424 *Hosp. Epidemiol.* **2008**, *29*, 996–1011.
- 425 4. Maree, C. L.; Daum, R.; Boyle-Vavra, S.; Matayoshi, K.; Miller, L. Community associated
426 methicillin-resistant *Staphylococcus aureus* isolates causing healthcare-associated infections.
427 *Emerg. Infect. Dis.* **2007**, *13*, 236-242.
- 428 5. Herold, B. C.; Immergluck, L. C.; Maranan, M. C.; Lauderdale, D. S.; Gaskin, R. E.; Boyle-
429 Vavra, S.; Leitch, C. D.; Daum, R. S. Community-acquired methicillin-
430 resistant *Staphylococcus aureus* in children with no identified predisposing risk. *JAMA* **1998**,
431 *279*, 593-598.

- 432 6. Lina, G.; Piémont, Y.; Godail-Gamot, F.; Bes, M.; Peter, M. O.; Gauduchon, V.; Vandenesch,
433 F.; Etienne, J. Involvement of Panton-Valentine leukocidin-producing *Staphylococcus aureus* in
434 primary skin infections and pneumonia. *Clin. Infect. Dis.* **1999**, *29*, 1128-1132.
- 435 7. Center for Disease Control and Prevention. Four pediatric deaths from community-acquired
436 methicillin-resistant *Staphylococcus aureus* – Minnesota and North Dakota, 1997-1999. *Morbid*
437 *Mortal Wkly Rep* **1999**, *52*, 88.
- 438 8. Dantes, R.; Mu, Y.; Belflower, R.; Aragon, D.; Dumyati, G.; Harrison, L. H.; Lessa, F. C.;
439 Lynfield, R.; Nadle, J.; Petit, S.; *et al.* National burden of invasive methicillin-resistant
440 *Staphylococcus aureus* infections, United States, 2011. *JAMA Intern. Med.* **2013**, *173*, 1970-
441 1978.
- 442 9. Pate, A. J.; Terribilini, R. G.; Ghobadi, F.; Azhir, A.; Barber, A.; Pearson, J. M.; Kalantari,
443 H.; Hassen, G. W. Antibiotics for methicillin-resistant *Staphylococcus aureus* skin and soft
444 tissue infections: the challenge of outpatient therapy. *Amer. J. Emerg. Med.* **2014**, *32*, 135-138.
- 445 10. Pendleton, J. N.; Gorman, S. P.; Gilmore, B. F. Clinical relevance of the ESKAPE
446 pathogens. *Expert Rev. Anti. Infect. Ther.* **2013**, *11*, 297-308.
- 447 11. Stryjewski, M. E.; Corey, G. R. Methicillin-resistant *Staphylococcus aureus*: an evolving
448 pathogen. *Clin. Infect. Dis.* **2014**, *58 Suppl*, S10-S19.
- 449 12. Bae, I. G.; Federspiel, J. J.; Miró, J. M.; Woods, C. W.; Park, L.; Rybak, M. J.; Rude, T. H.;
450 Bradley, S.; Bukovski, S.; de la Maria, C. G.; *et al.* Heterogeneous vancomycin-intermediate
451 susceptibility phenotype in bloodstream methicillin-resistant *Staphylococcus aureus* isolates
452 from an international cohort of patients with infective endocarditis: prevalence, genotype, and
453 clinical significance. *J. Infect. Dis.* **2009**, *200*, 1355-1366.

- 454 13. Gomes, D. M.; Ward, K. E.; LaPlante, K. L. Clinical implications of vancomycin
455 heteroresistant and intermediately susceptible *Staphylococcus aureus*. *Pharmacotherapy* **2015**,
456 35, 424-432.
- 457 14. Moise, P. A.; North, D.; Steenbergen, J. N.; Sakoulas, G. Susceptibility relationship
458 between vancomycin and daptomycin in *Staphylococcus aureus*: facts and assumptions. *Lancet*
459 *Infect. Dis.* **2009**, 9, 617-624.
- 460 15. Sader, H. S.; Jones, R. N.; Rossi, K. L.; Rybak, M. J. Occurrence of vancomycin-tolerant
461 and heterogeneous vancomycin-intermediate strains (hVISA) among *Staphylococcus aureus*
462 causing bloodstream infections in nine USA hospitals. *J. Antimicrob. Chemother.* **2009**, 64,
463 1024-1028.
- 464 16. Jones, R. N. Microbiological features of vancomycin in the 21st century: minimum
465 inhibitory concentration creep, bactericidal/static activity, and approved breakpoints to predict
466 clinical outcomes or detect resistant strains. *Clin. Infect. Dis.* **2006**, 42(Suppl. 1), S13-S24.
- 467 17. Traczewski, M. M.; Katz, B. D.; Steenbergen, J. N.; Brown, S. D. Inhibitory and
468 bactericidal activities of daptomycin, vancomycin, and teicoplanin against methicillin-resistant
469 *Staphylococcus aureus* isolates collected from 1985-2007. *Antimicrob. Agents Chemother.* **2009**,
470 53, 1735-1738.
- 471 18. Bassetti, M.; Righi, E. Development of novel antibacterial drugs to combat multiple
472 resistant organisms. *Langenbecks Arch. Surg.* **2015**, 400, 153-165.
- 473 19. Coates, A. R. M.; Halls, G.; Hu, Y. Novel classes of antibiotics or more of the same? *Br. J.*
474 *Pharmacol.* **2011**, 163, 184-194.

- 475 20. Infectious Diseases Society of America. The 10 X '20 initiative: pursuing a global
476 commitment to develop 10 new antibacterial drugs by 2020. *Clin. Infect. Dis.* **2010**, *50*, 1081-
477 1083.
- 478 21. Kabir, M.S.; Engelbrecht, K.; Polanowski, R.; Krueger, S.M.; Ignasiak, R.; Rott, M.;
479 Schwan, W.R.; Stemper, M.E.; Reed, K.D.; Sherman, D.; *et al.* New classes of Gram-positive
480 selective antibacterials: inhibitors of MRSA and surrogates of the causative agents of anthrax
481 and tuberculosis. *Bioorg. Med. Chem. Lett.* **2010**, *18*, 5745-5749.
- 482 22. Schwan, W. R.; Kabir, M. S.; Kallaus, M.; Krueger, S.; Monte, A.; Cook, J. M. Synthesis
483 and minimum inhibitory concentrations of SK-03-92 against *Staphylococcus aureus* and other
484 gram-positive bacteria. *J. Infect. Chemother.* **2012**, *18*, 124-126.
- 485 23. Schwan, W. R.; Kolesar, J.M.; Kabor, M.S.; Elder, E.J. Jr.; Williams, J.B.; Minerath, R.;
486 Cook, J.M.; Witzigmann, C. M.; Monte, A.; Flaherty T. Pharmacokinetic/toxicity properties of
487 the new anti-staphylococcal lead compound SK-03-92. *Antibiotics* **2015**, *4*, 617-626.
- 488 24. Lewis, K. Persister cells. *Annu Rev Microbiol* **2010**, *64*, 357-372.
- 489 25. Keren, I.; Shah, D.; Spoering, A.; Kaldalu, N.; Lewis, K. Specialized persister cells and the
490 mechanism of multidrug tolerance in *Escherichia coli*. *J. Bacteriol.* **2004**, *186*, 8172-8180.
- 491 26. Spoering, A. L.; Lewis, K. Biofilms and planktonic cells of *Pseudomonas aeruginosa* have
492 similar resistance to killing by antimicrobials. *J. Bacteriol.* **2001**, *183*, 6746-6751.
- 493 27. Stewart, P. S.; Costerton, J. W. Antibiotic resistance of bacteria in biofilms. *Lancet* **2001**,
494 *358*, 135-138.
- 495

496 28. Cohen, N. R.; Lobritz, M. A.; Collins, J. J. Microbial persistence and the road to drug
497 resistance. *Cell Host Microbe* **2013**, *13*, 632-642.

498 29. Conlon, B. P. *Staphylococcus aureus* chronic and relapsing infections: Evidence of a role
499 for persister cells: an investigation of persister cells, their formation and their role in *S. aureus*
500 disease. *Bioessays* **2014**, *36*, 991-996.

501 30. Lechner, S., Lewis, K. & Bertram, R. *Staphylococcus aureus* persists tolerant to
502 bactericidal antibiotics. *J. Mol. Microbiol. Biotechnol.* **2012**, *22*, 235-244.

503 31. Jang, H.; Nde, C.; Toghrol, F.; Bentley, W.E. Microarray analysis of toxicogenomic effects
504 of ortho-phenylphenol in *Staphylococcus aureus*. *BMC Genomics* **2008**, *9*, 411.

505 32. Lama, A.; Pané-Farré, J.; Chon, T.; Wiersma, A.M.; Sit, C.S.; Vederas, J.C.; Hecker, M.;
506 Nakano, M.M. Response of methicillin-resistant *Staphylococcus aureus* to ampicoumacin A.
507 *PLoS One* **2012**, *7*, e34037.

508 33. Muthaiyan, A.; Silverman, J.A.; Jayaswal, R.K.; Wilinon, B.J. Transcriptional profiling
509 reveals that daptomycin induces the *Staphylococcus aureus* cell wall stress stimulon and gene
510 responsive to membrane depolarization. *Antimicrob. Agents Chemother.* **2008**, *52*, 980-990.

511 34. Lechner, S.,; Prax, M.; Lange, B.; Huber, C.; Eisenreich, W.; Herbig, A.; Nieselt, K.;
512 Bertram, R. Metabolic and transcriptional activities of *Staphylococcus aureus* challenged with
513 high-doses of daptomycin. *Int. J. Med. Microbiol.* **2014**, *304*, 931-940. PMID:24980509

514 35. Pan, Z.; Agarwal, A. K.; Xu, T.; Feng, Q.; Baerson, S. R.; Duke, S. O.; Rimando, A. M.
515 Identification of molecular pathways affected by pterostilbene, a natural dimethylether analog of
516 resveratrol. *BMC Med. Genomics* **2008**, *20*, 1-7. PMID:18366703

517

- 518 36. Wang, Z.; Gu, Z.; Shen, Y.; Wang, Y.; Li, J.; Lv, H.; Huo, K. The natural product
519 resveratrol inhibits yeast cell separation by extensively modulating the transcriptional landscape
520 and reprogramming the intracellular metabolome. *PLoS One* **2016**, *11*, e0150156. doi:
521 10.1371/journal.pone.0150156.
- 522 37. Qin, N.; Tan, X.; Jiao, Y.; Liu, L.; Zhao, W.; Yang, S.; Jia, A. RNA-Seq-based
523 transcriptome analysis of methicillin-resistant *Staphylococcus aureus* biofilm inhibition by ursolic
524 acid and resveratrol. *Sci. Rep.* **2014**, *4*, 5467. PMID:24970710
- 525 38. Yeh, J.I., Chinte, U.; Du, S. Structure of glycerol-3-phosphate dehydrogenase, an essential
526 monotopic membrane enzyme involved in respiration and metabolism. *Proc. Nat. Acad. Sci.*
527 *USA* **2008**, *105*, 3280-3285.
- 528 39. Ramasamy, R.; Yan, S.F.; Schmidt, A.M. Methylglyoxal comes of AGE. *Cell* **2006**, *124*,
529 258-260.
- 530 40. Ackerman, R. S.; Cozzarelli, N. R.; Epstein, E. W. Accumulation of toxic concentrations of
531 methylglyoxal by wild-type *Escherichia coli* K-12. *J. Bacteriol.* **1974**, *119*, 357-362.
- 532 41. Rabbani, N.; Thornalley, P.J. Methylglyoxal, glyoxalase 1 and the dicarbonyl proteome.
533 *Amino Acids* **2012**, *42*, 1133-1142.
- 534 42. Spoering, A.L.; Vulić, M.; Lewis, K. GlpD and PlsB participate in persister cell formation in
535 *Escherichia coli*. *J. Bacteriol.* **2006**, *188*, 5136-5144.
- 536 43. Girgis, H.S.; Harris, K.; Tavazoie, S. Large mutational target size for rapid emergence of
537 bacterial persistence. *Proc. Nat. Acad. Sci. USA* **2012**, *109*, 12740-12745.
- 538 44. Cassat, J. E.; Skaar, E. P. Metal ion acquisition in *Staphylococcus aureus*: overcoming
539 nutritional immunity. *Semin, Immunopathol.* **2012**, *34*, 215-235. PMID:22048835
- 540

- 541 45. Bayles, K.W. Bacterial programmed cell death: making sense of a paradox. *Nat. Rev.*
542 *Microbiol.* **2014**, *12*, 63-69.
- 543 46. Tanouchi, Y.; Lee, A.J.; Meredith, H.; You, L. Programmed cell death in bacteria and
544 implications for antibiotic therapy. *Trends Microbiol.* **2013**, *21(6)*, 265-270.
- 545 47. Ranjit, D.K.; Endres, J.L.; Bayles, K.W. *Staphylococcus aureus* CidA and LrgA proteins
546 exhibit holin-like properties. *J. Bacteriol.* **2011**, *193(10)*, 2468-2476.
- 547 48. Sadykov, M.R.; Bayles, K. The control of death and lysis in staphylococcal biofilms: a
548 coordination of physiological signals. *Curr. Op. Microbiol.* **2012**, *15*, 211-215.
- 549 49. Yang, S. J.; Rice, K. C.; Brown, R. J.; Patton, T. G.; Liou, L. E.; Park, Y. H.; Bayles, K. W.
550 A LysR-type regulator, CidR, is required for induction of the *Staphylococcus aureus* *cidABC*
551 operon. *J. Bacteriol.* **2005**, *187*, 5893-5900. PMID:16109930
- 552 50. Chung, P. Y.; Chung, L. Y.; Navaratnam P. Identification, by gene expression profiling
553 analysis, of novel gene targets. *Res. Microbiol.* **2013**, *164*, 319-326.
- 554 51. Heath, R. J.; Rock, C. O. Roles of the FabA and FabZ beta-hydroxyacyl-acyl carrier protein
555 dehydratases in *Escherichia coli* fatty acid biosynthesis. *J. Biol. Chem.* **1996**, *271*, 27795-27801.
556 PMID:8910376
- 557 52. Brannon, D. R.; Mabe, J. A.; Fukuda, D. S. De-esterification of cephalosporin para-
558 nitrobenzyl esters by microbial enzymes. *J. Antibiot. (Tokyo)* **1976**, *29*, 121-124.
- 559 53. Somerville, G. A.; Proctor, R. P. At the crossroads of bacterial metabolism and virulence
560 factor synthesis in Staphylococci. *Microbiol. Mol. Biol. Rev.* **2009**, *73*, 233-248.
561 PMID:19487727
- 562 54. Wood, R. C., Steers, E. Study of the purine metabolism of *Staphylococcus aureus*. *J.*
563 *Bacteriol.* **1959**, *77*, 760-765.

- 564 55. Subramanian, D.; Natarajan, J. Network analysis of *S. aureus* response to ramoplanin
565 reveals modules for virulence factors and resistance mechanisms and characteristic novel genes.
566 *Gene* **2015**, *574*, 149-162.
- 567 56. Cuaron, J. A.; Dulal, S.; Song, Y.; Singh, A. K.; Montelongo, C. E.; Yu, W.; Nagarajan, V.;
568 Jayaswal, R. K.; Wilkinson, B. J.; Gustafson, J. E. Tea tree oil-induced transcriptional
569 alterations in *Staphylococcus aureus*. *Phytother. Res.* **2013**, *27*, 390-396.
- 570 57. Shen, F.; Tang, X.; Wang, Y.; Yang, Z.; Shi, .; Wang, C.; Zhang, Q.; An, Y.; Cheng, W.;
571 Jin, K.; Liu, M.; Guo, N.; Yu, L. Phenotype and expression prolife analysis of *Staphylococcus*
572 *aureus* biofilms and planktonic cells in response to licochalcone A. *Appl. Microbiol. Biotechnol.*
573 **2015**, *99*, 359-373.
- 574 58. Fung, D. K.; Chan, E. W.; Chin, M. L.; Chan, R. C. Delineation of a bacterial starvation
575 stress response network which can mediate antibiotic tolerance development. *Antimicrob.*
576 *Agents Chemother.* **2010**, *54*, 1082-1093.
- 577 59. Maisonneuve, E.; Gerdes, K. Molecular mechanisms underlying bacterial persisters. *Cell*
578 **2014**, *157*, 539-548.
- 579 60. Yee, R.; Cui, P.; Shi, W.; Feng, J.; Zhang, Y. Genetic screen reveals the role of purine
580 metabolism in *Staphylococcus aureus* persistence to rifampicin. *Antibiotics* **2015**, *4*, 627-642.
- 581 61. Blakely, R. L.; Vitols, E. The control of nucleotide biosynthesis. *Annu. Rev. Biochem.*
582 **1968**, *37*, 201-224.
- 583 62. Thorsness, P. E.; Fox, T. D. Nuclear mutations in *Saccharomyces cerevisiae* that affect the
584 escape of DNA from mitochondria to the nucleus. *Genetics* **1993**, *134*, 21-28.

585 63. Stauffer, L. T.; Steiert, P. S.; Steiert, J. G.; Stauffer, G. V. An *Escherichia coli* protein with
586 homology to the H-protein of the glycine cleavage enzyme complex from pea and chicken liver.
587 *DNA Seq.* **1991**, *2*, 13-17.

588 64. Raychaudhuri, S.; Conrad, J.; Hall, B. G.; Ofengand, J. A pseudouridine synthase required
589 for the formation of two universally conserved pseudouridines in ribosomal RNA is essential for
590 normal growth of *Escherichia coli*. *RNA* **1998**, *4*, 1407-1417. PMID 981461

591 65. Gemayel, R.; Fortpied, J.; Rzem, R.; Vertommen, D.; Veiga-da-Cunha, M.; Van
592 Schaftingen, E. Many fructosamine 3-kinase homologues in bacteria are
593 ribulosamine/erythrosamine 3-kinases potentially involved in protein deglycation. *FEBS J.*
594 **2007**, *274*, 4360-4374.

595 66. Bednarska, N.G.; Schymkowitz, J.; Rousseau, F.; Van Eldere, J. Protein aggregation in
596 bacteria: the thin boundary between functionality and toxicity. *Microbiology* **2013**, *159*, 1795-
597 1806.

598 67. Brelle, S.; Baronian, G.; Huc-Brandt, S.; Zaki, L. G.; Cohen-Gonsaud, M.; Bischoff, M.;
599 Molle, V. Phosphorylation-mediated regulation of the *Staphylococcus aureus* secreted tyrosine
600 phosphatase PtpA. *Biochem. Biophys. Res. Comm.*, **2016**, *469*, 619-625. PMID:26679607

601 68. Kwak, M.; Ku, M.; Kang, S. NAD⁺-linked alcohol dehydrogenase 1 regulates
602 methylglyoxal concentration in *Candida albicans*. *FEBS Lett.* **2014**, *588*, 1144-1153.

603 69. Rabbani, N.; Thornalley, P.J. Methylglyoxal, glyoxalase 1 and the dicarbonyl proteome.
604 *Amino Acids* **2012**, *42*, 1133-1142.

605 70. Kiser, K. B.; Bhasin, N.; Deng, L.; Lee, J. C. *Staphylococcus aureus cap5P* encodes a UDP-
606 N-acetylglucosamine 2-epimerase with functional redundancy. *J. Bacteriol.* **1999**, *181*, 4818-
607 4824. PMID:10438750.

608 71. Bierbaum, G.; Gotz, F.; Peschel, A.; Kupke, T.; van de Knap, M.; Sahl, H. G. The
609 biosynthesis of the lantibiotics epidermin, gallidermin, Pep5 and epilancin K7. *Antonie Van*
610 *Leeuwenhoek* **1996**, *69*, 119-127. PMID:8775972

611 72. Sarkar, S. K.; Bhattacharyya, A.; Mandal, S. S. YnfA, a SMP family efflux pump is
612 abundant in *Escherichia coli* isolates from urinary infection. *Indian J. Med. Microbiol.* **2015**, *33*,
613 139-142. PMID:25560019

614 73. Mazmanian, S. K.; Liu, G.; Ton-That, H.; Schneewind, O. *Staphylococcus aureus* sortase,
615 an enzyme that anchors surface proteins to the cell wall. *Science* **1999**, *285*, 760-763.

616 74. Altschul, S. F.; Madden, T. L.; Schäffer, A. A.; Zhang, J.; Zhang, Z.; Miller, W.; Lipman, D.
617 J. Gapped BLAST and PSI-BLAST: a new generation of protein database search programs.
618 *Nucleic Acids Res.* **1997**, *25*, 3389-3402.

619 75. Nikolskaya, A. N.; Galperin, M.Y. A novel type of conserved DNA-binding domain in the
620 transcriptional regulators of the AlgR/AgrA/LytR family. *Nucleic Acids Res.* **2002**, *30*, 2453–
621 2459.

622 76. Nicod, S. S.; Weinzierl, R. O.; Burchell, L.; Escalera-Maurer, A.; James, E. H.;
623 Wigneshweraraj, S. Systematic mutational analysis of the LytTR DNA binding domain of
624 *Staphylococcus aureus* virulence gene transcription factor AgrA. *Nucleic Acids Res* **2014**, *42*,
625 12523-12536.

626 77. Lan, L.; Cheng, A.; Dunman, P.M.; Missiakas, D.; He, C. Golden pigment production and
627 virulence gene expression are affected by metabolisms in *Staphylococcus aureus*. *J. Bacteriol.*
628 **2010**, *192*, 3068-3077.

629 78. Fuchs, S.; Pané-Farré, J.; Kohler, C.; Hecker, M.; Engelmann, S. Anaerobic gene expression
630 in *Staphylococcus aureus*. *J. Bacteriol.* **2007**, *189(11)*, 4275-4289.

- 631 79. Kadurugamuwa, J. L.; Sin, L.; Albert, E.; Yu, J.; Francis, K.; DeBoer, M.; Rubin, M.;
632 Bellinger-Kawahara, C.; Parr, T. R. Jr.; Contag, P. R. Direct continuous method for monitoring
633 biofilm infection in a mouse model. *Infect. Immun.* **2003**, *71*, 882-890.
- 634 80. Xiong, Y. Q.; Willard, J.; Kadurugamuwa, J. L.; Yu, J.; Francis, K. P.; Bayer, A. S. Real-
635 time in vivo bioluminescent imaging for evaluating the efficacy of antibiotics in a rat
636 *Staphylococcus aureus* endocarditis model. *Antimicrob. Agents Chemother.* **2005**, *49*, 380-387.
- 637 81. Marraffini, L. A.; DeDent, A. C.; Schneewind, O. Sortases and the art of anchoring
638 proteins to the envelopes of Gram-positive bacteria. *Microbiol Mol Biol Rev.* **2006**, *70*, 192-221.
- 639 82. Fischetti, V. A.; Pancholi, V.; Schneewind, O. Conservation of a hexapeptide sequence in
640 the anchor region of surface proteins from gram-positive bacteria. *Mol Microbiol.* **1990**, *4*,
641 1603-1605.
- 642 83. Boekhorst, J.; de Been, M. W.; Kleerebezem, M.; Siezen, R. J. Genome-wide detection and
643 analysis of cell wall-bound proteins with LPxTG-like sorting motifs. *J. Bacteriol.* **2005**, *187*,
644 4928-4934.
- 645 84. Ton-That, H.; Liu, G.; Mazmanian, S. K.; Faull, K. F.; Schneewind, O. Purification and
646 characterization of sortase, the transpeptidase that cleaves surface proteins of *Staphylococcus*
647 *aureus* at the LPXTG motif. *Proc. Natl. Acad. Sci. USA* **1999**, *96*, 12424-12429.
- 648 85. Foster, T. J.; Hook, M. Surface protein adhesins of *Staphylococcus aureus*. *Trends*
649 *Microbiol.* **1998**, *6*, 484-488.
- 650 86. Mazmanian, S. K.; Liu, G.; Jensen, E. R.; Lenoy, E.; Schneewind, O. *Staphylococcus*
651 *aureus* mutants defective in the display of surface proteins and in the pathogenesis of animal
652 infections. *Proc. Natl. Acad. Sci. USA* **2000**, *97*, 5510-5515.

653 87. Sibbald, M. J. J.; Yang, X.-M.; Tsompanidou, E.; Qu, D.; Hecker, M.; Becher, D.; Buist, G.;
654 Maarten van Dijl, J. Partially overlapping substrate specificities of staphylococcal group A
655 sortases. *Proteomics* **2012**, *12*, 3049-3062.

656 88. Jonsson, I. M.; Mazmanian, S. K.; Schneewind, O.; Bremell, T.; Tarkowski, A. The role of
657 *Staphylococcus aureus* sortase A and sortase B in murine arthritis. *Microbes Infect.* **2003**, *5*,
658 775-780.

659 89. Weiss, W. J.; Lenoy, E.; Murphy, T.; Tardio, L.; Burgio, P.; Projan, S. J.; Schneewind, O.;
660 Alksne, L. Effect of *srtA* and *srtB* gene expression on the virulence of *Staphylococcus aureus* in
661 animal infection. *J Antimicrob Chemother.* **2004**, *53*, 480-486.

662 90. Fey, P. D.; Endres, J. L.; Yajjala, V. K.; Widhelm, T. J.; Boissy, R. J.; Bose, J. L.; Bayles K.
663 W. A genetic resource for rapid and comprehensive phenotype screening of nonessential
664 *Staphylococcus aureus* genes. *mBio* **2013**, *4*, e00537012.

665 91. Xiao, Q.; Jiang, X.; Moore, K. J.; Shao, Y.; Pi, H.; Dubail, I.; Charbit, A.; Newton, S. M. ;
666 Klebba, P. E. Sortase independent and dependent systems for acquisition of haem and
667 haemoglobin in *Listeria monocytogenes*. *Mol. Microbiol.* **2011**, *80*, 1581-1597.

668 92. Voyich, J. M.; Braughton, K. R.; Sturdevant, D. E.; Whitney, A. R.; Saïd-Salim, B.; Porcella,
669 S. F.; Long, R. D.; Dorward, D. W.; Gardner, D. J.; Kreiswirth, B. N., *et al.* Insights into
670 mechanisms used by *Staphylococcus aureus* to avoid destruction by human neutrophils. *J.*
671 *Immunol.* **2005**, *175*, 3907-3919.

672 93. Baba, T.; Takeuchi, F.; Kuroda, M.; Yuzawa, H.; Aoki, K.; Oguchi, A.; Nagai, Y.; Iwama,
673 N.; Asano, K.; Naimi, T.; *et al.* Genome and virulence determinants of high virulence
674 community-acquired MRSA. *Lancet* **2002**, *359*, 1819-1827.

675 94. Bustin, S. S., Benes, V., Garson, J. A., Hellemans, J., Huggett, J., Kubista, M., Mueller, R.,
676 Nolan, T., Pfaffl, M. W., Shipley, G. L., *et al.* The MIQE guidelines: minimum information for
677 publication of quantitative real-time PCR experiments. *Clin. Chem.* **2009**, *55*, 611-622.

678 95. Livak, K. J.; Schmittgen, T. D. Analysis of relative gene expression data using real-time
679 quantitative PCR and the 2(-Delta Delta C(T)) Method. *Methods* **2001**, *25*, 402-408.

680 96. Clinical and Laboratory Standards Institute. Performance standards for antimicrobial
681 susceptibility testing, 16th informational supplement. NCCLS document M100-S16. **2006**,
682 National Committee for Clinical Laboratory Standards, Wayne, PA, USA.

683 97. Kamisango, K.; Saiki, I.; Tanio, Y.; Okumura, H.; Araki, Y.; Sekikawa, I.; Azuma, I.;
684 Yamamura, Y. Structures and biological activities of peptidoglycans of *Listeria monocytogenes*
685 and *Propionibacterium acnes*. *J. Biochem.* **1982**, *92*, 23-33.

686

687

688 Table 1. Bacterial strains used in this study

689

690 Bacterial strain Genotype Reference

691

692 *S. aureus*

693 MW2 USA400 wild-type [7]

694 JE2 USA300 wild-type [90]

695 NE272 JE2 *MW2284* mutant [90]

696 NE671 JE2 *MW2285* mutant [90]

697 NE1363 JE2 *srtB* mutant [90]

698 NE1787 JE2 *srtA* mutant [90]

699 *L. monocytogenes*

700 EGD Wild-type [97]

701 EGD *srtA* EGD *srtA* mutant [91]

702 EGD *srtB* EGD *srtB* mutant [91]

703

704

705 Table 2. Microarray analysis of genes dysregulated in *S. aureus* MW2 cells treated with 8X
 706
 707 the SK-03-92 MIC versus untreated cells
 708

709	Locus	Fold-difference	Description
710	<hr/>		
711	<u>Stress Response</u>		
712	<i>SACOL1759</i>	-2.3	universal stress protein family
713	<u>Transporter</u>		
714	<i>SACOL0086</i>	-2.0	drug transporter, putative
715	<i>SACOL0155</i>	-5.7	cation efflux family protein
716	<i>SACOL0178</i>	-2.9	PTS system, IIBC components (<i>scrBC</i>)
717	<i>SACOL0400</i>	-2.6	ascorbate-specific PTS system subunit IIC (<i>ulaA</i>)
718	<i>SACOL0454</i>	-2.3	sodium:dicarboxylate symporter family protein
719	<i>SACOL1018</i>	-2.3	sodium:alanine symporter family protein
720	<i>SACOL1872</i>	-3.0	epidermin immunity protein F (<i>epiE</i>)
721	<i>SACOL2146</i>	-2.7	PTS system, mannitol-specific IIBC components (<i>mtlA</i>)
722	<i>SACOL2333</i>	-2.8	YnfA family protein
723	<i>SACOL2573</i>	-3.2	copper ion binding protein (<i>copZ</i>)
724	<i>SACOL2664</i>	-2.3	mannose-6-phosphate isomerase (<i>manA</i>)
725	<i>SACOL2718</i>	-4.6	2-oxoglutarate/malate translocator, sodium sulfate
726			symporter
727	<u>Signaling/Regulation</u>		
728	<i>SACOL2360</i>	-14.1	LytTR family regulator protein
729	<i>SACOL2361</i>	-26.9	histidine kinase sensor membrane protein

730	<i>SACOL2340</i>	2.2	transcriptional regulator TetR-family
731	<u>Cell Wall Associated</u>		
732	<i>SACOL0151</i>	-2.7	UDP-N-acetylglucosamine 2-epimerase Cap5P (<i>cap5P</i>)
733	<i>SACOL0247</i>	-3.2	holin-like protein LrgA (<i>lrgA</i>)
734	<i>SACOL0612</i>	-2.1	glycosyl transferase, group 1 family protein
735	<i>SACOL1071</i>	-2.2	chitinase-related protein (<i>iraE</i>)
736	<i>SACOL2554</i>	-2.0	holin-like protein CidB (<i>cidB</i>)
737	<i>SACOL2539</i>	4.2	sortase A (<i>srtA</i>)
738	<u>Anabolism/Nucleic Acids</u>		
739	<i>SACOL0130</i>	-2.1	5' nucleotidase family protein
740	<i>SACOL1078</i>	-3.2	phosphoribosylformylglycinamide synthase II (<i>purL</i>)
741	<i>SACOL1082</i>	-2.5	bifunctional purine biosynthesis protein (<i>purH</i>)
742	<i>SACOL1083</i>	-2.6	phosphoribosylamine-glycine ligase (<i>purD</i>)
743	<i>SACOL2329</i>	-3.5	ribose 5-phosphate isomerase (<i>rpiA</i>)
744	<i>SACOL2111</i>	2.2	thymidine kinase (<i>tdk</i>)
745	<i>SACOL2377</i>	2.3	conserved hypothetical protein
746	<u>Anabolism/Proteostasis</u>		
747	<i>SACOL0085</i>	-2.5	peptidase, M20.M25/M40 family
748	<i>SACOL2605</i>	-9.6	ribulosamine 3-kinase
749	<i>SACOL0457</i>	2.6	conserved hypothetical protein, heat induced stress
750	<i>SACOL0590</i>	2.4	30S ribosomal protein L7 Ae
751	<i>SACOL0877</i>	2.5	glycine cleavage system H protein (<i>gcvH</i>)
752	<i>SACOL1907</i>	2.4	ribosomal large subunit pseudouridine synthase (<i>rluD</i>)

753	<i>SACOL1939</i>	2.3	phosphotyrosine protein phosphatase (<i>ptpA</i>)
754	<i>SACOL2596</i>	2.6	metallo-dependent amidohydrolase
755	<u>Lipid Metabolism</u>		
756	<i>SACOL2091</i>	-2.5	beta-hydroxyacyl-dehydratase FabZ (<i>fabZ</i>)
757	<i>SACOL2459</i>	-3.8	para-nitrobenzyl esterase (<i>pnbA</i>)
758	<i>SACOL1142</i>	10.0	aerobic glycerol-3-phosphate dehydrogenase (<i>glpD</i>)
759	<u>Catabolism</u>		
760	<i>SACOL0135</i>	-2.4	alcohol dehydrogenase, iron-containing (<i>adhE</i>)
761	<i>SACOL0660</i>	-3.4	alcohol dehydrogenase, zinc-containing (<i>adhA</i>)
762	<i>SACOL1158</i>	-2.5	succinate dehydrogenase, cytochrome b558 subunit (<i>sdhC</i>)
763	<i>SACOL1604</i>	-2.1	glucokinase (<i>glk</i>)
764	<i>SACOL2338</i>	-3.5	hypothetical protein (putative oxidoreductase)
765	<i>SACOL1713</i>	2.3	hypothetical protein, putative ammonia monooxygenase
766	<u>Unknown</u>		
767	<i>SACOL0089</i>	-4.4	myosin-reactive antigen, 67 kDa
768	<i>SACOL2315</i>	-3.8	conserved hypothetical protein
769	<i>SACOL2338</i>	-3.4	conserved hypothetical protein
770	<i>SACOL2491</i>	-2.9	conserved hypothetical protein
771	<i>SACOL0742</i>	3.1	conserved hypothetical protein
772	<i>SACOL1789</i>	2.4	conserved hypothetical protein

773 Table 3. Oligonucleotide primers used in this study
 774

775	776	777	778
Primer	Gene	Sequence	
779	SaFtsZ1	<i>ftsZ</i>	5'- GGTGTAGGTGGTGGCGGTAA - 3'
780			
781	SaFtsZ2		5'- TCATTGGCGTAGATTTGTC - 3'
782			
783	GuaBF1	<i>guaB</i>	5'- GCTCGTCAAGGTGGTTTAGGTG -3'
784			
785	GuaBR1		5'- TAAGACATGCACACCTGCTTCG -3'
786			
787	SrtA1	<i>srtA</i>	5'- TCGCTGGTGTGGTACTTATC - 3'
788			
789	SrtA2		5'- CAGGTGTTGCTGGTCCTGGA - 3'
790			
791	MW2284A	<i>MW2284</i>	5'- CAATGCAAATGAGACGGAATCT -3'
792			
793	MW2284B		5'- GAAGAATAGGTGTAGTGTGCAT -3'
794			
795	MW2285A	<i>MW2285</i>	5'- GTATGTTATTTGCAGACGGCAA -3'
796			
797	MW2285B		5'- AAAGGCAAGAATCCGACATACG -3'
798			
799	SA2043A	<i>tdk</i>	5'- CTTGTTCACTGACAGCCATCA -3'
800			
801	SA2043B		5'- ACGCACGACTTAACTAATGTTG -3'
802			
803	SaPurD1	<i>purD</i>	5'- CAGCCGCTAATTGATGGATTA -3'
804			
805	SaPurD2		5'- AGCACTTCTGGCTGCTTCAAT -3'
806			
807	SaPurH1	<i>purH</i>	5'- CCAGAAATAATGGATGGCCGT -3'
808			
809	SaPurH2		5'- TGCCGGATGTACAATTGTTGT -3'
810			
811	SaPurL1	<i>purL</i>	5'- GTTATGTGGAGTGAACATTGC -3'
812			
813	SaPurL2		5'- AGCCCAATAGAGACAATGTC -3'
814			

817 Table 4. MIC results for *S. aureus* and *L. monocytogenes* mutants and wild-type strains
 818 against SK-03-92

819

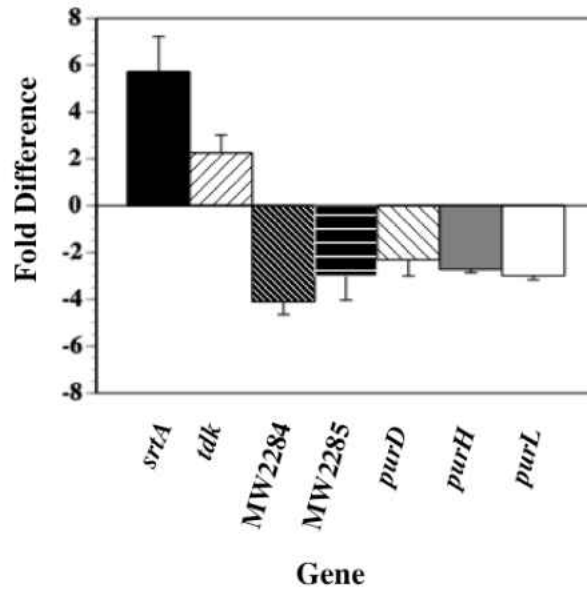
820

821 Strain	822 Genotype	823 MIC
824 <i>S. aureus</i>		
825 JE2	826 Wild-type	827 1 ^a
828 NE272	829 <i>MW2285</i>	830 1
831 NE671	832 <i>MW2284</i>	833 1
834 NE1363	835 <i>srtB</i>	836 1
837 NE1787	838 <i>srtA</i>	839 0.5
840 <i>L. monocytogenes</i>		
841 EGD	842 Wild-type	843 1
844 EGD <i>srtA</i>	845 <i>srtA</i>	846 0.125
847 EGD <i>srtB</i>	848 <i>srtB</i>	849 1

845 ^aMean±standard deviation from three separate runs.

848 Figure 1. Quantitative reverse transcribed-polymerase chain reaction results of *S. aureus*
849 MW2 cells treated with 8X the SK-03-92 MIC versus untreated cells

850

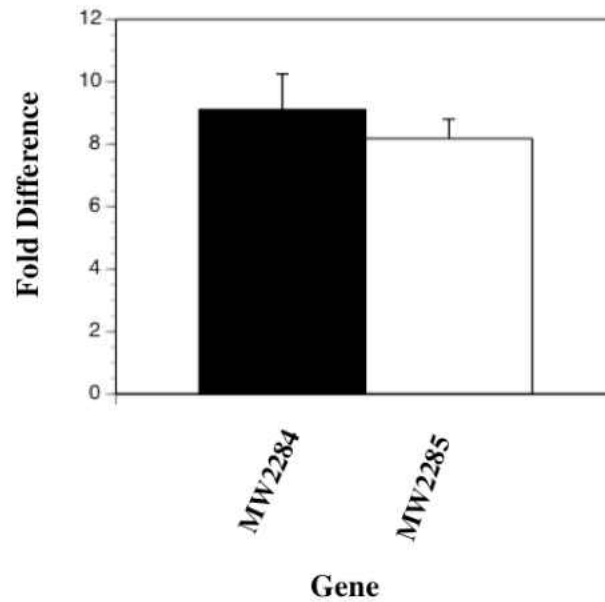


851
852
853
854
855
856
857
858
859

^aMean±standard deviation from three separate runs.

860 Figure 2. Quantitative reverse transcribed-polymerase chain reaction results of *S. aureus*
861 *srtA* transcription in wild-type bacteria compared to *MW2284* and *MW2285*
862 mutants

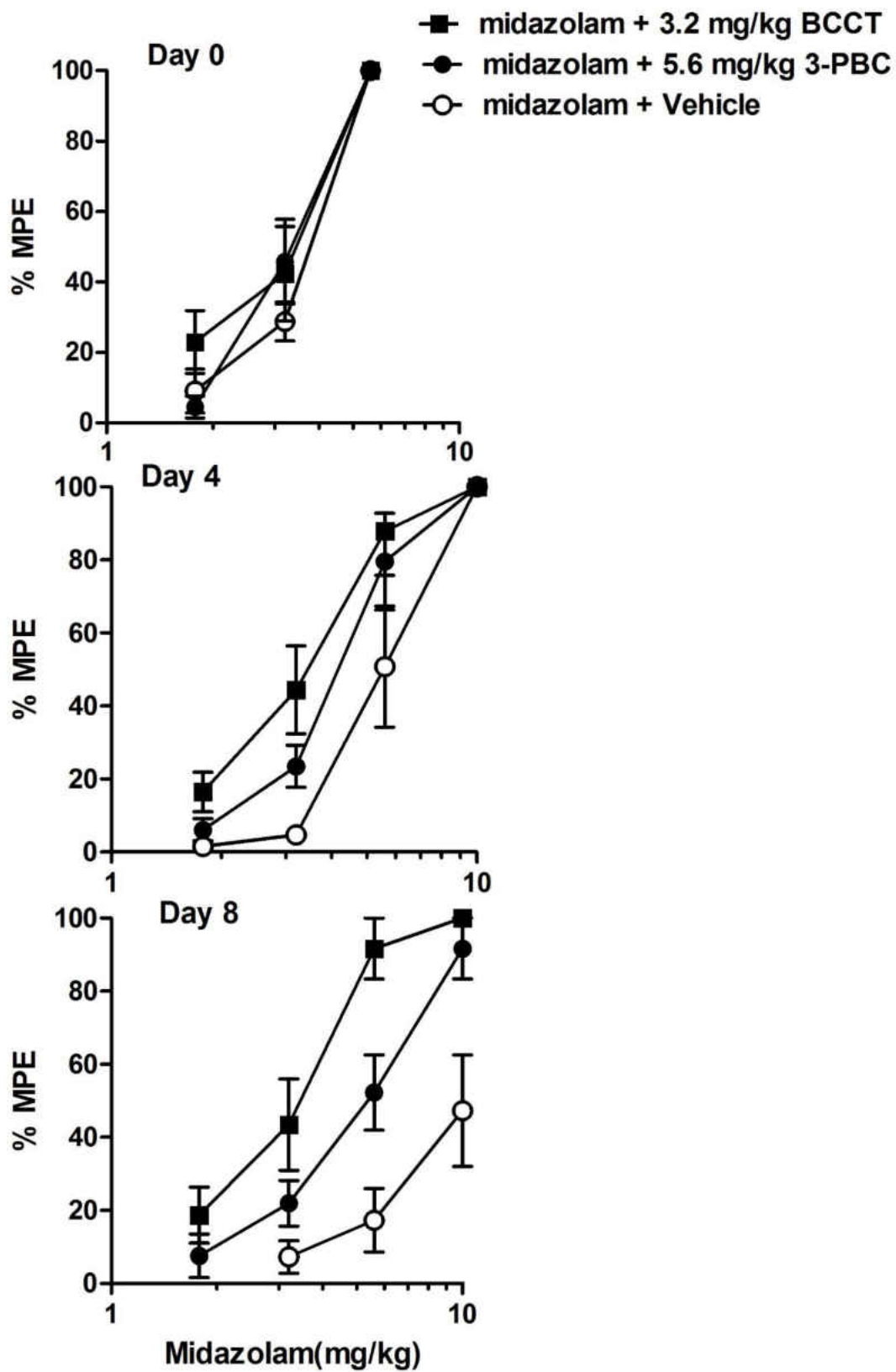
863
864
865



866
867
868
869
870
871
872
873
874
875
876

^aMean ± standard deviation from three separate runs.

APPENDIX B
MIDAZOLAM TOLERANCE DATA



APPENDIX C
SYNTHESIS AND BIOLOGY DATA FOR β -AND AZA- β -CARBOLINES



US008268854B2

(12) **United States Patent**
Cook et al.(10) **Patent No.:** US 8,268,854 B2
(45) **Date of Patent:** Sep. 18, 2012(54) **AZA-BETA-CARBOLINES AND METHODS OF USING SAME**(75) Inventors: **James M. Cook**, Whitefish Bay, WI (US); **Michael L. Van Linn**, Shorewood, WI (US); **Wenyuan Yin**, Milwaukee, WI (US)(73) Assignee: **The UWM Research Foundation, Inc.**, Milwaukee, WI (US)

(*) Notice: Subject to any disclaimer, the term of this patent is extended or adjusted under 35 U.S.C. 154(b) by 461 days.

(21) Appl. No.: 12/471,019

(22) Filed: **May 22, 2009**(65) **Prior Publication Data**

US 2009/0306121 A1 Dec. 10, 2009

Related U.S. Application Data

(60) Provisional application No. 61/055,334, filed on May 22, 2008.

(51) **Int. Cl.****C07D 471/12** (2006.01)**A61K 31/437** (2006.01)(52) **U.S. Cl.** **514/290**; 546/82; 546/85(58) **Field of Classification Search** 546/82, 546/85; 514/290

See application file for complete search history.

(56) **References Cited****U.S. PATENT DOCUMENTS**

2003/0176456 A1 9/2003 June et al.

FOREIGN PATENT DOCUMENTSEP 0030254 6/1981
WO 2007/085679 8/2007
WO 2008/132454 11/2008
WO 2009/143445 11/2009**OTHER PUBLICATIONS**

Dorwald F. A. Side Reactions in Organic Synthesis. 2005. Wiley: VCH, Weinheim p. IX of Preface.*

Allen, M.S. et al., "Predictive binding of beta-carboline inverse agonists and antagonists via the CoMFA/GoI.PF approach." J. Med. Chem. (1992) 35:4001-4010.

Allen, M.S. et al., "Synthesis of novel 3-substituted beta-carbolines as benzodiazepine receptor ligands: probing the benzodiazepine receptor pharmacophore." J. Med. Chem. (1988) 31:1854-1861.

Allen, M.S. et al., "Synthetic and computer-assisted analyses of the pharmacophore for the benzodiazepine receptor inverse agonist site." J. Med. Chem. (1990) 33:2343-2357.

Barberis, C. et al., "Cu(I)-catalyzed intramolecular cyclization of *cis*-carbamates: synthesis of indoles and pyrrolo [2,3-*c*] pyridines." Tetrahedron Lett. (2005) 46:8877-8880.

Bedford, R.B. et al., "N-H Carbazole synthesis from 2-chloroanilines via consecutive amination and C-H activation." J. Org. Chem. (2003) 71:9403-9410.

Bell, R.L. et al., "The alcohol-preferring P rat and animal models of excessive alcohol drinking." Addict Biol. (2006) 11:270-288.

Cao, R. et al., "beta-carboline alkaloids: biochemical and pharmacological functions." Curr. Med. Chem. (2007) 14:279-500.

Choudhary, M.S. et al., "Identification of receptor domains that modify ligand binding to 5-hydroxytryptamine₂ and 5-hydroxytryptamine_{1c} serotonin receptors." Mol. Pharmacol. (1992) 42:627-633.

Cox, F. et al., "beta1 receptor subtype specific ligands. Synthesis and biological properties of betaCC5, a beta1 receptor subtype specific antagonist." Med. Chem. Res. (1995) 5:710-718.

Driver, M.S. et al., "A second generation catalyst for aryl halide amination." J. Am. Chem. Soc. (1996) 118:7217-7218.

Eitel, L. et al., "Metalation:SRNI coupling in heterocyclic synthesis. A convenient methodology for ring functionalization." J. Org. Chem. (1988) 53:2740-2744.

Fuchs, K. et al., "Endogenous [3H] flunitrazepam binding in human embryonic kidney cell line 293." Eur. J. Pharmacol. (1995) 289:87-95.

Harvey, S. et al., "The GABA(A) receptor alpha1 subtype in the ventral pallidum regulates alcohol-seeking behaviors." J. Neuroscience (2002) 22:3765-3775.

Jonckers, T.H.M. et al., "Synthesis of isocryptolepine via a Pd-catalyzed 'amination-arylation' approach." Synlett. (2003) 615-617.

June, H.J. et al., "The reinforcing properties of alcohol are mediated by GABA(A) receptors in the ventral pallidum." Neuropsychopharmacol. (2003) 28:2124-2137.

Li, X. et al., "Synthesis of optically active tryptophans as IDO inhibitors." Tetrahedron Lett. (2004) 45:8569-8573.

Monguchi, Y. et al., "Pd/C-FT3N-mediated catalytic hydrochlorination of arnatic chlorides under mild conditions." Tetrahedron Lett. (2006) 62:7926-7933.

Namjoshi, O.A. et al., "Development of a two-step route to 3-PBC and betaCCt, two agents active against alcohol self-administration in rodent and primate models." J. Org. Chem. (2011) 76:4721-4727.

Roth, B.L. et al., "5-hydroxytryptamine₂ receptors coupled to phospholipase C in rat aorta: modulation of phosphoinositide turnover by phorbol ester." J. Pharmacol. Exp. Ther. (1986) 238:480-485.

Roth, B.L. et al., "Binding of typical and atypical antipsychotic agents to 5-hydroxytryptamine-6 and 5-hydroxytryptamine-7 receptors." J. Pharmacol. Exp. Ther. (1994) 268:1403-1410.

Savic, M. M. et al., "PW7-029, a compound with moderate inverse agonist functional selectivity at GABA(A) receptors containing alpha5 subunits, improves passive but not active avoidance learning in rats." Brain Res. (2008) 1208:150-159.

Sigel, E. et al., "The effect of subunit composition of rat brain GABA(A) receptors on channel function." Neuron (1990) 5:703-711.

Sigel, E., "Properties of single sodium channels translated by *Xenopus* oocytes after injection with messenger ribonucleic acid." J. Physiol. (1987) 386:73-90.

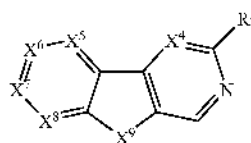
(Continued)

Primary Examiner — Rita Desai

(74) Attorney, Agent, or Firm — Michael Best & Friedrich L.L.P.

(57) **ABSTRACT**

Provided are compounds having the general structure according to formula (I):



(I)

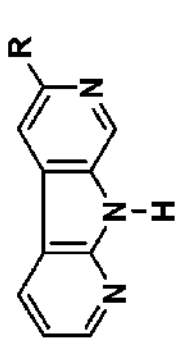
Further provided are pharmaceutical compositions comprising these compounds. The invention still further provides methods of treating alcoholism, methods of reducing alcohol intake, methods of treating anhedonia, and methods of treating anxiety using these compounds or the compositions containing them.

18 Claims, 21 Drawing Sheets

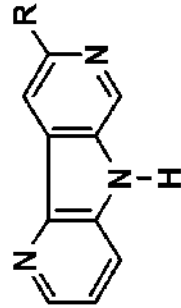
OTHER PUBLICATIONS

- Turner, J.A., "Regiospecific electrophilic substitution of aminopyridines: ortho lithiation of 2-, 3-, and 4-(pivaloylamino)pyridines," *J. Org. Chem.* (1983) 48:3401-3408.
- Yin, W. et al., "Search for benzodiazepine-GABA(A) subtype selective ligands that reverse alcohol self-administration," Abstracts of Papers, 224th ACS National Meeting, Boston, MA, Aug. 18-22, 2002, MFDD-244.
- Yin, W. et al., "Synthesis of bivalent ligands of beta-carboline-3-carboxylates via a palladium-catalyzed homo-coupling process," *Tetrahedron Lett.* (2005) 46:6363-6368.
- Yin, W., Ph.D. Thesis, "Part II. Design, synthesis and pharmacology of selective ligands for alpha1-containing GABAa/benzodiazepine receptor subtypes. SAR studies of beta-carbolines at positions-3 and -6 and their corresponding bivalent ligands," University of Wisconsin-Milwaukee, Milwaukee, WI (2007) 163-198.
- Yu, J. et al., "General approach for the synthesis of sarpagine indole alkaloids. Enantiospecific total synthesis of (+)-vellosimine, (+)-normacusine B, (-)-alkaloid A3, (-)-panarine, (+)-na-methyl-16-epipericyclivine," *J. Org. Chem.* (2003) 68:7565-7581.
- International Search Report and Written Opinion for Application No. PCT/US2009/045014 dated Oct. 29, 2009 (9 pages).

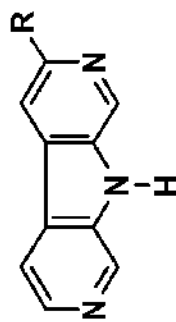
* cited by examiner



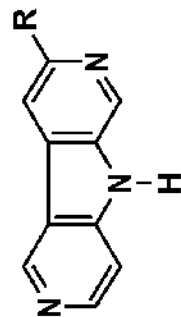
100, R = CO₂tBu
 101, R = OCH₂CH₂CH₃



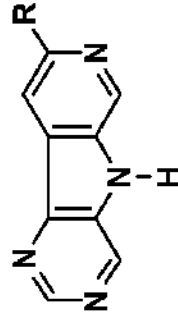
5, R = CO₂tBu
 6, R = OCH₂CH₂CH₃



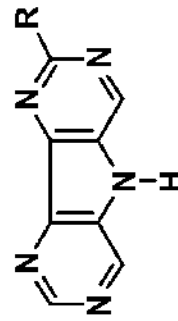
3, R = CO₂tBu
 4, R = OCH₂CH₂CH₃



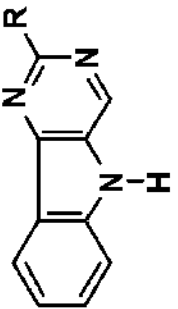
1, R = CO₂tBu
 2, R = OCH₂CH₂CH₃



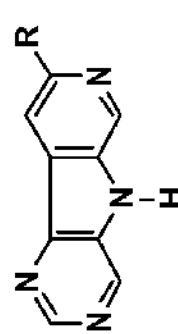
56, R = CO₂tBu
 57, R = OCH₂CH₂CH₃



54, R = CO₂tBu
 55, R = OCH₂CH₂CH₃,



52, R = CO₂tBu
 53, R = OCH₂CH₂CH₃



50, R = CO₂tBu
 51, R = OCH₂CH₂CH₃

FIG. 1

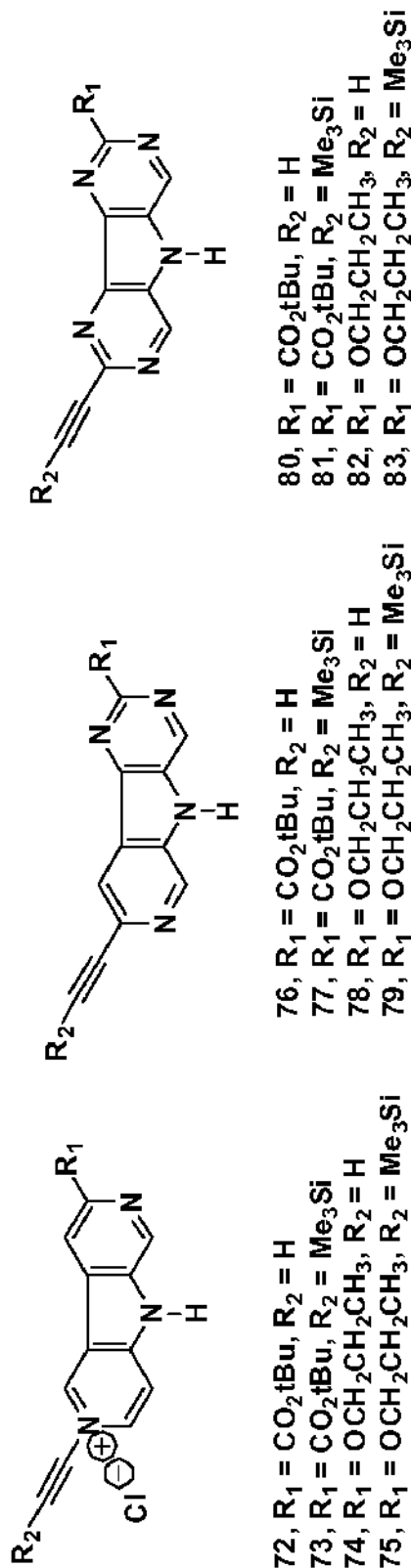
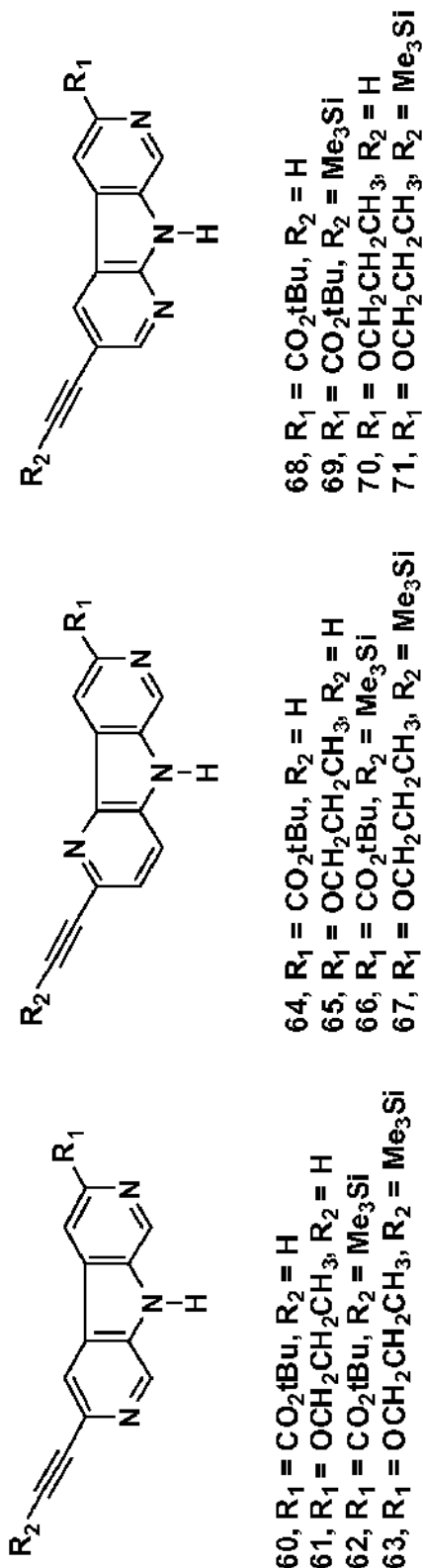


FIG. 2 (1 of 2)

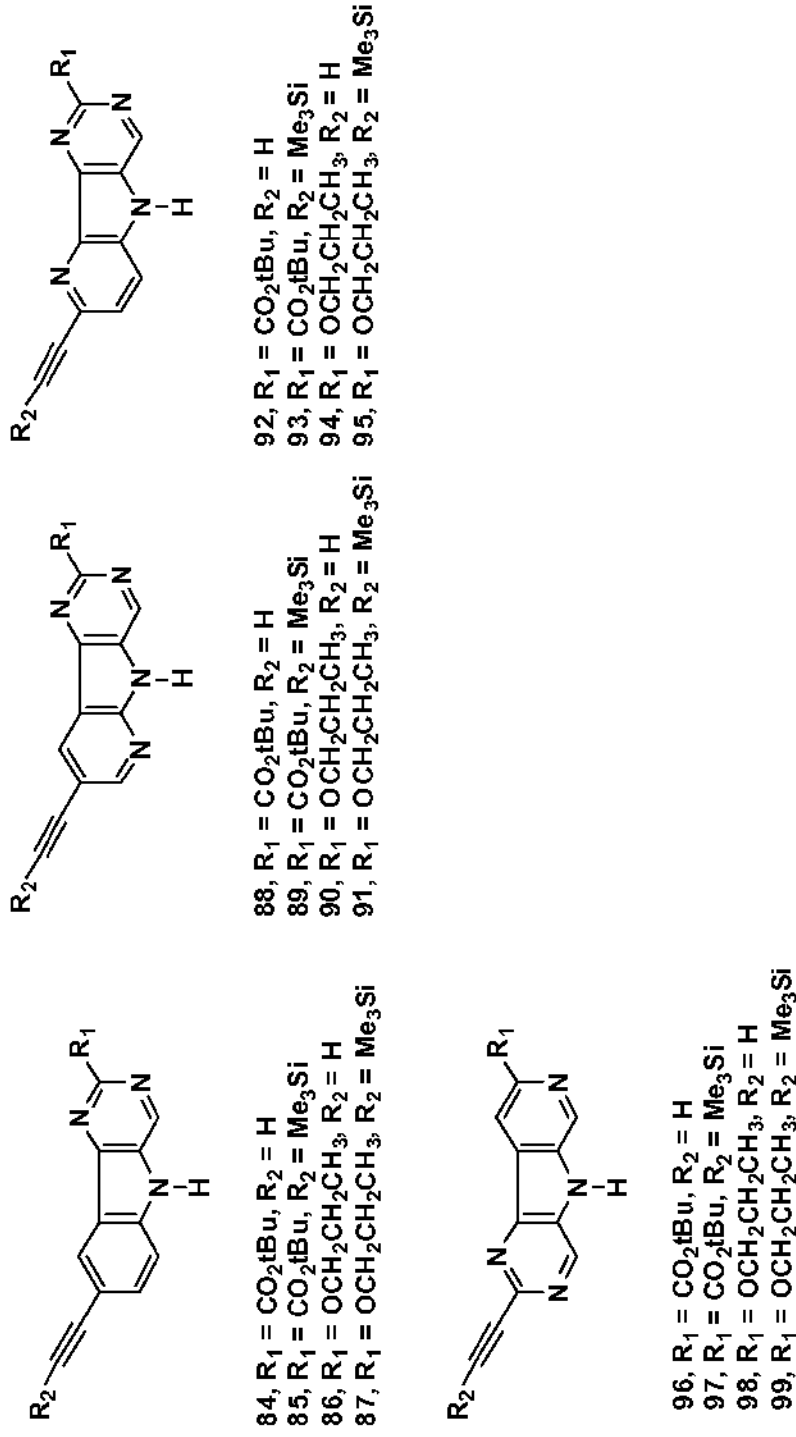


FIG. 2 (2 of 2)

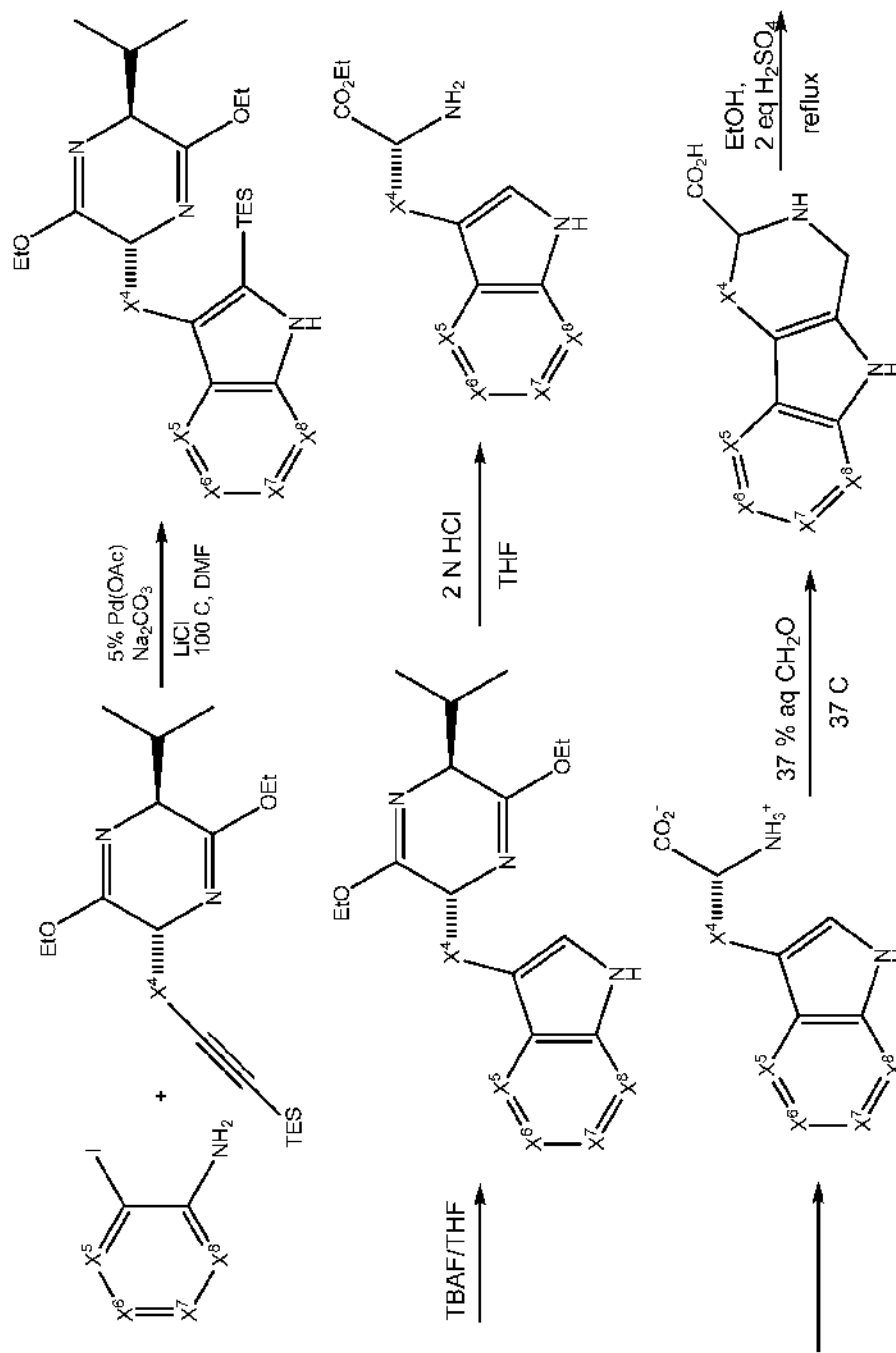
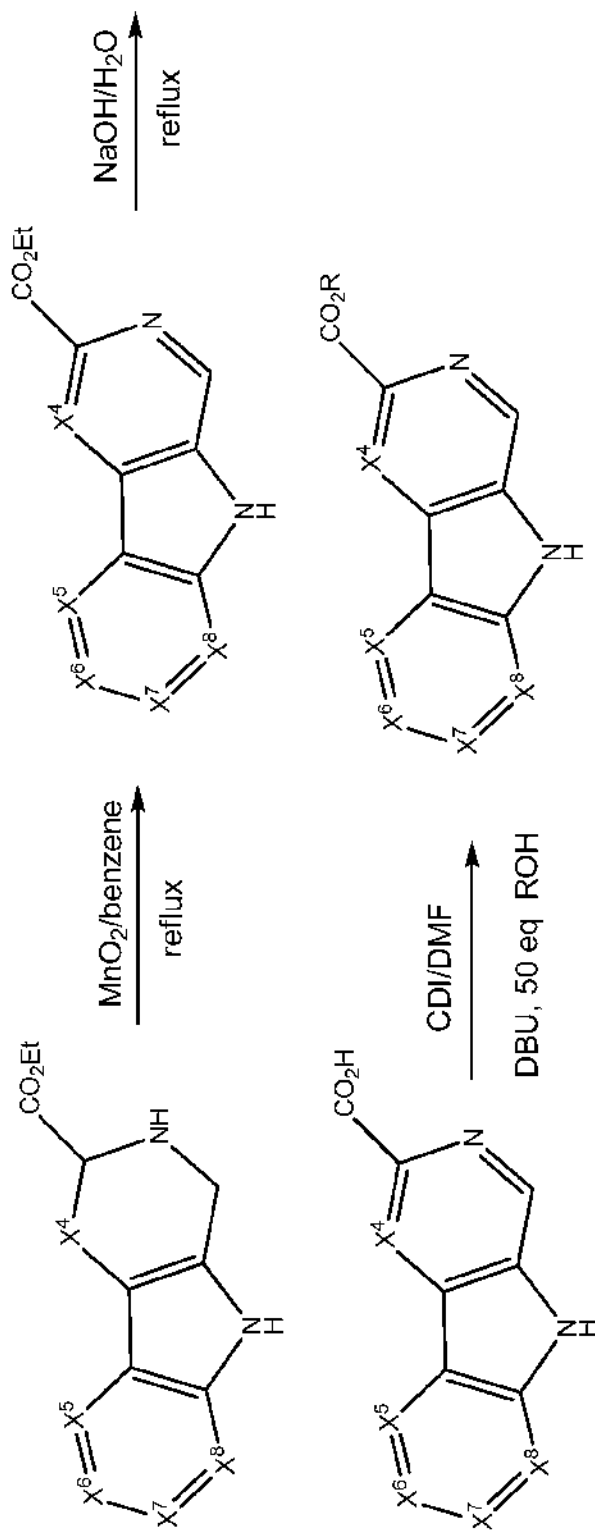


FIG. 3 (1 of 2)



where X⁴, X⁵, X⁶, X⁷, X⁸ and R are as defined for Formula (I).

FIG. 3 (2 of 2)

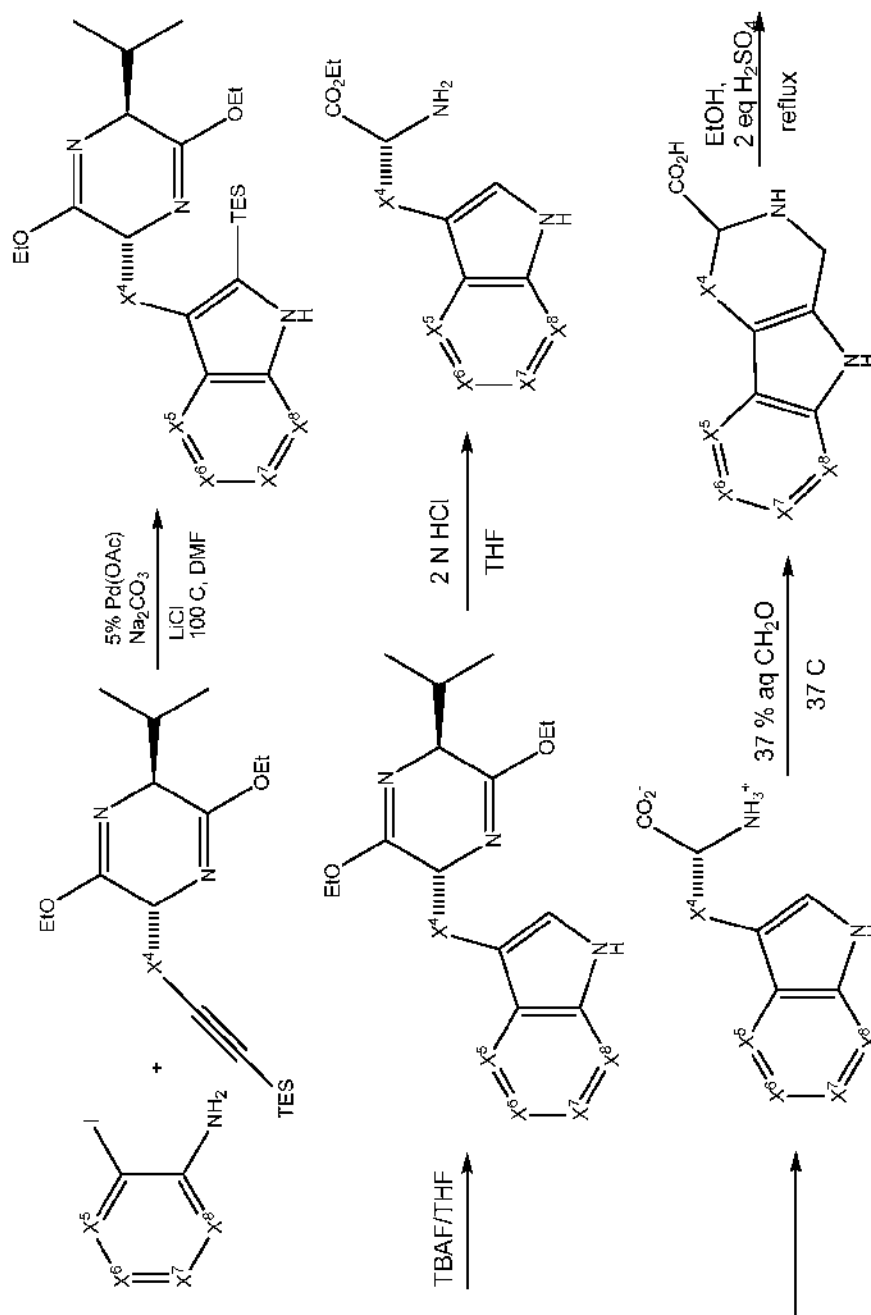
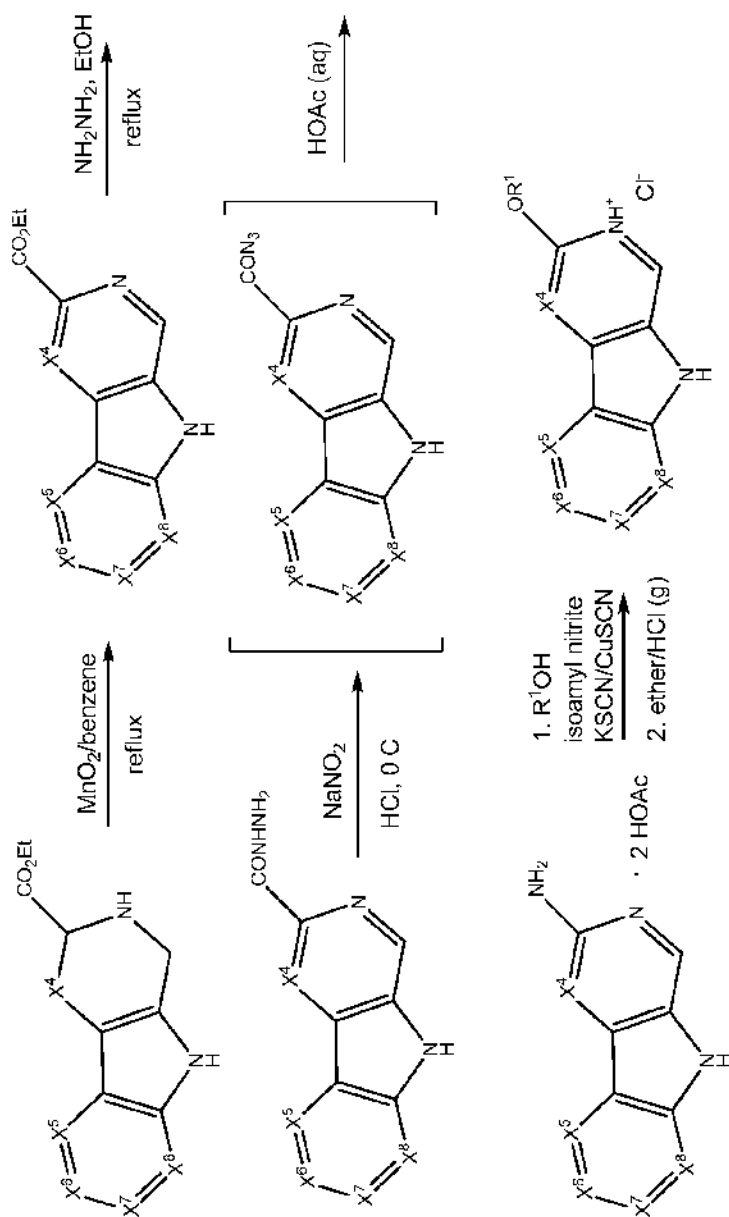
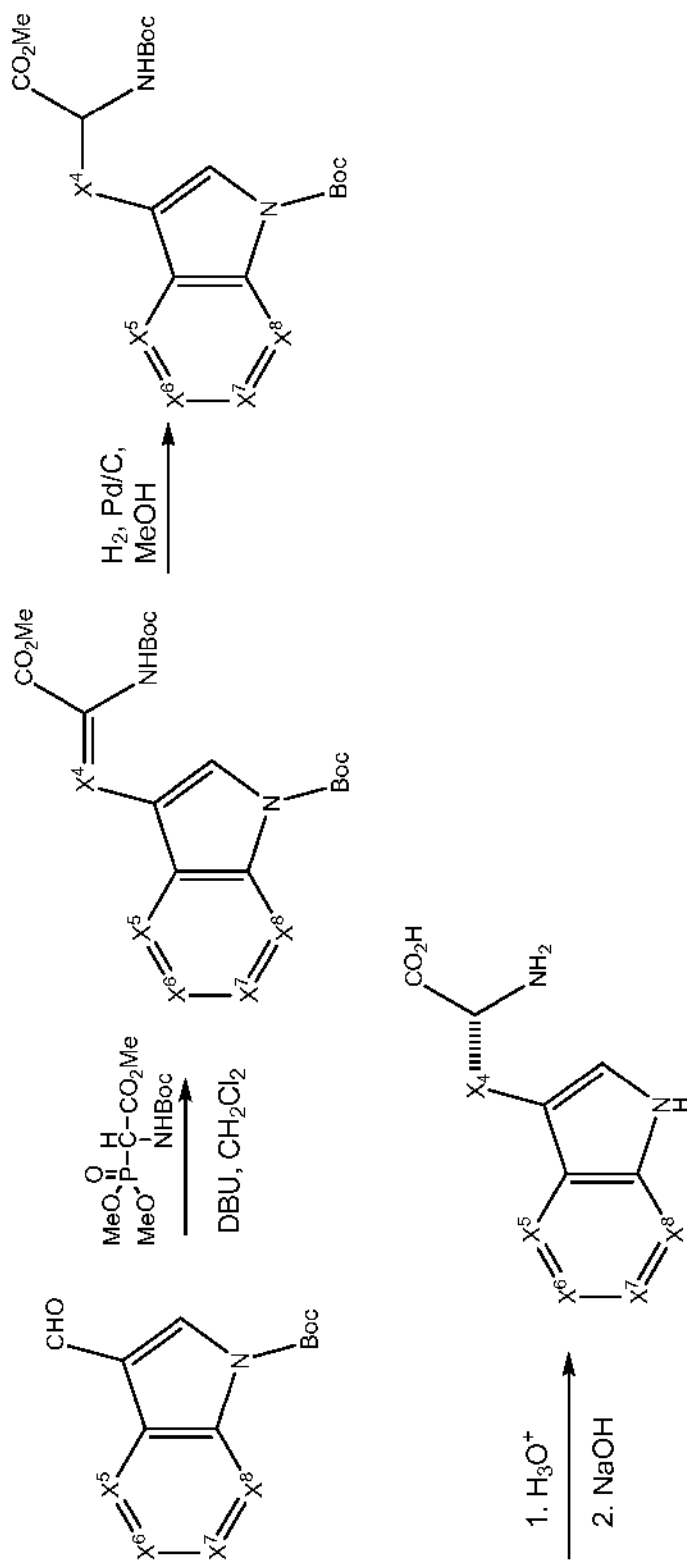


FIG. 4 (1 of 2)



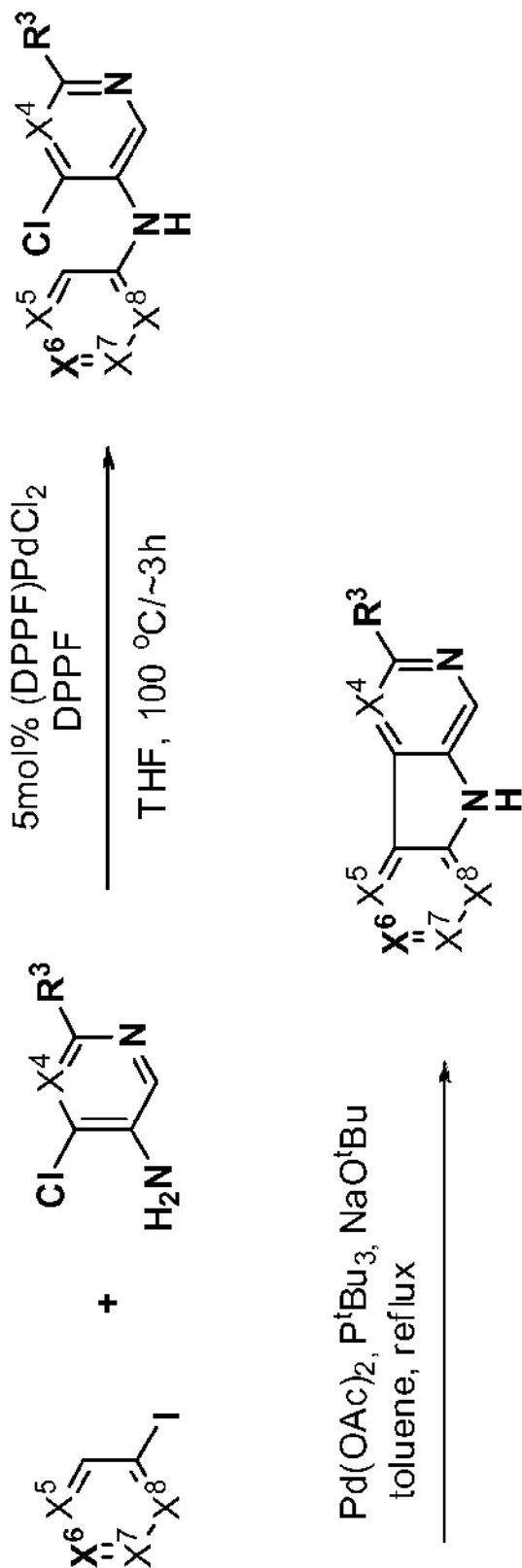
where X^4 , X^5 , X^6 , X^7 , X^8 and R are as defined for Formula (1).

FIG. 4 (2 of 2)



where X⁴ is CH, and X⁵, X⁶, X⁷, X⁸ and R are as defined for Formula (I).

FIG. 5



where X⁴, X⁵, X⁶, X⁷, X⁸ and R³ are as defined for Formula (I).

FIG. 6

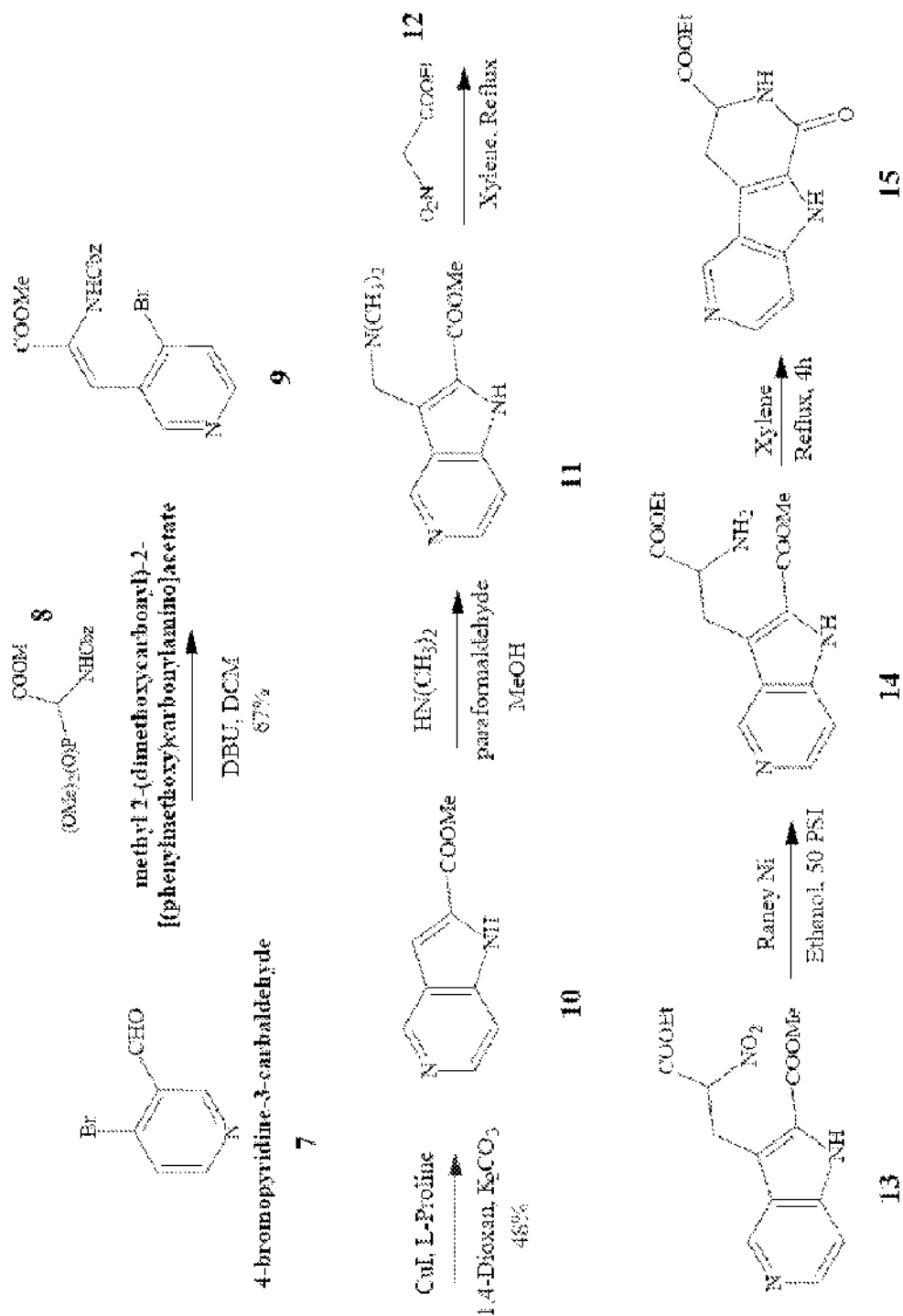


FIG. 7 (1 of 2)

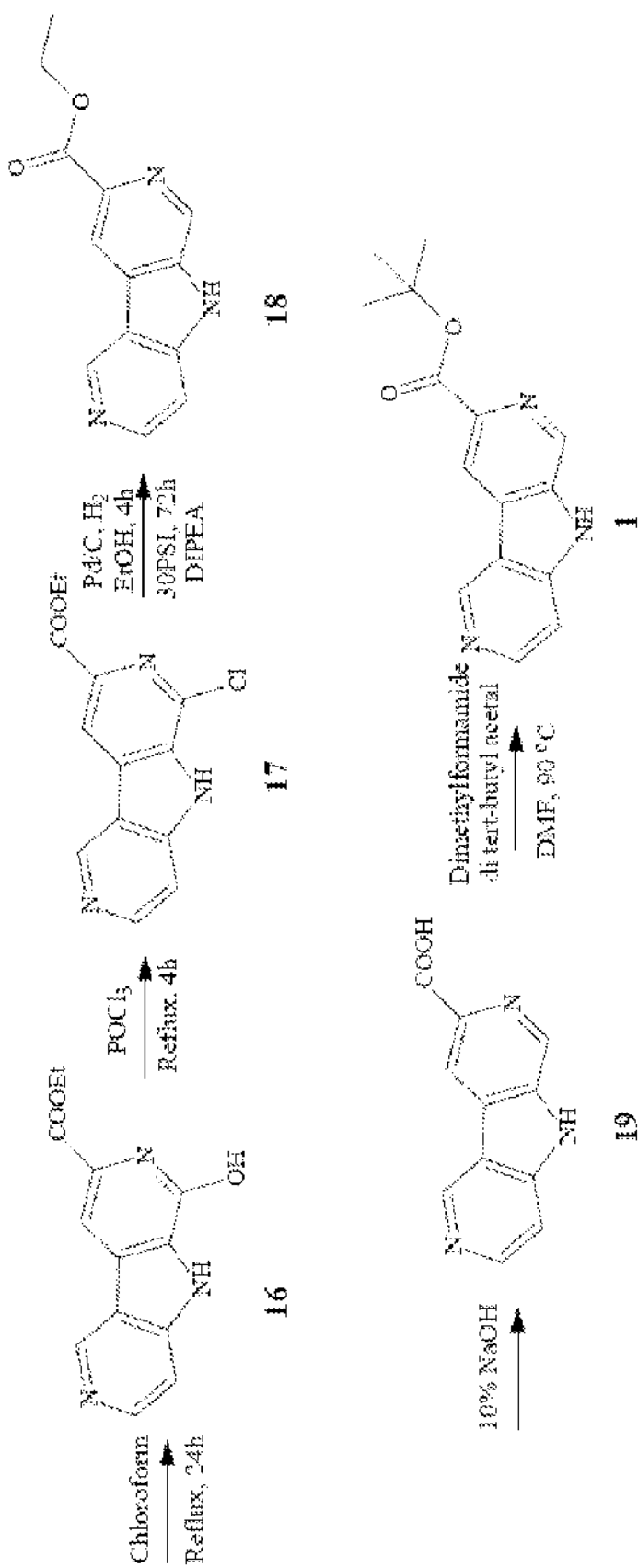


FIG. 7 (2 of 2)

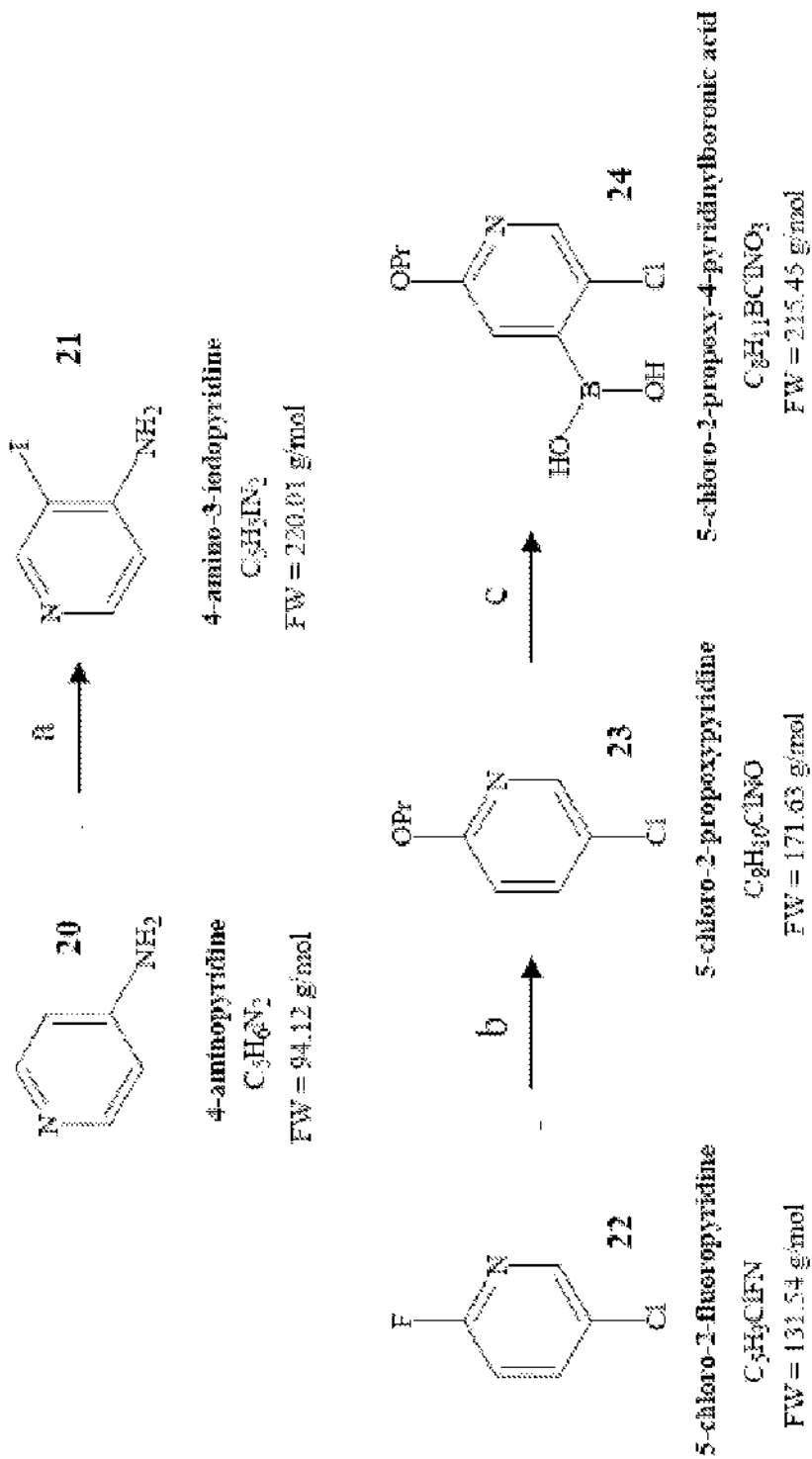


FIG. 8 (1 of 2)

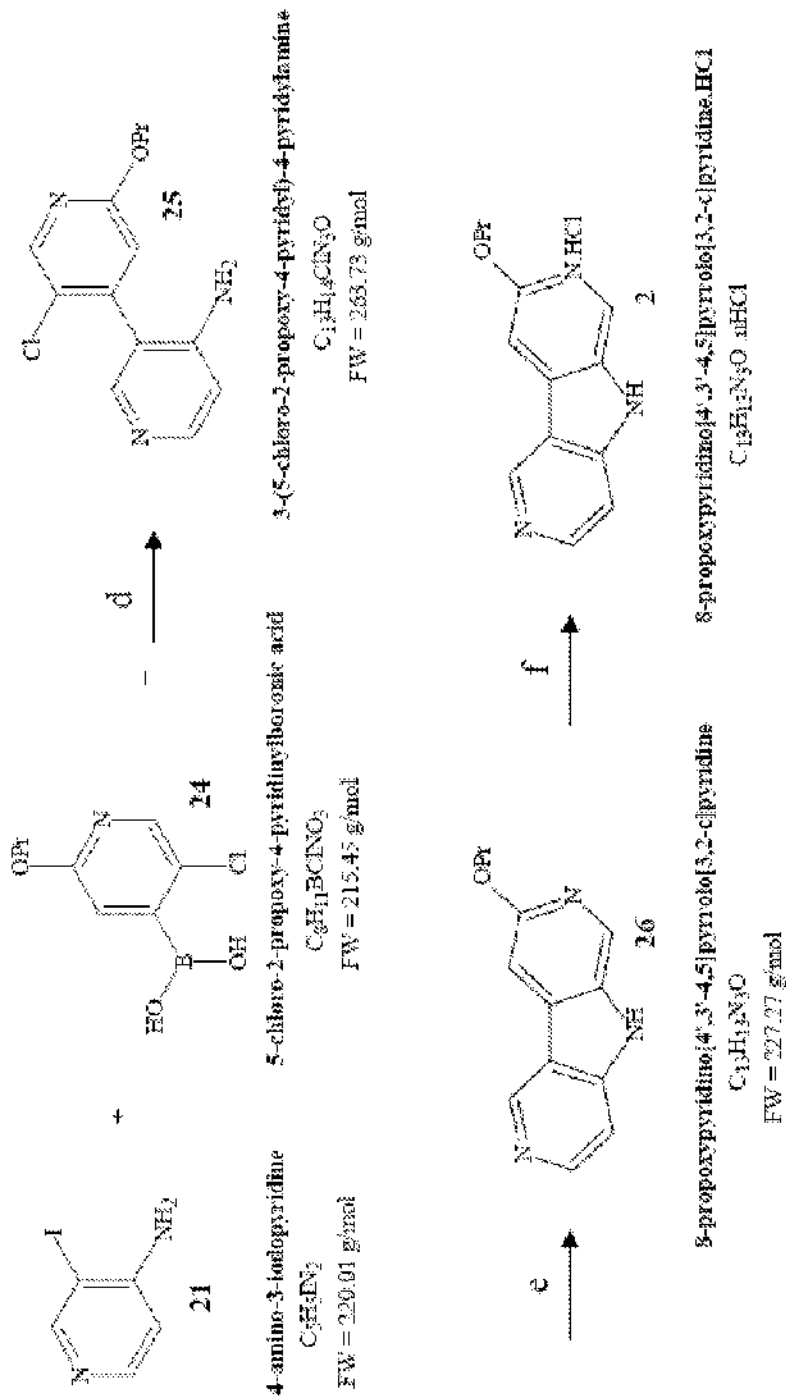


FIG. 8 (2 of 2)

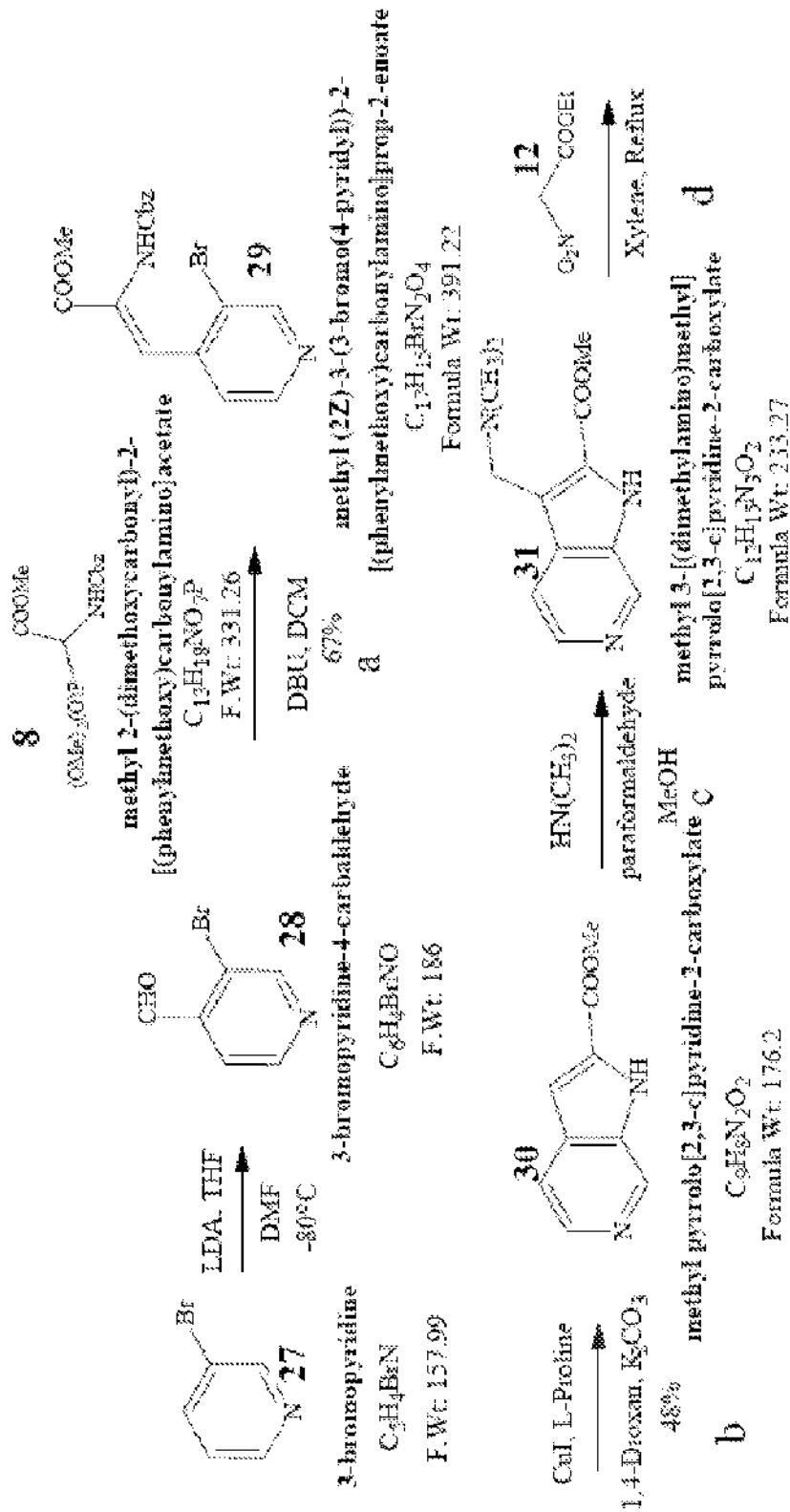


FIG. 9 (1 of 2)

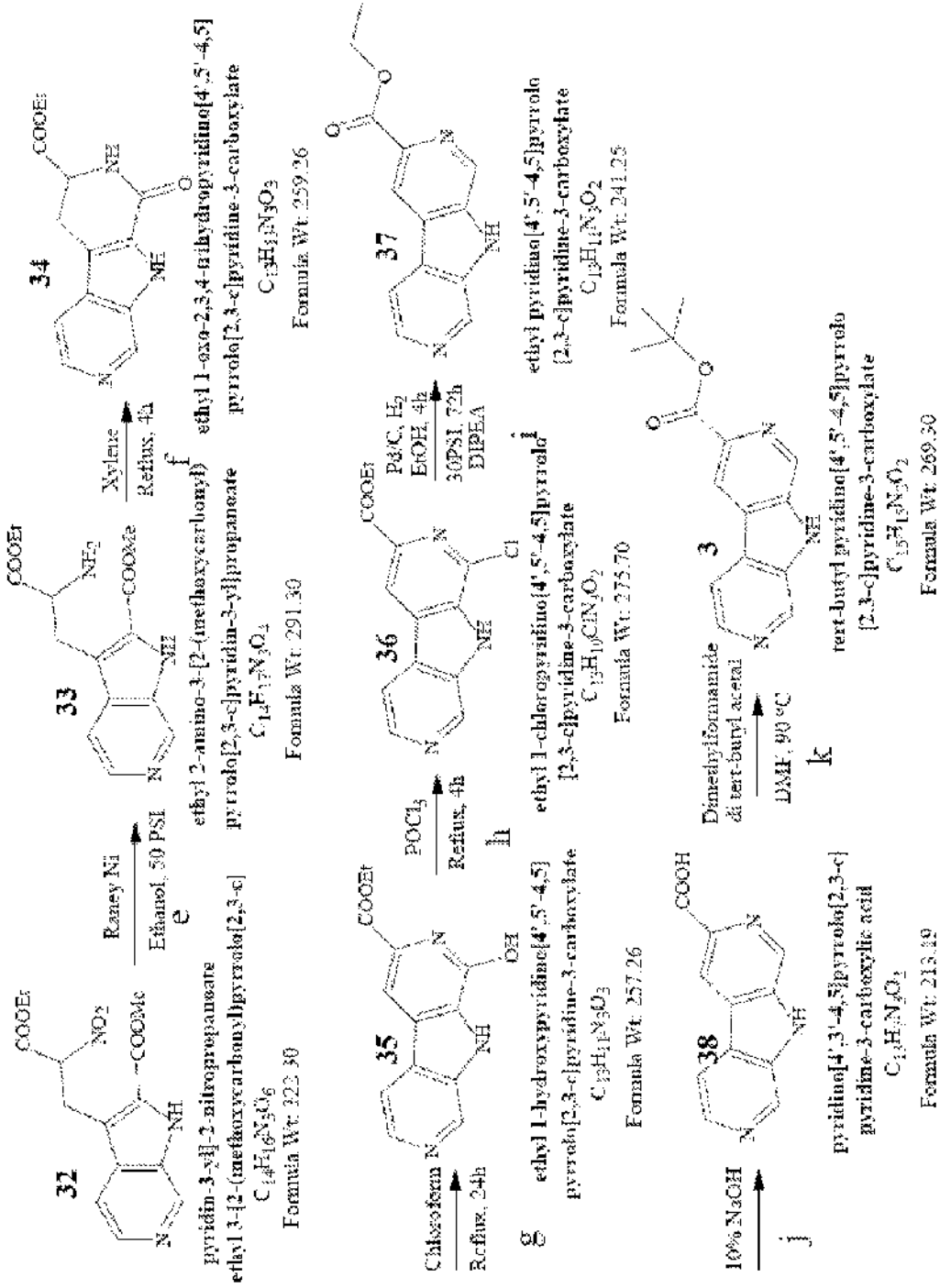


FIG. 9 (2 of 2)

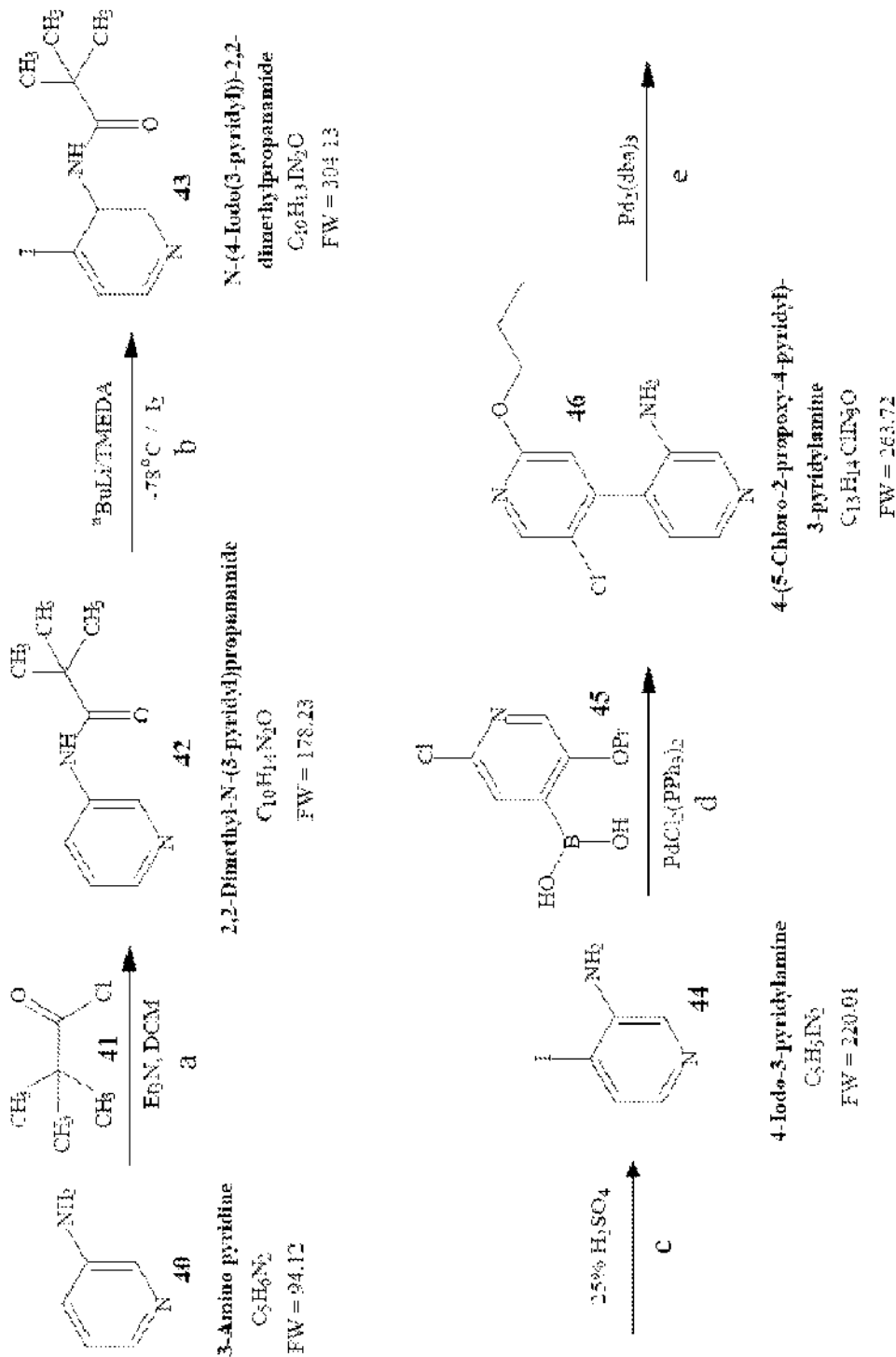
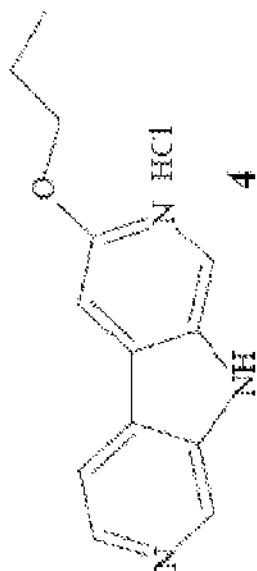
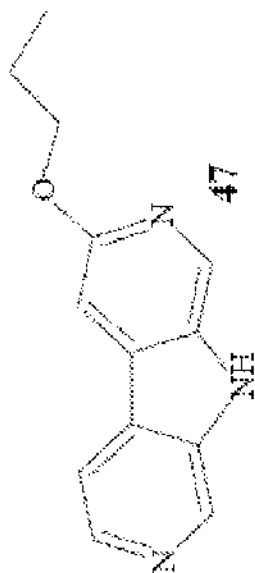
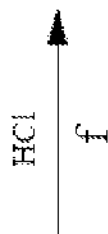


FIG. 10 (1 of 2)



3-Propoxytryptamine [4,3'-4,5]pyrrolo[2,3-c]pyridine hydrochloride
 $C_{13}H_{13}N_3O$

FW = 227.26



3-Propoxytryptamine [4,3'-4,5]pyrrolo[2,3-c]pyridine

$C_{13}H_{13}N_3O$

FW = 227.26

FIG. 10 (2 of 2)

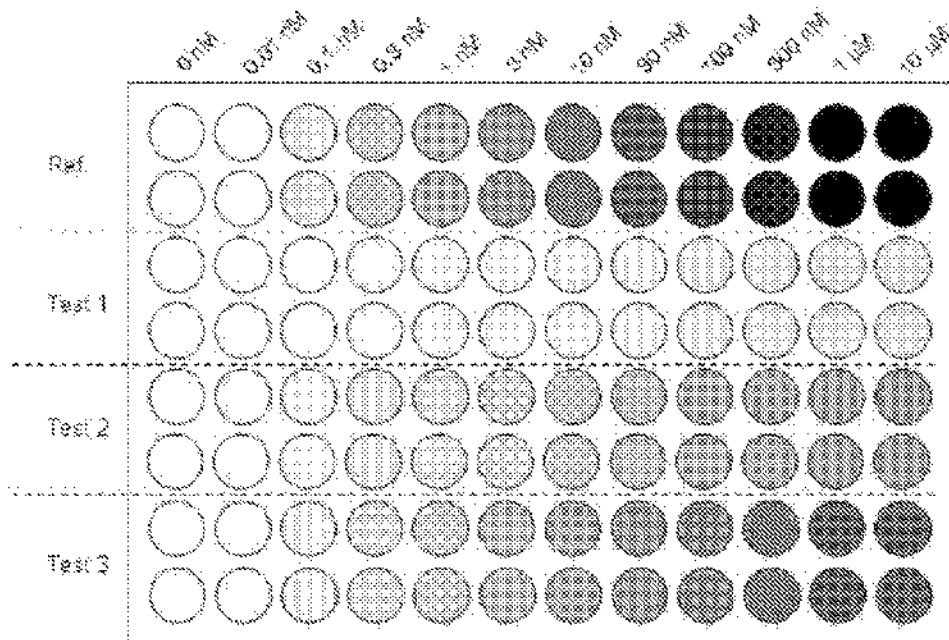


FIG. 11

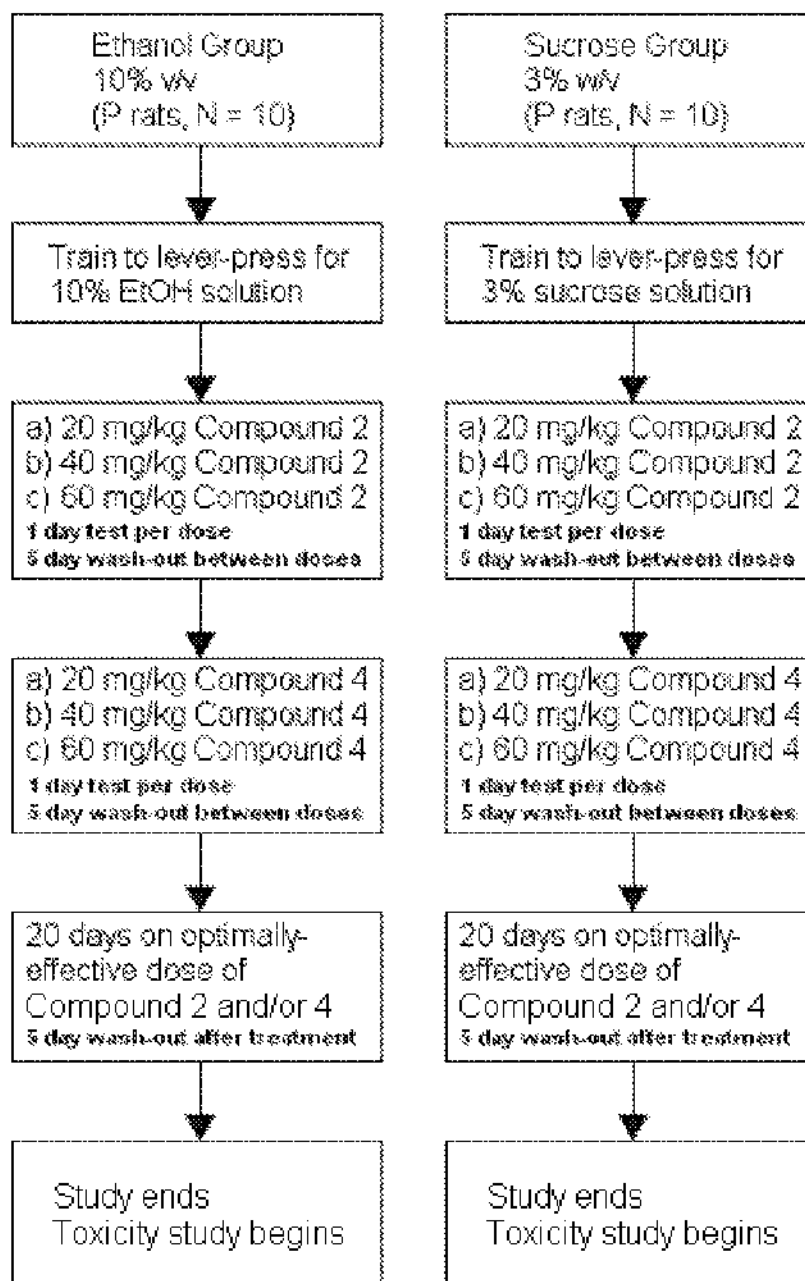


FIG. 12

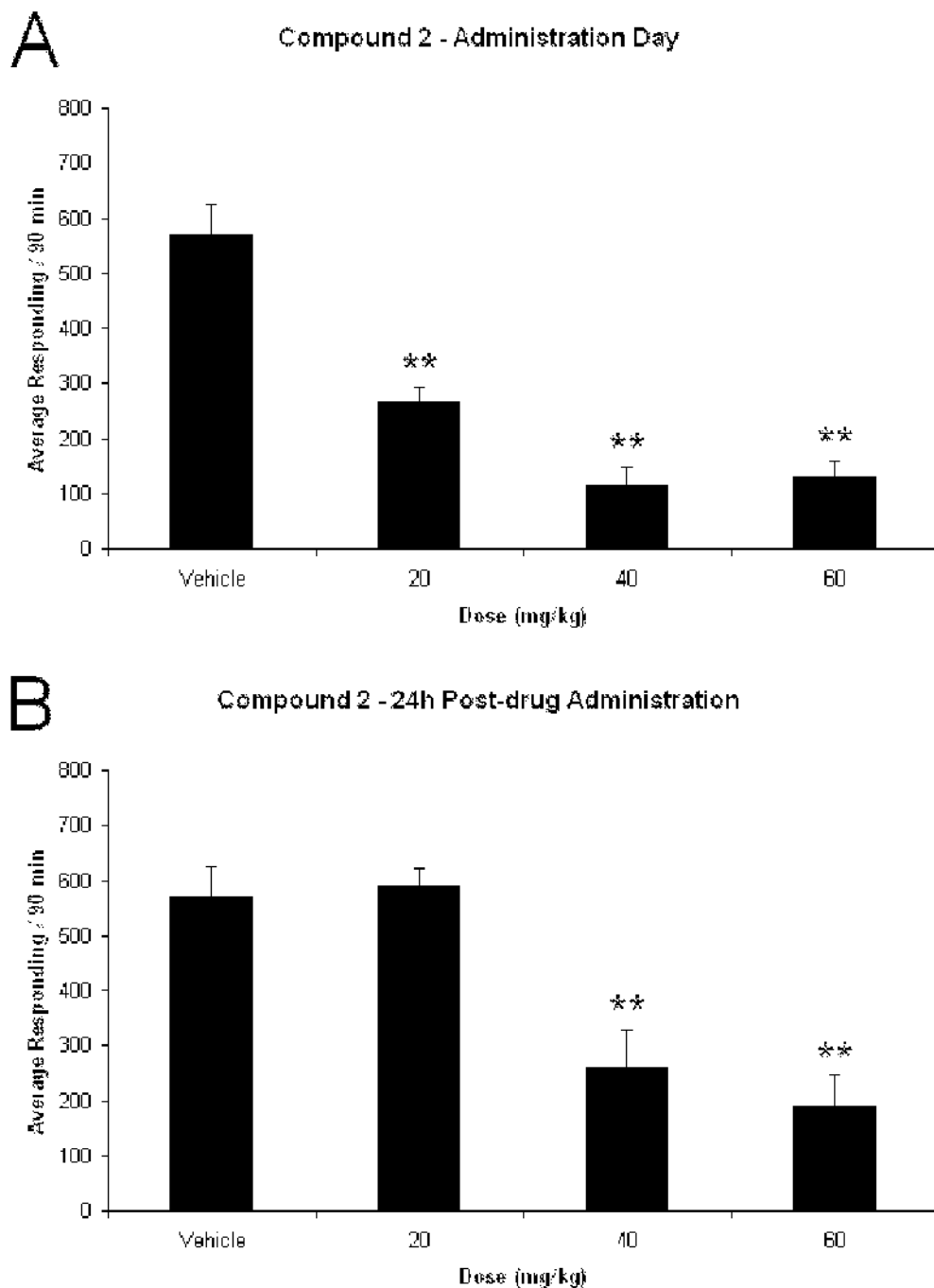


FIG. 13

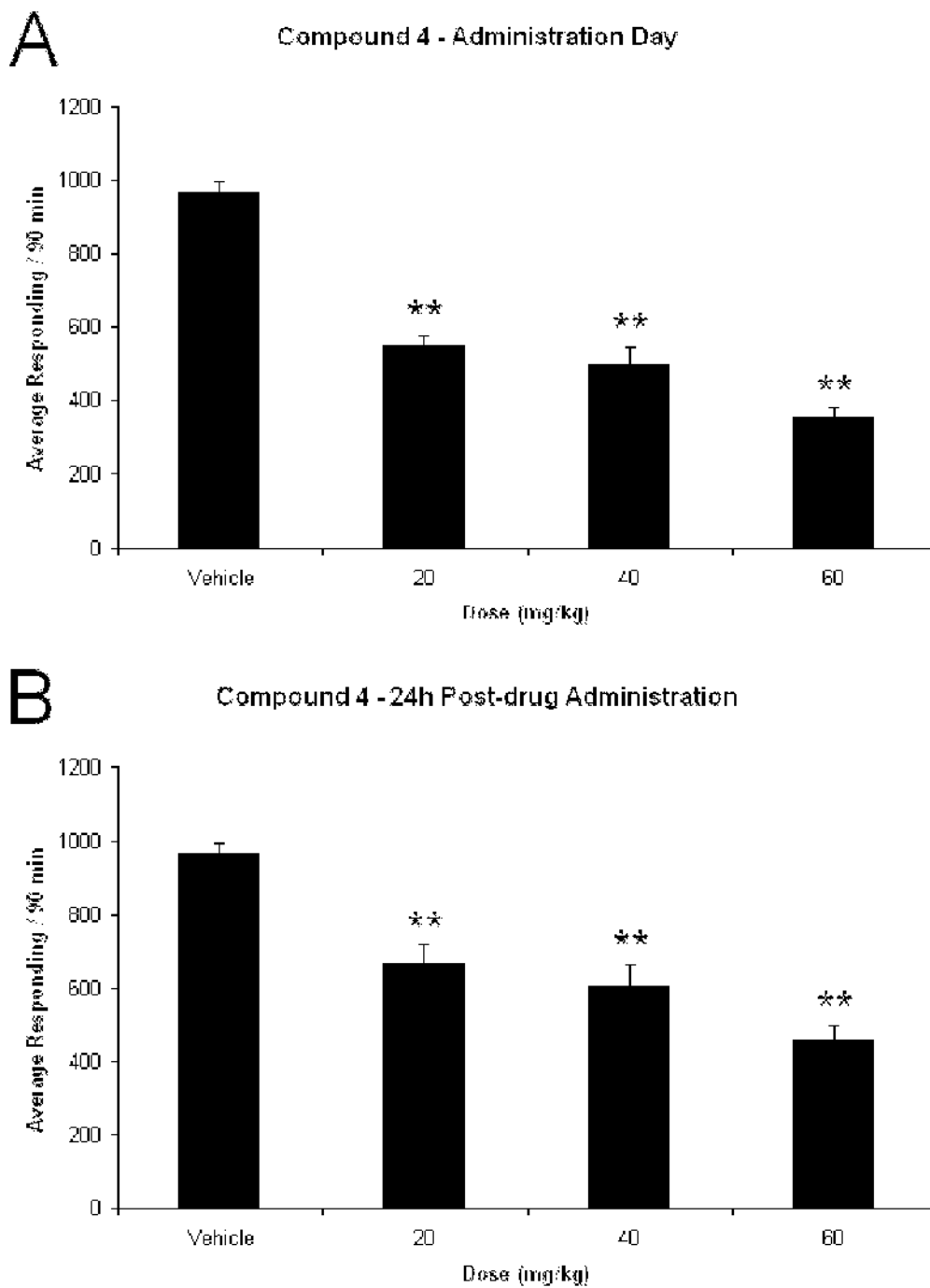


FIG. 14

1
AZA-BETA-CARBOLINES AND METHODS
OF USING SAME

CROSS-REFERENCE TO RELATED
 APPLICATIONS

This application claims the benefit of U.S. Application Ser. No. 61/055,334, filed May 22, 2008, which is incorporated by reference herein.

STATEMENT OF GOVERNMENT SUPPORT

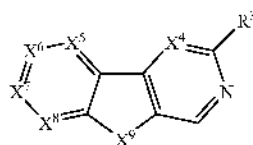
This invention was made with US Government support awarded by National Institute of Mental Health (NIMH), Grant No. MH 46851. The United States has certain rights in this invention.

BACKGROUND OF THE INVENTION

Drug and alcohol addiction and dependence remain a significant public health concern, impacting physical and mental well-being, family structure and occupational stability. While advances have been made in the development of novel therapies to treat alcoholism, alcohol-dependent individuals represent a heterogeneous group, and it is unlikely that a single pharmacological treatment will be effective for all alcoholics. Hence, a better understanding of the neuromechanisms which regulate alcohol seeking behaviors and the design of clinically safe and effective drugs that reduce drug and alcohol addiction and dependence remain a high priority. While the precise neuromechanisms regulating alcohol-seeking behaviors remain unknown, there is now compelling evidence that the GABA_A receptors within the striatopallidal and extended amygdala system are involved in the "acute" reinforcing actions of alcohol. The striatopallidal and extended amygdala system include the subnucleus extended amygdala [substantia innominata-ventral pallidum (VP)], shell of the nucleus accumbens, and central nucleus of the amygdala. Among the potential GABA(A) receptor isoforms within the VP regulating alcohol-seeking behaviors, GABA receptors containing the α1 receptor subtype (GABA_A1) appear preeminent. Acute alcohol administration selectively enhanced the effects of iontophoretically applied GABA in the VP. However, no effects were seen in the septum, VTA, and CA1 of the hippocampus. Further, a positive correlation was observed between alcohol-induced GABA enhancement and [³H] zolpidem binding (an α1 subtype selective agonist). A dense reciprocal projection from the VP to the NACC has been identified, and many of these have been found to be GABAergic neurons. The NACC is well established as a substrate that regulates the reinforcing properties of abused drugs. Finally, immunohistochemical and in situ hybridization studies have demonstrated that the VP contains one of the highest concentrations of mRNA encoding the α1 subunit in the CNS. These findings, together with pharmacological studies suggesting the VP plays a role in reward-mediated behaviors of psychostimulants and opiates suggest a possible role of the VP-α1 receptors in the euphoric properties of alcohol.

2
 SUMMARY OF THE INVENTION

The present invention relates to compounds having a structure according to Formula (I):



with variables as defined below.

The compounds of the present invention are useful for the treatment of a variety of diseases and conditions such as chemical addiction, e.g. alcoholism, nicotine addiction and opioid addiction, anhedonia, anxiety and other conditions associated with withdrawal from the chemical (e.g. alcohol, nicotine or opioid). Accordingly, the invention further provides pharmaceutical compositions comprising these compounds. The invention still further provides methods of treating chemical addiction, methods of treating alcoholism, methods of reducing alcohol intake, methods of treating anhedonia, and methods of treating anxiety using these compounds or the compositions containing them.

BRIEF DESCRIPTION OF THE DRAWINGS

FIG. 1 shows various compounds according to the present invention.

FIG. 2 shows various compounds according to the present invention.

FIG. 3 is a scheme to synthesize aza-β-carbolines according to the present invention.

FIG. 4 is a scheme to synthesize aza-β-carbolines according to the present invention.

FIG. 5 is a scheme to synthesize aza-tryptophans according to the present invention.

FIG. 6 is a scheme for Pd-mediated synthesis of aza-β-carbolines.

FIG. 7 is a scheme to synthesize compound 1 according to the present invention.

FIG. 8 is a scheme to synthesize compound 2 according to the present invention.

FIG. 9 is a scheme to synthesize compound 3 according to the present invention.

FIG. 10 is a scheme to synthesize compound 4 according to the present invention.

FIG. 11 is a schematic diagram of a binding assay plate for a radioligand binding assay.

FIG. 12 is a schematic diagram of administration of compounds according to the invention by oral gavage for an animal model of excessive alcohol consumption.

FIG. 13 is a graph of dose versus average responding, showing the effect of compound 2 on excessive alcohol consumption.

FIG. 14 is a graph of dose versus average responding, showing the effect of compound 4 on excessive alcohol consumption.

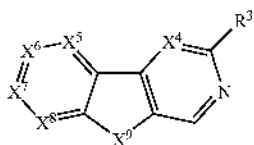
DETAILED DESCRIPTION OF THE INVENTION

Novel aza-β-carbolines have been developed. These compounds are designed to bind selectively at the α1 subtype GABA receptor and are suitably used as a treatment for

3

alcoholism. The invention also provides methods for reducing alcohol drinking and for reducing the anxiety and anhedonia associated with alcohol drinking and alcohol withdrawal. The invention further provides methods of treating anxiety and/or anhedonia.

Compounds according to the present invention include those shown in Formula (I):



or isomers, salts, solvates, chemically protected forms or prodrugs thereof;

wherein X^4 , X^5 , and X^8 may independently be chosen from N or Cl, X^6 may be N, $^+NR^6$ or CR^6 , and X^7 may be N, $^+NR^7$ or CR^7 , and wherein no more than any two of X^5 , X^6 , X^7 and X^8 is N;

wherein X^9 is NH, O or S;

wherein R^3 is CO_2R , or OR^1 or COR ;

wherein R^6 and R^7 are independently H, X, aryl, heteroaryl.

$C-CR^2$ lower alkyl, lower alkenyl, or lower alkynyl:

wherein R is $-C(CH_3)_{3-n}(CF_3)_m$, $-C(CH_3)_{3-n}(CH_2X_p)_{3-p}$, $-CH(CH_3)_{2-n}(CF_3)_m$, $-CH(CH_3)_{2-n}(CH_2X_p)_{2-p}$, aryl or heteroaryl;

wherein R^1 is $CH_2CH_2CH_3$, $CH(CH_3)_2$, $CH_2CH_2CH_2CH_3$, $CH_2CH(CH_3)_2$, $CH(CH_3)CH_2CH_3$, $-CH_2CH_2CH_2CH_2CH_3$, $-CH_2CH_2CH(CH_3)_2$, $-CH_2CH(CH_3)CH_2CH_3$, or $-CH(CH_3)CH_2CH_2CH_3$, wherein any of the hydrogens of R^1 may be replaced by X;

wherein R^2 is H, lower alkyl, Me_3Si , Et_3Si , $n-Pr_3Si$, $i-Pr_3Si$, aryl or heteroaryl;

wherein n is an integer from 0 to 3, m is an integer from 0 to 2, r is an integer from 1 to 3, p is an integer from 1 to 2, and t is an integer from 0 to 2; and

wherein X is independently selected from F, Cl, Br and I.

Some compounds according to formula (I) are shown in FIGS. 1-2. Suitably, the compounds of formula (I) bind selectively at the $\alpha 1$ subtype GABA receptor.

DEFINITIONS

Alkyl: The term "alkyl" as used herein, pertains to a monovalent moiety obtained by removing a hydrogen atom from a carbon atom of a hydrocarbon compound having from 1 to 20 carbon atoms (unless otherwise specified), which may be aliphatic or alicyclic, and which may be saturated or unsaturated (e.g., partially unsaturated, fully unsaturated). Thus, the term "alkyl" includes the sub-classes alkenyl, alkynyl, cycloalkyl, cycloalkenyl, cycloalkynyl, etc., discussed below.

In the context of alkyl groups, the prefixes (e.g., C_{1-4} , C_{1-7} , C_{1-20} , C_{2-7} , C_{3-7} , etc.) denote the number of carbon atoms, or range of number of carbon atoms. For example, the term " C_{1-4} alkyl" as used herein, pertains to an alkyl group having from 1 to 4 carbon atoms. Examples of groups of alkyl groups include C_{1-4} alkyl ("lower alkyl"), C_{1-7} alkyl, C_{1-20} alkyl and C_{1-30} alkyl. Note that the first prefix may vary according to other limitations; for example, for unsaturated alkyl groups, the first prefix must be at least 2; for cyclic and branched alkyl groups, the first prefix must be at least 3; etc.

4

Examples of saturated alkyl groups include, but are not limited to, methyl (C1), ethyl (C2), propyl (C3), butyl (C4), pentyl (C5), hexyl (C6), heptyl (C7), octyl (C8), nonyl (C9), decyl (C10), undecyl (C11), dodecyl (C12), tridecyl (C13), tetradecyl (C14), pentadecyl (C15), and eicododecyl (C20).

Examples of saturated linear alkyl groups include, but are not limited to, methyl (C1), ethyl (C2), n-propyl (C3), n-butyl (C4), n-pentyl (amyl) (C5), n-hexyl (C6), and n-heptyl (C7).

Examples of saturated branched alkyl groups include isopropyl (C3), iso-butyl (C4), sec-butyl (C4), tert-butyl (C4), iso-pentyl (C5), and neo-pentyl (C5).

Alkenyl: The term "alkenyl" as used herein, pertains to an alkyl group having one or more carbon-carbon double bonds. For example, the term " C_{2-4} alkenyl" as used herein, pertains to an alkenyl group having from 2 to 4 carbon atoms. Examples of groups of alkenyl groups include C_{2-4} alkenyl ("lower alkenyl"), C_{2-7} alkenyl, and C_{2-20} alkenyl.

Examples of alkenyl groups include, but are not limited to, ethenyl (vinyl, $-CH=CH_2$), 1-propenyl ($-CH=CH-CH_3$), 2-propenyl (allyl, $-CH=CH-CH_2$), isopropenyl (1-methylvinyl, $C(CH_3)=CH_2$), butenyl (C4), pentenyl (C5), and hexenyl (C6).

Alkynyl: The term "alkynyl" as used herein, pertains to an alkyl group having one or more carbon-carbon triple bonds. For example, the term " C_{2-4} alkynyl" as used herein, pertains to an alkynyl group having from 2 to 4 carbon atoms. Examples of groups of alkynyl groups include C_{2-4} alkynyl ("lower alkynyl"), C_{2-7} alkynyl, and C_{2-20} alkynyl.

Examples of alkynyl groups include, but are not limited to, ethynyl (ethynyl, $C-C\equiv C$) and 2-propynyl (propargyl, $CH_2-C\equiv C$).

Aryl: The term "aryl" as used herein, pertains to a monovalent moiety obtained by removing a hydrogen atom from an aromatic ring atom of an aromatic compound, which moiety has from 3 to 10 ring atoms (unless otherwise specified). Preferably, each ring has from 5 to 7 ring atoms.

In this context, the prefixes (e.g., C_{3-10} , C_{5-7} , C_{5-6} , etc.) denote the number of ring atoms, or range of number of ring atoms, whether carbon atoms or heteroatoms. For example, the term " C_{5-6} aryl" as used herein, pertains to an aryl group having 5 or 6 ring atoms. Examples of groups of aryl groups include C_{3-10} aryl, C_{5-10} aryl, C_{5-7} aryl, C_{5-6} aryl, C_5 aryl, and C_6 aryl.

The ring atoms may be all carbon atoms, as in "carboaryl groups". Examples of carboaryl groups include C_{3-10} carboaryl, C_{5-10} carboaryl, C_{5-7} carboaryl, C_{5-6} carboaryl and C_6 carboaryl.

Examples of carboaryl groups include, but are not limited to, those derived from benzene (i.e., phenyl) (C6), naphthalene (C10), and azulene (C10).

Examples of aryl groups which comprise fused rings, at least one of which is an aromatic ring, include, but are not limited to, groups derived from indane (e.g., 2,3-dihydro-1H-indene) (C9), indene (C9), isoindene (C9), and tetraline (1,2,3,4-tetrahydronaphthalene) (C10).

Alternatively, the ring atoms may include one or more heteroatoms, as in "heteroaryl groups". Examples of heteroaryl groups include C_{3-10} heteroaryl, C_{5-10} heteroaryl, C_{5-7} heteroaryl, C_{5-6} heteroaryl, C_5 heteroaryl, and C_6 heteroaryl.

Examples of monocyclic heteroaryl groups include, but are not limited to, those derived from:

N1: pyrrole (azole) (C5), pyridine (azine) (C6);

O1: furan (oxole) (C5);

S1: thiophene (thiole) (C5);

N1O1: oxazole (C5), isoxazole (C5), isoxazine (C6);

N2O1: oxadiazole (fuzazan) (C5);

N3O1: oxatriazole (C5);

5

N1S1: thiazole (C5), isothiazole (C5);

N2: imidazole (1,3-diazole) (C5), pyrazole (1,2-diazole) (C5), pyridazine (1,2-diazine) (C6), pyrimidine (1,3-diazine) (C6) (e.g., cytosine, thymine, uracil), pyrazine (1,4-diazine) (C6);

N3: triazole (C5), triazine (C6); and,

N4: tetrazole (C5).

Examples of heteroaryl groups which comprise fused rings, include, but are not limited to:

C9 heteroaryl groups (with 2 fused rings) derived from benzofuran (O1), isobenzofuran (O1), indole (N1), isoindole (N1), indolizine (N1), indoline (N1), isoindoline (N1), purine (N4) (e.g., adenine, guanine), benzimidazole (N2), indazole (N2), benzoxazole (N1O1), benzisoxazole (N1O1), benzodioxole (O2), benzofurazan (N2O1), benzotriazole (N3), benzothiofuran (S1), benzothiazole (N1S1), benzothiadiazole (N2S);

C10 heteroaryl groups (with 2 fused rings) derived from chromene (O1), isochromene (O1), chroman (O1), isochroman (O1), benzodioxan (O2), quinoline (N1), isoquinoline (N1), quinolizine (N1), benzoxazine (N1O1), benzodiazine (N2), pyridopyridine (N2), quinoxaline (N2), quinoxaline (N2), cinnoline (N2), phthalazine (N2), naphthyridine (N2), pteridine (N4);

C11 heteroaryl groups (with 2 fused rings) derived from benzodiazepine (N2);

C13 heteroaryl groups (with 3 fused rings) derived from carbazole (N1), dibenzofuran (O1), dibenzothiophene (S1), carboline (N2), perimidine (N2), pyridoindole (N2); and,

C14 heteroaryl groups (with 3 fused rings) derived from acridine (N1), xanthene (O1), thioxanthene (S1), oxanthrene (O2), phenoxathiin (O1S1), phenazine (N2), phenoxazine (N1O1), phenothiazine (N1S1), thianthrene (S2), phenanthridine (N1), phenanthroline (N2), phenazine (N2).

Heteroaryl groups which have a nitrogen ring atom in the form of an —NH— group may be N-substituted, that is, as

NR₁. For example, pyrrole may be N-methyl substituted, to give N-methylpyrrole. Examples of N-substituents include, but are not limited to C₁₋₇ alkyl, C₃₋₂₀ heterocyclyl, C₅₋₂₀ aryl, and acyl groups.

Heterocyclic groups (including heteroaryl groups) which have a nitrogen ring atom in the form of an —N— group may be substituted in the form of an N-oxide, that is, as N(→O)— (also denoted N+(=O)—). For example, quinoline may be substituted to give quinoline N-oxide; pyridine to give pyridine N-oxide; benzofurazan to give benzofurazan N-oxide (also known as benzofuroxan).

The above groups, whether alone or part of another substituent, may themselves optionally be substituted with one or more groups selected from themselves and the additional substituents listed below.

Halo: F, Cl, Br, and I.

Hydroxy: OH.

Ether: —OR, wherein R is an ether substituent, for example, a C₁₋₇ alkyl group (also referred to as a C₁₋₇ alkoxy group, discussed below), a C₃₋₂₀ heterocyclyl group (also referred to as a C₃₋₂₀ heterocycloxy group), or a C₅₋₂₀ aryl group (also referred to as a C₅₋₂₀ aryloxy group), preferably a C₁₋₇ alkyl group.

Alkoxy: —OR, wherein R is an alkyl group, for example, a C₁₋₇ alkyl group. Examples of C₁₋₇ alkoxy groups include, but are not limited to, OMe (methoxy), OEt (ethoxy),

O(nPr) (n-propoxy), O(iPr) (isopropoxy), O(nBu) (n-butoxy), —O(sBu) (sec-butoxy), —O(iBu) (isobutoxy), and —O(tBu) (tert-butoxy).

6

Oxo (keto, -one): —O.

Acyl (keto): C(=O)R, wherein R is an acyl substituent, for example, a C₁₋₇ alkyl group (also referred to as C₁₋₇ alkylacyl or C₁₋₇ alkanoyl), a C₃₋₂₀ heterocyclyl group (also referred to as C₃₋₂₀ heterocyclylacyl), a C₅₋₂₀ aryl group (also referred to as C₅₋₂₀ arylacyl), preferably a C₁₋₇ alkyl group or a halo. Examples of acyl groups include, but are not limited to, C(=O)CH₃ (acetyl), C(=O)CH₂CH₃ (propionyl), —C(=O)C(CH₃)₃ (t-butyl), —C(=O)Ph (benzoyl, phenone), —C(=O)Cl.

Carboxy (carboxylic acid): —C(=O)OH.

Ester (carboxylate, carboxylic acid ester, oxycarbonyl):

C(=O)OR, wherein R is an ester substituent, for example, a C₁₋₇ alkyl group, a C₃₋₂₀ heterocyclyl group, or a C₅₋₂₀ aryl group, preferably a C₁₋₇ alkyl group. Examples of ester groups include, but are not limited to, C(=O)OCH₃, C(=O)OCH₂CH₃, C(=O)OC(CH₃)₃, and C(=O)OPh.

Amino: —NR₂, wherein each R is independently an amino substituent, for example, hydrogen, a C₁₋₇ alkyl group (also referred to as C₁₋₇ alkylamino or di-C₁₋₇ alkylamino), a C₃₋₂₀ heterocyclyl group, or a C₅₋₂₀ aryl group, preferably H or a C₁₋₇ alkyl group, or, in the case of a “cyclic” amino group, both R's, taken together with the nitrogen atom to which they are attached, form a heterocyclic ring having from 4 to 8 ring atoms. Amino groups may be primary (—NH₂), secondary (—NH₂R), or tertiary (—NR₂), and in cationic form, may be quaternary (—NR₃⁺). Examples of amino groups include, but are not limited to, —NH₂, —NHCH₃, —NHC(CH₃)₂, N(CH₃)₂, N(CH₂CH₃)₂, and N(iPr). Examples of cyclic amino groups include, but are not limited to, aziridino, azetidino, pyrrolidino, piperidino, piperazino, morpholino, and thiomorpholino.

Amido (carbamoyl, carbamyl, aminocarbonyl, carboxamide): C(=O)NR₂, wherein each R is independently an amino substituent, as defined for amino groups. Examples of amido groups include, but are not limited to, C(=O)NH₂, —C(=O)NHCH₃, —C(=O)N(CH₃)₂, —C(=O)NHCH₂CH₃, and —C(=O)N(CH₂CH₃)₂, as well as amido groups in which both R's, together with the nitrogen atom to which they are attached, form a heterocyclic structure as in, for example, piperidinocarbonyl, morpholinocarbonyl, thiomorpholinocarbonyl, and piperazinocarbonyl.

Cyano (nitrile, carbonitrile): —CN.

Alkylsilyl groups: SiR₃, wherein each R is independently an alkyl group. Suitably the alkyl groups are lower alkyl groups such as methyl, ethyl or propyl.

Isomers, Salts, Solvates, Protected Forms, and Prodrugs

Certain compounds may exist in one or more particular geometric, optical, enantiomeric, diastereoisomeric, epimeric, stereoisomeric, tautomeric, conformational, or anomeric forms, including but not limited to, cis- and trans-forms; E- and Z-forms; c-, t-, and r-forms; endo- and exo-forms; R, S, and meso-forms; D- and L-forms; d- and l-forms; (+) and (−) forms; keto-, enol-, and enolate-forms; syn- and anti-forms; synclinal- and anticlinal-forms; α- and β-forms; axial and equatorial forms; boat-, chair-, twist-, envelope-, and halfchair-forms; and combinations thereof, hereinafter collectively referred to as “isomers” (or “isomeric forms”).

If the compound is in crystalline form, it may exist in a number of different polymorphic forms.

Note that, except as discussed below for tautomeric forms, specifically excluded from the term “isomers”, as used herein, are structural (or constitutional) isomers (i.e. isomers which differ in the connections between atoms rather than merely by the position of atoms in space). For example, a

reference to a methoxy group, —OCH₃, is not to be construed as a reference to its structural isomer, a hydroxymethyl group.

CH₂OH. Similarly, a reference to ortho-chlorophenyl is not to be construed as a reference to its structural isomer, meta-chlorophenyl. However, a reference to a class of structures may well include structurally isomeric forms falling within that class (e.g., C₁₋₇ alkyl includes n-propyl and isopropyl; butyl includes n-, iso-, sec-, and tert-butyl; methoxyphenyl includes ortho-, meta-, and para-methoxyphenyl).

The above exclusion does not pertain to tautomeric forms, for example, keto-, enol-, and enolate-forms, as in, for example, the following tautomeric pairs: keto/enol, imine/enamine, amide/imino alcohol, amidine/amidine, nitroso/oxime, thioketone/cythiol, N-nitroso/hydroxyazo, and nitro/aci-nitro.

Note that specifically included in the term "isomer" are compounds with one or more isotopic substitutions. For example, H may be in any isotopic form, including ¹H, ²H (D), and ³H (T); C may be in any isotopic form, including ¹²C, ¹³C, and ¹⁴C; O may be in any isotopic form, including ¹⁶O and ¹⁸O; and the like.

Unless otherwise specified, a reference to a particular compound includes all such isomeric forms, including (wholly or partially) racemic and other mixtures thereof. Methods for the preparation (e.g. asymmetric synthesis) and separation (e.g. fractional crystallisation and chromatographic means) of such isomeric forms are either known in the art or are readily obtained by adapting the methods taught herein, or known methods, in a known manner.

It may be convenient or desirable to prepare, purify, and/or handle the active compound in the form of a prodrug. The term "prodrug", as used herein, pertains to a compound which, when metabolised (e.g. in vivo), yields the desired active compound. Typically, the prodrug is inactive, or less active than the active compound, but may provide advantageous handling, administration, or metabolic properties.

It may be convenient or desirable to prepare, purify, and/or handle the active compound in the form of a salt. Suitable salts include those commonly used for pharmaceuticals, such as the hydrochloride salt.

Synthesis

Aza-β-carbolines according to the present invention can be prepared by the chemistry outlined in FIGS. 3-4. In brief, an aza-iodoaniline is reacted with an acetylene substituted Schöllkopf chiral auxiliary in the presence of a palladium catalyst to provide an aza indole. The triethylsilyl group is removed by stirring with TBAI followed by hydrolysis to provide an aza-tryptophan ethyl ester. This ester is reacted with formaldehyde and then converted to the desired aza-β-carboline as shown in FIGS. 3-4. See e.g., W. Yin, P. V. V. S. Sarma, J. Ma, D. Han, J. Chen and J. M. Cook, Synthesis of Bivalent Ligands of β-Carboline-3-Carboxylates via a Palladium-Catalyzed Homo-Coupling Process, *Tetrahedron Lett.*, 46, 6363-6368 (2005), which is incorporated by reference herein; E. Cox, T. Hagen, R. McKernan and J. M. Cook, Bz1 Receptor Subtype Specific Ligands, Synthesis and Biological Properties of βCC1, a Bz1 Receptor Subtype Specific Antagonist, *Med. Chem. Res.*, 5, 710-718 (1995), which is incorporated by reference herein; M. S. Allen, T. J. Hagen, M. L. Trudell, P. Skolnick and J. M. Cook, Synthesis of Novel 3-Substituted β-Carbolines as Benzodiazepine Receptor Ligands: Probing the Benzodiazepine Receptor Inverse Agonist Site," *J. Med. Chem.*, 31, 1854-1861 (1988), which is incorporated by reference herein; S. Harvey, K. Foster, P. McKay, M. Carroll, R. Seyoum, J. E. Woods II, C. Grey, C. Jones S. McCane, R. Cummings, D. Mason, C. Ma, J. M. Cook, and H. June, The GABA(A) Receptor α1 Subtype in the Ventral Pallidum Regulates Alcohol-Seeking Behaviors, *J. Neuroscience*, 22, 3765-3775 (2002), which is incorporated by reference herein; W. Yin, X. Liao, H. June and J. M.

Cook, Search for Benzodiazepine/GABA(A) Subtype Selective Ligands that Reverse Alcohol Self-Administration, Abstracts of Papers, 224th ACS National Meeting, Boston, Mass., August 18-22 (2002). M101-244, which is incorporated by reference herein; and H. June, C. Ma and J. M. Cook, Methods for Reducing Alcohol Cravings in Chronic Alcoholics, US Patent Application Publication No. US2003/0176456A1, Sep. 18, 2003; which is incorporated by reference herein.

The aza-tryptophans used in the above synthesis can also be synthesized by the route shown in FIG. 5. A Boc-protected formyl-aza-indole is reacted with a Wadsworth Horner Immons reagent in the presence of DBU to provide an aza-indole olefin. Reduction of the double bond, followed by hydrolysis provides an aza-tryptophan, set up for the steps depicted in FIGS. 3-4. See, e.g., X. Li, W. Yin, P. V. V. S. Sarma, H. Zhao, J. Ma and J. M. Cook, "Synthesis of Optically Active Tryptophans as IDO Inhibitors," *Tet. Lett.*, 45, 8569-8573 (2004), which is incorporated by reference herein; and J. Yu, T. Wang, X. Liu, J. Deschamps, J. Flippen-Anderson, X. Liao, J. M. Cook, "General Approach for the Synthesis of Sarpagine Indole Alkaloids. Enantioselective Total Synthesis of (+)-Velloximine, (+)-Normacusine B, (-)-Alkaloid Q3, (-)-Panarine, (+)-N₂-Methylvellosimine, and (+)-N_α-Methyl-16-epipericyclivine," *J. Org. Chem.*, 68, 7565-7581 (2003), which is incorporated by reference herein.

Aza-β-carbolines according to the present invention can also be prepared via a Pd-mediated synthesis shown presented in FIG. 6. In brief, an iodopyridine will be reacted with a 4-chloro-5-amino pyridine in the presence of a Buchwald-Hartwig amination catalyst to provide bipyridyl analog. This amine will be subjected to a Buchwald-type coupling process with the chloride to generate the desired aza-β-carboline. See, e.g., Driver, M. S. and Hartwig, J. F. A Second-Generation Catalyst for Aryl Halide Amination, *J. Am. Chem. Soc.*, 118, 7217-7218 (1996), which is incorporated by reference herein; Bedford, R. B. and Betham, M. N. II Carbazole Synthesis from 2-Chloroanilines via Consecutive Amination and C—H Activation, *J. Org. Chem.* 71, 9403-9410 (2006), which is incorporated by reference herein; and Jonckers, T. et al. *Syn. Lett.* 615-617 (2003), which is incorporated by reference herein.

Activity

In one embodiment, the present invention provides a method of treating chemical addiction comprising administering a therapeutically effective amount of a compound of formula (I) to a subject in need thereof. In some embodiments, the chemical may be alcohol, nicotine or opioids. In a further embodiment, the present invention provides a method of reducing chemical intake comprising administering a therapeutically effective amount of a compound of formula (I) to a subject in need thereof.

In another embodiment, the present invention provides a method of treating alcoholism comprising administering a therapeutically effective amount of a compound of formula (I) to a subject in need thereof. In another embodiment, the present invention provides a method for reducing alcohol intake comprising administering a therapeutically effective amount of a compound of formula (I) to a subject in need thereof.

In a further embodiment, the present invention provides a method for reducing anxiety comprising administering a therapeutically effective amount of a compound of formula (I) to a subject in need thereof. In yet another embodiment, the present invention provides a method of treating anhedonia comprising administering a therapeutically effective amount of a compound of formula (I) to a subject in need thereof. In some embodiments, the anxiety and/or anhedonia is associated with chemical withdrawal or reducing chemical intake.

In yet another embodiment, the invention provides a method of reducing physical symptoms (e.g., tremors and

seizures) associated with chemical withdrawal comprising administering a therapeutically effective amount of a compound according to formula (I) to a subject in need thereof.

The compounds of formula (I) may be administered alone or in combination with other active compounds, for example, those known to be useful in treating chemical addiction or alcoholism or anxiety or anhedonia, such as anxiolytics (e.g. diazepam, clonazepam, clorazepate, alprazolam, buspirone, and meprobamate), or alcoholism treatments (e.g. naltrexone, naltrexone hydrochloride, disulfiram, nalmefene, metadoxine, acamprosate calcium, and chlordiazepoxide hydrochloride). If administered in combination, the additional active compound can be administered simultaneously or sequentially with the compound of formula (I). In some embodiments, the additional active compound can be administered before or after the compound of formula (I).

GABA_A-receptors containing $\alpha 1$ subunits in the VP are thought to play an important role in regulating alcohol seeking behaviors. Without wishing to be bound by theory, it is thought that "competitive" benzodiazepine antagonists that exhibit binding selectivity at the $\alpha 1$ subtype, while concurrently displaying a partial agonist efficacy at non- $\alpha 1$ containing subtypes, may have important treatment implications in the design and development of novel pharmacotherapies for alcohol-dependent subjects. Thus, from a clinical perspective, $\alpha 1$ subtype antagonists capable of reducing alcohol intake, and capable of concurrently eliminating or attenuating the anxiety associated with abstinence or detoxification, would be useful pharmacotherapeutic agents in treating alcohol dependent individuals.

Administration

The compounds of this invention can be administered in a therapeutically effective amount by any of the accepted modes of administration for agents that serve similar utilities, e.g., oral, nasal, rectal and parenteral. As used herein, "parenteral" includes, but is not limited to, subcutaneous, intradermal, intravenous, intramuscular, intraperitoneal and intrathecal administration, such as by injection or infusion. The compounds of the invention may be administered separately or combined with each other or other agents known to be effective for the treatment of alcoholism or anxiety or anhedonia (e.g., naltrexone). The effective dose of the compounds of this invention, i.e., the active ingredient, will depend upon numerous factors such as the severity of the disease to be treated, the age, body weight, sex, diet and relative health of the subject, the potency of the compound used, the route and form of administration, and other factors. For example, it is well within the level of ordinary skill in the art to start doses at lower than those required to achieve the desired effect and to gradually increase the dosage until the desired effect is achieved.

Therapeutically effective amounts of the compounds may range from approximately 0.1-50 mg per kilogram body weight of the recipient per day; alternatively about 0.5-20 mg/kg/day can be administered. Thus, for administration to a 70 kg person, the dosage range could be about 40 mg to 1.4 g per day. In some embodiments, the compounds are administered more than once per day (e.g. 2x, 3x or 4x per day). In other embodiments, the compounds are administered once a day. Administration may also be less frequent than once a day, e.g., weekly, bi-weekly, monthly, etc. If desired, the effective daily dose may be divided into multiple doses for the purposes of administration.

Compositions containing aza- β -carbolines can be formulated according to known methods for preparing pharmaceutically useful compositions. In general, the compositions will be formulated such that an effective amount of the aza- β -carboline is combined with a suitable carrier in order to facilitate effective administration of the composition. The compositions of the invention may be prepared in various forms for administration. These include, for example, solid, semi-solid,

and liquid dosage forms, such as tablets, caplets, pills, powders, capsules, dragees, liquid solutions or suspension, suppositories, injectable and infusible solutions, and sprays. The form will depend on the intended mode of administration and therapeutic application. As used herein, "carrier" includes any and all solvents, excipients, diluents, other liquid vehicle, dispersion or suspension aids, surface active ingredients, preservatives, solid binders, lubricants, and the like, as suited to the particular dosage form desired. Remington's Pharmaceutical Sciences, Fifteenth Edition, E. W. Martin (Mack Publishing Co., Easton Pa. 1975) discloses various vehicles or carriers used in formulating pharmaceutical compositions and known techniques for the preparation thereof. Except insofar as any carrier is incompatible with the compounds of the invention, such as by producing any undesirable biological effect or otherwise interacting in a deleterious manner with any other component(s) of the pharmaceutical composition, its use is contemplated to be within the scope of the invention.

The pharmaceutical compositions may comprise between about 0.1% and 99%, and suitably between about 1 and 75% by weight of the total of one or more of the aza- β -carbolines of the present invention based on the weight of the total composition.

In some embodiments, the compositions described herein are formulated in dosage unit form for ease of administration and uniformity of dosage. A "dosage unit form" as used herein refers to a physically discrete unit of pharmaceutical composition for the patient to be treated. Each dosage should contain the quantity of active material calculated to produce the desired therapeutic effect either as such, or in association with the selected carrier.

The following examples are provided to facilitate the practice of the present invention. They are not intended to limit the invention in anyway.

EXAMPLES

Example 1

Synthesis of tert-Butyl pyridine[4',5'-4,5]pyrrolo[3,2-c]pyridine-8-carboxylate (1)

Tert-butyl pyridine[4',5'-4,5]pyrrolo[3,2-c]pyridine-8-carboxylate (1) is synthesized from commercially available 4-bromopyridine-3-carboxaldehyde (7) according to FIG. 7 ("bz" is benzene; "et" is ethyl). Commercially available reagents are used as received unless otherwise noted. Reactions requiring inert atmospheres are run under nitrogen unless otherwise noted.

Commercially available 4-bromopyridine-3-carboxaldehyde (7) is subjected to a Horner-Wadsworth-Emmons reaction with methyl 2-(dimethoxycarbonyl)-2-[(phenylmethoxy) carbonylamino]acetate (8) in dichloromethane (DCM) with 1,8-diazabicyclo[5.4.0]undec-7-ene (DBU) to give methyl (2Z)-3-(4-bromo(3-pyridyl))-2-[(phenylmethoxy)carbonyl amino]prop-2-enoate (9). This compound is cyclized with CuI and L-Proline in 1,4-dioxane and potassium carbonate (base) to yield methylpyrrolo[4,5-c]pyridine 2-carboxylate (10). This compound is converted to the gramine derivative, methyl 3-[(dimethylamino)methyl]pyrrolo[4,5-c]pyridine-2-carboxylate (11) by refluxing with dimethyl amine hydrochloride and paraformaldehyde in methanol. Reaction of this gramine with ethyl nitro acetate (12) yields the nitro ester product, ethyl 3-[2-(methoxycarbonyl)pyrrolo[3,2-c]pyridine-3-yl]-2-nitropropanoate (13). This is reduced to its corresponding amine (14) with Raney Ni in ethanol and further cyclized to give ethyl 6-oxo-7,8,9-trihydropyridino[4',5'-4,5]pyrrolo[3,2-c]pyridine-8-carboxylate (15) by refluxing in xylene. The cyclic amide is

11

aromatized with manganese dioxide in chloroform to give ethyl 6-hydroxypyridino[4',5'-4,5]pyrrolo[3,2-c]pyridine-8-carboxylate (16). Chlorination of this product with phosphorous oxychloride yields ethyl 6-chloropyridino[4',5'-4,5]pyrrolo[3,2-c]pyridine-8-carboxylate (17) which upon reduction

with Pd/C/H₂ in the presence of diisopropyl ethyl amine (as HCl scavenger) in ethanol gives ethyl pyridino[4',5'-4,5]pyrrolo[3,2-c]pyridine-8-carboxylate (18). The ethyl ester of this compound is hydrolyzed with 10% NaOH to give the corresponding acid product, pyridino[4',3'-4,5]pyrrolo[3,2-c]pyridine-8-carboxylic acid (19), which upon esterification with dimethylformamide di tert-butyl acetal in dimethylformamide (DMF) delivers the desired tert-butyl pyridino[4',5'-4,5]pyrrolo[3,2-c]pyridine-8-carboxylate (1).

To isolate the product (tert-butyl pyridino[4',5'-4,5]pyrrolo[3,2-c]pyridine-8-carboxylate, 1), the reaction mixture is cooled to ambient temperature and diluted with water (~30 mL). The reaction mixture is transferred to a separatory funnel and extracted with ethyl acetate (2x150 mL). The combined organic extracts are washed with water (30 mL) and saturated brine solution (60 mL), and then dried over magnesium sulfate. The mixture is filtered through a glass fiber filter,

12

inlet, and reflux condenser fitted with a drying tube and placed into a heating mantle. The flask was charged with glacial acetic acid (523 mL), and stirring was initiated. 4-aminopyridine (20, 95 g) was added to the reaction as a single portion, and the dissolution of the material was exothermic to ~30° C. Iodine monochloride (101 mL) was added slowly over a 2 hour period at a rate to keep the internal temperature below 45° C. At the end of the addition the temperature had reached ~42° C. After the complete addition of iodine monochloride, the exotherm was allowed to subside and then heating was applied to the reaction to maintain the temperature at 45-50° C. Stirring was continued at 45-50° C. overnight and continued for 10 days until the reaction was deemed to be complete. i.e., when no significant progress was being made towards product. The reaction was monitored by HPLC (MPP-IC1 (270)) by diluting an aliquot of the reaction mixture (~1 mL) at various time points with (1:1) acetonitrile/water (~2 mL) and submitting for analysis. The starting material eluted at 2.8 min, and the product eluted at 8.1 min. Materials used in the synthesis are detailed in Table 1.

TABLE 1

Materials used in synthesis of 4-amino-3-iodopyridine (21)					
Compound	MW (g/mol)	d (g/mL)	Equivalents	Amount	Lot #
Reaction					
4-Aminopyridine	94.12		1.0 eq.	95 g/101 mol	R11-2408-03
Iodine monochloride (ICl)	162.36	3.240	2.0 eq.	101 ml/2.02 mol	R03-0508-01
glacial Acetic acid	60.05	1.049	5.5 vols.	523 ml	
Isolation					
Water	18.02	1.000	41 vols.	3.9 L	RO water
50% Sodium hydroxide solution	40.00	1.515	—	As required	08-2208-01
Ethyl acetate	88.11	0.902	84 vols.	8 L	R09-0508-02
15% Sodium thiosulfate	—	—	42 vols.	4 L	R07-1107-06
Saturated brine solution	—	—	21 vols.	2 L	R08-1208-09

and the filtrate is concentrated under reduced pressure to complete dryness. The residue is triturated with methyl tert-butyl ether (MTBE) (6 mL) and filtered. The solid is dried under high vacuum overnight at room temperature.

Example 2

Synthesis of 8-Propoxy-pyridino[4,3'-5,4]pyrrolo[3,2-c]pyridine hydrochloride (2)

8-Propoxy-pyridino[4',3'-5,4]pyrrolo[3,2-c]pyridine hydrochloride (2) was synthesized from commercially available 4-aminopyridine (20) and 5-chloro-2-fluoropyridine (22) according to FIG. 8 ("Pr" is propyl). Commercially available reagents were used as received unless otherwise noted. Reactions requiring inert atmospheres were run under nitrogen unless otherwise noted.

Synthesis of 4-amino-3-iodopyridine (21. Step a)

A 2 L, three-neck round-bottom flask was equipped with a mechanical stirrer, thermocouple, addition funnel, nitrogen

To isolate 4-amino-3-iodopyridine (21), the reaction mixture was cooled to ambient temperature and diluted with 1.9 L of water. The solution was cooled in an ice/water bath to 0-5° C. and adjusted to pH ~10 with 50% sodium hydroxide solution and strong stirring. The addition of NaOH was strongly exothermic, and ice was added if required. During the pH adjustment brown solids formed. Ethyl acetate (4 L) was added, the biphasic solution was agitated, and the layers were allowed to separate. The brown solids dissolved during the extraction, by maintaining agitation and adding more ethyl acetate if needed. The aqueous layer was extracted with fresh ethyl acetate (4 L), the biphasic solution was agitated, and the layers were allowed to separate. The combined ethyl acetate extracts were washed sequentially with 15% sodium thiosulfate solution (2x2 L), water (2 L), and saturated brine solution (2 L), and then dried over sodium sulfate. The mixture was filtered through a glass microfiber filter, and the filtrate was evaporated under reduced pressure to give a brown solid. The solids were dissolved in 5% methanol in 1 L dichloromethane (DCM) and filtered through a 2" silica plug, washing with an additional 2 L of eluent. The solution was evaporated under reduced pressure to give a brown waxy solid. The solids were dried under vacuum at ambient temperature for a minimum of 12 h.

13

Results are shown in Table 2. 4-Amino-3-iodopyridine (21) (lot #1357-69-1) was a brown, waxy solid, synthesized with a yield of 173 g/78%. 4-Amino-3-iodopyridine (21) was analyzed using HPLC, and according to results, it was 92.3% pure. Mass spectrometry and ¹H-NMR (300 MHz, CDCl₃) were also used to analyze 4-amino-3-iodopyridine (21), confirming the identity of the compound.

TABLE 2

Lot summary for the preparation of 4-amino-3-iodopyridine (21)					
SM Lot #	SM Batch Size	Yield (g%)	Analysis	Product Lot #	Comments
R11-2408-03	5 g	8.6 g/74%	HPLC: 92.5%	1357-64-1	9 days reaction time
R11-2408-03	95 g	173 g/78%	HPLC: 92.3%	1357-69-1	10 days reaction time

Synthesis of 5-chloro-2-propoxypyridine (23, Step b)

A 12 L, three-neck round-bottom flask with a mechanical stirrer, thermocouple, addition funnel, nitrogen inlet, and a drying tube were equipped and placed into a cooling bath. An oversized flask was used due to the large amount of foaming and effervescence during the additions. The flask was charged with tetrahydrofuran (THF, 1.8 L), and stirring was initiated. Sodium hydride was added in portions. A mild exotherm was

14

below 5° C. The addition was strongly exothermic and accompanied by the evolution of hydrogen gas. There was a significant delay (~45 mins) to the hydrogen release, which was sudden and caused foaming. The cooling bath was allowed to expire naturally overnight. Stirring was continued at ambient temperature until the reaction was complete, i.e., typically after overnight stirring without the requirement for

additional reagents and when no starting material was observed. If reaction was not complete, it was cooled back to 0-5° C. and treated with fresh sodium hydride (0.5 eq.), the reaction was stirred at ambient temperature overnight, resampled, and the reaction was continued until deemed to be complete. The reaction was monitored by TLC (SiO₂, 25% ethyl acetate in heptanes, UV) by diluting an aliquot of reaction mixture (~1 mL) with water (~2 mL), extracting with ethyl acetate, and spotting the organic layer. The starting material had retention factor (Rf)=0.38; the product had Rf=0.45. Materials used in the synthesis are detailed in Table 3.

TABLE 3

Materials used in the synthesis of 5-chloro-2-propoxypyridine (23)					
Compound	MW (g/mol)	d (g/mL)	Equivalents	Amt/mol	Lot #
Reaction					
5-Chloro-2-fluoropyridine	131.54	1.311	1.0 eq.	86 g/0.65 mol	R11-2408-04
Sodium hydride (60% suspension on mineral oil)	24.0	—	2.0 eq.	52.3 g/1.31 mol	R03-1907-19
Propan-1-ol (anhydrous)	60.1	0.804	2.1 eq.	103 ml/1.37 mol	R10-0108-04
THF (anhydrous)	72.11	0.889	15 vols.	2.5 L	R10-2808-02
Isolation					
Ethyl acetate	88.11	0.902	46.5 vols.	4 L	R09-0508-02
Saturated ammonium chloride solution	—	—	11.6 vols.	1 L	R06-0808-04
Saturated brine solution	—	—	11.6 vols.	1 L	R08-1208-09

observed initially due to residual moisture in the solvent. After this had subsided the bulk of the material was added. The reaction mixture was cooled to 0-5° C. using an ice/water bath, and a solution of propanol (103 mL) in THF (350 mL) was added slowly over a 1 hour period at a rate to keep the internal temperature below 5° C. The addition was strongly exothermic and accompanied by the evolution of hydrogen gas. There was a significant delay (~45 mins) to the hydrogen release, which was sudden and caused foaming. After the complete addition of propanol, the reaction was stirred for a further 1 h. A solution of 5-chloro-2-fluoropyridine (22, 86 g) in tetrahydrofuran (THF, 350 mL) was added slowly over a 1.5 hour period at a rate to keep the internal temperature

To isolate 5-chloro-2-propoxypyridine (23), the reaction mixture was cooled to 0-5° C. using an ice/water bath. The reaction was quenched by the addition of a slow stream of saturated aqueous ammonium chloride solution (1 L). The addition was exothermic and may be accompanied by hydrogen gas evolution. The mixture was extracted with ethyl acetate (2x2 ml). The combined organic extracts were washed with saturated brine solution (1 L), dried over magnesium sulfate and charcoal, and filtered through a glass fiber filter. The filtrate was concentrated under reduced pressure to give a pale yellow liquid.

The reaction was successfully carried out on multi-gram scale giving both excellent yield and purity, and the results are shown in Table 4. 5-Chloro-2-propoxypyridine (23) (lot

15

#1357-96-1) was a pale yellow liquid, synthesized with a yield of 110 g/98%. 5-Chloro-2-propoxy pyridine (23) was analyzed using HPLC, and according to results, it was 99.0% pure. ¹H-NMR (300 MHz, CDCl₃) was also used to analyze 5-chloro-2-propoxy pyridine (23), confirming the identity of the compound.

TABLE 4

Lot summary for the preparation of 5-chloro-2-propoxy pyridine (23)					
SM Lot #	SM Batch Size	Yield (g%)	Analysis	Product Lot #	Comments
R11-2408-04	5 g	6.4 g/98%	HPLC: 98.2%	1357-75-1	None
R11-2408-04	25 g	32 g/98%	HPLC: 99.0%	1357-79-1	None
R11-2408-04	86 g	110 g/98%	NMR conforms	1357-96-1	None

Synthesis of 5-Chloro-2-propoxy-4-pyridinylboronic acid (24, Step c)

A 2 L, three-neck round-bottom flask was equipped with a mechanical stirrer, thermocouple, addition funnel, nitrogen

16

solids were present at this time. The reaction was stirred for a further 3 h. Water (500 mL) was added as a steady stream over about a 30 minute period at a rate to keep the internal temperature between -60 to -82° C. The addition was strongly exothermic. The reaction was allowed to reach ambient temperature, and it was stirred rapidly overnight. It was observed

that this reaction was highly temperature sensitive; it was maintained below -78° C. throughout. It was also observed that an increase in temperature, particularly during anion formation, could result in lower yields and byproduct formation. The materials used to synthesize 5-chloro-2-propoxy-4-pyridinylboronic acid (24) are shown in Table 5.

TABLE 5

Materials used in the synthesis of 5-chloro-2-propoxy-4-pyridinylboronic acid (24)					
Compound	MW (g/mol)	d (g/ml)	Equivalents	Amount	Lot #
Reaction					
5-Chloro-2-propoxy pyridine	171.63		1.0 eq.	32 g/0.18 mol	1357-79-1
Lithium diisopropylamide (2.0 M solution in THF/heptanes/ethyl benzene) (LDA)	107.12	0.812	1.2 eq.	112 mL/0.22 mol	R11-2408-05
Triisopropylborate (TPB)	188.08	0.878	2.05 eq.	88 mL/0.38 mol	R07-1007-03
THF (anhydrous)	72.11	0.889	20 vols.	600 mL	R10-2808-02
Isolation					
Water	18.02	1.000	15.6 vols.	500 mL	RO water
Diethyl ether	74.12	0.706	28.1 vols.	900 mL	NA
Ethyl acetate	88.11	0.902	65.6 vols.	2.1 L	R09-0508-02
50% Sodium hydroxide	40.00	1.515		As required	08-2208-01
48% Hydrobromic acid	80.91	1.490		As required	NA
Saturated brine solution			15.6 vols.	500 mL	R08-1208-09

inlet, and reflux condenser fitted with a drying tube and placed into a cooling bath. The flask was charged with a solution of 5-chloro-2-propoxy pyridine (23, 32 g) in THF (600 mL), and stirring was initiated. The solution was cooled in a dry ice/ether/acetone bath to -78 to -82° C. It was important to maintain this temperature throughout the entire reaction. Lithium diisopropylamide (LDA, 112 mL) was added as a slow stream over about a 1 hour period at a rate to keep the internal temperature between -78 to -82° C. The addition was mildly exothermic, leading to a clear orange-brown solution. The reaction was stirred for a further 2 h. Triisopropylborate (TPB, 88 mL) was added as a steady stream over about a 30 minute period at a rate to keep the internal temperature between -78 to -82° C. The addition was mildly exothermic, leading to an orange solution. Some

To isolate 5-chloro-2-propoxy-4-pyridinylboronic acid (24), the biphasic reaction mixture was transferred to a Buchi flask and concentrated under reduced pressure to remove the THF, leaving the aqueous residue. The pH of the aqueous layer was checked, and it was adjusted to pH ~10 with a small amount of 50% sodium hydroxide solution if needed. The aqueous mixture was extracted with diethyl ether (3x300 mL), and the organic extracts were discarded. The pH of the aqueous layer was adjusted to ~3-4 using 48% hydrobromic acid. The addition was exothermic, so ice cooling was used. The aqueous layer was extracted with ethyl acetate (3x700 mL), and the combined organic extracts were washed with saturated brine solution (500 mL) and dried over magnesium sulfate. The mixture was filtered through a glass microfiber filter, and the filtrate was evaporated under reduced pressure to give a sticky off-white solid. The solids were slurried in 15% (methyl tert-butyl ether, MTBE)/heptanes (300 mL) for

17

a minimum of 30 min. The solids were filtered onto a polypropylene filter pad and washed with fresh heptanes (100 mL). The solids were dried under vacuum at ambient temperature for a minimum of 12 h.

Results are shown in Table 6. 5-Chloro-2-propoxy-4-pyridinylboronic acid (24) (lot #1357-82-1) was a white solid, synthesized with a yield of 29.9 g/74%. 5-Chloro-2-propoxy-4-pyridinylboronic acid (24) was analyzed using HPLC, and according to results, it was 94.4% pure. ¹H-NMR (300 MHz, Acetone-*d*₆) was also used to analyze 5-chloro-2-propoxy-4-pyridinylboronic acid (24), confirming the identity of the compound.

TABLE 6

Lot summary for the preparation of 5-chloro-2-propoxy-4-pyridinylboronic acid (24)					
SM Lot #	SM Batch Size	Yield (g/%)	Analysis	Product Lot #	Comments
1357-75-1	5 g	2.36 g/38%	HPLC: 98.0%	1357-76-1	None
1357-79-1	32 g	29.9 g/74%	HPLC: 94.4%	1357-82-1	None
1357-96-1	125 g	82 g/52%	HPLC: 89.1%	1357-100-1	None

Synthesis of 3-(5-chloro-2-propoxy-4-pyridyl)-4-pyridylamine (25. Step d)

A 1 L three-necked round-bottomed flask was equipped with a magnetic bead, thermocouple, nitrogen inlet immer-

18

of K₃PO₄ (28.93 g) and water (136 mL). The addition of the base solution facilitated dissolution of the boronic acid which remained mostly in suspension until then. The solution was continued to be degassed for a minimum of 10 minutes. Dichlorobis(triphenyl phosphine)palladium (II) (3.19 g) was charged. The resulting orange color solution was heated to reflux (~89° C.) for a minimum of 20 hours. The reaction mixture continued to be stirred at reflux until the reaction was complete, i.e., when no significant progress was being made towards product. If the reaction was not complete, stirring was continued at 89° C. overnight, a sample was taken, and

stirring was continued until the reaction was deemed to be complete with addition of more boronic acid as needed. The reaction was monitored by HPLC (MPP-IC1 (270)) by diluting an aliquot of reaction mixture (~1 mL) with (1:1) acetonitrile/water (~2 mL) and submitting for analysis. The starting material eluted at 13.6 min, and the product eluted at 16.3 min. Materials used to synthesize 3-(5-chloro-2-propoxy-4-pyridyl)-4-pyridylamine (25) are shown in Table 7.

TABLE 7

Materials used to synthesize 3-(5-chloro-2-propoxy-4-pyridyl)-4-pyridylamine (25)					
Compound	MW (g/mol)	d (g/mL)	Equivalents	Amount	Lot #
Reaction					
4-Amino-3-iodopyridine	220.01		1.0 eq.	10 g/45.4 mmol	1357-69-1
5-Chloro-2-propoxy-4-pyridinylboronic acid	215.45		1.5 eq.	12471019.25/14.7 g/68.2 mmol	1357-100-1
Potassium phosphate tribasic (K ₃ PO ₄)	212.12		3.0 eq.	28.93 g/0.14 mol	R07-0808-03
Dichlorobis(triphenyl phosphine)palladium (II)	701.89		0.1 eq.	3.19 g/4.5 mmol	R09-1108-01
1,4-Dioxane	88.11	1.034	40.8 vols.	408 mL	R03-3007-06
Water	18.02	1.000	13.6 vols.	136 mL	RO water
Isolation					
Diethyl ether	74.12	0.706	10 vols.	100 mL	NA
2N Hydrochloric acid (HCl)				100 mL	NA
Potassium carbonate	138.21			As required	NA
Ethyl acetate	88.11	0.902	60 vols.	600 mL	R09-0508-02
Water	18.02	1.000	10 vols.	100 mL	RO water
Saturated brine solution			10 vols.	100 mL	R08-1208-09

sion tube, and reflux condenser and placed into a heating mantle. The flask was charged with 4-amino-3-iodopyridine (21, 10 g) and 1,4-dioxane (408 mL), and stirring was initiated. The resulting solution was degassed with nitrogen for 10 minutes. 5-Chloro-2-propoxy-4-pyridinylboronic acid (24, 14.7 g) was added as a single portion, followed by a solution

To isolate 3-(5-chloro-2-propoxy-4-pyridyl)-4-pyridylamine (25), the reaction mixture was cooled to ambient temperature and concentrated under reduced pressure at 40° C. The residue was partitioned between 2N hydrochloric acid (HCl) solution (100 mL) and ether (100 mL), and the mixture was stirred at ambient temperature for 20 minutes. The reaction mixture was transferred to a separatory funnel, and the

19

layers were allowed to separate. The ether extract was discarded. The pH of the aqueous layer was adjusted to ~pH 10 using potassium carbonate, and extracted with ethyl acetate (2x300 mL). The combined organic extracts were washed with water (100 mL), saturated brine solution (100 mL), and dried over magnesium sulfate. The mixture was filtered through a glass fiber filter, and the filtrate was concentrated under reduced pressure. The crude semisolid was loaded on top of a silica column (400 g) packed with DCM, using further DCM for loading. The column was eluted under gravity sequentially with DCM (1 L), 0.5% MeOH in DCM (0.5 L), 1% MeOH in DCM (0.5 L), and 1.5% MeOH in DCM (3 L), collecting fractions of ~150 mL. Increasing the methanol percentage in small increments helped facilitate effective purification. The column was eluted under gravity with 2% MeOH in DCM until complete removal of the clean product was observed by HPLC analysis. All fractions containing clean product were combined and concentrated under reduced pressure to give a yellow semi-solid. The impure fractions were kept aside for further purification if necessary.

Results are shown in Table 8. 3-(5-Chloro-2-propoxy-4-pyridyl)-4-pyridylamine (25) (lot #1457-16-1) was a yellow semi-solid, synthesized with a yield of 4.15 g/35%. 3-(5-Chloro-2-propoxy-4-pyridyl)-4-pyridylamine (25) was analyzed using HPLC, and according to results, it was 96.3% pure. Mass spectrometry and ¹H-NMR (300 MHz, CDCl₃) were used to confirm the identity of 3-(5-chloro-2-propoxy-4-pyridyl)-4-pyridylamine (25).

TABLE 8

Lot summary for the preparation of 3-(5-chloro-2-propoxy-4-pyridyl)-4-pyridylamine (25)					
SM Lot #	SM Batch Size	Yield (g/%)	Analysis	Product Lot #	Comments
1357-64-1	213 mg	110 mg/43%		1357-78-1	None
1357-64-1	1.36 g	N/A		1357-80-1	Combined for column
1357-69-1	5 g	4.4 g/74%	IIPLC: 89.6%	1357-94-1	Re-column gave 3.6 g clean
1357-69-1	9.5 g	9.02 g	HPLC: 73%	1457-9-1	None
1357-69-1	10 g	4.15 g/35%	IIPLC: 96.3%	1457-16-1	Impure materials kept aside
		4.7 g	HPLC: 82.1%	1457-16-2	

Synthesis of 8-propoxy-pyridino[4',3'-5,4]pyrrolo[3,2-c]pyridine (26, Step e)

A 250 mL thick-walled screw-capped reaction tube was charged with a solution of 3-(5-chloro-2-propoxy-4-pyridyl)-

20

4-pyridylamine (25, 2.8 g) in toluene (150 mL), and stirring was initiated. The reaction was carried out in a sealed tube, using a blast shield during the reaction. Sodium tert-butoxide (2.04 g) was added, and the resulting yellow slurry was degassed with nitrogen for 10 minutes. 2-Dicyclohexylphosphino-2'-(N,N-dimethylamino)biphenyl (DavePHOS, 1.09 g) was charged, and the solution was continued to be degassed for a minimum of 10 minutes. Tris(dibenzylidene acetone) palladium (0.97 g) was charged, and the tube was sealed. The resulting orange color solution was heated to ~95°C. in an oil bath for a minimum of 48 hours. Stirring was continued at ambient temperature until the reaction was complete, i.e., when <1% starting material remained, or no further progress towards product was being observed. If reaction was not complete, it was degassed with nitrogen, fresh ligand and catalyst were added, stirring was continued at 95°C. for a minimum of 48 h, another sample was taken, and the reaction was continued until deemed to be complete. The reaction was maintained at 95°C. for 6 days before isolation, and it required addition of fresh catalyst and ligand after 3 days. The reaction was monitored by HPLC (LIL-LC4e (220)), by cooling the sealed tube and opening it under a nitrogen stream,

diluting an aliquot of reaction mixture (~1 mL) with (1:1) 9:1 acetonitrile/water (~2 mL), and submitting for analysis. The starting material eluted at 9.2 min, and the product eluted at 8.2 min. Materials used for the synthesis of 8-propoxy-pyridino[4',3'-5,4]pyrrolo[3,2-c]pyridine (26) are shown in Table

TABLE 9

Materials used in the synthesis of 8-propoxy-pyridino[4',3'-5,4]pyrrolo[3,2-c]pyridine (26)					
Compound	MW (g/mol)	d (g/mL)	Equivalents	Amount (mmol)	Lot #
Reaction					
3-(5-Chloro-2-propoxy-4-pyridyl)-4-pyridylamine	263.5	—	1.0 eq.	2.8 g/10.6 mmol	1457-16-1
Sodium tert-butoxide	96.11	—	2.0 eq.	2.04 g/21.3 mmol	R09-0808-01
Tris(dibenzylidene acetone)palladium	915.7	—	0.1 eq.	0.97 g/1.1 mmol	R06-1808-01
2-Dicyclohexylphosphino-2'-(N,N-dimethylamino)biphenyl (DavePHOS)	342.51	—	0.3 eq.	1.09 g/3.3 mmol	R12-1907-57

TABLE 9-continued

Materials used in the synthesis of 8-propoxyppyridino[4',3'-5,4]pyrrolo[3,2-c]pyridine (26).					
Compound	MW (g/mol)	d (g/mL)	Equivalents	Amt/mol	Lot #
Toluene	92.14	0.865	54 vols. Isolation	150 mL	R09-1508-17
Ethyl acetate	88.11	0.902		350 mL	R09-0508-02
2N HCl solution	—	—		100 mL	NA
Potassium carbonate	138.21			As required	NA
Saturated brine solution				50 mL	R08-1208-09

15

To isolate 8-propoxyppyridino[4',3'-5,4]pyrrolo[3,2-c]pyridine (26), the reaction tube was allowed to cool to ambient temperature. The reaction was concentrated under reduced pressure to give the crude material. Material was combined with previous lots for purification. The crude material was partitioned between ethyl acetate (50 mL) and 1N HCl solution (100 mL), agitated, and the layers were allowed to separate. The aqueous layer was washed with further ethyl acetate (2x50 mL), and all the organic extracts were discarded. The aqueous layer was basified to pH ~8 using solid potassium carbonate and then extracted with ethyl acetate (2x100 mL). At this point solids precipitated which were insoluble in either phase, these were removed by filtration through a glass fiber filter. These solids contained some product, however, it was not possible to isolate the material from the residual catalyst and ligand, and this material was discarded. The organic layer was washed with saturated brine solution (50 mL), dried over magnesium sulfate, and concentrated to dryness under reduced pressure. The material was purified by column chromatography on silica gel [~200 g] eluting with an increasing percentage of methanol in dichloromethane (DCM) from 0-5%.

Results are shown in Table 10. 8-Propoxyppyridino[4',3'-5,4]pyrrolo[3,2-c]pyridine (26) (lot #1457-25-3) was a pale yellow solid, synthesized with a yield of 1.22 g/36%. 8-Propoxyppyridino[4',3'-5,4]pyrrolo[3,2-c]pyridine (26) was analyzed using HPLC, and according to results, it was 95.8% pure. ¹H-NMR (300 MHz, CDCl₃) was used to confirm the identity of 8-propoxyppyridino[4',3'-5,4]pyrrolo[3,2-c]pyridine (26).

20

25

30

35

40

45

TABLE 10

Lot summary for the preparation of 8-propoxyppyridino[4',3'-5,4]pyrrolo[3,2-c]pyridine (26)					
SM Lot #	SM Batch Size	Yield (g/%)	Analysis	Product Lot #	Comments
1457-16-1	100 mg	1.22 g/	N/A	1457-18-1	Materials combined for isolation as new
1457-16-1	1 g	36%	N/A	1457-22-1	
1457-16-1	2.8 g		NMR conforms HPLC: 95.8%	1457-24-1 1451-25-3.	

Synthesis of 8-propoxyppyridino[4',3'-5,4]pyrrolo[3,2-c]pyridine hydrochloride (2, Step f)

A 100 mL three-necked round-bottomed flask was equipped with a magnetic bead, thermocouple, nitrogen inlet, and drying tube and placed into a cooling bath. The flask was charged with 8-propoxyppyridino[4',3'-5,4]pyrrolo[3,2-c]pyridine (26, 1.2 g) and ether (50 mL), and stirring was initiated. Some solids were present at this time. The slurry was cooled to 0-5° C. using an ice/water bath, and HCl in ether (2 M solution, 7.93 mL) was added slowly over 5 minutes. A mild exotherm was observed, with yellow solids forming over time. The reaction was continued to be stirred at ambient temperature for 5 hours. Materials used to synthesize 8-propoxyppyridino[4',3'-5,4]pyrrolo[3,2-c]pyridine hydrochloride (2) are shown in Table 11.

TABLE 11

Materials used to synthesize 8-propoxyppyridino[4',3'-5,4]pyrrolo[3,2-c]pyridine hydrochloride (2)					
Compound	MW (g/mol)	d (g/mL)	Equivalents	Amt/mol	Lot #
Reaction					
8-Propoxyppyridino[4',3'-5,4]pyrrolo[3,2-c]pyridine	227.27		1.0 eq.	1.2 g/5.3 mmol	1457-25-3
2N HCl solution in diethyl ether	36.46	0.747	3.0 eq.	7.9 mL/15.9 mmol	R01-2609-01
Diethyl ether	74.12	0.706	42 vols.	50 mL	NA
Isolation					
Diethyl ether	74.12	0.706	12.5 vols.	15 mL	NA

23

To isolate 8-propoxypyridino[4',3'-5,4]pyrrolo[3,2-c]pyridine hydrochloride (2), the reaction mixture was cooled to 0-5° C. using an ice/water bath and stirred for a further 1 h. The solids were filtered onto a polypropylene filter pad and washed with fresh ether (15 mL) under a nitrogen atmosphere. The solids were dried under vacuum at 30° C. for a minimum of 24 h.

Results are shown in Table 12. 8-Propoxypyridino[4',3'-5,4]pyrrolo[3,2-c]pyridine hydrochloride (2) (lot #1457-26-1) was a yellow solid, synthesized with a yield of 1.49 g. 8-Propoxypyridino[4',3'-5,4]pyrrolo[3,2-c]pyridine hydrochloride (2) was analyzed using HPLC, and according to results, it was 95.8% pure. Mass spectrometry and ¹H-NMR (300 MHz, CDCl₃) were used to confirm the identity of 8-propoxypyridino[4',3'-5,4]pyrrolo[3,2-c]pyridine hydrochloride (2).

TABLE 12

Lot summary for the preparation of 8-propoxypyridino[4',3'-5,4]pyrrolo[3,2-c]pyridine hydrochloride (2)					
SM Lot #	SM Batch Size	Yield (g%)	Analysis	Product Lot #	Comments
1457-25-3	1.12 g	1.49 g	NMR conforms HPLC: 95.8%	1457-26-1	None

Example 3

Synthesis of Tert-Butyl pyridine[4',5'-5,4]pyrrolo[2,3-c]pyridine-3-carboxylate (3)

Tert-Butyl pyridine[4',5'-5,4]pyrrolo[2,3-c]pyridine-3-carboxylate (3) was synthesized from commercially available

24

Synthesis of methyl (2Z)-3-(3-bromo(4-pyridyl))-2-[(phenylmethoxy) carbonyl amino]prop-2-enoate (29. Step a)

The reaction was carried out according to a procedure previously published and as previously described (*Tetrahedron Lett.* 2005, 46, 8877). A 3 l. three-neck round-bottom flask was equipped with a mechanical stirrer, thermocouple, addition funnel, nitrogen inlet, and a drying tube and placed into a cooling bath. The flask was charged with methyl 2-(dimethoxycarbonyl)-2-[(phenylmethoxy)carbonylamino]acetate (8, 93.5 g) and dichloromethane (1000 mL). Stirring was initiated. The contents were cooled to 0° C. 1,8-diazabicyclo[5.4.0]undec-7-ene (44.22 mL) dissolved in dichloromethane (250 mL) was added dropwise over a period of 15 minutes. The solution was stirred at 0-5° C. for 30 minutes. The addition of the material was mildly exothermic to 5° C. 3-bromopyridine-4-carbaldehyde (28, 50 g) dissolved in dichloromethane (500 mL) was added as a slow steady stream through the addition funnel over a period of 30 minutes. The reaction mixture was exothermic to ~30° C. The reaction mixture was allowed to warm to room temperature and continued to stir for a minimum of 3 h. The reaction mixture was continued to be stirred at ambient temperature until the reaction was deemed complete, i.e., upon complete disappearance of 3-bromopyridine-4-carbaldehyde (28). If reaction was not complete, stirring was continued at room temperature for additional 3 h then monitored again. Typically, the reaction was complete within 3-4 h and formed a yellow clear solution. The reaction was monitored by TLC (SiO₂, [5:5] EtOAc:Hept. UV) by spotting the reaction mixture directly on a TLC plate. The reactant (3-bromopyridine-4-carbaldehyde, 28) had an R_F of 0.15, and the product (methyl (2Z)-3-(3-bromo(4-pyridyl))-2-[(phenylmethoxy)carbonyl amino]prop-2-enoate, 29) had an R_F of 0.35. Materials used to synthesize methyl (2Z)-3-(3-bromo(4-pyridyl))-2-[(phenylmethoxy) carbonyl amino]prop-2-enoate (29) are shown in Table 13.

TABLE 13

Materials used to synthesize methyl (2Z)-3-(3-bromo(4-pyridyl))-2-[(phenylmethoxy) carbonyl amino]prop-2-enoate (29)					
Compound	MW (g/mol)	d (g/mL)	Equivalents	Amt./mol	Lot #
Reaction					
3-bromopyridine-4-carbaldehyde	186	—	1.0 eq.	50 g/0.269 mol	1177-7-1
Methyl 2-(dimethoxycarbonyl)-2-[(phenylmethoxy)carbonyl amino]acetate	331.26	—	1.05 eq.	93.50 g/0.282 mol	R03-0909-01
1,8-diazabicyclo[5.4.0]undec-7-ene	152.24	1.018	1.1 vols.	44.22 mL/0.296 mol	R03-0909-05
dichloromethane	84.93	1.325	35 mL/1 g	1750 mL	CML bulk
Isolation					
dichloromethane	84.93	1.325	10 mL/1 g	500 mL	CML bulk
1N HCl	36.5	—	10 mL/1 g	500 mL/1M solution	CML bulk
Water	18.02	1.000	10 vols.	500 mL	RO water
Saturated brine solution	—	—	10 vols.	500 mL	CML bulk

3-bromopyridine-4-carbaldehyde (28) according to FIG. 9. Alternatively, 3-bromopyridine-4-carbaldehyde (28) may be prepared from 3-bromopyrimidine (27) as shown in FIG. 9. Commercially available reagents were used as received unless otherwise noted. Reactions requiring inert atmospheres were run under nitrogen unless otherwise noted.

To isolate the product (methyl (2Z)-3-(3-bromo(4-pyridyl))-2-[(phenylmethoxy) carbonyl amino]prop-2-enoate, 29), the reaction mixture was diluted with dichloromethane (500 mL) and transferred to a separatory funnel. The reaction mixture was washed with 1N HCl solution (2x250 mL) followed by washing with water (1x500 mL). The reaction mixture was washed with brine solution (1x500 mL). All the

25

aqueous layers were discarded. The organic layer was dried over magnesium sulfate and charcoal, and then filtered. The filtrate was concentrated to 1/10th volume (~200 mL). Heptane (~400 mL) was added, the mixture was heated to 40-50° C. on a rotary evaporator for 10 minutes, and stirring was continued at room temperature overnight. The solids were filtered and dried overnight under high vacuum at room temperature for a minimum of 12 h.

Results are shown in Table 14. Methyl (2Z)-3-(3-bromo(4-pyridyl))-2-[(phenylmethoxy)carbonyl amino]prop-2-enoate (29, lot #1458-75-11) was a light yellow solid, synthesized with a yield of 140 g/67% (yield from two batches of 50 g each). Methyl (2Z)-3-(3-bromo(4-pyridyl))-2-[(phenylmethoxy) carbonyl amino]prop-2-enoate (29) was analyzed using HPLC, and according to results, it was 92.3% pure. ¹H-NMR (300 MHz, CDCl₃) was used to confirm the identity of methyl (2Z)-3-(3-bromo(4-pyridyl))-2-[(phenylmethoxy) carbonyl amino]prop-2-enoate (29).

TABLE 14

Lot summary for the preparation of Methyl (2Z)-3-(3-bromo(4-pyridyl))-2-[(phenylmethoxy) carbonyl amino] prop-2-enoate (29)					
SM Lot #	SM Batch Size	Yield (g/%)	Analysis	Product Lot #	Comments
1177-7-1	20 g	25 g/60%	HPLC: 94.4%	1358-92-1	none
1177-7-1	50 g	72 g/68%	HPLC: 91.3%	1458-15-1	none
1177-7-1	2 x 50 g	140 g/67%	HPLC: 92.3%	1458-75-11	none

Synthesis of
methylpyrrolo[2,3-c]pyridine-2-carboxylate (30)
Step b)

A 2 L single neck round bottom flask was equipped with a magnetic bar and a rubber septum. The flask was charged with anhydrous 1,4-dioxane (~675 mL). Methyl (2Z)-3-(3-bromo(4-pyridyl))-2-[(phenylmethoxy) carbonyl amino]prop-2-enoate (29, 45 g) was added, followed by addition of potas-

26

repeated at least three times to ensure that the flask was free from oxygen. The rubber septum was opened and the reaction was charged with L-proline (2.64 g). The sealing and purging steps were repeated again at least three additional times to ensure that the flask was free from oxygen. The rubber septum was opened and the reaction was charged with copper iodide (99.999% purity, 2.2 g). The flask was sealed again, and the sealing and purging steps were repeated again at least three additional times to ensure that the flask was free from oxygen. The resulting slurry was heated at 100° C. for 24 h. Stirring was continued at 100° C. until the reaction was deemed complete, i.e., upon disappearance of starting material (methyl (2Z)-3-(3-bromo(4-pyridyl))-2-[(phenylmethoxy) carbonyl amino]prop-2-enoate, 29). If the reaction was not complete, 0.1 equivalent of CuI and 0.2 equivalents of L-proline were added, the reaction was degassed, nitrogen was purged,

the vessel was sealed, and stirring was continued at 100° C. for 12 h. Typically, the reaction was complete within 24 h and formed a yellow clear solution. The reaction was monitored by TLC (SiO₂, [5:95], MeOH:DCM:2-3 drops of aqueous NH₃, UV, two developments by diluting an aliquot (0.2 mL) with methanol (1 mL) and spotting the reaction mixture directly on a TLC plate. The starting material had an R_f of 0.8, and the product had an R_f of 0.35 (fluorescent spot). Materials used to synthesize methylpyrrolo[2,3-c]pyridine-2-carboxylate (30) are shown in Table 15.

TABLE 15

Materials used to synthesize methylpyrrolo[2,3-c]pyridine-2-carboxylate (30)					
Compound	MW (g/mol)	d (g/mL)	Equivalents	Amount	Lot #
Reaction					
Methyl (2Z)-3-(3-bromo(4-pyridyl))-2-[(phenylmethoxy)carbonyl amino] prop-2-enoate	391.22		1.0 eq.	45 g/0.115 mol	1458-75-11
Potassium carbonate	138.21		3.0 eq.	47.6 g/0.345 mol	CML bulk
Copper iodide, 99.999% purity	190.44	—	0.1 eq.	2.2 g/0.0115 mol	R03-1009-01
L-Proline	115.13		0.2 eq.	2.64 g/0.023 mol	R03-0909-02
1,4-dioxane		—	15 mL/1 g	675 mL	CML bulk
Isolation					
Tetrahydrofuran		—	16 mL/1 g	720 mL	CML bulk

sium carbonate (47.6 g) to the flask while stirring. The flask was sealed with rubber septum and degassed using an oil pump, and nitrogen was purged into the evacuated flask using needle/balloon technique. The sealing and purging steps were

To isolate the product (methylpyrrolo[2,3-c]pyridine-2-carboxylate, 30), the reaction mixture was cooled to room temperature. The reaction was concentrated under vacuum on a rotary evaporator to complete dryness. THF (~650 mL) was

27

added to the residue and heated to reflux. The slurry was maintained at reflux, while stirring, for 3-4 h. The insolubles were removed by hot filtration through a glass fiber filter. The filter cake was washed with hot THF (~50 mL). The filtrate was concentrated to 1/10th volume (~70 mL) and stirred overnight at room temperature. A light yellow solid precipitated. The yellow solid was filtered, washed with ice-cold THF (~25 mL), and dried under high vacuum overnight at room temperature.

Results are shown in Table 16. Methylpyrrolo[2,3-c]pyridine-2-carboxylate (30, lot #1458-83-1) was a pale yellow solid, synthesized with a yield of 10 g/49%. Methylpyrrolo[2,3-c]pyridine-2-carboxylate (30) was analyzed using HPLC, and according to results, it was 98.4% pure. ¹H-NMR (300 MHz, CD₃OD) was used to confirm the identity of methylpyrrolo[2,3-c]pyridine-2-carboxylate (30).

28

charged with methylpyrrolo[2,3-c]pyridine-2-carboxylate (30, 10 g) in methanol (40 mL), and stirring was initiated. Dimethylamine hydrochloride (8.3 g) was added followed by paraformaldehyde (3.05 g), and the tube was sealed. The sealed tube was heated, while stirring the slurry, to 72° C. for 24 h. Heating was stopped, and the reaction vessel was removed from the oil bath. The reaction was deemed complete upon disappearance of starting material (methylpyrrolo[2,3-c]pyridine-2-carboxylate (30). If reaction was not complete, 1 equivalent of both the reagents was added, the vessel was sealed, and stirring was continued overnight. Typically, reaction was complete within 24 h and formed a yellow clear solution. The reaction was monitored by TLC (SiO₂, [5:95], MeOH:DCM:2-3 drops of aqueous NH₃, UV, two developments) by diluting an aliquot (0.2 mL) with methanol (1 mL)

TABLE 16

Lot summary for the preparation of methylpyrrolo[2,3-c]pyridine-2-carboxylate (30)					
SM Lot #	SM Batch Size	Yield (g/%)	Analysis	Product Lot #	Comments
1358-92-1	6 g	50 mg/2%	NMR conforms	1358-95-1	None
1358-99-1	18 g	4.5 g/55%	HPLC: 99.9%	1358-99-1	None
1458-15-1	72 g	8 g/32%	NMR conforms	1458-18-1	Reaction done in a 3N RB flask with continuous N ₂ flow
1458-75-11	25 g	1.6 g/10%	NMR conforms	1458-76-1	Reaction done with continuous N ₂ bubbling into the reaction slurry.
1458-75-11	10 g	1 g/22%	NMR conforms	1458-77-1	Cesium carbonate was used as base instead of potassium carbonate
1458-75-11	20 g	3.1 g/34%	HPLC: 97.4%	1458-78-1	none
1458-75-11	50 g	9 g/40%	HPLC: 86.4%	1458-79-1	None
1458-75-11	45 g	10 g/49%	HPLC: 98.4%	1458-83-1	None

Synthesis of Methyl 3-[(dimethylamino)methyl]pyrrolo[2,3-c]pyridine-2-carboxylate (31, Step c)

An appropriately sized sealed tube was equipped with a magnetic bar and placed into an oil bath. The tube was

and spotting the reaction mixture directly on a TLC plate. The starting material had an R_F of 0.35, and the product had an R_F of 0.15. Materials used to synthesize methyl 3-[(dimethylamino)methyl]pyrrolo[2,3-c]pyridine-2-carboxylate (31) are shown in Table 17.

TABLE 17

Materials used to synthesize methyl 3-[(dimethylamino)methyl]pyrrolo[2,3-c]pyridine-2-carboxylate (31)					
Compound	MW (g/mol)	d (g/mL)	Equivalents	Amount/mol	Lot #
Reaction					
Methylpyrrolo[2,3-c]pyridine-2-carboxylate	176.2	—	1.0 eq.	10 g/0.0567 mol	1458-83-1
Dimethylamine hydrochloride	81.55	—	1.8 eq.	8.3 g/0.1017 mol	R01-0308-05
Paraformaldehyde	30	—	1.8 eq.	3.05 g/0.1017 mol	R01-0308-08
Methanol	—	—	4 vols.	40 mL	CML bulk

TABLE 17-continued

Materials used to synthesize methyl 3-[(dimethylamino)methyl]pyrrolo[2,3-c]pyridine-2-carboxylate (31)					
Compound	MW (g/mol)	d (g/mL)	Equivalents	Amt/mol	Lot #
Isolation					
Aq. Ammonia (15% in water)	17	—	2 vol.	20 mL	CML bulk
Ethyl acetate	88.11	0.902	100 vols.	1 L	CML bulk
Saturated brine solution			10 vols.	100 mL	CML bulk

To isolate methyl 3-[(dimethylamino)methyl]pyrrolo[2,3-c]pyridine-2-carboxylate (31), the reaction mixture was transferred immediately to a Büchi flask, and it was concentrated under reduced pressure to remove methanol. The residue was cooled to room temperature, ice (~5 mL) was added, and the mixture was diluted with aqueous ammonia (~15 mL). The pH was checked after complete dissolution of all the residue. If it was not basic (pH 8-10), an appropriate amount of aqueous ammonia was added to get pH 8-10. The aqueous mixture was extracted with ethyl acetate (5x200 mL). All the extracts were combined, washed with brine solution (~100 mL), dried over magnesium sulfate, and filtered. The result was concentrated to complete dryness. The result was triturated with MTBE (~10 mL), filtered, and dried in a vacuum oven overnight at room temperature.

Results are shown in Table 18. Methyl 3-[(dimethylamino)methyl]pyrrolo[2,3-c]pyridine-2-carboxylate (31, lot #1458-85-1) was a white/light yellow solid, synthesized with a yield of 7 g/50%. Methyl 3-[(dimethylamino)methyl]pyrrolo[2,3-c]pyridine-2-carboxylate (31) was analyzed using HPLC, and according to results, it was 94.4% pure. ¹H-NMR (300 MHz, CD₃OD) was used to confirm the identity of methyl 3-[(dimethylamino)methyl]pyrrolo[2,3-c]pyridine-2-carboxylate (31).

TABLE 18

Lot summary for the preparation of Methyl 3-[(dimethylamino)methyl]pyrrolo[2,3-c]pyridine-2-carboxylate (31)					
SM Lot #	SM Batch Size	Yield (g%)	Analysis	Product Lot #	Comments
1358-99-1	4.5 g	2.2 g/37%	HPLC: 98.4 g		none
1458-18-1					
1358-99-1	5.6 g	2.6 g/35%	HPLC: 97.3%	1458-37-1	none
1458-18-1					
1458-76-1	3 g	1.1 g/32%	NMR conforms	1458-82-1	In an attempt to improve the yield this reaction was attempted in ethanol:IPA:tBn(OH).
1458-78-1					None
1458-78-1	1 g	0.65 g/48%	NMR conforms	1458-82-1	None
1458-78-1	5 g	7.6 g/58%	HPLC: 91.7%	1458-84-1	None
1458-79-1	(two batches)				
1458-83-1	10 g	7 g/50%	HPLC: 98.5%	1458-85-1	None

Synthesis of Ethyl 3-[2-(methoxycarbonyl)pyrrolo[2,3-c]pyridine-3-yl]-2-nitropropanoate (32, Step d)

Ethyl 3-[2-(methoxycarbonyl)pyrrolo[2,3-c]pyridine-3-yl]-2-nitropropanoate (32) was synthesized according to a procedure previously published (*Synthetic Commun.* 1997, 27, 3201-3211). A 1 L single-necked round-bottomed flask

was equipped with a magnetic bead and a reflux condenser and placed into an oil bath. The flask was charged with methyl 3-[(dimethylamino)methyl]pyrrolo[2,3-c]pyridine-2-carboxylate (31, 8 g) and xylene (200 mL), and stirring was initiated. The solid did not dissolve in xylene and remained as a slurry. The resulting solution was degassed with nitrogen for 10 minutes. Ethyl nitroacetate (12, ~11.4 mL) was added as a single portion to the slurry. The solution was continued to be degassed with nitrogen for a minimum of 1 h while stirring. At this stage a slight change in the nature of the slurry was observed, probably due to the formation of the gramine salt of ethyl nitroacetate. The reaction mixture was heated to reflux (~156° C.) for 4 h. During reflux, the solid went into solution and simultaneously a white/light yellowish solid precipitated. The reaction mixture was continued to be stirred at reflux until the reaction was deemed complete, i.e., when no starting material peaks were observed on NMR. Indeed, the NMR matched with the NMR of pure product. If reaction was not complete, stirring was continued at 156° C. for another 3 h until the reaction was deemed to be complete, with additional ethyl nitroacetate added as required. This reaction was typi-

60

cally complete in 3-4 h. The reaction was monitored by NMR by taking an aliquot of reaction mixture (~1 mL), cooling to room temperature, filtering through a polypad, washing with diethyl ether (~2 mL), and submitting the solid for NMR analysis. Materials used to synthesize ethyl 3-[2-(methoxycarbonyl)pyrrolo[2,3-c]pyridine-3-yl]-2-nitropropanoate (32) are shown in Table 19.

TABLE 19

Materials used to synthesize ethyl 3-[2-(methoxycarbonyl)pyrrolo[2,3-c]pyridine-3-yl]-2-nitropropanoate (32)					
Compound	MW (g/mol)	d (g/mL)	Equivalents	Amt/mol	Lot #
Reaction					
Methyl 3-[(dimethylamino)methyl]pyrrolo[2,3-c]pyridine-2-carboxylate	233.27	—	1.0 eq.	8 g/0.034 mmol	1458-84-1 1458-85-1
Ethyl nitroacetate	133.1	1.203	3.0 eq.	11.4 mL/0.1026 mmol	R03-1609-01
Xylene	—	—	25 vol	200 mL	
Isolation					
Diethyl ether	74.12	0.706	10 vols.	80 mL	CML bulk

To isolate the product (ethyl 3-[2-(methoxycarbonyl)pyrrolo[2,3-c]pyridine-3-yl]-2-nitropropanoate, 32), the reaction mixture was cooled to 0° C. and stirred for at least 1 h (may be stirred overnight). The solid was filtered onto a polypad and washed with diethyl ether (~60 mL). Ether washings removed the color, and clean product was white/light yellow in color. The solid was dried under high vacuum for at least 24 h at room temperature.

Results are shown in Table 20. Ethyl 3-[2-(methoxycarbonyl)pyrrolo[2,3-c]pyridine-3-yl]-2-nitropropanoate (32, lot #1458-89-1) was an off-white solid, synthesized with a yield of 8 g/73%. Ethyl 3-[2-(methoxycarbonyl)pyrrolo[2,3-c]pyridine-3-yl]-2-nitropropanoate (32) was analyzed using HPLC, and according to results, it was 93.9% pure. ¹H-NMR (300 MHz, CD₃OD) was used to confirm the identity of ethyl 3-[2-(methoxycarbonyl)pyrrolo[2,3-c]pyridine-3-yl]-2-nitropropanoate (32).

TABLE 20

Lot summary for the preparation of Ethyl 3-[2-(methoxycarbonyl)pyrrolo[2,3-c]pyridine-3-yl]-2-nitropropanoate (32)					
SM Lot #	SM Batch Size	Yield (g-%)	Analysis	Product Lot #	Comments
1458-82-1	2.4 g	2.1 g/72%	NMR confirms	1458-86-1	None
1458-84-1	4.2 g	4 g/71%	HPLC: 92.9%	1458-88-1	None
1458-85-1	8 g	8 g/73%	HPLC: 93.9%	1458-89-1	None

Synthesis of Ethyl 1-oxo-2,3,4-trihydropyridino[4',5'-4.5]pyrrolo[2,3-c]pyridine-3-carboxylate (34, Steps e and f)

A small autoclave (~2 L capacity) was charged with ethyl 3-[2-(methoxy carbonyl)pyrrolo[2,3-c]pyridine-3-yl]-2-nitropropanoate (32) and ethanol (~1000 mL). The solid did not dissolve in ethanol. An approximate amount (~1 g) of Raney Ni was added to the solution, and the vessel was sealed. The autoclave was pressurized with nitrogen (30 to 40 psi), agitated briefly, and vented to hood. The nitrogen purge was repeated two additional times. The autoclave was pressurized with hydrogen (30 to 40 psi), agitated briefly, and vented to hood. The hydrogen purge was repeated two additional times. The autoclave was pressurized with hydrogen (60 psi), and stirring was initiated. The vessel was recharged as necessary to maintain a pressure of 60 psi. The vessel was heated to 42° C. The mixture was stirred for a minimum of 24 hours at 60 psi and 42° C. The reaction mixture was continued to be stirred at 42° C. until the reaction was deemed complete, i.e., when <2-3% starting material was observed by TLC. If the reaction was not complete, stirring was continued at 42° C. for an additional 6 h. Typically, the reaction was complete within 24 h. The reaction was monitored by TLC (SiO₂, [5:95], MeOH:DCM:2-3 drops of aqueous NH₃, UV, two developments) by directly spotting an aliquot of reaction mixture on a TLC plate. The starting material had an RF of 0.75, and the product had an RF of 0.3 (fluorescent spot). Materials used to synthesize ethyl 1-oxo-2,3,4-trihydropyridino[4',5'-4.5]pyrrolo[2,3-c]pyridine-3-carboxylate (34) are shown in Table 21.

TABLE 21

Materials used to synthesize ethyl 1-oxo-2,3,4-trihydropyridino[4',5'-4.5]pyrrolo[2,3-c]pyridine-3-carboxylate (34)					
Compound	MW (g/mol)	d (g/mL)	Equivalents	Amt/mol	Lot #
Reaction					
Ethyl 3-[2-(methoxy carbonyl)pyrrolo[2,3-c]pyridine-3-yl]-2-nitropropanoate	322.30	—	1.0 eq.	4 g/0.0124 mmol	1458-89-1
Raney Nickel	—	—	25% by wt	1 g	R02-0507-19
Ethanol	—	—	250 mL/1 g	1000 mL	CML bulk
Xylene	—	—	100 mL/1 g	400 mL	R04-0709-08

TABLE 21-continued

Materials used to synthesize ethyl 1-oxo-2,3,4-trihydropyridino[4',5'-4,5]pyrrolo[2,3-c]pyridine-3-carboxylate (34)					
Compound	MW (g/mol)	d (g/mL)	Equivalents	Amt/mol	Lot #
Isolation					
Ethyl acetate	88.11	0.902	60 vols.	600 mL	CML bulk

To isolate the product when the reaction was complete, the reaction mixture was cooled to room temperature and hydrogen was removed. The reaction was pressurized with nitrogen (30-40 psi) three times, and the reaction mixture was filtered through a glass-fiber filter pad. The filter cake was washed with hot absolute ethanol (1 L, ~70° C.). The filter cake was not allowed to dry. The filtrate was transferred to a single neck 2 L R13 flask and concentrated to complete dryness on a rotary evaporator. Xylene (~400 mL) was added to the flask. The solid residue did not dissolve in xylene. The resulting solution was degassed with nitrogen for 20 minutes while stirring. The reaction mixture was heated to reflux (~156° C.) and stirred for 4 h. Stirring was continued at reflux until the reaction was deemed complete, i.e. when <2-3% starting material was observed by TLC. If the reaction was not complete, stirring was continued at reflux for an additional 3 h. Typically, the reaction was complete within 4 h. The reaction was monitored by TLC (SiO₂, [5:95], MeOH:DCM:2-3 drops of aqueous NH₃, UV, two developments) by directly spotting an aliquot of the reaction mixture on a TLC plate. The starting material had an RF of 0.3, and the product had an RF of 0.35 (fluorescent spot). The reaction mixture was then cooled to room temperature and concentrated on a rotary evaporator under vacuum to complete dryness. The yellow solid was triturated with ethyl acetate (20 mL) and filtered. The solid was washed with ethyl acetate (~10 mL). The solids were dried under high vacuum overnight at room temperature. The impure material (filtrate) was kept aside for further purification if necessary.

Results are shown in Table 22. Ethyl 1-oxo-2,3,4-trihydropyridino[4',5'-4,5]pyrrolo[2,3-c]pyridine-3-carboxylate (34, lot #1458-91-1, a total of 13 g was hydrogenated and combined before the xylene reflux) was a yellow solid, synthesized with a yield of 4.6 g/44% (yield from 13 g of nitro ester). Ethyl 1-oxo-2,3,4-trihydropyridino[4',5'-4,5]pyrrolo[2,3-c]pyridine-3-carboxylate (34) was analyzed using HPLC, and according to results, it was 87.4% pure. ¹H-NMR (300 MHz, CD₃OD) was used to confirm the identity of Ethyl 1-oxo-2,3,4-trihydropyridino[4',5'-4,5]pyrrolo[2,3-c]pyridine-3-carboxylate (34).

TABLE 22

Lot summary for the preparation of ethyl 1-oxo-2,3,4-trihydropyridino[4',5'-4,5]pyrrolo[2,3-c]pyridine-3-carboxylate (34)					
SM Lot #	SM Batch Size	Yield (g/%)	Analysis	Product Lot #	Comments
1458-89-1	13 g	4.6 g/44%	HPLC:	1458-91-1	None
1458-88-1			87.4%		
1458-86-1					

25 Synthesis of Ethyl 1-hydroxypyridino[4',5'-4,5]pyrrolo[2,3-c]pyridine-3-carboxylate (35, Step g)

A 1 L three-necked round-bottomed flask was equipped with a magnetic bead, thermocouple, nitrogen inlet, and reflux condenser and placed into a heating mantle. The flask was charged with ethyl 1-oxo-2,3,4-trihydropyridino[4',5'-4,5]pyrrolo[2,3-c]pyridine-3-carboxylate (34, 4.5 g) and chloroform (300 mL), and stirring was initiated. The resulting solution was degassed with nitrogen for 10 minutes. Manganese dioxide (45 g) was added as a single portion, and the reaction mixture was heated to reflux for a minimum of 12 h. The solid did not dissolve in chloroform. The reaction mixture was continued to be stirred at reflux until the reaction was deemed complete, i.e., when <2-3% starting material was observed by TLC. If the reaction was not complete, stirring was continued at reflux for an additional 6 h. Typically, the reaction was complete within 12 h. The reaction was monitored by TLC (SiO₂, [5:95], MeOH:DCM:2-3 drops of aqueous NH₃, UV, two developments) by directly spotting an aliquot of the reaction mixture on a TLC plate. The starting material had an RF of 0.35 (fluorescent spot), and the product had an RF of 0.4 (fluorescent spot). Materials used to synthesize ethyl 1-hydroxypyridino[4',5'-4,5]pyrrolo[2,3-c]pyridine-3-carboxylate (35) are shown in Table 23.

TABLE 23

Materials used to synthesize ethyl 1-hydroxypyridino[4',5'-4,5]pyrrolo[2,3-c]pyridine-3-carboxylate (35)					
Compound	MW (g/mol)	d (g/mL)	Equivalents	Amt/mol	Lot #
Reaction					
Ethyl 1-oxo-2,3,4-trihydropyridino[4',5'-4,5]pyrrolo[2,3-c]pyridine-3-carboxylate	259.26		1.0 eq.	4.5 g/0.0174 mmol	1458-91-1
Manganese dioxide	86.94	—	10 times by Wt.	45 g	R10-1607-12
Chloroform			66 mL/1 g	300 mL	CML bulk

TABLE 23-continued

Materials used to synthesize ethyl 1-hydroxypyridino[4',5'-4,5]pyrrolo[2,3-c]pyridine-3-carboxylate (35)					
Compound	MW (g/mol)	d (g/mL)	Equivalents	Amt/mol	Lot #
Isolation					
Ethyl acetate	88.11	0.902	100 vols.	4500 mL	CML bulk

To isolate the product, (ethyl 1-hydroxypyridino[4',5'-4,5]pyrrolo[2,3-c]pyridine-3-carboxylate, 35), the reaction mixture was filtered, while hot, through a bed of celite (~3 g). The celite was washed with hot ethyl acetate (1 L, ~70° C.). The filtrate was kept aside. A 3 L three-necked round-bottomed flask was equipped with a magnetic bead, thermocouple, nitrogen inlet, and reflux condenser and placed into a heating mantle. The filter cake (MnO₂+Celite) was transferred to the flask along with ethyl acetate/MeOH mixture (9:1) (~2 L). The solution was heated to reflux for 4-5 h. The solution was filtered, while hot, through a glass fiber filter. Both the filtrates were combined and concentrated to complete dryness. The resulting solid was triturated with ethyl acetate (~20 ml.) and filtered. The solid was dried under high vacuum for 24 h overnight.

Results are shown in Table 24. Ethyl 1-hydroxypyridino[4',5'-4,5]pyrrolo[2,3-c]pyridine-3-carboxylate (35, lot #1458-94-1) was a yellow/semi-white solid, synthesized with a yield of 3.6 g/80%. Ethyl 1-hydroxypyridino[4',5'-4,5]pyrrolo[2,3-c]pyridine-3-carboxylate (35) was analyzed using HPLC, and according to results, it was 92% pure. Mass Spectrometry and ¹H-NMR (300 MHz, CD₃OD) were used to confirm the identity of ethyl 1-hydroxypyridino[4',5'-4,5]pyrrolo[2,3-c]pyridine-3-carboxylate (35).

TABLE 24

Lot summary for the preparation of Ethyl 1-hydroxypyridino[4',5'-4,5]pyrrolo[2,3-c]pyridine-3-carboxylate (35)					
SM Lot.#	SM Batch Size	Yield (g/%)	Analysis	Product Lot.#	Comments
1458-91-1	4.5 g	3.6 g/80%	HPLC: 92%	1458-94-1	None

Synthesis of ethyl 1-chloropyridino[4',5'-4,5]pyrrolo[2,3-c]pyridine-3-carboxylate (36, Step b)

A 1 L three-necked round-bottomed flask was equipped with a magnetic bead, thermocouple, nitrogen inlet, and reflux condenser and placed into a heating mantle. The flask was charged with ethyl 1-hydroxypyridino[4',5'-4,5]pyrrolo[2,3-c]pyridine-3-carboxylate (35, 3.6 g) and phosphorous oxychloride (30 ml.), and stirring was initiated. The solution was heated to 100° C. for 4 h. The reaction mixture was continued to be stirred at reflux until the reaction was deemed to be complete, i.e. when <2-3% starting material was observed by TLC. If reaction was not complete, stirring was continued at reflux for an additional 3 h. Typically, the reaction was complete within 4 h. The reaction was monitored by TLC (SiO₂, [5:95], MeOH:DCM:2-3 drops of aqueous NH₃, UV, two developments) by quenching an aliquot of reaction mixture (~1 ml.) with saturated NaHCO₃ (pH after quenching was 8), diluting with ethyl acetate (~2 ml.), and spotting the organic layer directly on TLC plate. The starting material had an RF of 0.4 (fluorescent spot), and the product had an RF of 0.6 (fluorescent spot). Materials used to synthesize ethyl 1-chloropyridino[4',5'-4,5]pyrrolo[2,3-c]pyridine-3-carboxylate (36) are shown in Table 25.

TABLE 25

Materials used to synthesize ethyl 1-chloropyridino[4',5'-4,5]pyrrolo[2,3-c]pyridine-3-carboxylate (36)					
Compound	MW (g/mol)	d (g/mL)	Equivalents	Amt/mol	Lot.#
Reaction					
Ethyl 1-hydroxypyridino[4',5'-4,5]pyrrolo[2,3-c]pyridine-3-carboxylate	257.26	—	1.0 eq.	3.6 g/0.0139 mmol	1458-94-1
Phosphorous oxychloride	153.33	1.675	24 eq.	30 ml./0.3358 mmol	R10-2507-01
Isolation					
Sat. sodium bicarbonate	—	—	—	As required	NA
Ethyl acetate	88.11	0.902	100 vols.	360 ml.	CML bulk

TABLE 25-continued

Materials used to synthesize ethyl 1-chloropyridino[4',5'-4,5]pyrrolo[2,3-c]pyridine-3-carboxylate (36)					
Compound	MW (g/mol)	d (g/mL)	Equivalents	Amt/mol	Lot #
Water	18.02	1.000	100 vols.	360 mL	RO water
Saturated brine solution	—	—	20 vols.	72 mL	CML bulk

To isolate the product (ethyl 1-chloropyridino[4',5'-4,5]pyrrolo[2,3-c]pyridine-3-carboxylate, 36), the reaction mixture was cooled to ambient temperature and concentrated under reduced pressure at 40° C. The residue was diluted with ice (~10 mL) and saturated NaHCO₃ (~20 mL, pH of the solution was basic). The aqueous layer was extracted with ethyl acetate (3×300 mL). The combined organic extracts were washed with water (100 mL), saturated brine solution (100 mL), and dried over magnesium sulfate. The mixture was filtered through a glass fiber filter, and the filtrate was concentrated under reduced pressure. The solid residue was triturated with ethyl acetate (~5 mL) and filtered. The solid was dried under high vacuum overnight at room temperature.

Results are shown in Table 26. Ethyl 1-chloropyridino[4',5'-4,5]pyrrolo[2,3-c]pyridine-3-carboxylate (36, lot #1458-97-1) was a yellow/semi-solid, synthesized with a yield of 3 g/79%. Ethyl 1-chloropyridino[4',5'-4,5]pyrrolo[2,3-c]pyridine-3-carboxylate (36) was analyzed using HPLC, and according to results, it was 94.2% pure. Mass Spectrometry and ¹H-NMR (300 MHz, CD₃OD) were used to confirm the identity of ethyl 1-chloropyridino[4',5'-4,5]pyrrolo[2,3-c]pyridine-3-carboxylate (36).

TABLE 26

Lot summary for the preparation of ethyl 1-chloropyridino[4',5'-4,5]pyrrolo[2,3-c]pyridine-3-carboxylate (36)					
SM Lot #	SM Batch Size	Yield (g/%)	Analysis	Product Lot #	Comments
1458-94-1	3.6 g	3 g	HPLC: 94.2%	1458-97-1	none

Synthesis of Ethyl pyridine[4',5'-4,5]pyrrolo[2,3-c]pyridine-3-carboxylate (37, Step i)

The synthesis was carried out according a procedure modified from a protocol previously published (*Tetrahedron Lett.* 2006, 62, 7926). To ethyl 1-chloropyridino[4',5'-4,5]pyrrolo[2,3-c]pyridine-3-carboxylate (36, 3 g) in EtOH (750 mL), diisopropyl ethylamine (~9.4 mL) is added in a small autoclave. The starting material did not always dissolve completely. Pd/C (10 wt %), ~50% wet (0.3 g, 0.1 g/g SM) was charged to the reaction mixture. The autoclave was purged with nitrogen (3×30 psi). At least 1 minute of stirring was allowed for each purge prior to venting. The autoclave was purged with hydrogen (1×30 psi). At least 1 minute of stirring was allowed for purge prior to venting. The autoclave was pressurized with hydrogen (30 psi), and it was hydrogenated at room temperature for 2436 hrs. The reaction mixture was continued to be stirred in the autoclave under 30 psi until it was determined that the reaction was complete, i.e. when <2-3% starting material was observed by TLC. If reaction was not complete, stirring at reflux was continued for an additional 6 h and the reaction was monitored again. This process was continued until the reaction was complete. Typically, reaction was complete within 24 h. The reaction was monitored by TLC (SiO₂, [5:95], MeOH:DCM:2-3 drops of aqueous NH₃, UV, two developments) by directly spotting an aliquot of the reaction mixture on the TLC plate. The starting material had an RF of 0.4 (fluorescent spot), and the product had an RF of 0.2 (fluorescent spot). Materials used to synthesize ethyl pyridine[4',5'-4,5]pyrrolo[2,3-c]pyridine-3-carboxylate (37) are shown in Table 27.

TABLE 27

Materials used to synthesize ethyl pyridine[4',5'-4,5]pyrrolo[2,3-c]pyridine-3-carboxylate (37)					
Compound	MW (g/mol)	d (g/mL)	Equivalents	Amt/mol	Lot #
Reaction					
Ethyl 1-chloropyridino[4',5'-4,5]pyrrolo[2,3-c]pyridine-3-carboxylate	275.7		1.0 eq.	3 g/0.011 mol	1458-97-1
10 wt. % Pd on carbon, ~50% wet	N/A	N/A	0.1 g/g SM	0.3 g	06-1807-2
Diisopropyl ethylamine	129.25	0.747	5.0 eq.	9.4 mL/0.0544 mol	R08-0707-12
Ethanol			250 mL/1 g	750 mL	CML bulk
Isolation					
Ethyl acetate	88.11	0.902	100 vols.	300 mL	CML bulk
Dichloromethane	84.93	1.325	10 mL/1 g	30 mL	CML bulk

39

To isolate the product (ethyl pyridine[4',5'-4,5]pyrrolo[2,3-c]pyridine-3-carboxylate, 37), the autoclave was purged with nitrogen (3x30 psi). At least 1 minute of stirring was allowed for each purge prior to venting. The catalyst was filtered off from the reaction mixture using a double glass fiber. The filter cake was rinsed with ethyl acetate (300 mL). The filtrate was concentrated under reduced pressure at 35/40° C. to dryness. The residue was triturated with dichloromethane (15 mL) and filtered. The solid was dried under high vacuum overnight at room temperature.

Results are shown in Table 28. Ethyl pyridine[4',5'-4,5]pyrrolo[2,3-c]pyridine-3-carboxylate (37, lot #1458-98-1) was an off-white solid, synthesized with a yield of 1.9 g/72%. Ethyl pyridine[4',5'-4,5]pyrrolo[2,3-c]pyridine-3-carboxylate (37) was analyzed using HPLC, and according to results, it was 97.2% pure. ¹H-NMR (300 MHz, CDCl₃) was used to confirm the identity of ethyl pyridine[4',5'-4,5]pyrrolo[2,3-c]pyridine-3-carboxylate (37).

TABLE 28

Lot summary for the preparation of ethyl pyridine[4',5'-4,5]pyrrolo[2,3-c]pyridine-3-carboxylate (37)					
SM Lot #	SM Batch Size	Yield (g/%)	Analysis	Product Lot #	Comments
1458-97-1	3 g	1.9 g	HPLC: 97.2%	1458-98-1	none

Synthesis of Pyridino[4',3'-4,5]pyrrolo[2,3-c]pyridine-3-carboxylic acid (38, Step j)

A 100 mL three-necked round-bottomed flask was equipped with a magnetic bead, thermocouple, and a nitrogen inlet and placed into a cooling bath. The flask was charged with ethyl pyridino[4',5'-4,5]pyrrolo[2,3-c]pyridine-3-carboxylate (37, 1.7 g) and 10% sodium hydroxide (17 mL), and stirring was initiated. The solid did not dissolve initially, but over a period of time (~1 h) it went into solution. Simultaneously, a solid started to precipitate. The solution was stirred for a minimum of 3 h at room temperature. The reaction mixture was continued to be stirred until the reaction was deemed to be complete, i.e., when no starting material was observed by TLC. If the reaction was not complete, stirring was continued at room temperature for an additional 3 h and monitored again. This process was continued until the reac-

40

tion was complete. Typically, the reaction was complete within 3 h. The reaction was monitored by TLC (SiO₂, [5:95], MeOH:DCM:2-3 drops of aqueous NH₃, UV, two developments) by directly spotting on a TLC plate an aliquot of a reaction mixture. The starting material had an R_F of 0.2 (fluorescent spot), and the product had an R_F of 0.0 (fluorescent spot). Materials used to synthesize pyridino[4',3'-4,5]pyrrolo[2,3-c]pyridine-3-carboxylic acid (38) are shown in Table 29.

TABLE 29

Materials used to synthesize pyridino[4',3'-4,5]pyrrolo[2,3-c]pyridine-3-carboxylic acid (38)					
Compound	MW (g/mol)	d (g/mL)	Equivalents	Amt/mol	Lot #
Reaction					
Ethyl pyridine[4',5'-4,5]pyrrolo[2,3-c]pyridine-3-carboxylate	241.25	—	1.0 eq.	1.7 g/0.007 mmol	1458-98-1
10% Sodium hydroxide solution	40.00	1.515	1 mL/0.1 g	17 mL	CML bulk
Isolation					
Conc. Hydrochloric acid	—	—	—	As required	CML bulk
Water	18.02	1.000	3 vols.	5 mL	RO water

To isolate the product (pyridino[4',3'-4,5]pyrrolo[2,3-c]pyridine-3-carboxylic acid, 38), the reaction mixture was cooled to 0° C. Concentrated HCl was added to the reaction mixture and the pH was monitored. HCl was continued to be added dropwise until the pH was 2-3. After reaching the pH, stirring was continued for 1 h and the pH was monitored. If the pH of the solution was acidic (2-3), the solid was filtered through a poly pad. If not, concentrated HCl was added until the mixture was pH 2-3. The solids were washed with water (~5 mL). The solids were dried under high vacuum at 40° C. for a minimum of 48 h.

The results are shown in Table 30. Pyridino[4',3'-4,5]pyrrolo[2,3-c]pyridine-3-carboxylic acid (38, lot #1458-101-1) was a light yellow solid, synthesized with a yield of 1.5 g/35%. ¹H-NMR (300 MHz, DMSO-*d*₆) was used to confirm the identity of pyridino[4',3'-4,5]pyrrolo[2,3-c]pyridine-3-carboxylic acid (38).

TABLE 30

Lot summary for the preparation of pyridino[4',3'-4,5]pyrrolo[2,3-c]pyridine-3-carboxylic acid (38)					
SM Lot #	SM Batch Size	Yield (g/%)	Analysis	Product Lot #	Comments
1357-64-1	213 mg	110 mg/43%		1357-78-1	None
1357-64-1	1.36 g	N/A		1357-80-1	Combined
1357-69-1	5 g	4.4 g/74%	IPLC: 89.6%	1357-94-1	for column
1357-69-1	9.5 g	9.02 g	HPLC: 73%	1457-9-1	Re-column gave 3.6 g clean
1357-69-1	10 g	4.15 g/35%	IPLC: 96.3%	1457-16-1	None
		4.7 g	IPLC: 82.1%	1457-16-2	Impure materials kept aside

41

Synthesis of tert-Butyl pyridine[4',5'-5,4]pyrrolo[2,3-c]pyridine-3-carboxylate (3, Step k)

A 250 ml. three-necked round-bottomed flask was equipped with a magnetic bead, thermocouple, nitrogen inlet immersion tube, and reflux condenser and placed into a heating mantle. The flask was charged with pyridino[4',3'-4,5]pyrrolo[2,3-c]pyridine-3-carboxylic acid (38, 1.5 g) and N,N-dimethylformamide (22.5 mL), and stirring was initiated. The resulting solution was degassed with nitrogen for 10 minutes. Dimethylformamide ditert-butyl acetal (17 mL) was added as a single portion, and the reaction was heated to 90° C. The reaction mixture was stirred at 90° C. for 2-3 h. The reaction was continued to be stirred until the reaction was

42

deemed to be complete, i.e., when no starting material was observed by TLC. If the reaction was not complete, stirring was continued at 90° C. for an additional 2 h and the reaction was monitored again. This process was continued until the reaction was complete. Typically, the reaction was complete within 3 h. The reaction was monitored by TLC (SiO₂, [5:95], MeOH:DCM:2-3 drops of aqueous NH₃, UV, two developments) by diluting an aliquot of reaction mixture (~0.5 mL) with water (~1 mL), extracting with ethyl acetate (~2 mL), and spotting the organic layer directly on TLC plate. The starting material had an RF of 0.0 (fluorescent spot), and the product had an RF of 0.4 (fluorescent spot). Materials used to synthesize tert-butyl pyridine[4',5'-5,4]pyrrolo[2,3-c]pyridine-3-carboxylate (3) are shown in Table 31.

TABLE 31

Materials used to synthesize tert-butyl pyridine[4',5'-5,4]pyrrolo[2,3-c]pyridine-3-carboxylate (3)					
Compound	MW (g/mol)	d (g/mL)	Equivalents	Am't/mol	Lot #
Reaction					
Pyridino[4',3'-4,5]pyrrolo[2,3-c]pyridine-3-carboxylic acid	213	—	1.0 eq.	1.5 g/0.007 mmol	1458-101-1
Dimethylformamide ditert-butyl acetal	203.33	0.848	10 eq.	17 mL / 0.0704 mmol	R04-2309-05
Dimethylformamide	73.09	0.944	15 mL/1 g isolation	22.5 mL	R04-2909-01
Water	18.02	1.000	40 vols.	60 mL	RO water
Ethyl acetate	88.11	0.902	200 vols.	300 mL	R09-0508-02
Saturated brine solution	—	—	40 vols.	60 mL	CML bulk
Methyl tert-butyl ether			4 vols.	6 mL	CML bulk

To isolate the product (tert-butyl pyridine[4',5'-5,4]pyrrolo[2,3-c]pyridine-3-carboxylate, 3), the reaction mixture was cooled to ambient temperature and diluted with water (~30 mL). The reaction mixture was transferred to a separatory funnel and extracted with ethyl acetate (2x150 mL). The combined organic extracts were washed with water (30 mL) and saturated brine solution (60 mL), and then dried over magnesium sulfate. The mixture was filtered through a glass fiber filter, and the filtrate was concentrated under reduced pressure to complete dryness. The residue was triturated with MTBE (6 mL) and filtered. The solid was dried under high vacuum overnight at room temperature.

Results are shown in Table 32. Tert-butyl pyridine[4',5'-5,4]pyrrolo[2,3-c]pyridine-3-carboxylate (3, lot #1458-102-1) was a light yellow solid, synthesized with a yield of 0.85 g/45%. Tert-butyl pyridine[4',5'-5,4]pyrrolo[2,3-c]pyridine-3-carboxylate (3) was analyzed using HPLC, and according to results, it was 98.5% pure. Mass spectrometry and ¹H-NMR (300 MHz, CDCl₃) were used to confirm the identity of tert-butyl pyridine[4',5'-5,4]pyrrolo[2,3-c]pyridine-3-carboxylate (3).

TABLE 32

Lot summary for the preparation of tert-butyl pyridine[4',5'-5,4]pyrrolo[2,3-c]pyridine-3-carboxylate (3)					
SM Lot #	SM Batch Size	Yield (g-%)	Analysis	Product Lot #	Comments
1357-69-1	66 mg	45 mg/54%	NMR conforms	1457-100-1	Scouting run

TABLE 32-continued

Lot summary for the preparation of tert-butyl pyridine[4',5'-5,4]pyrrolo[2,3-c]pyridine-3-carboxylate (3)					
SM Lot #	SM Batch Size	Yield (g-%)	Analysis	Product Lot #	Comments
1458-101-1	1.5 g	0.85 g	HPLC: 98.5%	1457-102-1	The starting material was recovered and subjected to the reaction again with same amount of equivalents. Both the product lots were combined.

Example 4

Synthesis of 3-Propoxy pyridino[4',3'-4,5]pyrrolo[2,3-c]pyridine hydrochloride (4)

3-Propoxy pyridino[4',3'-4,5]pyrrolo[2,3-c]pyridine hydrochloride (4) was synthesized from commercially available reagents including 3-amino pyridine (40) according to FIG. 10. Commercially available reagents were used as received unless otherwise noted. Reactions requiring inert atmospheres were run under nitrogen unless otherwise noted.

chloride (41, 36 ml.) in DCM (25 ml.) was added over at least a 30 minute period, keeping the temperature below 10° C. The reaction mixture was stirred continually at ambient temperature until the reaction was deemed complete, i.e., upon disappearance of 3-amino pyridine (40). If the reaction was not complete, it was stirred at room temperature for additional 3 h then monitored. Typically, the reaction was complete within 6 h. The reaction was monitored by TLC (SiO₂, [9:1] EtOAc:Hex, UV) by spotting an aliquot of the reaction mixture directly on a TLC plate. The reaction mixture was stirred continually overnight at room temperature, and the reactant (3-amino pyridine, 40) had an RF of 0.15, while the product (2,2-dimethyl-N-(3-pyridyl)propanamide, 42) had an RF of 0.35. The reaction mixture formed a dark brown clear solution. Materials used to synthesize 2,2-dimethyl-N-(3-pyridyl)propanamide (42) are shown in Table 33.

TABLE 33

Materials used to synthesize 2,2-dimethyl-N-(3-pyridyl)propanamide (42)					
Compound	MW (g/mol)	d (g/mL)	Equivalents	Amt/mol	Lot #
Reaction					
3-Amino pyridine	94.12	NA	1.00	25 g/0.265 mol	R12-1208-1
Trimethyl acetyl chloride	120.58	0.98	1.03	36 ml./0.292 mol	R11-1607-1
Triethyl amine (TEA)	101.19	0.726	1.25	46.2 mL/0.331 mol	R01-3108-10
Methylene chloride (DCM)	84.93	1.325	10 vol	250 ml.	R05-2208-1
Isolation					
Aq. NaHCO ₃ solution	NA	NA	20 vol	500 mL	R10-2308-1
Magnesium sulfate	NA	NA	0.33 g/g SM	8.2 g	R03-0408-4
Charcoal	NA	NA	0.05 g/g SM	1.25 g	R03-1308-4
Brine	NA	NA	10 vol	250 mL	R08-1208-9

Synthesis of 2,2-dimethyl-N-(3-pyridyl)propanamide (42, Step a)

The reaction was performed according to a procedure available in the literature (*J. Org. Chem.* 1983, 48, 3401-3408). A 1 L three-neck round-bottom flask was equipped with a mechanical stirrer, thermocouple, nitrogen inlet, and drying tube and placed in a cooling bath. The flask was charged with 3-amino pyridine (40, 25 g) and DCM (225 ml.), and stirring was initiated. The reaction mixture was cooled in an ice/water bath to 0-10° C. Triethyl amine (46.2 mL) was added over at least 5 minutes. Trimethyl acetyl

To isolate 2,2-dimethyl-N-(3-pyridyl)propanamide (42), the reaction mixture was washed with aqueous NaHCO₃ solution (2x250 ml.) and brine (250 ml.). The organic layer was dried over MgSO₄ and charcoal, filtered through glass fiber filter paper, and concentrated to dryness. The solids were slurried with MTBE:heptane (1:1, 150 mL) and filtered. The product was air-dried for 2 h and then dried under high vacuum at 40° C. to constant weight.

2,2-Dimethyl-N-(3-pyridyl)propanamide (42, lot #1358-74-1) was an off-white solid, synthesized with a yield of 40 g (84.5%). 2,2-Dimethyl-N-(3-pyridyl)propanamide (42) was analyzed using HPLC (MPP-LC1, 245 nm), and according to

45

results, it was 99.7% pure. ¹H-NMR (300 MHz, CDCl₃) was used to confirm the identity of 2,2-dimethyl-N-(3-pyridyl)propanamide (42).

Synthesis of N-(4-iodo(3-pyridyl))-2,2-dimethylpropanamide (43, Step b)

The reaction was performed according to a procedure in the literature (*J. Org. Chem.* 1988, 53, 2740-2744). A 3 L three-neck round-bottom flask was equipped with a mechanical stirrer, thermocouple, nitrogen inlet, and drying tube and placed in a cooling bath. The flask was charged with 2,2-dimethyl-N-(3-pyridyl)propanamide (42, 40 g), tetramethylethylenediamine (TMEDA, 84 mL) and THF (1400 mL), and stirring was initiated. The reaction mixture was cooled to -78° C. A suspension formed, n-Butyl lithium (224 mL) was added over at least a 15 minute period at a rate to keep the temperature below -65° C. The reaction mixture was stirred continually at -78° C. for 15 minutes before being stirred for 2 h at -10° C. A yellow to white precipitate slowly developed. The reaction mixture was cooled back to -78° C. A solution of iodine (142 g) in THF (480 mL) was added over 30 minutes. The temperature increased from -78° C. to -65° C. The reaction mixture was stirred continually for 2 h at -78° C. The reaction mixture was continually stirred at -78° C. until the reaction was deemed complete, i.e., upon disappearance of 2,2-dimethyl-N-(3-pyridyl)propanamide (42). If reaction was not complete, it was stirred continually at -78° C. for additional 1 h then monitored again. The reaction was monitored by TLC (SiO₂, [7:3] EtOAc:hexane, UV, two developments) by partitioning an aliquot of the reaction mixture (~1 mL) between EtOAc (1 mL) and saturated ammonium chloride solution (3 mL), agitating, allowing the layers to separate, and spotting the organic layer. The starting material (2,2-dimethyl-N-(3-pyridyl)propanamide, 42) had an R_F of 0.25, and the product (N-(4-iodo(3-pyridyl))-2,2-dimethylpropanamide, 43) had an R_F of 0.33. Typically, the reaction conversion was ~80% to product based on TLC. Materials used to synthesize N-(4-iodo(3-pyridyl))-2,2-dimethylpropanamide (43) are shown in Table 34.

TABLE 34

Materials used to synthesize N-(4-iodo(3-pyridyl))-2,2-dimethylpropanamide (43)					
Compound	MW (g/mol)	d (g/mL)	Equivalents	Amt/mol	Lot #
Reaction					
2,2-Dimethyl-N-(3-pyridyl)propanamide	178.23	NA	1.0	40 g/0.224 mol	1358-74-1
n-Butyl lithium (2.5 M in hexanes)	64.06	0.693	2.5	224 mL/0.561 mol	R10-3008-1
N,N,N',N'-Tetramethylethylenediamine (TMEDA)	116.20	0.775	2.5	84 mL/0.561 mol	11-2408-7
Iodine	253.81	NA	2.5	142 g/0.561 mol	R08-0207-7
Tetrahydrofuran (THF)	72.11	0.886	47 vol	1880 mL	R03-2808-3
Isolation					
Saturated (10%) ammonium chloride solution	NA	NA	2.5 vol	100 mL	R06-0808-4
Saturated (10%) sodium thiosulphate solution	NA	NA	5 vol	200 mL	R07-1107-6
Brine	NA	NA	5 vol	200 mL	R08-1208-9

46

To isolate the product (N-(4-iodo(3-pyridyl))-2,2-dimethylpropanamide, 43), the reaction mixture was poured into a saturated (10%) NH₄Cl solution (100 mL). The mixture was extracted with ethyl acetate (2x500 mL). The combined organic layer was washed with a saturated (10%) sodium thiosulfate solution (2x100 mL) to remove excess iodine and brine (200 mL). The organic layer was dried over MgSO₄ and charcoal, filtered through glass fiber filter paper, and concentrated to dryness. The above crude material was purified by passing through a silica plug (4 g of SiO₂/1 g of crude mixture), and eluting the plug with 10-50% ethyl acetate in heptanes. All fractions that contained compound were combined and concentrated under reduced pressure at 45° C. to yield a beige solid. The solid was dried under vacuum at 25° C. for a minimum of 5 hours.

N-(4-iodo(3-pyridyl))-2,2-dimethylpropanamide (43, lot #1358-77-1) was a beige solid, synthesized with a yield of 48 g (70%). N-(4-iodo(3-pyridyl))-2,2-dimethylpropanamide (43) was analyzed using HPLC (MPP-LC1, 240 nm), and according to results, it was 95.9% pure. ¹H-NMR (300 MHz, CDCl₃) was used to confirm the identity of N-(4-iodo(3-pyridyl))-2,2-dimethylpropanamide (43).

Synthesis of 4-iodo-3-pyridylamine (44, Step c)

The reaction was performed according to a procedure in the literature (*Tetrahedron Lett.* 2005, 46, 6363). A 1 L three-neck round-bottom flask was equipped with a mechanical stirrer, thermocouple, nitrogen inlet, and drying tube and placed in a heating mantle. The flask was charged with N-(4-iodo(3-pyridyl))-2,2-dimethylpropanamide (43, 45 g) and 25% sulfuric acid (270 mL). The solubility of starting material in 25% sulfuric acid was very high and formed light yellow clear solution. The reaction mixture was heated to 80° C. for 8 h. The reaction mixture was stirred continually at 80° C. until deemed to be complete, i.e., upon complete disappearance of starting material (N-(4-iodo(3-pyridyl))-2,2-dimethylpropanamide, 43). If reaction was not complete, stirring was continued at 80° C. for additional 6 h then monitored again, and repeated until complete. Typically, reaction was

47

complete within 4-6 h. The reaction was monitored by TLC (SiO₂, 100% EtOAc, UV) by partitioning an aliquot of reaction mixture (~1 mL) between 50% NaOH solution (2 mL) and EtOAc (4 mL), agitating, allowing the layers to separate, and spotting the organic layer on TLC. The starting material (N-(4-iodo(3-pyridyl))-2,2-dimethylpropanamide, 43) had an R_f of 0.55, and the product (4-iodo-3-pyridylamine, 44) had an R_f of 0.35. Materials used to synthesize 4-iodo-3-pyridylamine (44) are shown in Table 35.

TABLE 35

Materials used to synthesize 4-iodo-3-pyridylamine (44)					
Compound	MW (g/mol)	d (g/mL)	Equivalents	Amount	Lot #
Reaction					
N-(4-iodo(3-pyridyl))-2,2-dimethylpropanamide	304.13	NA	1.00	45 g/0.148 mol	1358-77-1
25% Sulfuric acid	98.01	1	6 vol	270 mL	R01-1909-2
Isolation					
50% NaOH solution	NA	1	1 vol	45 g	08-2208-1
EtOAc	NA	0.789	6.6 vol	300 mL	R09-0508-2
MTBE	NA	0.741	1.2 vol	60 mL	R10-2308-01

To isolate the product (4-iodo-3-pyridylamine, 44), the flask was cooled to -10° C. and the mixture was cautiously basified (pH 10-11) with 50% NaOH solution (45 g) while maintaining a temperature below 10° C. Additional ethyl acetate (200 mL) was added, the reaction was stirred for 10 minutes, and the layers were allowed to separate. The organic layer was collected, and the aqueous layer was extracted with ethyl acetate (2x50 mL). The combined organic layer was dried over MgSO₄ and charcoal, filtered through a glass fiber filter paper, and concentrated to dryness. The residue was diluted with MTBE (50 mL) and the solids were filtered, rinsing with MTBE (10 mL). The product was air-dried for 2 h and then dried under high vacuum at room temperature to constant weight.

4-Iodo-3-pyridylamine (44, lot #1358-86-1) was an off-white solid, synthesized with a yield of 24 g (75%). 4-Iodo-3-pyridylamine (44) was analyzed using HPLC (PLX-1.C3, 220), and according to results, it was 100% pure. ¹H-NMR (300 MHz, CDCl₃) was used to confirm the identity of 4-iodo-3-pyridylamine (44).

Synthesis of 4-(5-chloro-2-propoxy-4-pyridyl)-3-pyridyl amine (46, Step d)

A 1 L, three-necked round-bottomed flask was equipped with a mechanical stirrer, thermometer, glass immersion tube

48

for bubbling nitrogen, reflux condenser connected to a bubbler with silicone or mineral oil to monitor that a positive pressure of nitrogen was maintained in the reaction flask throughout the synthesis, and a heating mantle. The flask was charged with 3-amino-4-iodopyridine (44, 12.5 g), 5-chloro-2-propoxy-4-pyridinylboronic acid (45, 18.4 g), and dioxane (538 mL). Stirring was initiated. The resulting yellow solution was degassed by bubbling an intensive stream of nitrogen through the mixture for 10 minutes. Bubbling of nitrogen was

maintained throughout the entire synthesis. A solution of K₃PO₄ (36.18 g) and water (175 mL) was charged. The resulting solution was degassed by bubbling an intensive stream of nitrogen through the mixture for 10 minutes. PdCl₂(PPh₃)₂ (4 g) was charged. The nitrogen flow was reduced, and the resulting orange color solution was heated to reflux (at approximately 95° C.) with bubbling of nitrogen. The reaction mixture was stirred at reflux for a minimum of 24 hours. The reaction mixture was continued to be stirred at 95° C. until the reaction was deemed to be complete, i.e., when <10% starting material was observed by TLC. If reaction was not complete, stirring was continued at 80° C. for an additional 6 h. Typically, reaction was complete within 24 h. The reaction was monitored by TLC (SiO₂, [5:95], MeOH:DCM: 2-3 drops of aqueous NH₃, UV, three developments) by spotting an aliquot of reaction mixture directly on a TLC plate at various time points. The starting material had an R_f of 0.45, while the product had an R_f of 0.5, which was a fluorescent spot. The materials used to synthesize 4-(5-Chloro-2-propoxy-4-pyridyl)-3-pyridyl amine (46) are shown in Table 36.

TABLE 36

Materials used to synthesize 4-(5-chloro-2-propoxy-4-pyridyl)-3-pyridyl amine (46)					
Compound	MW (g/mol)	d (g/mL)	Equivalents	Amount	Lot #
Reaction					
3-Amino-4-iodopyridine	220.01	NA	1.00	12.5 g/0.058	1358-86-1
5-Chloro-2-propoxy-4-pyridinylboronic acid ¹	215.45	NA	1.5	18.4 g/0.085	1357-100-1
Potassium phosphate tri base (K ₃ PO ₄)	212.12	NA	3	36.18 g/0.17	R07-0808-3

TABLE 36-continued

Materials used to synthesize 4-(5-chloro-2-propoxy-4-pyridyl)-3-pyridyl amine (46)					
Compound	MW (g/mol)	d (g/mL)	Equivalents	Amt/mol	Lot #
PdCl ₂ (PPh ₃) ₂	701.89	NA	0.1	4 g/0.0058	R12-1907-57
1,4-Dioxane	NA	1.034	43 vol	538 mL	R03-3007-6
Water	NA	1	14	175 mL	RO water
Isolation					
Water	NA	1	10 vol	125 mL	RO water
EtOAc	NA	0.789	40 vol	500 mL	R09-0508-2

⁴This compound was not commercially available. It was prepared as reported in Example 2, the synthesis of 8-propoxy-pyridino [4',3'-5,4]pyrrolo[2,3-c]pyridine hydrochloride (2).

To isolate the product (4-(5-chloro-2-propoxy-4-pyridyl)-3-pyridyl amine, 46), the reaction mixture was cooled to 40° C. The reaction mixture was concentrated under reduced pressure at 40° C. to remove the majority of dioxane. The residue was diluted with water (125 mL) and EtOAc (300 mL), and the mixture was stirred at ambient temperature for 20 minutes. The reaction mixture was transferred to a separation funnel, the layers were allowed to separate, and the aqueous layer was extracted with EtOAc (2×100 mL). The organic layers were combined, washed with brine (200 mL), dried over MgSO₄ and charcoal, and filtered through a glass fiber filter. The filtrate was concentrated under vacuum to dryness (semi-solid, ~30 g). The crude semisolid was loaded on top of a silica plug (300 g) packed with DCM, using further DCM for loading. The column was eluted under gravity sequentially with DCM (1 L), 0.5% MeOH in DCM (0.5 L), 1% MeOH in DCM (0.5 L), and 1.5% MeOH in DCM (3 L) and collecting fractions of ~3 L. Increasing the methanol percentage in small increments helped facilitate effective purification. The column was eluted under gravity with 2% MeOH in DCM until complete removal of the clean product was observed by H.C. analysis. All fractions containing clean product were combined and concentrated under reduced pressure to give an off-white solid.

4-(5-Chloro-2-propoxy-4-pyridyl)-3-pyridyl amine (46, lot #1458-20-1) was an off-white solid, synthesized with a yield of 7.6 g (51%). 4-(5-Chloro-2-propoxy-4-pyridyl)-3-pyridyl amine (46) was analyzed using HPLC (PLX-LC3, 220), and according to results, it was 96% pure. ¹H-NMR

(300 MHz, CDCl₃) was used to confirm the identity of 4-(5-chloro-2-propoxy-4-pyridyl)-3-pyridyl amine (46).

Synthesis of 3-propoxy-pyridino[4',3'-4,5]pyrrolo[2,3-c]pyridine (47, Step c)

A 500 mL sealed tube was charged with 4-(5-chloro-2-propoxy-4-pyridyl)-3-pyridyl amine (46, 5 g), dioxane (200 mL), Cs₂CO₃ (20.1 g), and water (7 mL). Stirring was initiated. The resulting yellow solution was degassed by bubbling an intensive stream of nitrogen through the mixture for 10 minutes. S-PIIOS (1.56 g) was charged. The resulting solution was degassed by bubbling an intensive stream of nitrogen through the mixture for 10 minutes. Pd₂(dba)₂ (2.6 g) was charged. The resulting solution was degassed by bubbling an intensive stream of nitrogen through the mixture for 5 minutes. The tube was sealed. The reaction mixture was heated to approximately 95° C. at reflux for a minimum of 12 hours. Stirring of the reaction mixture was continued at 95° C. until it was deemed that the reaction was complete, i.e., when <15-20% of the starting material was observed by H.C. If the reaction was not complete, stirring was continued at 80° C. for an additional 6 h. Typically, the reaction was complete within 12 h. The reaction was monitored by TLC (SiO₂, [5:95], MeOH:DCM:2-3 drops of aqueous NH₃, UV, three developments) by spotting an aliquot of reaction mixture directly on H.C. plate. The starting material had an R_F of 0.5 (fluorescent spot), and the product had an R_F of 0.45 (fluorescent spot). Materials used to synthesize 3-propoxy-pyridino[4',3'-4,5]pyrrolo[2,3-c]pyridine (47) are shown in Table 37.

TABLE 37

Materials used to synthesize 3-propoxy-pyridino[4',3'-4,5]pyrrolo[2,3-c]pyridine (47)					
Compound	MW (g/mol)	d (g/mL)	Equivalents	Amt/mol	Lot #
Reaction					
4-(5-Chloro-2-propoxy-4-pyridyl)-3-pyridyl amine	263.73	NA	1.00	5 g/0.019	1358-86-1
Cesium carbonate (Cs ₂ CO ₃)	325.82	NA	3	20.1 g/ 0.057	
Tris(dibenzylideneacetone)palladium (Pd ₂ (dba) ₃)	915.7	NA	0.15	2.6 g/ 0.0028	R06-1808-01
2-Dicyclohexylphosphino-2',6'-dimethoxybiphenyl (S-PIIOS)	410.53	NA	0.2	1.56 g/ 0.0038	R10-0506-53
1,4-Dioxane	NA	1.034	40 vol	200 mL	R03-3007-6
Water	NA	1	1.4	7 mL	RO water

TABLE 37-continued

Materials used to synthesize 3-propoxyppyridino[4',3'-4,5]pyrrolo[2,3-c]pyridine (47)					
Compound	MW (g/mol)	d (g/mL)	Equivalents	Amt/mol	Lot #
Isolation					
Water	NA	1	20 vol	100 mL	RO water
EtOAc	NA	0.895	80 vol	400 mL	R07-0808-4

To isolate the product (3-propoxyppyridino[4',3'-4,5]pyrrolo[2,3-c]pyridine, 47), the reaction mixture was cooled to 40° C. The reaction mixture was concentrated under reduced pressure at 40° C. to remove the majority of dioxane. The residue was diluted with water (100 mL) and EtOAc (200 mL), and the mixture was stirred at ambient temperature for 20 minutes. The reaction mixture was transferred to an appropriate separation funnel, the layers were allowed to separate, and the aqueous layer was extracted with EtOAc (2×100 mL). The organic layers were combined, washed with brine (100 mL), dried over MgSO₄ and charcoal, and filtered through a glass fiber filter. The filtrate was concentrated under vacuum to dryness (~5 g). The crude semisolid was loaded on top of a silica plug (50 g) packed with DCM, using further DCM for

and drying tube and placed in a cooling bath. The flask was charged with 3-propoxyppyridino[4',3'-4,5]pyrrolo[2,3-c]pyridine (47, 1.2 g) and ether (30 mL). Stirring was initiated. A suspension formed. HCl in ether (2 M solution, 3.43 mL) was added slowly over 5 minutes. A mild exotherm was observed, with the temperature increasing from 18.0° C. to 19.4° C. The reaction mixture was continued to be stirred at room temperature for a minimum of 6 hours. No procedure was available to monitor the reaction, so the reaction was continued for a minimum of 6 hours, assuming that reaction was complete. Materials used to synthesize 3-propoxyppyridino[4',3'-4,5]pyrrolo[2,3-c]pyridine hydrochloride (4) are shown in Table 38.

TABLE 38

Materials used to synthesize 3-propoxyppyridino[4',3'-4,5]pyrrolo[2,3-c]pyridine hydrochloride (4)					
Compound	MW (g/mol)	d (g/mL)	Equivalents	Amt/mol	Lot #
Reaction					
3-Propoxyppyridino[4',3'-4,5]pyrrolo[2,3-c]pyridine	227.27	NA	1.0	1.2 g/5.28	1458-36-1
HCl in ether (2 M solution)	36.5	1	1.3	3.43 mL/6.86	R01-2609-01
Ether		1	25 vol	30 mL	NA
Isolation					
Ether		1	10 vol	12 mL	NA

loading. The column was eluted under gravity sequentially with DCM (0.5 L), 0.5% MeOH in DCM (0.5 L), 1% MeOH in DCM (0.5 L), and 1.5% MeOH in DCM (3 L), collecting fractions of ~3 L. Increasing the methanol percentage in small increments helped facilitate effective purification. The column was eluted under gravity with 3% MeOH in DCM until complete removal of the clean product was observed by HPLC analysis. All fractions containing clean product were combined and concentrated under reduced pressure to give an off-white solid.

3-Propoxyppyridino[4',3'-4,5]pyrrolo[2,3-c]pyridine (47, lot #1458-36-1) was a light yellow solid, synthesized with a yield of 2.6 g (60%). 3-Propoxyppyridino[4',3'-4,5]pyrrolo[2,3-c]pyridine (47) was analyzed using HPLC (LIL-LC4, 2230), and according to results, it was 99.9% pure. ¹H-NMR (300 MHz, CDCl₃) was used to confirm the identity of 3-propoxyppyridino[4',3'-4,5]pyrrolo[2,3-c]pyridine (47).

Synthesis of 3-propoxyppyridino[4',3'-4,5]pyrrolo[2,3-c]pyridine hydrochloride (4, Step 1)

A 100 mL three-necked round-bottomed flask was equipped with a magnetic bead, thermocouple, nitrogen inlet,

To isolate the product (3-propoxyppyridino[4',3'-4,5]pyrrolo[2,3-c]pyridine hydrochloride, 4), the reaction mixture was cooled to 0° C. The solids were filtered, the cake was washed with ether (12 mL), and the solids were dried under N₂ atmosphere for approximately 3 h until constant weight.

3-Propoxyppyridino[4',3'-4,5]pyrrolo[2,3-c]pyridine hydrochloride (4, lot #1458-45-1) was a yellow solid, synthesized with a yield of 1.25 g (90%). 3-Propoxyppyridino[4',3'-4,5]pyrrolo[2,3-c]pyridine hydrochloride (4) was analyzed using HPLC (LIL-LC4, 2230), and according to results, it was 99% pure. LC-MS and ¹H-NMR (300 MHz, DMSO-*d*₆) were used to confirm the identity of 3-propoxyppyridino[4',3'-4,5]pyrrolo[2,3-c]pyridine hydrochloride (4).

Reference Example 1

Psychoactive Drug Screening Program (PDSP)

Primary and secondary radioligand binding assays are performed. In general, the primary assay is run at very high ligand (compound) concentration as a broad screen to determine whether a compound binds to a particular receptor. If greater than 50% inhibition at 10 μM (high concentration of

53

compound) at a particular receptor is determined, a secondary assay is performed on that receptor. Data from the secondary assay is the binding affinity (K_i value). K_i values indicating selective binding of a compound to a receptor are generally less than 10 nM.

Primary Radioligand Binding Assay

A solution of the compound to be tested is prepared as a 1 mg/ml stock in Standard Binding Buffer or dimethyl sulfoxide (DMSO) according to its solubility. A similar stock of a reference compound (positive control) is also prepared. Eleven dilutions (5× assay concentration) of the test and reference (reference compounds are presented in Table 19) compounds are prepared in Standard Binding Buffer (buffer compositions are presented in Table 20) by serial dilution: 0.05 nM, 0.5 nM, 1.5 nM, 5 nM, 15 nM, 50 nM, 150 nM, 500 nM, 1.5 μM, 5 μM, 50 μM (thus, the corresponding assay concentrations span from 10 pM to 10 μM and include semi-log points in the range where high-to-moderate affinity ligands compete with radioligand for binding sites).

54

Radioligand (radioligands are presented in Table 39) is diluted to five times the assay concentration (assay concentrations are presented in Table 39) in Standard Binding Buffer. Typically, the assay concentration of radioligand is a value between one half the KD and the KD of a particular radioligand at its target. Aliquots (50 μL) of radioligand are dispensed into the wells of a 96-well plate (see FIG. 11) containing 100 μL of Standard Binding Buffer (Table 40). Then, duplicate 50 μL aliquots of the test and reference compound dilutions are added (see FIG. 11). According to FIG. 11, increasing concentrations (from left to right) of reference or test compound (diluted in buffer) are added (50 μL aliquots, in duplicate) from 5× stock solutions to wells containing 50 μL of 5× radioligand (fixed concentration, prepared in buffer) and 100 μL of buffer. Finally, 50 μL of receptor-containing membrane homogenate (5× suspension in buffer) are added to achieve a final assay volume of 250 μL. Final concentrations of reference or test compound are listed above the columns in FIG. 11.

TABLE 39

Assay conditions for primary radioligand binding assays.			
RECEPTOR	RADIOLIGAND (ASSAY CONC.)	REFERENCE	ASSAY BUFFER
5-HT1A	[³ H]8-OH-DPAT (0.5 nM)	Methysergide	Standard Binding Buffer
5-HT1B	[³ H]GR127543 (0.3 nM)	Ergotamine	Standard Binding Buffer
5-HT1D	[³ H]GR127543 (0.3 nM)	Ergotamine	Standard Binding Buffer
5-HT1E	[³ H]5-HT (3 nM)	5-HT	Standard Binding Buffer
5-HT2A	[³ H]Ketanserin (0.5 nM)	Chlorpromazine	Standard Binding Buffer
5-HT2B	[³ H]LSD (1 nM)	Methysergide	Standard Binding Buffer
5-HT3	[³ H]Mesulergine (0.5 nM)	Chlorpromazine	Standard Binding Buffer
5-HT5a	[³ H]LSD (1 nM)	Ergotamine	Standard Binding Buffer
5-HT6	[³ H]LSD (1 nM)	Chlorpromazine	Standard Binding Buffer
5-HT7	[³ H]LSD (1 nM)	Chlorpromazine	Standard Binding Buffer
D1	[³ H]SCH233930 (0.2 nM)	SKF38393	Dopamine Binding Buffer
D2	[³ H]N-methylspiperone (0.2 nM)	Haloperidol	Dopamine Binding Buffer
D3	[³ H]N-methylspiperone (0.2 nM)	Chlorpromazine	Dopamine Binding Buffer
D4	[³ H]N-methylspiperone (0.3 nM)	Chlorpromazine	Dopamine Binding Buffer
D5	[³ H]SCH233930 (0.2 nM)	SKF38393	Dopamine Binding Buffer
Delta OR	[³ H]DADLE (0.3 nM)	Naltrindole	Standard Binding Buffer
Kappa OR	[³ H]U-69593 (0.3 nM)	Salvinorin A	Standard Binding Buffer
Mu OR	[³ H]DAMGO (0.3 nM)	DAMGO	Standard Binding Buffer
H1	[³ H]Pyrilamine (0.9 nM)	Chlorpheniramine	Histamine Binding Buffer
H2	[³ H]Tiotidine (3 nM)	Cimetidine	Histamine Binding Buffer
H3	[³ H]alpha-methylhistamine (0.4 nM)	Histamine	Histamine Binding Buffer
H4	[³ H]Histamine (5 nM)	Clozapine	Histamine Binding Buffer
SERT	[³ H]Citalopram (0.5 nM)	Amitriptyline	Transporter Binding Buffer
NCT	[³ H]Nisoxetine (0.5 nM)	Desipramine	Transporter Binding Buffer
DAT	[³ H]WIN35428 (0.5 nM)	GBR12909	Transporter Binding Buffer

TABLE 39-continued

Assay conditions for primary radioligand binding assays.			
RECEPTOR	RADIOLIGAND (ASSAY CONC.)	REFERENCE	ASSAY BUFFER
V1	[³ H]Vasopressin (1 nM)	Vasopressin	Vasopressin Binding Buffer
V2	[³ H]Vasopressin (1 nM)	Vasopressin	Vasopressin Binding Buffer
V3	[³ H]Vasopressin (1 nM)	Vasopressin	Vasopressin Binding Buffer
EP3	[³ H]PGI ₂ (10 nM)	EP2	Prostaglandin Binding Buffer
EP4	[³ H]PGI ₂ (10 nM)	EP2	Prostaglandin Binding Buffer
PKCalpha	[³ H]PDBU (3 nM)	PDBU	PKC Binding Buffer
PKCbeta	[³ H]PDBU (3 nM)	PDBU	PKC Binding Buffer
PKCgamma	[³ H]PDBU (3 nM)	PDBU	PKC Binding Buffer
PKCdelta	[³ H]PDBU (3 nM)	PDBU	PKC Binding Buffer
PKCepsilon	[³ H]PDBU (3 nM)	PDBU	PKC Binding Buffer
A1	[³ H]NECA (5 nM)	NECA	Adenosine Binding Buffer
A2	[³ H]NECA (10 nM)	NECA	Adenosine Binding Buffer
VMAT2	[³ H]Tetrabenazine (1.5 nM)	Reserpine	VMAT Binding Buffer
GABAA	[³ H]Muscimol (1 nM)	GABA	50 mM Tris Acetate, pH 7.4
GABAB	[³ H]Baclofen (20 nM)	GABA	50 mM Tris Acetate, pH 7.4
PBR	[³ H]PK11195 (1 nM)	PK11195	50 mM Tris HCl, pH 7.4
AMPA	[³ H]AMPA (1 nM)	Glutamic Acid	50 mM Tris HCl, 2.5 mM CaCl ₂ , pH 7.4
BZP	[³ H]Flunitrazepam (0.5 nM)	Diazepam	50 mM Tris HCl, 2.5 mM CaCl ₂ , pH 7.4
Kainate	[³ H]Kainic Acid	Glutamic Acid	50 mM Tris HCl, 2.5 mM CaCl ₂ , pH 7.4
Na Channel	[³ H]Batrachotoxin	Veratridine	Na Channel Buffer
NMDA	[³ H]MK801 (1 nM)	MK801	5 mM Tris, pH 7.4
Oxytocin	[³ H]Oxytocin	Oxytocin	Oxytocin Binding Buffer
Alpha1A	[³ H]Prazosin (0.7 nM)	Urapidil	Alpha1 Binding Buffer
Alpha1B	[³ H]Prazosin (9.7 nM)	Corynanthine	Alpha1 Binding Buffer
Alpha2A	[³ H]Clonidine (1 nM)	Oxymetazoline	Alpha2 Binding Buffer
Alpha2B	[³ H]Clonidine (1 nM)	Prazosin	Alpha2 Binding Buffer
Alpha2C	[³ H]Clonidine (1 nM)	Prazosin	Alpha2 Binding Buffer
Beta1	[¹²⁵ I]Iodopindolol (0.1 nM)	Atenolol	Beta Binding Buffer
Beta2	[¹²⁵ I]Iodopindolol (9.1 nM)	ICI118551	Beta Binding Buffer
Beta3	[¹²⁵ I]Iodopindolol (0.1 nM)	ICI118551	Beta Binding Buffer
M1	[³ H]QNB (0.5 nM)	Atropine	Muscarinic Binding Buffer
M2	[³ H]QNB (0.5 nM)	Atropine	Muscarinic Binding Buffer
M3	[³ H]QNB (0.5 nM)	Atropine	Muscarinic Binding Buffer
M4	[³ H]QNB (0.5 nM)	Atropine	Muscarinic Binding Buffer
M5	[³ H]QNB (0.5 nM)	Atropine	Muscarinic Binding Buffer
Alpha2Beta2	[³ H]Epibatidine (0.5 nM)	(-)-Nicotine	50 mM Tris HCl, pH 7.4
Alpha2Beta4	[³ H]Epibatidine (0.5 nM)	(-)-Nicotine	50 mM Tris HCl, pH 7.4
Alpha3Beta2	[³ H]Epibatidine (0.5 nM)	(-)-Nicotine	50 mM Tris HCl, pH 7.4
Alpha3Beta4	[³ H]Epibatidine (0.5 nM)	(-)-Nicotine	50 mM Tris HCl, pH 7.4
Alpha4Beta2	[³ H]Epibatidine (0.5 nM)	(-)-Nicotine	50 mM Tris HCl, pH 7.4
Alpha4Beta4	[³ H]Epibatidine (0.5 nM)	(-)-Nicotine	50 mM Tris HCl, pH 7.4

TABLE 39-continued

Assay conditions for primary radioligand binding assays.			
RECEPTOR	RADIOLOGAND (ASSAY CONC.)	REFERENCE	ASSAY BUFFER
Alpha4Beta2 (endog.)	[³ H]Epibatidine (0.5 nM)	(-)-Nicotine	50 mM Tris HCl, pH 7.4
CB1	[³ H]CP55940	CP55940	Cannabinoid Binding Buffer
CB2	[³ H]CP55940	CP55940	Cannabinoid Binding Buffer
Sigma1	[³ H]Pentazocine (3 nM)	Haloperidol	Sigma Binding Buffer
Sigma2	[³ H]DTG (3 nM)	Haloperidol	Sigma Binding Buffer
AT1	[¹²⁵ I]ATII (0.1 nM)	Candesartan	Angiotensin Binding Buffer
AT2	[¹²⁵ I]ATII (0.1 nM)	PD123319	Angiotensin Binding Buffer
Ca++ Channel	[³ H]Nifedipine (0.1 nM)	Nifedipine	Calcium Channel Buffer
Imidazoline1	[¹²⁵ I]Clonidine (0.1 nM)	Naphazoline	Imidazoline Binding Buffer
NT1	[³ H]Neurotensin (2 nM)	Neurotensin	50 mM Tris HCl, 0.2% BSA, pH 7.4
NT2	[³ H]Neurotensin (2 nM)	Neurotensin	50 mM Tris HCl, 0.2% BSA, pH 7.4

TABLE 40

Buffer compositions for primary radioligand binding assays	
BUFFER	COMPOSITION
Standard Binding Buffer	50 mM Tris HCl, 10 mM MgCl ₂ , 0.1 mM EDTA, pH 7.4
Dopamine Binding Buffer	50 mM HEPES, 50 mM NaCl, 5 mM MgCl ₂ , 0.5 mM EDTA, pH 7.4
Histamine Binding Buffer	50 mM Tris HCl, 0.5 mM EDTA, pH 7.4
Transporter Binding Buffer	50 mM Tris HCl, 150 mM NaCl, 5 mM KCl, pH 7.4
Vasopressin Binding Buffer	20 mM Tris HCl, 100 mM NaCl, 10 mM MgCl ₂ , 0.1 mg/ml bacitracin, 1 mg/ml BSA, pH 7.4
Prostaglandin Binding Buffer	25 mM Tris HCl, 10 mM MgCl ₂ , 1 mM EDTA, pH 7.4
PKC Binding Buffer	50 mM Tris HCl, 1 mM CaCl ₂ , 4 mg/ml BSA, 100 µg/ml phosphatidylserine, pH 7.4
Adenosine Binding Buffer	50 mM Tris HCl, 1 U/ml adenosine deaminase, pH 7.4
VMA1 Binding Buffer	50 mM HEPES, 300 mM sucrose, pH 8.0
Na Channel Buffer	130 mM choline chloride, 5.4 mM KCl, 0.8 MgSO ₄ , 5.5 mM glucose, 50 mM HEPES, 1 µM tetrodotoxin, 1 mg/ml BSA, 30 µg/well scorpion venom, pH 7.4 at 37 degrees centigrade
Oxytocin Binding Buffer	50 mM HEPES, 10 mM MnCl ₂ , pH 7.4
Alpha1 Binding Buffer	20 mM Tris HCl, 145 mM NaCl, pH 7.4
Alpha2 Binding Buffer	50 mM Tris HCl, 5 mM MgCl ₂ , pH 7.7
Beta Binding Buffer	50 mM Tris HCl, 3 mM MnCl ₂ , pH 7.7
Muscarinic Binding Buffer	50 mM Tris HCl, pH 7.7
Cannabinoid Binding Buffer	50 mM Tris HCl, 1 mM EDTA, 3 mM MgCl ₂ , 5 mg/ml fatty acid-free BSA, pH 7.4
Sigma Binding Buffer	50 mM Tris HCl, pH 8.0
Angiotensin Binding Buffer	50 mM Tris HCl, 5 mM MgCl ₂ , 150 mM NaCl, 0.5 mg/ml BSA, 100 mM bacitracin, protease inhibitor, pH 7.4
Calcium Channel Buffer	50 mM Tris HCl, 50 mM NaCl, 1 mM CaCl ₂ , pH 7.4
Imidazoline Binding Buffer	5 mM Tris HCl, 5 mM HEPES, 0.5 mM EDTA, 0.5 mM MgCl ₂ , pH 8.0

Finally, crude membrane fractions of cells expressing recombinant target (prepared from 10 cm plates by harvesting phosphate buffered saline (PBS)-rinsed monolayers, resuspending and lysing in chilled, hypotonic 50 mM Tris-HCl, pH 7.4, centrifuging at 20,000xg, decanting the supernatant and storing at -80° C.; typically, one 10 cm plate provides sufficient material for 24 wells) are resuspended in 3 ml of chilled Standard Binding Buffer and homogenized by several passages through a 26 gauge needle, and then 50 µL are dispensed into each well.

The 250 µL reactions are incubated at room temperature and shielded from light (to prevent photolysis of light-sensitive ligands) for 1.5 hours, then harvested by rapid filtration onto Whatman GF/B glass fiber filters pre-soaked with 0.3% polyethyleneimine using a 96-well Brandel harvester. Four rapid 500 µL washes are performed with chilled Standard Binding Buffer to reduce non-specific binding. Filters are placed in 6 ml scintillation tubes and allowed to dry overnight. The next day, 4 ml of BeckoScint scintillation cocktail (National Diagnostics) are added to each tube. The tubes are capped, labeled, and counted by liquid scintillation counting.

For higher throughput assays, bound radioactivity is harvested onto 0.3% polyethyleneimine-treated, 96-well filter mats using a 96-well filtermate harvester. The filter mats are dried, then scintillant is melted onto the filters, and the radioactivity retained on the filters is counted in a Microbeta scintillation counter.

Raw data (dpm) representing total radioligand binding (i.e., specific+non-specific binding) are plotted as a function of the logarithm of the molar concentration of the competitor (i.e., test or reference compound). Non-linear regression of the normalized (i.e., percent radioligand binding compared to that observed in the absence of test or reference compound) raw data is performed in Prism 4.0 (GraphPad Software) using the built-in three parameter logistic model describing ligand competition binding to radioligand-labeled sites:

$$y = \text{bottom} + \frac{(\text{top} - \text{bottom})}{1 + 10^{-(\log IC_{50} - x)}}$$

where bottom equals the residual radioligand binding measured in the presence of 10 μM reference compound (i.e., non-specific binding) and top equals the total radioligand binding observed in the absence of competitor. The $\log IC_{50}$ (i.e., the log of the ligand concentration that reduces radioligand binding by 50%) is thus estimated from the data and used to obtain the K_i by applying the Cheng-Prusoff approximation:

$$K_i = IC_{50} / (1 + [\text{ligand}] / K_D)$$

where [ligand] equals the assay radioligand concentration and K_D equals the affinity constant of the radioligand for the target receptor.

Secondary Radioligand Binding Assay

This assay is used to test binding to receptors such as the serotonin receptors: 5-HT_{1A}, 5-HT_{1B}, 5-HT_{1D}, 5-HT_{1E}, 5-HT_{2A}, 5-HT_{2B}, 5-HT_{2C}, 5-HT₃, 5-HT_{5A}, 5-HT₆ and 5-HT₇. The protocol is adapted from Roth et al. *J. Pharmacol. Exp. Ther.* 1986, 238, 480-485 and Roth et al. *J. Pharmacol. Exp. Ther.* 1994, 268, 1403-1410. The assay buffer is Standard Binding Buffer (50 mM Tris-HCl, 10 mM MgCl₂, 0.1 mM EDTA, pH 7.4). The membrane fraction source is transiently or stably transfected cell lines (e.g., HEK293, COS, CHO, NIH3T3).

A solution of the compound to be tested is prepared as a 1 mg/ml stock in Standard Binding Buffer or DMSO according to its solubility. A similar stock of a reference compound (positive control) is also prepared. Eleven dilutions (5 \times assay concentration) of the test and reference (see Table 41) compounds are prepared in Standard Binding Buffer by serial dilution: 0.05 nM, 0.5 nM, 1.5 nM, 5 nM, 15 nM, 50 nM, 150 nM, 500 nM, 1.5 μM , 5 μM , 50 μM (thus, the corresponding assay concentrations span from 10 pM to 10 μM and include semilog points in the range where high-to-moderate affinity ligands compete with radioligand for binding sites).

Radioligand (see Table 41) is diluted to five times the assay concentration (see Table 21) in Standard Binding Buffer. Typically, the assay concentration of radioligand is a value between one half the K_D and the K_D of a particular radioligand at its target. Aliquots (50 μL) of radioligand are dispensed into the wells of a 96-well plate (see FIG. 11) containing 100 μL of Standard Binding Buffer. Then, duplicate 50 μL aliquots of the test and reference compound dilutions are added (see FIG. 11).

TABLE 41

Radioligands, radioligands assay concentrations, and reference compounds for secondary radioligand binding assay		
RECEPTOR	RADIOLIGAND (ASSAY CONC.)	REFERENCE COMPOUND
5-HT _{1A}	[³ H]8-OH-PPAT (0.5 nM)	Methysergide
5-HT _{1B}	[³ H]GR125743 (0.3 nM)	Ergotamine
5-HT _{1D}	[³ H]GR125743 (0.3 nM)	Ergotamine
5-HT _{1E}	[³ H]5-HT (3 nM)	5-HT
5-HT _{2A}	[³ H]Ketsanserin (0.5 nM)	Chlorpromazine
5-HT _{2B}	[³ H]LSD (1 nM)	5-HT
5-HT _{2C}	[³ H]Mesulergine (0.5 nM)	Chlorpromazine
5-HT ₃	[³ H]LY278584 (0.3 nM)	LY278584
5-HT _{5A}	[³ H]LSD (1 nM)	Ergotamine
5-HT ₆	[³ H]LSD (1 nM)	Chlorpromazine
5-HT ₇	[³ H]LSD (1 nM)	Chlorpromazine

Finally, crude membrane fractions of cells expressing recombinant target (prepared from 10-cm plates by harvesting PBS-rinsed monolayers, resuspending and lysing in chilled, hypotonic 50 mM Tris-HCl, pH 7.4, centrifuging at 20,000 \times g, decanting the supernatant and storing at -80 $^{\circ}$ C.; typically, one 10 cm plate provides sufficient material for 24 wells) are resuspended in 3 mL of chilled Standard Binding Buffer and homogenized by several passages through a 26 gauge needle, and then 50 μL are dispensed into each well.

The 250 μL reactions are incubated at room temperature and shielded from light (to prevent photolysis of light-sensitive ligands) for 1.5 hours, then harvested by rapid filtration onto Whatman GF/B glass fiber filters pre-soaked with 0.3% polyethyleneimine using a 96-well Brandel harvester. Four rapid 500 μL washes are performed with chilled Standard Binding Buffer to reduce non-specific binding. Filters are placed in 6 mL scintillation tubes and allowed to dry overnight. The next day, 4 mL of BeckoScint scintillation cocktail (National Diagnostics) are added to each tube. The tubes are capped, labeled, and counted by liquid scintillation counting. For higher throughput assays, bound radioactivity is harvested onto 0.3% polyethyleneimine-treated, 96-well filter mats using a 96-well Filtermate harvester. The filter mats are dried, then scintillant is melted onto the filters, and the radioactivity retained on the filters is counted in a Microbeta scintillation counter.

Raw data (dpm) representing total radioligand binding (i.e., specific+non-specific binding) are plotted as a function of the logarithm of the molar concentration of the competitor (i.e., test or reference compound). Non-linear regression of the normalized (i.e., percent radioligand binding compared to that observed in the absence of test or reference compound) raw data is performed in Prism 4.0 (GraphPad Software) using the built-in three parameter logistic model describing ligand competition binding to radioligand-labeled sites:

$$y = \text{bottom} + \frac{(\text{top} - \text{bottom})}{1 + 10^{-(\log IC_{50} - x)}}$$

where bottom equals the residual radioligand binding measured in the presence of 10 μM reference compound (i.e., non-specific binding) and top equals the total radioligand binding observed in the absence of competitor. The $\log IC_{50}$ (i.e., the log of the ligand concentration that reduces radioligand binding by 50%) is thus estimated from the data and used to obtain the K_i by applying the Cheng-Prusoff approximation:

$$K_i = IC_{50} / (1 + [\text{ligand}] / K_D)$$

where [ligand] equals the assay radioligand concentration and K_D equals the affinity constant of the radioligand for the target receptor.

61

Example 5

Psychoactive Drug Screening Program (PDSP)
Analysis of 8-Propoxy pyridino[4,3'-5,4]pyrrolo[3,2-c]pyridine hydrochloride (2) and 3-Propoxy pyridino[4',3'-4,5]pyrrolo[2,3-c]pyridine hydrochloride (4)

8-Propoxy pyridino[4',3'-5,4]pyrrolo[3,2-c]pyridine hydrochloride (2) and 3-propoxy pyridino[4',3'-4,5]pyrrolo[2,3-c]pyridine hydrochloride (4) were tested for binding to receptors according to Reference Example 1. Results are presented in Table 42, where data represent mean percentage inhibition (with n = 4 determinations) for the compound tested at receptor subtypes. Data shown in Table 42 are results from primary assays, except numbers in parentheses are the K_i values in nM as determined from secondary assays. Significant inhibition was considered to be >50% in primary assays. Where negative inhibition (-) was seen, it represented a stimulation of binding, as in some cases, compounds at high concentration non-specifically increase binding. The concentration of compound in primary assays was 10 μ M.

8-Propoxy pyridino[4',3'-5,4]pyrrolo[3,2-c]pyridine hydrochloride (2) demonstrated <50% binding at 10 μ M in primary receptor binding assays, i.e., the compounds did not bind to the receptor, at the following receptors: Serotonin 5ht1a (human); Serotonin 5ht1b (human); Serotonin 5ht5a (human); Serotonin 5ht6 (human); Serotonin 5ht7 (human); Adrenergic Beta1 (human); Dopamine D1 (human); Dopamine D3 (rat); Dopamine D5 (human); Opiate DOR; Histamine H1 (human); Histamine H2 (human); Histamine H3 (human); Opiate KOR; Muscarinic (acetylcholine) M3 (human); and Opiate MOR. 8-Propoxy pyridino[4',3'-5,4]pyrrolo[3,2-c]pyridine hydrochloride (2) demonstrated >50% binding at 10 μ M in primary receptor binding assays at the Dopamine D2 (human) and Dopamine D4 (human) receptors, so secondary assay binding data was determined for these two receptors. The K_i for binding of compound 2 at Dopamine D2 (human) and Dopamine D4 (human) receptors was found to be >10,000 nM and 7,503 nM, respectively, which indicated that compound 2 does not significantly bind these receptors.

3-Propoxy pyridino[4',3'-4,5]pyrrolo[2,3-c]pyridine hydrochloride (4) demonstrated <50% binding at 10 μ M in primary receptor binding assays, i.e., the compounds did not bind to the receptor, at the following receptors: Serotonin 5ht1a (human); Serotonin 5ht1b (human); Serotonin 5ht3 (human); Serotonin 5ht5a (human); Serotonin 5ht6 (human); Serotonin 5ht7 (human); Adrenergic Beta1 (human); Dopamine D1 (human); Dopamine D5 (human); Opiate DOR; Histamine H1 (human); Histamine H2 (human); Histamine H3 (human); Histamine H4 (human); Opiate KOR; Muscarinic (acetylcholine) M3 (human); Opiate MOR; NET transporter; and SERT transporter. 3-Propoxy pyridino[4',3'-4,5]pyrrolo[2,3-c]pyridine hydrochloride (4) demonstrated >50% binding at 10 μ M in primary receptor binding assays at the Dopamine D2 (human) receptor, so secondary assay binding data was determined for this receptor. The K_i for binding of compound 4 at Dopamine D2 (human) receptor was found to be >10,000 nM, which indicated that compound 4 does not significantly bind this receptor.

62

TABLE 42

Results of Psychoactive Drug Screening Program (PDSP) Analysis of 8-propoxy pyridino[4',3'-5,4]pyrrolo[3,2-c]pyridine hydrochloride (2) and 3-propoxy pyridino[4',3'-4,5]pyrrolo[2,3-c]pyridine hydrochloride (4)		
RECEPTOR ^a	COMPOUND 2	COMPOUND 4
Adrenergic receptor Beta1	3.2	3.5
Dopamine receptor D1	-8.8	-14
Dopamine receptor D2	(>10,000) ^b	50 (>10,000) ^b
Dopamine receptor D3	31.8	24.1
Dopamine receptor D4	(7,503) ^b	-18.1
Opiate receptor DOR	13.6	10
Histamine receptor H1	17.1	9.3
Histamine receptor H2	31.4	26.8
Histamine receptor H3	21	11.3
Histamine receptor H4		4.9
Opiate receptor KOR	-10.2	-6.1
Opiate receptor MOR	5.6	1.2
Muscarinic receptor M3	15.6	2.4
Serotonin receptor 5ht1a	6.1	16.4
Serotonin receptor 5ht1b	47	4.1
Serotonin receptor 5ht3		20.7
Serotonin receptor 5ht5a	15	8.3
Serotonin receptor 5ht6	10.4	15.3
Serotonin receptor 5ht7	6.4	-12.1
NET transporter		36.8
SERT transporter	22.1	17.6

^aBased on the primary (and secondary, if determined) binding assays, compounds 2 and 4 did not significantly bind to the receptors shown here.

^bSecondary binding assay was performed, with the number in parentheses being the K_i value in nM.

Example 6

Psychoactive Drug Screening Program (PDSP)
Analysis of tert-Butyl pyridine[4',5'-4,5]pyrrolo[3,2-c]pyridine-8-carboxylate (1) and tert-Butyl pyridine [4',5'-5,4]pyrrolo[2,3-c]pyridine-3-carboxylate (3)

tert-Butyl pyridine[4',5'-4,5]pyrrolo[3,2-c]pyridine-8-carboxylate (1) and tert-butyl pyridine[4',5'-5,4]pyrrolo[2,3-c]pyridine-3-carboxylate (3) are tested for binding to receptors as described in Reference Example 1 and are shown to bind to GABA_A receptor.

Reference Example 2

Competition Binding Assays

Competition binding assays are performed as described in Choudhary, M. S. et al. *Mol. Pharmacol.* 1992, 42, 627-633. Competition binding assays are performed in a total volume of 0.5 ml, at 4° C. for 1 hour using [³H]flunitrazepam as the radiolabelled ligand. A total of 6 μ g of cloned human GABA_A receptor DNA containing desired α subtype along with β 2 and γ 2 subunits are used for transfecting HEK293 cell line using Eugene 6 (Roche Diagnostic) transfecting reagent. Cells are harvested 48 hrs after transfection, washed with Tris-C1 buffer (pH 7.0) and Tris-Acetate buffer (pH 7.4), and the resulting pellets are stored at -80° C. until assayed. On the day of the assay, pellets containing 20-50 μ g of GABA_A receptor protein are resuspended in 50 mM Tris-acetate pH 7.4 at 4° C. and incubated with the radiolabel as previously described (Choudhary et al., 1992). Nonspecific binding is defined as radioactivity bound in the presence of 100 μ M compound and represents less than 20% of total binding. Membranes are harvested with a Brandel cell harvester followed by three ice-cold washes onto polyethylenimine-pre-treated (0.3%) Whatman GF/C filters. Filters are dried overnight and then soaked in Ecocint A liquid scintillation

63

cocktail (National Diagnostics; Atlanta, Ga.). Bound radioactivity is quantified by liquid scintillation counting. Membrane protein concentrations are determined using an assay kit from Bio-Rad (I Hercules, Calif.) with bovine serum albumin as the standard.

Example 7

Competition Binding Assay Analysis of Compounds (2), (3) and (4)

8-Propoxy pyridino[4',3'-5,4]pyrrolo[3,2-c]pyridine hydrochloride (2), tert-butyl pyridine[4',5'-5,4]pyrrolo[2,3-c]pyridine-3-carboxylate (3) and 3-propoxy pyridino[4',3'-4,5]pyrrolo[2,3-c]pyridine hydrochloride (4) were tested for binding to the BzR/GABA_A-ergic receptors as detailed in Reference Example 2. As shown in Table 43, the compounds bind potently at the BzR/GABA_A-ergic receptors.

TABLE 43

Results of Competition Binding Assay Analysis of Compounds (2), (3) and (4)				
Compound	GABA _A RECEPTOR BINDING (nM)			
	α1	α2	α3	α5
2	9.861	0.33	4.04	12.21
3	2.9	2.5	3.4	3.7
4	5.785	6.308	1.49	43.06

Example 8

Competition Binding Assay Analysis of tert-Butyl pyridine[4',5'-4,5]pyrrolo[3,2-c]pyridine-8-carboxylate (1)

Tert-butyl pyridine[4',5'-4,5]pyrrolo[3,2-c]pyridine-8-carboxylate (1) is tested for binding to the BzR/GABA_A-ergic receptors as described in Reference Example 2, and results indicate the compound potently binds to the BzR/GABA_A-ergic receptors.

Reference Example 3

Analysis of the In Vivo Effects

Electrophysiological Experiments

GABA_A receptor subunits α1, α3, and α2 are cloned into pCDM8 expression vectors (Invitrogen, CA) as been described elsewhere (Fuchs et al. *Eur. J. Pharmacol.* 1995, 289, 87-95). cDNAs for subunits α2, α3 and α5 are subcloned into pCI-vector. After linearizing the cDNA vectors with appropriate restriction endonucleases, capped transcripts are produced using the mMessage mMachine 17 transcription kit (Ambion, Tex.). The capped transcripts are polyadenylated using yeast poly(A) polymerase (USB, OH) and are diluted and stored in diethylpyrocarbonate-treated water at -70° C.

The methods used for isolating, culturing, injecting and defolliculating of the oocytes are identical as described previously (Sigel, E. *J. Physiol.* 1987, 386, 73-90; Sigel, E. et al. *Neuron* 1990, 5, 703-711.). Briefly, mature female *Xenopus laevis* (Nasco, Wis.) are anaesthetized in a bath of ice-cold 0.17% Tricain (Ethyl-m-aminobenzoate, Sigma, Mo.) before decapitation and removal of the frogs ovary. Stage 5 to 6 oocytes with the follicle cell layer around them are singled out of the ovary using a platinum wire loop. Oocytes are stored

64

and incubated at 18° C. in modified Barths' Medium (MB, containing 88 mM NaCl, 10 mM HEPES-NaOH (pH 7.4), 2.4 mM NaHCO₃, 1 mM KCl, 0.82 mM MgSO₄, 0.41 mM CaCl₂, 0.34 mM Ca(NO₃)₂) that is supplemented with 100 U/ml penicillin and 100 µg/mL streptomycin. Oocytes with follicle cell layers still around them are injected with a total of 2.25 µg of cRNA. cRNA ratio used is 1:1:5 for the α subunits, β3, and γ2, respectively. After injection of cRNA, oocytes are incubated for at least 36 hours before the enveloping follicle cell layers are removed. To this end, oocytes are incubated for 20 min at 37° C. in MB that contains 1 mg/mL collagenase type IA and 0.1 mg/ml trypsin inhibitor I-S (both Sigma). This is followed by osmotic shrinkage of the oocytes in doubly concentrated MB medium supplied with 4 mM Na-EGTA and manually removing the follicle cell layer. After peeling off the follicle cell layer, the cells are allowed to recover overnight before being used in electrophysiological experiments.

For electrophysiological recordings, oocytes are placed on a nylon-grid in a bath of *Xenopus* Ringer solution (XR, containing 90 mM NaCl, 5 mM HEPES-NaOH (pH 7.4), 1 mM MgCl₂, 1 mM KCl and 1 mM CaCl₂). The oocytes are constantly washed by a flow of 6 ml/min XR which can be switched to XR containing GABA and/or the compounds. The compounds are diluted into XR from DMSO-solutions resulting in a final concentration of 0.1% DMSO perfusing the oocytes. Compounds are preapplied for 30 sec before the addition of GABA, which is coapplied with the drugs until a peak response is observed. Between two applications, oocytes are washed in XR for up to 15 min to ensure full recovery from desensitization. For measurements the oocytes are impaled with two microelectrodes (2-3 MΩ) which are filled with 2 mM KCl. All recordings are performed at room temperature at a holding potential of -60 mV using a Warner OC-725C two-electrode voltage clamp (Warner Instruments, Hamden, Conn.). Data are digitized, recorded, and measured using a Digidata 1322A data acquisition system (Axon Instruments, Union City, Calif.). Results of concentration response experiments are graphed using GraphPad Prism 4.00 (GraphPad Software, San Diego, Calif.). Data are graphed as mean±SEM of at least four oocytes from at least two batches.

Behavioral Experiments

Experiments are carried out on male Wistar rats (Military Farm, Belgrade, Serbia), weighing 220-250 g. All procedures in the study conform to EEC Directive 86/609 and are approved by the Ethical Committee on Animal Experimentation of the Faculty of Pharmacy in Belgrade. The rats are housed in transparent plastic cages, six animals per cage, and have free access to food pellets and tap water. The temperature of the animal room is 22±1° C., the relative humidity 40-70%, the illumination 120 lux, and the 12/12 h light/dark period (light on at 6:00 h). All handling and testing takes place during the light phase of the diurnal cycle. Separate groups of animals are used for three behavioral paradigms. The behavior is recorded by a ceiling-mounted camera and analyzed by the ANY-maze Video Tracking System software (Stoelting Co., Wood Dale, Ill., USA). The compounds are dissolved/suspended with the aid of sonication in a solvent containing 85% distilled water, 14% propylene glycol, and 1% Tween 80, and are administered intraperitoneally in a volume of 2 ml/mL, 20 min before behavioral testing.

Measurement of Locomotor Activity

Twenty minutes after receiving the appropriate treatment, single rats are placed in a clear Plexiglas chamber (40×25×35 cm). Activity under dim red light (20 lux) is recorded for a total of 30 min or 45 min, without any habituation period, using ANY-maze software. Besides the total distance trav-

eled, behavior is analyzed by dividing the locomotor activity data into 5-min bins. For purposes of improving data analysis, the central 20% of the chamber (200 cm²) may be virtually set as a central zone. An entry into a zone is counted when 70% of the animal's body has crossed the zone border. An exit from the zone is counted when more than 50% of the animal's body has left the zone.

Locomotor influences of a compound dosed for example, at 30 mg/kg, are assessed in comparison with a reference compound. The dose response curve for the compound (for example, at 0; 2.5; 5; 10; 20 and 40 mg/kg) is determined. Examples of this characterization of other compounds may be found in Savić, M. M. et al. *Brain Res.* 2008, 1208, 150-159, which is incorporated by reference herein.

Behavior in the Elevated Plus Maze

The apparatus is constructed of sheet metal, with a black rubber floor. It consists of a maze elevated to a height of 50 cm with two open (50×10 cm) and two enclosed arms (50×10×40 cm), connected by a junction area (central platform) measuring 10×10 cm. A ledge of sheet metal (0.3 cm high) surrounding the open arms is added. The illumination in the experimental room consists of one red neon tube fixed on the ceiling, giving light intensity of 10 lux on the surface of the closed arms. At the beginning of the experiment, single rats are placed in the center of the maze, facing one of the enclosed arms, and their behavior is recorded for 5 min. An entry into an open or closed arm is scored when 90% of the animal crossed the virtual line separating the central square of the maze from the arm, whereas an exit occurs when more than 90% of the animal left the respective arm. After each trial, the maze is cleaned with dry and wet towels. The dose response curve for the compound is determined. Examples of this dose response curve characterization of other compounds may be found in Savić, M. M. et al. *Brain Res.* 2008, 1208, 150-159, which is incorporated by reference herein.

Behavior in the Morris Water Maze

The water maze consists of a black cylindrical pool (diameter: 200 cm, height: 60 cm), with a uniform inner surface. The pool is filled to a height of 30 cm with 23° C. (±1° C.) water. The escape platform made of black plastic (15×10 cm) is submerged 2 cm below the water surface. The platform is made invisible to rats by having it painted the same color as the pool wall. There are many distal cues in the testing room (doors, pipes on the walls and the ceiling, cupboards). An indirect illumination in the experimental room is provided by white neon tubes fixed on the walls near the pool.

The rats receive the appropriate treatment 20 min before a swimming block, each day for 5 consecutive days of spatial acquisition. Each block consists of 4 trials, lasting a maximum time of 120 s, the inter-trial interval being 60 s. For each trial the rat is placed in the water facing the pool at one of four pseudorandomly determined starting positions. As during spatial learning the platform is hidden in the middle of the NE quadrant, the four distal start locations are chosen: S, W, NW and SE. Once the rat finds and mounts the escape, it is permitted to remain on the platform for 15 s. The rat is guided to the platform by the experimenter if it does not locate the escape within 120 s. To assess the long-term spatial memory at the end of learning, a probe trial for 60 s, with the platform omitted, is given 24 h after the last acquisition day. The probe trial, starting from the novel, most distant SW location, is performed without any pre-treatment. The tracking software virtually divides the pool into four quadrants, three concentric annuli and a target region consisting of the intersection of the platform quadrant and the platform (middle) annulus. The

central annulus is set up to 10% of the whole area; the platform annulus equals 40%, whereas the area of the peripheral annulus is 50% of the whole.

Dependent variables chosen for tracking during the acquisition trials are: latency to platform (time from start to goal), total distance swam (path length), average swim speed and path efficiency (the ratio of the shortest possible path length to actual path length). All these indices are, to a lesser or greater degree, related to goal-directed behavior, i.e. spatial learning. As thigmotaxis (the tendency to swim or float near the pool wall) represents a factor which accounts for much of the variance in the water maze performance, and normally weakens during consecutive trials, the persistence of the thigmotaxis in the target (NE) quadrant is quantified. The loss of thigmotaxis is related to the procedural component of acquisition, and the percent of the distance swam in the target region (away from the wall) of the target quadrant may be seen as a measure of procedural learning. The indices of memory, assessed during the probe trial, include the distance and time in the platform (target) quadrant, platform ring and target region, as well as the number of entries and distance swam in the area where the platform used to be during training. In addition, the distance swam during 60 sec in the probe trial is taken as a measure of overall activity, while peripheral ring parameters (distance and time) are connected to the thigmotactic behavior. The dose-response curve for the compound at various dosages is determined.

Statistical Analysis

All numerical data will be given as the mean±SEM. For electrophysiological data Student's t-test is used. Data from the activity assay and elevated plus maze are assessed by a one-way ANOVA, whereas the results from the water maze test are analyzed using a two-way ANOVA with repeated measures. Where applicable, Student-Newman-Keuls or Dunnett's test (post hoc comparisons) and analysis of covariance are also used. Statistical analyses are performed with ANY-maze Video Tracking System software (Stoelting Co., Wood Dale, Ill., USA).

Reference Example 4

Effect of Compounds on Excessive Alcohol Consumption

Subjects

Male P rats are used as subjects. All animals are individually housed in shoebox cages in a temperature- and humidity-controlled room on a 12 h:12 h light/dark cycle (lights on at 8:00 AM, off at 8:00 PM) with food and water available ad libitum. All behavioral training and testing take place between 8:00 AM and 10:00 AM. All procedures are conducted in accordance with the NIH Guide for the Care and Use of Laboratory Animals.

Systemic Drug Administration and Oral Solutions

10% (v/v) DMSO and 3% (w/v) sucrose solutions are prepared using previously published procedures (Harvey et al. *J. Neurosci.* 2002, 22, 3765-3775; June et al. *Neuropsychopharmacology* 2003, 28, 2124-2137) with deionized water. The solutions are prepared daily. Compounds are administered by oral gavage (20-60 mg/kg) in all studies (e.g., alcohol responding, sucrose responding) as indicated in FIG. 12. The compounds are mixed in deionized water and administered by gavage in an injection volume of 1 ml/kg 25 min prior to the behavioral task.

Animal Model of Excessive Alcohol Consumption

To initiate excessive "binge" alcohol drinking, a multiple-scheduled-access protocol is employed (Bell et al. *Addict*

67

Biol. 2006, 11, 270-288, which is incorporated by reference herein) with P rats. First, the procedure entails adapting 20 P rats to a 12 h:12 h light/dark cycle which begins at 8:00 AM (lights on) and lasts to 8:00 PM (lights off). Beginning at 8:00 AM, one cohort of rats (N=10) are placed in the operant chamber for 30 min and presented with 10% (v/v) alcohol on both levers. After the initial 30 min session has elapsed, rats are then placed in the home cage with food and water ad libitum for 1 h. Rats then receive two additional 30 min alcohol access periods, spaced 1 h apart. In total, animals receive three 30 min access periods spaced 1 h apart across the cycle. Using this protocol, the P rats are expected to produce consistent blood alcohol concentration (BACs) of approximately 144±22 mg %, while the HAD rats in the homecage procedure are expected to produce consistent BACs of approximately 158±15 mg %. Fluid deprivation is performed during the initiation period (1-2 days); this is discontinued after 1-2 days of successful lever pressing. Another cohort of rats (N=10) is trained in a similar manner; however, they lever press for a 3% (w/v) sucrose concentration. The sucrose control rats allow for evaluation of reinforcer specificity following administration of a compound. The duration of the binge period is 21 days, and responding is expected to increase over the 3 week period from 280 lever presses per 90 min to 500-750 lever presses per 90 min. BAC levels are taken immediately after the first two 30 min sessions every third day over the 21 day period. Data is collected every day of the 21 day period.

Behavioral testing is conducted in 20 standard operant chambers (Coulbourn Instruments, Allentown, Pa.), each equipped with two removable levers and two dipper fluid delivery systems enclosed in sound-attenuated cubicles as previously described (Harvey et al., *J. Neurosci.* 2002, 22, 3765-3775).

To ensure that animals are consuming pharmacologically-relevant amounts of alcohol during the binge operant sessions, BACs are collected in all animals on days that they do not receive drug treatment. Approximately 100 µL of whole blood is collected from a rat's tail tip into a heparin-coated microsample tube. The BAC samples are collected at select time points, depending on the experimental protocol. After collection, the whole blood is immediately centrifuged for 5 min at 1100 rpm. The results are calculated in units of mg/dL and printed within 20 s of each trial as previously reported (Harvey et al., *J. Neurosci.* 2002, 22, 3765-3775; June et al. *Neuropsychopharmacology* 2003, 28, 2124-2137). Measures are collected during the 2nd and 3rd week in the protocol after the 2nd 30 min session.

Compounds are tested for ability to effectively attenuate excessive/heavy alcohol drinking in binge-inducing models using the P rat. Separate cohorts of P rats (n=10/dosage group) undergo training for either the binge alcohol or sucrose drinking protocols. A power analysis reveals that this sample size is quite sufficient to detect independent variable manipulation for binge drinking. Following dose-response studies (for example, at 20, 40, and 60 mg/kg per compound) of each compound, the most effective dose (assuming efficacy) of the compound on binge alcohol drinking is tested for chronic treatment over a 20 day period as noted above. Efficacy is operationally defined as an agent which selectively reduces alcohol responding by >30% with little if any reduction (i.e., >than 10%) of a 3% sucrose concentration.

Data from the operant self-administration is analyzed using between-group analysis of variance (ANOVA) to determine the effects of the compounds on EtOH or sucrose responding. Any significant ANOVA is further analyzed by the use of an appropriate post-hoc test.

68

Example 9

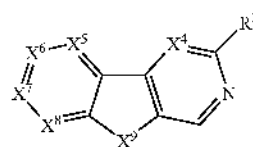
Compounds 2 and 4 Reduce Excessive Alcohol Consumption

Compounds 2 and 4 were tested for their effect on excessive alcohol consumption as described in Example 10. Male P rats [N=5 per compound] were trained to lever press for alcohol under the excessive binge alcohol drinking model. Each cohort of rats received an oral gavage administration of compound 2 or 4, with at least 5 days in between for washout periods. Results for compound 2 are shown in FIG. 13, and results for compound 4 are shown in FIG. 14. The compounds remained effective in reducing excessive alcohol consumption 24 hr after compound administration.

The present invention is not limited to the embodiments specifically described above, but is capable of variation and modification without departure from the scope of the appended claims.

The invention claimed is:

1. A compound according to Formula (I):



(I)

or isomers, or salts thereof;

wherein X⁴, X⁵, and X⁸ are CH, X⁶ may be N, *NR⁶ or CR⁶, and X⁷ may be N, *NR⁶ or CR⁷, and wherein either X⁶ or X⁷ is N;

wherein X⁹ is NH;

wherein R³ is CO₂R, or OR¹ or COR;

wherein R⁶ and R⁷ are independently H, X, —C=CR², lower alkyl, lower alkenyl, or lower alkynyl;

wherein R is C(CH₃)_{3-n}(CH₃)_n, C(CH₃)_{3-n}(CH_{3-p}X_p)_n, CH(CH₃)_{2-m}(CH₃)_m, or CH(CH₃)_{2-n}(CH_{3-p}X_p)_n;

wherein R¹ is —CH₂CH₂CH₃, —CH(CH₃)₂, —CH₂CH₂CH₂CH₃, —CH₂CH(CH₃)₂, —CH(CH₃)CH₂CH₃, —CH₂CH₂CH₂CH₂CH₃, —CH₂CH₂CH₂CH(CH₃)CH₃, —CH₂CH₂CH₂CH(CH₃)₂, —CH₂CH(CH₃)CH₂CH₃, or CH(CH₃)CH₂CH₂CH₃, wherein any of the hydrogens of R¹ may be replaced by X;

wherein R² is H, lower alkyl, Me₃Si, Et₃Si, n-Pr₃Si, or i-Pr₃Si;

wherein n is an integer from 0 to 3, m is an integer from 0 to 2, r is an integer from 1 to 3, p is an integer from 1 to 2, and t is an integer from 0 to 2; and

wherein X is independently selected from F, Cl, Br and I.

2. A compound according to claim 1, wherein X⁶ is N.

3. A compound according to claim 2, wherein X⁷ is CH.

4. A compound according to claim 1, wherein X⁷ is N.

5. A compound according to claim 4, wherein X⁶ is CH.

6. A compound according to claim 1, wherein R³ is CO₂R.

7. A compound according to claim 6, wherein R is —C(CH₃)₃.

8. A compound according to claim 1, wherein R³ is OR¹.

9. A compound according to claim 8, wherein R¹ is CH₂CH₂CH₃.

10. A compound according to claim 1, wherein X⁴ is CH, X⁵ is CH, X⁶ is N, X⁷ is CH, X⁹ is CH, X⁹ is NH, and R¹ is —CO₂C(CH₃)₃.

69

11. A compound according to claim 1, wherein X⁴ is CH, X⁵ is CH, X⁶ is N, X⁷ is CH, X⁸ is CH, X⁹ is NH, and R¹ is OCH₂CH₂CH₃.

12. A compound according to claim 1, wherein X⁴ is CH, X⁵ is CH, X⁶ is CH, X⁷ is N, X⁸ is CH, X⁹ is NH, and R¹ is CO₂C(CH₃)₃.

13. A compound according to claim 1, wherein X⁴ is CH, X⁵ is CH, X⁶ is CH, X⁷ is N, X⁸ is CH, X⁹ is NH, and R¹ is —OCH₂CH₂CH₃.

14. A pharmaceutical composition comprising a compound according to claim 1 and a carrier.

15. The composition according to claim 14, further comprising an additional active agent.

70

16. The composition according to claim 15, wherein the additional active agent is an anxiolytic.

17. The composition according to claim 15, wherein the additional active agent treats a chemical addiction.

18. The composition according to claim 15, wherein the additional active agent is selected from the group consisting of diazepam, clonazepam, lorazepam, alprazolam, buspirone, meprobamate, naltrexone, naltrexone hydrochloride, disulfiram, nalmefene, metadoxine, acamprosate calcium, and chlordiazepoxide hydrochloride.

* * * * *

UNITED STATES PATENT AND TRADEMARK OFFICE
CERTIFICATE OF CORRECTION

PATENT NO. : 8,268,854 B2
APPLICATION NO. : 12/471019
DATED : September 18, 2012
INVENTOR(S) : James M. Cook et al.

Page 1 of 1

It is certified that error appears in the above-identified patent and that said Letters Patent is hereby corrected as shown below:

In the Specification

Column 1, line 15

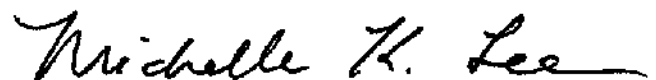
Replace:

[[This invention was made with US Government support awarded by the National Institute of Mental Health (NIMH), Grant No. MH 46851. The United States as certain rights in this invention.]]

with:

--This invention was made with government support under MH 46851 awarded by the National Institutes of Health (NIH). The government has certain rights in the invention.--

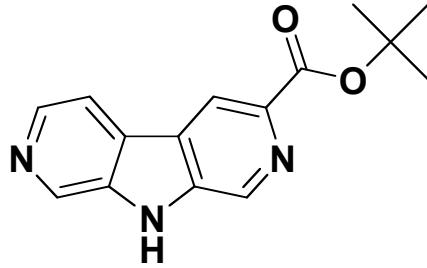
Signed and Sealed this
Fourteenth Day of April, 2015



Michelle K. Lee

Director of the United States Patent and Trademark Office

Compound 3 (a.k.a. MVL-VI-52)

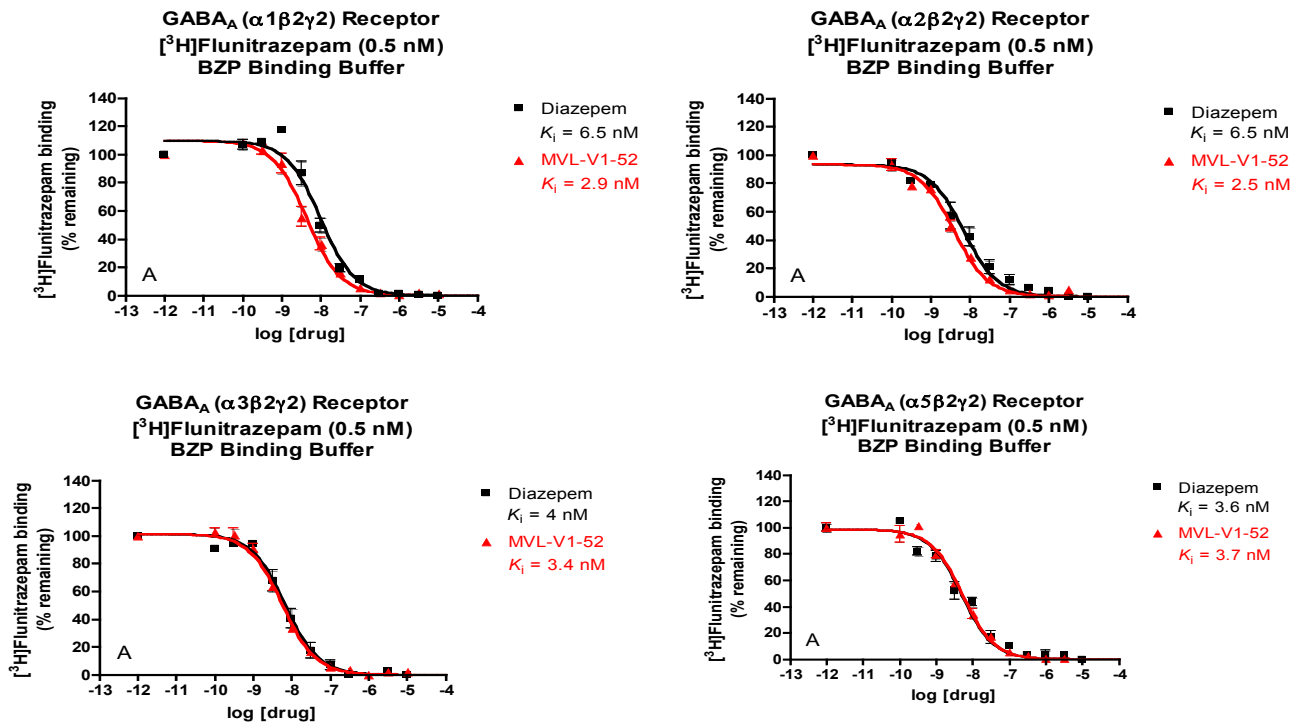


$C_{15}H_{15}N_3O_2$
 Exact Mass: 269.1164
 Mol. Wt.: 269.2986
 C, 66.90; H, 5.61; N, 15.60; O, 11.88

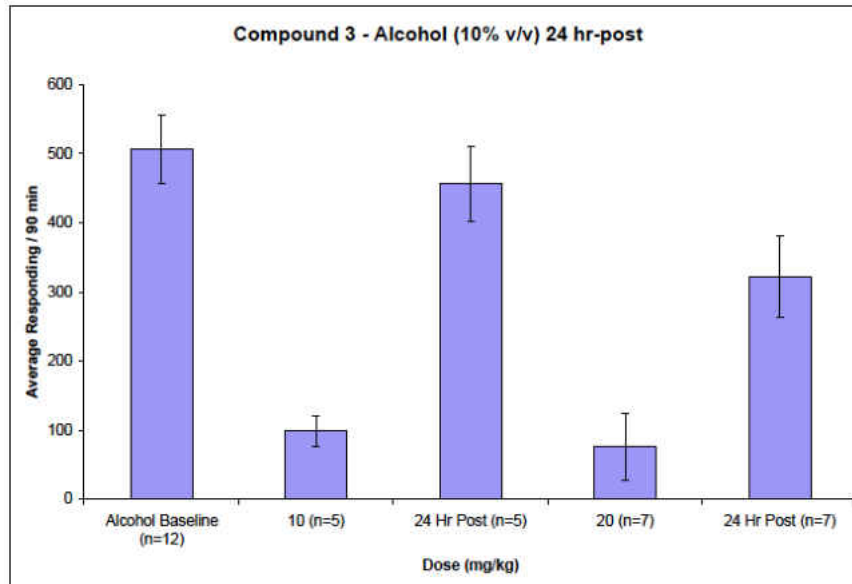
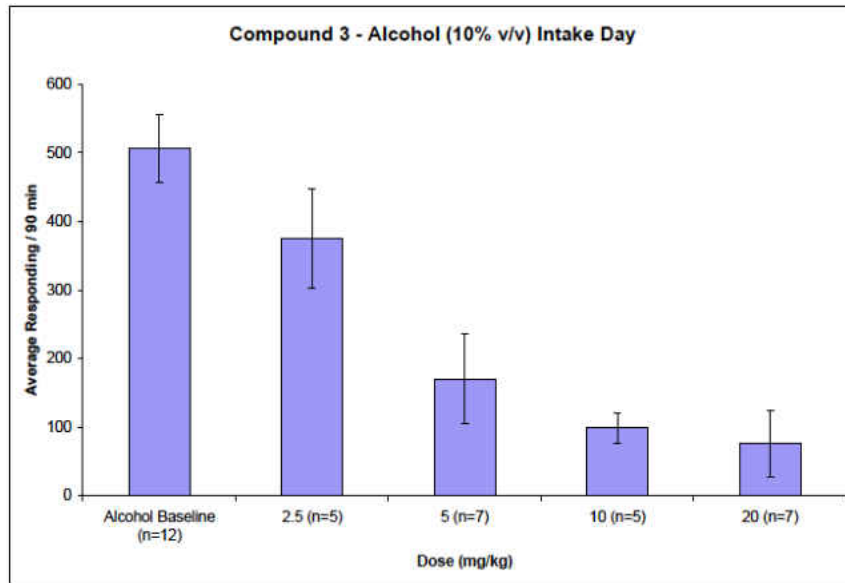
Subtype Binding Data at $\alpha_x\beta_2\gamma_2$ (nM)

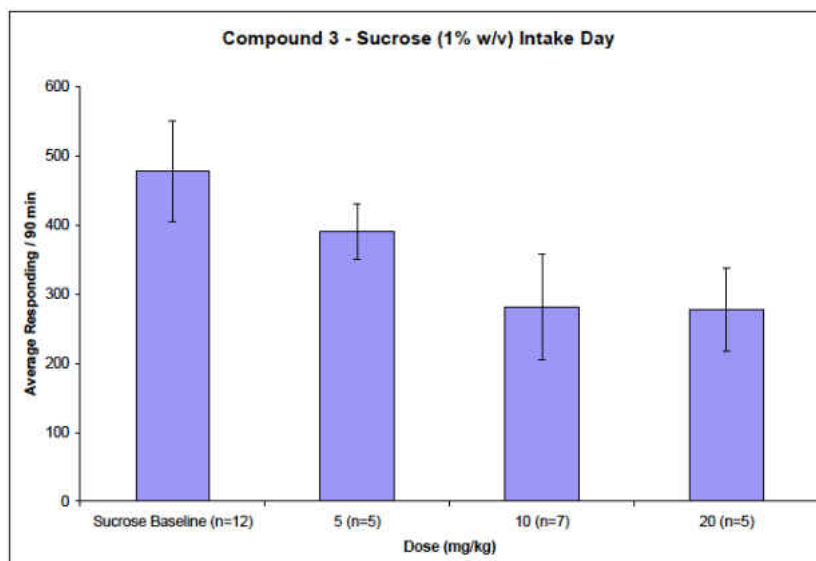
$\alpha 1$	$\alpha 2$	$\alpha 3$	$\alpha 5$
2.9	2.5	3.4	3.7

Efficacy Data



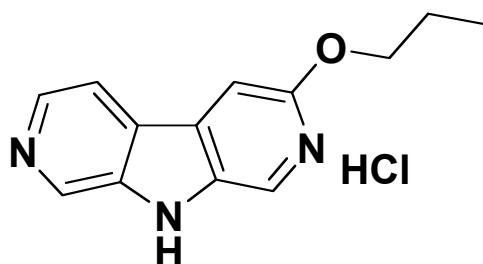
Rodent Model Data





Compound 3 binds to the $\alpha_{1,2,3,5}\beta_2\gamma_2$ GABA_A/BzR receptor subtypes with high affinity. This data suggests that Compound 3 could effectively reduce alcohol self-administration as it binds to the appropriate receptors that are thought to be involved in alcohol seeking behaviors. The efficacy data shows similar pharmacological profiles to that of diazepam, which is a well-known, active GABA_A allosteric modulator. Since the data for Compound 3 is similar to that of diazepam, Compound 3 would be expected to produce a pharmacological effect at the cellular level. In rodent models, Compound 3 effectively reduced alcohol self-administration in a dose-dependent manner (dose range was 2.5 mg/kg to 20 mg/kg). In addition, a reduction in alcohol-seeking behavior was observed 24 hours post-administration at the 10 mg/kg dose. This observation shows promise that the drug (Compound 3) remains active over time.

Compound 4 (a.k.a. MVL-VI-34)

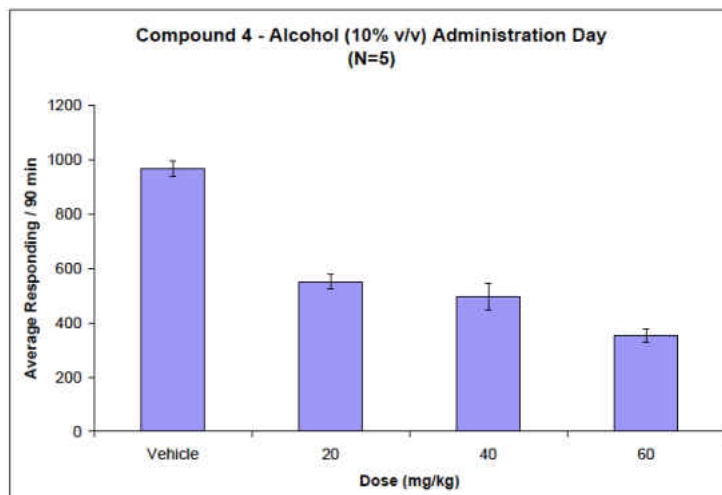


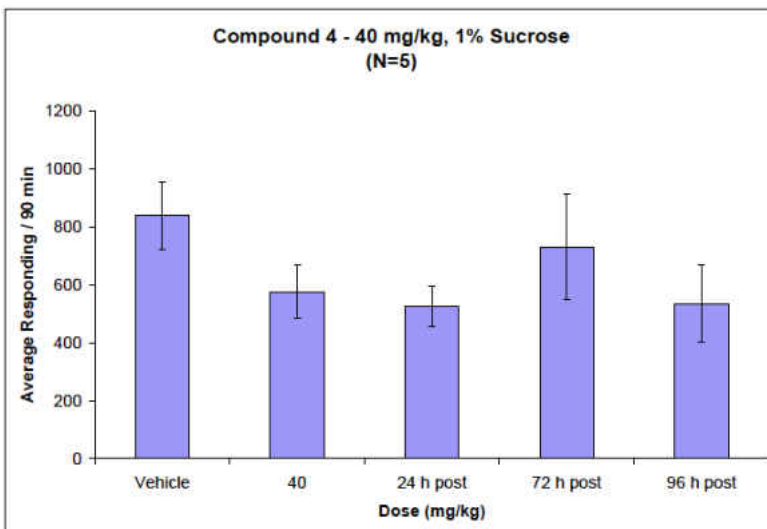
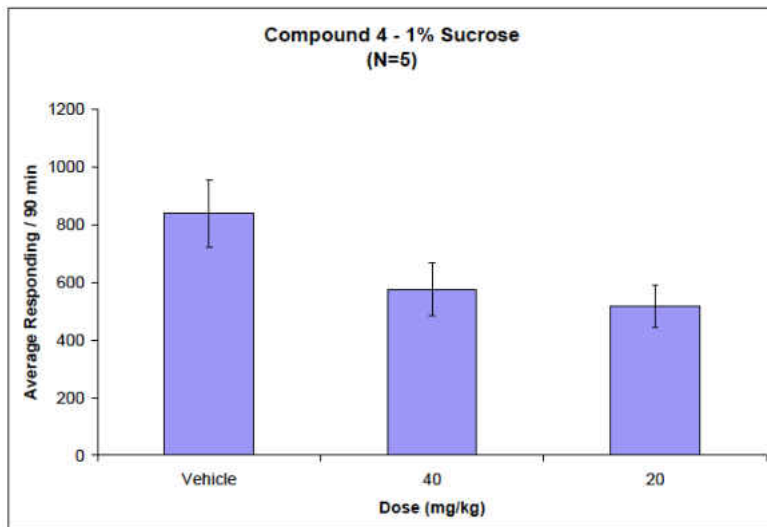
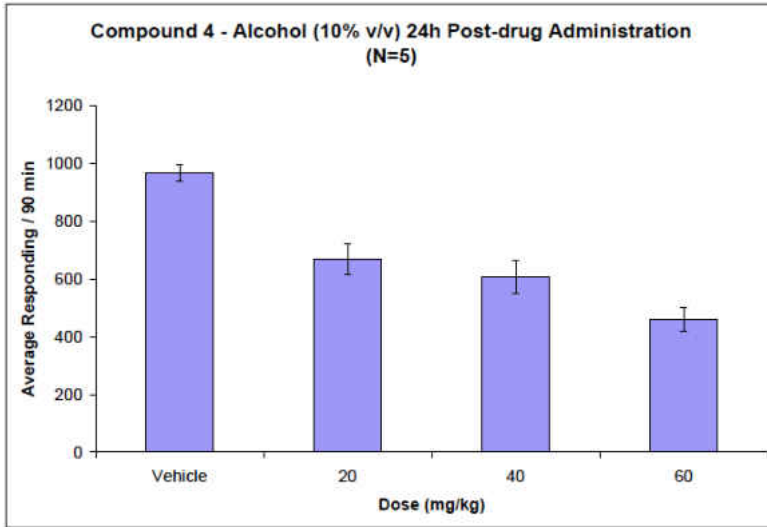
C₁₃H₁₄ClN₃O
Exact Mass: 263.08
Mol. Wt.: 263.72
C, 59.21; H, 5.35; Cl, 13.44; N, 15.93; O, 6.07

Subtype Binding Data at $\alpha_x\beta_2\gamma_2$ (nM)

α_1	α_2	α_3	α_5
5.785	6.308	1.49	43.06

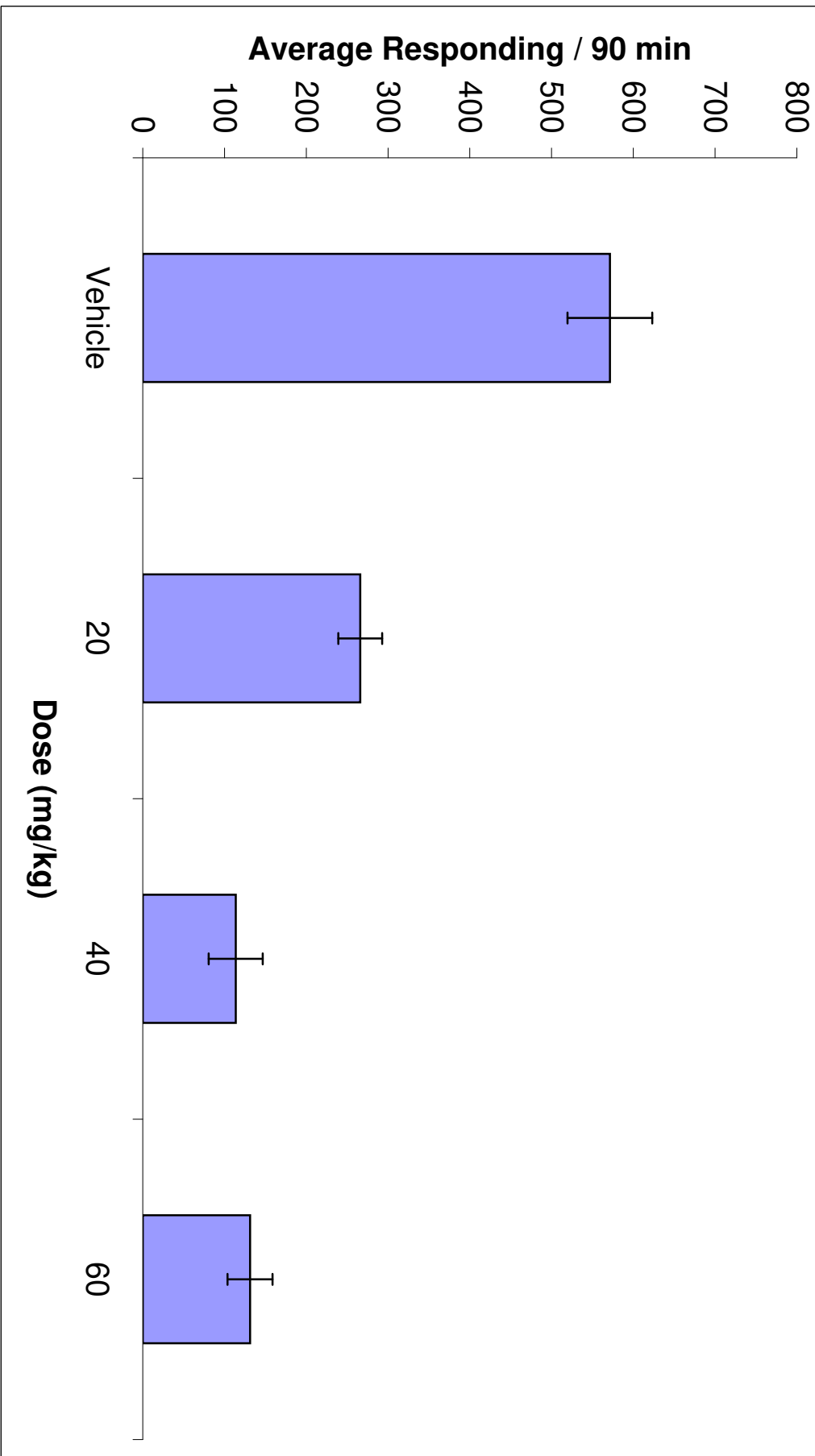
Rodent Model Data



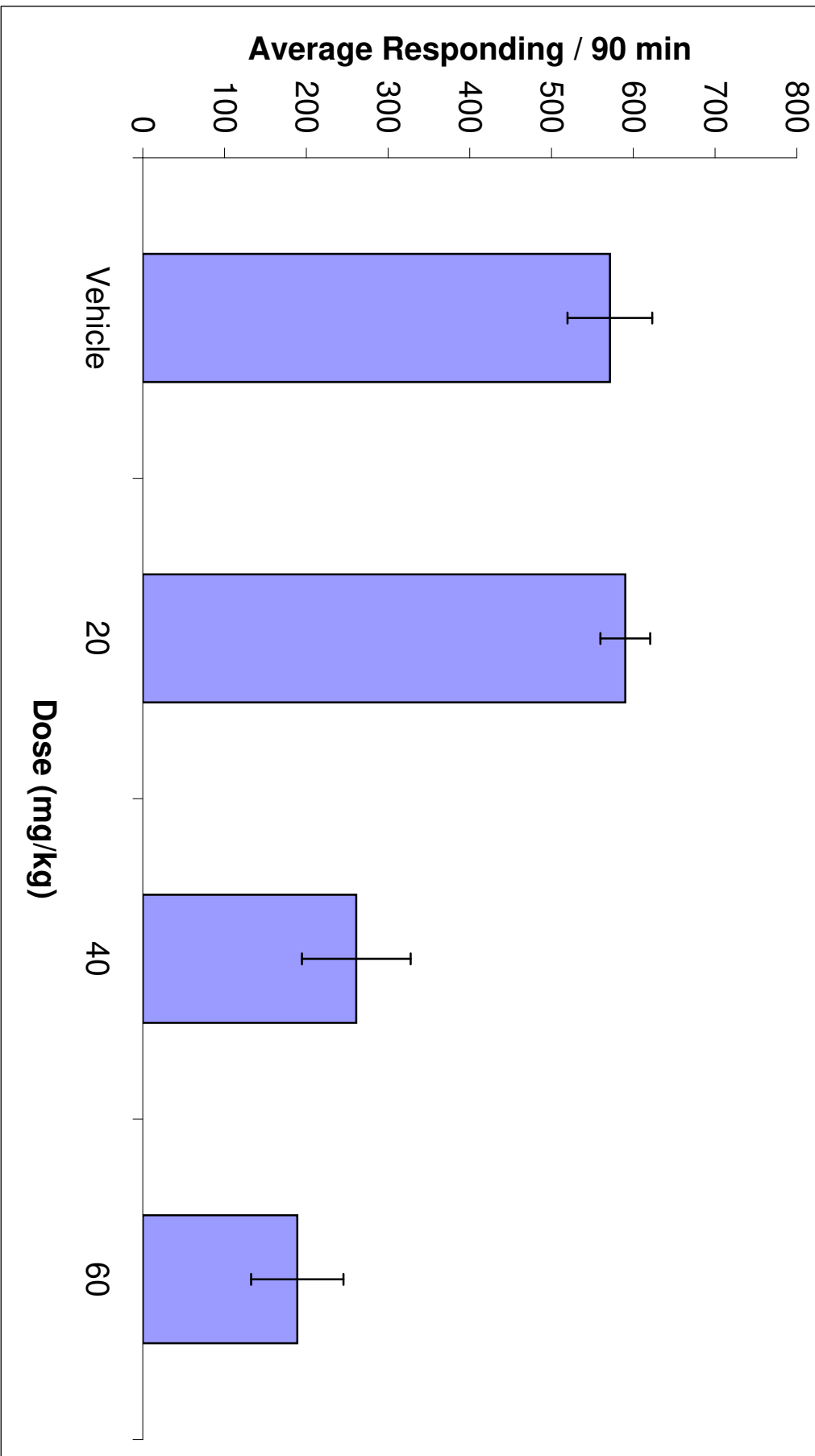


Compound 4 binds to the $\alpha_{1,2,3,5}\beta_2\gamma_2$ GABA_A/BzR receptor subtypes with high affinity, similar to Compound 3. This data suggests that Compound 4 could effectively reduce alcohol self-administration as it binds to the appropriate receptors that are thought to be involved in alcohol seeking behaviors. In rodent models, Compound 4 effectively reduced alcohol self-administration in a dose-dependent manner (dose range was 20 mg/kg to 60 mg/kg). The administered dose of Compound 4 was higher than that given for the same experiments using Compound 3. This shows that Compound 4 is active in reducing alcohol self-administration but not as potent as Compound 3. Compound 4 was also dose-dependent in remaining active 24 hours post-administration. This observation shows promise that the drug (Compound 4) remains active over time.

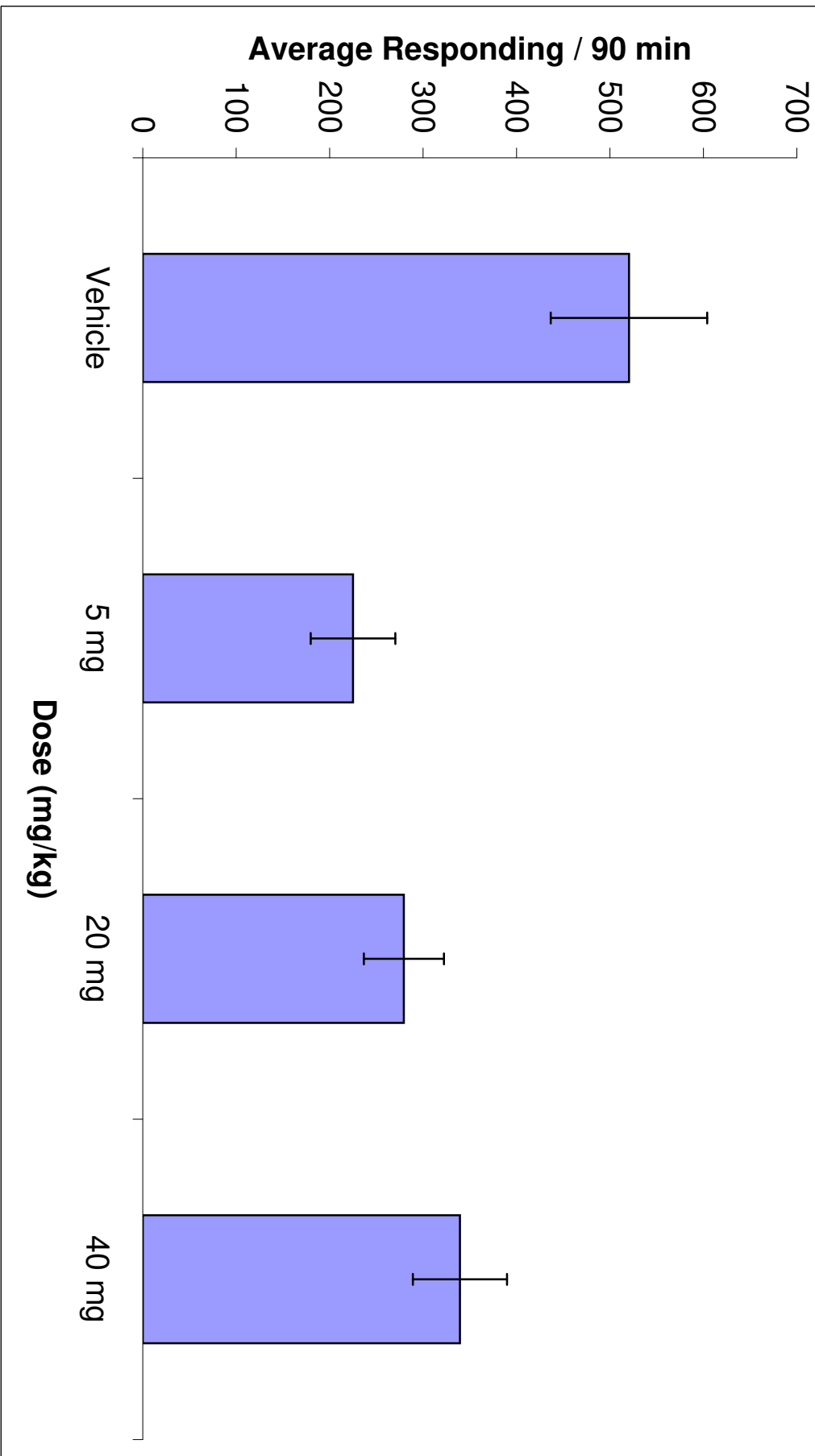
**Compound 2 - Alcohol (10% v/v) - Administration Day
(N=7)**



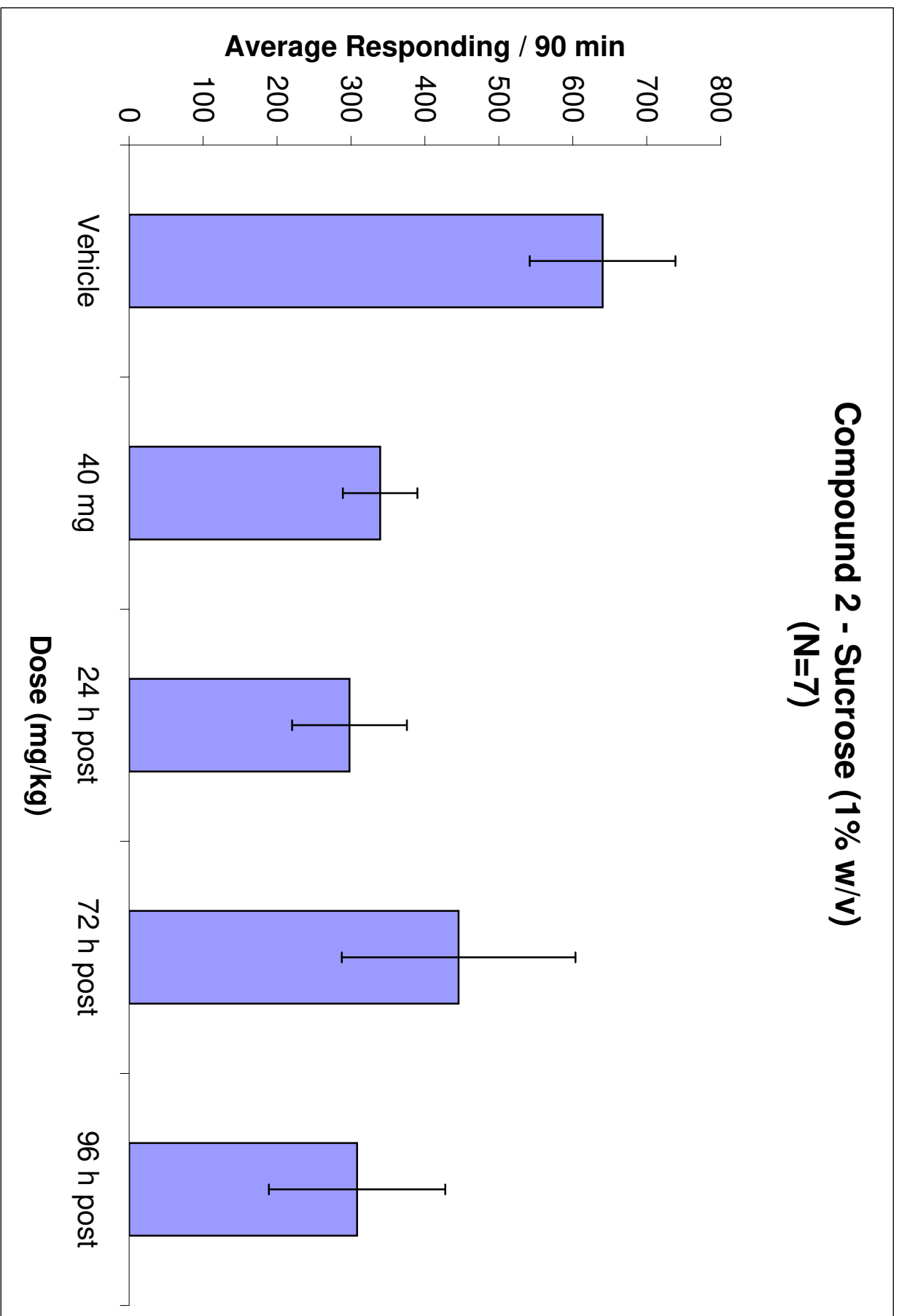
Compound 2 - Alcohol (10% v/v) 24h Post-drug Administration (N=7)



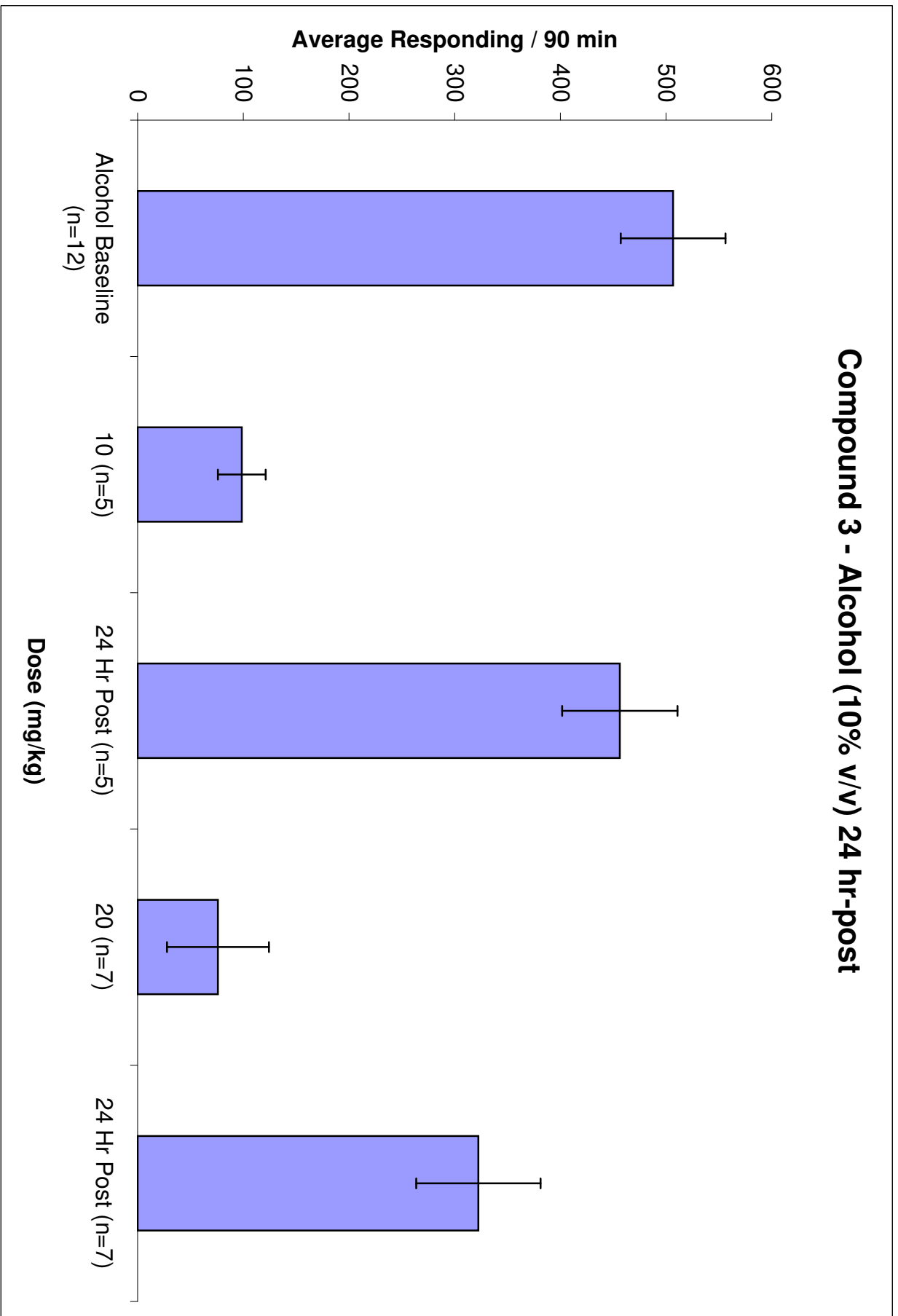
**Compound 2 - Sucrose (1% w/v) Intake Day
(N=7)**



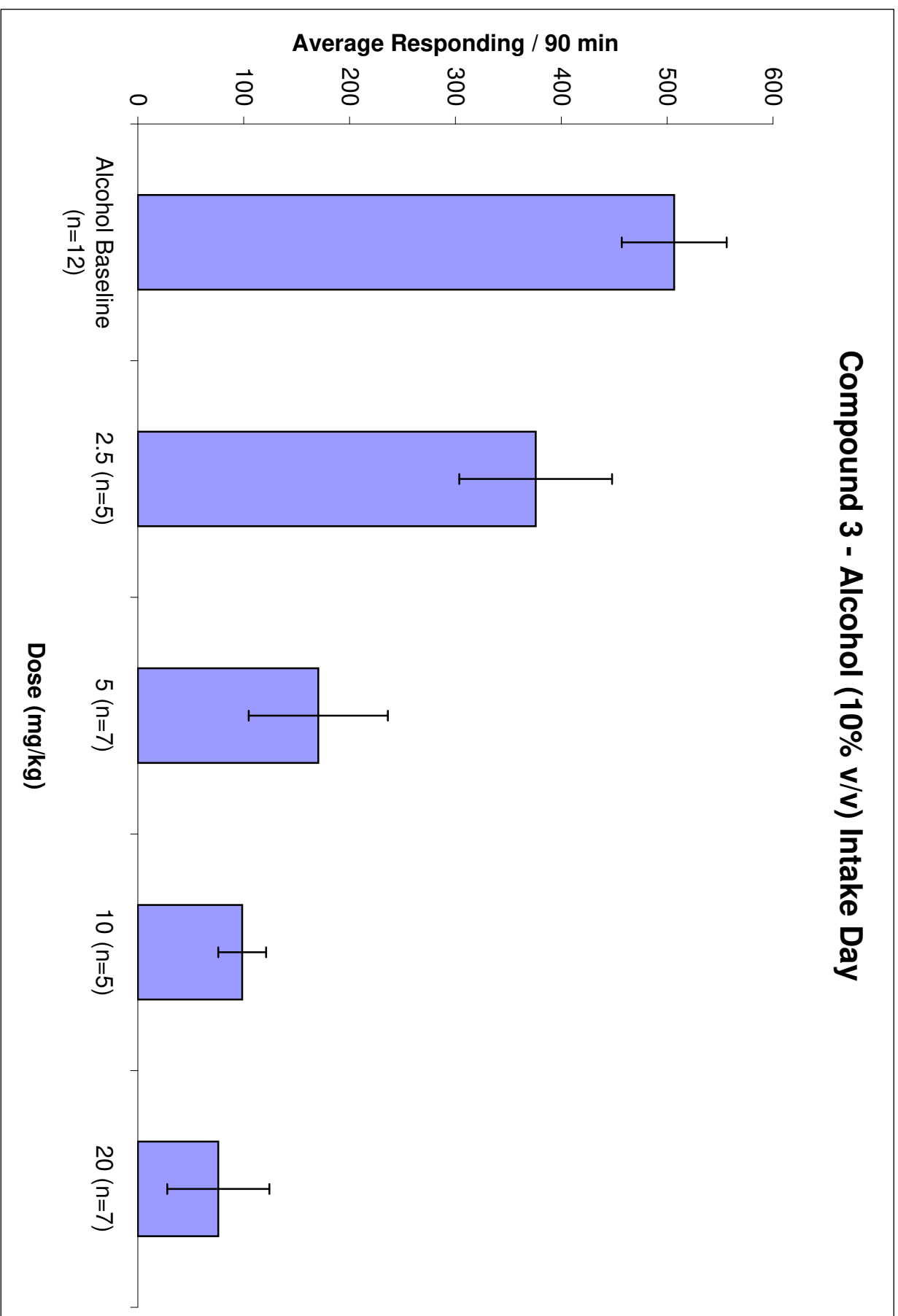
**Compound 2 - Sucrose (1% w/v)
(N=7)**



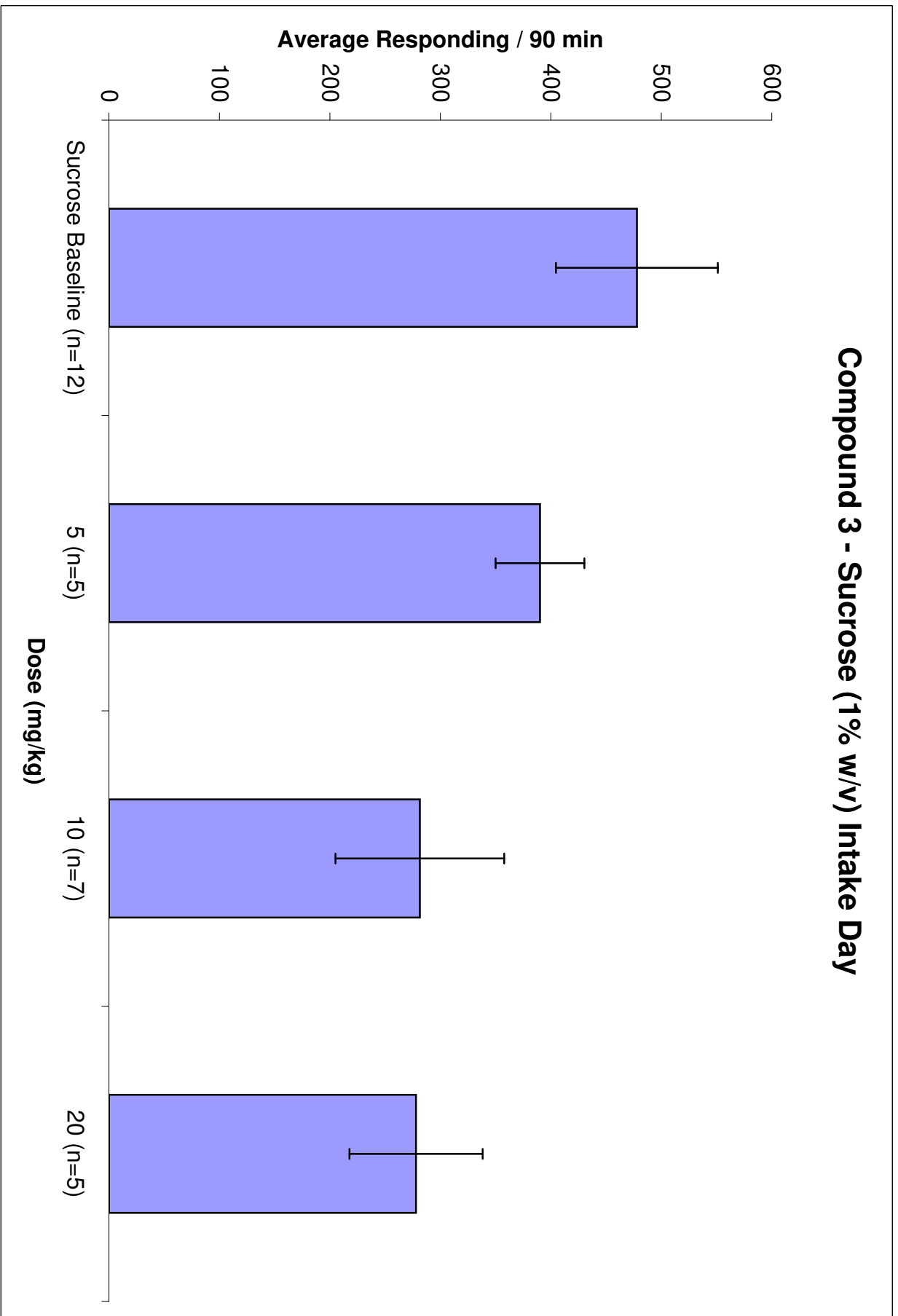
Compound 3 - Alcohol (10% v/v) 24 hr-post



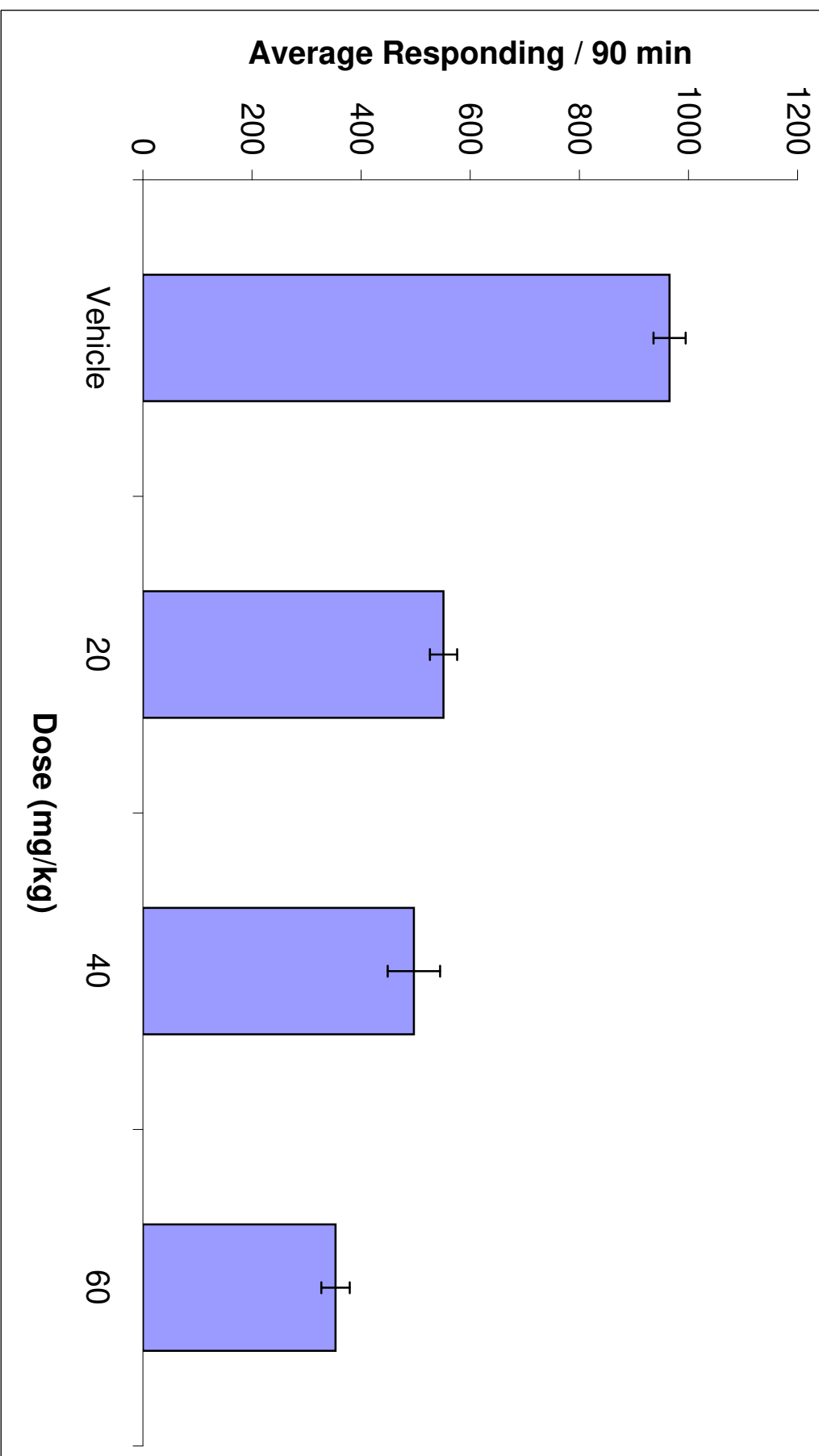
Compound 3 - Alcohol (10% v/v) Intake Day



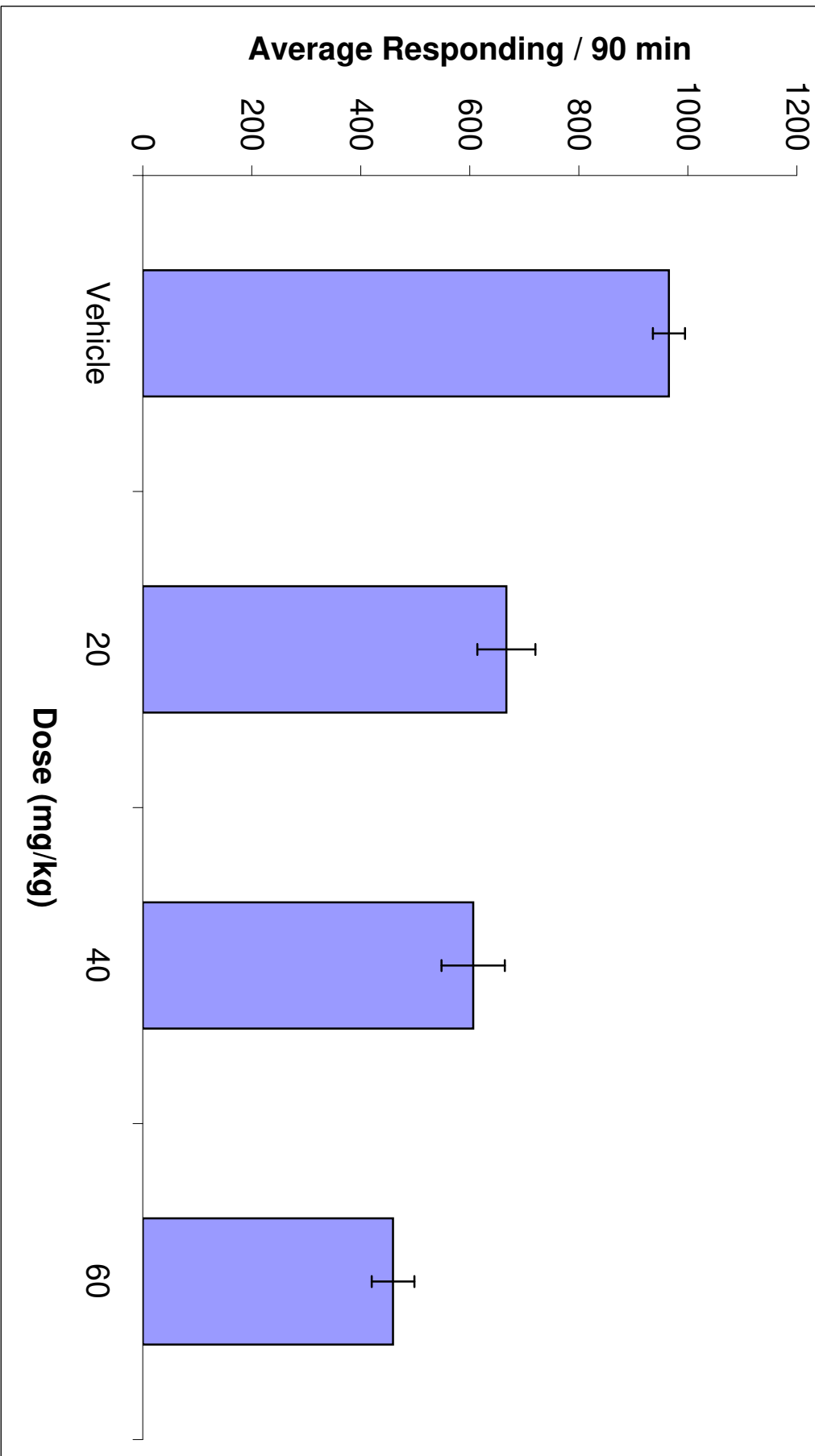
Compound 3 - Sucrose (1% w/v) Intake Day



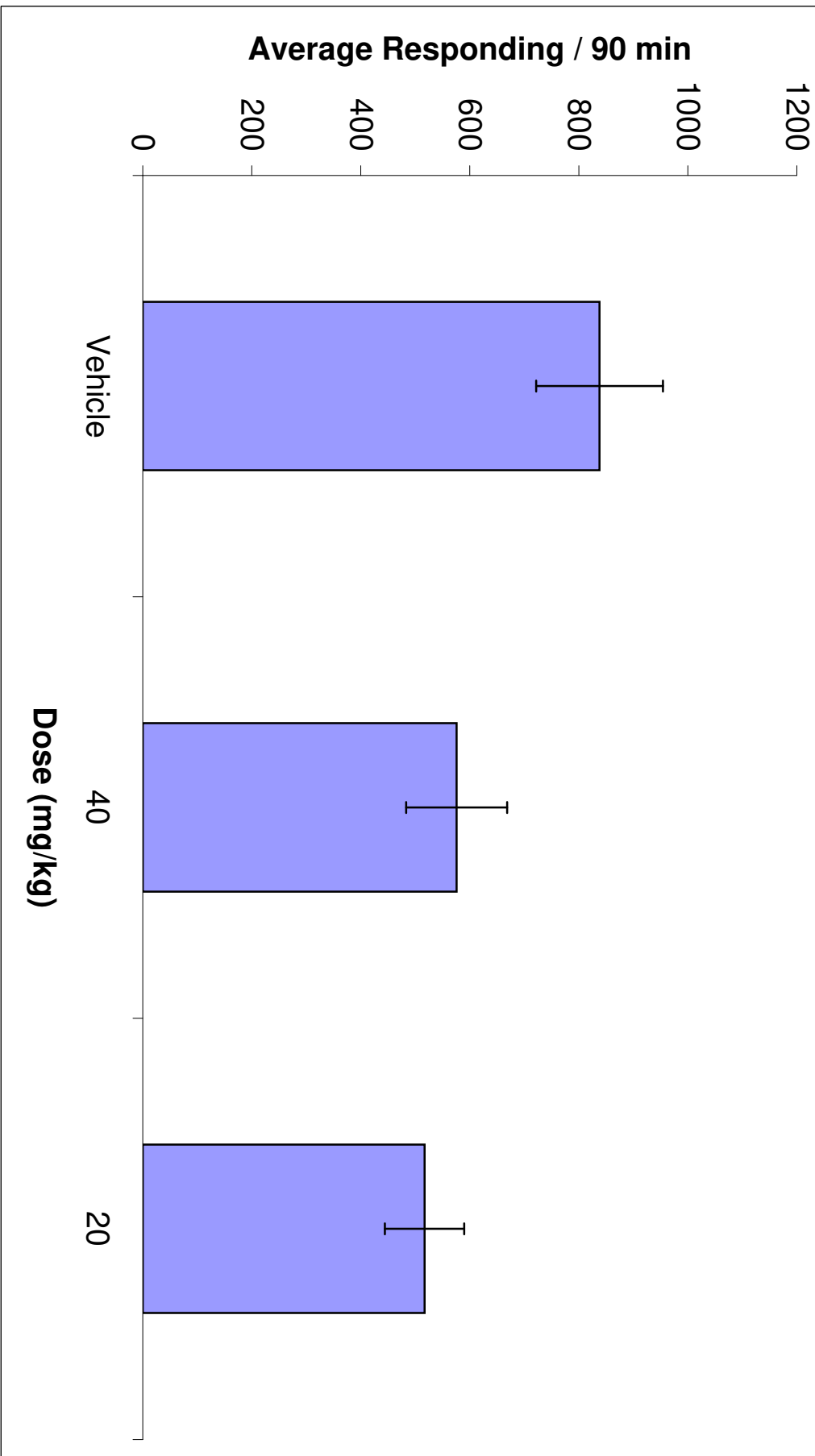
**Compound 4 - Alcohol (10% v/v) Administration Day
(N=5)**



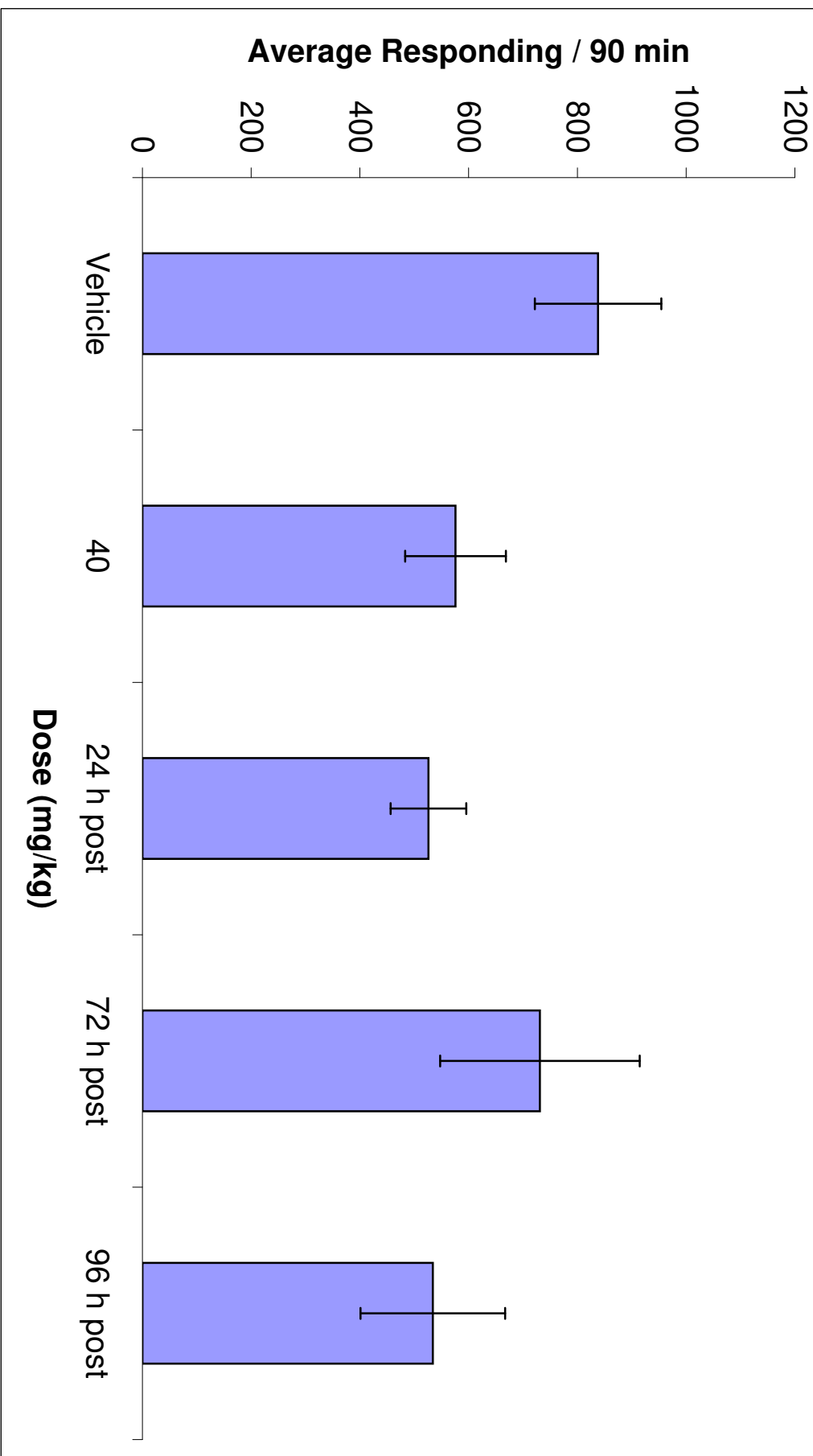
**Compound 4 - Alcohol (10% v/v) 24h Post-drug Administration
(N=5)**



**Compound 4 - 1% Sucrose
(N=5)**



**Compound 4 - 40 mg/kg, 1% Sucrose
(N=5)**



Effects of the benzodiazepine GABA_A α 1-preferring ligand, 3-propoxy- β -carboline hydrochloride (3-PBC), on alcohol seeking and self-administration in baboons

Barbara J. Kaminski · Michael L. Van Linn ·
James M. Cook · Wenyuan Yin · Elise M. Weerts

Received: 4 June 2012 / Accepted: 1 December 2012 / Published online: 28 December 2012
© Springer-Verlag Berlin Heidelberg 2012

Abstract

Rationale The various α subtypes of GABA_A receptors have been strongly implicated in alcohol reinforcement and consumption.

Objectives The effects of the GABA_A α 1-preferring ligand, 3-propoxy- β -carboline hydrochloride (3-PBC), on seeking and self-administration responses were evaluated in two groups of baboons trained under a 3-component chained schedule of reinforcement (CSR).

Methods Alcohol (4 %w/v; $n=5$; alcohol group) or a preferred nonalcoholic beverage ($n=4$; control group) was available for self-administration only in component 3 of the CSR. Responses in component 2 provided indices of motivation to drink (seeking). 3-PBC (1.0–30.0 mg/kg) and saline were administered before drinking sessions under both acute and 5-day dosing conditions.

Results Repeated, and not acute, doses of 3-PBC significantly decreased total self-administration responses ($p<0.05$), volume consumed ($p<0.05$), and gram per kilogram of alcohol ($p<0.05$) in the alcohol group. In the control group, 5-day administration of 3-PBC significantly decreased total self-

administration responses ($p<0.05$) but produced nonsignificant decreases in volume consumed. Within-session pattern of drinking was characterized by a high level of drinking in the first 20 min of the session for both groups, which was significantly ($p<0.05$) decreased by all doses of 3-PBC (1.0–18.0 mg/kg) only in the alcohol group. In contrast, the first drinking bout in the control group was only reduced at the highest doses of 3-PBC (10.0 and 18.0 mg/kg).

Conclusions The results support the involvement of the GABA_A α 1 subtype receptor in alcohol reinforcement and consumption.

Keywords Alcohol · 3-Propoxy- β -carboline hydrochloride · 3-PBC · Self-administration · Baboon

Introduction

gamma-Aminobutyric acid (GABA) is the major inhibitory neurotransmitter and a primary inhibitor of dopamine (DA) neuronal activity in mesolimbic regions (Enoch 2008). The actions of GABA in the central nervous system are mediated by at least two receptors, GABA_A and GABA_B, which have different distributions in the brain (Chu et al. 1990). The GABA system has been implicated in the maintenance of and relapse to chronic alcohol drinking (for recent reviews, see Enoch 2008; Heilig et al. 2011; Lobo and Harris 2008). Alcohol modulates the GABA receptor complex allosterically to open the coupled chloride (Cl⁻) channel and either hyperpolarize cells or potentiate the hyperpolarization produced by GABA (Blair et al. 1988; Koob 2004), subsequently modulating release of DA. GABA_A receptors are important therapeutic targets given their involvement in many of the direct behavioral effects of alcohol including motor incoordination, sedation, tolerance, and withdrawal in laboratory animals (for reviews, see Davies 2003; Korpi 1994; Nevo and Haman

B. J. Kaminski · E. M. Weerts
Division of Behavioral Biology,
Department of Psychiatry and Behavioral Sciences,
Johns Hopkins University School of Medicine,
5510 Nathan Shock Drive,
Baltimore, MD 21224, USA

M. L. Van Linn · J. M. Cook · W. Yin
Department of Chemistry and Biochemistry,
University of Wisconsin-Milwaukee,
Milwaukee, WI 53201, USA

E. M. Weerts (✉)
Johns Hopkins Bayview Campus, Behavioral Biology Research
Center, 5510 Nathan Shock Drive, Suite 3000,
Baltimore, MD 21224, USA
e-mail: eweerts@jhmi.edu

1995) as well as alcohol reinforcement and consumption (for reviews, see Chester and Cunningham 2002; Davies 2003).

GABA_A receptors have a pentameric structure: five subunits, which form an ionophore. There are seven classes of subunits of GABA_A receptors and multiple isoforms (e.g., α 1–6, β 1–3, γ 1–3, δ , ϵ , π , θ) (for a review, see D'Hulst et al. 2009). Coexpression of the α , β , and γ subunits is required for the formation of a GABA_A receptor that has a benzodiazepine (BZ)-binding site (Richter et al. 2012), and this basic combination, with variations in subunit isoform, is most prevalent in the brain (Olsen and Sieghart 2008). In addition to their primary uses as anxiolytics and sleep aides, BZs are the standard treatment to alleviate alcohol withdrawal symptoms (Amato et al. 2011) that are thought to be due, in part, to a compensatory decrease in GABAergic inhibitory function that occurs after discontinuation of the chronic activation of GABA receptors by alcohol (Malcolm 2003). Activation of GABA/BZ receptor complex seems to play an important role in modulating alcohol reinforcing effects, as evidenced by reduction in alcohol self-administration (under limited access conditions) following acute pretreatment with GABA/BZ antagonists and inverse agonists (Chester and Cunningham 2002; Koob 2004).

GABA/BZ receptors containing α 1, α 2, α 3, or α 5 subunits appear to be especially relevant to inherited risks of alcohol. In humans, genetic variations in GABA_A α 1 and α 2 subunits have been associated with alcohol dependence (Ittiwut et al. 2011; Johnson et al. 1992; Lydall et al. 2011) and with differences in the subjective effects of alcohol intoxication (Roh et al. 2011; Uhart et al. 2012), suggesting that these subunits may be particularly important in alcohol abuse and dependence. Rat strains specifically bred for high alcohol drinking (HAD) and for alcohol preference (P) show elevations of GABA_A receptors in the nucleus accumbens (Murphy et al. 2002) and recent studies in these inbred rat lines suggest that the GABA_A α 1 subunit is involved in modulation of a variety of alcohol-related behaviors including binge drinking (Yang et al. 2011), alcohol reinforcement (Harvey et al. 2002; June et al. 2003), and alcohol-induced loss of righting reflex (Boehm et al. 2006).

Isolation of the precise roles of the specific GABA receptor subtypes is currently being investigated using a series of β -carboline ligands that bind preferentially to the α 1 receptor subtype (Yin et al. 2010; Namjoshi et al. 2011). One promising ligand, 3-propoxy- β -carboline hydrochloride (3-PBC), displays tenfold selectivity for the α 1 subtype over the α 2 and α 3 receptors as well as over 150-fold selectivity for the α 1 subtype over the α 5 subtype (Harvey et al. 2002). Further, it shows a higher binding affinity for the α 1 receptor (5.3 nM) than the prototypical α 1-preferring BZ agonist zolpidem (29.6 nM). In behavioral studies, 3-PBC typically displays a GABA_A-competitive antagonist profile (Gourley et al. 2005; Lelas et al. 2002; Rowlett et al. 2003), while an in vitro study has reported low partial

agonist efficacy at recombinant diazepam-sensitive receptors (i.e., BZ receptors containing α 1, α 2, or α 3 subunits; Harvey et al. 2002), leading to a classification as a mixed BZ partial agonist/antagonist (Yin et al. 2010). In P rats, both systemic administration (parenteral, IP) and bilateral microinfusion of 3-PBC in the anterior and medial ventral pallidum selectively produced marked reductions in alcohol-maintained responding (Harvey et al. 2002).

GABA/BZ α 1-preferring antagonists have been proposed as potential pharmacotherapies for treatment of human alcohol abuse disorders, based largely on data in rodents (Yin et al. 2010). While the studies in rodents are highly informative and provide a basis for the current studies, it is important to recognize that these studies were done in rodent lines selectively bred for alcohol preference and/or high alcohol consumption and genetics is only one factor in alcoholism risk. Chronic alcohol exposure induces compensatory adaptations in the GABA system, including decreases in α 1 subunits in rats (Grobin et al. 1998; Ortiz et al. 1995) and nonhuman primate (Floyd et al. 2004). Thus, it is important to examine the effects of potential treatment medications in outbred subjects, particularly in nonhuman primates which are closer in phylogenetic origin than rodents and will consume high levels of alcohol daily and over prolonged periods. Self-administration of alcohol over long periods (i.e., years) more closely models the long-term use characteristics of alcohol abuse in humans. The current study augments the data collected in rodents to provide cross-species validation and bridge the translational research gap between rodents and humans.

In the current studies, 3-PBC was administered before sessions consisting of a chained schedule of reinforcement (CSR) composed of distinct, sequential contingencies (“components”), each of which is correlated with a different stimulus (Kaminski et al. 2008; Weerts et al. 2006). The use of the chain schedule allows examination of drug effects on responding in the presence of alcohol-related stimuli that is maintained by conditioned reinforcement (i.e., responding that produces access to alcohol or “seeking”) as well as alcohol self-administration (consumption) within the same session. This study is the first to examine the effects of 3-PC on alcohol-seeking behaviors. 3-PBC was administered under acute and repeated administration (5 days). In order to determine the specificity of effects on alcohol-related behaviors, repeated treatment with 3-PBC was also administered to baboons that self-administered a preferred, nonalcoholic beverage.

Methods and materials

Subjects

Nine singly-housed adult male baboons (*Papio anubis*; Southwest Foundation for Biomedical Research, San

Antonio, TX, USA) weighing 27.2 kg kg (+4.6 SD) served as subjects. Baboons were housed under conditions previously described (Kaminski et al. 2012). For the alcohol group ($N=5$), the reinforcer delivered was 4 % alcohol w/v. For the control group ($N=4$), the reinforcer delivered was a preferred non-alcohol beverage (orange-flavored, sugar-free Tang[®]), diluted to a concentration that functioned as a comparable reinforcer (Duke et al. 2012). All baboons had extensive histories of self-administration of the reinforcer under the CSR. Baboons received standard primate chow (50–73 kcal/kg), fresh fruit or vegetables, and a children's chewable multivitamin daily. Drinking water was available ad libitum except during sessions. Facilities were maintained in accordance with United States Department of Agriculture (USDA) and Association for Assessment and Accreditation of Laboratory Animal Care International (AAALAC) standards. The protocol was approved by the Johns Hopkins University (JHU) Animal Care and Use Committee and followed the Guide for the Care and Use of Laboratory Animals (1996).

Apparatus

Each baboon's cage was modified to also function as the experimental chamber (for details, see Weerts et al. 2006) and contained (1) a panel with three colored “cue” lights; (2) an intelligence panel with two vertically operated levers and two different colored “jewel” lights; (3) a “drinkometer” connected to a calibrated 1,000-ml bottle; and (4) a speaker, mounted above the cage, which presented auditory tones. A computer interfaced with Med Associates hardware and software remotely controlled the experimental conditions and data collection.

Drugs

All solutions for oral consumption were mixed using reverse osmosis (RO) purified drinking water. Ethyl alcohol (190 Proof, Pharmco-AAPER, Brookville CT, USA) was diluted with RO water to 4 %w/v alcohol. Orange-flavored, sugar-free, Tang[®] powder (Kraft Foods) was dissolved in RO water as described previously (Kaminski et al. 2012). 3-PBC was synthesized in the laboratory of Dr. James Cook (University of Wisconsin-Milwaukee; Yin et al. 2010). Doses of 3-PBC (1.0–30.0 mg/kg) were dissolved in a vehicle of 50 % propylene glycol and 50 % saline and administered via the intramuscular (IM) route (2–4 ml/injection). 3-PBC vehicle tests were completed using the same volume and procedures as detailed below.

CSR procedure

For all sessions, fluids were available only via the drinkometer. The CSR procedures have been described in detail previously (Kaminski et al. 2008; Kaminski et al. 2012) and were identical for the alcohol and control groups.

Daily sessions (7 days/week for both groups) were initiated at the same time (8:30 AM) and were signaled by a 3-s tone. During component 1 (C1), a red cue light was illuminated and all instrumental responses were recorded but had no consequence. After 20 min, C1 was terminated and component 2 (C2) was initiated, as signaled by illumination of the yellow cue light. During the first link of C2 (C2-Link 1), the yellow jewel light over the left lever was continuously illuminated and a concurrent fixed interval 10 min, fixed time 20 min (FI 10-min FT 20-min) schedule was in effect. In C2-Link 2, the jewel light over the lever flashed and a fixed ratio (FR 10) schedule was in effect on the left lever for transition to component 3 (C3). If the FR 10 requirement was not completed, the session terminated without transitioning to C3 (i.e., no access to alcohol or the nonalcoholic beverage for the day). C3 began with the illumination of the blue cue light. A blue jewel light over the right lever was also illuminated, and drinks of the alcohol or the nonalcoholic beverage were available under an FR 10 schedule on the right lever followed by contact with the drinkometer spout. Fluid was delivered for the duration of spout contact or for a programmed duration (5 s), whichever came first. C3 (and the session) ended after 120 min. Previously, we have demonstrated that Tang and alcohol concentrations used in the current study maintained similar breakpoints (i.e., functioned as equivalent reinforcers (see Duke et al 2012)).

3-PBC test procedures

The CSR baseline (BL) criterion was defined as stable self-administration of alcohol or nonalcoholic beverage (i.e., ± 20 %) for three consecutive CSR sessions. To evaluate acute effects of 3-PBC on alcohol-related behaviors and to verify the safety of the dose range, in experiment 1, doses of 3-PBC (1.0–30.0 mg/kg) or its vehicle were administered acutely in the alcohol group only. The CSR was established and CSR BL criterion was met before each test dose of 3-PBC. Doses were tested in mixed order, with active doses tested no more than once per week. In addition, the results of experiment 1 were used to determine a safe dose range for repeated administration. In experiment 2, doses of 3-PBC (1.0–18.0 mg/kg) or vehicle were administered daily for five consecutive days to baboons in both groups. Only four of the five baboons from the alcohol group participated in experiment 2; one baboon had been removed for health reasons unrelated to the study. For both experiments, doses of 3-PBC were administered 10 min before CSR sessions. For both experiments, stable BL intake was sometimes disrupted after drug treatments and required additional time to stabilize before testing the next dose (e.g., 2 weeks).

Data analysis

The grand mean of the 3 days that preceded each test condition for each baboon was used as the BL for comparison with vehicle and doses of 3-PBC, except when otherwise noted. In experiment 2, data analyzed were the last three of the 5 days of 3-PBC administration. Data were analyzed using separate statistical analysis of variance (ANOVA) for each group (alcohol or control) with 3-PBC dose (BL, 0–30.0 mg/kg) as a repeated measure. Bonferroni's *t* tests were used for pairwise comparisons of BL with vehicle and 3-PBC doses. Total gram per kilogram of alcohol was calculated based on individual body weights and total volume of alcohol consumed. Change in gram per kilogram of alcohol consumed was calculated as test dose (vehicle or 3-PBC)—BL and doses of 3-PBC were compared to vehicle.

Temporal pattern of drinking was analyzed as number of drinks in sequential 20-min bins using two-way repeated measures ANOVA (Time × Dose) for each group given 5 days of 3-PBC dosing (experiment 2). Post hoc Bonferroni pairwise comparisons examined differences between vehicle and doses of 3-PBC.

Results

Stable, reliable drinking was observed in all baboons in both groups. During criterion BL sessions preceding test sessions, baboons in both groups reliably completed the CSR. The number of sessions required to satisfy the BL stability criterion varied. Following drug treatment, BL intake was sometimes unsystematically disrupted and required 2 weeks or longer to meet the stability criterion. The volume of each drink, within the constraints described above, was under the control of the baboon. Average milliliter per drink (total volume consumed/number of drinks in the session) was approximately 30 ml/drink and did not vary systematically as a function of 3-PBC administration (data not shown). Few or no responses were recorded on the inactive operanda (all operanda in C1, right lever and drinkometer in C2, left lever in C3).

To determine if there were any differences in BL responding in the alcohol and control groups, BL session responding in experiment 2 was compared for the two groups (BL sessions of the alcohol group in experiment 1 are not included because corresponding control group sessions were not conducted). During BL sessions, systematic differences between the groups were not observed for C1 and C2 measures. In C3, both alcohol and the nonalcoholic beverage maintained self-administration responses (right lever responses; drink contacts) and high intake (milliliter). During the BL sessions preceding tests, the grand mean

(+SEM) alcohol intake was 625.6 (31.2) ml and 1.13 (0.09)g/kg, comparable to intake that has previously been reported to produce blood alcohol levels (BAL) of > .08 % in baboons (Kaminski et al. 2008). The grand mean nonalcoholic beverage intake during BL sessions was 1,000.0 (0.0) ml. Despite having previously demonstrated comparable reinforcement of 4 %w/v alcohol and the nonalcoholic beverage under BL conditions via a progressive ratio procedure (Duke et al. 2012), volume of intake of the nonalcoholic beverage was greater than volume of alcohol ($t(4)=24.6, p<.001$) under BL conditions.

Experiment 1: effects of acutely administered 3-PBC on seeking and self-administration under the CSR

Acute administration of 3-PBC did not result in significant changes in any of the measures of seeking (C2-Link 1: FI responses, latency to complete the FI requirement; C2-Link 2: FR responses rate (*r/s*)) or self-administration (C3: FR responses, volume consumed, gram per kilogram consumed) (Table 1). The data and unsystematic observation by laboratory personnel confirmed that administration of doses up to and including 30.0 mg/kg was safe and did not produce severe adverse effects. The highest dose (30.0 mg/kg) did, however, suppress daily food intake (i.e., technicians reported that a large proportion of daily free food ration was not consumed). As a result, this dose was not tested under 5-day administration conditions (experiment 2). Because 3-PBC did not systematically reduce seeking and self-administration in the alcohol group, it was not tested in the control group under acute administration conditions.

Experiment 2: effects of repeated administration of 3-PBC on seeking and self-administration under the CSR

In the alcohol group, significant changes in C2 seeking measures (left lever responses) were not observed as a function of repeated administration of 3-PBC (Table 2). However, in the control group, the C2-L2 response rate was significantly decreased as a function of dose, with both 10.0 and 18.0 mg/kg differing significantly from BL. Although the number of C2-L1 FI responses was significantly increased in the control group because this effect was also observed during vehicle administration, it does not appear to be directly related to 3-PBC effects but may be related to the procedure for injections per se.

As shown in Fig. 1a, in the alcohol group, 3-PBC dose-dependently decreased the number of right lever responses (i.e., self-administration responses) in C3 ($F(4,12)=4.98, p<0.05$), with a significant decrease relative to BL at 18.0 mg/kg. Both volume of alcohol consumed and gram per kilogram consumed decreased as a function of 3-PBC

Table 1 Experiment 1. Effects of acute 3-PBC (10-min pretreatment) on seeking (C2-L1 and C2-L2) and self-administration (C3) responses for alcohol under the CSR. BL is the grand mean of the 3 baseline days preceding each acute administration

			3-PBC dose						F(5,15)
			BL	0.3	1.0	3.0	10.0	30.0	
C2-L1	Left levFI resp	Mean	92.4	130.6	66.6	38.6	256.2	205.8	0.57
		SEM	47.5	80.2	47.5	18.0	206.9	155.0	
	Left lev FI resp Latency (s)	Mean	647.7	621.3	648.6	613.5	639.9	670.1	0.85
		SEM	17.9	11.3	21.7	3.4	20.9	41.9	
C2-L2	Left lev FR Resp rate (r/s)	Mean	2.2	3.2	2.7	1.0	2.3	3.2	1.88
		SEM	0.3	0.8	0.9	0.4	0.5	0.6	
C3	Right lev FR resp	Mean	194.4	196.0	182.0	184.0	190.0	130.0	1.48
		SEM	15.1	31.7	24.8	12.1	24.9	20.3	
	Volume (ml)	Mean	554.2	677.0	484.0	480.0	631.1	436.0	1.91
		SEM	61.0	147.2	57.1	60.4	83.2	79.4	
	g/kg Alc consumed	Mean	1.03	1.27	0.88	0.88	1.10	0.75	1.65
		SEM	0.1	0.3	0.1	0.1	0.2	0.1	

Data shown are group means (and SEM) for baseline (BL) and each 3-PBC dose (mg/kg)

FI fixed interval, FR fixed ratio, Lev lever, Resp response, Alc alcohol

dose (Table 2). Similarly, change in gram per kilogram alcohol consumed (compared to BL) was significantly decreased as a function of dose ($F(4,12)=3.53, p<0.05$), with 18.0 mg/kg differing significantly from vehicle (Fig. 1b).

In the control group, 3-PBC produced a significant decrease in the number of right lever operant responses during C3 ($F(4,12)=6.18, p<0.05$) with a significant decrease relative to BL at 10 mg/kg (Fig. 1a). A nonsignificant decrease

Table 2 Experiment 2. Effects of repeated administration (5-day) of vehicle (V) and doses of 3-PBC (10-min pretreatment) on seeking (C2-L1, C2-L2) for alcohol (alcohol group) and a nonalcohol beverage

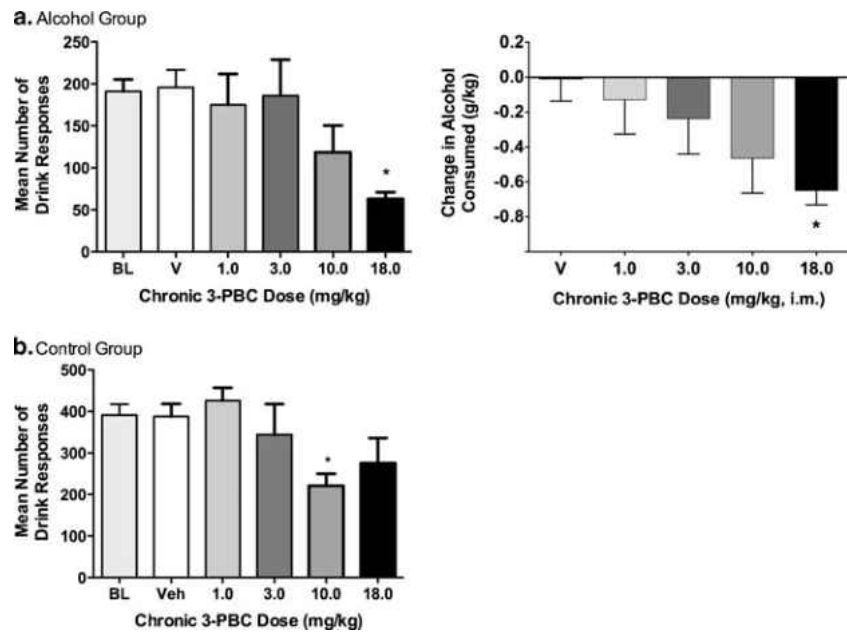
(control group) under the CSR. All data are the mean of days 3–5 of each condition. BL is the grand mean of the 3 baseline days preceding each chronic condition

			3-PBC dose						F(5,15)
Alcohol group			BL	V	1.0	3.0	10.0	18.0	
C2-L1	Left lev FI resp	Mean	144.7	169.4	106.9	115.5	36.8	116.3	0.48
		SEM	84.8	102.8	60.1	84.0	23.7	50.3	
	Left lev FI resp Latency (s)	Mean	630.2	606.2	695.8	712.3	697.8	739.0	1.60
		SEM	13.7	2.1	53.4	35.0	32.3	57.6	
C2-L2	Left lev FR Resp rate (r/s)	Mean	3.1	3.2	2.7	2.2	2.1	2.1	1.40
		SEM	0.3	0.5	0.5	0.3	0.7	0.7	
C3	Volume (ml)	Mean	625.6	674.8	576.7	489.6	355.4	283.3	<u>4.86</u>
		SEM	31.2	85.1	115.0	110.6	76.5	71.2	
	gkg Alc consumed	Mean	1.13	1.12	1.00	0.90	0.67	0.48	<u>3.85</u>
		SEM	0.1	0.1	0.2	0.1	0.2	0.1	
Control group									
C2-L1	Left lev FI resp	Mean	93.4	234.5	306.7	115.4	74.2	101.3	5.30
		SEM	21.5	73.8	129.1	44.3	49.4	72.6	
	Left lev FI esp Latency (s)	Mean	606.8	610.7	616.4	710.1	711.0	676.9	0.96
		SEM	0.9	2.52	12.4	56.2	87.8	70.1	
C2-L2	Left lev FR resp Rate (r/s)	Mean	3.1	2.9	2.5	2.1	1.5	1.7	<u>3.78</u>
		SEM	0.3	0.4	0.2	0.2	0.3	0.4	
C3	Volume (ml)	Mean	1000	1000	979.2	825.0	772.9	775.0	1.84
		SEM	0.0	0.0	20.8	175.0	88.2	125.2	

Data shown are group means (and SEM) for baseline (BL) and each 3-PBC dose (mg/kg). An underlined F ratio indicates a significant ($p<0.05$ ANOVA), numbers in bold indicate a significant ($p<0.05$) Bonferroni's post hoc test compared to vehicle

FI fixed interval, FR fixed ratio, Lev lever, Resp response, Alc alcohol

Fig. 1 Experiment 2: the effects of repeated (5-day) administration of 3-PBC on self-administration in C3 of the CSR in **a** the alcohol group and **b** the control group. Data shown are the group means (\pm SEM) of right (self-administration) responses (*left panels*) and for the alcohol group, change in gram per kilogram of alcohol consumed (*right panel*). * $p < 0.05$ for pairwise comparison for each dose vs. baseline



in the volume consumed (Table 1) was also obtained in the control group. Individual data showed that 3-PBC decreased volume consumed for all four baboons at 10.0 and 18.0 mg/kg, while lower doses (1.0 and 3.0 mg/kg) produced a decrease in only one of the baboons.

During BL, in both the alcohol and control groups, the majority of drinks occurred in the first 20 min of availability, followed by a lower rate across the subsequent 20-min bins. Despite this general similarity, a greater proportion of drinks occurred during the first 20-min bin in the control group (>95 %) compared to the alcohol group (>75 %) (Fig. 2). All doses (1.0–18.0 mg/kg) of 3-PBC significantly ($p < 0.05$) decreased the number of drinks during the first 20 min in the alcohol group, with larger decreases observed at the higher (10.0 and 18.0 mg/kg) doses. In the control group, only the highest doses (10 and 18.0 mg/kg) significantly decreased drinking during the first 20 min of drinking.

Discussion

Targets for therapeutic agents to treat alcohol abuse and dependence include the reduction of alcohol intake and attenuation of the motivation or desire to consume alcohol. In the current model, this would be reflected in decreases in alcohol self-administration responses and gram per kilogram intake (consumption in C3), and disruption of responses directed towards obtaining the opportunity to drink (seeking in C2). Several important findings were identified in the current study. First, repeated (5-day), but not acute, administration of the GABA_A $\alpha 1$ -preferring ligand 3-PBC reduced ongoing alcohol self-administration in baboons with long-term alcohol self-administration experience. Second,

3-PBC did not disrupt the established pattern of alcohol seeking and self-administration but reduced the magnitude of intake, particularly during the initial drinking bout. Third,

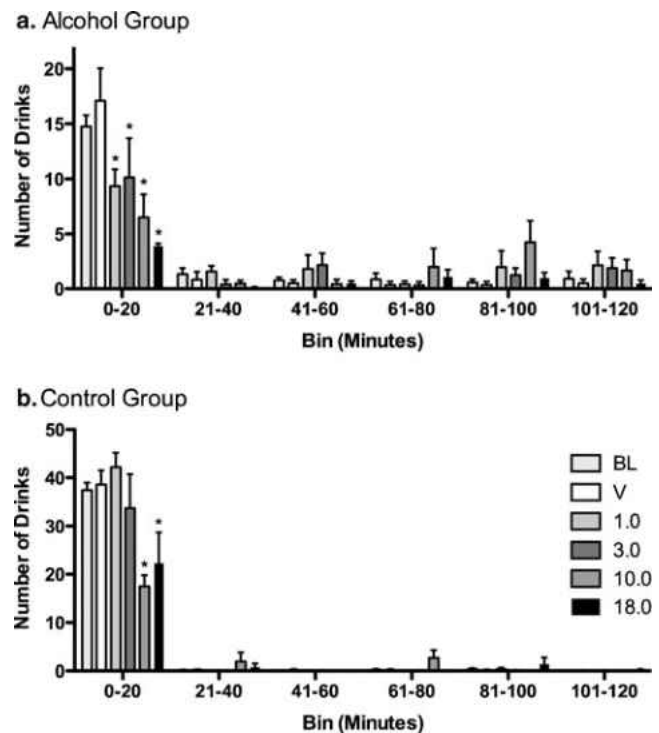


Fig. 2 Experiment 2: the effects of repeated (5-day) administration of 3-PBC on the pattern and number of drinks per 20-min interval of the 120-min self-administration period (C3) in the **a** alcohol group and **b** the control group. Data shown are group mean drinks (\pm SEM) for each successive time bin of availability of alcohol or the nonalcoholic beverage, and * $p < 0.05$ for pairwise comparison for each 3-PBC dose vs. vehicle within each time bin

3-PBC also suppressed responding maintained by a nonalcoholic beverage, albeit at higher doses than required to suppress alcohol. Each of these findings is discussed below.

The finding that 3-PBC decreased alcohol-maintained responding and consumption in primates provides further evidence of a role of $\alpha 1$ GABA_A subtype in alcohol abuse and dependence. The involvement of the GABA_A receptor in the behavioral actions of alcohol is complex, with different subtypes differentially involved in the various effects of alcohol. Studies with subtype-preferring compounds and in modified mouse models have shown that several of the subtypes ($\alpha 1$, $\alpha 2$, $\alpha 3$, and $\alpha 5$) may have involvement in alcohol reinforcement (Atack 2003; Cook et al. 2005; Stephens et al 2005; for a review see Kumar et al 2009). 3-PBC exhibits binding preference for the GABA_A $\alpha 1$ receptor (Cox et al. 1998; Huang et al. 2000). The current findings are consistent with studies in rats selectively bred for P or HAD. Specifically, administration of the $\alpha 1$ -preferring ligands 3-PBC or β -carboline-3-carboxylate-t-butylester (β CCt) decreased ongoing alcohol consumption in P rats when administered systemically or via microinfusion into the ventral pallidum (Harvey et al 2002; June et al. 2003). Taken together with the current findings, the $\alpha 1$ GABA_A subtype-preferring ligand 3-PBC reduces alcohol-maintained behaviors and daily alcohol intake in both genetically predisposed animals and outbred animals with long-term drinking experience.

In the present study, high doses of 3-PBC also produced a decrease in self-administration of a palatable nonalcoholic beverage, which suggests that 3-PBC effects may not be specific to alcohol. Although 3-PBC typically displays a BZ antagonist-like profile in most behavioral tasks, in an *in vitro* analysis, 3-PBC exhibited a low partial agonist efficacy at recombinant diazepam-sensitive receptors (Harvey et al 2002). The decreased component 2 FR (C2-L2) response rate in the control group is consistent with a rate-suppressing agonist effect. However, responding was not also suppressed during the FI link of C2 in the control group (and, in fact, was increased at lower doses), suggesting that a general rate-decreasing effect cannot account for the non-specific effects obtained.

Nonspecific effects have also been reported in other studies. For example, $\alpha 1$ receptor knockout mice consumed less ethanol in a two-bottle choice procedure, but also less saccharin, when compared to wild type mice (Blednov et al. 2003; June et al. 2007). $\alpha 1$ -GABA_A receptor knockout mice also showed decreased operant responding for both ethanol and sucrose (June et al. 2007). However, Harvey et al. (2002) reported that only the highest IP administered dose (20 mg/kg) of 3-PBC significantly suppressed saccharin-maintained responding and did so throughout the drinking period. As 3-PBC does bind to other α -receptor subtypes to some degree, the authors suggested there may be a

saturation of all α -receptor subtypes following the highest dose. Similarly, in the present study, acute administration of the highest dose of 3-PBC (30 mg/kg) in the alcohol group disrupted daily food intake and repeated administration of the highest doses (10 and 18 mg/kg) suppressed responding for a highly preferred beverage during the initial 20 min of the session in the control group. The highest dose tested under the 5-day dosing conditions in the present study (18 mg/kg) is roughly equivalent (via interspecies conversion, Dews 1976; Mordenti and Chappell 1989) to 78 mg/kg in the rat, a dose that is substantially higher than that evaluated by Harvey et al. (2002). Thus, it is possible that receptor saturation may account for the decrease in non-alcohol beverage in the present study.

This is the first study to examine the effects of 3-PBC on responses to gain access to alcohol (seeking). 3-PBC did not significantly decrease seeking during either C2 link in the alcohol group. Alcohol-related cues maintain seeking behavior even under conditions of alcohol abstinence and are highly resistant to change. For example, studies in rats have shown that stimuli previously paired with alcohol continue to maintain responding for many sessions (e.g., Ciccocioppo et al. 2001; Zironi et al. 2006). Likewise, in Kaminski et al. (2008), presentation of alcohol-related cues in the CSR maintained C2 responding for an extended period (i.e., 30 consecutive sessions) after water was substituted for alcohol in C3 (i.e., during extinction). In addition, when alcohol was available for consumption in C3, high levels of seeking responses were maintained (>600 responses in C2 Link 2) under conditions in which the response requirement was progressively increased to obtain the daily supply of alcohol (Kaminski et al. 2008). In the alcohol group, then, the strength of C2 seeking responding, which is maintained by transition to C3 where alcohol is available for consumption, appears to have mitigated the C2 (seeking) response suppression observed in the control group. This suggests that 3-PBC suppression of alcohol-maintained responding obtained in C3 is a function of changes in the reinforcing effects of alcohol upon consumption.

Within each daily session, in both the alcohol and control groups, the majority of BL drinking occurred within the first 20 min of the 2 h of availability. Drinks in the first 20 min was tightly clustered (i.e., a single drinking bout). 3-PBC did not disrupt this pattern of intake but dose-dependently decreased the number of drinks in this initial drinking bout in the alcohol group. Consistent with the results of Harvey et al. (2002), after the initial suppression of intake, 3-PBC did not reduce the low levels of alcohol drinking during later portions of the session. As a result, the effects of 3-PBC on self-administration measures for the entire 2-h drinking period differed from BL only at the highest doses of 3-PBC. The suppression of alcohol intake during the first drinking bout of the CSR, with BL levels of alcohol intake later in the

session, is similar to that previously reported for naltrexone (Kaminski et al. 2012). Naltrexone is one of the current Food and Drug Administration (FDA)-approved treatments to reduce drinking and promote abstinence in alcohol-dependent persons and numerous clinical trials have demonstrated its effectiveness for treatment of alcohol dependence (Johnson 2008). Studies have suggested that naltrexone's clinical effectiveness is due, in part, to preventing drinking episodes from becoming a full-fledged relapse to heavy drinking (Anton et al. 1999; O'Malley and Froehlich 2003; Pettinati et al. 2006).

There are a number of strengths of the current study that increase the translational value of these findings. First, recent reviews have emphasized the importance of animal models with sufficient alcohol intake to achieve a biologically relevant BAL of 0.08 mg/dl or more for better medication development (Egli 2005; Grant and Bennett 2003). In the alcohol group, baboons drank approximately 1 g/kg/day of alcohol. Mean BAL of 88.2 mg/dl (>0.08 %) were previously determined in these same baboons after comparable alcohol intake (mean volume 0.93 g/kg) (Kaminski et al. 2008). A BAL of 0.08 % is defined as intoxication with regard to National Institute on Alcohol Abuse and Alcoholism (NIAAA) definitions and for driving violations in most of the USA. Second, the current procedure models key elements of human problematic drinking. In humans, drinking to intoxication (e.g., 0.8 to 1 g/kg, BAL > 0.08 %) within a single drinking period (binge) and regular drinking at this level across days (heavy drinking) is characterized as problem drinking with higher risk for alcoholism (Rethinking Drinking, NIH). The baboons in the current study had long-term self-administration experience (i.e., years) under the CSR with either alcohol or, for the control group, the nonalcoholic beverage. Thus, based on NIAAA definitions, baboon drinking in the current study models problem drinking in humans. Third, our study is the first to show that a GABA_A α 1-preferring ligand reduces alcohol self-administration behaviors and gram per kilogram consumption in long-term heavy drinking primates under a CSR. Use of the CSR is novel, as it allows, within the same session, evaluation of drug effects on responding in the presence of alcohol-related stimuli maintained by conditioned reinforcement as well as alcohol self-administration (consumption) and, thus, provides a measure of the motivation to drink. Fourth, the inclusion of the control group allowed the examination of specificity of 3-PBC effects on alcohol-related behaviors.

Previously, we have shown that alcohol-seeking behaviors maintained by alcohol-associated cues are highly resistant to change and are sensitive to duration of abstinence and alcohol availability (Kaminski et al. 2008; 2012; Weerts et al 2006). In the present study, 3-PBC did not decrease C2 seeking measures but did produce time-dependent changes in alcohol self-administration behaviors in C3. As indicated previously, ideal therapeutic agents for alcohol abuse and

dependence would reduce alcohol seeking and self-administration in the current model. Thus, the present results suggest that, like naltrexone, GABA_A α 1-preferring ligands, such as 3-PBC, may have clinical utility in reducing the severity of drinking episodes when they do occur but are less likely to affect the motivation or desire to consume alcohol. With the recent development of ligands selective for each of the α subtypes, future research can further clarify the role of the GABA receptors in alcohol abuse and dependence.

Acknowledgments This research was supported by NIH/NIAAA R01AA15971 (Weerts), MH046851 (Cook), and The Lynde and Harry Bradley Foundation (Cook).

Conflict of interest The authors have no conflicts to disclose.

References

- Amato L, Minozzi S, Davoli M (2011) Efficacy and safety of pharmacological interventions for the treatment of the alcohol withdrawal syndrome. *Cochrane Database Syst Rev* 6:CD008537
- Anton RF, Moak DH, Waid LR, Latham PK, Malcolm RJ, Dias JK (1999) Naltrexone and cognitive behavioral therapy for the treatment of outpatient alcoholics: results of a placebo-controlled trial. *Am J Psychiatry* 156:1758–1764
- Atack JR (2003) Anxiolytic compounds acting at the GABA_A receptor benzodiazepine binding site. *Curr Drug Targets CNS Neural Disord* 2:213–232
- Blair LA, Levitan ES, Marshall J, Dionne VE, Barnard EA (1988) Single subunits of the GABA_A receptor form ion channels with properties of the native receptor. *Science* 242:577–579
- Blednov YA, Walker D, Alva H, Creech K, Findlay G, Harris RA (2003) GABA_A receptor α 1 and β 2 subunit null mutant mice: behavioral responses to ethanol. *J Pharmacol Exp Ther* 305(3):854–863
- Boehm SL, Ponomarev I, Blednov YA, Harris RA (2006) From gene to behavior and back again: new perspectives on GABA_A receptor subunit selectivity of alcohol actions. *Adv Pharmacol* 54:171–203
- Chester JA, Cunningham CL (2002) GABA(A) receptor modulation of the rewarding and aversive effects of ethanol. *Alcohol* 26(3):131–143
- Chu DC, Albin RL, Young AB, Penney JB (1990) Distribution and kinetics of GABA_B binding sites in rat central nervous system: a quantitative autoradiographic study. *Neurosci* 34:341–357
- Ciccocioppo R, Angeletti S, Weiss F (2001) Long-lasting resistance to extinction of response reinstatement induced by ethanol-related stimuli: role of genetic ethanol preference. *Alcohol Clin Exp Res* 25:1414–1419
- Cook JB, Foster KL, Eiler WJ 2nd, McKay PF, Woods J 2nd, Harvey SC, Garcia M, Grey C, McCane S et al (2005) Selective GABA_A α 5 benzodiazepine inverse agonist antagonizes the neurobiological actions of alcohol. *Alcohol Clin Exp Res* 29:1390–1401
- Cox ED, Diaz-Araujo H, Huang Q, Reddy MS, Harris B, McKernan RM, Skolnick P, Cook JM (1998) Synthesis and evaluation of analogues of the partial agonist 6-(propyloxy)-4-(methoxymethyl)-beta-carboline-3-carboxylic acid ethyl ester (6-PBC) and the full agonist 6-(benzyloxy)-4-(methoxymethyl)-beta-carboline-3-carboxylic acid ethyl ester (Zk 93423) at wild type and recombinant GABA(A) receptors. *J Med Chem* 41:2537–2552

- Davies M (2003) The role of GABAA receptors in mediating the effects of alcohol in the central nervous system. *J Psychiatry Neurosci* 28(4):263–274
- Dews PB (1976) Interspecies differences in drug effects: behavioral. In: Usdin E, Forrest IS (eds) *Psychotherapeutic drugs, part I*. Marcel Dekker, New York, pp 175–214
- D'Hulst C, Atack JR, Kooy RF (2009) The complexity of the GABA_A receptor shapes unique pharmacological profiles. *Drug Discov Today* 14:866–875
- Duke AN, Kaminski BJ, Weerts EM (2012) Baclofen effects on alcohol seeking, self-administration and extinction of seeking responses in a within-session design in baboons. *Addict Biol* 28. doi:10.1111/j.1369-1600.2012.00448.x
- Enoch MA (2008) The role of GABA(A) receptors in the development of alcoholism. *Pharmacol Biochem Behav* 90:95–104
- Egli M (2005) Can experimental paradigms and animal models be used to discover clinically effective medications for alcoholism? *Addict Biol* 10:309–310
- Floyd DW, Friedman DP, Daunais JB, Pierre PJ, Grant KA, McCool BA (2004) Long-term ethanol self-administration by cynomolgus macaques alters the pharmacology and expression of GABAA receptors in basolateral amygdala. *J Pharmacol Exp Ther* 311:1071–1079
- Gourley SL, DeBold JF, Yin W, Cook J, Miczek KA (2005) Benzodiazepines and heightened aggressive behavior in rats: reduction by GABAA/α1 receptor antagonists. *Psychopharmacol* 178:232–240
- Grant KA, Bennett AJ (2003) Advances in nonhuman primate alcohol abuse and alcoholism research. *Pharmacol Ther* 100:235–255
- Grobin AC, Matthews DB, Devaud LL, Morrow AL (1998) The role of GABA(A) receptors in the acute and chronic effects of ethanol. *Psychopharmacol* 139:2–19
- Harvey SC, Foster KL, McKay PF, Carroll MR, Seyoum R, Woods JE, Grey C, Jones CM, McCane S, Cummings R, Mason D, Ma CR, Cook JM, June HL (2002) The GABA(A) receptor alpha(1) subtype in the ventral pallidum regulates alcohol-seeking behaviors. *J Neurosci* 22(9):3765–3775
- Heilig M, Goldman D, Berrettini W, O'Brien CP (2011) Pharmacogenetic approaches to the treatment of alcohol addiction. *Nat Rev Neurosci* 12(11):670–684
- Huang Q, He XH, Ma CR, Liu RY, Yu S, Dayer CA, Wenger GR, McKernan R, Cook JM (2000) Pharmacophore/receptor models for GABA(A)/BzR subtypes (α1β3γ2, α5β3γ2, α6β3γ2) via a comprehensive ligand-mapping approach. *J Med Chem* 43(1):71–95
- Ittiwut C, Yang BZ, Kranzler HR, Anton RF, Hirunsatit R, Weiss RD, et al (2011) GABRG1 and GABRA2 variation associated with alcohol dependence in African Americans. *Alcohol Clin Exp Res Epub* 2011/09/17.
- Johnson BA (2008) Update on neuropharmacological treatment for alcoholism: scientific basis and clinical findings. *Biochem Pharmacol* 75:34–56
- Johnson KJ, Sander T, Hicks AA, van Marle A, Janz D, Mullan MJ et al (1992) Confirmation of the localization of the human GABAA receptor alpha 1-subunit gene (GABRA1) to distal 5q by linkage analysis. *Genomics* 14(3):745–748
- June HL, Foster KL, McKay PF, Seyoum R, Woods JE, Harvey SC et al (2003) The reinforcing properties of alcohol are mediated by GABA(A1) receptors in the ventral pallidum. *Neuropsychopharmacol* 28(12):2124–2137
- June HL Sr, Foster KL, Eiler WJ 2nd, Goergen J, Cook JB, Johnson N, Mensah-Zoe B, Simmons JO, June HL Jr, Yin W, Cook JM, Homanics GE (2007) Dopamine and benzodiazepine-dependent mechanisms regulate the EtOH-enhanced locomotor stimulation in the the GABAA alpha1 subunit null mutant mice. *Neuropsychopharm* 32:137–152
- Kaminski BJ, Goodwin AK, Wand G, Weerts EM (2008) Dissociation of alcohol-seeking and consumption under a chained schedule of oral alcohol reinforcement. *Alcohol Clin Exp Res* 32:1–9
- Kaminski BJ, Duke AN, Weerts EM (2012) Effects of naltrexone on alcohol drinking patterns and extinction of alcohol seeking in baboons. *Psychopharmacology* 223:55–66
- Korpi ER (1994) Role of GABAA receptors in the actions of alcohol and in alcoholism: recent advances. *Alcohol Alcohol* 29(2):115–129
- Koob GF (2004) A role for GABA mechanisms in the motivational effects of alcohol. *Biochem Pharmacol* 68:1515–1525
- Kumar S, Porcu P, Werner DF, Matthews DB, Diaz-Granados JL, Helfand RS, Morrow AL (2009) The role of GABAA receptors in the acute and chronic effects of ethanol: a decade of progress. *Psychopharmacology* 205:529–564
- Lelas S, Rowlett JK, Spealman RD, Cook JM, Ma CR, Li XY, Yin WY (2002) Role of GABAA/benzodiazepine receptors containing α1 and α5 subunits in the discriminative stimulus effects of triazolam in squirrel monkeys. *Psychopharmacology* 161:180–188
- Lobo IA, Harris RA (2008) GABA(A) receptors and alcohol. *Pharmacol Biochem Behav* 90(1):90–94
- Lydall GJ, Saini J, Ruparelia K, Montagnese S, McQuillin A, Guerrini I et al (2011) Genetic association study of GABRA2 single nucleotide polymorphisms and electroencephalography in alcohol dependence. *Neurosci Lett* 500(3):162–166
- Malcolm RJ (2003) GABA systems, benzodiazepines, and substance dependence. *J Clin Psychiatry* 64(Suppl 3):36–40
- Mordenti J, Chappell W (1989) The use of interspecies scaling in toxicokinetics. In: Yacobi A, Kelly J, Batra V (eds) *Toxicokinetics and new drug development*. Pergamon, New York, pp 42–96
- Murphy JM, Stewart RB, Bell RL, Badia-Elder NE, Carr LG, McBride WJ, Lumeng L, Li TK (2002) Phenotypic and genotypic characterization of the Indiana University rat lines selectively bred for high and low alcohol preference. *Behav Genet* 32(5):363–388
- Namjoshi OA, Gryboski A, Fonseca GO, Van Linn ML, Wang Z, Deschamps JR, Cook JM (2011) Development of a two-step route to 3-PBC and βCCt, two agents active against alcohol self-administration in rodent and primate models. *J Org Chem* 76:4721–4727
- Nevo I, Hamon M (1995) Neurotransmitter and neuromodulatory mechanisms involved in alcohol abuse and alcoholism. *Neurochem Int* 26(4):305–336
- Olsen RW, Sieghart W (2009) GABA A receptors: subtypes provide diversity of function and pharmacology. *Neuropharmacology* 56(1):141–148
- O'Malley SS, Froehlich JC (2003) Advances in the use of naltrexone: an integration of preclinical and clinical findings. *Recent Dev Alcohol* 16:217–245
- Ortiz J, Fitzgerald LW, Charlton M, Lane S, Trevisan L, Guitart X et al (1995) Biochemical actions of chronic ethanol exposure in the mesolimbic dopamine system. *Synapse* 21:289–298
- Pettinati HM, O'Brien CP, Rabinowitz AR, Wortman SP, Oslin DW, Kampman KM, Dackis CA (2006) The status of naltrexone in the treatment of alcohol dependence: specific effects on heavy drinking. *J Clin Psychopharmacol* 26:610–625
- Richter L, de Graaf C, Sieghart W, Varagic Z, Mörzinger M, de Esch IJP, Ecker GF, Ernst M (2012) Diazepam-bound GABA_A receptor models identify new benzodiazepine binding-site ligands. *Chem Biol* 25 March 2012, doi 10.1038 [Epub ahead of print].
- Roh S, Matsushita S, Hara S, Maesata H, Matsui T, Suzuki G et al (2011) Role of GABRA2 in moderating subjective responses to alcohol. *Alcohol Clin Exp Res* 35(3):400–407
- Rowlett JK, Spealman RD, Lelas S, Cook JM, Yin W (2003) Discriminative stimulus effects of zolpidem in squirrel monkeys: role of GABAA/α1 receptors. *Psychopharmacology* 165:209–215

- Stephens DN, Pistocakova J, Worthing L, Atack JR, Dawson GR (2005) Role of GABAA alpha5-containing receptors in ethanol reward: the effects of targeted gene deletion, and a selective inverse agonist. *Eur J Pharmacol* 5:240–250
- Uhart M, Weerts EM, McCaul ME, Guo X, Yan X, Kranzler HR, Li N, Wand GS (2012) GABRA2 markers moderate the subjective effects of alcohol. *Addict Biol* Apr 13. doi:10.1111/j.1369-1600.2012.00457.x
- Weerts EM, Goodwin AK, Kaminski BJ, Hienz RD (2006) Environmental cues, alcohol seeking, and consumption in baboons: effects of response requirement and duration of alcohol abstinence. *Alcohol Clin Exp Res* 30:2026–2036
- Yang AR, Liu J, Yi HS, Warnock KT, Wang M, June HL Jr, Puche AC, Elnabawi A, Sieghart W, Aurelian L, June HL Sr (2011) Binge drinking: in search of its molecular target via the GABA(A) receptor. *Front Neurosci* 5:123
- Yin W, Majumder S, Clayton T, Petrou S, VanLinn ML, Namjoshi OA et al (2010) Design, synthesis, and subtype selectivity of 3,6-disubstituted beta-carbolines at Bz/GABA (a)ergic receptors. SAR and studies directed toward agents for treatment of alcohol abuse. *Bioorg Med Chem* 8 (21):7548–7564
- Zironi I, Burattini C, Aicardi G, Janak PH (2006) Context is a trigger for relapse to alcohol. *Behav Brain Res* 167:150–155

Copyright of Psychopharmacology is the property of Springer Science & Business Media B.V. and its content may not be copied or emailed to multiple sites or posted to a listserv without the copyright holder's express written permission. However, users may print, download, or email articles for individual use.



Full length article

Effects of the benzodiazepine GABA_A α 1-preferring antagonist 3-isopropoxy- β -carboline hydrochloride (3-ISOPBC) on alcohol seeking and self-administration in baboons



August F. Holtyn^a, V.V.N. Phani Babu Tiruveedhula^b, Michael Rajesh Stephen^b, James M. Cook^b, Elise M. Weerts^{a,*}

^a Johns Hopkins University School of Medicine, Division of Behavioral Biology, 5510 Nathan Shock Dr, Baltimore, MD 21224, USA

^b University of Wisconsin-Milwaukee, Department of Chemistry & Biochemistry, 3210 N Cramer St, Milwaukee, WI 53201, USA

ARTICLE INFO

Article history:

Received 12 July 2016

Received in revised form 28 October 2016

Accepted 28 October 2016

Available online 4 November 2016

Keywords:

Alcohol

3-Isopropoxy- β -carboline hydrochloride

3-ISOPBC

Self-administration

Baboon

ABSTRACT

Background: The major inhibitory neurotransmitter, gamma-aminobutyric acid (GABA), modulates many of the behavioral effects of alcohol, including sedation, tolerance, and withdrawal. The α 1 subunit of the benzodiazepine GABA_A receptor is the most widely expressed alpha subunit in the brain, and has been implicated in the reinforcing- and abuse-related effects of alcohol. The aim of the present study was to examine whether treatment with a benzodiazepine GABA_A α 1-preferring ligand, 3-isopropoxy- β -carboline hydrochloride (3-ISOPBC), selectively decreases alcohol seeking and consumption.

Methods: Eight baboons self-administered alcohol (4% w/v; n=5; alcohol group) or a non-alcoholic beverage (n=3; control group) in Component 3 of a chained schedule of reinforcement. Responses in Component 2 provided indices of motivation to drink (seeking). Doses of 3-ISOPBC (5.0–30.0 mg/kg) and vehicle were administered before drinking sessions under both acute and chronic (5 day) conditions.

Results: Chronic, and not acute, administration of 3-ISOPBC significantly decreased self-administration responses, g/kg alcohol consumed, and the number of drinks in and duration of the first drinking bout in the alcohol group. In the control group, chronic administration of 3-ISOPBC did not significantly decrease any of these measures at any of the doses.

Conclusions: The GABA_A α 1-preferring ligand 3-ISOPBC may have therapeutic potential in the treatment of alcohol use disorder due to its ability to selectively reduce alcohol use.

© 2016 Elsevier Ireland Ltd. All rights reserved.

1. Introduction

Gamma-aminobutyric acid (GABA) is the major inhibitory neurotransmitter in the central nervous system and is an important target in the development of pharmacotherapies for alcohol use disorder. GABA binds to type A receptors, which have been implicated in the acute and chronic effects of alcohol, including sedation, tolerance, and withdrawal as well as the motivational effects of alcohol, including alcohol reinforcement and consumption (for reviews, see Enoch, 2008; Kumar et al., 2009; Lobo and Harris, 2008). GABA_A receptors are composed of five subunits that form a central chloride channel and can belong to different subunit classes: α (1–6), β (1–3), γ (1–3), δ , ϵ , π , θ , and ρ (1–3). While many GABA_A recep-

tors are composed of one γ , two α , and two β subunits, the various subunit classes allow for extensive heterogeneity in receptor subunit composition. The subunit composition is a major determinant of the pharmacological profile of the receptor and the presence or absence of certain subunits may regulate specific behavioral effects of drugs such as alcohol (Olsen and Sieghart, 2009).

The α 1 subunit of the GABA_A receptor may play a role in the reinforcing- and abuse-related effects of alcohol. Knockout mice without the GABA_A α 1 receptor have been shown to consume less alcohol under a two-bottle alcohol versus water choice procedure and to respond less for alcohol under an operant self-administration procedure, although these were accompanied by reductions in saccharin and sucrose consumption (Blednov et al., 2003; June et al., 2007). In rodents bred for high alcohol intake, benzodiazepine GABA_A α 1-preferring antagonists, 3-propoxy- β -carboline hydrochloride (3-PBC) and β -carboline-3-carboxylate-*tert*-butyl ester (β CCCT), decreased alcohol intake when administered systemically or through microinfusions into

* Corresponding author. Johns Hopkins Bayview Campus, Behavioral Biology Research Center, 5510 Nathan Shock Drive, Suite 3000, Baltimore, MD, 21224, USA.
E-mail address: eweerts@jhmi.edu (E.M. Weerts).

the ventral palladium (Harvey et al., 2002; June et al., 2003). In primates, chronic administration of 3-PBC significantly decreased self-administration responses, volume consumed, and g/kg alcohol intake but also had some effects on self-administration of a non-alcoholic reinforcer in one study (Kaminski et al., 2013). In another study, chronic administration of 3-PBC and β CCT did not decrease alcohol intake or blood alcohol levels (Sawyer et al., 2014).

It is clear from the work of Licata et al. (2009) in primates, June et al. (2003) and Harvey et al. (2002) in rodents, and Platt et al. (2002) in rhesus macaques, that both β CCT and 3-PBC have been shown to be α 1-preferring antagonists *in vivo*. Moreover, both β CCT and 3-PBC have been shown to be potent antagonists *in vitro* (Harvey et al., 2002; Yin et al., 2010). Based on these and the above data, the synthesis of an analog of 3-PBC, 3-isopropoxy- β -carboline hydrochloride (3-ISOPBC), was undertaken (Tiruveedhula et al., 2015). This choice was guided by molecular modeling (He et al., 2000; Huang et al., 2000) wherein it is well established that a major change in the structure of a benzodiazepine GABA_A (α 1-6 β 2/3 γ 2) receptor subunit selective ligand can dramatically alter the subunit selectivity (Clayton et al., 2007, 2015). 3-ISOPBC displays a 7-fold selectivity for the α 1 subunit over the α 2 and α 3 subunits as well as a 30-fold selectivity over the α 5 subunit (supplemental Table 1s). 3-PBC binding affinities have been published previously (Harvey et al., 2002). 3-ISOPBC did not bind to any other receptors in the 43 receptor panel tested (supplemental Table 2s) in the psychoactive drug screening program (UNC, B. Roth; Besnard et al., 2012; Huang et al., 2010), analogous to the ligand 3-PBC. In addition, 3-ISOPBC did not exhibit sedative nor ataxic activity, as illustrated by results from rotarod testing (supplemental Fig. 1s). Even though 3-ISOPBC binds more potently to α 1 receptors (supplemental Table 1s), it is clear from the rotarod data that it does not affect positive allosteric modulation at benzodiazepine α 1 GABA_A receptors. The ligand 3-PBC also had no agonist activity at α 1 subunits, even though it binds more potently to the α 1 subunit than other DS sites (Yin et al., 2010). The choice of 3-ISOPBC was also based on the structure of the branched isopropyl group, which would hinder metabolism by beta (omega-1) oxidation. Since 3-ISOPBC may undergo phase 1 metabolism by cytochrome P450 enzymes—potentially by beta (omega-1) oxidation of the linear *n*-propyl group in 3-PBC (Foye et al., 2013) – at a much slower rate than 3-PBC, it was hypothesized that this would increase the duration of action and provide a ligand more active *in vivo* than 3-PBC.

The present study investigated whether acute and chronic administration of 3-ISOPBC could selectively reduce alcohol seeking and self-administration in baboons. The baboons consumed alcohol daily under a chained schedule of reinforcement at levels that produce blood alcohol levels exceeding 0.08%. The use of the chain schedule allows for examination of drug effects on responding in the presence of alcohol-related cues that is maintained by conditioned reinforcement (i.e., responding that produces access to alcohol or “seeking”), as well as alcohol self-administration within the same session. To determine the specificity of effects on alcohol-related behaviors, chronic administration of 3-ISOPBC was also conducted with baboons that self-administered a preferred, non-alcoholic beverage under the chained schedule.

2. Material and methods

2.1. Subjects

Eight singly-housed adult male baboons (*Papio anubis*; Southwest Foundation for Biomedical Research, San Antonio, TX) weighing on average 28.1 kg (+4.2 SD) served as subjects. For the alcohol group (N=5), the reinforcer delivered was 4% w/v alcohol. For the control group (N=3), the reinforcer delivered was a pre-

ferred non-alcohol beverage (orange-flavored, sugar-free Tang[®]), diluted to a concentration that functioned as a comparable reinforcer (Duke et al., 2014). All baboons had extensive histories of self-administration of either alcohol or the non-alcoholic beverage under the chained schedule of reinforcement as reported previously (Duke et al., 2014; Holtyn et al., 2014; Kaminski and Weerts, 2014; Kaminski et al., 2008, 2012, 2013). Each day, the baboons were fed standard primate chow that was adjusted to maintain sufficient caloric intake for normal baboons of their size, age, and activity level (about 50–73 kcal/kg); fresh fruit or vegetables; and a children’s chewable multivitamin. Water was available *ad libitum* except during sessions. The housing room was maintained under a 12-hour light/dark cycle (lights on at 6:00 AM). Facilities were maintained in accordance with USDA and AAALAC standards. The protocol was approved by the JHU Animal Care and Use Committee and followed the *Guide for the Care and Use of Laboratory Animals* (2011).

2.2. Apparatus

Sessions were conducted in modified primate cages as described in detail previously (Kaminski et al., 2008; Weerts et al., 2006) and contained (1) a panel with three colored “cue” lights, (2) an intelligence panel with two vertically operated levers and two different colored “jewel” lights each located above one of the levers, (3) a “drinkometer” connected to a calibrated 1000-ml bottle, and (4) a speaker mounted above the cages for presentation of auditory stimuli (tones). A computer interfaced with Med Associates hardware and software remotely controlled the experimental conditions and data collection.

2.3. Chained schedule of reinforcement procedure

Sessions were conducted seven days per week and began at the same time (8:30 AM) each day. The start of a session and the onset of Component 1 was signaled by a 3-s tone. During Component 1, a red cue light was illuminated and all instrumental responses were recorded but had no programmed consequence. After 20 min, Component 1 ended and Component 2 was initiated.

Component 2 was signaled by the illumination of a yellow cue light and consisted of two links. During the first link, the jewel light over the left lever was turned on, and a concurrent fixed interval 10 min, fixed time 20 min (FI 10-min FT 20-min) schedule was in effect. The first link ended either a) with the first response on the left lever after 10 min elapsed or b) automatically after 20 min, whichever occurred first. During the second link, the jewel light over the left lever flashed and a fixed-ratio (FR) 10 schedule was in effect on the left lever. Completion of the FR response requirement ended Component 2; the yellow cue light and the jewel light were turned off and Component 3 was initiated. If the FR 10 requirement was not completed within 90 min, the session terminated without transitioning to Component 3 (i.e., no access to alcohol or the non-alcoholic beverage for the day).

Component 3 was signaled by the illumination of the blue cue light. A blue jewel light over the right lever was also illuminated, and the opportunity to self-administer alcohol or the non-alcoholic beverage (depending on group assignment) was available under an FR 10 schedule on the right lever. Completion of each FR and subsequent contact with the drinkometer spout delivered fluid for the duration of spout contact or for a programmed duration (5 s), whichever came first. This defined a single drink. Component 3 and the session ended after 120 min.

Table 1

Experiment 1. Effects of acute administration of vehicle (V) and doses of 3-ISOPBC on seeking in Component 2 (C2) and consumption in Component 3 (C3) for alcohol under the chained schedule of reinforcement. Baseline (BL) is the grand mean of the 3 days preceding each acute administration.

			BL	V	3-ISOPBC dose (mg/kg)			F (4,16)	
					10.0	20.0	30.0		
C2	Left Lever	Mean	125.5	574.8	582.8	272.0	417.0	1.91	
	FI Resp	SEM	48.0	270.1	307.3	166.6	236.6		
	Left Lever FI Resp	Mean	632.3	625.4	615.1	629.9	613.6		0.46
	Latency (s)	SEM	24.8	19.2	13.7	13.2	10.7		
C3	Right Lever	Mean	117.9	126.2	108.0	109.4	106.0	0.82	
	FR Resp	SEM	14.6	12.6	13.0	16.1	19.5		
	g/kg Alc Consumed	Mean	1.1	1.2	1.1	1.0	1.0		0.60
		SEM	0.1	0.1	0.1	0.1	0.1		

Note: FI, Fixed Interval; FR, Fixed Ratio; Resp, Response; Alc, Alcohol.

2.4. Drugs

All solutions for oral consumption were mixed using reverse osmosis (RO) purified drinking water. Ethyl alcohol (190 Proof, Pharmco-AAPER, Brookville CT) was diluted with RO water to 4% w/v alcohol. Orange-flavored, sugar-free, Tang® powder (Kraft Foods) was dissolved in RO water as described previously (Duke et al., 2014). The 3-ISOPBC was synthesized in the laboratory of Dr. James Cook (University of Wisconsin-Milwaukee; Tiruveedhula et al., 2015). Doses of 3-ISOPBC (5.0–30.0 mg/kg) were dissolved in a vehicle of 50% saline, 37.5% propylene glycol, and 12.5% ethanol and administered via the intramuscular route (2–3 mls/injection). Vehicle tests were completed using the same volume and procedures as detailed below.

2.5. 3-ISOPBC test procedures

The baseline stability criterion was defined as stable self-administration of alcohol or non-alcoholic beverage (i.e., $\pm 20\%$) for three consecutive sessions. To evaluate acute effects of 3-ISOPBC on alcohol-related behaviors and to verify the safety of the dose range, in Experiment 1, doses of 3-ISOPBC (10.0–30.0 mg/kg) or its vehicle were administered acutely in the alcohol group only. The baseline stability criterion was met before each test dose of 3-ISOPBC. Doses were tested in mixed order, with active doses tested no more than once per week. In Experiment 2, doses of 3-ISOPBC (5.0–20.0 mg/kg) or vehicle were administered daily for 5 consecutive days to baboons in both groups. For both experiments, doses of 3-ISOPBC were administered 30 min before sessions.

2.6. Data analysis

The primary variables of interest included measures of seeking (Component 2: FI responses and latency to complete the FI requirement) and measures of consumption (Component 3: FR self-administration responses, drink contacts, and volume consumed). Total g/kg and ml/kg consumed were calculated based on individual body weights and the total volume of alcohol or non-alcoholic beverage consumed, respectively. The patterning of drinking was analyzed as a function of drinking “bouts” as in our previous study (Kaminski and Weerts, 2014). A drinking bout was defined as 2 or more drinks with less than 5 min between each drink, beginning with the first drink.

For each baboon, the mean of the 3 sessions that preceded each test condition was used as the baseline for comparison with doses of 3-ISOPBC and vehicle. To determine whether there were any differences in baseline responding in the alcohol and control groups, baseline responding in Experiment 2 was compared using independent-samples *t*-tests (baseline responding of the alcohol group in Experiment 1 is not included because corresponding con-

trol group sessions were not conducted). In Experiment 2, data analyzed were the last 3 of the 5 days of 3-ISOPBC or vehicle administration. Data were analyzed using separate statistical analysis of variance (ANOVA) for each group (Alcohol or Control) with 3-ISOPBC dose (BL, 0.0–30.0 mg/kg) as a repeated measure. Bonferroni post-hoc tests were used for pair-wise comparisons of vehicle with 3-ISOPBC doses.

3. Results

During baseline sessions, stable drinking was observed in all baboons, in both groups and few or no responses were recorded on the inactive operanda (all operanda in Component 1, right lever and drinkometer in Component 2, and left lever in Component 3). Systematic differences between the groups during baseline sessions were not observed for measures of seeking (Component 2: FI responses and latency to complete the FI requirement). During the baseline sessions preceding drug test sessions, the grand mean (+SEM) latency to complete the FI schedule was 639.5 (20.2) seconds for the alcohol group and 609.7 (5.3) seconds for the control group [$t(6) = 1.09, p = 0.317$]. The grand mean (+SEM) number of FI responses was 141.2 (68.4) for the alcohol group and 144.9 (96.2) for the control group [$t(6) = 0.03, p = 0.975$].

During baseline sessions, the grand mean (+SEM) alcohol intake was 748.1 (78.6) ml and 1.07 (0.07) g/kg, comparable to intake which has previously been reported to produce blood-alcohol levels (BAL) of $>0.08\%$ in baboons (Holtyn et al., 2014; Kaminski et al., 2008). The grand mean non-alcoholic beverage intake during baseline sessions was 1000.0 (0.0) ml. While volume of intake of the non-alcoholic beverage was higher than the volume of intake of alcohol [$t(6) = 2.40, p = 0.053$], we have previously demonstrated that 4% w/v alcohol and the non-alcoholic beverage function as equivalent reinforcers (i.e., maintain similar breaking points under a progressive ratio procedure) despite the fact that they maintain different intake volumes (Duke et al., 2014).

3.1. Experiment 1: effects of acute administration of 3-ISOPBC

Table 1 shows effects of acute administration of 3-ISOPBC on alcohol seeking and consumption under the chained schedule of reinforcement. Acute administration of 3-ISOPBC did not significantly change any of the measures of seeking (Component 2: FI responses and latency to complete the FI requirement) or consumption (Component 3: FR self-administration responses and g/kg alcohol consumed). Behavioral observations conducted by laboratory personnel that included the recording of any signs or symptoms of drug side effects (e.g., sedation, muscle relaxation, motor incoordination, gastro-intestinal symptoms, etc.) confirmed that administration of doses up to and including 30.0 mg/kg were safe and did not produce adverse effects. However, there was some

Table 2
Experiment 2. Effects of chronic (5 day) administration of vehicle (V) and doses of 3-ISOPBC on seeking in Component 2 (C2) for alcohol (Alcohol Group) and a non-alcoholic beverage (Control Group) under the chained schedule of reinforcement. Baseline (BL) is the grand mean of the 3 days preceding each chronic condition.

Alcohol Group			BL	V	3-ISOPBC dose (mg/kg)			F(4,16)
					5.0	10.0	20.0	
C2	Left Lever	Mean	141.2	394.5	212.3	161.5	198.2	1.93
	FI Resp	SEM	68.4	217.4	118.1	107.4	113.1	
	Left Lever FI Resp	Mean	639.5	620.4	706.0	676.5	755.3	
	Latency (s)	SEM	20.2	10.8	58.1	52.0	93.2	
Control Group C2	Left Lever	Mean	144.9	128.2	200.4	154.8	75.0	F(4,8)
	FI Resp	SEM	96.2	55.3	131.1	85.1	37.7	
	Left Lever FI Resp	Mean	609.7	674.6	612.8	624.7	735.0	
	Latency (s)	SEM	5.3	20.7	11.3	18.3	95.1	

Note: FI, Fixed Interval; FR, Fixed Ratio; Resp, Response; Alc, Alcohol.

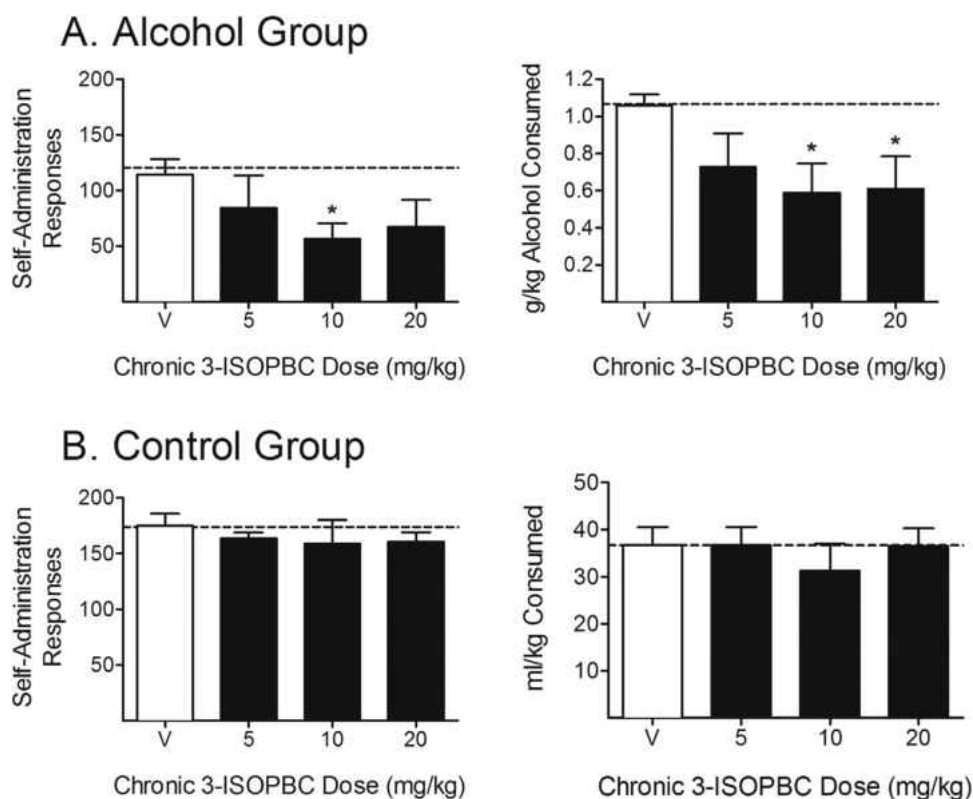


Fig. 1. Experiment 2. Effects of chronic (5 day) administration of 3-ISOPBC (5.0–20.0 mg/kg) on consumption in Component 3 of the chained schedule of reinforcement in the (A) Alcohol Group and (B) Control Group. Data shown are the group means (+SEM) of self-administration responses (left panels), and g/kg alcohol consumed for the alcohol group and ml/kg consumed for the control group (right panel). Baseline responding is indicated by the horizontal, dashed lines. *indicates $p < 0.05$ for pair-wise comparison for each 3-ISOPBC dose vs. vehicle.

difficulty with solubility at the 30.0 mg/kg dose. Because of this, in combination with the difficulty in synthesizing the large quantities needed for testing in baboons, the 30.0 mg/kg dose was not tested under chronic conditions. Acute administration of 3-ISOPBC was not conducted in the control group because it did not significantly reduce seeking or consumption in the alcohol group.

3.2. Experiment 2: effects of chronic administration of 3-ISOPBC

Table 2 shows effects of chronic administration of 3-ISOPBC on seeking for alcohol and the non-alcoholic beverage under the chained schedule of reinforcement. Chronic administration of 3-ISOPBC did not significantly change any of the measures of seeking (Component 2: FI responses and latency to complete the FI requirement) in both the alcohol and control groups.

Fig. 1 shows effects of chronic administration of 3-ISOPBC on consumption. In the alcohol group, chronic administration of 3-ISOPBC decreased the number of self-administration responses (Component 3: FR responses), with a significant decrease relative to vehicle at the 10.0 mg/kg dose. Chronic administration of 3-ISOPBC decreased g/kg alcohol consumed, with significant decreases relative to vehicle at the 10.0 and 20.0 mg/kg doses. In the control group, 3-ISOPBC did not reduce the number of self-administration responses or ml/kg consumed at any of the doses.

Fig. 2 shows effects of chronic administration of 3-ISOPBC on the pattern of drinking in the first drinking bout. In the alcohol group, chronic administration of 3-ISOPBC decreased the number of drinks in the first drinking bout, with a significant decrease relative to vehicle at the 10.0 and 20.0 mg/kg doses. Chronic administration of 3-ISOPBC decreased the duration of the first drinking bout, with significant decreases relative to vehicle at the 20.0 mg/kg dose. In

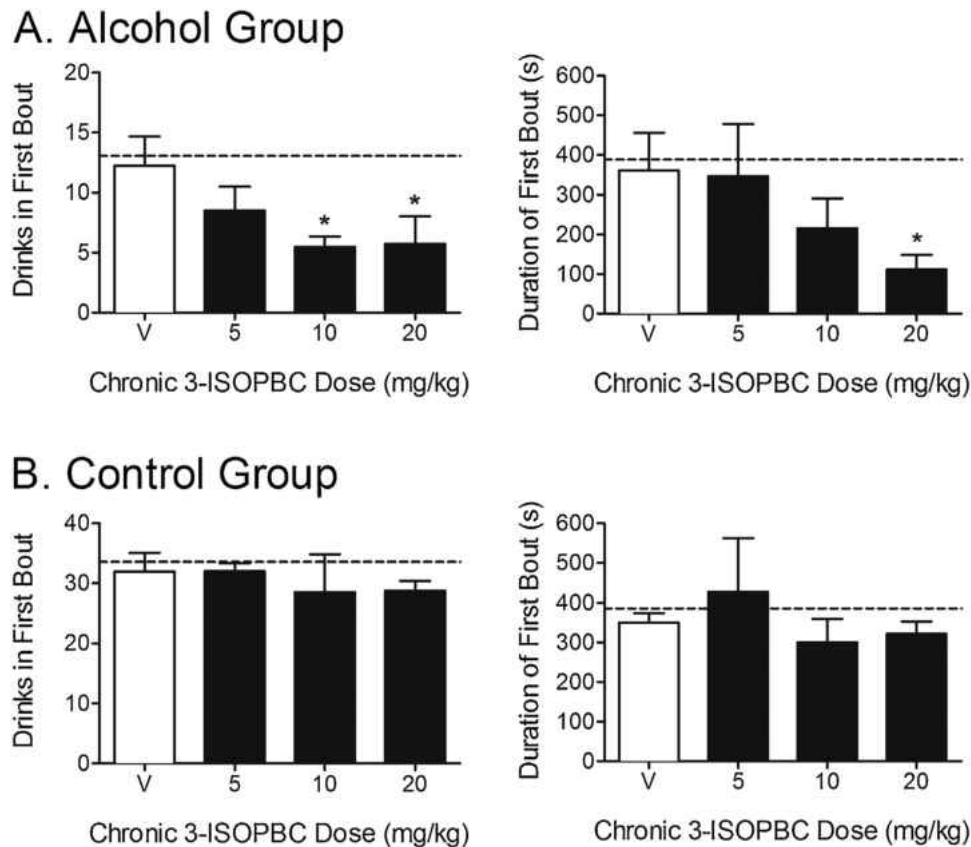


Fig. 2. Experiment 2. Effects of chronic (5 day) administration of 3-ISOPBC (5.0–20.0 mg/kg) on the pattern of drinking in the first drinking bout in Component 3 of the chained schedule of reinforcement in the (A) Alcohol Group and (B) Control Group. Data shown are the group means (+SEM) of the number of drinks in the first drinking bout (left panels), and the duration (seconds) of the first drinking bout (right panels). Baseline responding is indicated by the horizontal, dashed lines. *indicates $p < 0.05$ for pair-wise comparison for each 3-ISOPBC dose vs. vehicle.

the control group, 3-ISOPBC did not reduce the number of drinks in or the duration of the first drinking bout at any of the doses.

4. Discussion

The $\alpha 1$ subunit of the GABA_A receptor has been implicated in the reinforcing- and abuse-related effects of alcohol in some studies (Blednov et al., 2003; Harvey et al., 2002; June et al., 2007; Kaminski et al., 2013). The present study investigated whether acute and chronic administration of the benzodiazepine GABA_A $\alpha 1$ -preferring ligand 3-ISOPBC could selectively reduce alcohol seeking and self-administration in baboons. Pretreatment with 3-ISOPBC did not reduce alcohol seeking in a group that self-administered alcohol or in a control group that self-administered a non-alcoholic beverage. This is consistent with a prior similar study in which acute and chronic administration of 3-PBC did not reduce alcohol seeking in baboons responding under a chained schedule of alcohol reinforcement (Kaminski et al., 2013). Chronic, and not acute, administration of 3-ISOPBC reduced alcohol consumption in the alcohol group without reducing consumption of the non-alcoholic reinforcer in the control group. Thus, 3-ISOPBC may have therapeutic potential in the treatment of alcohol use disorder due to its ability to selectively reduce alcohol use.

Identification of the precise role of the GABA_A $\alpha 1$ receptor in alcohol reinforcement and consumption is ongoing. Knockout mice without the GABA_A $\alpha 1$ receptor have been shown to consume less alcohol under a two-bottle alcohol versus water choice procedure (Blednov et al., 2003) and an operant self-administration procedure (June et al., 2007). The GABA_A $\alpha 1$ -preferring antagonist 3-PBC has been shown to decrease alcohol self-administration in rodents

bred for high alcohol intake (Harvey et al., 2002), as well as binge-like drinking in a maternally deprived rodent model (Gondré-Lewis et al., 2016). A similar reduction in alcohol maintained responding was observed following administration of 3-ISOPBC in the maternal deprivation model (Tiruveedhula et al., 2015). In baboons, 3-PBC reduced self-administration of alcohol, but also had some effects on self-administration of a non-alcoholic reinforcer (Kaminski et al., 2013). In contrast to the findings in rodents and baboons, both 3-PBC and β CCT failed to attenuate alcohol drinking in rhesus macaques (Sawyer et al., 2014). The reason for this contradictory result is unclear; however, the highest dose of 3-PBC tested in Sawyer et al.'s study (10.0 mg/kg) was lower than that which reduced total g/kg alcohol intake in the baboon model (18.0 mg/kg). The choice of 3-ISOPBC for the present study was based on the structure of the branched isopropyl group, which would hinder metabolism by beta (ω -1) oxidation. It was hypothesized that this would increase the duration of action and provide a ligand more active *in vivo* than 3-PBC; this appears to be the case. In the present study, 3-ISOPBC selectively reduced alcohol drinking.

In both the alcohol and control groups, the majority of drinks occurred within the first drinking bout. Prior studies also have shown rats (Samson et al., 2000), baboons (Weerts et al., 2006), and other primates (Boyle et al., 1998) to engage in "loading," wherein the highest rate of alcohol drinking occurs early in the alcohol self-administration period followed by lower rates of drinking for the remainder of the period. Chronic administration of 3-ISOPBC reduced the number of drinks in, and the duration of, the first drinking bout in the alcohol group, but not in the control group. This suggests that 3-ISOPBC may reduce alcohol intake once consumption is initiated, which could be important in pre-

venting drinking episodes from becoming a full relapse to heavy drinking. Chronic administration of 3-PBC also has been shown to decrease the number of drinks during the first 20 min of alcohol availability in Component 3 of the chained schedule (Kaminski et al., 2013). In Kaminski et al.'s (2013) study, the highest doses of 3-PBC tested (10.0 and 18.0 mg/kg) also decreased the number of drinks in the first 20 min in a control group that self-administered a non-alcoholic beverage. Harvey et al. (2002) observed a decrease in saccharin-maintained responding when the highest dose of 3-PBC (20.0 mg/kg) was administered to rodents. The authors suggested that the non-selective effects at higher doses of 3-PBC may be due to a saturation of all α receptors as 3-PBC binds to other α receptors to some degree. It is worth emphasizing, however, that in both studies, responding maintained by the non-alcoholic reinforcer was reduced at higher doses than required to suppress alcohol self-administration. In the present study, effects of 3-ISOPBC were selective for alcohol. The mechanism by which 3-ISOPBC selectively attenuated alcohol response in the present study is not known. Possible differences between 3-PBC and 3-ISOPBC include differences in metabolism or ligand transport.

Although the mechanisms of action of the $\alpha 1$ -preferring antagonists are not well understood, one possibility rests on the tonic control in the central nervous system by opposing systems, including GABA. It is possible that these $\alpha 1$ -preferring antagonists simply stabilize the benzodiazepine $\alpha 1$ GABA receptor system in the antagonist conformation, the result of which would be to slightly decrease the normal flow of chloride ions through the $\alpha 1\beta_{2/3}\gamma 2$ ion channel. The effect via the projections from the ventral tegmental area (Harvey et al., 2002) to the nucleus accumbens would then effect the levels of dopamine release; this slight decrease may be why Warnock, June et al. (personal communication) did observe a decrease in alcohol self-administration in a binge drinking model (rodents) in the complete absence of anhedonia or depression. Tiruveedhula et al. (2015) reported that 3-ISOPBC decreased alcohol consumption in a maternally deprived rodent model. Gondré-Lewis et al. (2016) reported a similar effect with 3-PBC and proposed some involvement of $\alpha 2$ -receptor subunits; however, this effect could not be reversed by administration of flumazenil. Consequently, this cannot be due to an effect at $\alpha 2\beta_{2/3}\gamma 2$ benzodiazepine GABA_A receptors. It is possible that the observed effect was mediated by a different set of $\alpha 2$ -related receptors (Gondré-Lewis et al., 2016) or to the $\alpha 1$ -preferring antagonist effect at benzodiazepine $\alpha 1$ GABA_A receptors. Much work remains to understand this observation. Nevertheless, the real strength of the use of $\alpha 1$ -preferring antagonists in the treatment of alcohol use disorder stems from the fact that this type of ligand lacks sedating, amnesic, and ataxic properties (Ator et al., 2010; Licata et al., 2009) because it is an antagonist at this $\alpha 1$ benzodiazepine GABA_A site.

The present study examined whether the GABA_A $\alpha 1$ -preferring ligand 3-ISOPBC possesses therapeutic potential in regard to its ability to selectively reduce alcohol seeking and consumption. Alcohol use disorders are heterogeneous and development of more efficacious and safe pharmacotherapies is needed to expand the number of individuals who may benefit from treatment. In the present study, 3-ISOPBC did not decrease alcohol seeking, but did selectively reduce alcohol self-administration and consumption by primarily altering the pattern of drinking. 3-ISOPBC selectively reduced the number of drinks and the duration of drinks in the first alcohol drinking bout. No changes in drinking patterns were found for the non-alcoholic reinforcer. These data suggest that 3-ISOPBC may be clinically useful for reducing alcohol use.

Conflict of interest

The authors have no conflicts of interest to declare.

Role of funding source

This work was supported by the National Institutes of Health under grant numbers R01AA15971 (Weerts), R01MH096463 (Cook), and R01NS076517 (Cook). The grants provided financial support for the conduct of the research and the preparation of the article. The funding sponsors were not involved in study design; in the collection, analysis and interpretation of data; in the writing of the report; and in the decision to submit the article for publication.

Contributions

All authors have contributed to the research and the article preparation. Holtyn performed the data analyses, wrote the first draft of the manuscript, and incorporated edits from the co-authors. Weerts contributed to the original conceptualization and design of the experiments, directed the present experiments, and edited the manuscript. Cook directed the development of the novel compound used in these experiments and contributed to the original conceptualization and design of the experiments. Tiruveedhula and Stephen synthesized the novel compound used in the experiments and edited the manuscript. All authors have approved the final manuscript.

Acknowledgements

The authors thank Margot Ernst, Petra Scholze, and Xenia Simeone for providing data on the binding affinity of 3-ISOPBC. Psychoactive drug screening program data were generously provided by the National Institute of Mental Health's Psychoactive Drug Screening Program, Contract # HHSN-271-2013-00017-C (NIMH PDSP). The NIMH PDSP is Directed by Bryan L. Roth, MD, PhD at the University of North Carolina at Chapel Hill and Project Officer Jamie Driscoll at NIMH, Bethesda, MD.

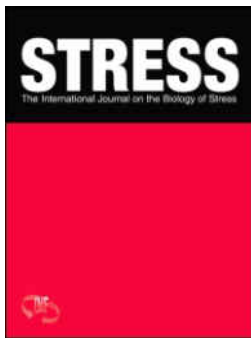
Appendix A. Supplementary data

Supplementary data associated with this article can be found, in the online version, at <http://dx.doi.org/10.1016/j.drugalcdep.2016.10.036>.

References

- Ator, N.A., Atack, J.R., Hargreaves, R.J., Burns, H.D., Dawson, G.R., 2010. Reducing abuse liability of GABA_A/benzodiazepine ligands via selective partial agonist efficacy at $\alpha 1$ and $\alpha 2/3$ subtypes. *J. Pharmacol. Exp. Ther.* 332, 4–16.
- Besnard, J., Ruda, G.F., Setola, V., Abecassis, K., Rodriguiz, R.M., Huang, X.P., Norval, S., Sassano, M.F., Shin, A.I., Webster, L.A., Simeons, F.R., Stojanovski, L., Prat, A., Seidah, N.G., Constam, D.B., Bickerton, G.R., Read, K.D., Wetsel, W.C., Gilbert, I.H., Roth, B.L., Hopkins, A.L., 2012. Automated design of ligands to polypharmacological profiles. *Nature* 492, 215–220.
- Blednov, Y.A., Walker, D., Alva, H., Creech, K., Findlay, G., Harris, R.A., 2003. GABA_A receptor $\alpha 1$ and $\beta 2$ subunit null mutant mice: behavioral responses to ethanol. *J. Pharmacol. Exp. Ther.* 305, 854–863.
- Boyle, A.E.L., Stewart, R.B., Macenski, M.J., Spiga, R., Johnson, B.A., Meisch, R.A., 1998. Effects of acute and chronic doses of naltrexone on ethanol self-administration in rhesus monkeys. *Alcohol. Clin. Exp. Res.* 22, 359–366.
- Clayton, T., Chen, J.L., Ernst, M., Richter, L., Cromer, B.A., Morton, C.J., Ng, H., Kaczorowski, C.C., Helmstetter, F.J., Furtmuller, R., Ecker, G., Parker, M.W., Sieghart, W., Cook, J.M., 2007. An updated unified pharmacophore model of the benzodiazepine binding site on gamma-aminobutyric acid(a) receptors: correlation with comparative models. *Curr. Med. Chem.* 14, 2755–2775.
- Clayton, T., Poe, M.M., Rallapalli, S., Biawat, P., Savić, M.M., Rowlett, J.K., Gallos, G., Emala, C.W., Kaczorowski, C.C., Stafford, D.C., Arnold, L.A., 2015. A review of the updated pharmacophore for the alpha 5 GABA (A) benzodiazepine receptor model. *Int. J. Med. Chem.*, 1–54.
- Duke, A.N., Kaminski, B.J., Weerts, E.M., 2014. Baclofen effects on alcohol seeking, self-administration and extinction of seeking responses in a within-session design in baboons. *Addict. Biol.* 19, 16–26.
- Enoch, M.A., 2008. The role of GABA(A) receptors in the development of alcoholism. *Pharmacol. Biochem. Behav.* 90, 95–104.
- Foye, W.O., Lemke, T.L., Williams, D.A., 2013. *Foye's Principles of Medicinal Chemistry*. Lippincott Williams & Wilkins.

- Gondré-Lewis, M.C., Warnock, K.T., Wang, H., June Jr., H.L., Bell, K.A., Rabe, H., Tiruveedhula, V.P., Cook, J.M., Lüddens, H., Aurelian, L., June Sr., H.L., 2016. Early life stress is a risk factor for excessive alcohol drinking and impulsivity in adults and is mediated via a CRF/GABAA mechanism. *Stress* 19, 235–247.
- Harvey, S.C., Foster, K.L., McKay, P.F., Carroll, M.R., Seyoum, R., Woods, J.E., Grey, C., Jones, C.M., McCane, S., Cummings, R., Mason, D., Ma, C.R., Cook, J.M., June, H.L., 2002. The GABA(A) receptor α 1 subtype in the ventral pallidum regulates alcohol-seeking behaviors. *J. Neurosci.* 22, 3765–3775.
- He, X., Huang, Q., Ma, C., Yu, S., McKernan, R., Cook, J.M., 2000. Pharmacophore/receptor models for GABA(A)/BzR α 2 β 3 γ 2, α 3 β 3 γ 2 and α 4 β 3 γ 2 recombinant subtypes. Included volume analysis and comparison to α 1 β 3 γ 2, α 5 β 3 γ 2, and α 6 β 3 γ 2 subtypes. *Drug Des. Discov.* 17, 131–171.
- Holtyn, A.F., Kaminski, B.J., Wand, G.S., Weerts, E.M., 2014. Differences in extinction of cue-maintained conditioned responses associated with self-administration: alcohol versus a nonalcoholic reinforcer. *Alcohol. Clin. Exp. Res.* 38, 2639–2646.
- Huang, Q., He, X., Ma, C., Liu, R., Yu, S., Dayer, C.A., Wenger, G.R., McKernan, R., Cook, J.M., 2000. Pharmacophore/receptor models for GABAA/BzR subtypes (α 1 β 3 γ 2, α 5 β 3 γ 2, and α 6 β 3 γ 2) via a comprehensive ligand-mapping approach. *J. Med. Chem.* 43, 71–95.
- Huang, X.P., Mangano, T., Hufeisen, S., Setola, V., Roth, B.L., 2010. Identification of human ether-a-go-go related gene modulators by three screening platforms in an academic drug-discovery setting. *Assay Drug Dev. Technol.* 8, 727–742.
- June, H.L., Foster, K.L., McKay, P.F., Seyoum, R., Woods II, J.E., Harvey, S.C., Eiler II, W.J.A., Grey, C., Carroll, M.R., McCane, S., Jones, C.M., Yin, W., Mason, D., Cummings, R., Garcia, M., Ma, C., Sarma, P.V., Cook, J.M., Skolnick, P., 2003. The reinforcing properties of alcohol are mediated by GABA(A1) receptors in the ventral pallidum. *Neuropsychopharmacol* 28, 2124–2137.
- June, H.L., Foster, K.L., Eiler, W.J., Goergen, J., Cook, J.B., Johnson, N., Mensah-Zoe, B., Simmons, J.O., Yin, W., Cook, J.M., Homanics, G.E., 2007. Dopamine and benzodiazepine-dependent mechanisms regulate the EtOH-enhanced locomotor stimulation in the GABAA α 1 subunit null mutant mice. *Neuropsychopharmacol* 32, 137–152.
- Kaminski, B.J., Weerts, E.M., 2014. The effects of varenicline on alcohol seeking and self-administration in baboons. *Alcohol. Clin. Exp. Res.* 38, 376–383.
- Kaminski, B.J., Goodwin, A.K., Wand, G., Weerts, E.M., 2008. Dissociation of alcohol-seeking and consumption under a chained schedule of oral alcohol reinforcement. *Alcohol. Clin. Exp. Res.* 32, 1–9.
- Kaminski, B.J., Duke, A.N., Weerts, E.M., 2012. Effects of naltrexone on alcohol drinking patterns and extinction of alcohol seeking in baboons. *Psychopharmacol* 223, 55–66.
- Kaminski, B.J., Van Linn, M.L., Cook, J.M., Yin, W., Weerts, E.M., 2013. Effects of the benzodiazepine GABAA α 1-preferring ligand, 3-propoxy- β -carboline hydrochloride (3-PBC), on alcohol seeking and self-administration in baboons. *Psychopharmacology (Berl)* 227, 127–136.
- Kumar, S., Porcu, P., Werner, D.F., Matthews, D.B., Diaz-Granados, J.L., Helfand, R.S., Morrow, A.L., 2009. The role of GABAA receptors in the acute and chronic effects of ethanol: a decade of progress. *Psychopharmacology (Berl)* 205, 529–564.
- Licata, S.C., Platt, D.M., Cook, J.M., Van Linn, M.L., Rowlett, J.K., 2009. Contribution of α 1 subunit-containing gamma-aminobutyric acidA (GABAA) receptors to motor-impairing effects of benzodiazepines in squirrel monkeys. *Psychopharmacol* 203, 539–546.
- Lobo, I.A., Harris, R.A., 2008. GABA(A) receptors and alcohol. *Pharmacol. Biochem. Behav.* 90, 90–94.
- National Research Council, 2011. Guide For The Care And Use Of Laboratory Animals, eighth edition. The National Academies Press, Washington, DC.
- Olsen, R.W., Sieghart, W., 2009. GABA A receptors: subtypes provide diversity of function and pharmacology. *Neuropharmacology* 56, 141–148.
- Platt, D.M., Rowlett, J.K., Spealman, R.D., Cook, J., Ma, C., 2002. Selective antagonism of the ataxic effects of zolpidem and triazolam by the GABAA/ α 1-preferring antagonist beta-CCT in squirrel monkeys. *Psychopharmacol* 164, 151–159.
- Samson, H.H., Czachowski, C.L., Slawecki, C.J., 2000. A new assessment of the ability of oral ethanol to function as a reinforcing stimulus. *Alcohol. Clin. Exp. Res.* 24, 766–773.
- Sawyer, E.K., Moran, C., Sirbu, M.H., Szafir, M., Linn, M., Namjoshi, O., Phani Babu Tiruveedhula, V.V.N., Cook, J.M., Platt, D.M., 2014. Little evidence of a role for the α 1GABAA subunit-containing receptor in a rhesus monkey model of alcohol drinking. *Alcohol. Clin. Exp. Res.* 38, 1108–1117.
- Tiruveedhula, V.P., Methuku, K.R., Deschamps, J.R., Cook, J.M., 2015. Synthesis of aza and carbocyclic β -carbolines for the treatment of alcohol abuse. Regiospecific solution to the problem of 3, 6-disubstituted β - and aza- β -carboline specificity. *Org. Biomol. Chem.* 13, 10705–10715.
- Weerts, E.M., Goodwin, A.K., Kaminski, B.J., Hienz, R.D., 2006. Environmental cues, alcohol seeking, and consumption in baboons: effects of response requirement and duration of alcohol abstinence. *Alcohol. Clin. Exp. Res.* 30, 2026–2036.
- Yin, W., Majumder, S., Clayton, T., Petrou, S., VanLinn, M.L., Namjoshi, O.A., Ma, C., Cromer, B.A., Roth, B.L., Platt, D.M., Cook, J.M., 2010. Design, synthesis, and subtype selectivity of 3,6-disubstituted beta-carbolines at Bz/GABA(A)ergic receptors. SAR and studies directed toward agents for treatment of alcohol abuse. *Bioorg. Med. Chem.* 8, 7548–7564.



Early life stress is a risk factor for excessive alcohol drinking and impulsivity in adults and is mediated via a CRF/GABA_A mechanism

Marjorie C. Gondré-Lewis, Kaitlin T. Warnock, Hong Wang, Harry L. June Jr, Kimberly A. Bell, Holger Rabe, Veera Venkata Naga Phani Babu Tiruveedhula, James Cook, Hartmut Lüddens, Laure Aurelian & Harry L. June Sr

To cite this article: Marjorie C. Gondré-Lewis, Kaitlin T. Warnock, Hong Wang, Harry L. June Jr, Kimberly A. Bell, Holger Rabe, Veera Venkata Naga Phani Babu Tiruveedhula, James Cook, Hartmut Lüddens, Laure Aurelian & Harry L. June Sr (2016): Early life stress is a risk factor for excessive alcohol drinking and impulsivity in adults and is mediated via a CRF/GABA_A mechanism, *Stress*, DOI: [10.3109/10253890.2016.1160280](https://doi.org/10.3109/10253890.2016.1160280)

To link to this article: <http://dx.doi.org/10.3109/10253890.2016.1160280>



Published online: 29 Mar 2016.



Submit your article to this journal [↗](#)



Article views: 5



View related articles [↗](#)



View Crossmark data [↗](#)

ORIGINAL RESEARCH REPORT

Early life stress is a risk factor for excessive alcohol drinking and impulsivity in adults and is mediated via a CRF/GABA_A mechanism

Marjorie C. Gondré-Lewis^{1,2}, Kaitlin T. Warnock², Hong Wang¹, Harry L. June Jr², Kimberly A. Bell², Holger Rabe³, Veera Venkata Naga Phani Babu Tiruveedhula⁴, James Cook⁴, Hartmut Lüddens³, Laure Aurelian⁵, and Harry L. June Sr²

¹Department of Anatomy, Howard University College of Medicine, Washington, DC, USA, ²Department of Psychiatry and Behavioral Sciences, Howard University College of Medicine, Washington, DC, USA, ³Department of Psychiatry, University of Mainz, Mainz, UK, ⁴Department of Chemistry and Biochemistry, University of Wisconsin-Milwaukee, Milwaukee, WI, USA, and ⁵Department of Pharmacology and Experimental Therapeutics, University of Maryland School of Medicine, Baltimore, MD, USA

Abstract

Childhood stress and trauma are associated with substance use disorders in adulthood, but the neurological changes that confer increased vulnerability are largely unknown. In this study, maternal separation (MS) stress, restricted to the pre-weaning period, was used as a model to study mechanisms of protracted effects of childhood stress/traumatic experiences on binge drinking and impulsivity. Using an operant self-administration model of binge drinking and a delay discounting assay to measure impulsive-like behavior, we report that early life stress due to MS facilitated acquisition of binge drinking and impulsivity during adulthood in rats. Previous studies have shown heightened levels of corticotropin releasing factor (CRF) after MS, and here, we add that MS increased expression levels of GABA_A α 2 subunit in central stress circuits. To investigate the precise role of these circuits in regulating impulsivity and binge drinking, the CRF1 receptor antagonist antalarmin and the novel GABA_A α 2 subunit ligand 3-PBC were infused into the central amygdala (CeA) and medial prefrontal cortex (mPFC). Antalarmin and 3-PBC at each site markedly reduced impulsivity and produced profound reductions on binge-motivated alcohol drinking, without altering responding for sucrose. Furthermore, whole-cell patch-clamp studies showed that low concentrations of 3-PBC directly reversed the effect of relatively high concentrations of ethanol on α 2 β 3 γ 2 GABA_A receptors, by a benzodiazepine site-independent mechanism. Together, our data provide strong evidence that maternal separation, i.e. early life stress, is a risk factor for binge drinking, and is linked to impulsivity, another key risk factor for excessive alcohol drinking. We further show that pharmacological manipulation of CRF and GABA receptor signaling is effective to reverse binge drinking and impulsive-like behavior in MS rats. These results provide novel insights into the role of the brain stress systems in the development of impulsivity and excessive alcohol consumption.

Keywords

GABA, alpha-2 receptor, corticotropin releasing factor, benzodiazepine, central amygdala, medial prefrontal cortex, antalarmin, 3-PBC, limbic, neuropsychiatric

History

Received 30 July 2015
Revised 11 January 2016
Accepted 20 February 2016
Published online 28 March 2016

Introduction

Individuals differ in the risk for developing drug addiction such that even after chronic usage, only a fraction of individuals develop drug dependence (Everitt et al., 2008). The rationale for this discrepancy is poorly understood; however, stress during the perinatal period is correlated to behavioral phenotypes linked to mood disorders and increased addiction risk during adulthood (Deminere et al., 1992; Marinelli & Piazza, 2002). The experience of stress during infancy causes long-lasting modulation of neurons in the limbic system, as well as hyperactivity of the hypothalamus-

pituitary-adrenal (HPA) axis, which leads to elevated circulating levels of corticosterone, other glucocorticoids, and their metabolites (Koe et al., 2014) with widespread biochemical consequences.

Even less is known about the neuronal mechanisms that render the stressed offspring vulnerable to initiate binge drinking and to exhibit abnormal impulsivity. Binge drinking as defined by the National Institutes of Health is alcohol intake which increases blood alcohol level to ≥ 80 mg% within a 2-hour period (Crabbe et al., 2011; NIH-NIAAA, 2004); a definition used by researchers and clinicians alike to investigate the brain circuits involved in this type of excessive alcohol intake (Gilpin et al., 2012; Vargas et al., 2014). Cognitive impulsivity is a core deficit present in many psychiatric conditions including drug addiction (Robinson et al., 2009). While there are increasingly more

Correspondence: Dr Marjorie C. Gondré-Lewis, Associate Professor, Department of Anatomy, Laboratory for Neurodevelopment, Howard University College of Medicine, 520 W Street, NW, Washington, DC 20059, USA. Tel: 202-806-5274. E-mail: Mgondre-lewis@howard.edu

categorizations of impulsivity related to risky behavior and decision-making with various underlying neurochemical and neuroanatomical bases, it is generally accepted that impulsivity is the tendency to respond prematurely without foresight or regard for the consequences (Dalley et al., 2011). Although the behavioral task in this study focuses on impulsive choice where animals exhibit the temporal discounting of reward, response disinhibition involving the regulation of GABA signaling system in the cortico-limbic system is an important factor in impulsivity (Dick et al., 2013), and thus GABA dysregulation and modulation in MS is important.

Non-human primates (Huggins et al., 2012) and rodents exposed to MS, will self-administer ethanol during adolescence and adulthood (Cruz et al., 2008; Garcia-Gutierrez et al., 2015; Moffett et al., 2007; Romano-Lopez et al., 2012). Although the mechanism for stress-induced binge drinking is unknown, studies show that MS permanently alters expression of various GABA_A receptor subunits [e.g. $\alpha 1$, $\alpha 2$, $\gamma 2$] and their mRNA in the amygdala and hippocampus (Caldji et al., 2000; Edenberg et al., 2004; Hsu et al., 2003). The GABA receptors, especially the GABA_A $\alpha 1$ receptor, has been extensively studied in relation to alcohol biochemistry, but recent human linkage studies also implicate the GABRA2 gene, encoding the GABA_A $\alpha 2$ receptor in regulating excessive drinking and impulsivity, and reduced GABA levels in human frontal lobes are associated with significant levels of impulsivity in adolescents (Dick et al., 2006, 2013; Edenberg et al., 2004; Enoch et al., 2010). The approach in the present study focuses on the role of GABA_A $\alpha 2$ subunit in modulating excessive drinking and impulsivity in adults exposed to MS.

Studies in MS models reveal elevated CRF in stress loci (Nemeroff, 2004a,b; O'Malley et al., 2011). This effect of MS can result in structural changes in neurons of the PFC and significantly affect development of neurons in reward and emotional memory circuits including nucleus accumbens and hippocampus (Gondré-Lewis et al., 2016; Monroy et al., 2010; Wang & Gondré-Lewis, 2013; Yang et al., 2015). In addition, pharmacological and genetic studies support the hypothesis that *excessive alcohol consumption* and binge drinking is mediated by elevated CRF, via activation of the CRF1 receptor [CRF1R] (Heilig et al., 2011; Koob, 2008, 2014; Phillips et al., 2015). Blockade of CRF1R in rodents, attenuates alcohol intake in dependent rodents (Funk et al., 2007; Gehlert et al., 2007; Koob, 2008; Lowery-Gionta et al., 2012). The literature supports a model where CRF signaling in the central amygdala (CeA) functions as a key regulator of binge drinking (Lowery-Gionta et al., 2012), recruited during excessive alcohol intake *prior* to the development of dependence, with CRF as a mediator of the transition to dependence.

A genetic polymorphism in the CRF1R gene was significantly linked to binge alcohol drinking in humans (Treutlein et al., 2006). Following exposure to stressful stimuli, adolescents expressing this polymorphism displayed a predisposition to excessive drinking leading to dependence in adulthood (Blomeyer et al., 2008). Moreover, early life adversity interacted with CRF to increase alcohol intake in primates (Barr et al., 2009). Indeed, addiction-related changes

in prefrontal cortex CRF systems and their association with executive (George et al., 2012) or drinking phenotypes (Glaser et al., 2014) were reported; however, research to support a mechanism for the CRF system in impulsivity is lacking. Given that the experience of MS results in elevated CRF (Nemeroff, 2004b; O'Malley et al., 2011) and permanent alterations in GABA levels in stress circuits during adulthood (Caldji et al., 2000; Hsu et al., 2003), combined with the finding that MS results in long-term increases in alcohol in rodents (Cruz et al., 2008; Moffett et al., 2007), we hypothesized that the CeA and the mPFC, two loci of the stress circuits and important for cognitive processing, could influence vulnerability to initiate binge drinking or impulsivity following MS. Thus, the aim of this study was first to investigate the extent of binge alcohol drinking and impulsive-like behavior in our MS model, and second to determine if the action of pharmacological agents acting at CRF or GABA receptors in the CeA or mPFC could revert these behaviors to control levels.

Methods

Animals

Pregnant Sprague-Dawley dams were obtained from Harlan Laboratories (Frederick, MD) and offspring used in this study were born onsite at the veterinary facility. They were subjected to the MS paradigm as described below, and were tested for drinking and impulsivity behaviors as adults. Equivalent number of males and females were used in the binge drinking and impulsivity studies. Subjects were housed in groups of 2–3 per plastic cage until drinking studies began. The vivarium was maintained at an ambient temperature of 21 °C and was on a reverse 12-h light/dark cycle. All rats were provided *ad libitum* access to food and water. All training and experimental sessions for all subjects took place between 8:30 AM and 5:30 PM. The treatment of all subjects was approved by the IACUC of the Howard University College of Medicine and all procedures were conducted in strict adherence with the National Institutes of Health *Guide for the Care and Use of Laboratory Animals*.

MS regimen

The maternal separation (MS) paradigm was performed as previously published (Roceri et al., 2002; Wang & Gondré-Lewis, 2013; Gondré-Lewis et al., 2016), and was meant to emulate recurrent stressful experiences during the neonatal period. The number of pups in each litter ranged from 10 to 14 pups. To prevent litter effects, pups were sexed, culled to $n=10$ with equal number of males and females, and redistributed to nursing dams at P1. Beginning at P2 until weaning at P21, the separation comprised of removal of pups from their nursing mothers. They were brought to a designated room, separated from the mother, where the temperature was monitored and maintained at 29 °C. Each pup was placed in a cage located on a warmed pad, and visual access to other pups was blocked with cardboard. These conditions were maintained for 3 h per day from 11:00 AM to 2:00 PM. After the 3 h separation time, they were returned to their home cage and rooms. Non-MS (CTL) pups were not

separated from their mothers and were treated according to standard animal facility regulations.

Use of animals

Forty adult rats from 21 litters were used; 12 for western blotting and 28 for the behavioral studies, used over several months. Although these studies are not aimed at examining sex differences, both males and females were always represented. Therefore, this is a mixed-sex study. In any behavioral experiment, to control for litter effects, the maximum number of pups used from a single mother was one male and one female. Therefore, for an $n = 10$ as an example, the minimum number of dams was 5 for each condition. For the operant binge drinking paradigm in Figure 2, there were $n = 10$ controls (5F, 5M) and $n = 10$ MS (5M, 5F); 75% of these same animals were re-used and added to other animals for the delay discounting experiments; $n = 9$ controls (5F, 4M) and $n = 11$ for MS (8F, 3M). For Western blotting analysis, a different cohort of animals was used with the same principle of heterogeneity to reduce litter effects; $n = 5-6$ controls (2-3F, 3M) and $n = 6$ for MS (3F and 3M). For drug dosage studies, some animals used in Figure 2 were combined with other rats of the same age that had undergone similar sustained operant training to have a sufficient number for surgical implantation of the cannulae and subsequent behavioral testing, $n = 5$ for CeA drug infusion (3F, 2M) and $n = 4$ for mPFC studies.

Tissue preparation and immunoblotting

Naïve, randomly-selected adult rats at P70 were sacrificed and neural tissue was harvested for immunoblotting to semi-quantitatively evaluate baseline levels of GABA_A $\alpha 2$ and CRF proteins in the CeA and mPFC of MS [$N = 4-6$] and CTL [$N = 5-6$] rats. The brain was removed from each animal and frozen, then sliced on a microtome in 300 μ m sections. CeA and mPFC tissue sections were collected by 1.0 mm micropunch (Ted Pella, Redding, CA) from the right and left hemispheres and pooled. Tissue micropunches were lysed with CelLytic MT (dialyzable mild detergent, bicine, and 150 mM NaCl; Sigma-Aldrich, St Louis, MO) according to manufacturer's instructions. Total protein was determined by the bicinchoninic assay (BCA) (Pierce, Rockford, IL). Proteins were resolved by SDS-polyacrylamide gel electrophoresis and transferred to nitrocellulose membranes. Blots were exposed to primary antibody overnight at 4 °C followed by horseradish peroxidase (HRP)-labeled goat anti-mouse or anti-rabbit secondary antibody for 1 h at room temperature (RT) (Cell Signaling). Detection was with the ECL kit reagents (Amersham Life Science/GE Healthcare, Pittsburg, PA) followed by exposure to high-performance chemiluminescence film (Hyperfilm ECL; Amersham Life Science/GE Healthcare, Pittsburg, PA), and quantitation was by densitometric scanning with a Bio-Rad GS-700 imaging densitometer (Bio-Rad Laboratories, Hercules, CA). Each lane represents an individual animal. The optical density (O.D.) of protein bands on each digital image was normalized to the O.D. of the loading control, and the animals for a given condition were averaged and expressed as densitometric units \pm SE. Normalized values across three blots were used for graph and analyzed with a Student's *t*-test.

Antibodies and reagents

The generation and specificity of the rabbit-derived GABA_A $\alpha 2$ antibody was previously described (Liu et al., 2011; Pirker et al., 2000). The GABA_A $\alpha 2$ antibody was a gift from Dr W. Sieghart (Department of Biochemistry and Molecular Biology, Center for Brain Research, Medical University Vienna, A-1090 Vienna, Austria). It was raised in rabbits against peptides corresponding to amino acids 322-357 of the $\alpha 2$ protein coupled to keyhole-limpet hemocyanin, affinity purified and extensively characterized by various methods, including immunoprecipitation, western blotting and immunocytochemistry (Pirker et al., 2000). The Mouse anti-GAPDH (0411, Cat# sc-47724) antibody was from Santa Cruz Biotechnology (Santa Cruz, CA) and is well characterized and used in numerous studies including our own previous publications (Liu et al., 2011).

Stereotaxic implantation of cannulae for microinfusions

Adult MS rats were anesthetized via isofluorane/oxygen gas inhalation and placed in a stereotaxic apparatus to allow for bilateral implantation of 22-gauge guide cannulae into the CeA or mPFC. The cannulae were anchored to the skull by four stainless steel screws and dental acrylic. A stylet was inserted into each cannula to maintain its viability and was only removed during infusion times. The coordinates were based on the rat brain atlas of Paxinos and Watson as follows: CeA: AP, -2.0 mm; ML, ± 3.6 mm; DV, -8.5 mm from bregma; mPFC: AP, +2.7 mm; ML, ± 1.45 mm; DV, -2.5 mm from bregma at a 16° angle to the midline. Each cannula was placed 1.0 mm above the intended target. This allowed the injector tip to extend below the cannula tip. The animals were given a 3-day recovery period before re-stabilization on the delay discounting or operant drinking paradigms. After behavioral experiments, cannula placement was confirmed visually by examination of cryostat-generated 300 μ m brain slices post-sacrifice.

Drugs and microinfusion procedure

3-propoxy-9H-pyrido[3,4-b]indole hydrochloride, commonly known as 3-propoxy- β -carboline hydrochloride (3-PBC), acting at the GABA_A $\alpha 1/\alpha 2$ receptor, was obtained from Dr James Cook at the University of Wisconsin-Milwaukee (Milwaukee, WI) (Namjoshi et al., 2011). Antalarmin hydrochloride, a CRF antagonist, was obtained from R&D Systems Inc. (Minneapolis, MN). The drugs were mixed into 1 mL of sterile PBS with Tween-20 added dropwise until dissolved, and then bilaterally infused into the CeA or mPFC at a rate of 0.1 μ L/min for 5 min using a Harvard infusion pump. The overall design of experiments was such that doses of vehicle, 2, and 4 μ g of antalarmin, or 20 or 40 μ g of 3-PBC were injected immediately prior to animals being placed in the operant or delay discounting chambers. Animals rested 1-3 days between doses. The antalarmin infusion studies occurred before the 3-PBC infusion studies, and were at least 2 weeks apart for any given animal. Different animals were used for the CeA and mPFC infusions. Antalarmin and 3-PBC were administered to MS rats to test their effects on the heightened

operant responding and impulsivity profile of MS, whereas CTL rats do not consume significant levels of alcohol at baseline, nor do their impulsivity profile differ significantly at 8 s compared to 0 s delay.

Delay discounting [impulsivity]

The impulsivity paradigm was executed as described by Oberlin & Grahame (2009). Impulsivity is operationally defined as choosing a smaller, immediate reward to the exclusion of a larger delayed reward (Rachlin & Green, 1972), and was quantified using the adjusted amount delay discounting (DD) assay (Wilhelm & Mitchell, 2008). Operant boxes consisted of a nosepoke light, two levers, a cue light above each lever, a house light, and a 10 mL descending sipper tube for saccharin reinforcement [0.03% w/v]. Control of the operant boxes and data collection was with the MedPC IV software (MedAssociates, St. Albans, VT). Prior to actual testing, rats underwent four stages of behavioral shaping: Stage 1 is run for 1 session, and all center nose pokes are reinforced on a fixed ratio 1 (FR1) schedule with 20 s sipper access, where 1 lever press is required for sipper access. At stage 2, center nose pokes are reinforced on a FR1 schedule with 10 s sipper access, and the animal must complete 20 trials to move on to next stage. Stage 3 also requires 20 trials, but all trials are cued with a center light illuminated for 20 s. There is a 10 s intertrial interval. At stage 4, a nose poke and lever press is required for the 10-second sipper access, and both right and left levers are reinforced equally, 20 trials with a 10 s intertrial interval in 60 min is required (Oberlin & Grahame, 2009).

After shaping, side bias was assessed by averaging the last 3 days' choices on each side. The large reinforcer was then assigned to their non-preferred side, to counter any initial side bias. After shaping was completed, rats were assessed at 0 s delay. This time point is used as a task to assess discrimination of reinforcer (saccharin) magnitude prior to introduction of any delay to the larger reward. Immediate reward amount started at 1 s of saccharin access, and was adjusted upwards and downwards by 0.1 s based on the rat's choices, i.e. an immediate choice resulted in down-adjustment of the sipper access time by 0.1 s on the next trial, whereas a delay choice resulted in up-adjustment of the sipper access time by 0.1 s in the next trial. The total adjustments in access were restricted to a minimum of 0 s and a maximum of 2 s. Average adjusted amounts of the reward over the last 20 trials of the session served as the measure of adjusted amount. All rats received 2-hour water access in their home cages at the end of daily testing (Oberlin & Grahame, 2009).

Phase 1: Following behavioral shaping rats, were tested in the delay discounting paradigm at 0, 1, 4, 8, 12, 16 and 20 s delays. Each delay was tested for two consecutive sessions and the two-day data for each delay was averaged.

Phase 2: Following completion of Phase 1, rats were randomly separated into treatment groups and bilaterally implanted with cannulae in the mPFC or CeA. After re-stabilization on the DD paradigm at a delay of 8 s, rats were infused with 3-PBC [20 or 40 μ g] or antalarmin [2 or 4 μ g] as described above and run in the impulsivity paradigm with an 8 s delay.

Operant drinking apparatus

Animals were tested in 11 standard operant chambers (Coulbourn Instruments, Inc., Lehigh Valley, PA) enclosed in an isolated chamber as previously described (Liu et al., 2011). The operant apparatus contained two levers, two dipper manipulanda, triple cue lights over each lever, and a house light. The dipper cup size which contained the 10% (v/v) alcohol or 3% (w/v) sucrose reinforcers was 0.1 mL. The Coulbourn Graphic State "3" operant software (Coulbourn, Whitehall, PA) was used.

Drinking in the dark multiple scheduled access paradigm

To initiate excessive "binge" alcohol drinking, we employed a modification of the drinking-in-the-dark-multiple-scheduled-access (DIDMSA) protocol (Bell et al., 2014; Liu et al., 2011). First, the procedure entailed adapting the rats to a reverse 12 h/12 h light/dark cycle which began at 7:00 PM [lights on] and lasted to 7:00 AM [lights off]. Rats were trained to orally self-administer EtOH daily for two 45 min sessions with 30 min rest in between under an FR1 schedule employing the sucrose fading technique (Harvey et al., 2002). After a period of stabilization on the FR1 schedule, the response requirement was then increased to an FR4 schedule, where 4 lever presses are required for access to the reinforcer. For each schedule, responding was considered stable when responses were within $\pm 20\%$ of the average responses for five consecutive days. Stabilization on the FR4 schedule took ~ 8 days. During the stabilization procedures, the animals were never deprived of food or fluid. These procedures are well established in our laboratory (Gondré-Lewis et al., 2016; June & Eiler, 2007; Liu et al., 2011). Other cohorts of rats were given a 3% [w/v] concentration of sucrose and trained in an identical manner under the FR1, then FR4, schedule. Following stabilization on the FR4 schedule for EtOH/sucrose, the DIDMSA protocol began using an FR4 schedule where the rats were given access to 10% alcohol, or 3% sucrose on both the left and right levers. To initiate the DIDMSA protocol during the dark phase, rats were given a 45 min operant session. After the session had elapsed, rats were then placed in the home cage with food and water *ad libitum* for 30 min. Rats were then given a second 45 min operant session and subsequently returned to their home cage. Rats engaged in the alcohol drinking for 21 consecutive days. Using this protocol, the MS rats in our laboratory produced consistent BACs of 99 ± 3 mg%. Sucrose control rats were trained in a similar manner; but lever pressed for a 3% sucrose solution instead of ethanol. The sucrose control rats allowed for evaluation of reinforcer specificity following MS and drug treatments.

Following 21 days of alcohol or sucrose drinking, rats were surgically implanted with bilateral cannulae into the CeA or mPFC. Rats ($N = 5/6$) were then infused with 3-PBC [20 or 40 μ g] or antalarmin [2 or 4 μ g] as described above and were immediately placed in the operant chambers to respond for alcohol or sucrose. A 2-hour session consisted of two 45 min (90 min) access and 30 min of rest. Figure 1 shows the timeline of experiments.

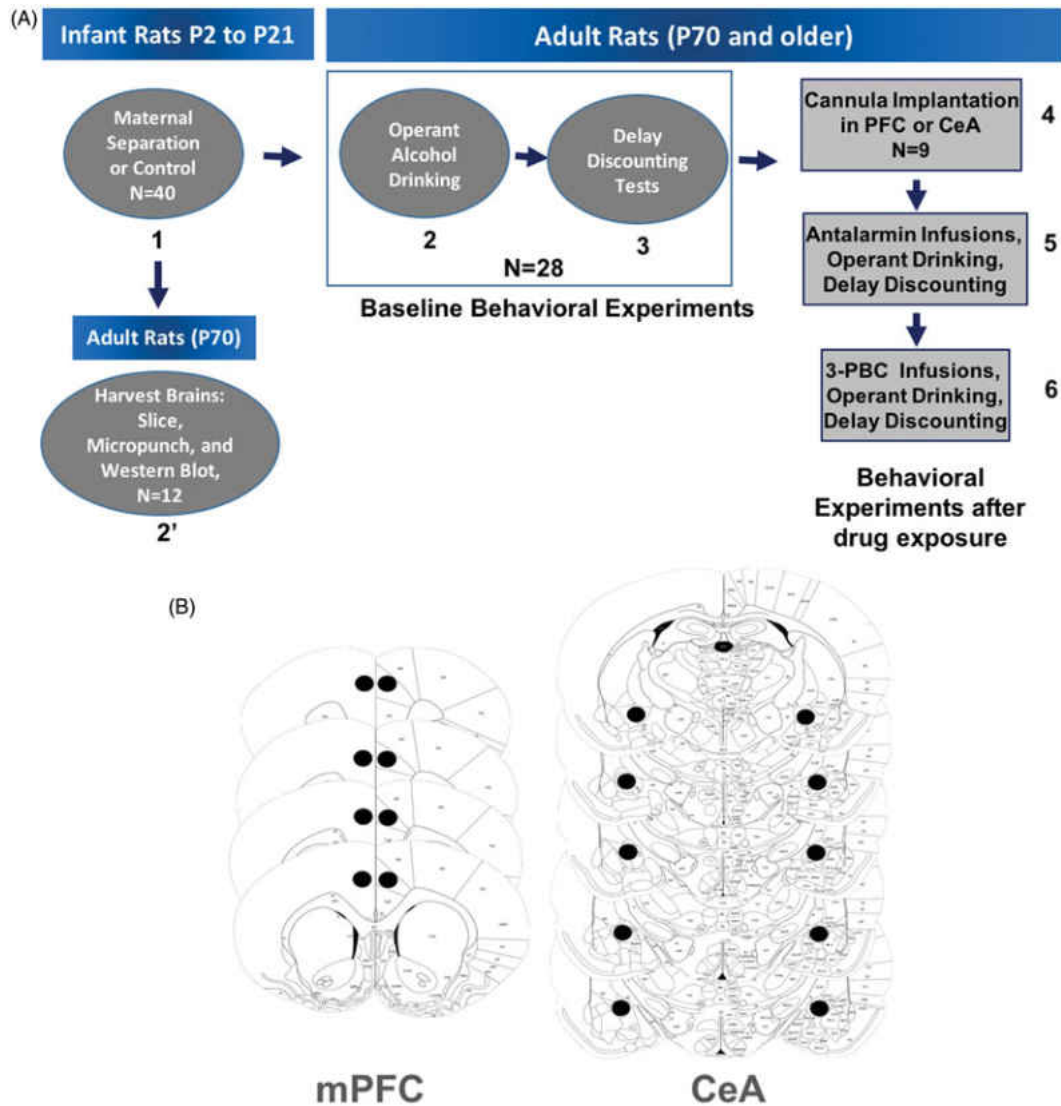


Figure 1. Map of behavioral experiments and locations of cannula implantation for animal studies. Panel A shows order of experiments demarcated by the numbers in bold and the direction of arrows. Panel B shows the location in the mPFC and the CeA where cannula were implanted for experiments in Figures 3, 4, and 6. Each slice represents a different animal.

Blood alcohol concentration measurement

To ensure animals were consuming pharmacologically relevant amounts of EtOH to model human binge drinking (Bell et al., 2006; Naimi et al., 2003; NIH-NIAAA, 2004), ~100 μ L of whole blood was collected from the tail vein of MS and CTL rats [$N = 4/\text{treatment group}$] into a heparin-coated tube. After collection, the whole blood was immediately centrifuged for 5 min at 1100 rpm. Plasma samples of 5 μ L were analyzed in a GL-5 Analyzer (Analox Instruments, Luxenburg, MA). Microanalysis consisted of measuring the oxygen consumption in the reaction between the sample of alcohol and alcohol oxidase using a Clark-type amperometric oxygen electrode. Alcohol reagent buffer solutions (pH 7.4) and alcohol oxidase enzymes were used in all samples tested. BACs were determined in duplicates after 90 min of drinking.

Cell culturing and cell transfection

HEK 293 cells plated on 15-cm plates in 15 mL of Minimum Essential Medium (MEM, Gibco, Karlsruhe, Germany)

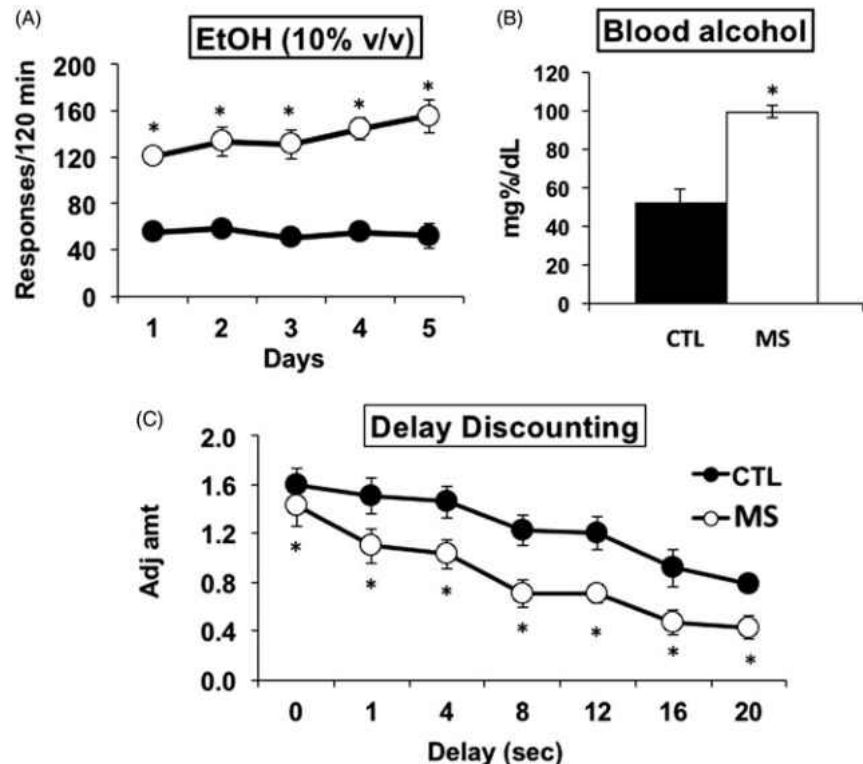
supplemented with 158 mg/L sodium bicarbonate, 2 mM glutamine (Gibco, Karlsruhe, Germany), 100 U/mL penicillin-streptomycin (Gibco, Karlsruhe, Germany), and 10% fetal calf serum (Gibco, Karlsruhe, Germany). Cultures were maintained at 37 °C in a humidified 95% O₂/5% CO₂ atmosphere for two days. Transfection with recombinant rat GABA_A receptors were carried out as described in detail (Korpi & Luddens, 1993). Briefly, HEK 293 cells were transfected using the phosphate precipitation method with rat GABA_A receptor cDNAs in eukaryotic expression vectors [pRK5] for $\alpha 2$. For optimal receptor expression, final concentrations [μ g vector DNA per 15 mm tissue culture plate] were: $\alpha 2$, 12.5 μ g.

Electrophysiology

Two days after transfection, single coverslips containing HEK 293 cells were placed in a recording chamber mounted on the movable stage of a fluorescence microscope (Olympus IX70, Tokyo, Japan) and perfused at room temperature with a defined saline solution containing (in

mM): 130 NaCl, 5.4 KCl, 2 CaCl₂, 2 MgSO₄, 10 glucose, 5 sucrose, and 10 HEPES (free acid), pH adjusted to 7.35, with about 35 mM NaOH. Transfected cells were identified by the fluorescence of the co-expressed enhanced green fluorescent protein (eGFP). The amplitudes of peak currents were measured from recorded traces. The GABA concentration response curve was analyzed with a sigmoidal non-linear regression fit, using the formula $I = (I_{\max}[L]^{nH}) / (EC_{50}^{nH} + [L]^{nH})$, where I_{\max} is the maximal induced current, L is the concentration of the agonist, and nH the Hill coefficient. Ligand-mediated membrane currents of these cells were studied in the whole-cell configuration (Hamill et al., 1981). Patch clamp pipettes were pulled from hard borosilicate capillary glass (0.5 mm ID, 1.5 mm OD, Vitrex, Science Products GmbH, Hofheim, Germany) using a horizontal puller (model P-97, Sutter Instruments, Novato, CA) in a multi-stage process. Using a fast Y-tube application system, the recombinant receptors were tested for EtOH mediated effects on the receptor current response with the approximate receptor subtype specific GABA EC₁₀, and GABA EC₁₀ plus 30 mM or 100 mM EtOH. Furthermore, both EtOH concentrations were tested together with the GABA EC₁₀ and 1 nM and 30 nM 3-PBC. The responses of the cells were recorded by a patch clamp amplifier (EPC-8, HEKA-Electronic, Lambrecht, Germany) and the pClamp 8.1 software package (Axon Instruments, Foster City, CA). The standard holding potential for the cells was -40 mV. Whole cell currents were low pass-filtered by an eight-pole Bessel filter at 5 or 3 kHz before being digitized by a Digidata 1322A interface (Axon Instruments) and recorded by the computer at a sampling rate of at least 1 kHz.

Figure 2. Baseline operant responding for alcohol, blood alcohol concentration and delay discounting (impulsivity) of MS versus CTL rats. (A) Responding for alcohol is increased in maternally separated [MS] rats [$N=10$] compared to control [CTL] rats [$N=10$]. (B) BACs of MS rats [$N=4$] were elevated above those of CTL rats [$N=4$] and were >80 mg%/dL following 2 h of drinking. (C) Adjusted amount is decreased [impulsivity is elevated] in MS rats [$N=11$] compared to CTL SD rats [$N=9$]. $*p \leq 0.05$ by ANOVA followed by *post-hoc* tests.



Statistical analyses

Data obtained using antalarmin and 3-PBC were analyzed by separate univariate ANOVAs for binge alcohol or sucrose drinking followed by Newman-Keuls *post hoc* tests. A two-tailed *t*-test was used to analyze the HEK cell data. A Student's *t*-test was used for western blotting analysis. All analyses were performed using the Sigma Plot 11.2 software program (Systat Software Inc., San Jose, CA).

Results

MS facilitates acquisition of binge drinking and impulsivity during adulthood

We tested if the experience of chronic 3-hour daily postnatal MS, as a model of early life stress and childhood trauma, could have protracted effects on alcohol drinking and impulsivity-like behavior in adults. After stabilization on the FR4 schedule for 8 days, responding for alcohol within a 2-hour period was recorded as presented in Figure 2(A). MS rats showed significantly elevated levels of responding for alcohol compared to CTL rats (Figure 2A) with a significant main effect of Group [$F_{(9,90)} = 78.169, p < 0.001$]. *Post-hoc* analyses confirmed the elevated responding for alcohol by MS rats for all 5 days tested [$p \leq 0.05$]. BACs measured after the two 45 min drinking sessions were 99.3 ± 3.2 mg%/dL for MS animals and 52.9 ± 6.2 mg%/dL in CTL rats (Figure 2B). A significant main effect of Group [$F_{(1,6)} = 46.547, p < 0.001$] was confirmed with *post-hoc* analysis [$p \leq 0.05$].

While “impulsivity” is a complex behavioral phenotype (Dick et al., 2010), in the present study, it was defined as choosing a smaller, immediate reward to the exclusion of a larger delayed reward (Rachlin & Green, 1972), and was

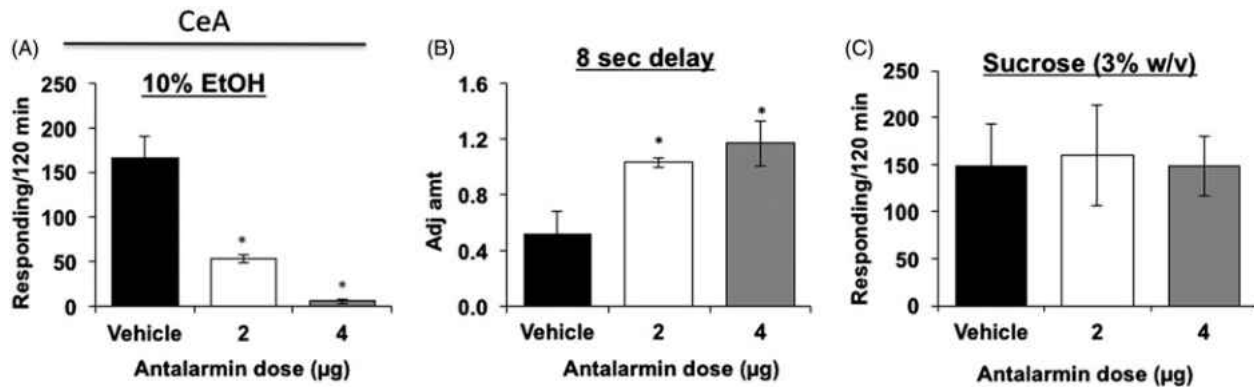


Figure 3. Effects of antalarmin injected into the CeA on delay discounting, operant binge drinking, sucrose drinking. (A) Both doses of antalarmin [$N=6$ /dosage group] reduced operant responding for alcohol of MS rats compared to vehicle-treated MS rats [$N=6$]. (B) Both 2 and 4 µg doses of antalarmin [$N=6$ /dosage group] microinjected into the CeA of MS rats elevated adjusted amount [decreased impulsivity] compared to vehicle treatment in MS rats [$N=6$]. (C) Both doses of antalarmin in the CeA [$N=5$ /dosage group] did not alter the responding of MS rats for sucrose compared to vehicle [$N=5$]. $*p \leq 0.05$ by ANOVA.

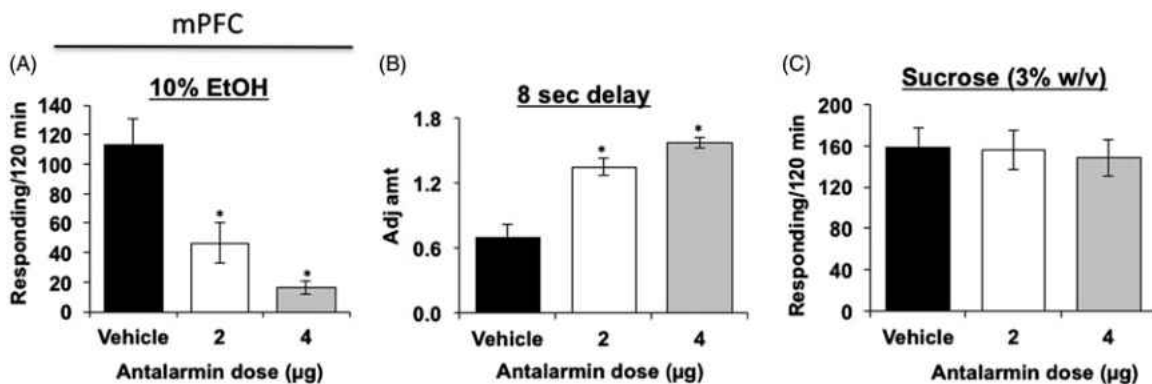


Figure 4. Effects of antalarmin injected into the mPFC on delay discounting, operant binge drinking and sucrose drinking. (A) Both 2 and 4 µg doses of antalarmin microinjected into the mPFC decreased impulsivity [elevated adjusted amount] in MS rats [$N=6$ /dosage group] compared to vehicle treatment [$N=6$]. (B) Both doses of antalarmin also reduced responding of MS rats [$N=4$ /dosage group] for alcohol compared to vehicle [$N=4$]. (C) Both doses of antalarmin in the mPFC [$N=5$ /dosage group] did not alter the responding of MS rats for sucrose compared to vehicle [$N=5$]. $*p \leq 0.05$ by ANOVA.

quantified using the adjusted amount delay discounting (DD) assay (Wilhelm & Mitchell, 2008). The smaller the amount of the reward, the greater is the impulsive inference. The MS rats showed significantly increased levels of impulsivity [lower adjusted amounts] compared with CTL rats (Figure 2C), with significant main effects of Group [$F_{[1,108]}=31.134$, $p < 0.001$] and Delay [$F_{[6,108]}=14.764$, $p < 0.001$]. *Post-hoc* analyses confirmed the increased impulsivity of MS rats compared to CTL rats for 1, 4, 8, 12, 16 and 20 s delays [$p \leq 0.05$]. These data are consistent with other findings that genetically bred high alcohol drinking (HAD) rats discounted delayed and probabilistic rewards more steeply than LAD rats (Wilhelm & Mitchell, 2008).

Antalarmin decreases impulsivity and binge alcohol drinking in MS rats

Because of the elevated levels of CRF in the CeA and mPFC of MS rats, we directly microinjected antalarmin, a CRF antagonist, into the CeA or mPFC of animals previously subjected to ethanol drinking or the delay discounting assay, to determine its effects on impulsivity and alcohol binge

drinking, as well as the role CRF may play in regulating these two behaviors. When directly infused into the CeA of MS rats, antalarmin significantly reduced operant responding for alcohol [Figure 3A; $F_{[2,15]}=31.082$; $p < 0.001$] and impulsivity [Figure 3B; $F_{[2,15]}=6.667$; $p = 0.008$] compared to vehicle-treated MS rats. *Post hoc* analyses confirmed the reduction of impulsivity and operant responding by both 2 µg and 4 µg intracranial doses of antalarmin [$p \leq 0.05$].

To confirm that the antalarmin-induced reduction in operant responding for alcohol was not due to an overall reduction in the consumption of fluid or the drug's potential sedative effects, we evaluated the effect of antalarmin on operant responding for sucrose in MS rats. Antalarmin did not reduce sucrose responding [Figure 3C; $F_{[2,12]}=0.0222$; $p = 0.978$] compared to vehicle-treated MS rats.

Similar reductions of impulsivity and alcohol binge drinking were observed when antalarmin was microinjected into the mPFC. Antalarmin significantly reduced operant responding for alcohol [Figure 4A; $F_{[2,9]}=8.974$; $p = 0.007$] and impulsivity [Figure 4B; $F_{[2,30]}=30.464$; $p < 0.001$] compared to vehicle-treated MS rats. *Post hoc* analyses confirmed the reduction of impulsivity and operant

responding by both 2 μ g and 4 μ g intracranial doses of antalarmin [$p \leq 0.05$]. Antalarmin injected into mPFC did not reduce responding for sucrose [Figure 4C; $F_{[2,12]} = 0.0843$; $p = 0.920$] compared to vehicle-treated MS rats.

GABA_A $\alpha 2$ is elevated in the CeA and mPFC of naïve MS rats

GABA_A $\alpha 2$ receptors have been implicated in the mechanisms associated with excessive alcohol drinking behavior in genetically alcohol-preferring rats. To determine if MS rats share biochemical features of P rats, naïve MS rats, never exposed to any behavioral or alcohol drinking tests were examined for expression of GABA_A $\alpha 2$ subunit because elevations of this receptor subunit is associated with excessive drinking. Compared with CTL rats, MS rats showed significantly elevated levels of GABA_A $\alpha 2$ in the CeA and mPFC [Figure 5A and B; $p \leq 0.05$].

3-PBC decreases impulsivity and binge alcohol drinking in MS rats

Because of the importance of GABA_A receptors in modulating the effects of stress and alcohol and the importance of the CeA and mPFC in stress, impulsivity, and addiction processes, we microinjected *in vivo*, 3-PBC, a GABA receptor modulator, directly into the CeA or mPFC of MS rats that were previously subjected to alcohol drinking or impulsivity. 3-PBC significantly reduced impulsivity [Figure 6A; $F_{[2,12]} = 7.013$; $p = 0.010$] and operant responding for alcohol [Figure 6B; $F_{[2,12]} = 31.399$; $p < 0.001$] compared to vehicle-treated MS rats. *Post hoc* analyses confirmed the reduction of impulsivity and operant responding by both 20 μ g and 40 μ g intracranial doses of 3-PBC [$p \leq 0.05$]. 3-PBC in the CeA did not reduce sucrose responding [Figure 6C; $F_{[2,12]} = 0.0537$; $p = 0.948$] compared to vehicle-treated MS rats.

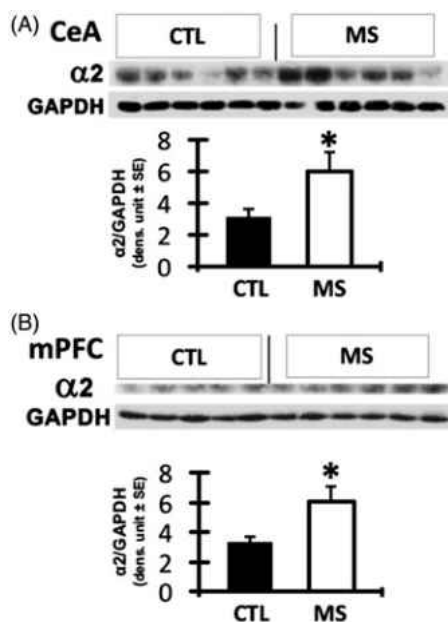


Figure 5. GABA_A $\alpha 2$ protein concentration in CeA and mPFC of MS versus CTL rats. The levels of GABA_A $\alpha 2$ expression were significantly higher in the CeA (A) and mPFC (B) of MS rats [$N = 6$] compared to CTL rats [$N = 5$ for mPFC, $n = 6$ for CeA]. * $p \leq 0.05$ by ANOVA.

Similar reductions of impulsivity and alcohol binge drinking were observed when 3-PBC was microinjected into the mPFC. Because 40 μ g of 3-PBC was shown to completely reverse excessive drinking and impulsive choice in the CeA, this single dose was used in the mPFC. It significantly reduced impulsivity [Figure 6D; $F_{[1,20]} = 22.135$; $p < 0.001$] and operant responding for alcohol [Figure 6E; $F_{[1,6]} = 15.474$; $p = 0.008$] compared to vehicle-treated MS rats. *Post hoc* analyses confirmed the reduction of impulsivity and operant responding by the 40 μ g intracranial dose of 3-PBC [$p \leq 0.05$]. 3-PBC in the mPFC also did not reduce responding for sucrose [Figure 6F; $F_{[2,12]} = 0.0600$; $p = 0.942$] compared to vehicle-treated MS rats.

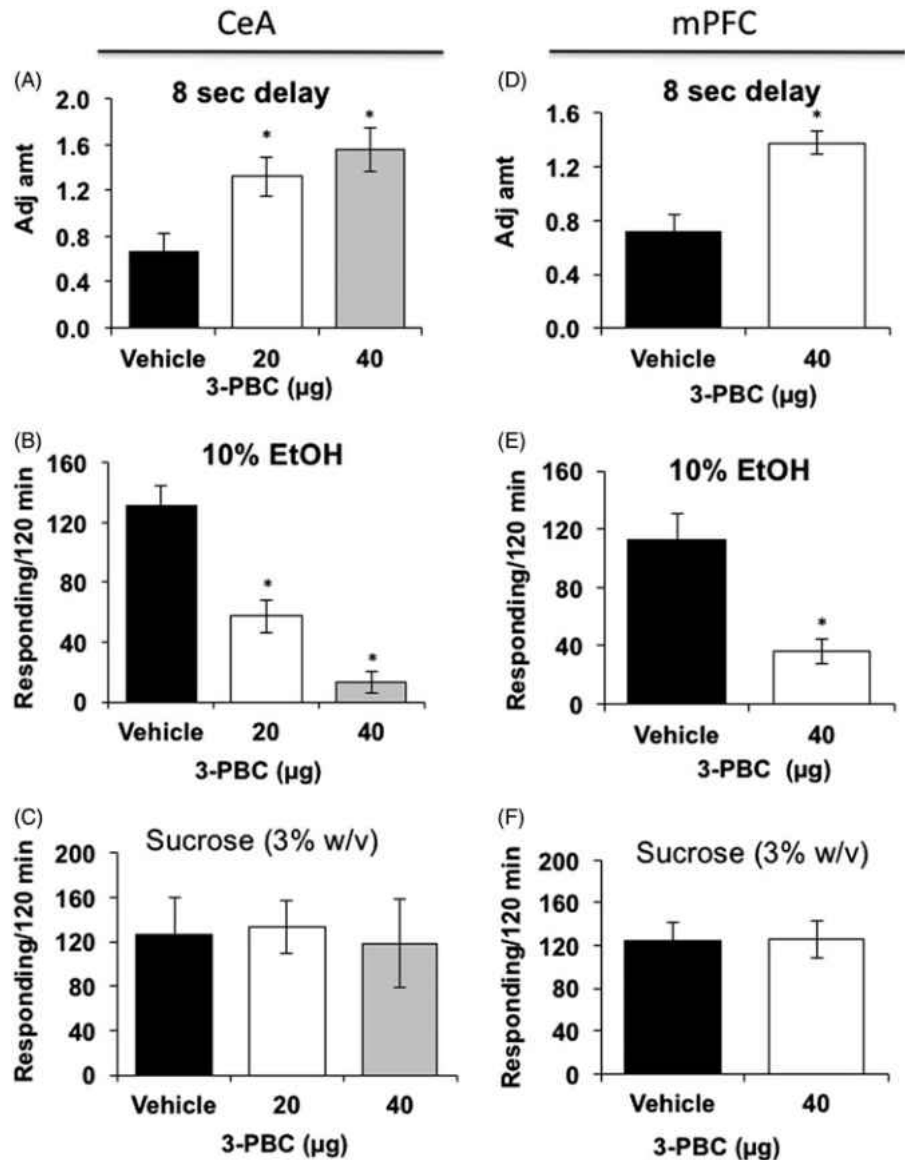
3-PBC modulates alcohol action *in vitro* at a non-benzodiazepine binding site

Given the consistent finding that 3-PBC is an antagonist of alcohol motivated behaviors as shown here and in the literature (Harvey et al., 2002; Kaminski et al., 2013), we evaluated the capacity of this ligand to block alcohol's action at the GABA_A $\alpha 2$ -containing receptor subtype using electrophysiological whole cell recordings in HEK cells. Recent work has implicated the GABA_A $\alpha 2$ -receptor subtype as a direct substrate for the effects of alcohol. Figure 7(A) shows that low doses of 3-PBC, at 30 nM, reduced the low and high dose (30 and 100 mM) alcohol enhancement of currents at GABA_A $\alpha 2\beta 3\gamma 2$ receptors [$p \leq 0.05$] in HEK293 cells. To determine if 3-PBC binds at the benzodiazepine-specific binding site of GABA receptors, $\alpha 2\beta 3\gamma 2$ and $\alpha 5\beta 3\gamma 2$ expressing HEK cells were treated with either Diazepam or 3-PBC at varying doses. As expected, diazepam greatly potentiated the effects of GABA on whole cell currents beginning at 0.1 μ M, an effect which was effectively blocked by Ro15-1788 (flumazenil), a specific antagonist for the BDZ site (Figure 7B and C). By contrast, the potentiating effects of 1 to 100 μ M 3-PBC on $\alpha 2\beta 3\gamma 2$ but not $\alpha 5\beta 3\gamma 2$ were resistant to Ro15-1788 (Figure 6D and E). These findings suggest that the action site on $\alpha 2\beta 3\gamma 2$ at which 3-PBC blocks alcohol's effects is distinct from the BDZ site.

Discussion

Despite the pervasive human clinical literature linking impulsivity and binge drinking during adolescence and young adulthood (Dick et al., 2006, 2013), little direct behavioral or neurobiological evidence exists to support this hypothesis. In the present study, MS, restricted to the early postnatal pre-weaning period, directly led to increased addiction risk illustrated by enhanced acquisition and maintenance of binge drinking during adulthood in rodents, with BACs ≥ 95 mg% dL . While MS was previously reported to cause long-term increases in alcohol self-administration in adult animals (Cruz et al., 2008; Moffett et al., 2007), subjects did not approximate the binge alcohol levels that have been reported in human alcoholics (Liu et al., 2011; Yang et al., 2011). Thus, the study emulates human binge drinking due to protracted effects of childhood stress on adult alcohol-drinking behavior. MS also facilitated acquisition of cognitive impulsivity during adulthood.

Figure 6. Effects of 3-PBC in the CeA and mPFC on delay discounting, operant binge drinking, and sucrose drinking. (A) Both 20 and 40 μg doses of 3-PBC microinjected into the CeA, elevated adjusted amounts [decreased impulsivity] in MS rats [$N=5$ /dosage group] compared to vehicle treatment [$N=5$]. (B) Both doses of 3-PBC also reduced operant responding of MS rats [$N=5$ /dosage group] for alcohol compared to vehicle [$N=5$]. (C) Neither dose of 3-PBC in the CeA [$N=5$ /dosage group] altered the responding of MS rats for sucrose compared to vehicle [$N=5$]. (D) The 40 μg dose of 3-PBC microinjected into the mPFC, elevated adjusted amount [decreased impulsivity] in MS rats [$N=4$] compared to vehicle treatment [$N=4$]. (E) 40 μg of 3-PBC also reduced operant responding of MS rats [$N=4$] for alcohol compared to vehicle [$N=4$]. (F) 3-PBC in the mPFC [$N=5$] did not alter the responding of MS rats for sucrose compared to vehicle [$N=5$]. * $p \leq 0.05$ by ANOVA.



Impulsivity is a behavioral phenotype associated with vulnerability to alcohol use initiation, onset of binge drinking behaviors, early-stage alcohol problems, and end-stage diagnoses of alcohol dependence and abuse (Dick et al., 2010; Lejuez et al., 2010; Rubio et al., 2008). Therefore, this behavior may be an important target of therapeutic intervention. As illustrated in Figure 2(C), MS produced a remarkable impulsivity phenotype across each of the 8 delay intervals tested, with the 16 s interval reaching the maximal level of impulsivity detectable. However, it is not known if binge drinking facilitated acquisition of the impulsivity phenotype, or vice versa. Nevertheless, our findings suggest, MS is a powerful factor in the initiation of both binge drinking and impulsivity, and may influence vulnerability to their comorbidity.

The MS model employed here is well established (Hulshof et al., 2011; Monroy et al., 2010; Wang & Gondre-Lewis, 2013; Wang et al., 2015), and uses repeated 3-hour separation of newborns from the dams and their littermates over a 20-21 day period, with controls for temperature (room kept at 29°C) and conditions that diminish potential auditory

stressors. We prefer this MS model to others that use 6 h of MS (MS360) or a single 24 h maternal separation at P9 (Nylander & Roman, 2013; Penasco et al., 2015) because these prolonged means of inducing maternal deprivation disrupt the infant's key metabolic needs for feeding, hydration, and warmth, necessary for survival. Additionally, in many reports, bodily contact (if any) between siblings is not specified, and this factor could introduce inconsistent outcomes across studies. These and other MS paradigms using 2-4 bottle free choice show results that range from no statistical difference in alcohol consumption compared to control animal facility reared animals whether MS was for 15 min or 360 min (Daoura et al., 2011; Gustafsson et al., 2005; Jaworski et al., 2005), to a reduction in alcohol intake, depending on the rat background and sex (Roman et al., 2003). However, many recent free-choice studies report a clear preference of MS animals for ethanol with MS180 (Huot et al., 2001) or a 24 h deprivation at P9 (Penasco et al., 2015). Therefore, although different MS paradigms or alcohol exposure regimen may influence the findings for MS-induced alcohol preference (Huot et al., 2001; Penasco et al., 2015;

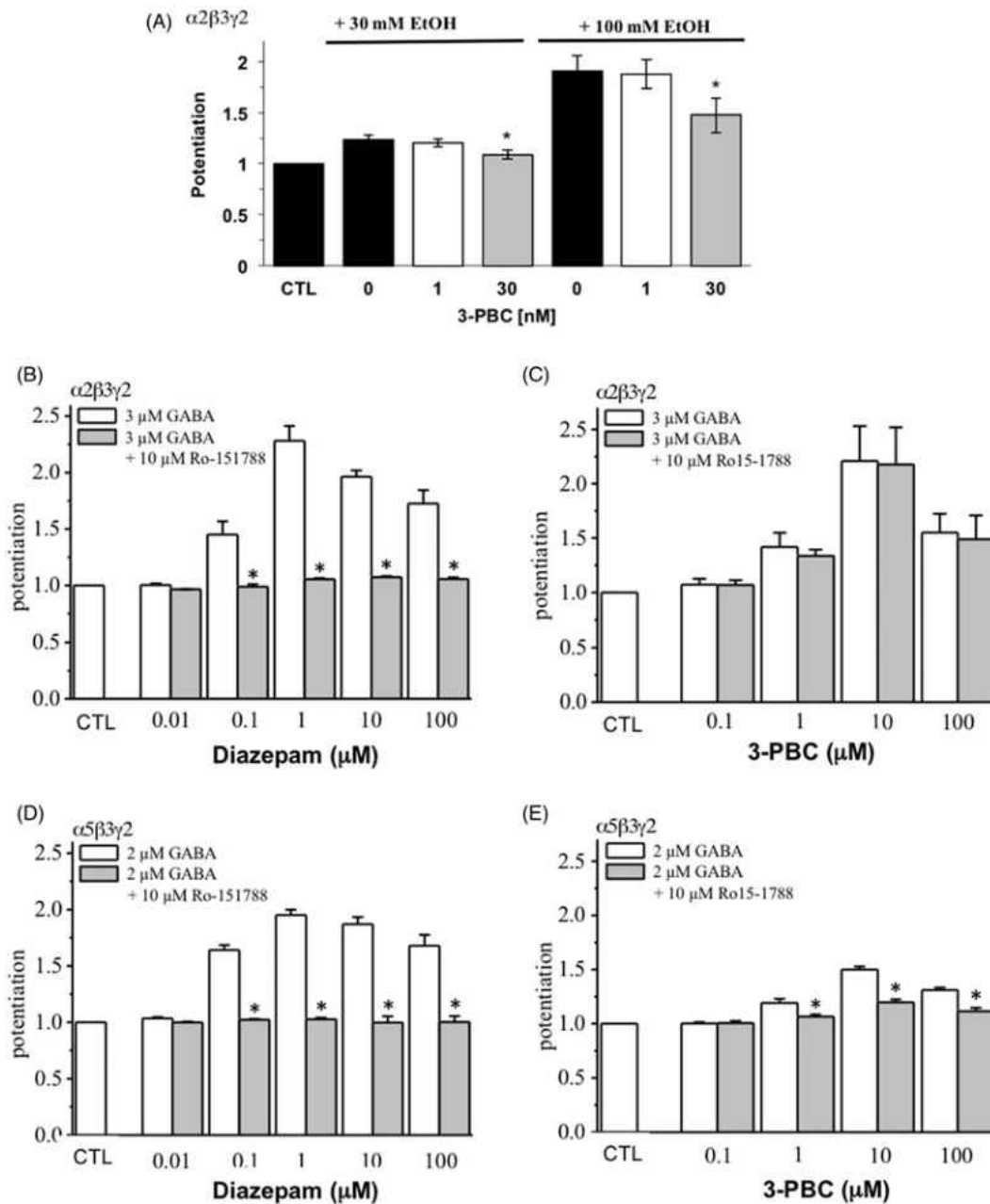


Figure 7. Effects of 3-PBC *in vitro* on attenuating alcohol-mediated actions via a benzodiazepine-independent manner. (A) Whole-cell recordings of HEK 293 cells expressing recombinant rat $\alpha 2\beta 3\gamma 2$ GABA_A receptors were performed. Currents were normalized to the GABA concentration specific for the receptor subtype EC10 under *in vitro* conditions. Two concentrations of EtOH [30 mM and 100 mM] in the absence or presence of 1 nM and 30 nM 3-PBC, respectively, were co-applied with 1.5 μ M GABA. Asterisks [*] denote $p \leq 0.05$ in a two-sided *t*-test, compared to 0 or 1 nM PBC. (B-E) Increasing concentrations of diazepam (B, C) or 3-PBC (D, E) in the absence (white) or presence (gray) of 10 μ M Ro15-1788 were co-applied with the receptor specific GABA concentrations at about the EC20. Asterisks (*) denote $p < 0.05$ in a two-sided *t*-test comparing diazepam and 3-PBC plus Ro15-1788 to the test compounds alone. Error bars indicate the standard error of the mean (\pm SEM) for at least four cells.

Roman et al., 2003), in the current study in which the animals must press the lever 4 times (i.e., work) for the 10% ethanol reinforcement, we clearly demonstrate here and elsewhere (Gondré-Lewis et al., 2016) that MS exposure enhances the propensity for alcohol self-administration. Further, using this same MS model for assessment of delay-discounting, we show that MS causes impulsive-like behavior compared to controls.

Persistent elevations of adult CRF levels are present in brain regions that modulate stress both after maternal separation, (O'Malley et al., 2011) and in non-stressed high

alcohol drinking rodents (Sommer et al., 2008; Zorrilla et al., 2013). Elevations in CRF are purported to regulate binge drinking in rodents (Lowery-Gionta et al., 2012) and humans (Treutlein et al., 2006), and were suggested to play a salient role in the transition to dependence (Koob, 2008). However, the role of CRF in regulating binge drinking and cognitive impulsivity in rodents triggered by stress/negative affective states has not been investigated. To test the hypothesis, the CRF1 receptor antagonist antalarmin was infused in the CeA and mPFC. Antalarmin in each locus produced profound and selective reductions on binge drinking and markedly reduced

impulsivity-like responding. These findings provide strong evidence that CRF is a major neuronal regulator of binge drinking and cognitive impulsivity induced by MS. Hence, as with alcohol-dependent subjects (Heilig et al., 2011; Koob, 2008; Lowery & Thiele, 2010) CRF1R antagonists may represent an important therapeutic intervention for psychiatric disorders due to sustained uncontrollable stressors, such as childhood trauma.

When applied directly into the CeA and mPFC, two brain regions that exhibit a high density of the GABA_A $\alpha 2$ subunit protein (Fritschy & Mohler, 1995; Kaufmann et al., 2003), 3-PBC markedly reduced alcohol drinking in MS rats (Figure 6), but sucrose drinking was undiminished between groups, indicative of a reinforcement specific behavior of MS rats, and also that 3-PBC was not acting as a sedative (Harvey et al., 2002). Consistent with naïve alcohol-preferring rats, which exhibited elevated GABA_A $\alpha 2$ protein compared to non-preferring rats (Liu et al., 2011), the current study reveals *increased* baseline levels of GABA_A $\alpha 2$ protein in MS relative to controls (Figure 3). This could indicate similar modes of induction of binge drinking in both P and neonatally stressed rat models. We show that modulation of the $\alpha 2$ receptor is sufficient to attenuate binge drinking in MS as was shown in alcohol preferring rats (Harvey et al., 2002; Liu et al., 2011). In addition to the GABA_A receptor functions, reductions in overall cortical GABA levels in human adolescents and young adults are highly associated with “cognitive impulsivity” and response inhibition (Silveri et al., 2013). In the current study on the stressed rat model, we do not directly measure the levels of the GABA neurotransmitter, but this could be an important next step in further characterizing the MS model for alcohol, impulsivity and other neuropsychiatric presentations. Indeed, in the current study, the pups were isolated from each other as well as from their mother during the 3-hour separation, thus the possibility exists that infant peer isolation could interact with maternal separation to elicit the effects reported.

We tested the effectiveness of alcohol alone to modulate the GABA_A $\alpha 2\beta 3\gamma 2$ receptors, and 3-PBC to modulate alcohol's action at this GABA_A receptor in HEK cells *in vitro*. The magnitude of the 100 mM concentration suggests a response sensitivity of the GABA_A $\alpha 2\beta 3\gamma 2$ receptors to moderate and high doses of alcohol. These data provide compelling evidence that 3-PBC was highly effective in attenuating alcohol's agonistic effects on whole cell currents, particularly at the 30 nM concentration. Because benzodiazepine action at the GABA site is well known for its sedative and anti-psychotic effects, the term binds at the “benzodiazepine receptor” or “benzodiazepine site” is promiscuously employed when there is an effect on the GABA receptor. However, our data in HEK cells show that 3-PBC does not seem to act via the classical benzodiazepine receptor because the potentiation of GABA at its EC₅₀ by 3-PBC was not blocked by the universal GABA_A receptor null modulator Ro 15-1788, also known as flumazenil (Figure 7). It is increasingly evident that the GABA_A receptor demonstrates specific sensitivity to many molecules aside from GABA, including ethanol (Borghese et al., 2014), dopamine (Hoerbelt et al., 2015) and BDZ (Sieghart, 2015), among others. Thus, although our data demonstrates a potent reduction of alcohol's

effects on $\alpha 2\beta 3\gamma 2$ by 3-PBC, and the association of GABA_A $\alpha 2$ with impulsive behavior in alcoholics (Villafuerte et al., 2012), indicating that 3-PBC can specifically act at the $\alpha 2$ site, in a BDZ-independent manner, we cannot rule out the possibility that 3-PBC might interact with more than one binding site at the GABA_A receptor. Additional studies are needed to further characterize the actions of 3-PBC in MS.

However, 3-PBC was shown to be a safe ligand devoid of untoward effects when given orally and did not work additively/synergistically with alcohol, or other benzodiazepine agonists (Harvey et al., 2002; June & Eiler, 2007). Hence, therapeutically, 3-PBC may represent a safe ligand to evaluate for stress-induced binge drinking and cognitive impulsivity induced by stressful life events such as childhood trauma. Although these results are compelling, there are sex-based differences in behavior, brain function and even alcohol clearance that cannot be resolved in the mixed-sex design of the current study. Future studies aimed at addressing sex differences in response to stress are necessary to enlighten a potential heterogeneity in ensuing psychoaffective behaviors following the experience of maternal separation or other early life stress. Further, other more common agonists and antagonists to GABA receptors as well as triple uptake inhibitors should be tested to expand our understanding of neurophysiological (dys) function after undergoing early life stress.

Conclusions

In summary, our data provide strong evidence that MS is a major risk factor for excessive drinking and impulsivity. These behaviors are greatly attenuated by the GABA_A ligand, 3-PBC, and the CRF antagonist, antalarmin. These results provide novel insights into the role of the brain stress systems, especially CRF, in the development of impulsivity and concomitant excessive drinking. Therapeutically, these drugs represent two putative therapeutic agents demonstrated here to be effective in attenuating both binge drinking and cognitive impulsivity induced by stressful life events.

Declaration of interest

The authors have no conflict of interest to disclose. This research was supported in part by NIH grant NS076517 to JC and AA021262 to LA and MGL.

References

- Barr CS, Dvoskin RL, Gupte M, Sommer W, Sun H, Schwandt ML, Lindell SG, et al. (2009). Functional CRH variation increases stress-induced alcohol consumption in primates. *Proc Natl Acad Sci USA* 106:14593–8.
- Bell RL, Rodd ZA, Engleman EA, Toalston JE, McBride WJ. (2014). Scheduled access alcohol drinking by alcohol-preferring (P) and high-alcohol-drinking (HAD) rats: modeling adolescent and adult binge-like drinking. *Alcohol* 48:225–34.
- Bell RL, Rodd ZA, Lumeng L, Murphy JM, McBride WJ. (2006). The alcohol-preferring P rat and animal models of excessive alcohol drinking. *Addict Biol* 11:270–88.
- Blomeyer D, Treutlein J, Esser G, Schmidt MH, Schumann G, Laucht M. (2008). Interaction between CRHR1 gene and stressful life events predicts adolescent heavy alcohol use. *Biol Psychiatry* 63:146–51.
- Borghese CM, Hicks JA, Lapid DJ, Trudell JR, Harris RA. (2014). GABA(A) receptor transmembrane amino acids are critical for alcohol action: disulfide cross-linking and alkyl methanethiosulfonate

- labeling reveal relative location of binding sites. *J Neurochem* 128: 363–75.
- Caldji C, Francis D, Sharma S, Plotsky PM, Meaney MJ. (2000). The effects of early rearing environment on the development of GABA_A and central benzodiazepine receptor levels and novelty-induced fearfulness in the rat. *Neuropsychopharmacology* 22:219–29.
- Crabbe JC, Harris RA, Koob GF. (2011). Preclinical studies of alcohol binge drinking. *Ann N Y Acad Sci* 1216:24–40.
- Cruz FC, Quadros IM, Planeta Cda S, Miczek KA. (2008). Maternal separation stress in male mice: long-term increases in alcohol intake. *Psychopharmacology (Berl)* 201:459–68.
- Dalley JW, Everitt BJ, Robbins TW. (2011). Impulsivity, compulsivity, and top-down cognitive control. *Neuron* 69:680–94.
- Daoura L, Haaker J, Nylander I. (2011). Early environmental factors differentially affect voluntary ethanol consumption in adolescent and adult male rats. *Alcohol Clin Exp Res* 35:506–15.
- Deminieri JM, Piazza PV, Guegan G, Abrous N, Maccari S, Le Moal M, Simon H. (1992). Increased locomotor response to novelty and propensity to intravenous amphetamine self-administration in adult offspring of stressed mothers. *Brain Res* 586:135–9.
- Dick DM, Aliev F, Latendresse S, Porjesz B, Schuckit M, Rangaswamy M, Hesselbrock V, et al. (2013). How phenotype and developmental stage affect the genes we find: GABRA2 and impulsivity. *Twin Res Hum Genet* 16:661–9.
- Dick DM, Bierut L, Hinrichs A, Fox L, Bucholz KK, Kramer J, Kuperman S, et al. (2006). The role of GABRA2 in risk for conduct disorder and alcohol and drug dependence across developmental stages. *Behav Genet* 36:577–90.
- Dick DM, Smith G, Olausson P, Mitchell SH, Leeman RF, O'Malley SS, Sher K. (2010). Understanding the construct of impulsivity and its relationship to alcohol use disorders. *Addict Biol* 15:217–26.
- Edenberg HJ, Dick DM, Xuei X, Tian H, Almasy L, Bauer LO, Crowe RR, et al. (2004). Variations in GABRA2, encoding the alpha 2 subunit of the GABA(A) receptor, are associated with alcohol dependence and with brain oscillations. *Am J Hum Genet* 74:705–14.
- Enoch MA, Hodgkinson CA, Yuan Q, Shen PH, Goldman D, Roy A. (2010). The influence of GABRA2, childhood trauma, and their interaction on alcohol, heroin, and cocaine dependence. *Biol Psychiatry* 67:20–7.
- Everitt BJ, Belin D, Economidou D, Pelloux Y, Dalley JW, Robbins TW. (2008). Review. Neural mechanisms underlying the vulnerability to develop compulsive drug-seeking habits and addiction. *Philos Trans R Soc Lond B Biol Sci* 363:3125–35.
- Fritschy JM, Mohler H. (1995). GABA_A-receptor heterogeneity in the adult rat brain: differential regional and cellular distribution of seven major subunits. *J Comp Neurol* 359:154–94.
- Funk CK, Zorrilla EP, Lee MJ, Rice KC, Koob GF. (2007). Corticotropin-releasing factor 1 antagonists selectively reduce ethanol self-administration in ethanol-dependent rats. *Biol Psychiatry* 61: 78–86.
- Garcia-Gutierrez MS, Navarrete F, Aracil A, Bartoll A, Martinez-Gras I, Lanciego JL, Rubio G, Manzanares J. (2015). Increased vulnerability to ethanol consumption in adolescent maternal separated mice. *Addict Biol*. [Epub ahead of print]. doi: 10.1111/adb.12266.
- Gehlert DR, Cipitelli A, Thorsell A, Le AD, Hipskind PA, Hamdouchi C, Lu J, et al. (2007). 3-(4-Chloro-2-morpholin-4-yl-thiazol-5-yl)-8-(1-ethylpropyl)-2,6-dimethyl-imidazo [1,2-b]pyridazine: a novel brain-penetrant, orally available corticotropin-releasing factor receptor 1 antagonist with efficacy in animal models of alcoholism. *J Neurosci* 27:2718–26.
- George O, Sanders C, Freiling J, Grigoryan E, Vu S, Allen CD, Crawford E, et al. (2012). Recruitment of medial prefrontal cortex neurons during alcohol withdrawal predicts cognitive impairment and excessive alcohol drinking. *Proc Natl Acad Sci U S A* 109:18156–61.
- Gilpin NW, Karanikas CA, Richardson HN. (2012). Adolescent binge drinking leads to changes in alcohol drinking, anxiety, and amygdalar corticotropin releasing factor cells in adulthood in male rats. *PLoS One* 7:e31466.
- Glaser YG, Zubieta JK, Hsu DT, Villafuerte S, Mickey BJ, Trucco EM, Burmeister M, et al. (2014). Indirect effect of corticotropin-releasing hormone receptor 1 gene variation on negative emotionality and alcohol use via right ventrolateral prefrontal cortex. *J Neurosci* 34: 4099–107.
- Gondré-Lewis MC, Darius PJ, Wang H, Allard JA. (2016). Stereological analyses of reward system nuclei in maternally deprived/separated alcohol drinking rats. *J Chem Neuroanat*. [Epub ahead of print]. doi: http://dx.doi.org/10.1016/j.jchemneu.2016.02.004.
- Gustafsson L, Ploj K, Nylander I. (2005). Effects of maternal separation on voluntary ethanol intake and brain peptide systems in female Wistar rats. *Pharmacol Biochem Behav* 81:506–16.
- Hamill OP, Marty A, Neher E, Sakmann B, Sigworth FJ. (1981). Improved patch-clamp techniques for high-resolution current recording from cells and cell-free membrane patches. *Pflugers Arch* 391: 85–100.
- Harvey SC, Foster KL, McKay PF, Carroll MR, Seyoum R, Woods 2nd JE, Grey C, et al. (2002). The GABA(A) receptor alpha1 subtype in the ventral pallidum regulates alcohol-seeking behaviors. *J Neurosci* 22:3765–75.
- Heilig M, Goldman D, Berrettini W, O'Brien CP. (2011). Pharmacogenetic approaches to the treatment of alcohol addiction. *Nat Rev Neurosci* 12:670–84.
- Hoerbel P, Lindsley TA, Fleck MW. (2015). Dopamine directly modulates GABA_A receptors. *J Neurosci* 35:3525–36.
- Hsu FC, Zhang GJ, Raol YS, Valentino RJ, Coulter DA, Brooks-Kayal AR. (2003). Repeated neonatal handling with maternal separation permanently alters hippocampal GABA_A receptors and behavioral stress responses. *Proc Natl Acad Sci U S A* 100:12213–18.
- Huggins KN, Mathews TA, Locke JL, Szeliga KT, Friedman DP, Bennett AJ, Jones SR. (2012). Effects of early life stress on drinking and serotonin system activity in rhesus macaques: 5-hydroxyindoleacetic acid in cerebrospinal fluid predicts brain tissue levels. *Alcohol* 46: 371–6.
- Hulshof HJ, Novati A, Sgoifo A, Luiten PG, den Boer JA, Meerlo P. (2011). Maternal separation decreases adult hippocampal cell proliferation and impairs cognitive performance but has little effect on stress sensitivity and anxiety in adult Wistar rats. *Behav Brain Res* 216:552–60.
- Huot RL, Thirivikraman KV, Meaney MJ, Plotsky PM. (2001). Development of adult ethanol preference and anxiety as a consequence of neonatal maternal separation in Long Evans rats and reversal with antidepressant treatment. *Psychopharmacology (Berl)* 158:366–73.
- Jaworski JN, Francis DD, Brommer CL, Morgan ET, Kuhar MJ. (2005). Effects of early maternal separation on ethanol intake, GABA receptors and metabolizing enzymes in adult rats. *Psychopharmacology (Berl)* 181:8–15.
- June HL, Eiler WJA. (2007). Dopaminergic and GABAergic regulation of alcohol-motivated behaviors: novel neuroanatomical substrates. In: Sibley DR, Hanin I, Kuhar M, Skolnick P, editors. *Handbook of contemporary neuropharmacology*. Hoboken, NJ: Wiley & Sons, Inc. doi: 10.1002/9780470101001.hcn036.
- Kaminski BJ, van Linn ML, Cook JM, Yin W, Weerts EM. (2013). Effects of the benzodiazepine GABA_A α1-preferring ligand, 3-propoxy-β-carboline hydrochloride (3-PBC), on alcohol seeking and self-administration in baboons. *Psychopharmacology (Berl)* 227: 127–36.
- Kaufmann WA, Humpel C, Alheid GF, Marksteiner J. (2003). Compartmentation of alpha 1 and alpha 2 GABA(A) receptor subunits within rat extended amygdala: implications for benzodiazepine action. *Brain Res* 964:91–9.
- Koe AS, Salzberg MR, Morris MJ, O'Brien TJ, Jones NC. (2014). Early life maternal separation stress augmentation of limbic epileptogenesis: the role of corticosterone and HPA axis programming. *Psychoneuroendocrinology* 42:124–33.
- Koob GF. (2008). Corticotropin-releasing factor, neuroplasticity (sensitization), and alcoholism. *Proc Natl Acad Sci USA* 105:8809–10.
- Koob GF. (2014). Neurocircuitry of alcohol addiction: synthesis from animal models. *Handb Clin Neurol* 125:33–54.
- Korpi ER, Luddens H. (1993). Regional gamma-aminobutyric acid sensitivity of t-butylbicyclopophosphoro[35S]thionate binding depends on gamma-aminobutyric acidA receptor alpha subunit. *Mol Pharmacol* 44:87–92.
- Lejuez CW, Magidson JF, Mitchell SH, Sinha R, Stevens MC, de Wit H. (2010). Behavioral and biological indicators of impulsivity in the development of alcohol use, problems, and disorders. *Alcohol Clin Exp Res* 34:1334–45.
- Liu J, Yang AR, Kelly T, Puche A, Esoga C, June Jr HL, Elnabawi A, et al. (2011). Binge alcohol drinking is associated with GABA_A α2-regulated Toll-like receptor 4 (TLR4) expression in the central amygdala. *Proc Natl Acad Sci USA* 108:4465–70.

- Lowery EG, Thiele TE. (2010). Pre-clinical evidence that corticotropin-releasing factor (CRF) receptor antagonists are promising targets for pharmacological treatment of alcoholism. *CNS Neurol Disord Drug Targets* 9:77–86.
- Lowery-Gionta EG, Navarro M, Li C, Pleil KE, Rinker JA, Cox BR, Sprow GM, et al. (2012). Corticotropin releasing factor signaling in the central amygdala is recruited during binge-like ethanol consumption in C57BL/6J mice. *J Neurosci* 32:3405–13.
- Marinelli M, Piazza PV. (2002). Interaction between glucocorticoid hormones, stress and psychostimulant drugs. *Eur J Neurosci* 16: 387–94.
- Moffett MC, Vicentic A, Kozel M, Plotsky P, Francis DD, Kuhar MJ. (2007). Maternal separation alters drug intake patterns in adulthood in rats. *Biochem Pharmacol* 73:321–30.
- Monroy E, Hernandez-Torres E, Flores G. (2010). Maternal separation disrupts dendritic morphology of neurons in prefrontal cortex, hippocampus, and nucleus accumbens in male rat offspring. *J Chem Neuroanat* 40:93–101.
- Naimi TS, Brewer RD, Mokdad a, Denny C, Serdula MK, Marks JS. (2003). Binge drinking among US adults. *JAMA* 289:70–5.
- Namjoshi OA, Gryboski A, Fonseca GO, van Linn ML, Wang ZJ, Deschamps JR, Cook JM. (2011). Development of a two-step route to 3-PBC and β CcT, two agents active against alcohol self-administration in rodent and primate models. *J Org Chem* 76:4721–7.
- Nemeroff CB. (2004a). Neurobiological consequences of childhood trauma. *J Clin Psychiatry* 65 Suppl 1:18–28.
- Nemeroff CC. (2004b). Early-life adversity, CRF dysregulation, and vulnerability to mood and anxiety disorders. *Psychopharmacol Bull* 38:14–20.
- NIH-NIAAA. (2004). NIAAA council approves definition of binge drinking. NIAAA Newsletter No. 3.
- Nylander I, Roman E. (2013). Is the rodent maternal separation model a valid and effective model for studies on the early-life impact on ethanol consumption? *Psychopharmacology (Berl)* 229:555–69.
- O'Malley D, Dinan TG, Cryan JF. (2011). Neonatal maternal separation in the rat impacts on the stress responsivity of central corticotropin-releasing factor receptors in adulthood. *Psychopharmacology (Berl)* 214:221–9.
- Oberlin BG, Grahame NJ. (2009). High-alcohol preferring mice are more impulsive than low-alcohol preferring mice as measured in the delay discounting task. *Alcohol Clin Exp Res* 33:1294–303.
- Penasco S, Mela V, Lopez-Moreno JA, Viveros MP, Marco EM. (2015). Early maternal deprivation enhances voluntary alcohol intake induced by exposure to stressful events later in life. *Neural Plast* 2015:342761.
- Phillips TJ, Reed C, Pastor R. (2015). Preclinical evidence implicating corticotropin-releasing factor signaling in ethanol consumption and neuroadaptation. *Genes Brain Behav* 14:98–135.
- Pirker S, Schwarzer C, Wieselthaler A, Sieghart W, Sperk G. (2000). GABA(A) receptors: immunocytochemical distribution of 13 subunits in the adult rat brain. *Neuroscience* 101:815–50.
- Rachlin H, Green L. (1972). Commitment, choice and self-control. *J Exp Anal Behav* 17:15–22.
- Robinson ES, Eagle DM, Economidou D, Theobald DE, Mar AC, Murphy ER, Robbins TW, Dalley JW. (2009). Behavioural characterisation of high impulsivity on the 5-choice serial reaction time task: specific deficits in 'waiting' versus 'stopping'. *Behav Brain Res* 196: 310–16.
- Roceri M, Hendriks W, Racagni G, Ellenbroek BA, Riva MA. (2002). Early maternal deprivation reduces the expression of BDNF and NMDA receptor subunits in rat hippocampus. *Mol Psychiatry* 7: 609–16.
- Roman E, Hyytia P, Nylander I. (2003). Maternal separation alters acquisition of ethanol intake in male ethanol-preferring AA rats. *Alcohol Clin Exp Res* 27:31–7.
- Romano-Lopez A, Mendez-Diaz M, Ruiz-Contreras AE, Carrisoza R, Prospero-Garcia O. (2012). Maternal separation and proclivity for ethanol intake: a potential role of the endocannabinoid system in rats. *Neuroscience* 223:296–304.
- Rubio G, Jimenez M, Rodriguez-Jimenez R, Martinez I, Avila C, Ferre F, Jimenez-Arriero MA, et al. (2008). The role of behavioral impulsivity in the development of alcohol dependence: a 4-year follow-up study. *Alcohol Clin Exp Res* 32:1681–7.
- Sieghart W. (2015). Allosteric modulation of GABA_A receptors via multiple drug-binding sites. *Adv Pharmacol* 72:53–96.
- Silveri MM, Sneider JT, Crowley DJ, Covell MJ, Acharya D, Rosso IM, Jensen JE. (2013). Frontal lobe γ -aminobutyric acid levels during adolescence: associations with impulsivity and response inhibition. *Biol Psychiatry* 74:296–304.
- Sommer WH, Rimondini R, Hansson AC, Hipskind PA, Gehlert DR, Barr CS, Heilig MA. (2008). Upregulation of voluntary alcohol intake, behavioral sensitivity to stress, and amygdala *crhr1* expression following a history of dependence. *Biol Psychiatry* 63:139–45.
- Treutlein J, Kissling C, Frank J, Wiemann S, Dong L, Depner M, Saam C, et al. (2006). Genetic association of the human corticotropin releasing hormone receptor 1 (CRHR1) with binge drinking and alcohol intake patterns in two independent samples. *Mol Psychiatry* 11:594–602.
- Vargas WM, Bengston L, Gilpin NW, Whitcomb BW, Richardson HN. (2014). Alcohol binge drinking during adolescence or dependence during adulthood reduces prefrontal myelin in male rats. *J Neurosci* 34:14777–82.
- Villafuente S, Heitzeg MM, Foley S, Yau WY, Majczenko K, Zubieta JK, Zucker RA, Burmeister M. (2012). Impulsiveness and insula activation during reward anticipation are associated with genetic variants in GABRA2 in a family sample enriched for alcoholism. *Mol Psychiatry* 17:511–19.
- Wang H, Gondre-Lewis MC. (2013). Prenatal nicotine and maternal deprivation stress de-regulate the development of CA1, CA3, and dentate gyrus neurons in hippocampus of infant rats. *PLoS One* 8: e65517.
- Wang Q, Shao F, Wang W. (2015). Maternal separation produces alterations of forebrain brain-derived neurotrophic factor expression in differently aged rats. *Front Mol Neurosci* 8:49.
- Wilhelm CJ, Mitchell SH. (2008). Rats bred for high alcohol drinking are more sensitive to delayed and probabilistic outcomes. *Genes Brain Behav* 7:705–13.
- Yang AR, Liu J, Yi HS, Warnock KT, Wang M, June Jr HL, Puche Sr AC, et al. (2011). Binge drinking: in search of its molecular target via the GABA(A) receptor. *Front Neurosci* 5:123.
- Yang XD, Liao XM, Uribe-Marino A, Liu R, Xie XM, Jia J, Su YA, et al. (2015). Stress during a critical postnatal period induces region-specific structural abnormalities and dysfunction of the prefrontal cortex via CRF. *Neuropsychopharmacology*. 40:1203–15.
- Zorrilla EP, Heilig M, de Wit H, Shaham Y. (2013). Behavioral, biological, and chemical perspectives on targeting CRF(1) receptor antagonists to treat alcoholism. *Drug Alcohol Depend* 128: 175–86.

Triple monoamine uptake inhibitors demonstrate a pharmacologic association between excessive drinking and impulsivity in high-alcohol-preferring (HAP) mice

David S. O'Tousa^{1*}, Kaitlin T. Warnock^{2*}, Liana M. Matson¹, Ojas A. Namjoshi³, Michael Van Linn³, Veera Venkata Tiruveedhula³, Meredith E. Halcomb¹, James Cook³, Nicholas J. Grahame¹ & Harry L. June^{2,4}

Department of Psychology, Indiana University-Purdue University, Indianapolis, IN, USA¹, Neuropsychopharmacology Laboratory, Department of Psychiatry and Behavioral Sciences, Howard University College of Medicine, Washington, DC, USA², Department of Chemistry, University of Wisconsin-Milwaukee, Milwaukee, WI, USA³ and Department of Pharmacology, Howard University College of Medicine, Washington, DC, USA⁴

ABSTRACT

Approximately 30% of current drinkers in the United States drink excessively, and are referred to as problem/hazardous drinkers. These individuals, who may not meet criteria for alcohol abuse or dependence, comprise binge, heavy drinkers, or both. Given their high prevalence, interventions that reduce the risk of binge and heavy drinking have important public health implications. Impulsivity has been repeatedly associated with excessive drinking in the clinical literature. As impulsivity is correlated with, and may play a critical role in, the initiation and maintenance of excessive drinking, this behavior may be an important target for therapeutic intervention. Hence, a better understanding of pharmacological treatments capable of attenuating excessive drinking and impulsivity may markedly improve clinical outcomes. The high-alcohol-preferring (HAP) mice represent a strong rodent model to study the relationship between impulsivity and excessive alcohol drinking, as recent evidence indicates they consume high levels of alcohol throughout their active cycle and are innately impulsive. Using this model, the present study demonstrates that the triple monoamine uptake inhibitors (TUIs) amitifadine and DOV 102, 677 effectively attenuate binge drinking, heavy drinking assessed via a 24-hour free-choice assay, and impulsivity measured by the delay discounting procedure. In contrast, 3-PBC, a GABA_A α 1 preferring ligand with mixed agonist-antagonist properties, attenuates excessive drinking without affecting impulsivity. These findings suggest that in HAP mice, monoamine pathways may predominate as a common mechanism underlying impulsivity and excessive drinking, while the GABAergic system may be more salient in regulating excessive drinking. We further propose that TUIs such as amitifadine and DOV 102, 677 may be used to treat the co-occurrence of impulsivity and excessive drinking.

Keywords Alcohol use disorders, delay discounting, HAP mice, impulsivity, triple uptake inhibitor.

Correspondence to: Harry L. June, Director of Substance Abuse Research, Department of Psychiatry and Behavioral Sciences, Department of Pharmacology, Howard University College of Medicine, 2041 Georgia Ave. NW Suite #5B02, Washington, DC 20060, USA. E-mail: harry.june@howard.edu; Nicholas J. Grahame, Department of Psychology, 426 N Blackford St., LD #124, Indiana University-Purdue University, Indianapolis, IN 46202, USA. E-mail: ngrahame@iupui.edu

INTRODUCTION

Excessive alcohol drinking is the third leading lifestyle-related cause of death in the United States, and has been suggested to kill approximately 75 000 people annually. It results in 2.3 million years of potential life lost, about 30 years of life lost per death (Center for Disease Control

and Prevention 2001; Chikritzhs *et al.* 2001; Town *et al.* 2006). Excessive drinkers are considered to be binge drinkers, heavy drinkers or both (Town *et al.* 2006). Binge drinkers include men who consume five or more drinks and women who consume four or more drinks on one or more occasions in the past month. For the typical adult, this pattern often results in a blood alcohol

*The authors contributed equally to this article.

concentration (BAC) of 0.08 gram percent or above in a 2-hour period (NIAAA 2004). Heavy drinking includes those who have consumed 60 drinks in the past month for men, and 30 for women (Town *et al.* 2006). While excessive drinkers are at significantly increased risks for serious medical conditions (e.g. hypertension, cardiomyopathy, obesity and liver diseases) (Center for Disease Control and Prevention 2001; Chikritzhs *et al.* 2001), most excessive drinkers do not meet criteria for alcohol abuse or dependence (Dawson, Grant & Li 2005). Moreover, emerging evidence suggests that, in contrast to alcohol dependence, excessive drinking contributes to most alcohol-related problems in the United States (Institute of Medicine 1990; Town *et al.* 2006; Dawson *et al.* 2005; Courtney & Polich 2009). However, few medications have been investigated for treatment of such populations despite the high prevalence of excessive drinking.

Interestingly, the trait of impulsivity is correlated with addiction to virtually all drugs of abuse (Kirby, Petry & Bickel 1999; Hoffman *et al.* 2006), but particularly with dimensions of excessive alcohol drinking (Rubio *et al.* 2008; Dick *et al.* 2010; Vanderveen, Cohen & Watson 2012). Impulsivity is involved in vulnerability to alcohol use initiation, onset of binge drinking behaviors, early-stage alcohol problems, and end-stage diagnoses of alcohol dependence and abuse (reviewed in Lejuez *et al.* 2010). Therefore, this behavior may be an important target of therapeutic intervention. However, current clinical treatments are ineffective in treating both impulsivity and excessive alcohol drinking (Oberlin *et al.* 2010). Thus, a better understanding of the pharmacological treatments capable of regulating excessive alcohol drinking as well as impulsivity may improve clinical outcomes.

Research in our laboratories has focused on impulsive choice, also referred to as 'cognitive impulsivity' (Rachlin & Green 1972; Winstanley *et al.* 2004). This definition is experimentally assessed using a task called delay discounting (DD). The DD task is widely used in human and animal studies, and is similar between species, lending good face validity to assessments of impulsivity in experimental animal models (Richards *et al.* 1997; Bickel, Odum & Madden 1999; Petry 2001). In the present study, we focused on investigating the potential pharmacological overlap between cognitive impulsivity and two modes of excessive drinking: binge drinking and heavy drinking assessed via 24-hour free choice. Both types of excessive drinking have been shown to result in alcohol dependence/use disorders in some individuals (King *et al.* 2011).

Preclinical research employing alcohol-preferring rodent lines has consistently demonstrated that the association between impulsivity and alcohol use is genetically mediated (e.g. Wilhelm & Mitchell 2008; Oberlin &

Grahame 2009). Employing high-alcohol-drinking (HAD) and low-alcohol-drinking (LAD) rats, Wilhelm & Mitchell (2008), using the DD assay, demonstrated that HAD rats were more impulsive than LAD rats. Using replicate selected lines of outbred high-alcohol-preferring (HAP) mice, Oberlin & Grahame (2009) showed that both HAP2 and HAP1 lines of mice were more impulsive than the LAP2 and HS/Ibg lines, respectively. Together, these results in naïve, alcohol-preferring rodents suggest that impulsivity is a heritable difference that precedes the initiation of alcohol use. However, despite the genotypic correlation of impulsivity and alcohol use, no research has been able to identify a single therapeutic modality capable of attenuating both phenotypes (Mitchell *et al.* 2007; Oberlin *et al.* 2010). Hence, it is plausible that differential, though genetically linked, neurobiological mechanisms contribute to the development of impulsivity and alcohol drinking.

In an effort to identify both neurochemical targets and a single pharmacotherapy capable of attenuating both excessive drinking and impulsivity, our laboratories have employed a series of compounds referred to as both 'broad spectrum' antidepressants (ADs) and triple uptake inhibitors (TUIs) (Skolnick & Basile 2007). Unlike currently available ADs, these agents inhibit the uptake of dopamine (DA), norepinephrine (NE) and serotonin (5-HT), with varying potencies at their respective monoaminergic transporters. The exact neural mechanisms regulating cognitive impulsivity are not known; however, the monoamines DA, NE and 5-HT are widely implicated in modulating impulsivity based on the clinical effects of drugs that increase the activity of the relevant pathways, and by evidence that dopaminergic, noradrenergic and/or serotonergic neurotransmission is deficient in patients and animal models of impulse control disorders (Bevilacqua *et al.* 2010; Economidou *et al.* 2012). Further evidence suggests that hypo-functional mesolimbic monoaminergic pathways contribute to the clinical manifestations of alcoholism (Johnson 2008; Simon O'Brien *et al.* 2011). The γ -amino butyric acid_A (GABA_A) receptors are also an established target for excessive drinking (Harris, Trudell & Mihic 2008). Recent research indicates a significant role for both the GABA α 1 and α 2 subunits in regulating binge drinking (Liu *et al.* 2011; Yang *et al.* 2011). Significant support for the role of these subunits in regulating excessive drinking in the clinical literature is also well established (see Liu *et al.* 2011). However, few studies have investigated a pharmacologic association between excessive drinking and impulsivity using GABAergic and monoaminergic ligands. Because of the critical role of impulsivity in alcohol use disorders, this behavior may be an important target of therapeutic intervention, and hence improve clinical outcomes.

In the present research, based on our previous findings that the two TUIs, amitifadine (formerly DOV 21, 947) and DOV 102, 677, and 3-PBC, a GABA_A α 1 preferring ligand with mixed agonist-antagonist properties (Harvey *et al.* 2002), reduced excessive drinking in alcohol-preferring (P) rats (June & Eiler 2007; Warnock *et al.* 2012; Yang *et al.* 2012), we hypothesized that the three ligands would reduce two modes of excessive drinking (i.e. binge drinking and heavy drinking) and impulsivity in HAP mice. The HAP mouse model was an optimal model to use for these studies, because these mice are both excessive drinkers and 'innately' impulsive (Oberlin & Grahame 2009; Matson & Grahame 2011).

MATERIALS AND METHODS

Experiment 1: effects of amitifadine, DOV 102, 677, and 3-PBC on binge alcohol and sucrose drinking

Subjects

Two cohorts of male and female HAP2/HAP3 mice ($N = 105$) were used to model binge alcohol drinking in humans using the reverse light cycle as previously reported in rats (Liu *et al.* 2011; Warnock *et al.* 2012). The first cohort comprised 27 male and 20 female HAP2 mice of the 34th generation, and 14 male and 14 female HAP2 mice of the 37th generation. The second cohort comprised 15 male HAP2 mice of the 35th generation, and 15 male HAP3 mice of the 14th generation. The second cohort, while drug naïve, had previously participated in a study evaluating affect-related behaviors (see Can, Grahame & Gould 2012). The amount of time between the two studies was approximately 4 weeks. Animals were approximately 4–5 months of age at the beginning of the experiments. All subjects for all experiments were individually housed. The treatment of subjects for experiment 1 was approved by the institutional review board of the University of Maryland School of Medicine.

Compounds

Amitifadine and DOV 102, 677 were obtained from DOV Pharmaceutical (Somerset, NJ, USA). 3-PBC was obtained from Dr. James Cook of the University of Wisconsin-Milwaukee (Milwaukee, WI, USA). Drug formulations were prepared immediately before each test session in a volume of 10 ml/kg using deionized (DI) water. They were administered by oral gavage 25 minutes prior to binge and locomotor activity experiments due to the half-life/estimated half-life in the previously published studies (see June & Eiler 2007; Tizzano *et al.* 2008). Animals were habituated to the gavage procedures by administering DI water alone over a number of experimental sessions.

Equipment

Binge drinking procedures were tested in standard mouse operant chambers (Coulbourn Instruments, Inc., Lehigh Valley, PA, USA) as previously described (June & Eiler 2007; June *et al.* 2007). The dipper cup size was 0.1 ml, and contained 10% (v/v) alcohol or 1% (w/v) sucrose reinforcers. The Coulbourn Graphic State '3' operant software was used (June & Eiler 2007; June *et al.* 2007).

Drinking in the dark multiple-scheduled access (DIDMSA) paradigm

The DIDMSA protocol was used to initiate binge drinking with HAP mice. Identical and complete training procedures have recently been employed in P rats (Liu *et al.* 2011; Warnock *et al.* 2012). To initiate the DIDMSA protocol in mice, the subjects were given a 30-minute operant session using an FR-4 schedule. After the initial 30-minute session had elapsed, mice were placed in the home cage with food and water *ad libitum* for 1 hour. Mice then received two additional 30 minutes of alcohol access periods, spaced 1 hour apart over the 21 consecutive days time course. In total, animals received three daily 30-minute access periods, each spaced 1 hour apart. Other cohorts of mice were trained in an identical manner for 1% (w/v) sucrose. The sucrose concentration was selected so response rates would be relatively similar, eliminating the potential confound of a difference in reinforcer efficacy (June & Gilpin 2010).

BAC measurement

To ensure that the HAP mice were consuming pharmacologically relevant amounts of ethanol to effectively model human binge drinking (e.g. Naimi *et al.* 2003), BACs were taken as previously reported (June & Eiler 2007; June *et al.* 2007) on day 21 from a subset of mice randomized into the drug treatment groups. The BAC levels at 90 minutes were consistent with the NIAAA definition of binge alcohol consumption in humans (NIAAA 2004).

Procedural summary

On day 22, mice in the drug treatment groups were randomly administered their respective treatments to evaluate effects on binge alcohol drinking. A total of 28 mice comprising 24 males and four females of the 34th generation were selected to receive amitifadine. Mice were randomly divided into four ($n = 7$) dosage groups (vehicle, 25, 50 and 75 mg/kg). After completion of the amitifadine treatment for binge alcohol drinking and a 7-day washout period, 24 of the 28 mice that participated in the alcohol study were then randomly divided into four ($n = 6$) dosage groups (vehicle, 25, 50 and 75 mg/kg), and retrained on the binge drinking procedure using sucrose as a reinforcer.

Thirty-five mice comprising three males and 16 females of the 34th generation HAP2 line, and 14 males and two females of the 37th generation HAP2 line were tested using DOV 102, 677. Mice were randomly divided into five ($n = 7$) dosage groups (vehicle, 12.5, 25, 50 and 75 mg/kg). After completion of the DOV 102, 677 treatment for binge alcohol drinking and a 7-day washout period, the 35 mice that participated in the alcohol study were then randomly divided into five ($n = 7$) dosage groups (vehicle, 12.5, 25, 50 and 75 mg/kg) and retrained using sucrose.

Forty-two mice comprising 15 females of the 35th generation HAP2 line, 12 females of the 37th generation HAP2 line and 15 males of the 14th generation HAP3 line were tested using 3-PBC. Mice were then randomly divided into seven ($n = 6$) dosage groups (vehicle, 30, 60, 80, 100, 200 and 300 mg/kg). After completion of the 3-PBC treatment for binge alcohol drinking and a 10-day washout period, 35 of the mice that participated in the alcohol study were randomly divided into six ($n = 7$) sucrose dosage groups (vehicle, 60, 80, 100, 200 and 300 mg/kg) and retrained using sucrose.

Statistical analysis

Given the number of male and female mice in the DOV 102, 677 and 3-PBC treatment groups, responding was initially analyzed using a mixed analysis of variance (ANOVA) for sex \times dose (2×4) collapsed over generation. However, because no sex or interaction effects were seen, data were reanalyzed using a univariate ANOVA for only dose. Thus, data obtained using amitifadine, DOV 102, 677 and 3-PBC were analyzed by separate univariate ANOVAs for binge alcohol or sucrose drinking followed by Dunnett's *post hoc* tests. BAC and responding were analyzed by Pearson correlation and repeated measures ANOVAs. The dissimilar composition of male/female mice selected to receive amitifadine in experiment 1 was due to the availability of mice at the time the experiment was being conducted, many of whom were obtained from a moderately large study evaluating affect-related behaviors (see Can *et al.* 2012) at one of the researchers' institutions.

Effects of amitifadine on locomotor activity

Amitifadine effects on locomotor activity were evaluated using mice randomly selected from the three binge sucrose experiments (see Supporting Information Fig. S1).

Experiment 2: effects of amitifadine and DOV 102, 677 on heavy (free-choice) drinking

Subjects

Thirty-six male and female HAP1 mice from the 44th generation were tested using amitifadine and a separate

cohort of 36 male and female HAP1 mice from the 49th generation were tested using DOV 102, 677. Lights were on from 8:00 PM to 8:00 AM, and drinking was measured during the dark part of the cycle using red illumination. Mice had ad-lib access to food and water. Procedures were approved by the Institutional Animal Care and Use Committee of Indiana University-Purdue University Indianapolis, and were conducted in strict adherence with the National Institutes of Health *Guide for the Care and Use of Laboratory Animals* at all institutions.

Compounds

Amitifadine was dissolved in isotonic saline to concentrations of 0.8–2.5 mg/ml. 3-PBC was first dissolved in 0.1 ml dimethyl sulfoxide (DMSO) and then brought to concentrations of 0.4–1.2 mg/ml in 1% DMSO/saline vehicle. DOV 102, 677 was dissolved in saline to concentrations of 1.5, 3.0 and 4.0 mg/ml. Injection volumes of all agents were 10 ml/kg administered *i.p.*

Procedural summary

Prior to administration of compounds, mice were given free-choice access to 10% alcohol for 3 weeks. Intakes were read and bottles side switched every other day. During drug testing, alcohol drinking was measured in the home cage beginning at the start of the dark part of the cycle. Drugs were given 30 minutes prior to measuring drinking. Intakes were measured directly on the cage to ± 0.05 ml every 2 hours from 8:00 AM to 2:00 PM using graduated sipper tubes. A single dose of amitifadine (0–25 mg/kg) was given on Tuesday and Thursday, while each dose of DOV 102, 677 (0–40 mg/kg) was given to all subjects in a Latin square design on Mondays and Thursdays.

Statistical analysis

Daily bihourly and overall drinking data were analyzed by mixed ANOVAs for dose \times time \times sex ($4 \times 4 \times 2$) to examine the effects of amitifadine on g/kg alcohol and ml/kg water drinking. Dose \times sex (4×2) repeated measures ANOVAs were used to analyze DOV 102, 677 drinking on g/kg alcohol and ml/kg water drinking due to the Latin square design. A repeated measures ANOVA of the bihourly data examined the changes in these variables with time for each compound. Dunnett's *post hoc* tests were performed to assess individual dose–response effects in comparison to saline control in amitifadine testing, and planned pairwise comparisons were used in DOV 102, 677 testing. All analyses for experiments 3 and 4 were performed using SPSS version 18 (IBM, Chicago, IL, USA).

Experiment 3: effects of amitifadine, DOV 102, 677, and 3-PBC on DD

Subjects

Forty-eight male and female HAP2 mice from 39th generation were tested using all three compounds. Amitifadine study required an additional 49 male and female HAP2 mice from the 37th generation following the observation of a trend toward an effect after the first cohort. Half of these mice had previously received alcohol access and were counterbalanced considering this factor. All mice were counterbalanced across sex and litter for run order and drug treatment and otherwise handled identically to those in experiment 2.

Compounds

Amitifadine was dissolved in isotonic saline to concentrations of 0.4–1.2 mg/ml, while DOV 102, 677 was used in concentrations of 3.0 and 4.0 mg/ml in saline. 3-PBC was first dissolved in 0.1 ml DMSO and then brought to concentrations of 1.5–6.0 mg/ml in 1% DMSO/saline vehicle. Injection volumes were 10 ml/kg administered i.p.

Procedural summary

Operant boxes consisted of a nose poke light, two levers, a house light and a descending sipper tube for saccharin reinforcement (0.032% w/v) (for details, see Oberlin & Grahame 2009). Boxes were controlled using MedPC IV software (Med Associates, Georgia, VT, USA). Mice underwent five stages of behavioral shaping, with the final, fifth stage serving as 0-second delay testing (Oberlin & Grahame 2009), serving as a reinforcer magnitude discrimination task prior to introduction of any delay to the large reward. Immediate reward amount started at 1 second of saccharin access, and was adjusted upward and downward by 0.1 second based on the mouse's choices. Forced trials of the non-selected reward followed two consecutive identical choices. Average adjusted amounts of the reward over the last 20 trials of the session served as the measure of adjusted amount. If mice failed to complete 20 trials during stages 1–4 of shaping, or achieve adjusted amounts of 1.6 seconds or higher on 3 consecutive days during stage 5, they were excluded from testing. Additionally, a sixth stage with a 10-second delay was performed to acclimate mice to the 10-second delay to the large reward used during drug testing. To ensure stable responding, mice that failed to achieve adjusted amounts of 0.6 second or lower on 3 consecutive days were excluded from testing. Use of a long delay to the large reinforcer ensured an impulsive baseline of behavior on which to detect any drug-induced attenuation of impulsivity (Oberlin *et al.* 2010).

All mice received 2-hour water access in their home cage at the end of daily testing. Mice received only one dose of each compound, but all mice received all compounds, except for replication 2 of amitifadine that only received this compound. Animals were injected immediately prior to placement in operant boxes and the commencement of DD testing. 3-PBC was first administered to mice in doses of 0–120 mg/kg, but the 120 mg/kg group was reduced to a 15 mg/kg dose following the observation of markedly decreased responding on the first day of testing. 3-PBC was tested for 4 days, as the 15 mg/kg group was run on one additional day to have equal data points for all groups. Amitifadine was administered in 0–12 mg/kg doses for 4 days during each replicate. DOV 102, 677 was tested for 4 days at 0–40 mg/kg doses.

Statistical analysis

Adjusted amounts were analyzed using factorial ANOVA of sex \times dose (2×4) using SPSS. As no sex or interaction effects were seen, data were reexamined by collapsing across sex using a univariate ANOVA for evaluation of dose. Dunnett's *post hoc* tests were performed to assess individual dose–response effects. The second replicate of amitifadine testing was analyzed separately to assess any alcohol pre-exposure effects, then in tandem with the first to assess effects of replication.

RESULTS

Experiment 1: operant binge drinking and BACs

Amitifadine dose dependently reduced binge alcohol responding rates, as shown by a significant dose effect [$F(3,18) = 15.284$, $P < 0.001$] (Fig. 1a). In contrast, sucrose responding was not significantly altered by any of the doses (Fig. 1b). DOV 102, 677 also dose dependently reduced responding rates, as shown by a significant dose effect [$F(4,24) = 7.604$, $P < 0.001$] (Fig. 2a). As with amitifadine, responding maintained by sucrose was not affected with DOV 102, 677 (Fig. 2b). Similar to the TUIs, 3-PBC also dose dependently reduced binge alcohol responding [$F(6,36) = 27.457$, $P < 0.001$] (Fig. 3a). However, responding maintained by sucrose was not affected, $P > 0.05$ (Fig. 3b).

Compared with BACs ($N = 6$) taken after the initial 30-minute session, there was a profound increase in BAC after the final 90-minute session [$F(1,5) = 200.13$, $P < 0.001$] (Fig. 4a). Responding maintained by alcohol was also markedly increased from the initial 30-minute to the final 90-minute session [$F(1,5) = 63.12$, $P < 0.001$] (Fig. 4b). To further evaluate the relationship between BAC and responding, Pearson product correlations were performed between BACs and level of responding for the

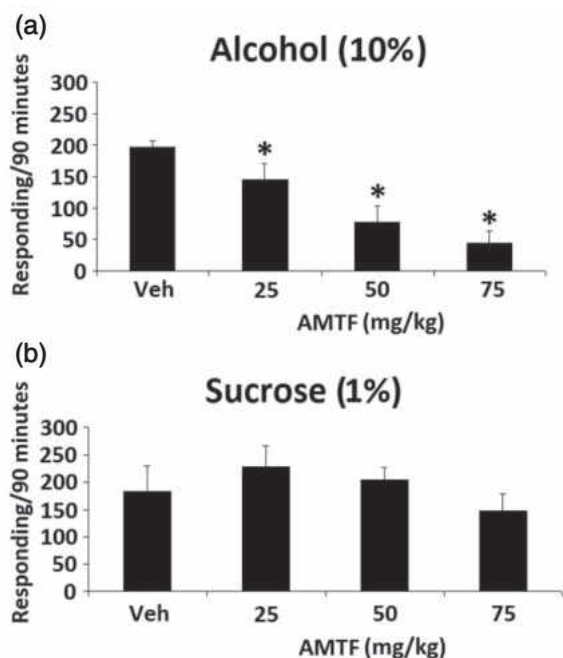


Figure 1 Amitifadine dose response on binge alcohol (10% v/v) responding with the vehicle and 25–75 mg/kg doses ($N=7$ per dose group) (a), and sucrose (1% w/v) responding with the vehicle and 25–75 mg/kg doses ($N=6$ per dose group) (b) in HAP mice. Data were analyzed by between-group ANOVAs and Dunnett's *post hoc* test. Drinking is measured as lever presses over 90 minutes (three 30-minute sessions), and the data are presented as mean \pm SEM. * $P \leq 0.05$, compared with vehicle control

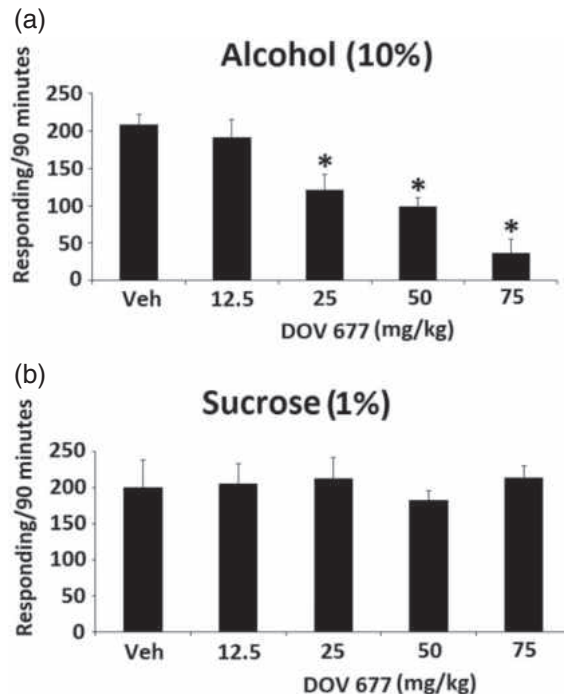


Figure 2 DOV 102, 677 dose response on binge alcohol (10% v/v) responding with the vehicle and 12.5–75 mg/kg doses ($N=7$ per dose group) (a), and sucrose (1% w/v) responding with the vehicle and 12.5–75 mg/kg doses ($N=7$ per dose group) (b) in HAP mice. Data were analyzed by between-group ANOVAs, and Dunnett's *post hoc* test. Drinking is measured as lever presses over 90 minutes (three 30-minute sessions), and the data are presented as mean \pm SEM. * $P \leq 0.05$, compared with vehicle control

first 30-minute and total 90-minute sessions. Significant positive correlations were observed between the BACs and level of responding for the first 30-minute session ($r = 0.849$, $P < 0.03$), and the total 90-minute session ($r = 0.774$, $P < 0.05$).

Supporting Information Fig. S1 illustrates the effects of oral amitifadine on horizontal activity (A) and stereotypy (B) 30 minutes prior to exposure in the open field. Amitifadine was without effect on either type of activity.

Experiment 2: heavy (free-choice) drinking

Over the course of 12 hours of drinking, amitifadine dose dependently reduced alcohol consumption, as shown by a main effect of dose [$F(3,28) = 25.95$, $P < 0.001$], with no effect of sex and/or interaction (Fig. 5a). *Post hoc* tests showed that the 8, 14 and 25 mg/kg doses all decreased alcohol intake relative to saline ($P < 0.01$). Effects of amitifadine were most pronounced early in the dark cycle, and began to wane over time; a repeated measures ANOVA showed an hour \times dose interaction on g/kg/hour [$F(15,160) = 5.44$, $P < 0.001$], justifying follow-up one-way ANOVAs at each timepoint, which revealed dose-dependent effects as indicated by the symbols in Fig. 5b. Interestingly, as alcohol intake decreased, mice appeared

to compensate by increasing water intake, as demonstrated by a main effect of dose on ml/kg water intake [$F(3,28) = 11.31$, $P < 0.001$], and Dunnett's *post hoc* tests showing that the 14 and 25 mg/kg doses increased water intake relative to saline ($P < 0.001$; Fig. 5c).

Six mice were lost during data collection using DOV 102, 677 to unknown illness (final $n = 18$). Similar to amitifadine, DOV 102, 677 decreased alcohol intake as demonstrated by a dose main effect in a repeated measures ANOVA on g/kg/day [$F(3,51) = 64.208$, $P < 0.001$] (Fig. 6a). Pairwise comparisons showed that the 15, 30 and 40 mg/kg doses all differed from saline ($P < 0.001$). A sex effect was observed [$F(1,17) = 6.600$, $P = 0.020$], consistent with prior data demonstrating that female mice drink more alcohol, and a dose \times sex interaction was also seen [$F(3,51) = 4.456$, $P = 0.007$]; however, this effect was driven by the higher baseline consumption of females, as a repeated measures ANOVA run without the saline dose revealed no interaction effect. Thus, data were collapsed across sex for additional analyses. Effects were again most pronounced early in the dark cycle; a repeated measures ANOVA showed an hour \times dose interaction [$F(15,270) = 7.754$, $P < 0.001$], justifying

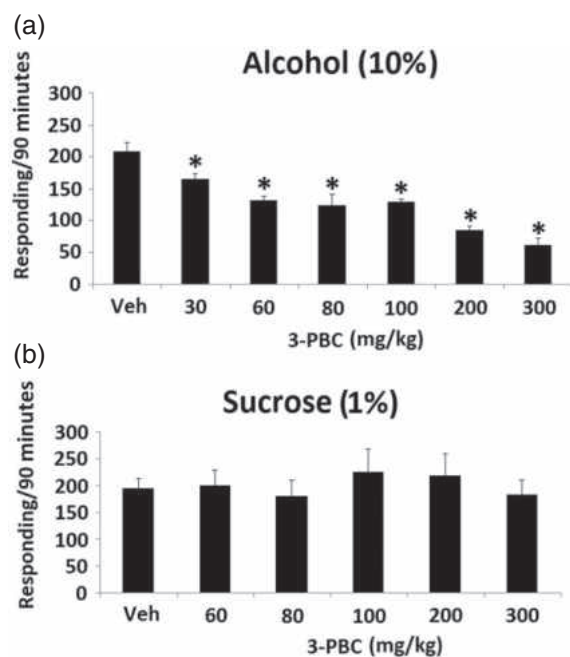


Figure 3 3-PBC dose response on binge alcohol (10% v/v) responding with the vehicle, and 30–300 mg/kg doses ($N=6$ per dose group) (a), and sucrose (1% w/v) responding with the vehicle, and 60–300 mg/kg doses ($N=7$ per dose group) (b) in HAP mice. Data were analyzed by between-group ANOVAs, and Dunnett's *post hoc* test. Drinking is measured as lever presses over 90 minutes (three 30-minute sessions), and the data are presented as mean \pm SEM. * $P \leq 0.05$, compared with vehicle control

pairwise comparisons of saline to all doses at all times of day which revealed dose-dependent effects as indicated by the symbols in Fig. 6b. Similar to amitifadine, DOV 102, 677 caused increased water intake that appeared to compensate for reduced alcohol consumption. A repeated measures ANOVA on ml/kg/day showed a main effect of dose [$F(3,51) = 2.990$, $P = 0.039$], and pairwise comparisons showed that the 30 and 40 mg/kg doses were significantly different from saline ($P < 0.05$; Fig. 6c).

Experiment 3: DD

Three subjects were excluded from the experiment after stage 4 of shaping due to an inability to complete a sufficient number of trials to generate adjusted amount data. Additionally, animals that did not complete 20 trials on at least 2 days of drug testing were excluded, resulting in the *ns* listed in the figure captions. 3-PBC did not affect impulsivity, as shown by no effect of dose on adjusted amount ($P > 0.5$) (Fig. 7c). Amitifadine did reduce impulsivity, as shown by a main effect of dose on adjusted amount [$F(3,71) = 3.92$, $P = 0.012$]. Dunnett's *post hoc* testing showed that the 8 mg/kg dose increased the adjusted amount relative to saline, demonstrative of decreased impulsivity ($P \leq 0.005$) (Fig. 7a). Surprisingly, the 12 mg/kg dose did not differ from saline, suggesting a

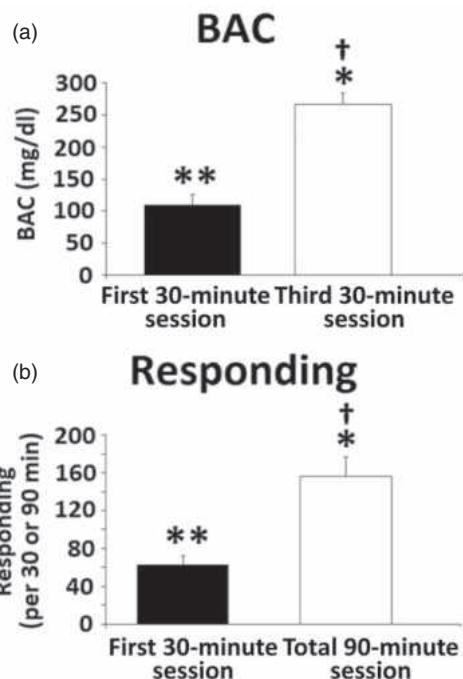


Figure 4 (a) BAC of HAP2 mice after the first and third 30-minute operant binge alcohol drinking sessions ($N=6$). (b) Number of lever presses of mice during the first 30-minute session ($N=6$) and the total responding after the entire 90-minute session. Data are presented as mean \pm SEM. Data were analyzed using repeated measures ANOVA with Dunnett's *post hoc* test. Pearson correlations were also performed. ** $P < 0.01$, compared with first 30-minute session. †Positive correlation between BAC and responding for first 30-minute session, $P < 0.03$. †Positive correlation between BAC and responding after entire 90-minute session, $P < 0.05$

non-dose-dependent effect for this compound. In contrast, DOV 102, 677 dose dependently decreased impulsivity as indicated by increases in the adjusted amount (Fig. 7b). This was supported by the main effect of dose [$F(2,23) = 6.33$, $P = 0.006$], and *post hoc* tests showing higher adjusted amounts in both the 30 and 40 mg/kg doses compared with the vehicle condition ($P < 0.005$) (Fig. 7b). No sex effects or interaction effects were seen.

DISCUSSION

Using an established model of binge alcohol drinking (Liu *et al.* 2011; Warnock *et al.* 2012), the present study demonstrated that the TUIs, amitifadine and DOV 102, 677, and the GABA_A $\alpha 1$ preferring ligand, 3-PBC, which exerts agonist effects on some, but antagonist effects at other GABA receptor subunits (Harvey *et al.* 2002; June & Eiler 2007), effectively reduce binge alcohol, but not binge sucrose drinking in HAP mice. These results indicate that increased activity in the dopaminergic, noradrenergic and serotonergic pathways may cause marked attenuation of binge drinking. In addition, given

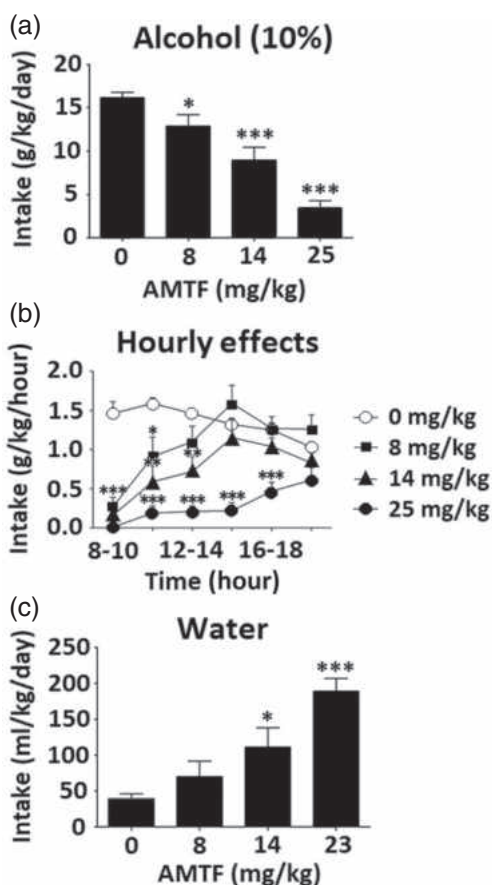


Figure 5 Effects of amitifadine on ethanol intake ($N=12$) (a), hourly alcohol (10% v/v) intake ($N=12$) (b), and water intake ($N=12$) (c). Data expressed as mean \pm SEM; significance expressed as compared with saline. * $P < 0.05$, ** $P < 0.01$, *** $P < 0.001$

the modulatory actions of 3-PBC (Harvey *et al.* 2002; June & Eiler 2007), along with the recent siRNA findings in P and HAD rats (Liu *et al.* 2011; Yang *et al.* 2011), the findings with 3-PBC provide critical support for the hypothesis that the GABA_A $\alpha 1$ subunit is important in the regulation of binge drinking.

Similar to the findings with binge drinking, both TUIs produced a selective dose-dependent reduction on free-choice drinking, which was used to emulate heavy drinking. These findings were accompanied by a concomitant dose-related elevation of water intake. The concomitant elevation in water intake provides support for the behavioral specificity of these compounds on alcohol consumption, consistent with specificity on binge drinking. While we did not assess BACs during free-choice drinking, intake amounts and patterns in saline-treated animals were similar to our prior reports where BAC levels exceeded 100 mg/dl by 2 hours after the onset of drinking (Matson & Grahame 2011). In the present study, because mice continuously had access to alcohol, we were able to accurately measure the duration of action of

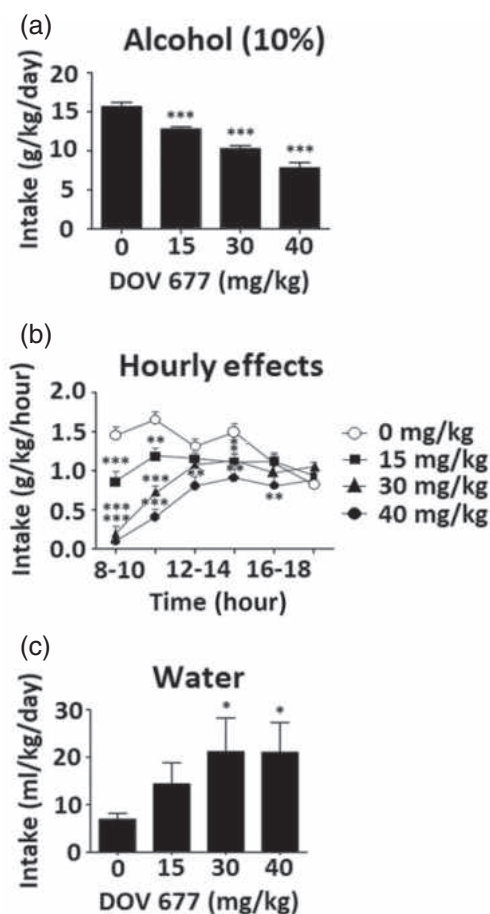


Figure 6 Effects of DOV 102, 677 on ethanol intake ($N=12$) (a), hourly alcohol (10% v/v) intake ($N=12$) (b), and water intake ($N=12$) (c). Data expressed as mean \pm SEM; significance expressed as compared with saline. * $P < 0.05$, ** $P < 0.01$, *** $P < 0.001$

these drugs. All DOV 102, 677 doses significantly suppressed alcohol intake for up to 6 hours, while all amitifadine doses reduced intake for up to 8 hours. Amitifadine was the most efficacious antagonist of the two compounds, reducing drinking by 70–100% of control levels early in the 12-hour period. To our knowledge, no approved AD has produced such potent, prolonged and selective suppression on excessive alcohol drinking. Given the microdialysis time course for the three monoamines following administration of the two agents (approximately 4 hours) (Popik *et al.* 2006; Golembiowska, Kowalska & Bymaster 2012), the prolonged duration of suppression on alcohol drinking for amitifadine and DOV 102, 677 may suggest the utility of further evaluation of both TUIs as putative alcohol antagonists in humans. Furthermore, the compensatory dose-related elevations in water intake with the TUIs in the heavy drinking model suggest the absence of toxic effects.

Consistent with their effects on binge and free-choice drinking, the two TUIs significantly attenuated cognitive

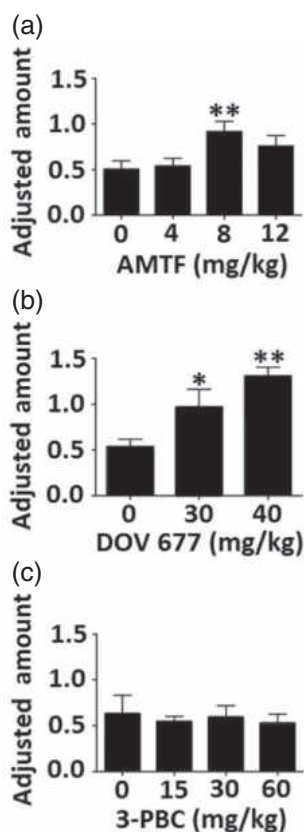


Figure 7 Effects of the three pharmacologically active compounds on delay discounting. Adjusted amounts are listed in seconds; a higher adjusted amount is representative of decreased impulsivity. [Ns for each group: (a) 7, 19, 23, 12; (b) 9, 10, 7; (c) 9, 10, 10, 9]. Data expressed as mean \pm SEM; significance expressed as compared with saline. * $P < 0.05$, ** $P < 0.01$, *** $P < 0.001$

impulsivity. However, while the effective dose response profiles for impulsivity, free-choice and binge drinking were relatively similar for DOV 102, 677, a different profile emerged for amitifadine. Specifically, the lowest effective amitifadine dose in reducing impulsivity and free-choice drinking was 8 mg/kg, while the lowest effective dose in suppressing binge drinking was 25 mg/kg. This difference in dose response for amitifadine may in part be explained by the usage of i.p. dosing in the impulsivity and free-choice drinking studies compared with using oral dosing in the binge studies. It is well documented that i.p. and oral routes differ significantly with respect to the absolute magnitude and the time course of increases in extracellular catecholamines and behavioral effects. Intraperitoneal injection has been reported to be twice as potent, as oral in increases in extracellular catecholamines such as DA, and neurobehavioral effects (Gerasimov *et al.* 2000). In addition, it is also well established that the quantitatively different response profiles between oral and i.p. are a function of bioavailability (Chan *et al.* 1981). Specifically, the lower bioavailability

for the oral route is presumably due to the slower absorption from the gastrointestinal tract, and a greater degree of metabolism. Nevertheless, while more research is required to clarify the differences in dose response profiles of amitifadine across behavioral assays and genotypes, the seminal oral dose–response function that produced AD-like effects (5–20 mg/kg) (Skolnick 2012) was comparable to i.p. doses that produced effectiveness in the impulsivity and free-choice drinking studies in mice. Hence, these findings suggest that in some behavioral assays, comparable potency is observed with amitifadine, independent of route of drug administration and rodent used. Interestingly, the dose–response function seen in our data for DOV 102, 677 on impulsivity, free-choice and binge drinking was similar across routes of administration.

Amitifadine is an unbalanced TUI, showing preferential inhibition to the 5-HT transporter (i.e. SERT, NET and DAT; 1:2:8) (Skolnick & Basile 2007). Amitifadine (10 mg/kg) markedly increases extracellular levels of DA, NE and 5-HT in the prefrontal cortex to 208, 274 and 412%, above baseline 100 minutes after administration, respectively. Unlike amitifadine, DOV 102, 677 is a balanced inhibitor of DA, NE and 5-HT transporters with potency close to a 1:1:1 ratio (Popik *et al.* 2006). DOV 102, 677 (20 mg/kg i.p.) increased extracellular levels of 5-HT and DA in the prefrontal cortex to 280 and 320%, respectively, above baseline 100 minutes after administration (Popik *et al.* 2006). NE levels increased linearly to a maximum of 348% at 240 minutes post-dosing. Thus, relative to amitifadine, DOV 102, 677 is a preferential DAT inhibitor, and our results are consistent with dopaminergic agonists that decrease impulsivity (Sagvolden 2000; Oberlin *et al.* 2010). Thus, taken together, while route of administration may be a salient factor to explain the differential dose response between the two TUIs, amitifadine's capacity to modulate both DA and 5-HT, and the capacity of DOV 102, 677 to primarily modulate DA may also contribute to the differential dose response function. Moreover, it is well established that 5-HT regulates the activity of many neurotransmitters, particularly DA neurons of the mesoaccumbens circuitry (Fink & Göthert 2007; Dalley & Roiser 2012). Hence, given the greater activity of 5-HT, along with the i.p. route, lower amitifadine doses would be needed to attenuate impulsivity and heavy drinking in the present study.

A general consensus in the preclinical and clinical studies is that a reduction in brain 5-HT appears to be important for increasing impulsivity (Bevilacqua *et al.* 2010; Dalley & Roiser 2012). In the present study, the TUIs may decrease impulsive behavior via increasing release of DA/NE via serotonergic activity in addition to their direct effects on the neurotransmitter transporters (see Skolnick & Basile 2007). Furthermore, increased

5-HT tone has been associated with a reduced potential for reinforcement among drugs that increase monoaminergic neurotransmission, lessening abuse potential (Wee, Carroll & Woolverton 2006). The failure of amitifadine to exert activating effects in the present study is also consistent with a greater engagement of the 5-HT transporters relative to DA, suggesting that amitifadine may be a good candidate for impulsivity reduction without motor or rewarding side effects (Howell *et al.* 2007). The lack of motor activating effects is also consistent with a recent preclinical report from others (Golembiowska *et al.* 2012) as well as our laboratory (Warnock *et al.* 2012).

The inverted U-shaped dose–response curve observed with amitifadine on impulsivity, however, is worth noting, and similar effects on cognitive-related behaviors have been reported in the literature (Baldi & Bucherelli 2005) with agents used to treat impulsivity (Tannock, Schachar & Logan 1995). Unfortunately, it is not easy to elucidate the mechanisms on which this effect is based (see Baldi & Bucherelli 2005). However, in relation to the present study, it is possible the neuropharmacological effects related to the descending limb of the dose–response curve may be related to stereotypy, non-specific excitation or serotonergic related effects unrelated to impulsivity. Any, or several of the neuropharmacological effects noted, may have interfered with the attenuation of impulsivity.

In contrast to the TUIs, the GABA_A α 1 preferring ligand, 3-PBC, was ineffective in altering cognitive impulsivity. The rationale for this is not clear at present; however, it may reflect the fact that the neural mechanism(s) regulating impulsivity in the HAP mice may be mediated via monoamines only, while excessive drinking in the HAP mice may be regulated via GABA, monoamines, as well as other neurotransmitters (see McBride & Li 1998). Nevertheless, the finding with 3-PBC in the present study contrasts the report by Murphy *et al.* (2012) where the GABA_A receptor antagonist bicuculline blocked the increase in impulsivity produced by the agonist muscimol. However, it should be noted that this study used a five-choice serial reaction time task, which measures motor impulsivity, unlike the cognitive impulsivity-based DD assay of the present study. Different measures of impulsivity may have distinct underlying neuropharmacological profiles (Dalley & Roiser 2012).

In conclusion, the data of the present study provide compelling evidence that a pharmacologic association exists between two modes of excessive drinking (i.e. binge and heavy drinking) and cognitive impulsivity using two TUIs, while a dissociation exists using a GABAergic ligand. These findings suggest that while the neuronal mechanism(s) that regulate excessive drinking may directly involve DA, NE, 5-HT and GABAergic activity, the

neuronal mechanism(s) regulating cognitive impulsivity appear to involve only DA, NE and 5-HT activity. Furthermore, the data from the present and our previous study (Yang *et al.* 2012) provide support for the hypothesis that elevations in 5-HT and DA neurotransmission may be critical in the prolonged suppression of alcohol drinking, as the highest TUI doses were effective in the free-choice model for 6–8 hours. From a clinical perspective, these findings are important because a ‘single’ TUI dose may be capable of sustained reduction of heavy drinking in the absence of untoward effects, increasing efficacy in human alcoholics (Yang *et al.* 2012). Finally, given the safety profile of amitifadine and DOV 102, 677 (Skolnick 2012; Tran *et al.* 2012), and their proposed low abuse liability, we hypothesize that both agents would be effective in treating the co-occurrence of excessive drinking and impulsivity in humans.

Acknowledgements

Experiments 1 and 2 were financed by grant AA10406 to HLJ from the National Institute of Alcohol Abuse and Alcoholism (NIAAA). HAP mice were provided by AA015512 to Lawrence Lumeng. Experiments 3 and 4 were supported by grant AA017611 to David Crabb.

DISCLOSURE

The authors declare that over the past 5 years, DOV Pharmaceutical, Inc., the original manufacturer of amitifadine (DOV 21, 947) and DOV 102, 677, has provided funding for past projects performed in the laboratory of HLJ; however, it provided no funds for any of the studies included in this article. HLJ is currently a consultant for Euthymics Bioscience, the current licensee of amitifadine and DOV 102, 677.

References

- Baldi E, Bucherelli C (2005) The inverted ‘u-shaped’ dose-effect relationships in learning and memory: modulation of arousal and consolidation. *Nonlinearity Biol Toxicol Med* 3:9–21.
- Bevilacqua L, Doly S, Kaprio J, Yuan Q, Tikkanen R, Paunio T, Zhou Z, Wedenoja J, Maroteaux L, Diaz S, Belmer A, Hodgkinson CA, Dell’osso L, Suvisaari J, Coccaro E, Rose RJ, Peltonen L, Virkkunen M, Goldman D (2010) A population-specific HTR2B stop codon predisposes to severe impulsivity. *Nature* 468:1061–1066.
- Bickel WK, Odum AL, Madden GJ (1999) Impulsivity and cigarette smoking: delay discounting in current, never, and ex-smokers. *Psychopharmacology (Berl)* 146:447–454.
- Can A, Grahame NJ, Gould TD (2012) Affect-related behaviors in mice selectively bred for high and low voluntary alcohol consumption. *Behav Genet* 42:313–322.
- Center for Disease Control and Prevention (2001) Alcohol-related mortality and years lost. US, [1990–2000]. *MMWR Morb Mortal Wkly Rep* 50:1064–1065.

- Chan K, Davison SC, Dehghan A, Hyman N (1981) The effect of neostigmine on pyridostigmine bioavailability in myasthenic patients after oral administration. *Methods Find Exp Clin Pharmacol* 3:291–296.
- Chikritzhs TN, Jonas HA, Stockwell TR, Heal PF, Dietze PM (2001) Mortality and life-years lost due to alcohol: a comparison of acute and chronic causes. *Med J Aust* 174:281–284.
- Courtney KE, Polich J (2009) Binge drinking in young adults: data, definitions, and determinants. *Psychol Bull* 135:142–156.
- Dalley JW, Roiser JP (2012) Dopamine, serotonin and impulsivity. *Neuroscience* 215:42–58.
- Dawson DA, Grant BF, Li T-K (2005) Quantifying the risks associated with exceeding recommended drinking limits. *Alcohol Clin Exp Res* 34:1334–1345.
- Dick DM, Smith G, Olausson P, Mitchell SH, Leeman RF, O'Malley SS, Sher K (2010) Understanding the construct of impulsivity and its relationship to alcohol use disorders. *Addict Biol* 15:217–226.
- Economidou D, Theobald DE, Robbins TW, Everitt BJ, Dalley JW (2012) Norepinephrine and dopamine modulate impulsivity on the five-choice serial reaction time task through opponent actions in the shell and core sub-regions of the nucleus accumbens. *Neuropsychopharmacology* 37:2057–2066.
- Fink KB, Göthert M (2007) 5-HT receptor regulation of neurotransmitter release. *Pharmacol Rev* 59:360–417.
- Gerasimov MR, Franceschi M, Volkow ND, Gifford A, Gatley SJ, Marsteller D, Molina PE, Dewey SL (2000) Comparison between intraperitoneal and oral methylphenidate administration: a microdialysis and locomotor activity study. *J Pharmacol Exp Ther* 295:51–57.
- Golembiowska K, Kowalska M, Bymaster FP (2012) Effects of the triple reuptake inhibitor amitifadine on extracellular levels of monoamines in rat brain regions and on locomotor activity. *Synapse* 66:435–444.
- Harris RA, Trudell JR, Mihic SJ (2008) Ethanol's molecular targets. *Sci Signal* 1:re7.
- Harvey SC, Carroll MR, Foster KL, McKay PF, Collette Grey C, McCane S, Rancia C, Mason D, Seyoum R, Jones CM, Ma C, Cook JM, June HL (2002) The GABA_A receptor α 1 subtype in the ventral pallidum regulates alcohol-seeking behaviors. *J Neurosci* 22:3765–3775.
- Hoffman WF, Moore M, Templin R, McFarland B, Hitzemann RJ, Mitchell SH (2006) Neuropsychological function and delay discounting in methamphetamine-dependent individuals. *Psychopharmacology (Berl)* 188:162–170.
- Howell LL, Carroll FI, Votaw JR, Goodman MM, Kimmel HL (2007) Effects of combined dopamine and serotonin transporter inhibitors on cocaine self-administration in rhesus monkeys. *J Pharmacol Exp Ther* 320:757–765.
- Institute of Medicine (1990) *Broadening the Base of Treatment for Alcohol Problems*. Washington, DC: National Academy Press.
- Johnson BA (2008) Update on neuropharmacological treatments for alcoholism: scientific basis and clinical findings. *Biochem Pharmacol* 75:34–56.
- June HL, Eiler WLA (2007) Dopaminergic and GABAergic regulation of alcohol-motivated behaviors: novel neuroanatomical substrates. In: Sibley DR, Hanin I, Kuhar M, Skolnick P, eds. *Handbook of Contemporary Neuropharmacology*, pp. 1–72. Hoboken, NJ: Wiley & Sons.
- June HL, Gilpin NW (2010) Operant self-administration models for testing the neuropharmacological basis of ethanol consumption in rats. *Curr Protoc Neurosci*. Chapter 9: Unit 9.12.1–26. doi: 10.1002/0471142301.ns0912s51.
- June HL Sr., Foster KL, Eiler WJ 2nd, Goergen J, Cook JB, Johnson N, Mensah-Zoe B, Simmons JO, June HL Jr., Yin W, Cook JM, Homanics GE (2007) Dopamine and benzodiazepine-dependent mechanisms regulate the EtOH-enhanced locomotor stimulation in the GABAA α 1 subunit null mutant mice. *Neuropsychopharmacology* 32:137–152.
- King AC, de Wit H, McNamara PJ, Cao D (2011) Rewarding, stimulant, and sedative alcohol responses and relationship to future binge drinking. *Arch Gen Psychiatry* 68:389–399.
- Kirby KN, Petry NM, Bickel WK (1999) Heroin addicts have higher discount rates for delayed rewards than non-drug-using controls. *J Exp Psychol Gen* 128:78–87.
- Lejuez CW, Magidson JF, Mitchell SH, Sinha R, Stevens MC, de Wit H (2010) Behavioral and biological indicators of impulsivity in the development of alcohol use, problems, and disorders. *Alcohol Clin Exp Res* 34:1334–1345.
- Liu J, Yang AR, Kelly T, Puche A, Esoga C, June HL Jr., Elnabawi A, Merchenthaler I, Sieghart W, June HL Sr., Aurelian L (2011) Binge alcohol drinking is associated with GABAA α 2-regulated toll-like receptor 4 (TLR4) expression in the central amygdala. *Proc Natl Acad Sci U S A* 108:4465–4470.
- Matson LM, Grahame NJ (2011) Pharmacologically relevant intake during chronic, free-choice drinking rhythms in selectively bred high alcohol-preferring mice. *Addict Biol*. doi: 10.1111/j.1369-1600.2011.00412.x.
- McBride WJ, Li TK (1998) Animal models of alcoholism: neurobiology of high alcohol-drinking behavior in rodents. *Crit Rev Neurobiol* 12:339–369.
- Mitchell JM, Tavares VC, Fields HL, D'Esposito M, Boettiger CA (2007) Endogenous opioid blockade and impulsive responding in alcoholics and healthy controls. *Neuropsychopharmacology* 32:439–449.
- Murphy ER, Fernando AB, Urcelay GP, Robinson ES, Mar AC, Theobald DE, Dalley JW, Robbins TW (2012) Impulsive behaviour induced by both NMDA receptor antagonism and GABAA receptor activation in rat ventromedial prefrontal cortex. *Psychopharmacology (Berl)* 219:401–410.
- Naimi TS, Brewer RD, Mokdad A, Denny C, Serdula MK, Marks JS (2003) Binge drinking among US adults. *JAMA* 289:70–75.
- NIAAA (2004) National Institute on Alcohol Abuse and Alcoholism Council approves definition of binge drinking. NIAAA Newsletter, Vol. 3. Available at: http://pubs.niaaa.nih.gov/publications/Newsletter/winter2004/Newsletter_Number3.pdf. Accessed 27 September 2013.
- Oberlin BG, Grahame NJ (2009) High alcohol preferring mice are more impulsive than low alcohol preferring mice as measured in the delay discounting task. *Alcohol Clin Exp Res* 33:1–10.
- Oberlin BG, Bristow RE, Heighton ME, Grahame NJ (2010) Pharmacologic dissociation between impulsivity and alcohol drinking in high alcohol preferring mice. *Alcohol Clin Exp Res* 34:1363–1375.
- Petry NM (2001) Delay discounting of money and alcohol in actively using alcoholics, currently abstinent alcoholics, and controls. *Psychopharmacology (Berl)* 154:243–250.
- Popik P, Krawczyk M, Golembiowska K, Nowak G, Janowsky A, Skolnick P, Lippa A, Basile AS (2006) Pharmacological profile of the 'triple' monoamine neurotransmitter uptake inhibitor, DOV 102 677. *Cell Mol Neurobiol* 26:857–873.
- Rachlin H, Green L (1972) Commitment, choice and self-control. *J Exp Anal Behav* 17:15–22.

- Richards JB, Mitchell SH, de Wit H, Seiden LS (1997) Determination of discount functions in rats with an adjusting-amount procedure. *J Exp Anal Behav* 67:353–366.
- Rubio G, Jiménez M, Rodríguez-Jiménez R, Martínez I, Avila C, Ferre F, Jiménez-Arriero MA, Ponce G, Palomo T (2008) The role of behavioral impulsivity in the development of alcohol dependence: a 4-year follow-up study. *Alcohol Clin Exp Res* 32:1681–1687.
- Sagvolden T (2000) Behavioral validation of the spontaneously hypertensive rat (SHR) as an animal model of attention-deficit/hyperactivity disorder (AD/HD). *Neurosci Biobehav Rev* 24:31–39.
- Simon O'Brien E, Legastelois R, Houchi H, Vilpoux C, Alaux-Cantin S, Pierrefiche O, André E, Naassila M (2011) Fluoxetine, desipramine, and the dual antidepressant milnacipran reduce alcohol self-administration and/or relapse in dependent rats. *Neuropsychopharmacology* 36:1518–1530.
- Skolnick P (2012) Triple-uptake inhibitors (broad spectrum antidepressants). In: Peters JU, ed. *Polypharmacology in Drug Discovery*, pp. 361–380. New York: Wiley & Sons Inc.
- Skolnick P, Basile AS (2007) Triple reuptake inhibitors ('broad spectrum' antidepressants). *CNS Neurol Disord Drug Targets* 6:141–149.
- Tannock R, Schachar R, Logan G (1995) Methylphenidate and cognitive flexibility: dissociated dose effects in hyperactive children. *J Abnorm Child Psychol* 23:235–266.
- Tizzano JP, Stribling DS, Perez-Tilve D, Strack A, Frassetto A, Chen RZ, Fong TM, Shearman L, Krieter PA, Tschöp MH, Skolnick P, Basile AS (2008) The triple uptake inhibitor (1R,5S)-(+)-1-(3,4-dichlorophenyl)-3-azabicyclo[3.1.0]hexane hydrochloride (DOV 21947) reduces body weight and plasma triglycerides in rodent models of diet-induced obesity. *J Pharmacol Exp Ther* 324:1111–1126.
- Town M, Naimi TS, Mokdad AH, Brewer RD (2006) Health care access among U.S. adults who drink alcohol excessively: missed opportunities for prevention. *Prev Chronic Dis* 3: A53.
- Tran P, Skolnick P, Czobor P, Huang NY, Bradshaw M, McKinney A *et al.* (2012) Efficacy and tolerability of the novel triple reuptake inhibitor amitifadine in the treatment of patients with major depressive disorder: a randomized, double-blind, placebo-controlled trial. *J Psychiatr Res* 46:64–71.
- Vanderveen JW, Cohen LM, Watson NL (2012) Utilizing a multimodal assessment strategy to examine variations of impulsivity among young adults engaged in co-occurring smoking and binge drinking behaviors. *Drug Alcohol Depend* 127:150–155.
- Warnock KT, Yang AR, Yi HS, June HL Jr., Kelly T, Basile AS, Skolnick P, June HL (2012) Amitifadine, a triple monoamine uptake inhibitor reduces binge drinking and negative affect in an animal model of co-occurring alcoholism and depression symptomatology. *Pharmacol Biochem Behav* 103:111–118.
- Wee S, Carroll FI, Woolverton WL (2006) A reduced rate of in vivo dopamine transporter binding is associated with lower relative reinforcing efficacy of stimulants. *Neuropsychopharmacology* 31:351–362.
- Wilhelm CJ, Mitchell SH (2008) Rats bred for high alcohol drinking are more sensitive to delayed and probabilistic outcomes. *Genes Brain Behav* 7:705–713.
- Winstanley CA, Dalley JW, Theobald DE, Robbins TW (2004) Fractionating impulsivity: contrasting effects of central 5-HT depletion on different measures of impulsive behavior. *Neuropsychopharmacology* 29:1331–1343.
- Yang AR, Liu J, Yi HS, Warnock KT, Wang M, June HL Jr., Puche AC, Elnabawi A, Sieghart W, Aurelian L, June HL Sr. (2011) Binge drinking: in search of its molecular target via the GABA(A) receptor. *Front Neurosci* 5:1–9.
- Yang AR, Yi HS, Warnock KT, Mamczarz J, June HL Jr., Mallick N, Krieter PA, Tonelli L, Skolnick P, Basile AS, June HL Sr. (2012) Effects of the triple monoamine uptake inhibitor DOV 102 677 on alcohol-motivated responding and antidepressant activity in alcohol-preferring (P) rats. *Alcohol Clin Exp Res* 36:863–873.

SUPPORTING INFORMATION

Additional Supporting Information may be found in the online version of this article at the publisher's web-site:

Figure S1 Effects of amitifadine on HAP mice at the 12–50 mg/kg doses compared with vehicle on horizontal activity (A) and stereotypy (B) for a 45-minute open field session ($N = 7$ per dose group).



Cite this: *Org. Biomol. Chem.*, 2015, **13**, 10705

Received 29th July 2015,
Accepted 3rd September 2015

DOI: 10.1039/c5ob01572c

www.rsc.org/obc

Synthesis of aza and carbocyclic β -carbolines for the treatment of alcohol abuse. Regiospecific solution to the problem of 3,6-disubstituted β - and aza- β -carboline specificity†

V. V. N. Phani Babu Tiruveedhula,^a Kashi Reddy Methuku,^a Jeffrey R. Deschamps^b and James M. Cook^{*a}

A novel two step protocol was developed to gain regiospecific access to 3-substituted β - and aza- β -carbolines, 3-PBC (**1**), 3-ISOPBC (**2**), β CCt (**3**), 6-aza-3-PBC (**4**) and 6-aza-3-ISOPBC (**5**). These β -carbolines (**1–3**) are potential clinical agents to reduce alcohol self-administration, especially 3-ISOPBC·HCl (**2·HCl**) which appears to be a potent anti-alcohol agent active against binge drinking in a rat model of maternally deprived (MD) rats. The method consists of two consecutive palladium-catalyzed reactions: a Buchwald–Hartwig amination followed by an intramolecular Heck-type cyclization in high yield.

Introduction

β -Carbolines, aza- β -carbolines and their derivatives are important targets in synthetic chemistry.¹ In addition, they are found in a large number of natural products, many of which demonstrate novel biological activity, especially in regard to the reduction of alcohol self-administration [binge drinking (BD)]. This is proposed to be due to the activity at the benzodiazepine site of the GABA_A receptor.² Surprisingly, BD kills six people a day, most of which are men, and approximately 88 000 people die from alcohol related issues annually making it the third leading preventable cause of death in the United States.³ In 2006, this alcohol misuse cost the US government approximately \$223.5 billion dollars.³ BD (Blood-alcohol level ≥ 0.08 g% in a 2 hour period) is one form of excessive drinking and because of it, alcohol addiction and dependence remain a significant public health concern.⁴ Maternal separation and early life events can cause profound neurochemical and behavioral alterations in childhood that persist into adulthood, enhance the risk to develop alcohol use disorders and excessive drinking.^{5–7} Consequently, the development of clinically safe and cost effective therapeutic agents to reduce alcohol

addiction and dependence remain essential for the future treatment of alcoholism.^{8,9}

One influence on alcohol abuse is known to be mediated by GABA_A receptors, the major inhibitory chloride ion gated channels with γ -aminobutyric acid (GABA) as the endogenous ligand in the central nervous system. It plays a vital role in several neuronal disorders including anxiety, epilepsy, insomnia, depression, bipolar disorder, schizophrenia, as well as mild cognitive impairments and Alzheimer's disease.^{10–15} The pentameric structure of the GABA_A receptor is made up of 2 α , 2 β and 1 γ subunits, with a higher distribution of the α 1-subunit in the mesolimbic system of the ventral pallidum (VP) possibly playing an important role in regulating alcohol abuse.^{16–20} However, the precise neuromechanisms of regulating alcohol-seeking behavior remain unknown. In addition to the ventral pallidum, there is now compelling evidence that the GABA_A receptors within the striatopallidal and extended amygdala system are involved in the 'acute' reinforcing actions of alcohol.^{21–23}

To evaluate the role of the α 1 receptor in regulating alcohol reinforcement, the orally active β -carbolines 3-propoxy- β -carboline hydrochloride **1·HCl** (3-PBC·HCl) and β -carboline-3-carboxylate-*tert*-butyl ester **3** (β CCt), the mixed benzodiazepine (BDZ) agonist-antagonists with binding selectivity at the α 1 Bz/GABA_A receptor were developed (see Fig. 1).^{18,24,25} Behavioral studies in several species (*e.g.*, rats, mice, primates) show that these ligands were BDZ antagonists, at the α 1 Bz/GABA_A subtype exhibiting competitive binding-site interactions with BDZ agonists over a broad range of doses.^{18,24,26} In studies which involved the α 1 subtype, they were shown to selectively reduce alcohol-motivated behaviors and more importantly,

^aDepartment of Chemistry and Biochemistry, University of Wisconsin-Milwaukee, Milwaukee, WI 53201, USA. E-mail: capncook@uwm.edu

^bCenter for Biomolecular Science and Engineering, Naval Research Laboratory, Code 6930, Washington, D. C. 20375, USA

† Electronic supplementary information (ESI) available: Copies of spectra and crystallographic information files in CIF format. CCDC 1040831–1040833 and 1044936. For ESI and crystallographic data in CIF or other electronic format see DOI: 10.1039/c5ob01572c

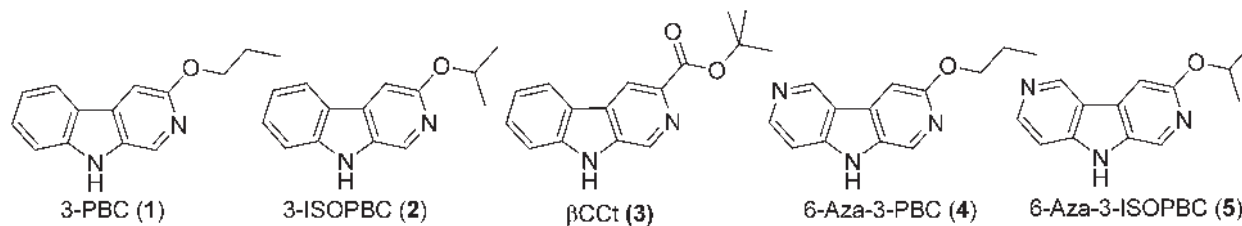


Fig. 1 Structures of 3-PBC (1), 3-ISOPBC (2), βCct (3), 6-aza-3-PBC (4) and 6-aza-3-ISOPBC (5).

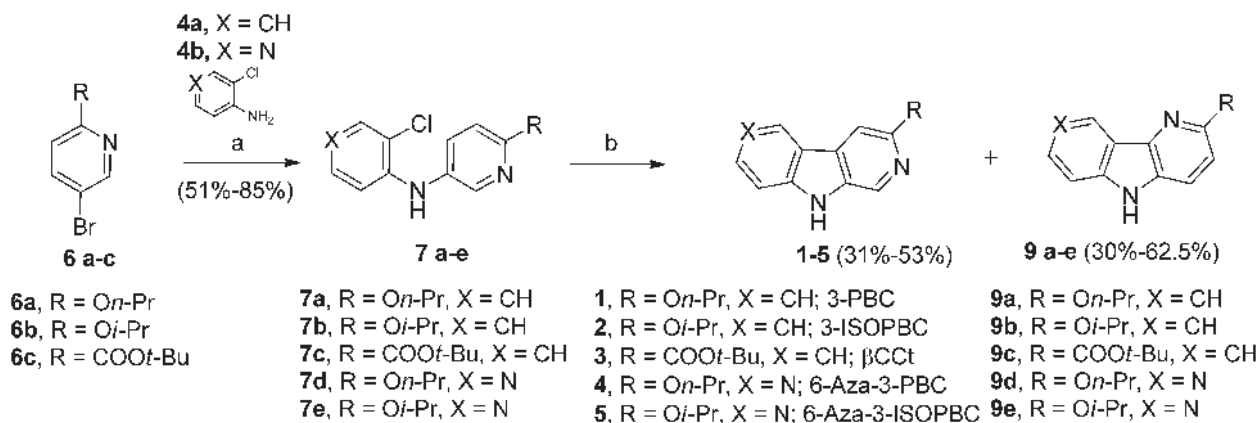
3-PBC·HCl significantly reduced alcohol self-administration and reduced craving in baboons.²⁶ β-Carbolines **1·HCl** and **3** displayed mixed weak agonist-antagonist profiles *in vivo* in alcohol preferring (P) and high alcohol drinking (HAD) rats.^{18,26–28} Therefore, in addition to their use to study the molecular basis of alcohol reinforcement, α1 Bz β-carboline ligands which display mixed pharmacological antagonist-agonist activity in alcohol P and HAD rats may be capable of reducing alcohol intake while eliminating or greatly reducing the anxiety associated with habitual alcohol, abstinence or detoxification.^{18,28–30} Consequently, these types of ligands may be ideal clinical agents for the treatment of alcohol dependent individuals.

Results and discussion

Previously, the β-carbolines **1** and **3** have been synthesized from DL-tryptophan. The overall yield of **1** (*via* 6 steps) as reported previously was 8%, while the combined yield of **3** (5 steps) was 35%. A few key steps occurred in low yields which was something of which we sought to improve on^{31–34} in a continued effort to find more potent subtype selective ligands for GABA_A receptors. This interest resulted in a short and concise synthesis of **1** and **3**. In 2011, a palladium catalyzed two-step protocol for the synthesis of **1**, and **3** as well as analogs of **1** was reported.³⁵ In the search for a more potent subtype selec-

tive ligand for the GABA_A receptor, with the knowledge that many 3-substituted β-carbolines and more water soluble aza-β-carbolines might exhibit greater subtype selectivity at α1β_{2/3}γ2 BZR/GABAergic receptors,^{31–33,36–38} the ligands 3-ISOPBC (**2**), 6-aza-3-PBC (**4**), and 6-aza-3-ISOPBC (**5**) were designed (see Fig. 1) and synthesized using a two-step protocol (Scheme 1).

As shown in Scheme 1, bromopyridines **6a–c**^{39,40} were reacted with anilines **4a–b** in toluene at 100–140 °C in the presence of 5 mol% Pd(OAc)₂ and 7.5 mol% X-Phos to obtain the corresponding diarylamines **7a–e** in moderate to good yields. Unfortunately, the intramolecular Heck cyclization [Pd(OAc)₂, (*t*-Bu)₃P·HBF₄, K₂CO₃, DMA, 120 °C] of **7a–e** afforded both the β-carbolines **1–5** (individually) and their regioisomeric δ-carbolines **9a–e**, respectively. Carbolines **2**, **3**, **9a**, and **9d** were subjected to X-ray crystallographic analysis (see Fig. 2, Scheme 4, and the ESI†) to confirm the regiochemistry. Although this protocol permitted synthesis of β-carbolines on gram scale for *in vivo* studies, occasionally the first step in the Buckwald–Hartwig coupling failed to give complete conversion into the carboline. This complicated purification for the diarylamine was difficult to purify *via* column chromatography because the diarylamine and one of the starting anilines had almost identical *R_f* values. Furthermore, in the case of the water soluble aza-β-carboline the yields (51%) were very poor and importantly, since the second step was not regioselective, this required careful purification to remove the unwanted δ-carboline present in 30 to 62.5% yield (Scheme 1). Interest-



Scheme 1 Synthesis of substituted carboline analogues. Reagents and conditions: (a) Pd(OAc)₂, X-Phos, Cs₂CO₃, toluene, 100–140 °C, 15–24 h (b) Pd(OAc)₂, (*t*-Bu)₃P·HBF₄, K₂CO₃, DMA, 120 °C, 16 h.

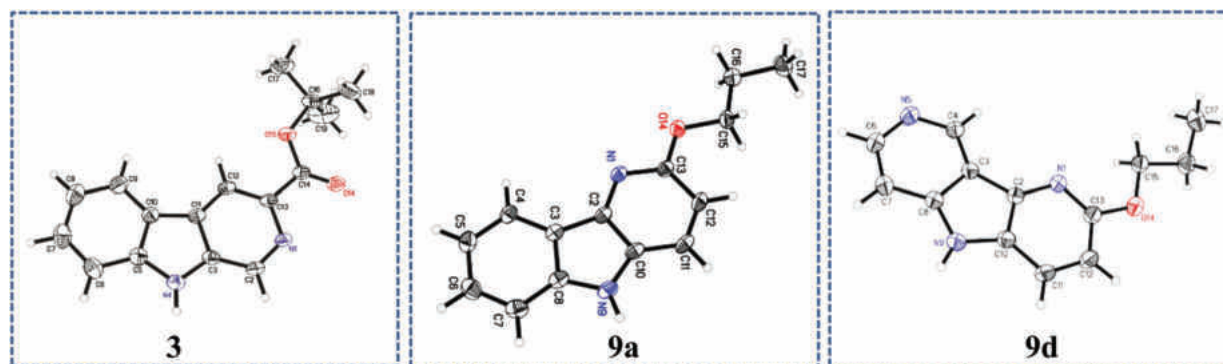
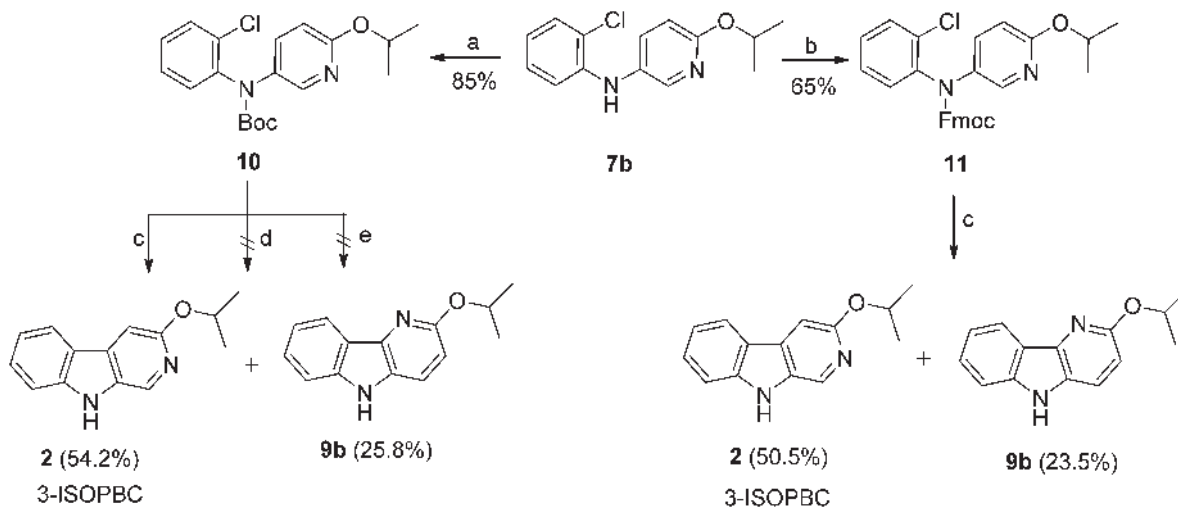


Fig. 2 ORTEP view of the crystal structure of substituted carbolines **3**, **9a**, and **9d** (displacement ellipsoids are at the 50% level (β -carboline numbering not followed).

ingly, the *in vivo* results (unpublished) for 3-isopropoxy- β -carboline hydrochloride **2**·HCl (3-ISOPBC·HCl) carried out in maternally deprived rats for binge drinking decreased dramatically this self-administration compared to **1**·HCl without affecting the overall activity of the rats (*i.e.* no sedation). This important finding led to the interest in a regiospecific synthesis of 3-ISOPBC (**2**) on large scale.

The revised synthetic strategy for the regiospecific synthesis of **2** began with the protection of the intermediate amine **7b** (N_a -H) with bulkier groups such as *tert*-butyloxycarbonyl (Boc) **10** or a fluorenylmethyloxy group (Fmoc) **11**, which might block the formation of the Pd^{II} π -complex that is required to obtain the undesired regioisomeric δ -carboline. The Boc protected amine **10** was easily accessible by treating the amine **7b** with di-*tert*-butyl dicarbonate (Boc)₂O and 4-(dimethylamino)pyridine (DMAP) in good yield (85%). The Fmoc protected amine **11** was synthesized under solvent free conditions by reaction of the amine **7b** and Fmoc-Cl by microwave

irradiation at 80 °C in moderate yield (65%, Scheme 2).⁴¹ Once protected, diarylamines **10** and **11** were subjected to a palladium catalyzed Heck-type cyclization using similar conditions to those from above. Unfortunately, both reactions afforded the deprotected regioisomers 3-ISOPBC (**2**) and δ -isomer **9b** in approximately the same 2 : 1 ratio, as compared to cyclization with the previously unprotected diarylamine **7b** (see Scheme 1 above). It was felt that deprotection of the carbamate occurred once the indole ring had formed (Scheme 2) which provided the better indole leaving group. To test the thermal stability of the carbamate starting materials, diarylamines **10** and **11** were heated at 120 °C in DMA; they were stable to these conditions. In addition, the cyclization with PdCl₂(PPh₃)₂ as a palladium source was also attempted using standard Heck-type reaction conditions with a milder base (NaOAc), but this failed to give the cyclized product. We also explored the reaction by varying the water content using NaOAc·3H₂O as a base; however, there was no cyclization (Scheme 2).



Scheme 2 Synthesis of the carbamate protected analogs from intermediate **7b**. Reagents and conditions: (a) (Boc)₂O, DMAP, THF, rt, 24 h; (b) Fmoc-Cl, 80 °C, microwave, 1 h; (c) Pd(OAc)₂, (t-Bu)₃P·HBF₄, K₂CO₃, DMA, 120 °C, 16 h; (d) PdCl₂(PPh₃)₂, NaOAc·3H₂O, DMA, 120 °C, 14 h; (e) PdCl₂(PPh₃)₂, NaOAc, DMA, 120 °C, 14 h.

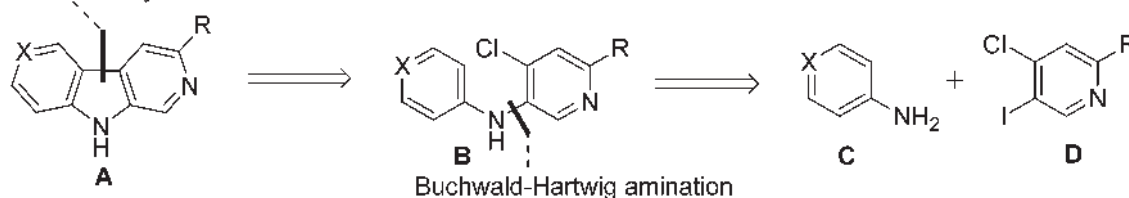
The second approach rested on the important switch of the chlorine atom from the benzene ring to the pyridine ring in amine **7b**. Retrosynthetically, it was envisioned that the core structure of 3,6-disubstituted β -carboline **A** could be obtained from diarylamine **B** via an intramolecular Heck cyclization and it was anticipated that diarylamine **B** could arise from a substituted aniline **C** and a substituted pyridine derivative **D** via a Buchwald–Hartwig amination (Scheme 3).

At this point it was decided to explore the regioselective palladium catalyzed Buchwald–Hartwig coupling between aniline and pyridine **14**⁴² for the synthesis of diarylamine **16** (Table 1). With the previous history in mind,³⁵ the initial attempt was made with 5 mol% Pd(OAc)₂, 7.5 mol% X-Phos and Cs₂CO₃ (1.5 equiv.) in toluene at 110 °C which gave only 18% of the diarylamine **16** with a large excess of unreacted starting material even after heating for 24 hours (Table 1, entry 1). However, the catalyst based on the combination of Pd₂(dba)₃, Xantphos and Pd(OAc)₂, Xantphos with Cs₂CO₃ in toluene and dioxane gave the desired product diarylamine **16** in up to 62% yield (Table 1, entries 2–3). The ligand Xantphos has been shown to be efficient in cross coupling reactions of C–N bond formation because of a wider bite angle,⁴³ which facilitates the reductive elimination. In addition, the excess base may also

play a role in the improvement of the yield.⁴³ In recent years rapid synthesis with microwave technology has attracted a considerable amount of attention for C–N bond formation.^{44–46} All three previous cyclizations were attempted with microwave irradiation (for 1 hour) in order to decrease the duration of the reaction time, as well as increase the selectivity under similar reaction conditions. However, the results were the same except that in the Xantphos-based ligand systems the cyclizations were completed in 1 hour. During continuation of the study of this selective amination, recent reports from Buchwald and co-workers⁴⁷ demonstrated air- and moisture-stable palladacyclic precatalysts, when employed with aryl iodides and heteroaryl iodides were attractive substrates in Pd-catalyzed C–N cross-coupling reactions. This process works by preventing formation of the stable bridging iodide dimers and also using a solvent system in which iodide salts were insoluble. These complexes easily undergo deprotonation and reductive elimination to generate LPd(0) along with relatively inert indoline (for generation of 1) or carbazole (for generation of 2 and 3). These conditions also permit the successful coupling of aryl iodides with amines at ambient temperature.^{47–50}

The first attempt in this modification was to use the Buchwald 3rd generation palladacycle precatalyst (BrettPhos Pd G3)

Intramolecular Heck Cyclization



Scheme 3 Retrosynthetic analysis of 3,6-disubstituted β -carbolines.

Table 1 Optimization of conditions for regioselective synthesis of intermediate **16** from **14**^a

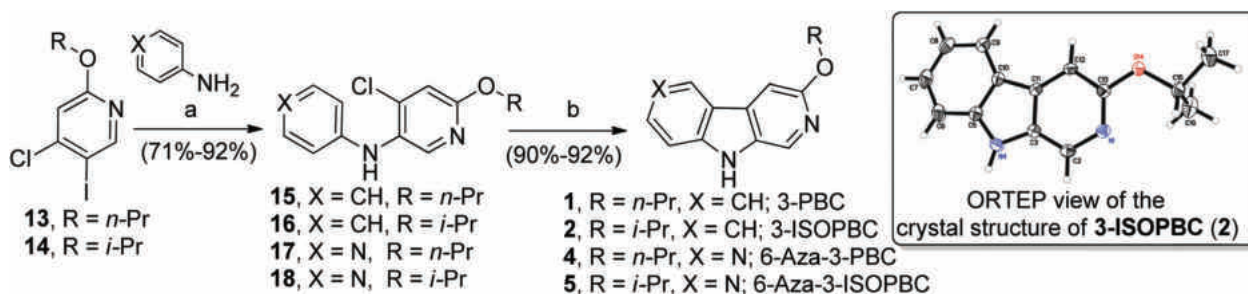
Entry	Pd source	Ligand	Base (equiv.)	Solvent	Temp (time)	Yield ^b (%)
1	Pd(OAc) ₂	X-Phos	Cs ₂ CO ₃ (1.5)	Toluene	110 °C (24 h)	18 ^c
2	Pd ₂ (dba) ₃	Xantphos	Cs ₂ CO ₃ (2)	Dioxane	110 °C (6 h)	51
3	Pd(OAc) ₂	Xantphos	Cs ₂ CO ₃ (4)	Toluene	110 °C (6 h)	62
4	BrettPhos Pd G3	BrettPhos	Cs ₂ CO ₃ (1.5)	Toluene	110 °C (14 h)	45
5	BrettPhos Pd G3	BrettPhos	Cs ₂ CO ₃ (3)	Toluene	110 °C (5 h)	66
6	BrettPhos Pd G3	BrettPhos	NaOt-Bu (1.5)	Toluene	110 °C (5 h)	52
7	BrettPhos Pd G3	BrettPhos	Cs ₂ CO ₃ (5)	Toluene	110 °C (5 h)	0 ^e
8	Pd ₂ (dba) ₃	Xantphos	Cs ₂ CO ₃ (5)	Toluene	110 °C (3 h)	74
9	Pd(OAc) ₂	<i>rac</i> -BINAP	Cs ₂ CO ₃ (5)	Toluene	110 °C (5 h)	80
10	Pd(OAc) ₂	<i>rac</i> -BINAP	K ₂ CO ₃ (5)	Toluene	110 °C (24 h)	22
11	Pd(OAc)₂	<i>rac</i> -BINAP	Cs ₂ CO ₃ (5)	Toluene	110 °C (5 h)	92^d

^a **14** (0.1 mmol), aniline (0.12 mmol), Pd (3 mol%), ligand (3 mol%), base, and solvent (1 mL). ^b Isolated yields. ^c Pd (5 mol%), ligand (7.5 mol%). ^d Aniline (0.1 mmol). ^e 90% of diaminated product [6-isopropoxy-*N*³,*N*⁴-diphenylpyridine-3,4-diamine] was observed.

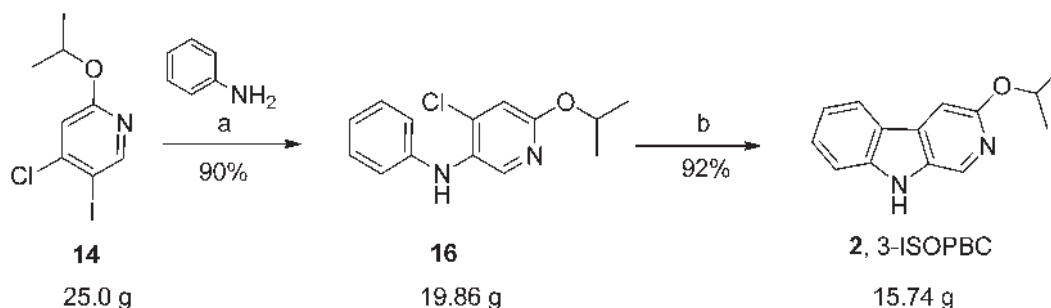
with the BrettPhos ligand in the presence of Cs_2CO_3 or NaOt-Bu in toluene at room temperature. This failed to give the desired product and there was no consumption of starting material. Following this attempt, the temperature was raised to reflux, with the addition of 3 equivalents of Cs_2CO_3 and the reaction went to completion within 5 hours. However, it only gave the desired amine **16** in 66% yield (Table 1, entry 5). When the same experiment was performed using only 1.5 equiv. of Cs_2CO_3 the process took a longer time to go to completion with an isolated yield of 45% of the desired amine **16**. This was accompanied by the diaminated product [6-isopropoxy- N^3,N^4 -diphenylpyridine-3,4-diamine] in ~18% yield (Table 1, entry 4). Unfortunately, when the stronger base NaOt-Bu was employed comparable results to the above reaction (Table 1, entry 4) were obtained accompanied by more decomposed material [TLC(silica gel; Table 1, entry 6)]. The use of excess base (Cs_2CO_3) gave only the unwanted diaminated product in 90% yield (Table 1, entry 7). It was found the $\text{Pd}(\text{OAc})_2$, *rac*-BINAP and K_2CO_3 combination, unfortunately, did not lead to full conversion even after heating for 24 hours (Table 1, entry 10). Interestingly, the catalyst system $\text{Pd}_2(\text{dba})_3$ and Xantphos with a large excess of base [Cs_2CO_3 (5 equiv.)] gave 74% yield of **16**, whereas the catalyst system $\text{Pd}(\text{OAc})_2$, *rac*-BINAP under similar reaction conditions yielded 80% (Table 1, entry 8 and 9) of the desired amine **16**. Remarkably, these data indicated a large excess of mild base was essential to obtain good yields, as well as selectivity. Furthermore, a rate-limiting interphase deprotonation of the Pd(II)-amine complex inter-

mediate has occurred in the catalytic cycle.^{51–53} Encouraged by these promising results, efforts turned toward lowering the aniline loading from 1.2 equivalents to 1 equivalent for regioselectivity. In doing so we achieved selective amination of pyridine **14** with aniline. Interestingly, neither a 4- nor 4,5-diaminated pyridine product was obtained. Using this catalyst-base combination in refluxing toluene, the desired cross-coupling proceeded smoothly to provide the desired anilino-pyridine **16** in excellent yield (92%, Table 1, entry 11). Interestingly, the same reaction conditions gave good yields in the case of the more polar starting 4-amino pyridine (Scheme 4); however, the temperature was necessarily increased to 140 °C to increase the solubility of the starting material, 4-amino pyridine. In contrast, when a polar solvent such as DMA was employed, the result was either inferior yields and/or deiodination of pyridine **16**, as mentioned above.

Once the diarylamines **15–18** were in hand in good to excellent yields, the previously applied Heck-type conditions [$\text{Pd}(\text{OAc})_2$, (*t*-Bu)₃P-HBF₄, K_2CO_3 , DMA, 120 °C] were employed for cyclization. Gratifyingly, this catalyst system gave excellent yields of 91–92% and 90–92% for β -carboline **1–2** and aza- β -carboline **4–5**, respectively (Scheme 4). The switch of the chlorine position from the benzene ring to the pyridine ring worked regiospecifically and completely eliminated the corresponding unwanted δ regioisomer. This completely eliminated the difficult chromatography required to separate β and δ carbolines. The 3-ISOPBC **2** has now been prepared on 15–25 gram scale for studies *in vivo* (Scheme 5) and it is very



Scheme 4 Regiospecific synthesis of β -carboline (**1–2**) and aza- β -carboline (**4–5**). Reagents and conditions: (a) $\text{Pd}(\text{OAc})_2$, *rac*-BINAP, Cs_2CO_3 , toluene, 110–140 °C, 5–6 h (b) $\text{Pd}(\text{OAc})_2$, (*t*-Bu)₃P-HBF₄, K_2CO_3 , DMA, 120 °C, 16 h.



Scheme 5 Large-scale regiospecific synthesis of β -carboline 3-ISOPBC (**2**). Reagents and conditions: (a) $\text{Pd}(\text{OAc})_2$, *rac*-BINAP, Cs_2CO_3 , toluene, 110 °C, 15 h (b) $\text{Pd}(\text{OAc})_2$, (*t*-Bu)₃P-HBF₄, K_2CO_3 , DMA, 120 °C, 16 h.

easy to scale up to 50–100 gram level. Finally, the overall yield increased from 43% to 84% compared to the previous syntheses.^{33,35}

Conclusions

In conclusion, a novel two-step regioselective route to the four anti-alcohol agents of biological interest, 3-PBC (**1**), 3-ISOPBC (**2**), 6-aza-3-PBC (**4**) and 6-aza-3-ISOPBC (**5**), has been developed. The process provided improved yields when compared to the earlier reported syntheses.^{33,35} This two-step protocol consists of the combination of a regioselective Buchwald–Hartwig amination and an intramolecular Heck-type cyclization. The first step, regioselective arylamination, was achieved by using a Pd-BINAP catalytic system in combination with a large excess of Cs₂CO₃, while the latter intramolecular Heck-type cyclization went smoothly with Pd(OAc)₂ in combination with the air-stable monodentate ligand (*t*-Bu)₃·HBF₄ and K₂CO₃. These conditions permit the presence of base sensitive functional groups in the substrates. Regioselective synthesis of β - and aza- β -carbolines was achieved by simply changing the chlorine position from the benzene ring to the pyridine derivatives. Importantly, these reactions are capable of scale-up to multigram quantities and were performed on 25 gram scale level for *in vivo* biology. We observed similar results except in the case of the Buchwald–Hartwig amination step, where it required an increase of the catalyst loading from 3 to 6 mol% whenever the starting material was not consumed. This new process reported here provides the material necessary to study alcohol self-administration and reduction thereof in MD rats and in primates. This regioselective two-step synthetic protocol increased the overall yield from 43% to 84% in the case of β -carbolines **1–2** and from 16% to 66% for aza- β -carbolines **4–5** respectively, and negated the need for a difficult chromatographic step.

Experimental

General considerations

All reactions were carried out in oven-dried, round-bottom flasks or in resealable screw-cap test tubes or heavy-wall pressure vessels under an argon atmosphere. The solvents were anhydrous unless otherwise stated. Stainless steel syringes were used to transfer air-sensitive liquids. Organic solvents were purified when necessary by standard methods or purchased from commercial suppliers. Anhydrous solvents of toluene, dioxane and *N,N*-dimethylacetamide (DMA) were subjected to the freeze-thaw method to render them oxygen free to execute the Buchwald–Hartwig coupling and intramolecular Heck reactions. All chemicals purchased from commercial suppliers were employed as is, unless stated otherwise in regard to purification. Silica gel (230–400 mesh) for flash chromatography was utilized to purify the analogues. The ¹H and ¹³C NMR data were obtained on an NMR spectrometer (300 MHz/500 MHz) instrument with chemical shifts in δ (ppm) reported

relative to TMS. The HRMS were obtained on a LCMS-IT-TOF mass spectrometer by Dr Mark Wang.

General procedure for the Buchwald–Hartwig coupling reaction between substituted anilines and substituted pyridines: representative procedure for the synthesis of *N*-(2-chlorophenyl)-6-propoxy pyridin-3-amine (**7a**)

A heavy-wall pressure tube was equipped with a magnetic stir bar and fitted with a rubber septum. It was then charged with 5-bromo-2-propoxy pyridine **6a** (1.3 g, 6 mmol), Pd(OAc)₂ (67.4 mg, 0.3 mmol), X-Phos (214 mg, 0.45 mmol) and Cs₂CO₃ (2.34 g, 7.2 mmol). The vessel was evacuated and backfilled with argon (this process was repeated a total of 3 times). The 2-chloroaniline **4a** (0.8 g, 6.3 mmol) and freeze-thawed toluene (20 mL) was injected into the tube with a degassed syringe under a positive pressure of argon. The rubber septum was replaced with a screw-cap by quickly removing the rubber septum under the flow of argon and the sealed tube was introduced into a pre-heated oil bath at 110 °C. The reaction mixture was maintained at this temperature for 15 h. At the end of this time period, the pressure tube was allowed to cool to rt. The reaction mixture was filtered through a short pad of celite, and the pad was washed with ethyl acetate (until no more product could be obtained; \approx 100 mL; TLC, silica gel). The combined organic fractions were washed with water (100 mL), brine (100 mL), dried (Na₂SO₄) and concentrated under reduced pressure. The crude product was purified by flash column chromatography (silica gel, 20 : 1 hexanes/ethyl acetate) to afford **7a** (0.64 g, 81%) as a pale yellow oil: ¹H NMR (300 MHz, CDCl₃) δ 8.04 (d, *J* = 2.6 Hz, 1H), 7.47 (dd, *J* = 8.8, 2.8 Hz, 1H), 7.33 (dd, *J* = 7.9, 1.4 Hz, 1H), 7.12–7.02 (m, 1H), 6.84 (dd, *J* = 8.2, 1.3 Hz, 1H), 6.74 (dd, *J* = 11.5, 5.1 Hz, 2H), 5.88 (br, 1H), 4.24 (t, *J* = 6.7 Hz, 2H), 1.90–1.72 (m, 2H), 1.04 (t, *J* = 7.4 Hz, 3H); ¹³C NMR (75 MHz, CDCl₃) δ 161.2, 142.1, 141.9, 135.3, 131.0, 129.7, 127.6, 120.1, 119.5, 113.5, 111.4, 67.9, 22.4, 10.6; HRMS (ESI-TOF) (*m/z*): [M + H]⁺ calcd for C₁₄H₁₆ClN₂O: 263.0951, found: 263.0958.

N-(2-Chlorophenyl)-6-isopropoxy pyridin-3-amine (**7b**)

Following the general procedure, 5-bromo-2-isopropoxy pyridine **6b** (0.44 g, 2.0 mmol) with 2-chloroaniline **4a** (0.268 g, 2.1 mmol), Pd(OAc)₂ (22.4 mg, 0.1 mmol), X-Phos (71.4 mg, 0.15 mmol), and Cs₂CO₃ (0.78 g, 2.4 mmol) were heated to 110 °C in toluene. After flash chromatography (silica gel, 20 : 1 hexane/ethyl acetate), the process afforded **7b** (0.215 g, 82%) as a pale yellow oil: ¹H NMR (300 MHz, CDCl₃) δ 8.06 (d, *J* = 2.7 Hz, 1H), 7.47 (dd, *J* = 8.7, 2.8 Hz, 1H), 7.34 (dd, *J* = 7.9, 1.3 Hz, 1H), 7.13–7.04 (m, 1H), 6.87 (dd, *J* = 8.2, 1.2 Hz, 1H), 6.81–6.67 (m, 2H), 5.90 (br, 1H), 5.36–5.24 (m, 1H), 1.39 (d, *J* = 6.2 Hz, 6H); ¹³C NMR (75 MHz, CDCl₃) δ 160.6, 142.3, 142.0, 135.3, 130.7, 129.6, 127.6, 120.1, 119.5, 113.5, 111.9, 68.2, 22.1; HRMS (ESI-TOF) (*m/z*): [M + H]⁺ calcd for C₁₄H₁₆ClN₂O: 263.0951, found: 263.0935.

tert-Butyl 5-[(2-chlorophenyl)amino]picolinate (**7c**)

Following the general procedure, *tert*-butyl 5-bromopicolinate **6c** (5 g, 19.4 mmol) with 2-chloroaniline **4a** (2.6 g, 20.3 mmol),

Pd(OAc)₂ (0.22 g, 0.97 mmol), X-Phos (0.69 g, 1.45 mmol), and Cs₂CO₃ (7.59 g, 23.3 mmol) was heated to 110 °C in toluene. After flash chromatography (silica gel, 5 : 1 hexanes/ethyl acetate), this process afforded **7c** (5.02 g, 85%) as an off-white solid; mp 148–149 °C: ¹H NMR (300 MHz, CDCl₃) δ 8.54 (d, *J* = 2.7 Hz, 1H), 8.00 (d, *J* = 8.6 Hz, 1H), 7.45 (dd, *J* = 8.1, 1.7 Hz, 2H), 7.39 (dd, *J* = 8.1, 1.2 Hz, 1H), 7.27–7.20 (m, 1H), 7.02 (td, *J* = 7.9, 1.4 Hz, 1H), 6.45 (br, 1H), 1.65 (s, 9H); ¹³C NMR (75 MHz, CDCl₃) δ 163.8, 141.5, 141.3, 139.3, 137.3, 130.3, 127.7, 125.9, 124.6, 123.7, 122.6, 118.8, 81.9, 28.2; HRMS (ESI-TOF) (*m/z*): [M + Na]⁺ calcd for C₁₆H₁₇ClN₂O₂Na: 327.0876, found: 327.0857.

N-(3-Chloropyridin-4-yl)-6-propoxy-pyridin-3-amine (**7d**)

Following the general procedure for 24 h at 140 °C, 5-bromo-2-propoxy-pyridine **6a** (13.45 g, 62.50 mmol) was heated with 4-amino-3-chloropyridine **4b** (8.0 g, 62.5 mmol), Pd(OAc)₂ (697 mg, 3.1 mmol), X-Phos (1.46 g, 3.1 mmol) and Cs₂CO₃ (40.6 g, 125 mmol) in refluxing toluene to yield the crude diaza material **7d**. After flash chromatography (silica gel, 1 : 1 ethyl acetate/hexane), this afforded the pure diaza material **7d** (8.29 g, 51%) as a white solid; mp 71.6–72.6 °C: ¹H NMR (300 MHz, CDCl₃): δ 8.35 (s, 1H), 8.10–8.07 (m, 2H), 7.48 (dd, *J* = 6.0, 3.0 Hz, 1H), 6.80 (d, *J* = 6.0 Hz, 1H), 6.60 (d, *J* = 6.0 Hz, 1H), δ 6.45 (br, 1H), 4.25 (t, *J* = 6.9 Hz, 2H), 1.87–1.75 (m, 2H), 1.03 (t, *J* = 7.2 Hz, 3H); ¹³C NMR (75 MHz, CDCl₃): δ 162.3, 148.8, 148.3, 148.2, 144.0, 136.56, 128.2, 117.1, 111.7, 106.9, 68.0, 22.3, 10.5; HRMS (ESI-TOF) (*m/z*): [M + H]⁺ calcd for C₁₃H₁₅ClN₃O 264.0904, found 264.0893.

N-(3-Chloropyridin-4-yl)-6-isopropoxy-pyridin-3-amine (**7e**)

Following the general procedure for 24 h at 140 °C, 5-bromo-2-isopropoxy-pyridine **6b** (8.09 g, 37.20 mmol) was heated with 4-amino-3-chloropyridine **4b** (4.74 g, 37.20 mmol), Pd(OAc)₂ (419 mg, 1.87 mmol), X-Phos (608 mg, 1.87 mmol), Cs₂CO₃ (15.25 g, 46.80 mmol) in refluxing toluene to afford a crude solid which was purified by flash chromatography (silica gel, 1 : 1 ethyl acetate/hexane) to furnish a white solid **7e** (5.20 g, 52.4%); mp 76–78 °C: ¹H NMR (300 MHz, CDCl₃): δ 8.35 (s, 1H), 8.10–8.06 (m, 2H), 7.46 (dd, *J* = 6.0, 3.0 Hz, 1H), 6.74 (d, *J* = 6.0 Hz, 1H), 6.61 (d, *J* = 6.0 Hz, 1H), 6.42 (br s, 1H), 5.35–5.23 (m, 1H), 1.36 (d, *J* = 6.0 Hz, 6H); ¹³C NMR (75 MHz, CDCl₃): δ 161.7, 148.7, 148.3, 144.0, 136.5, 127.9, 117.0, 112.2, 106.9, 68.5, 22.0; HRMS (ESI-TOF) (*m/z*): [M + H]⁺ calcd for C₁₃H₁₅ClN₃O 264.0904, found 264.0909.

General procedure for the intramolecular Heck cyclization: representative procedure for the synthesis of 3-propoxy-9*H*-pyrido[3,4-*b*]indole (3-PBC, **1**) and 2-propoxy-5*H*-pyrido[3,2-*b*]indole (**9a**)

A heavy-wall pressure tube was equipped with a magnetic stir bar and fitted with a rubber septum and loaded with *N*-(2-chlorophenyl)-6-propoxy-pyridin-3-amine **7a** (526 mg, 2.0 mmol), Pd(OAc)₂ (44.8 mg, 0.2 mmol), (*t*-Bu)₃P-HBF₄ (116 mg, 0.4 mmol) and K₂CO₃ (552 mg, 4.0 mmol). The vessel was evacuated and backfilled with argon (this process was

repeated a total of 3 times) and degassed DMA (8 mL) was injected into the tube with a degassed syringe under a positive pressure of argon. The rubber septum was replaced with a screw-cap by quickly removing the rubber septum under the flow of argon and the sealed tube was introduced into a pre-heated oil bath at 120 °C. The reaction mixture was maintained at this temperature for 16 h. At the end of this period, the reaction mixture was allowed to cool to rt. The dark brown mixture which resulted was then passed through a short pad of celite. The celite pad was further washed with ethyl acetate (150 mL) until no more product (TLC; silica gel) was detected in the eluent. The combined filtrate was washed with water (100 mL × 3), brine (100 mL), dried (Na₂SO₄) and concentrated under reduced pressure. The crude product was purified by flash column chromatography (silica gel, 5 : 1 hexanes/ethyl acetate) to afford 3-PBC (**1**) (235 mg, 52%) as an off white solid. mp 120.5–121.5 °C (lit.³⁵ mp 119.3–120.5 °C): **1**, ¹H NMR (300 MHz, CDCl₃) δ 8.66 (br, 1H), 8.42 (s, 1H), 8.05 (d, *J* = 7.9 Hz, 1H), 7.50 (t, *J* = 7.6 Hz, 1H), 7.45–7.38 (m, 1H), 7.35 (s, 1H), 7.21 (t, *J* = 7.4 Hz, 1H), 4.28 (t, *J* = 6.7 Hz, 2H), 1.94–1.78 (m, 2H), 1.06 (t, *J* = 7.4 Hz, 3H); ¹³C NMR (75 MHz, CDCl₃) δ 157.9, 142.4, 133.8, 132.7, 128.9, 128.7, 122.0, 121.4, 119.5, 111.5, 99.1, 68.6, 22.7, 10.6; HRMS (ESI-TOF) (*m/z*): [M + H]⁺ calcd for C₁₄H₁₅N₂O: 227.1184, found: 227.1174. A hydrochloride salt of **1** was prepared by the reported method³¹ to obtain 3-PBC-HCl (**1·HCl**): yellow solid; mp 194.5–195.5 °C (lit.³¹ 194.0–195.0 °C). The spectral data for this **1·HCl** were in excellent agreement with the reported values (mp, ¹H NMR).³¹

9a (145 mg, 32%) as a white solid; mp 125–126 °C: ¹H NMR (300 MHz, CDCl₃) δ 8.28 (t, *J* = 8.8 Hz, 1H), 8.20 (br, 1H), 7.60 (d, *J* = 8.7 Hz, 1H), 7.51–7.34 (m, 2H), 7.27 (t, *J* = 7.3 Hz, 1H), 6.83 (d, *J* = 8.7 Hz, 1H), 4.46 (t, *J* = 6.7 Hz, 2H), 1.99–1.80 (m, 2H), 1.10 (t, *J* = 7.4 Hz, 3H); ¹³C NMR (75 MHz, CDCl₃) δ 159.5, 140.2, 138.2, 128.4, 126.8, 122.3, 121.6, 120.6, 119.7, 111.3, 108.6, 67.9, 22.6, 10.7; HRMS (ESI-TOF) (*m/z*): [M + H]⁺ calcd for C₁₄H₁₅N₂O: 227.1184, found: 227.1180.

3-Isopropoxy-9*H*-pyrido[3,4-*b*]indole (3-ISOPBC, **2**) and 3-isopropoxy-5*H*-pyrido[3,2-*b*]indole (**9b**)

Following the general procedure for the intramolecular Heck cyclization, **7b** (526 mg, 2.0 mmol) was heated with Pd(OAc)₂ (45 mg, 0.2 mmol), (*t*-Bu)₃P-HBF₄ (116 mg, 0.4 mmol) and K₂CO₃ (552 mg, 4.0 mmol) in DMA at 120 °C to afford a mixture of regioisomers **2** and **9b**. After flash chromatography (silica gel, 5 : 1 hexanes/ethyl acetate), this procedure yielded pure 3-ISOPBC (**2**) and the byproduct **9b**.

2 (239.5 mg, 53%): off-white solid; mp 134–136 °C: ¹H NMR (300 MHz, CDCl₃) δ 8.41 (s, 1H), 8.19 (br, 1H), 8.04 (d, *J* = 7.8 Hz, 1H), 7.50 (t, *J* = 7.6 Hz, 1H), 7.40 (d, *J* = 8.1 Hz, 1H), 7.34 (s, 1H), 7.21 (t, *J* = 7.4 Hz, 1H), 5.35–5.23 (m, 1H), 1.40 (d, *J* = 6.1 Hz, 6H); ¹³C NMR (75 MHz, CDCl₃) δ 157.4, 142.1, 133.7, 132.5, 128.9, 128.8, 122.0, 121.6, 119.5, 111.3, 100.5, 68.6, 22.3; HRMS (ESI-TOF) (*m/z*): [M + H]⁺ calcd for C₁₄H₁₅N₂O: 227.1184, found: 227.1184. A hydrochloride salt of **2** was prepared by the reported method³⁷ to obtain 3-ISOPBC-HCl (**2·HCl**): light greenish yellow solid; mp

169–171 °C (lit.³⁷ 168–172 °C). The data for this compound matched in all respects (¹H NMR, mp) with that reported in the literature.³⁷

9b (163.1 mg, 36%): light brown solid; mp 110.4–111.5 °C: ¹H NMR (300 MHz, CDCl₃) δ 8.27 (d, *J* = 7.8 Hz, 1H), 7.99 (br, 1H), 7.67 (d, *J* = 8.7 Hz, 1H), 7.49–7.45 (m, 2H), 7.30–7.25 (m, 1H), 6.79 (d, *J* = 8.7 Hz, 1H), 5.60–5.48 (m, 1H), 1.45 (d, *J* = 6.1 Hz, 6H); ¹³C NMR (75 MHz, CDCl₃) δ 158.9, 140.1, 138.4, 128.1, 126.7, 122.6, 121.3, 120.5, 119.7, 111.1, 109.4, 67.9, 22.2; HRMS (ESI-TOF) (*m/z*): [M + H]⁺ calcd for C₁₄H₁₅N₂O: 227.1184, found: 227.1185.

tert-Butyl 9H-pyrido[3,4-*b*]indole-3-carboxylate (βCCT; 3) and tert-butyl 5H-pyrido[3,2-*b*]indole-3-carboxylate (9c)

Following the general procedure for the intramolecular Heck cyclization, **7c** (2 g, 16.4 mmol), was heated with Pd(OAc)₂ (147 mg, 0.656 mmol), (*t*-Bu)₃P·HBF₄ (380 mg, 0.4 mmol) and K₂CO₃ (1.8 g, 13.12 mmol) in DMA at 120 °C to afford crude **3** and **9c**. After flash chromatography (silica gel, 1:1 hexanes/ethyl acetate), this afforded pure βCCT (**3**) and **9c**.

3 (885 mg, 50%), white solid; mp 302.5–304.5 °C (lit.³³ 301–303 °C): ¹H NMR (300 MHz, CDCl₃) δ 10.35 (br, 1H), 9.23 (s, 1H), 8.86 (s, 1H), 8.25 (d, *J* = 7.9 Hz, 1H), 7.80 (d, *J* = 8.3 Hz, 1H), 7.66–7.61 (m, 1H), 7.38 (t, *J* = 7.5 Hz, 1H), 1.75 (s, 9H); ¹³C NMR (75 MHz, CD₃COCD₃) δ 164.9, 141.2, 139.2, 137.7, 133.4, 128.6, 128.1, 121.8, 121.5, 120.3, 116.9, 112.2, 80.1, 27.6; HRMS (ESI-TOF) (*m/z*): [M + H]⁺ calcd for C₁₆H₁₇N₂O₂: 269.1290, found: 269.1286. The spectral data are in excellent agreement with the published values.³³

9c (531 mg, 30%), fluffy white solid; mp 216.0–218.2 °C: ¹H NMR (300 MHz, CDCl₃) δ 9.46 (br, 1H), 8.38 (d, *J* = 7.8 Hz, 1H), 8.18 (d, *J* = 8.5 Hz, 1H), 7.82 (d, *J* = 8.5 Hz, 1H), 7.53–7.49 (m, 2H), 7.25–7.23 (m, 1H), 1.67 (s, 9H); ¹³C NMR (75 MHz, CDCl₃) δ 164.9, 142.4, 141.4, 141.1, 134.7, 128.6, 122.0, 121.9, 121.0, 120.8, 117.4, 111.5, 81.9, 28.2; HRMS (ESI-TOF) (*m/z*): [M + H]⁺ calcd for C₁₆H₁₇N₂O₂: 269.1290, found: 269.1289.

8-Propoxy-5H-pyrrolo[2,3-*c*:4,5-*c'*]dipyridine (6-aza-3-PBC, 4) and 2-propoxy-5H-pyrrolo[3,2-*b*:4,5-*c'*]dipyridine (9d)

Following the general procedure for the intramolecular Heck cyclization, the diaza compound **7d** (3.0 g, 11.30 mmol) was heated with Pd(OAc)₂ (255.0 mg, 1.13 mmol), (*t*-Bu)₃P·HBF₄ (657.0 mg, 2.26 mmol) and K₂CO₃ (3.2 g, 22.60 mmol) in DMA at 120 °C to afford crude **4** and **9d**. After flash chromatography (silica gel, 1:24 methanol/dichloromethane) this process afforded the pure regioisomers 6-aza-3-PBC (**4**) and **9d** as white solids.

4 (820 mg, 31.8%): mp 166–168 °C: ¹H NMR (300 MHz, CD₃SO) δ 12.13 (br, 1H), 9.51 (s, 1H), 8.57 (br, 2H), 7.68 (s, 1H), 7.61 (d, *J* = 5.7 Hz, 1H), 4.26 (t, *J* = 6.0 Hz, 2H), 1.83–1.71 (m, 2H), 1.01 (t, *J* = 6.0 Hz, 3H); ¹³C NMR (75 MHz, CD₃SO) δ 158.4, 147.0, 144.5, 143.4, 133.0, 131.5, 130.7, 118.2, 108.1, 100.4, 68.0, 22.5, 10.9; HRMS (ESI-TOF) (*m/z*): [M + H]⁺ calcd for C₁₃H₁₄N₃O: 228.1137, found: 228.1144.

9d (1.62 g, 62.5%): mp 192–194 °C: ¹H NMR (300 MHz, CD₃SO) δ 11.70 (s, 1H), 9.25 (s, 1H), 8.43 (d, *J* = 6.0 Hz, 1H),

7.94 (d, *J* = 9.0 Hz, 1H), 7.51 (d, *J* = 6.0 Hz, 1H), 6.93 (d, *J* = 9.0 Hz, 1H), 4.36 (t, *J* = 6.0 Hz, 2H), 1.84–1.77 (m, 2H), 1.03 (t, *J* = 6.0 Hz, 3H); ¹³C NMR (75 MHz, CD₃SO) δ 159.7, 145.2, 143.8, 142.8, 136.0, 128.8, 123.5, 118.5, 110.2, 107.6, 67.4, 22.4, 11.0; HRMS (ESI-TOF) (*m/z*): [M + H]⁺ calcd for C₁₃H₁₄N₃O: 228.1137, found: 228.1140.

8-Isopropoxy-5H-pyrrolo[2,3-*c*:4,5-*c'*]dipyridine (6-aza-3-ISOPBC, 5) and 2-isopropoxy-5H-pyrrolo[3,2-*b*:4,5-*c'*]dipyridine (9e)

Following the general procedure for the intramolecular Heck cyclization, pyridine **7e** (3.0 g, 11.30 mmol) was heated with Pd(OAc)₂ (255.0 mg, 1.13 mmol), (*t*-Bu)₃P·HBF₄ (657.0 mg, 2.26 mmol) and K₂CO₃ (3.2 g, 22.60 mmol) in DMA at 120 °C to afford crude **5** and **9e**. After flash chromatography (silica gel, 1:24 methanol/dichloromethane) this afforded the regioisomeric 6-aza-3-ISOPBC (**5**) and **9e** as white solids.

5 (800 mg, 31.0%): mp 180.2–183.2 °C: ¹H NMR (300 MHz, CD₃SO) δ 11.66 (s, 1H), 9.37 (s, 1H), 8.51 (s, 1H), 8.48 (d, *J* = 6.0 Hz, 1H), 7.56 (s, 1H), 7.46 (d, *J* = 6.0 Hz, 1H), 5.32–5.20 (m, 1H), 1.32 (d, *J* = 6.0 Hz, 6H); ¹³C NMR (125 MHz, CD₃SO) δ 157.4, 147.3, 146.3, 145.4, 132.7, 131.6, 130.1, 118.2, 107.4, 100.0, 68.0, 22.6; HRMS (ESI-TOF) (*m/z*): [M + H]⁺ calcd for C₁₃H₁₄N₃O: 228.1137, found: 228.1150.

9e (1.6 g, 62.3%): mp 207.4–208.6 °C: ¹H NMR (500 MHz, CD₃SO) δ 11.85 (s, 1H), 9.28 (s, 1H), 8.44 (d, *J* = 3.0 Hz, 1H), 7.94 (d, *J* = 6.0 Hz, 1H), 7.55 (d, *J* = 3.0 Hz, 1H), 6.89 (d, *J* = 6.0 Hz, 1H), 5.49–5.41 (m, 1H), 1.36 (d, *J* = 3.0 Hz, 6H); ¹³C NMR (125 MHz, CD₃SO) δ 159.2, 144.2, 144.0, 142.1, 136.0, 128.9, 123.7, 111.1, 107.8, 67.8, 22.4; HRMS (ESI-TOF) (*m/z*): [M + H]⁺ calcd for C₁₃H₁₄N₃O: 228.1137, found: 228.1140.

tert-Butyl (2-chlorophenyl)(6-isopropoxy-pyridin-3-yl)-carbamate (10)

To the amine **7b** (275 mg, 1.05 mmol) in THF (6 mL) was added the di-*tert*-butyl dicarbonate (320 mg, 1.46 mmol) and 4-(dimethylamino)pyridine (DMAP) (51.1 mg, 0.42 mmol) and this mixture was stirred at rt for 24 h. The organic solvent was removed under reduced pressure and the crude product which resulted was purified by flash column chromatography (silica gel, 1:9 ethylacetate/hexane) to give the pure BOC protected amine **10** (323 mg, 85%).

¹H NMR (300 MHz, CDCl₃) δ 8.03 (d, *J* = 2.6 Hz, 1H), 7.60 (s, 1H), 7.44 (dd, *J* = 8.1, 5.9 Hz, 1H), 7.32–7.20 (m, 3H), 6.62 (d, *J* = 8.9 Hz, 1H), 5.30–5.16 (m, 1H), 1.43 (s, 9H), 1.31 (d, *J* = 6.2 Hz, 6H); ¹³C NMR (75 MHz, CDCl₃) δ 160.9, 153.3, 143.9, 139.8, 136.7, 133.3, 132.2, 130.4, 130.3, 128.6, 127.7, 111.1, 81.6, 68.2, 28.1; HRMS (ESI-TOF) (*m/z*): [M + H]⁺ calcd for C₁₉H₂₄ClN₂O₃: 363.1475, found: 363.1469.

(9H-Fluoren-9-yl)methyl (2-chlorophenyl)(6-isopropoxy-pyridin-3-yl)carbamate (11)

The microwave tube was loaded with amine **7b** (300 mg, 1.14 mmol) and Fmoc chloride (325 mg, 1.25 mmol). The tube was sealed and placed into a microwave apparatus (with a

power of 100 W) at 80 °C for 1 h with stirring. At the end of this period, the reaction was directly purified, without quenching, by flash column chromatography (silica gel, 1 : 4 ethylacetate/hexane) to give pure Fmoc protected pyridine **11** (360 mg, 65%).

$^1\text{H NMR}$ (300 MHz, CDCl_3) δ 8.08 (d, $J = 2.7$ Hz, 1H), 7.70 (d, $J = 7.6$ Hz, 3H), 7.50 (d, $J = 3.8$ Hz, 1H), 7.42–7.28 (m, 5H), 7.20–7.06 (m, 4H), 6.64 (d, $J = 8.5$ Hz, 1H), 5.33–5.15 (m, 1H), 4.49–4.41 (m, 2H), 4.16–4.09 (m, 1H), 1.34 (d, $J = 6.1$ Hz, 6H); $^{13}\text{C NMR}$ (75 MHz, CDCl_3) δ 154.3, 143.6, 141.3, 139.2, 139.1, 131.6, 130.60, 130.5, 129.2, 127.9, 127.7, 126.9, 125.0, 119.9, 111.4, 68.4, 68.2, 46.9, 22.1; HRMS (ESI-TOF) (m/z): $[\text{M} + \text{Na}]^+$ calcd for $\text{C}_{29}\text{H}_{25}\text{ClN}_2\text{O}_3\text{Na}$: 507.1451, found: 507.1448.

4-Chloro-6-isopropoxy-*N*-phenylpyridin-3-amine (16)

A heavy-wall pressure tube was equipped with a magnetic stir bar and fitted with a rubber septum that had been charged with 4-chloro-5-iodo-2-isopropoxy-pyridine **14** (75 mg, 0.252 mmol), aniline (27.6 μL , 0.256 mmol) and Cs_2CO_3 (410 mg, 1.26 mmol). The vessel was evacuated and backfilled with argon (this process was repeated a total of 3 times) and degassed toluene (1 mL) was injected into the tube with a degassed syringe under a positive pressure of argon. In another round bottom flask fitted with a rubber septum, $\text{Pd}(\text{OAc})_2$ (1.7 mg, 0.0076 mmol) and *rac*-BINAP (4.7 mg, 0.0076 mmol) was charged. This flask was evacuated and backfilled with argon (this process was repeated a total of 3 times) and then degassed toluene (0.5 mL) was added under a positive pressure of argon. This mixture was stirred for 10 min and then the mixture which resulted was added to the above pressure tube. The rubber septum was replaced with a screw-cap by quickly removing the rubber septum under the flow of argon and the sealed tube was introduced into a pre-heated oil bath at 110 °C. The reaction mixture was maintained at this temperature for 5 h. At the end of this time period the pressure tube was allowed to cool to rt. The reaction mixture was filtered through a short pad of celite, and the pad was washed with ethyl acetate (until no more product could be obtained; ≈ 50 mL). The combined organic eluents were washed with water (50 mL), brine (50 mL), dried (Na_2SO_4) and concentrated under reduced pressure. The crude product was purified by flash column chromatography (silica gel, 20 : 1 hexanes/ethyl acetate) to afford only **16** (61 mg, 92%) as a pale yellow oil.

$^1\text{H NMR}$ (300 MHz, CDCl_3) δ 8.18 (s, 1H), 7.28 (t, $J = 7.9$ Hz, 2H), 6.98–6.92 (m, 3H), 6.83 (s, 1H), 5.52 (s, 1H), 5.29–5.17 (m, 1H), 1.36 (d, $J = 6.2$ Hz, 6H); $^{13}\text{C NMR}$ (75 MHz, CDCl_3) δ 159.2, 143.5, 139.1, 138.2, 130.4, 129.5, 121.1, 116.8, 111.9, 68.8, 22.1; HRMS (ESI-TOF) (m/z): $[\text{M} + \text{H}]^+$ calcd for $\text{C}_{14}\text{H}_{16}\text{ClN}_2\text{O}$: 263.0951, found: 263.0958.

4-Chloro-6-propoxy-*N*-phenylpyridin-3-amine (15)

Following the above general procedure for 5 h at 110 °C, 4-chloro-5-iodo-2-propoxy-pyridine **13** (75 mg, 0.252 mmol), aniline (27.6 μL , 0.256 mmol), $\text{Pd}(\text{OAc})_2$ (1.7 mg, 0.0076 mmol), *rac*-BINAP (4.7 mg, 0.0076 mmol) and Cs_2CO_3 (410 mg, 1.26 mmol) were heated in toluene at reflux to afford

a crude liquid which was purified by flash chromatography (silica gel, 20 : 1 hexanes/ethyl acetate) to furnish a pale yellow oil **15** (60.33 mg, 91%).

$^1\text{H NMR}$ (300 MHz, CDCl_3) δ 8.20 (s, 1H), 7.28 (t, $J = 7.9$ Hz, 2H), 6.98–6.93 (m, 3H), 6.89 (s, 1H), 5.57 (s, 1H), 4.26 (t, $J = 6.6$ Hz, 2H), 1.89–1.77 (m, 2H), 1.06 (t, $J = 7.2$ Hz, 2H); $^{13}\text{C NMR}$ (75 MHz, CDCl_3) δ 159.9, 143.6, 139.3, 138.1, 130.6, 129.5, 121.1, 116.7, 111.4, 68.1, 22.4, 10.5; HRMS (ESI-TOF) (m/z): $[\text{M} + \text{H}]^+$ calcd for $\text{C}_{14}\text{H}_{16}\text{ClN}_2\text{O}$: 263.0951, found: 263.0946.

4-Chloro-6-propoxy-*N*-(pyridin-4-yl)pyridine-3-amine (17)

Following the above general procedure for 6 h at 140 °C, 4-chloro-5-iodo-2-propoxy-pyridine **13** (214 mg, 0.72 mmol), 4-aminopyridine (68.8 mg, 0.73 mmol), $\text{Pd}(\text{OAc})_2$ (4.8 mg, 0.0216 mmol) and *rac*-BINAP (13.4 mg, 0.0216 mmol) as well as Cs_2CO_3 (1.17 g, 3.6 mmol) were heated in toluene at reflux to afford a crude solid which was purified by flash chromatography (silica gel, ethyl acetate) to furnish a white solid **17** (137 mg, 72%); mp 119–120 °C, $^1\text{H NMR}$ (300 MHz, CDCl_3): δ 8.28 (d, $J = 4.8$ Hz, 2H), 8.19 (s, 1H), 6.92 (s, 1H), 6.65 (d, $J = 5.4$ Hz, 2H), 6.18 (br, 1H), 4.27 (t, $J = 6.6$ Hz, 2H), 1.88–1.76 (m, 2H), 1.04 (t, $J = 7.5$ Hz, 2H); $^{13}\text{C NMR}$ (75 MHz, CDCl_3): δ 162.3, 151.7, 150.0, 144.6, 142.0, 126.9, 111.9, 108.9, 68.4, 22.3, 10.5; HRMS (ESI-TOF) (m/z): $[\text{M} + \text{H}]^+$ calcd for $\text{C}_{13}\text{H}_{15}\text{ClN}_3\text{O}$ 264.0904, found 264.0898.

4-Chloro-6-isopropoxy-*N*-(pyridin-4-yl)pyridine-3-amine (18)

Following the above general procedure for 6 h at 140 °C, 4-chloro-5-iodo-2-isopropoxy-pyridine **13** (214 mg, 0.72 mmol), 4-aminopyridine (68.8 mg, 0.73 mmol), $\text{Pd}(\text{OAc})_2$ (4.8 mg, 0.0216 mmol) and *rac*-BINAP (13.4 mg, 0.0216 mmol) as well as Cs_2CO_3 (1.17 g, 3.6 mmol) were heated in toluene at reflux to afford a crude solid which was purified by flash chromatography (silica gel, ethyl acetate) to furnish a white solid **18** (135 mg, 71%); $^1\text{H NMR}$ (300 MHz, CDCl_3): δ 8.24 (d, $J = 4.2$ Hz, 2H), 8.18 (s, 1H), 6.87 (s, 1H), 6.74 (d, $J = 5.7$ Hz, 2H), 5.36–5.23 (m, 1H), 1.37 (d, $J = 6.3$ Hz, 6H); $^{13}\text{C NMR}$ (75 MHz, CDCl_3): δ 161.9, 152.4, 148.9, 144.8, 142.1, 126.4, 112.4, 108.9, 69.3, 22.0; HRMS (ESI-TOF) (m/z): $[\text{M} + \text{H}]^+$ calcd for $\text{C}_{13}\text{H}_{15}\text{ClN}_3\text{O}$ 264.0904, found 264.0910.

3-Propoxy-9*H*-pyrido[3,4-*b*]indole (3-PBC, 1)

Following the general procedure for the Heck cyclization for 16 h at 120 °C, 4-chloro-6-propoxy-*N*-phenylpyridin-3-amine **15** (526 mg, 2.0 mmol), $\text{Pd}(\text{OAc})_2$ (44.8 mg, 0.2 mmol), (*t*-Bu) $_3\text{P}$ -HBF $_4$ (116 mg, 0.4 mmol) and K_2CO_3 (552 mg, 4.0 mmol) were heated to give a solid which was purified by a wash column (silica gel, 5 : 1 hexanes/ethyl acetate) to yield 3-PBC **1** (416.80 mg, 92%).

3-Isopropoxy-9*H*-pyrido[3,4-*b*]indole (3-ISOPBC, 2)

Following the general procedure for the Heck cyclization for 16 h at 120 °C, 4-chloro-6-isopropoxy-*N*-phenylpyridin-3-amine **16** (526 mg, 2.0 mmol), $\text{Pd}(\text{OAc})_2$ (44.8 mg, 0.2 mmol), (*t*-Bu) $_3\text{P}$ -HBF $_4$ (116 mg, 0.4 mmol) and K_2CO_3 (552 mg,

4.0 mmol) were heated to give a solid which was purified by a wash column (silica gel, 5 : 1 hexanes/ethyl acetate) to yield 3-ISOPBC 2 (412.30 mg, 91%).

8-Propoxy-5H-pyrrolo[2,3-c:4,5-c']dipyridine (6-aza-3-PBC, 4)

Following the general procedure for the Heck cyclization for 16 h at 120 °C, 4-chloro-6-propoxy-*N*-(pyridin-4-yl)pyridine-3-amine **17** (125 mg, 0.475 mmol), Pd(OAc)₂ (10.7 mg, 0.047 mmol), (*t*-Bu)₃P·HBF₄ (27.6 mg, 0.095 mmol) and K₂CO₃ (131.3 mg, 0.95 mmol) were heated to give a solid which was purified by a wash column (silica gel, 1 : 24 methanol/dichloromethane) to yield 6-aza-3-PBC **4** (97.15 mg, 90%).

8-Isopropoxy-5H-pyrrolo[2,3-c:4,5-c']dipyridine (6-aza-3-ISOPBC, 5)

Following the general procedure for the Heck cyclization for 16 h at 120 °C, 4-chloro-6-isopropoxy-*N*-(pyridin-4-yl)pyridine-3-amine **18** (125 mg, 0.475 mmol), Pd(OAc)₂ (10.7 mg, 0.047 mmol), (*t*-Bu)₃P·HBF₄ (27.6 mg, 0.095 mmol) and K₂CO₃ (131.3 mg, 0.95 mmol) were heated to give a solid which was purified by a wash column (silica gel, 1 : 24 methanol/dichloromethane) to yield 6-aza-3-ISOPBC **5** (99.31 mg, 92%).

Large-scale synthesis of 3-ISOPBC (2)

Step 1: Synthesis of 4-chloro-6-isopropoxy-*N*-phenylpyridin-3-amine (16). 4-Chloro-5-iodo-2-isopropoxy-pyridine **14** (25 g, 84.03 mmol), aniline (7.65 mL, 84.03 mmol), Pd(OAc)₂ (0.57 g, 2.52 mmol) and *rac*-BINAP (1.57 g, 2.52 mmol) as well as Cs₂CO₃ (136.84 g, 420 mmol) were added to a three-neck flask with a reflux condenser. The flask was evacuated and back-filled with argon. Degassed toluene (300 mL) was added *via* a cannula, and the flask was introduced into a preheated oil bath at 110 °C. After 15 h at 110 °C the reaction mixture was cooled to rt and filtered through a short pad of celite, and the pad was washed with ethyl acetate. The combined organic eluents were washed with water and brine, dried (Na₂SO₄), and concentrated under reduced pressure. The crude product was purified by flash chromatography (silica gel, 20 : 1 hexanes/ethyl acetate) to afford only **16** (19.86 g, 90%) as a pale yellow oil.

Step 2: Synthesis of 3-isopropoxy-9H-pyrido[3,4-*b*]indole (2). A heavy-wall pressure tube was equipped with a magnetic stir bar and fitted with a rubber septum loaded with 4-chloro-6-isopropoxy-*N*-phenylpyridin-3-amine **16** (19.86 g, 75.58 mmol), Pd(OAc)₂ (1.70 g, 7.558 mmol), (*t*-Bu)₃P·HBF₄ (4.39 g, 15.12 mmol) and K₂CO₃ (20.89 g, 151.16 mmol). The vessel was evacuated and backfilled with argon (this process was repeated a total of 3 times) and degassed DMA (200 mL) was added to this vial *via* a cannula. The rubber septum was replaced with a screw-cap by quickly removing the rubber septum under the flow of argon and the sealed tube was introduced into a pre-heated oil bath at 120 °C. The reaction mixture was maintained at this temperature for 16 h. At the end of this period, the reaction mixture was allowed to cool to rt. The dark brown mixture which resulted was then passed through a short pad of celite. The celite pad was further

washed with ethyl acetate until no product (TLC; silica gel) was detected in the eluent. The combined filtrate was washed with water, brine, dried (Na₂SO₄) and concentrated under reduced pressure. The solid product was purified by a wash column (silica gel, 5 : 1 hexanes/ethyl acetate) to afford 3-ISOPBC (**2**) (15.74 g, 92%) as an off white solid.

Acknowledgements

We thank the NIMH (1R01MH096463-01A1), NIAAA (7R01AA-016179) and NINDS (5R01NS076517-03) for generous financial support. The X-ray crystallographic work was supported by NIDA through Interagency Agreement #ADA 12003 with the Naval Research Laboratory (NRL). We also wish to acknowledge the Bradley-Herzfeld Foundation and The Milwaukee Institute for Drug Discovery for support.

References

- R. Cao, W. Peng, Z. Wang and A. Xu, *Curr. Med. Chem.*, 2007, **14**, 479–500.
- P. Venault and G. Chapouthier, *Sci. World J.*, 2007, **7**, 204–223.
- M. Stahre, J. Roeber, D. Kanny, R. D. Brewer and X. Zhang, *Prev. Chronic Dis.*, 2014, **11**, E109.
- A. R. Yang, J. Liu, H. S. Yi, K. T. Warnock, M. Wang, H. L. June Jr., A. C. Puche, A. Elnabawi, W. Sieghart, L. Aurelian and H. L. June Sr., *Front. Neurosci.*, 2011, **5**, 123.
- M. C. Moffett, A. Vicentic, M. Kozel, P. Plotsky, D. D. Francis and M. J. Kuhar, *Biochem. Pharmacol.*, 2007, **73**, 321–330.
- I. Nylander and E. Roman, *Psychopharmacology*, 2013, **229**, 555–569.
- J. N. Jaworski, D. D. Francis, C. L. Brommer, E. T. Morgan and M. J. Kuhar, *Psychopharmacology*, 2005, **181**, 8–15.
- B. A. Johnson and N. Ait-Daoud, *Psychopharmacology*, 2000, **149**, 327–344.
- H. R. Kranzler, *Alcohol Alcohol.*, 2000, **35**, 537–547.
- M. Davies, *J. Psychiatry Neurosci.*, 2003, **28**, 263–274.
- G. Kalsi, C. A. Prescott, K. S. Kendler and B. P. Riley, *Trends Genet.*, 2009, **25**, 49–55.
- G. F. Koob, *Biochem. Pharmacol.*, 2004, **68**, 1515–1525.
- W. Sieghart and M. Ernst, *Curr. Med. Chem.: Cent. Nerv. Syst. Agents*, 2005, **5**, 217–242.
- M. M. Silveri, J. T. Sneider, D. J. Crowley, M. J. Covell, D. Acharya, I. M. Rosso and J. E. Jensen, *Biol. Psychiatry*, 2013, **74**, 296–304.
- S. Kumar, P. Porcu, D. F. Werner, D. B. Matthews, J. L. Diaz-Granados, R. S. Helfand and A. L. Morrow, *Psychopharmacology*, 2009, **205**, 529–564.
- L. Churchill, A. Bourdelais, M. C. Austin, S. J. Lolait, L. C. Mahan, A. M. O'Carroll and P. W. Kalivas, *Synapse*, 1991, **8**, 75–85.
- G. E. Duncan, G. R. Breese, H. E. Criswell, T. J. McCown, J. S. Herbert, L. L. Devaud and A. L. Morrow, *Neuroscience*, 1995, **64**, 1113–1128.

- 18 S. C. Harvey, K. L. Foster, P. F. McKay, M. R. Carroll, R. Seyoum, J. E. Woods 2nd, C. Grey, C. M. Jones, S. McCane, R. Cummings, D. Mason, C. Ma, J. M. Cook and H. L. June, *J. Neurosci.*, 2002, **22**, 3765–3775.
- 19 W. Wisden, D. J. Laurie, H. Monyer and P. H. Seeburg, *J. Neurosci.*, 1992, **12**, 1040–1062.
- 20 J. Liu, A. R. Yang, T. Kelly, A. Puche, C. Esoga, H. L. June Jr., A. Elnabawi, I. Merchenthaler, W. Sieghart, H. L. June Sr. and L. Aurelian, *Proc. Natl. Acad. Sci. U. S. A.*, 2011, **108**, 4465–4470.
- 21 G. F. Koob and M. Le Moal, *Nat. Neurosci.*, 2005, **8**, 1442–1444.
- 22 G. F. Koob, A. J. Roberts, G. Schulteis, L. H. Parsons, C. J. Heyser, P. Hyytia, E. Merlo-Pich and F. Weiss, *Alcohol. Clin. Exp. Res.*, 1998, **22**, 3–9.
- 23 W. J. McBride and T. K. Li, *Crit. Rev. Neurobiol.*, 1998, **12**, 339–369.
- 24 H. L. June, K. L. Foster, P. F. McKay, R. Seyoum, J. E. Woods II, S. C. Harvey, W. J. A. Eiler, II, C. Grey, M. R. Carroll, S. McCane, C. M. Jones, W. Yin, D. Mason, R. Cummings, M. Garcia, C. Ma, P. V. V. S. Sarma, J. M. Cook and P. Skolnick, *Neuropsychopharmacology*, 2003, **28**, 2124–2137.
- 25 E. D. Cox, T. J. Hagen, R. M. Mckernan and J. M. Cook, *Med. Chem. Res.*, 1995, **5**, 710.
- 26 E. K. Sawyer, C. Moran, M. H. Sirbu, M. Szafir, M. Van Linn, O. Namjoshi, V. V. N. P. B. Tiruveedhula, J. M. Cook and D. M. Platt, *Alcohol. Clin. Exp. Res.*, 2014, **38**, 1108–1117.
- 27 D. S. O'Tousa, K. T. Warnock, L. M. Matson, O. A. Namjoshi, M. V. Linn, V. V. Tiruveedhula, M. E. Halcomb, J. Cook, N. J. Grahame and H. L. June, *Addict. Biol.*, 2015, **20**, 236–247.
- 28 J. K. Rowlett, R. D. Spealman, S. Lelas, J. M. Cook and W. Yin, *Psychopharmacology*, 2003, **165**, 209–215.
- 29 J. Kovacevic, T. Timic, V. V. Tiruveedhula, B. Batinic, O. A. Namjoshi, M. Milic, S. Joksimovic, J. M. Cook and M. M. Savic, *Brain Res. Bull.*, 2014, **104**, 1–6.
- 30 J. Divljakovic, M. Milic, O. A. Namjoshi, V. V. Tiruveedhula, T. Timic, J. M. Cook and M. M. Savic, *Brain Res. Bull.*, 2013, **91**, 1–7.
- 31 M. S. Allen, T. J. Hagen, M. L. Trudell, P. W. Coddington, P. Skolnick and J. M. Cook, *J. Med. Chem.*, 1988, **31**, 1854–1861.
- 32 T. J. Hagen, F. Guzman, C. Schultz, J. M. Cook, P. Skolnick and H. E. Shannon, *Heterocycles*, 1986, **24**, 2845–2855.
- 33 W. Yin, S. Majumder, T. Clayton, S. Petrou, M. L. VanLinn, O. A. Namjoshi, C. Ma, B. A. Cromer, B. L. Roth, D. M. Platt and J. M. Cook, *Bioorg. Med. Chem.*, 2010, **18**, 7548–7564.
- 34 W. Yin, P. V. V. S. Sarma, J. Ma, D. Han, J. L. Chen and J. M. Cook, *Tetrahedron Lett.*, 2005, **46**, 6363–6368.
- 35 O. A. Namjoshi, A. Gryboski, G. O. Fonseca, M. L. Van Linn, Z.-j. Wang, J. R. Deschamps and J. M. Cook, *J. Org. Chem.*, 2011, **76**, 4721–4727.
- 36 M. S. Allen, A. J. LaLoggia, L. J. Dorn, M. J. Martin, G. Costantino, T. J. Hagen, K. F. Koehler, P. Skolnick and J. M. Cook, *J. Med. Chem.*, 1992, **35**, 4001–4010.
- 37 M. S. Allen, Y. C. Tan, M. L. Trudell, K. Narayanan, L. R. Schindler, M. J. Martin, C. Schultz, T. J. Hagen, K. F. Koehler, P. W. Coddington, P. Skolnick and J. M. Cook, *J. Med. Chem.*, 1990, **33**, 2343–2357.
- 38 J. M. Cook, M. L. Van Linn and W. Yin, *U. S. Patent*, 8268854, 2012.
- 39 J. M. Bailey, G. Bruton, A. Huxley, P. H. Milner and B. S. Orlek, *PCT Int. Patent*, 2005014571, 2005.
- 40 J.-R. Jansen, M. Fuesslein, W. Hallenbach, O. Ort, C. Arnold, E.-M. Franken, O. Malsam, U. Reckmann, E. Sanwald and U. Goergens, *PCT Int. Patent*, 2009068194, 2009.
- 41 M. Godoi, G. V. Botteselle, J. Rafique, M. S. T. Rocha, J. M. Pena and A. L. Braga, *Asian J. Org. Chem.*, 2013, **2**, 746–749.
- 42 T. Heffron, B. Safina, S. Staben, D. P. Sutherlin, B. Wei, R. Elliott, R. Heald, E. M. Seward, E. Gancia and B. Waskowycs, *US Patent*, 20120245144, 2012.
- 43 M.-N. Birkholz, Z. Freixa and P. W. N. M. van Leeuwen, *Chem. Soc. Rev.*, 2009, **38**, 1099–1118.
- 44 K. T. J. Loones, B. U. W. Maes, G. Rombouts, S. Hostyn and G. Diels, *Tetrahedron*, 2005, **61**, 10338–10348.
- 45 S. Hostyn, B. U. W. Maes, G. Van Baelen, A. Gulevskaya, C. Meyers and K. Smits, *Tetrahedron*, 2006, **62**, 4676–4684.
- 46 C. O. Kappe, *Angew. Chem., Int. Ed.*, 2004, **43**, 6250–6284.
- 47 N. C. Bruno and S. L. Buchwald, *Org. Lett.*, 2013, **15**, 2876–2879.
- 48 B. P. Fors, N. R. Davis and S. L. Buchwald, *J. Am. Chem. Soc.*, 2009, **131**, 5766–5768.
- 49 B. P. Fors, D. A. Watson, M. R. Biscoe and S. L. Buchwald, *J. Am. Chem. Soc.*, 2008, **130**, 13552–13554.
- 50 J. P. Wolfe and S. L. Buchwald, *J. Org. Chem.*, 1997, **62**, 6066–6068.
- 51 B. U. W. Maes, K. T. J. Loones, T. H. M. Jonckers, G. L. F. Lemièrre, R. A. Dommissie and A. Haemers, *Synlett*, 2002, 1995–1998.
- 52 C. Meyers, B. U. W. Maes, K. T. J. Loones, G. Bal, G. L. F. Lemièrre and R. A. Dommissie, *J. Org. Chem.*, 2004, **69**, 6010–6017.
- 53 Y. Sunesson, E. Limé, S. O. Nilsson Lill, R. E. Meadows and P.-O. Norrby, *J. Org. Chem.*, 2014, **79**, 11961–11969.

Anxiety and alcoholism: Effects of GABA_A benzodiazepine agonists on the comorbid condition

Running title: GABA BDZ agonists reduce binge drinking and anxiolytic states

The intended authors were:

Marjorie Gondre-Lewis¹, Kaitlin T. Warnock¹, V. V. N. Phani Babu Tiruveedhula², Ojas Namjoshi³, James Cook² and Harry L. June, Sr.^{1, 4*}

But, we will certainly have to revise and re-order if we choose to put this forth.

¹Neuropsychopharmacology Laboratory, Department of Psychiatry and Behavioral Sciences, Howard University College of Medicine, Washington, DC 20060 USA

²Department of Chemistry and Biochemistry, University of Wisconsin-Milwaukee, Milwaukee, WI 53211, USA

³RTI International, Center for Drug Discovery, Research Triangle Park, NC 27513, USA

⁴Department of Pharmacology and Experimental Therapeutics, Howard University College of Medicine Washington, DC 20060, USA

Dear Jim,

This is a manuscript that Harry was working on as late as October of 2013. I think this was intended as a major publication between your and his laboratory. I think you are well-versed in the specific drugs used for anxiety treatment. If you would like, I can help bring this to fruition in the next few months as it still needs a lot of work. What are your thoughts?

Marjorie Gondré-Lewis

ABSTRACT

INTRODUCTION

Alcohol dependence and anxiety frequently co-occur in psychiatric patients and can significantly complicate treatment outcomes (Kushner et al., 2000; Tiet and Mausbach, 2007). Regier et al. (1990) reported that in the Epidemiological Catchment Area (ECA) survey, those with “any anxiety disorder,” as compared to the rest of the sample, had a 50% higher probability of being diagnosed with an alcohol disorder. Also, men and women with a generalized anxiety disorder (GAD) were 4 and 3 times, respectively, more likely to be diagnosed with alcohol dependence. Together, these studies suggest that “all or most anxiety disorders have a highly significant relationship to alcohol use disorders (AUDs)” (Kushner et al., 2000).

Additionally, substantial clinical studies show that anxiety disorders contribute to a poorer outcome in alcoholism treatment and an increase in the risk of relapse across a range of AUDs (LaBounty et al., 1992; Tomasson and Vaglum, 1996; Driessen et al., 2001). Thus, successfully treating comorbid anxiety disorders in even the “most standard alcoholic” would be expected to improve alcoholism treatment outcomes (Fals-Stewart and Schafer, 1992; Tollefson et al., 1992).

A critical review of the psychiatry literature from 1996 to 2007 identified only five randomized control studies which evaluated a drug treatment for comorbid alcoholism and anxiety. Of these, four employed the atypical anti-anxiety agent buspirone (a non-BDZ 5-HT_{1a} agonist/D2 dopamine agonist), and one used the SSRI paroxetine (Tiet and Mausbach, 2007). While paroxetine significantly reduced both fear/anxiety, no significant effects were observed on alcohol drinking (Randall et al., 2001). Tollefson et al. (1992) found that participants receiving buspirone showed significant reductions in anxiety scores; however, no significant medication effect was observed for physician-rated change in drinking. Kranzler et al. (1994) and Malcolm et al. (1992) reported negative findings with buspirone on anxiety and alcohol drinking in patients with nonspecific anxiety related disorders (i.e., GAD, phobia, etc). Given the lack of

effectiveness of the existing pharmacotherapies, researchers realized a clear need for new therapies to treat the comorbid condition (Swift, 1999; Tiet and Mausbach, 2007).

Research suggests that alterations occur in the GABAA receptor subunits once the animal transitions from the nondependent to dependent phases (Koob, 2004). Chronic alcohol consumption (i.e., diet) produces decreases in $\alpha 1$ subunit protein expression levels (Charlton et al., 1997; Devaud et al., 1997; Grobin et al., 2000) and increases in the $\alpha 4$ subunit in both the cerebral cortex and hippocampus of the rat (Devaud et al., 1997; Grobin et al., 2000; Matthews et al., 1998). Morrow and colleagues suggest that, with chronic ethanol consumption, the GABAA receptor $\alpha 1$ subunit is substituted by the $\alpha 4$ subunit (Devaud et al., 1995, 1997) and may contribute to both excessive alcohol drinking behavior and the development of ethanol dependence.

Previous research suggests that $\alpha 2$ -containing GABAA receptor subunits regulate the anxiolytic actions of BDZs (Low et al., 2000). However, new evidence using $\alpha 2$ -knockin mice suggests a role for the $\alpha 3$ -containing GABAA receptors (Dias et al., 2005). Finally, the discovery of a new anxiolytic ligand (ocinaplon) with significant efficacy at the $\alpha 1$ subunit suggests an important role for the $\alpha 1$ receptors (Lippa et al., 2005). Thus, the $\alpha 1$ – $\alpha 3$ -containing GABAA receptor subunits *all* seem to play a critical role in mediating the anxiolytic actions of BDZs. Much evidence suggests that, in rodents, the BLA is critical for the acquisition of fear/anxiety responses (Killcross et al., 1997), as well as innate expression of anxiety (Sajdyk and Shekhar, 1997). This locus contains high levels of both the $\alpha 1$ and $\alpha 2$ subunits (Fritschy and Mohler, 1995; Kaufmann et al., 2003).

In three highly-cited papers (Harvey et al., 2002; June et al., 2003, Foster et al., 2004), our lab has shown that systemic and direct infusion of mixed BDZ agonist-antagonist ligands with binding preference/selectivity for the $\alpha 1$ receptor (e.g., β CCt or 3-PBC) into the VP or CeA produces remarkably selective reduction in alcohol responding in nondependent P and HAD rats. Because the VP primarily contains GABA receptors of the $\alpha 1$ subtype (Churchill et al.,

1991; Kaufmann et al., 2003), and the CeA contains $\alpha 2$ and $\alpha 3$ subtypes (Fritschy and Mohler, 1995; Kaufmann et al., 2003), we hypothesized that the reduction in alcohol responding following microinfusion into the VP and CeA was due primarily to modulation of the $\alpha 1$ and $\alpha 2 - \alpha 3$ receptor subtypes, respectively (see June and Eiler, 2007). However, the HEK cell data presented in this manuscript allowed us to understand and exploit the molecular mechanism of action of our compounds. Given that $\alpha 2$ has been associated with anxiety, we wanted to further evaluate our compounds for regulation via the GABA $\alpha 2$ receptor.

MATERIALS AND METHODS

Subjects: P rats (males; N = X) were used to model binge alcohol drinking in humans (Bell et al., 2006; Nami et al., 2005). Animals were approximately 3 – 4 months of age at the beginning of the experiment.

Oral drugs and administration procedures: 3-PBC and β CCt (Dr. James Cook, University of Wisconsin-Milwaukee, Milwaukee, WI) were mixed immediately before the experimental test sessions in a volume of 1 ml/kg in deionized (DI) water. Drugs were given by oral gavage 25 min prior to all experimental sessions.

Binge Drinking Apparatus: Animals were tested in standard operant chambers (Coulbourn Instruments, Inc., Lehigh Valley, PA) enclosed in an isolation chamber as previously described (June et al., 2007). The dipper cup size was 0.1 mL, and contained the 10% (v/v) alcohol or 0.1% (w/v) sucrose reinforcers. The Coulbourn Graphic State “3” operant software was used (June et al., 2007).

Drinking in the Dark Multiple Scheduled Access (DIDMSA) Paradigm: The DIDMSA protocol (Bell et al., 2006) was used to initiate binge drinking with P rats. Identical and complete training procedures have been employed previously (Warnock et al., 2012). To initiate the DIDMSA protocol, the subjects were given a 30 min operant session using an FR-4 schedule after training. After the initial 30 min session had elapsed, rats were placed in the home cage with food and water ad libitum for 1 h. Rats then received two additional 30 min alcohol access periods, spaced 1 h apart. In total, animals received three daily 30 min access periods, each spaced 1 h apart. Other cohorts of rats were trained in an identical manner for 0.1% (w/v) sucrose. During the non-session binge period, rats received food and water ad libitum. Based

on preliminary data illustrating that sustainable and highly reliable measures of BACs produced negative affective measures of withdrawal following abstinence (Warnock et al., 2012), the P rats were engaged in binge drinking for 21 consecutive days. Using this protocol, BAC measurements exceeded ≥ 80 mg %/dL at the 90 min operant session.

Blood Alcohol Concentration (BAC) Measurement: To ensure that the P rats were consuming pharmacologically relevant amounts of ethanol to effectively model human binge drinking (Naimi et al., 2003), BACs were taken on day 21 from a subset of rats randomized into the drug treatment groups. BACs were determined in duplicates at the 30 and 90 min operant sessions as previously reported (June et al., 2007). The BAC measurements at 90 min were consistent with the NIAAA definition of binge alcohol consumption in humans (NIAAA, 2004; Bell et al., 2006).

Prolonged Repeated Alcohol Deprivation (PRAD) Paradigm: Rats were trained on the DIDMSA paradigm to binge drink for a full 6 weeks using the 90 min exposure regimen, with each 30 min session separated by 1 h, on a modification of the Rodd et al., (2003) paradigm. Following a 6 week period, rats were initially deprived of alcohol for 2 weeks. All animals were then re-exposed to the experimental chambers and allowed to respond on an FR4 schedule on both levers for alcohol [10%, v/v] for 2 weeks. Following this re-exposure period, all 4 of the deprived groups were once again deprived of alcohol for two more weeks before being given access to the operant chamber for an additional two weeks. Thus, all rats had 2 deprivation periods with each followed by a 2 week access (see **Table 1**).

Elevated Plus Maze (EPM) Paradigm: In order to measure anxiety we employed the EPM. The fully automated plus-maze (Acuscan Electronics, Columbus, OH) utilizes an apparatus with two

open arms without sides, at right angles to two closed arms with sides, and raised about four feet from the floor. When allowed to shuttle freely among the arms, rats spend less time on the open arms than on the closed arms, presumably reflecting a fear of height and open spaces. Forced confinement to the open arms is associated with increased plasma corticosterone concentrations and treatment with anxiolytic drugs increases the time rats spend on the open arms compared with un-drugged controls (Pellow et al., 1985; File, 1995).

Functional evaluation of ligands: The HEK cell data discussed below used standard methods from Dr. Ludden's laboratory. These procedures will be described prior to discussion of binding and functionality.

Statistical Analyses: Data were analyzed by between-group ANOVAs. Significant ANOVAs were followed by the Newman-Keuls *post-hoc* tests. All analyses were performed using the Sigma Plot 11.2 software program (Systat Software Inc., San Jose, CA).

EXPERIMENTAL DESIGN

Experiment 1: Evaluation of 3-PBC and β CCt on binge drinking

After 21 days of binge drinking alcohol/sucrose rats (N = 40) were randomly divided into 3-PBC (25, 40, or 75 mg/kg) or vehicle (DI water) groups (N = 5/group), and on Day 22, received their respective treatments. Similarly constructed cohorts received β CCt (25, 40, or 75 mg/kg) or vehicle (N = 5 – 8/group). BACs were taken on *day 21* from select 3-PBC or β CCt-treated rats.

Experiment 2: Evaluation of β CCt on the PRAD Paradigm

Following the 6 week training period 5 cohorts of P rats were randomly divided into treatment groups (N = 5/group) and withdrawn from alcohol as described above. Animals were

orally administered β CCt (25, 40 or 75 mg/kg) or vehicle 25 min before their 90 min binge session for 5 days post-deprivation, and responding was measured after the first 30 min and full 90 min sessions (see **Table 1**).

Experiment 3: Effect of β CCt on EPM

After the 21 days of binge drinking, 12 h after their last 30 min binge alcohol session (withdrawal), P (N = 5-6/group) and HAD (N = 6-8/group) rats were given β CCt (25, 40 or 75 mg/kg) or DI water 20 min prior to the 5 min plus maze session. Time spent on the open arms was measured and compared to respective pre-withdrawn groups (N = 6-7/group).

Experiment 4: Evaluation of β CCt on ICSS.

Phase I. Alcohol withdrawal time course. Following stabilization on an FR6 ICSS schedule, P rats were trained to binge drink alcohol (N = 6) or sucrose (N = 6). Following 21 days of binge drinking, abstinence was induced and ICSS parameters were measured over a 6 to 84 h period. During the abstinence period, both groups were given DI water.

Phase II. Effects of β CCt on alcohol withdrawal. To evaluate the effects of β CCt, five additional cohorts of P rats were stabilized on the FR6 ICSS schedule. Following 21 days of binge drinking, they were randomly divided into a sucrose control [N = 9], non-alcohol withdrawn [N = 9], alcohol withdrawal [N = 9], 20 mg/kg + withdrawal [N = 9], and 40 mg/kg + withdrawal [N = 9] groups. ICSS parameters were measured at 12 and 24 h withdrawal. Immediately, prior to the 12 and 24 h abstinence periods, oral β CCt [20, and 40 mg/kg] or vehicle was administered. The six cohorts were then compared with the sucrose control and non-alcohol withdrawn groups.

Experiment 5

Phase I. Expression of recombinant GABAA receptors. For electrophysiological recordings HEK 293 cells were passaged and re-plated on 12-mm glass cover slips located in 9.6 cm plastic dishes filled with 10 mL of Minimum Essential Medium (MEM, Gibco) supplemented with 158 mg/L sodium bicarbonate, 2 mM glutamine (Gibco), 100 U/mL penicillin-streptomycin (Gibco), and 10% fetal calf serum (Gibco). Cultures were maintained at 37° C in a humidified 95% O₂/5% CO₂ atmosphere for 2 – 3 days. Transfection of HEK 293 cells was carried out using the phosphate precipitation method as described elsewhere in detail (1). Rat wild-type subunit cDNAs of the GABAA receptor in the eukaryotic expression vector pRK5 were co-transfected in varying combination. For optimal receptor expression (1) the following final concentrations (µg vector DNA per 9.6 cm tissue culture plate) were used: α1, 2; α2, 4.8; α3, 1.2; α4, 10; α5, 0.8; α6, 2; β2, 10; β3, 0.4; γ2S, 0.5, and δ, 2. The γ2S variant is abbreviated γ2 in the remainder of the text. To facilitate the identification of transfected cells, 1 µg/ plate of pEGFPN1 vector (Clontech, Saint-Germain-en-Laye, France) was added.

Phase II. Electrophysiology. Two days after transfection, single coverslips containing HEK 293 cells were placed in a recording chamber mounted on the movable stage of a fluorescence microscope (Olympus IX70) and perfused at room temperature with a solution containing (in mM): 130 NaCl, 5.4 KCl, 2 CaCl₂, 2 MgSO₄, and 10 HEPES (free acid), pH adjusted to 7.35 with about 35 mM NaOH. Transfected cells were identified by their EGFP fluorescence, and ligand-mediated membrane currents of these cells were studied in the whole-cell configuration of the patch-clamp technique (2) with an electrophysiological set-up and procedure as described in detail elsewhere (3). To assess the concentration-response effects of βCCt and 3-PBC, increasing concentrations (0.01–100 µmol/L) of one of these compounds were co-applied to the cells with the approximate receptor subtype specific GABA EC₂₀. with a fast application system

(SF-77B, Perfusion Fast Step; Warner Instruments, LLC, Hamden, CT, USA) which enables rapid solution changes with maximal current rise times of < 1 ms for a liquid junction current on pipette tips, although the exchange around cells is probably slower. Maximal GABA-induced currents were determined by 1 mmol/L GABA. β CCt and 3-PBC were additionally tested at all concentrations in the presence of 10 μ M Ro15-1788 and GABA at its respective EC20.

Ethanol mediated effects on the receptor current response were tested with the approximate receptor subtype specific GABA EC10, and GABA EC10 with 30 mM or 100 mM ethanol. Furthermore, both ethanol concentrations were tested together with GABA EC10 and 1 nM or 30 nM of β CCt and 3-PBC, respectively. All compounds were additionally tested at the concentrations used here in the presence of GABA at its respective EC10 (data not shown).

The amplitudes of peak currents were measured from recorded traces. The GABA concentration–response curve was analyzed with a sigmoidal non-linear regression fit, using the formula $I = (I_{max}x[L]^nH)/(EC50^nH+[L]^nH)$, where I_{max} is the maximal induced current, L is the concentration of the agonist, and n the Hill coefficient. Current activation was depicted with the current rise-time by measuring the time needed from 10-90% of the peak current at the individual GABA concentration. Kinetics of current desensitization and current deactivation were fitted to standard exponential functions with one to three terms using the Chebyshev searching routines of ClampFit 8.1.

RESULTS

Experiment 1: 3-PBC and β CCt reduce binge drinking

Figures 1A and **C**, respectively, illustrate rates of responding maintained by impulsive binge alcohol (e.g., DIDMSA) drinking following oral administration of β CCt or 3-PBC (25, 40 and 75 mg/kg). Using the binge model, P rats produced consistent BACs of 144 ± 22 mg%/dL. The effects of β CCt and 3-PBC on binge sucrose responding, following identical drug treatments, are illustrated in **Figures 1B** and **D**, respectively. All doses of β CCt and 3-PBC markedly suppressed alcohol responding compared to vehicle (**Figs. 1A, 1C**) [β CCt, $F(2,14) = 11.546$, $p = 0.001$], [3-PBC, $F(2,8) = 53.053$, $p < 0.001$]. Neither β CCt nor 3-PBC (**Figs. 1B, 1D**) altered sucrose responding [β CCt, $F(2,8) = 0.0615$, $p > 0.05$] [3-PBC, $F(2,16) = 0.0187$, $p > 0.05$].

Experiment 2: Evaluation of β CCt on the PRAD Paradigm

In addition to the DIDMSA binge model, we employed the PRAD model to examine the effects of β CCt on the relapse/craving domain of alcohol dependence. Animals were initially trained on an FR4 schedule for 10% (v/v) alcohol for 6 weeks, using a 90 min operant session (Rodd et al., 2003). They were then subjected to either a single two week deprivation period - 2 week alcohol access period (**Figure 2**, 2 week ADE group), two cycles of this treatment (**Figure 2**, PRAD group), or PRAD exposure with β CCt treatment (**Figure 2**; 25, 50, or 75 mg β CCt group). β CCt was given during the initial 5 days of alcohol access for the last alcohol exposure phase. **Figures 2A and 2B** shows significant effects for Treatment [$F(4,5) = 21.065$, $p < 0.001$; $F(4,5) = 11.641$, $p < 0.001$], Day [$F(5,20) = 5.333$, $p < 0.001$; $F(5,20) = 10.032$, $p < 0.001$], and the treatment x day interaction [$F(20,149) = 2.377$, $p < 0.005$; $F(20,149) = 2.260$, $p < 0.005$] for the 30 min and 90 min sessions, respectively, for P rats on a 2 week PRAD paradigm. During the initial 6 week baseline period, all animals responded at relatively similar levels at the 30 and

90 min drinking sessions. More importantly, the PRAD group showed a marked elevation of responding above basal levels for all 5 post-deprivation days [$p < 0.05$ for both 30 and 90 min]; BACs were well above 110 mg%/dL and 138 mg%/dL at the 30 and 90 min sessions, respectively. These PRAD effects were markedly reduced by chronic treatment with β CCt [$p < 0.001$ for both 30 and 90 min]. Taken together, it is possible that the β CCt agent may be an effective treatment for both binge- and relapse-induced drinking.

Experiment 3: Effect of β CCt on EPM

Previous research has shown that withdrawal from drugs of abuse increased anxiety in the elevated plus maze (Koob, 2004). Thus, we evaluated this hypothesis after both P and HAD rats had binge-consumed high levels of alcohol for 21 days. On day 22, 12 h after the rats' last 30 min binge alcohol session, we performed the standard 5 min test in control- and β CCt- (25 – 75 mg/kg) treated HAD and P rats. **Figures 3A – B** show that, compared with the control (non-alcohol treated) animals, alcohol abstinence produced a significant reduction in time spent in the open arms in HAD and P rats. However, rats given the β CCt treatment exhibited a markedly enhanced duration of time on the open arms of the plus maze. [HAD rats, $F(3,22) = 2.859$, $p \leq 0.05$; P rats, $F(4,22) = 7.783$, $p < 0.001$]. These data are in agreement with other studies which show that treatments that augment GABAergic activity reduced the anxiogenic actions on the plus maze following alcohol abstinence (for review see Rassnick et al., 1993; Koob, 2004).

Experiment 4: Evaluation of β CCt on ICSS.

Phase I. Alcohol withdrawal time course.

Figure 4A illustrates time-dependent threshold elevations in P rats after withdrawal from alcohol following 21 consecutive days of intake using the home cage DIDMSA protocol (Bell et al., 2006). The BACs on Day 21 were 148 ± 32 mg%/dL in P rats. Significant main effects of Time [$F(8,40) = 5.046$, $p < 0.001$], Treatment [$F(1,5) = 21.910$, $p = 0.005$], and the interaction of

Time x Treatment [$F(8,40) = 3.852, p = 0.002$] were seen for withdrawn vs. control groups. At the 6 h abstinence period, threshold elevations began to emerge, and by 12 h post-alcohol administration, the elevations were markedly above the level of the control animals in the Baseline 1 and 2 conditions [$p \leq 0.05$]. By 84 h post-alcohol administration, the threshold elevation effects had dissipated. Thus, as in outbred rats using the alcohol vapor chamber (Schulteis et al., 1994), alcohol-induced abstinence effects can also be observed in alcoholic rats following *oral* binge alcohol intake using the ICSS model.

Phase II. Effects of β CCt on alcohol withdrawal.

Though chronic alcohol exposure produced no ICSS threshold lowering effects on either the minimum frequency or EF_{50} parameters [**Figures 4B and C**], [$p > 0.05$], alcohol-abstinent P rats displayed a markedly enhanced elevation in ICSS threshold [$p < 0.05$ for minimum frequency at 12 hr, EF_{50} at 24 hr] [**Figures 4A and B**]. When the abstinent rats were pre-treated with the 20 and 40 mg/kg oral doses of β CCt, a marked reduction in both the minimum [$p < 0.05$ for 40 mg/kg at 12 and 24 h] [**Figure 4B**] and EF_{50} [$p < 0.05$ for both doses on both days] [**Figure 4C**] threshold measures was observed. Thus, β CCt may “normalize” GABA, or an interaction at monoaminergic neurotransmission, in the abstinent P rats, restoring the alcohol-deficient GABA/monoamine systems to appropriately regulate reward-related behaviors.

Experiment 5

Phase I. Expression of recombinant GABA_A receptors

As illustrated by Harvey et al. (2002) and Yin et al. (2005), an examination of the potencies of a series of compounds across GABA_A receptor subtypes by radioligand binding (including both “diazepam sensitive” [DS] types [α 1-,2-, 3-, and 5-containing] as well as a “diazepam insensitive” [DI] subtype [α 4 and α 6-containing]) reveals selectivity at GABA_A α 1 receptors for β CCt and 3-PBC, relative to the prototypic α 1-preferring compounds zolpidem and

CL 218,872. For example, β CCt and 3-PBC exhibit ~15 – 26-fold higher affinity for α 1 relative to other subtypes examined. Both zolpidem and CL 218,872 exhibit no more than a 10-fold selectivity at α 1 relative to the other GABA_A receptor subtypes examined. Note that there are no remarkable differences in the potency of the prototypic benzodiazepine diazepam among GABA_A α 1-, 2-, 3-, and 5-containing receptors.

The electrophysiological studies using recombinant receptors provide insights into the functional pharmacology of drugs at specific GABA_A receptor subtypes. **Figure 5** illustrates the efficacy of β CCt and 3-PBC across the GABA_A α 1-2 receptor subtypes. It is clear that the novel compounds exhibit efficacies lower than diazepam across the 0.01 – 100 μ M dose range. A similar profile of effects occurred at the α 3 and 5 receptor subtypes (data not shown). The predicted α 2-mediated anxiolytic profile of diazepam would likely be accommodated by a greater number of unwanted side effects due to the greater augmentation of GABA at the α 1- and α 5-mediated sedative subunits (Barnard et al., 1998). This contrasts with the anxiolytic effects of the novel ligands. Also, unlike diazepam, at the α 1 and α 2 subunits, the GABA-mediated effects do not appear to be mediated via the normal BDZ site, as Ro15-1788 (flumazenil) partially/completely fails to block the GABA potentiation of β CCt and 3-PBC (**Figure 5**). At the α 6 subtype, little if any efficacy occurred with any of the four ligands (data not shown).

Harvey et al. (2002) and Yin et al. (2005) show that the affinity of β CCt is about 21 – 26-fold higher at GABA_A α 1 relative to GABA_A α 2 and α 3, respectively. In electrophysiological studies, the EC₅₀ values for β CCt (at an EC₂₀ of GABA) are 0.21 μ M, 9.43 μ M, and 3.14 μ M at GABA_A α 1, 2, and 3, respectively (Rabe and Lüddens, unpublished). By comparison, the EC₅₀ values of diazepam across these three isoforms are 0.07 μ M, 0.18 μ M, and .08 μ M respectively. This illustrates that diazepam is nonselective across these receptor isoforms, while β CCt is relatively selective at the GABA_A α 1 subtype. Hence, these findings illustrate that the affinity ratio determined by radioligand binding techniques as summarized in Harvey et al. (2002) and Yin et al. (2005) are not generally indicative of “the functional consequences of these ligands at

GABA_A receptors” because they do not measure the compounds’ efficacies, but only their relative potencies. Thus, electrophysiological studies are used: to provide some insight into the pharmacological effects of compounds at specific receptor subtypes. The preliminary efficacy data in **Figure 5** illustrates this point. Radioligand binding studies would not have predicted the Ro 15-1788-insensitive augmentation of GABA currents by β CCt and 3-PBC. Thus, radioligand binding studies clearly do not reflect “functional consequences.” Inspection of the binding and functional data for the DI α 4-containing subtype shows that β CCt and 3-PBC augments GABA at the α 4 β 3 γ 2 subtype at the 1 and 10 μ M concentrations (**Figure 5**). Moreover, at the α 4 β 2 δ subtype, dramatic modulation on alcohol mediated GABA currents was observed by β CCt (**Figure 5**). However, the potencies of these compounds, as determined by radioligand binding techniques and summarized in Harvey et al. (2002) and Yin et al. (2005), are silent (i.e., very low affinity). Clearly, the binding constants at these receptors do not predict their functional consequences. In summary, binding constants for our novel ligands are generally not reflective of the potential functional consequences resulting from a ligand-receptor interaction, although there are a few exceptions.

β CCt and 3-PBC in vitro.

Unexpectedly, 3-PBC potentiated GABA-induced currents of GABA_A receptors consisting of α - and β - subunits only. On α 1 β 3 and on α 6 β 3 50 μ M of the drug enhanced GABA-induced currents up to the GABA EC90 (**Fig. 6**). Since α 4 β 2/3 and α 6 β 2/3 receptors seem to be extra synaptic (McKernan and Whiting, 1996), these findings might play a physiological role, i.e. by enhancing the GABA sensitivity of these extra synaptic receptors. In both cases 1 μ M of ZK 93426 completely antagonized the 3-PBC effect. On the other hand, β CCt had no significant effects of the GABA induced currents.

β CCt and 3-PBC Modulate Alcohol Action in vitro

Given the consistent reports in our laboratory that both β CCt and 3-PBC are selective antagonists of alcohol motivated behaviors and are also anxiolytics (June and Eiler, 2007; also see below), we evaluated the capacity of these ligands to block alcohol's action at the α 2 subtype. **Figure 7** shows that low doses of both 3-PBC and β CCt (1 – 30 nM) dose-dependently reduced the low and high dose (30 and 100 mM) alcohol enhancement at the α 2 receptors. Taken together, we hypothesize that WYS8, β CCt and 3-PBC may reduce excessive alcohol drinking (see below) via an anxiolytic action, particularly because of the role of the α 2 subunit in anxiety (Low et al., 2000).

DISCUSSION

In an attempt to find an agent active in treating anxiety and alcoholism, we employed P and HAD rats (McBride and Li, 1998; Murphy et al., 2002) to model the effectiveness of the α 1-preferring BDZs, 3-PBC and β CCt, on binge alcohol self-administration, craving/relapse, anxiety (using the EPM) and negative affective states (as seen with anhedonia in the ICSS).

In vitro, 3-PBC and β CCt act primarily at the α 1, α 2 and α 3 receptors, diazepam sensitive sites, (**Fig. 5**) by potentiating GABA across different concentrations that are equivalent to the doses of 3-PBC and β CCt given orally to our rats during the behavioral studies. This is consistent with our previous work (Liu et al., 2011) that used siRNA viral vectors to show that GABA α 1 and α 2 receptor subunits play a significant role in regulating binge alcohol drinking. Additionally, the compounds potentiate GABA at the α 4 receptor, a diazepam insensitive site (**Fig. 5**). We initially hypothesized that our compounds work only at the diazepam sensitive sites, α 1, α 2 and α 3, but we show that our compounds may also be acting at the diazepam insensitive site, α 4, which has been shown to regulate social drinking (Janek, PNAS 2011). The α 2 receptor is particularly involved in antagonizing alcohol binge drinking (Liu et al., 2011; June and Eiler, 2007). Both low and high concentrations of alcohol potentiate GABA at the α 2 subunit (**Fig. 7**). This is important because it contrasts the Olsen et al., (date) manuscript that shows that only low doses of alcohol potentiate GABAergic activity at these subunits. Both 3-PBC and β CCt alone do not potentiate the GABA α 2 subunit at small doses. However, when given in combination with alcohol, both compounds dose-dependently reduce the GABA potentiation by alcohol (**Fig. 7**). These data are consistent with the role of α 2 in regulating binge drinking showing by Liu et al. (2011) in PNAS. Given that the α 2 subunit has been shown to play a role in anxiety (Low et al., 2000), this data strongly suggests that our ligands may be reducing binge drinking as well as negative affect.

Alcohol dependence and anxiety frequently co-occur in psychiatric patients and can significantly complicate treatment outcomes (Kushner et al., 2000; Tiet and Mautsach, 2007).

Using an established binge model (Bell et al., 2006; Liu et al., 2011), we demonstrated the GABA α 1-preferring ligands, 3-PBC and β CCt, effectively and dose dependently reduce binge alcohol, but not binge sucrose drinking. The sucrose concentration was selected so response rates would be relatively similar to both alcohol and sucrose, eliminating the potential confound of a “difference in reinforcer efficacy” (June et al., 2003; June and Gilpin, 2010). The failure of both β CCt and 3-PBC to alter sucrose responding strongly suggests that these agents would not disrupt normal ingestive behaviors (June and Gilpin, 2003). These results agree with another study done by June and Eiler (2007) where the efficacies of both β CCt and 3-PBC in selectively reducing alcohol responding and producing anxiolytic effects were demonstrated in P and HAD rats following oral administration (June and Eiler, 2007). Taken together, these data indicate that 3-PBC and β CCt selectively suppress alcohol-motivated behaviors in alcohol-dependent rats. Additionally, our findings are supported by the work of Boem and colleagues (year) with other GABA-selective compounds. However, unlike the compounds used in the Boem studies, our GABA compounds can be used in a clinical population.

Previous research has shown that withdrawal from drugs of abuse increase anxiety in the elevated plus maze (Koob, 2004); decreased time spent on the open arms of the EPM approximates increased anxiety (citation needed). In our study, compared with the control (non-alcohol treated) animals, alcohol abstinence produced a significant reduction in time spent in the open arms in HAD and P rats. However, rats given the β CCt treatments exhibited markedly increased time spent on the open arms of the plus maze (**Fig. 3**). Our also data strongly support the capacity of our BDZ compounds to attenuate the anxiolytic effects of alcohol withdrawal. These data are in agreement with other abstinence studies which show treatments that augment GABA reduced the anxiolytic actions of withdrawal on plus maze activity (Rassnick et al., 1993; Koob, 2004).

Elevations in ICSS threshold parallel anhedonia (Paterson and Markou, 2007), a condition characterized by a diminished pleasure or interest (American Psychiatric Association

(APA), 2000). Anhedonia is a core symptom of depression and drug withdrawal (Markou et al., 1998; Paterson and Markou, 2007), and thus, elevations in ICSS threshold have been used to model negative affective states (Der-Avakian and Markou, 2012). As observed in both depressed and drug-withdrawn states, ICSS measures of total responding also provide an assessment of psychomotor performance (Eiler et al., 2005; Paterson and Markou, 2007). In our study, we showed that there is a significant elevation of minimum frequency following 12 to 72 h of alcohol withdrawal as compared to a sucrose control group (**Fig. 4A**). Furthermore, we showed that β CCt is effective in attenuating the increase in minimum frequency and EF_{50} parameters caused by 12 or 24 h of withdrawal (**Fig. 4B**; **Fig. 4C**). Anhedonia has been suggested as a key component of the abstinence symptomatology (Gawin and Kleber, 1986), and as an important factor in relapse (Koob and Le Moal, 2001). In the ICSS model, β CCt was effective in reducing alcohol-induced negative affective states which have been suggested to emulate depression-like behaviors in humans (Heinz et al., 1994; Paterson and Markou, 2007). While anxiety is addressed with the effects of β CCt on withdrawal in the EPM, the fact that β CCt also significantly attenuates withdrawal symptomatology in the ICSS paradigm suggests our compounds may also be effective in regulating the mechanisms of depression.

A critical review of the psychiatry literature from 1996 to 2007 identified only five randomized control studies which evaluated a drug treatment for comorbid alcoholism and anxiety. Of these, four employed the atypical anti-anxiety agent buspirone (a non-BDZ 5-HT 1a agonist/D2 dopamine agonist), and one used the SSRI paroxetine (Tiet and Mausbach, 2007). Randall et al. (2001) examined the efficacy of paroxetine for the treatment of social anxiety and alcohol abuse or dependence (Randall et al., 2001). All five studies reported significant effects on anxiety, but no effects on alcohol drinking (Tiet and Mausbach, 2007). Given the ineffectiveness of the existing pharmacotherapies, researchers have come to the realization that there is a clear need for new drug therapies to treat the comorbid condition (Swift, 1999; Tiet and Mausbach, 2007). Based on our binge alcohol drinking and negative affect data, our α 1-

preferring ligands represent significant, novel pharmacotherapies for treating the comorbid condition of alcoholism and anxiety.

Rodd et al. (2003) contend that the drinking patterns of human alcoholics are segmented by multiple periods of abstinence and intake, also known as relapse (Hilbrom, 1990; McMillen, 1997). Relapse drinking, similar to binge drinking, is an excessive model of drinking that produce hazardous effects in adolescents (citation needed) as well as the adult population (citation needed). Substantial epidemiological work suggests these excessive models are the most devastating alcohol patterns to society (citation needed), in contrast to traditional DSM-IV definition alcohol dependence (APA, 1994). In this study, we used the PRAD paradigm (Rodd et al., 2003) to illustrate craving/relapse in an animal model of alcohol abuse. As with the DIDMSA model, the PRAD model produces dependence in P and HAD rats, though it has also been suggested to be a relapse model. Because we see a significant attenuation of responding for alcohol during the relapse period by β CCt compared with relapse alone (**Fig. 2**), this suggests that our BDZs represent promising pharmacotherapies for alcohol craving and relapse. Unlike binge drinking, very few studies have looked at GABA agents and relapse drinking. Our data suggest that our compounds can be used not only to antagonize binge drinking, but also relapse drinking. Because our compounds act at primarily the GABA α 1, α 2 and α 3 subunits, our data also suggest that these GABA subunits may be involved in the regulation of alcohol craving/relapse in addition to the regulation of binge alcohol drinking.

In summary, both 3-PBC and β CCt were effective in attenuating binge alcohol drinking, and β CCt was effective in regulating craving/relapse. In addition, β CCt was effective in attenuating two measures of negative affect induced by abstinence: anxiety and anhedonia (Paterson and Markou, 2007). The responding profiles in the ICSS assay suggest that the effects of β CCt on negative affective states are not secondary to altering general activity. Thus, given the ability of the EPM and ICSS to model aspects of the anxiolytic and depressive symptomatology (Paterson and Markou, 2007), we propose that our compounds may be

effective in attenuating anxiety/depression secondary to alcohol-induced abstinence. Given the effectiveness of our compounds for treating the comorbid condition, the failure/reduced capacity of our compounds to show additive sedative effects with alcohol (June et al., 2003), and the need for pharmacotherapies that affect both alcohol consumption and anxiety (Swift, 1999; Tiet and Mausbach, 2007), we propose β CCt and 3-PBC would be effective in treating the co-occurrence of alcoholism and anxiety at doses that are safe and well tolerated in humans.

ACKNOWLEDGEMENTS

The studies in this manuscript were financed by a grant AA017963 to HLJSr from the National Institute of Alcohol Abuse and Alcoholism (NIAAA). Generous financial support for JMC was provided by NIH (AA016179, NS076517). The authors acknowledge support from the Milwaukee Institute for Drug Discovery, Analytical Instrumentation support was provided by UW-Milwaukee's Shimadzu Laboratory for Advanced Applied and Analytical Chemistry.

DISCLOSURE

The authors declare no conflict of interest.

REFERENCES

- Harvey, S. C.; Foster, K. L.; McKay, P. F.; Carroll, M. R.; Seyoum, R.; Woods, J. E., 2nd; Grey, C.; Jones, C. M.; McCane, S.; Cummings, R.; Mason, D.; Ma, C.; Cook, J. M.; June, H. L. *J. Neurosci.* **2002**, *22*, 3765-3775.
- Yin, W.; Sarma, P. V. V. S.; Ma, J.; Han, D.; Chen, J. L.; Cook, J. M. *Tetrahedron Lett.* **2005**, *46*, 6363-6368.
- Rowlett, J. K.; Spealman, R. D.; Lelas, S.; Cook, J. M.; Yin, W. *Psychopharmacology* **2003**, *165*, 209-215.
- Yin, W.; Majumder, S.; Clayton, T.; Petrou, S.; VanLinn, M. L.; Namjoshi, O. A.; Ma, C.; Cromer, B. A.; Roth, B. L.; Platt, D. M.; Cook, J. M. *Biorg. Med. Chem.* **2010**, *18*, 7548-7564.

FIGURE LEGENDS

Figure 1. Effects of β CCt and 3-PBC (25, 40 and 75 mg/kg) on binge alcohol (**A, C**) and sucrose (**B, D**) responding in P rats (N = 5-8/dose), * $p \leq 0.05$.

Figure 2. Effects of orally-administered β CCt on a 2 week PRAD paradigm over (**A**) 30 min and (**B**) 90 min in P rats. (N = 5 – 9/group; Total N = 36). BL = baseline; ## $p \leq 0.05$ compared with 25, 40 and 75 mg β CCt PRAD groups, ‡ $p \leq 0.05$ compared with 2 week ADE group.

Figure 3. The effects of withdrawal from binge alcohol consumption in (**A**) HAD and (**B**) P rats in the elevated plus maze test for normal (non-alcohol treated), binge alcohol-withdrawn, and β CCt-treated rats (N = 6 – 8/treatment group). The plus maze test was 5 min and the treatments were given orally immediately prior to evaluation. **, $p \leq 0.05$ compared with withdrawn condition, ††, $p \leq 0.05$ compared with vehicle.

Figure 4. (**A**) Time-dependent elevation of ICSS during alcohol withdrawal in P rats (N = 6/group). Rats were withdrawn from alcohol for 6 – 84 h after 21 days of consecutive binge alcohol intake. Min Freq (**B**) and EF_{50} (**C**) of P rats (N = 9/group) in ICSS pre-withdrawal, during withdrawal, and with β CCt treatment. *, $p \leq 0.05$ compared with the vehicle-treated “withdrawn” rats.

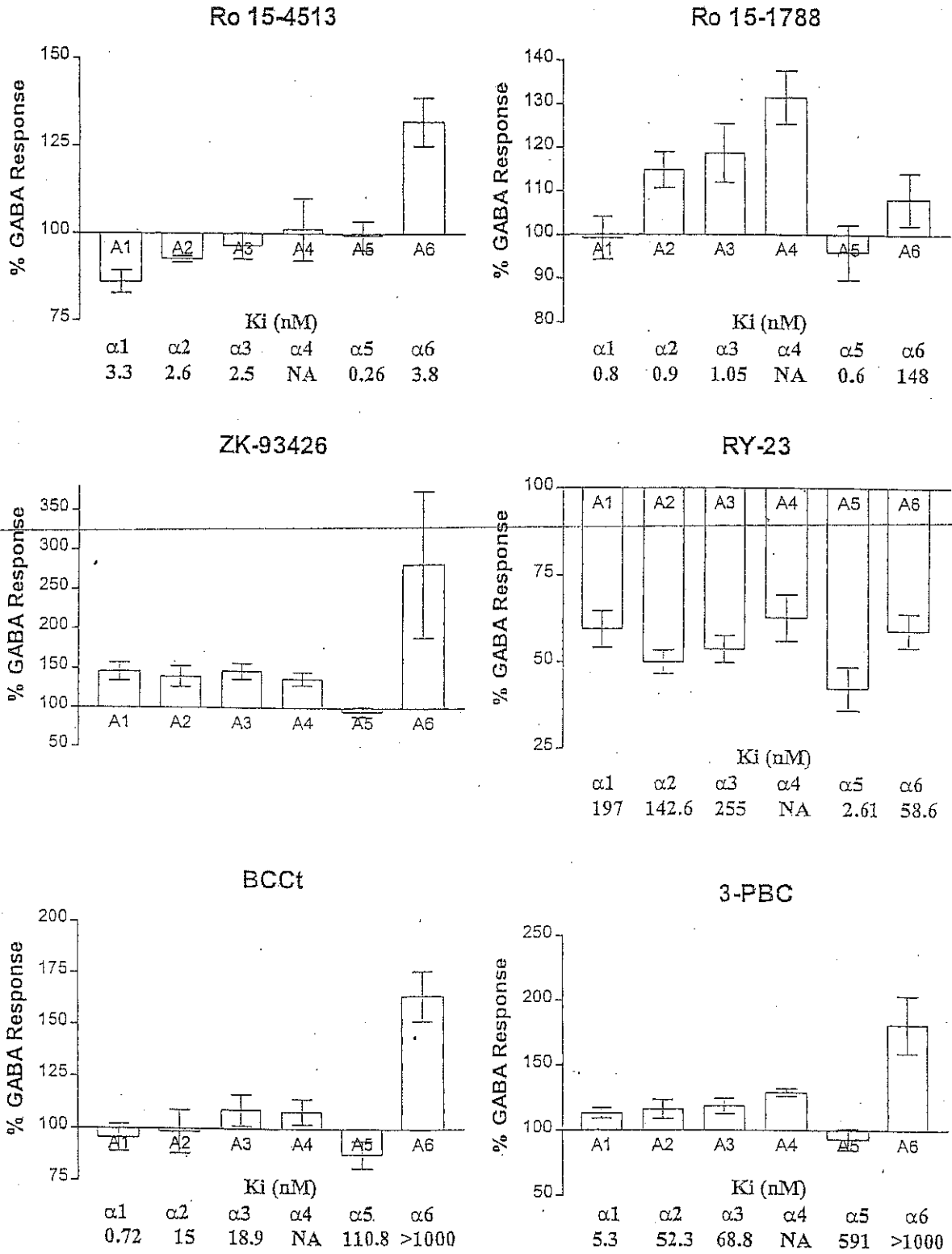
Figure 5. Whole-cell recordings of HEK 293 cells expressing recombinant rat $\alpha 1\beta 3\gamma 2$, $\alpha 2\beta 3\gamma 2$, $\alpha 3\beta 3\gamma 2$, $\alpha 4\beta 3\gamma 2$, $\alpha 5\beta 3\gamma 2$ and $\alpha 6\beta 3\gamma 2$ (GABA_A) receptors for diazepam (DZ), β CCt, and 3-PBC at doses of 0.1 – 100 μ M interacting with Ro15-1788 (10 μ M) at the EC₂₀ level. Asterisk (*), plus (+), and number (#) symbols denote $p < 0.05$ in a two-sided t-test. * indicates significance of DZ, β CCt or 3-PBC compared to GABA control; +, of DZ, β CCt or 3-PBC plus Ro15-1788

compared to treatments alone; and #, of DZ, β CCt or 3-PBC plus Ro15-1788 compared to GABA control. Error bars indicate the standard error of the mean (\pm SEM) for at least four cells.

Figure 6. Effects of 3-PBC (A) and β CCt (B) on GABA-induced currents to GABA_A receptors consisting of α - and β - subunits only. Currents were normalized to the GABA concentration specific for the receptor subtype under *in vitro* conditions. On α 1 β 3, 50 μ M of 3-PBC (A) enhances the GABA-induced currents up to the GABA EC₉₀. β CCt (B) had no significant effects of the GABA induced currents. Error bars indicate the standard error of the mean (\pm SEM) for at least four cells. p-values were calculated with the students t-test (paired).

Figure 7. Whole-cell recordings of HEK 293 cells expressing recombinant rat α 2 β 3 γ 2 GABA_A receptors. Currents were normalized to the GABA concentration specific for the receptor subtype EC10 under *in vitro* conditions. (A) Two concentrations of ethanol (30 mM and 100 mM) in the absence or presence of 1 nM and 30 nM β CCt, respectively, were co-applied with 1.5 μ M GABA. (B) An identical set of experiments was performed with 3-PBC. Asterisk (*), plus (+), and number (#) symbols denote $p < 0.05$ in a two-sided t-test. * indicates significance compared to GABA control; +, of GABA plus ethanol compared to GABA plus ethanol plus β -carboline; and #, of GABA plus ethanol plus 1 nM β -carboline compared to GABA plus ethanol plus 30 nM β -carboline. Error bars indicate the standard error of the mean (\pm SEM) for four cells.

Efficacy of GABA_A Receptor Modulators



Percent modulation of GABA-evoked current responses in voltage clamped *Xenopus* oocytes expressing recombinant GABA_A receptors. Each oocyte was injected with cRNA of indicated α subunit together with cRNA of $\beta 3$ and $\gamma 2$ subunits. GABA concentration is at the EC₅₀ for each receptor subunit combination. Concentration of indicated modulator is saturating (1-10 μ M). The peak whole cell current response from application of GABA and modulator is reported as the percentage of the peak response to GABA alone (% GABA Response). Each value is the mean \pm standard deviation for 3 or more separate oocytes (Harvey, June, Cook et. al. in press).^{19-22, 55}

METHODS

Materials. *Xenopus laevis* frogs were purchased from Xenopus-1 (Dexter, MI). Collagenase B was from Boehringer Mannheim (Indianapolis, IN). GABA was from RBI, all other compounds were synthesized by James Cook (UW)

cDNA clones. The rat GABA receptor alpha 1-5, beta 3 and gamma 2 clones were gifts from Dr. Luddens (Department of Psychiatry, University of Mainz, Germany).

Injection of in vitro synthesized RNA into Xenopus oocytes. Capped cRNA was synthesized from linearized template cDNA encoding the subunits using mMMESSAGE mMACHINE kits (Ambion, Austin, TX). Oocytes were injected with the alpha, beta and gamma subunits in a molar ratio of 1:1:1 as determined by UV absorbance.

Mature *X. laevis* frogs were anesthetized by submersion in 0.1% 3-aminobenzoic acid ethyl ester, and oocytes were surgically removed. Follicle cells were removed by treatment with collagenase B for 2 hr. Each oocyte was injected with 50-100 ng of cRNA in 50 nl of water and incubated at 19° C in modified Barth's saline (88 mM NaCl, 1mM KCl, 2.4 mM NaHCO₃, 0.41 mM CaCl₂, 0.82 mM MgSO₄, 100 µg/ml gentamicin, and 15 mM HEPES, pH 7.6). Oocytes were recorded from after 3 to 10 days post-injection.

Electrophysiological recordings. Oocytes were perfused at room temperature in a Warner Instruments oocyte recording chamber #RC-5/18 (Hamden, CT) with perfusion solution (115 mM NaCl, 1.8 mM CaCl₂, 2.5 mM KCl, 10 mM HEPES, pH 7.2). Perfusion solution was gravity fed continuously at a rate of 15 ml/min. Compounds were diluted in perfusion solution, and applied until a peak current was reached.

V. V. N. Phani Babu Tiruveedhula, Ph.D.

3495 N Oakland Ave, Apt # 310

Milwaukee, Wisconsin - 53211

Education:

- **Ph. D.** in Synthetic Organic and Medicinal Chemistry
Advisor: **Dr. James M. Cook**, University Distinguished Professor
University of Wisconsin-Milwaukee, Milwaukee, WI, USA 2010 – 2017
Dissertation title: Part I – Development of a two-step regiospecific synthetic route for multigram-scale synthesis of β -carboline analogs for studies in primates as anti-alcohol agents
Part II – Design and synthesis of novel antimicrobials for the treatment of drug resistant bacterial infections
Part III – A novel synthetic method for the synthesis of the key quinine metabolite (3*S*)-3-Hydroxy-quinine
- **M.Sc.**, Organic Chemistry, Acharya Nagarjuna University, India 2005-2007
- **B.Sc.**, (Maths, Physics, Chemistry), Acharya Nagarjuna University, India 2002-2005

Experience:

Industry:

- Research Associate (R&D Division), Sreeni labs Pvt. Ltd., Hyderabad, India 2007-2010
 - Worked on different projects for synthesizing API's and pharmaceutical intermediates from milligram to multi-kilogram scale, process optimization and impurities characterization using analytical tools (TLC, NMR, HPLC, GC, FTIR, LC-MS etc.,)
 - Led the group of chemists as a team leader to meet the deadlines and mentored the new chemists in process research development

Doctoral Student:

- Designed novel synthetic routes for acrylic acid derivatives and different heterocyclic molecules including β -carboline, indole, and process optimization for (3*S*)-3-hydroxyquinine
- Designed regioselective metal-catalyzed cross coupling reactions and its applications
- Synthesized over 100 new acrylic acid derivatives as well as heterocyclic molecules for *in vitro* and *in vivo* screening for antimicrobial and anti-alcohol abuse activity
- Designing of multi-step synthetic process for indole natural products Macrodasine A-G from commercially available starting material D-Tryptophan
- Active involvement in drug design and interpretation of SAR
- Mentored two undergraduates, two new graduate students in research and two post-doctoral associates for conducting the reactions under oxygen free environment for metal-catalyzed cross coupling reactions
- Optimized the protocols for cytotoxicity, DNA intercalating and gel electrophoresis studies
- Rodent Studies for sedation, ataxia, toxicity and behavioral effects
- Discovery of novel approach to identify target proteins responsible for antimicrobial activity of TI-I-100 using Click chemistry with LC-MS/MS (Shimadzu, Agilent technologies)
- Protein purification by affinity and size exclusion chromatography techniques using FPLC
- Purchasing coordinator for Cook group to maintain the stock of chemicals, solvents and other supplies to conduct research and getting the best price from different vendors
- Research Assistant/Teaching Assistant, Department of Chemistry and Biochemistry, UW-Milwaukee 2010-2017
- Mentor for new graduate students on teaching skills for four consecutive semesters, Department of Chemistry and Biochemistry, UW-Milwaukee 2012-2014

Awards and Honors:

- **The Research on Alcoholism was selected for the UWM News Report and presented in UWM home page “Taking Depression Out of treating alcoholism”** June, 2016
- **UWM – Chemistry and Biochemistry Department Research Award “Dr. Sosnovsky Award for Excellence in Graduate Research”** April, 2015
- **American Chemical Society (ACS) Division of Medicinal Chemistry Travel grant** for attending ACS National Meeting, San Diego, CA, March 13-17, 2016
- **ACS (The world’s largest scientific society) selected the abstract “Design and Regiospecific Synthesis of 3-Substituted β -carbolines as a GABA_A subtype Selective Agents for the Treatment of Alcohol Abuse” for press release at 250th ACS National Meeting, Boston, MA** August 19th, 2015
- **The above research work was published in Chemical and Engineering news magazine by ACS and published in Chemistry world news magazine by Royal Society of Chemistry** August 24th, 2015
- Graduate Student Council Travel Award; Awarded by the Center for Student Involvement, University of Wisconsin-Milwaukee June, 2015 and January, 2016
- Chancellor’s Graduate Fellowship; Awarded by the University of Wisconsin- Milwaukee 2010-2013
- Mentoring Travel Award; Awarded by the University of Wisconsin- Milwaukee New Graduate Student Mentor Program 2012-2014
- Student Travel Award; Awarded by the Milwaukee section of the **American Chemical Society** 2014
- Graduate Student Travel Award; Awarded by the Graduate School at the University of Wisconsin – Milwaukee 2013-2014

Publications:

- “Concise Total Synthesis of Sarpagine and Macroline Oxindole Alkaloids (-)-Affinisine Oxindole, (+)-Isoalstonisine, (+)-Alstofoline, (-)-Macrogentine, (+)-N(1)-Demethylalstonisine, and (-)-Alstonoxine A as well as an improved Total Synthesis of (+)-Alstonisine” Stephen, Michael Rajesh.; Rahman, M. Toufiqur.; **Tiruvedhula, V. V. N. Phani Babu.**; Fonseca, German. O.; Deschamps, J.R.; Cook, James. *Chem. Eur. J.* **2017**, *Manuscript under review*
- “Neurobiological correlates of State-Dependent Context Fear”, Meyer, M. A. A.; Corconran, K. A.; Chen, H. J.; Gallego, S.; Li, G.; **Tiruvedhula, V. V. N. Phani Babu.**; Cook, J. M.; Radulovic, J. *Learning and Memory.* **2017**, *Manuscript accepted*
- “Evidence that sedative effects of benzodiazepines involve unexpected GABA_A receptor subtypes: Quantitative observation studies in rhesus monkeys” Meng, Zhiqiang.; Duke, Angela N.; Platt, Donna M.; **Tiruvedhula, V. V. N. Phani Babu.**; Li, Guanguan.; Stephen, Michael Rajesh.; Cook, J. M.; Rowlett, James K. *Neuropsychopharmacology.* **2017**, *Manuscript under review*
- “Identification of *Staphylococcus aureus* cellular pathways affected by the stilbenoid lead drug SK-03-92 using a microarray” Schwan, William R.; Polanowski Rebecca.; Dunman Paul M.; Medina-Bielski Sara.; Lane Michelle.; **Tiruvedhula, V. V. N. Phani Babu.**; Witzigmann, C. M.; Rott Marc.; Lipker Lauren.; Monte, Aaron.; James M. Cook.; Somerville, Greg A.; Mikel, Cassandra. *The Journal of Antibiotics*, **2017**, *Manuscript under review*
- “Synthesis of Bisindole Alkaloids from the Apocynaceae Which Contain a Macroline or Sarpagine Unit: A Review” Rahman, Md Toufiqur.; **Tiruvedhula, V. V. N. Phani Babu.**; Cook, James M. *Molecules*, **2016**, *21*, 1525
- “Effects of the benzodiazepine GABA_A α 1-preferring antagonist 3-isopropoxy- β -carboline hydrochloride (3-ISOPBC) on alcohol seeking and self-administration in baboons” Holtyn, August F.;

Tiruvedhula, V. V. N. Phani Babu.; Stephen, Michael Rajesh.; Cook, James M.; Weerts, Elise M. *Drug and Alcohol Dependence*, **2017**, *170*, 25

- “Early life stress is a risk factor for excessive alcohol drinking and impulsivity in adults and is mediated via a CRF/GABA_A mechanism” Gondre-Lewis, Marjorie C.; Warnock, Kaitlin T.; Wang, Hong.; June jr. Harry L.; Bell, Kimberly A.; Rabe, Holger.; **Tiruvedhula, V. V. N. Phani Babu.**; Cook, James M.; Luddens, Hartmut.; Aurelian, Laure.; June Sr., Harry L. *Stress*. **2016**, *19*, 235
- “Synthesis of Aza and Carbocyclic β -Carbolines for Treatment of Alcohol Abuse. Regiospecific Solution to The Problem of 3,6-Disubstituted β -Carbolines Specificity” **Tiruvedhula, V. V. N. Phani Babu.**; Methuku, Kashi Reddy.; Deschamps, J.R.; Cook, J.M. *Org. Biomol. Chem.* **2015**, *13*, 10705
- “Triple monoamine uptake inhibitors demonstrate a pharmacologic association between excessive drinking and impulsivity in high-alcohol-preferring (HAP) mice” O'Tousa, D. S.; Warnock, K. T.; Matson, L. M.; Namjoshi, O. A.; Linn, M. V.; **Tiruvedhula, V.V.N. Phani Babu.**; Halcomb, M. E.; Cook, J.; Grahame, N. J.; June, H. L. *Addiction Biology*. **2015**, *20*, 236
- “Stereospecific Total Synthesis of the Indole Alkaloid Ervincidine. Establishment of the C-6 Hydroxyl Stereochemistry” Rallapalli, S.K.; Namjoshi, O.A.; **Tiruvedhula, V.V.N. Phani Babu.**; Deschamps, J.R.; Cook, J.M. *J. Org. Chem.* **2014**, *79*, 3776
- “Little evidence of a role for the $\alpha 1$ GABA_A subunit-containing receptor in a rhesus monkey model of alcohol drinking” Sawyer, E. K.; Moran, C.; Sirbu, M. H.; Szafir, M.; Van Linn, M.; Namjoshi, O.; **Tiruvedhula, V.V.N. Phani Babu.**; Cook, J. M.; Platt, D. M. *Alcohol Clin Exp Res*. **2014**, *38*, 1108
- “Duration of treatment and activation of $\alpha 1$ -containing GABA_A receptors variably affect the level of anxiety and seizure susceptibility after diazepam withdrawal in rats” Kovačević, J.; Timić, T.; **Tiruvedhula, V.V.N. Phani Babu.**; Batinić, B.; Namjoshi, O. A.; Milić, M.; Joksimović, S.; Cook, J. M.; Savić, M. M. *Brain research bulletin*. **2014**, *104*, 1
- “Design and synthesis of novel antimicrobials with activity against Gram-positive bacteria and mycobacterial species, including *M. tuberculosis*” **Tiruvedhula, V.V.N. Phani Babu.**; Witzigmann, C. M.; Verma, R.; Kabir, M. S.; Rott, M.; Schwan, W. R.; Medina-Bielski, S.; Lane, M.; Close, W.; Polanowski, R. L.; Sherman, D.; Monte, A.; Deschamps, J.R.; Cook, J.M. *Bioorg. Med. Chem.* **2013**, *21*, 7830
- “ β CCT, an antagonist selective for $\alpha 1$ GABA_A receptors, reverses diazepam withdrawal-induced anxiety in rats” Divljaković, J.; Milić, M.; Namjoshi, O. A.; **Tiruvedhula, V.V.N. Phani Babu.**; Timić, T.; Cook, J. M.; Savić, M. M. *Brain research bulletin*. **2013**, *91*, 1
- “Base-mediated stereospecific synthesis of aryloxy and amino substituted ethyl acrylates” Kabir, M.S.; Namjoshi, O. A.; Verma, R.; Lorenz, M.; **Tiruvedhula, V.V.N. Phani Babu.**; Monte, A.; Bertz, S. H.; Schwabacher, A. W.; Cook, J. M. *J. Org. Chem.* **2012**, *77*, 300

Patents:

- “Stereospecific synthesis of acrylate ethers and amines for industrial and medicinal applications” Cook, J. M.; Witzigmann, C.; **Tiruvedhula, V.V.N. Phani Babu.**; Monte, A.; Rott, M.; Schwan, W.; US Provisional Patent Application No. 61/610,574.
- “Novel Combination Therapy for Anxiety Disorders, Epilepsy, and Pain” Cook, J. M.; **Tiruvedhula, V.V.N. Phani Babu.**; Li, Jun-Xu. US Provisional Patent Application No. 62414363.

Manuscripts in Preparation:

- “Synthesis of Novel Acrylates as an Antimicrobials with Activity Against Drug Resistant Strains of *M. tuberculosis* and MRSA” **Tiruvedhula, V.V.N. Phani Babu.**; Witzigmann, C. M.; Rott, M.; Schwan, W. R.; Medina-Bielski, S.; Lane, M.; Close, W.; Polanowski, R. L.; Monte, A.; Cook, J.M. *European Journal of Medicinal Chemistry*.
- “Identifying of the Molecular Target for the Potent Antimicrobial Agent TI-I-100 to Treat Drug Resistance Bacteria”, **Tiruvedhula, V. V. N. Phani Babu.**; Kodali, Revathi.; Han Lanlan.; Bardy, Sonia L; Mirza, Shama P; Silvaggi, Nicholas R.; Stafford, Douglas.; Arnold, Leggy A.; Cook, James M.

ACS Chemical Biology.

- “A Novel synthetic method for the synthesis of the key quinine metabolite (3*S*)-3-Hydroxy-quinine” **Tiruvedhula, V. V. N. Phani Babu.**; Cook, James M. *J. Org. Chem.*

Presentations:

- “Identifying of the Molecular Target for the Potent Antimicrobial Agent TI-I-100 to Treat Drug Resistance Bacteria”, V. V. N. Phani Babu Tiruveedhula, Revathi Kodali, Lanlan Han, Sonia L. Bardy, Shama P. Mirza, Nicholas R. Silvaggi, Douglas Stafford, Leggy A. Arnold, James M. Cook. Research Symposium, Department of Chemistry and Biochemistry, UW-Milwaukee, May 23, 2017.
- “Synthesis of novel β -carboline as a GABA_A subtype selective agents for the treatment of alcohol abuse. Regiospecific solution to the problem of 3,6-disubstituted β - and aza- β -carboline specificity”, **V. V. N. Phani Babu Tiruveedhula**, Kaitlin Warnock, Harry June, Xenia Simeone, Margot Ernst, Marjorie C. Gondre-Lewis, James M Cook. 251st ACS National Meeting, San Diego, California, March 13-17, (Abst. MEDI 111), 2016.
- “Design and regiospecific synthesis of 3-substituted β -carbolines as a GABA_A subtype selective agents for the treatment of alcohol abuse”, **V. V. N. Phani Babu Tiruveedhula**, Kaitlin T. Warnock, Harry L. June, Margot Ernst, Marjorie C. Gondre-Lewis, and James M. Cook, 250th ACS National Meeting, Boston, Massachusetts, August 16-20, (Abst. MEDI 433), 2015.
- “Design and synthesis of novel β -carbolines as a Potential Anti Alcohol Agents”, **V. V. N. Phani Babu Tiruveedhula**, Kashi Reddy Methuku, Kaitlin Warnock, Harry June, James M Cook. Research Symposium, Department of Chemistry and Biochemistry, UW-Milwaukee, April 3, 2015.
- “Design and synthesis of novel β -carbolines as a Potential Anti Alcohol Agents”, **V. V. N. Phani Babu Tiruveedhula**, Kashi Reddy Methuku, Kaitlin Warnock, Harry June, James M Cook. The 7th Yao Yuan Biotech Pharma Symposium, University of Illinois, April 18, 2015.
- “Design and synthesis of novel β -carbolines as a GABA_A subtype selective agents for the treatment of alcohol abuse”, **V. V. N. Phani Babu Tiruveedhula**, Kashi Reddy Methuku, Kaitlin Warnock, Harry June, James M Cook. 248th ACS National Meeting, San Francisco, California, August 10-14, (Abst. MEDI 0128), 2014.
- “Design and synthesis of novel antimicrobials for the treatment of drug resistance bacterial infections, including *M. tuberculosis*”, **V. V. N. Phani Babu Tiruveedhula**, Christopher M Witzigmann, Marc Rott, William R Schwan, Aaron Monte, James M Cook, UWM Department of Chemistry and Biochemistry Awards Day Ceremony, Milwaukee, WI, April 18, 2014 (2014).
- “Design and synthesis of novel antimicrobials for the treatment of drug resistance bacterial infections, including *M. tuberculosis*”, **V. V. N. Phani Babu Tiruveedhula**, Christopher M Witzigmann, Marc Rott, William R Schwan, Aaron Monte, James M Cook. 247th ACS National Meeting, Dallas TX, March 16-20, (Abst. MEDI 263), 2014.
- “Design and Synthesis of novel antimicrobials with activity against Gram-positive and mycobacterial species, including *M.tuberculosis*”, **V. V. N. Phani Babu Tiruveedhula**, Christopher M Witzigmann, Marc Rott, William R Schwan, Aaron Monte, James M Cook. UWM Department of Chemistry and Biochemistry Awards Day Ceremony, Milwaukee, WI, April 20, 2013.
- “Design and Synthesis of novel antimicrobials with activity against Gram-positive and mycobacterial species, including *M.tuberculosis*”, **V. V. N. Phani Babu Tiruveedhula**, Christopher M Witzigmann, Marc Rott, William R Schwan, Aaron Monte, James M Cook. From Abstract of Papers, 245th ACS National Meeting and Exposition, New Orleans, LA, United States, April 7-11, 2013 (2013), MEDI-390.